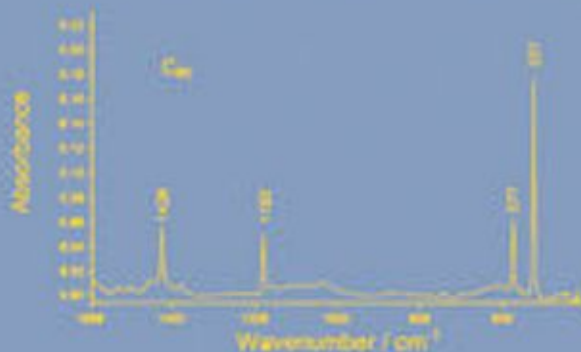


SIXTH EDITION

Infrared and Raman Spectra of Inorganic and Coordination Compounds

Part A

THEORY AND APPLICATIONS IN
INORGANIC CHEMISTRY



KAZUO NAKAMOTO

*Infrared and Raman
Spectra of Inorganic and
Coordination Compounds*

Infrared and Raman Spectra of Inorganic and Coordination Compounds

*Part A: Theory and Applications
in Inorganic Chemistry*

Sixth Edition

Kazuo Nakamoto

Wehr Professor Emeritus of Chemistry
Marquette University



A JOHN WILEY & SONS, INC., PUBLICATION

Copyright © 2009 by John Wiley & Sons, Inc. All rights reserved

Published by John Wiley & Sons, Inc., Hoboken, New Jersey
Published simultaneously in Canada

No part of this publication may be reproduced, stored in a retrieval system, or transmitted in any form or by any means, electronic, mechanical, photocopying, recording, scanning, or otherwise, except as permitted under Section 107 or 108 of the 1976 United States Copyright Act, without either the prior written permission of the Publisher, or authorization through payment of the appropriate per-copy fee to the Copyright Clearance Center, Inc., 222 Rosewood Drive, Danvers, MA 01923, (978) 750-8400, fax (978) 750-4470, or on the web at www.copyright.com. Requests to the Publisher for permission should be addressed to the Permissions Department, John Wiley & Sons, Inc., 111 River Street, Hoboken, NJ 07030, (201) 748-6011, fax (201) 748-6008, or online at <http://www.wiley.com/go/permission>.

Limit of Liability/Disclaimer of Warranty: While the publisher and author have used their best efforts in preparing this book, they make no representations or warranties with respect to the accuracy or completeness of the contents of this book and specifically disclaim any implied warranties of merchantability or fitness for a particular purpose. No warranty may be created or extended by sales representatives or written sales materials. The advice and strategies contained herein may not be suitable for your situation. You should consult with a professional where appropriate. Neither the publisher nor author shall be liable for any loss of profit or any other commercial damages, including but not limited to special, incidental, consequential, or other damages.

For general information on our other products and services or for technical support, please contact our Customer Care Department within the United States at (800) 762-2974, outside the United States at (317) 572-3993 or fax (317) 572-4002.

Wiley also publishes its books in a variety of electronic formats. Some content that appears in print may not be available in electronic formats. For more information about Wiley products, visit our web site at www.wiley.com.

Library of Congress Cataloging-in-Publication Data is available.

ISBN 978-0-471-74339-2

Printed in the United States of America

10 9 8 7 6 5 4 3 2 1

Contents

PREFACE TO THE SIXTH EDITION	ix
ABBREVIATIONS	xi
Chapter 1. Theory of Normal Vibrations	1
1.1. Origin of Molecular Spectra / 1	
1.2. Origin of Infrared and Raman Spectra / 5	
1.3. Vibration of a Diatomic Molecule / 9	
1.4. Normal Coordinates and Normal Vibrations / 15	
1.5. Symmetry Elements and Point Groups / 21	
1.6. Symmetry of Normal Vibrations and Selection Rules / 25	
1.7. Introduction to Group Theory / 34	
1.8. The Number of Normal Vibrations for Each Species / 39	
1.9. Internal Coordinates / 46	
1.10. Selection Rules for Infrared and Raman Spectra / 49	
1.11. Structure Determination / 56	
1.12. Principle of the GF Matrix Method / 58	
1.13. Utilization of Symmetry Properties / 65	
1.14. Potential Fields and Force Constants / 71	
1.15. Solution of the Secular Equation / 75	
1.16. Vibrational Frequencies of Isotopic Molecules / 77	
1.17. Metal–Isotope Spectroscopy / 79	

1.18. Group Frequencies and Band Assignments /	82
1.19. Intensity of Infrared Absorption /	88
1.20. Depolarization of Raman Lines /	90
1.21. Intensity of Raman Scattering /	94
1.22. Principle of Resonance Raman Spectroscopy /	98
1.23. Resonance Raman Spectra /	101
1.24. Theoretical Calculation of Vibrational Frequencies /	106
1.25. Vibrational Spectra in Gaseous Phase and Inert Gas Matrices /	109
1.26. Matrix Cocondensation Reactions /	112
1.27. Symmetry in Crystals /	115
1.28. Vibrational Analysis of Crystals /	119
1.29. The Correlation Method /	124
1.30. Lattice Vibrations /	129
1.31. Polarized Spectra of Single Crystals /	133
1.32. Vibrational Analysis of Ceramic Superconductors /	136
References /	141

Chapter 2. Applications in Inorganic Chemistry

149

2.1. Diatomic Molecules /	149
2.2. Triatomic Molecules /	159
2.3. Pyramidal Four-Atom Molecules /	173
2.4. Planar Four-Atom Molecules /	180
2.5. Other Four-Atom Molecules /	187
2.6. Tetrahedral and Square–Planar Five-Atom Molecules /	192
2.7. Trigonal–Bipyramidal and Tetragonal–Pyramidal XY_5 and Related Molecules /	213
2.8. Octahedral Molecules /	221
2.9. XY_7 and XY_8 Molecules /	237
2.10. X_2Y_4 and X_2Y_6 Molecules /	239
2.11. X_2Y_7 , X_2Y_8 , X_2Y_9 , and X_2Y_{10} Molecules /	244
2.12. Metal Cluster Compounds /	250
2.13. Compounds of Boron /	254
2.14. Compounds of Carbon /	258
2.15. Compounds of Silicon, Germanium, and Other Group IVB Elements /	276
2.16. Compounds of Nitrogen /	279
2.17. Compounds of Phosphorus and Other Group VB Elements /	285
2.18. Compounds of Sulfur and Selenium /	292

2.19. Compounds of Halogen /	296
References /	299

Appendixes	355
-------------------	------------

I. Point Groups and Their Character Tables /	355
II. Matrix Algebra /	368
III. General Formulas for Calculating the Number of Normal Vibrations in Each Species /	373
IV. Direct Products of Irreducible Representations /	377
V. Number of Infrared- and Raman-Active Stretching Vibrations for MX_nY_m -Type Molecules /	378
VI. Derivation of Eq. 1.113 /	379
VII. The G and F Matrix Elements of Typical Molecules /	382
VIII. Group Frequency Charts /	388
IX. Correlation Tables /	393
X. Site Symmetry for the 230 Space Groups /	407

Index	415
--------------	------------

Preface to the Sixth Edition

Since the fifth edition was published in 1996, a number of new developments have been made in the field of infrared and Raman spectra of inorganic and coordination compounds. The sixth edition is intended to emphasize new important developments as well as to catch up with the ever-increasing new literature. Major changes are described below.

Part A. Chapter 1 (“Theory of Normal Vibrations”) includes two new sections. Section 1.24 explains the procedure for calculating vibrational frequencies on the basis of density functional theory (DFT). The DFT method is currently used almost routinely to determine molecular structures and to calculate vibrational parameters. Section 1.26 describes new developments in matrix cocondensation techniques. More recently, a large number of novel inorganic and coordination compounds have been prepared by using this technique, and their structures have been determined and vibrational assignments have been made on the basis of results of DFT calculations. Chapter 2 (“Applications in Inorganic Chemistry”) has been updated extensively, resulting in a total number of references of over 1800. In particular, sections on triangular X_3 - and tetrahedral X_4 -type molecules have been added as Secs. 2.2 and 2.5, respectively. In Sec. 2.8, the rotational–vibrational spectrum of the octahedral UF_6 molecule is shown to demonstrate how an extremely small metal isotope shift by $^{235}U/^{238}U$ substitution (only 0.6040 cm^{-1}) can be measured. Section 2.14 (“Compounds of Carbon”) has been expanded to show significant applications of vibrational spectroscopy to the structural determination of fullerenes, endohedral fullerenes, and carbon nanotubes. Vibrational data on a number of novel inorganic compounds prepared most recently have been added throughout Chapter 2.

Part B. Chapter 3 (“Applications in Coordination Chemistry”) contains two new Sections: Sec. 3.6 (“Metallochloins, Chlorophylls, and Metallophthalocyanines”)

and Sec. 3.19 (“Complexes of Carbon Dioxide”). The total number of references has approached 1700 because of substantial expansion of other sections such as Secs. 3.5, 3.18, 3.20, 3.22, and 3.28. Chapter 4 (“Applications in Organometallic Chemistry”) includes new types of organometallic compounds obtained by matrix cocondensation techniques (Sec. 4.1). In Chapter 5 (“Applications in Bioinorganic Chemistry”), a new section (Sec. 5.4) has been added, and several sections such as Secs. 5.3, 5.7, and 5.9 have been expanded to include many important new developments.

I would like to express my sincere thanks to all who helped me in preparing this edition. Special thanks go to Prof. E. L. Varetto (University of La Plata, Argentina), Prof. S. Guha (University of Missouri, Columbia), and Prof. L. Andrews (University of Virginia) for their help in writing new sections in Chapter 1 of Part A. My thanks also go to all the authors and publishers who gave me permission to reproduce their figures in this and previous editions.

Finally, I would like to thank the staff of John Raynor Science Library of Marquette University for their help in collecting new references.

Milwaukee, Wisconsin
March 2008

KAZUO NAKAMOTO

Abbreviations

Several different groups of acronyms and other abbreviations are used:

1. IR, infrared; R, Raman; RR, resonance Raman; *p*, polarized; *dp*, depolarized; *ap*, anomalous polarization; *ia*, inactive.
2. ν , stretching; δ , in-plane bending or deformation; ρ_w , wagging; ρ_r , rocking; ρ_t , twisting; π , out-of-plane bending. Subscripts, *a*, *s*, and *d* denote antisymmetric, symmetric, and degenerate modes, respectively. Approximate normal modes of vibration corresponding to these vibrations are given in Figs. 1.25 and 1.26.
3. DFT, density functional theory; NCA, normal coordinate analysis; GVF, generalized valence force field; UBF, Urey–Bradley force field.
4. M, metal; L, ligand; X, halogen; R, alkyl group.
5. g, gas; l, liquid; s, solid; m or mat, matrix; sol'n or sl, solution; (gr) or (ex), ground or excited state.
6. Me, methyl; Et, ethyl; Pr, propyl; Bu, butyl; Ph, phenyl; Cp, cyclopentadienyl; OAc, acetate ion; py, pyridine; pic, picoline; en, ethylenediamine. Abbreviations of other ligands are given when they appear in the text.

In the tables of observed frequencies, values in parentheses are calculated or estimated values unless otherwise stated.

Chapter 1

Theory of Normal Vibrations

1.1. ORIGIN OF MOLECULAR SPECTRA

As a first approximation, the energy of the molecule can be separated into three additive components associated with (1) the motion of the electrons in the molecule,* (2) the vibrations of the constituent atoms, and (3) the rotation of the molecule as a whole:

$$E_{\text{total}} = E_{\text{el}} + E_{\text{vib}} + E_{\text{rot}} \quad (1.1)$$

The basis for this separation lies in the fact that electronic transitions occur on a much shorter timescale, and rotational transitions occur on a much longer timescale, than 10 vibrational transitions. The translational energy of the molecule may be ignored in this discussion because it is essentially not quantized.

If a molecule is placed in an electromagnetic field (e.g., light), a transfer of energy from the field to the molecule will occur when Bohr's frequency condition is satisfied:

$$\Delta E = h\nu \quad (1.2)$$

*Hereafter the word *molecule* may also represent an *ion*.

where ΔE is the difference in energy between two quantized states, h is Planck's constant (6.625×10^{-27} erg s), and ν is the frequency of the light. Here, the frequency is the number of electromagnetic waves in the distance that light travels in one second:

$$\nu = \frac{c}{\lambda} \quad (1.3)$$

where c is the velocity of light (3×10^{10} cm s $^{-1}$) and λ is the wavelength of the electromagnetic wave. If λ has the units of cm, ν has dimensions of (cm s $^{-1}$)/cm = s $^{-1}$, which is also called "Hertz (Hz)."

The wavenumber ($\tilde{\nu}$) defined by

$$\tilde{\nu} = \frac{1}{\lambda} \quad (1.4)$$

is most commonly used in vibrational spectroscopy. It has the dimension of cm $^{-1}$. By combining Eqs. 1.3 and 1.4, we obtain

$$\tilde{\nu} = \frac{1}{\lambda} = \frac{\nu}{c} \quad \text{or} \quad \nu = \frac{c}{\lambda} = c\tilde{\nu} \quad (1.5)$$

Although the dimensions of ν and $\tilde{\nu}$ differ from one another, it is convenient to use them interchangeably. Thus, an expression such as "a frequency shift of 5 cm $^{-1}$ " is used throughout this book.

Using Eq. 1.5, Bohr's condition (Eq. 1.2) is written as

$$\Delta E = hc\tilde{\nu} \quad (1.6)$$

Since h and c are known constants, ΔE can be expressed in units such as*

$$\begin{aligned} 1(\text{cm}^{-1}) &= 1.99 \times 10^{-16}(\text{erg} \cdot \text{molecule}^{-1}) \\ &= 2.86(\text{cal} \cdot \text{mol}^{-1}) \\ &= 1.24 \times 10^{-4}(\text{eV} \cdot \text{molecule}^{-1}) \end{aligned}$$

Suppose that

$$\Delta E = E_2 - E_1 \quad (1.7)$$

where E_2 and E_1 are the energies of the excited and ground states, respectively.

Then, the molecule "absorbs" ΔE when it is excited from E_1 to E_2 and "emits" ΔE when it reverts from E_2 to E_1 . Figure 1.1 shows the regions of the electromagnetic spectrum where ΔE is indicated in $\tilde{\nu}$, λ , and ν . In this book, we are concerned mainly with vibrational transitions which are observed in infrared (IR) or Raman (R) spectra.

*Use conversion factors such as

$$\begin{aligned} \text{Avogadro's number } N_0 &= 6.023 \times 10^{23}(\text{mol}^{-1}) \\ 1(\text{cal}) &= 4.1846 \times 10^7(\text{erg}) \\ 1(\text{eV}) &= 1.6021 \times 10^{-12}(\text{erg} \cdot \text{molecule}^{-1}) \end{aligned}$$

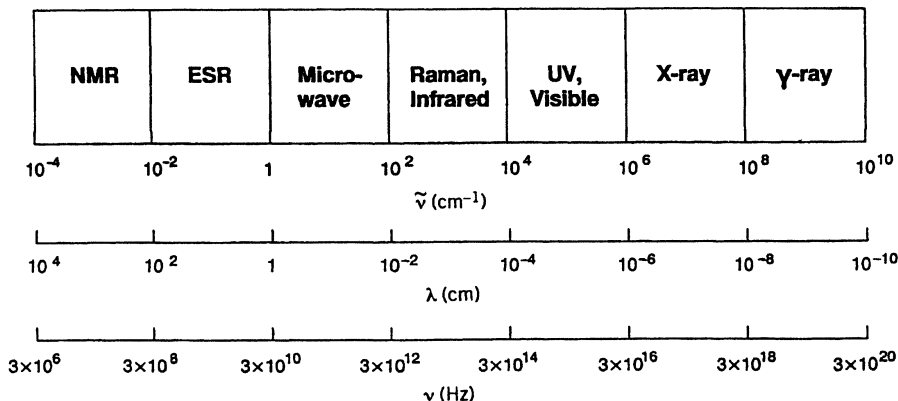


Fig. 1.1. Regions of the electromagnetic spectrum and energy units.

These transitions appear in the $10^2 \sim 10^4 \text{ cm}^{-1}$ region, and originate from vibrations of nuclei constituting the molecule. Rotational transitions occur in the $1\text{--}10^2 \text{ cm}^{-1}$ region (microwave region) because rotational levels are relatively close to each other, whereas electronic transitions are observed in the $10^4\text{--}10^6 \text{ cm}^{-1}$ region (UV-visible region) because their energy levels are far apart. However, such division is somewhat arbitrary, for pure rotational spectra may appear in the far-infrared region if transitions to higher excited states are involved, and pure electronic transitions may appear in the near-infrared region if electronic levels are closely spaced.

Figure 1.2 illustrates transitions of the three types mentioned for a diatomic molecule. As the figure shows, rotational intervals tend to increase as the rotational quantum number J increases, whereas vibrational intervals tend to decrease as the vibrational quantum number v increases. The dashed line below each electronic level indicates the “zero-point energy” that must exist even at a temperature of absolute zero as a result of Heisenberg’s uncertainty principle:

$$E_0 = \frac{1}{2} h\nu \quad (1.8)$$

It should be emphasized that not all transitions between these levels are possible. To see whether the transition is “allowed” or “forbidden,” the relevant selection rule must be examined. This, in turn, is determined by the symmetry of the molecule.

As expected from Fig. 1.2, electronic spectra are very complicated because they are accompanied by vibrational as well as rotational fine structure. The rotational fine structure in the electronic spectrum can be observed if a molecule is simple and the spectrum is measured in the gaseous state under high resolution. The vibrational fine structure of the electronic spectrum is easier to observe than the rotational fine structure, and can provide structural and bonding information about molecules in electronic excited states.

Vibrational spectra are accompanied by rotational transitions. Figure 1.3 shows the rotational fine structure observed for the gaseous ammonia molecule. In most polyatomic molecules, however, such a rotational fine structure is not observed

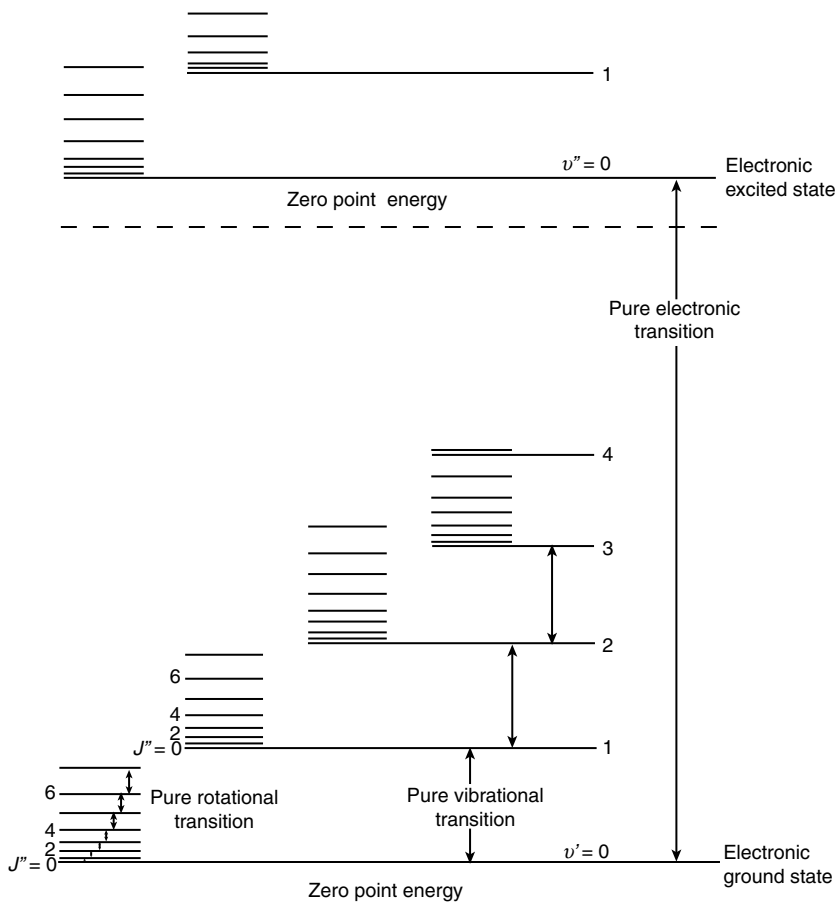


Fig. 1.2. Energy level of a diatomic molecule (the actual spacings of electronic levels are much larger, and those of rotational levels are much smaller, than that shown in the figure).

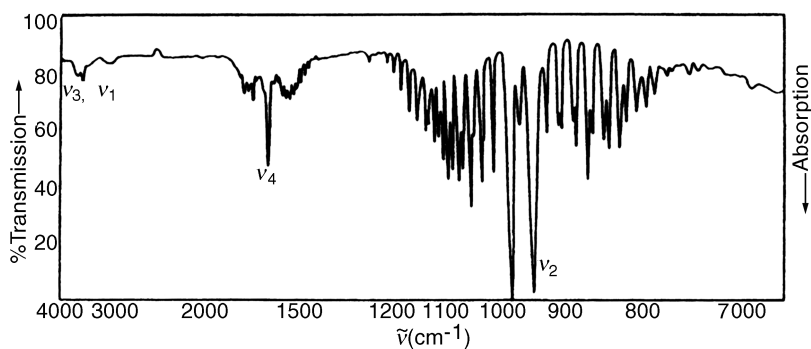


Fig. 1.3. Rotational fine structure of gaseous NH_3 .

because the rotational levels are closely spaced as a result of relatively large moments of inertia. Vibrational spectra obtained in solution do not exhibit rotational fine structure, since molecular collisions occur before a rotation is completed and the levels of the individual molecules are perturbed differently.

The selection rule allows any transitions corresponding to $\Delta v = \pm 1$ if the molecule is assumed to be a harmonic oscillator (Sec. 1.3). Under ordinary conditions, however, only the *fundamentals* that originate in the transition from $v = 0$ to $v = 1$ in the electronic ground state can be observed. This is because the Maxwell-Boltzmann distribution law requires that the ratio of population at $v = 0$ and $v = 1$ states is given by

$$R = \frac{P(v = 1)}{P(v = 0)} = e^{-\Delta E_v/kT} \quad (1.9)$$

where ΔE_v is the vibrational frequency (cm^{-1}) and $kT = 208 \text{ (cm}^{-1}\text{)}$ at room temperature. In the case of H_2 , $\Delta E_v = 4160 \text{ cm}^{-1}$ and $R = 2.16 \times 10^{-9}$. Thus, almost all molecules are at $v = 0$. However, the population at $v = 1$ increases as ΔE_v becomes small. For example, $R = 0.36$ for I_2 ($\Delta E_v = 213 \text{ cm}^{-1}$). Then, about 27% of the molecules are at $v = 1$ state, and the transition from $v = 1$ to $v = 2$ can be observed as a “hot band.”

In addition to the harmonic oscillator selection rule, another restriction results from the symmetry of the molecule (Sec. 1.10). Thus, the number of allowed transitions in polyatomic molecules is greatly reduced. *Overtones and combination bands** of these fundamentals are forbidden by the selection rule. However, they are weakly observed in the spectrum because of the anharmonicity of the vibration (Sec. 1.3). Since they are less important than the fundamentals, they will be discussed only when necessary.

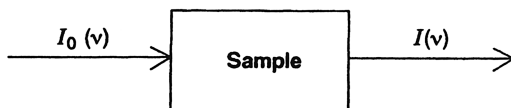
1.2. ORIGIN OF INFRARED AND RAMAN SPECTRA

As stated previously, vibrational transitions can be observed as infrared (IR) or Raman spectra.[†] However, the physical origins of these two spectra are markedly different. Infrared (absorption) spectra originate in photons in the infrared region that are absorbed by transitions between two vibrational levels of the molecule in the electronic ground state. On the other hand, Raman spectra have their origin in the electronic polarization caused by ultraviolet, visible, and near-IR light. If a molecule is irradiated by monochromatic light of frequency ν (laser), then, because of electronic polarization induced in the molecule by this incident beam, the light of frequency ν (“Rayleigh scattering”) as well as that of frequency $\nu \pm \nu_i$ (“Raman scattering”) is scattered where ν_i represents a vibrational frequency of the molecule. Thus, Raman spectra are presented as *shifts* from the incident frequency in the ultraviolet, visible, and near-IR region. Figure 1.4 illustrates the difference between IR and Raman techniques.

*Overtones represent some multiples of the fundamental, whereas combination bands arise from the sum or difference of two or more fundamentals.

[†]Raman spectra were first observed by C. V. Raman [*Indian J. Phys.* **2**, 387 (1928)] and C. V. Raman and K. S. Krishnan [*Nature* **121**, 501 (1928)].

IR



Raman

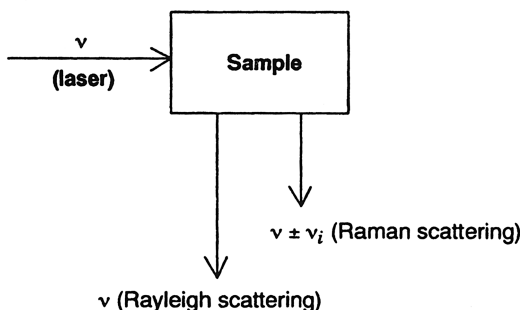


Fig. 1.4. Mechanisms of infrared absorption and Raman scattering.

Although Raman scattering is much weaker than Rayleigh scattering (by a factor of 10^{-3} – 10^{-5}), it is still possible to observe the former by using a strong exciting source. In the past, the mercury lines at 435.8 nm ($22,938\text{ cm}^{-1}$) and 404.7 nm ($24,705\text{ cm}^{-1}$) from a low-pressure mercury arc were used to observe Raman scattering. However, the advent of lasers revolutionized Raman spectroscopy. Lasers provide strong, coherent monochromatic light in a wide range of wavelengths, as listed in Table 1.1. In the case of resonance Raman spectroscopy (Sec. 1.22), the exciting frequency is chosen so as to fall inside the electronic absorption band. The degree of resonance enhancement varies as a function of the exciting frequency and reaches a maximum when the exciting frequency coincides with that of the electronic absorption maximum. It is possible to change the exciting frequency continuously by pumping dye lasers with powerful gas or pulsed lasers.

The origin of Raman spectra can be explained by an elementary classical theory. Consider a light wave of frequency ν with an electric field strength E . Since E fluctuates at frequency ν , we can write

$$E = E_0 \cos 2\pi\nu t \quad (1.10)$$

where E_0 is the amplitude and t the time. If a diatomic molecule is irradiated by this light, the dipole moment P given by

$$P = \alpha E = \alpha E_0 \cos 2\pi\nu t \quad (1.11)$$

TABLE 1.1. Some Representative Laser Lines for Raman Spectroscopy

Laser ^a	Mode	Wavelength (nm)	$\tilde{\nu}$ (cm ⁻¹)
Gas lasers			
Ar-ion	CW	488.0 (blue)	20491.8
		514.5 (green)	19436.3
Kr-ion	CW	413.1 (violet)	24207.2
		530.9 (green/yellow)	18835.9
		647.1 (red)	15453.6
He-Ne	CW	632.8 (red)	15802.8
He-Cd	CW	441.6 (blue/violet)	22644.9
Nitrogen	Pulsed	337.1 (UV)	29664.7
Excimer (XeCl)		308 (UV)	32467.5
Solid-state lasers			
Nd:YAG ^b	CW or pulsed	1064 (near-IR)	9398.4
Liquid lasers			
A variety of dye solutions are pumped by strong CW or pulsed-laser sources; a wide range (440–800 nm) can be covered continuously by choosing proper organic dyes			

^aAcronym of *light amplification by stimulated emission of radiation*.

^bAcronym of *neodymium-doped yttrium aluminum garnet*.

Source: For more information, see Nakamoto and colleagues [21,26].

is induced. Here α is a proportionality constant and is called the *polarizability*. If the molecule is vibrating with frequency ν_i , the nuclear displacement q is written as

$$q = q_0 \cos 2\pi\nu_i t \quad (1.12)$$

where q_0 is the vibrational amplitude. For small amplitudes of vibration, α is a linear function of q . Thus, we can write

$$\alpha = \alpha_0 + \left(\frac{\partial \alpha}{\partial q} \right)_0 q \quad (1.13)$$

Here, α_0 is the polarizability at the equilibrium position, and $(\partial\alpha/\partial q)_0$ is the rate of change of α with respect to the change in q , evaluated at the equilibrium position. If we combine Eqs. 1.11–1.13, we have

$$\begin{aligned}
 P &= \alpha E_0 \cos 2\pi\nu t \\
 &= \alpha_0 E_0 \cos 2\pi\nu t + \left(\frac{\partial \alpha}{\partial q} \right)_0 q_0 E_0 \cos 2\pi\nu t \cos 2\pi\nu_i t \\
 &= \alpha_0 E_0 \cos 2\pi\nu t \\
 &\quad + \frac{1}{2} \left(\frac{\partial \alpha}{\partial q} \right)_0 q_0 E_0 \{ \cos[2\pi(\nu + \nu_i)t] + \cos[2\pi(\nu - \nu_i)t] \}
 \end{aligned} \quad (1.14)$$

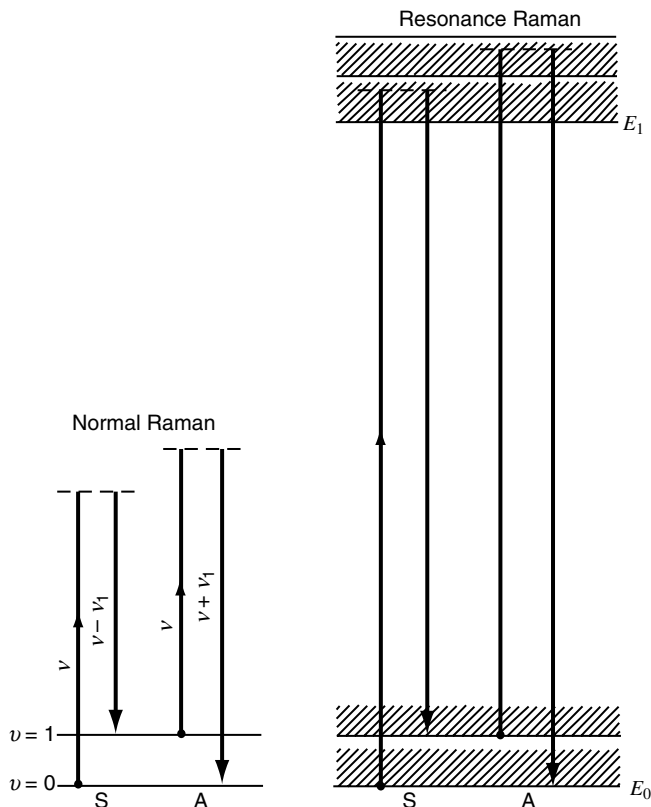


Fig. 1.5. Mechanisms of normal and resonance Raman scattering. S and A denote Stokes and anti-Stokes scattering, respectively. The shaded areas indicate the broadening of rotational-vibrational levels in the liquid and solid states (Sec. 1.22).

According to classical theory, the first term describes an oscillating dipole that radiates light of frequency ν (Rayleigh scattering). The second term gives the Raman scattering of frequencies $\nu + \nu_i$ (*anti-Stokes*) and $\nu - \nu_i$ (*Stokes*). If $(\partial\alpha/\partial q)_0$ is zero, the second term vanishes. Thus, the vibration is not Raman-active unless the polarizability changes during the vibration.

Figure 1.5 illustrates the mechanisms of *normal* and *resonance Raman (RR) scattering*. In the former, the energy of the exciting line falls far below that required to excite the first electronic transition. In the latter, the energy of the exciting line coincides with that of an electronic transition.* If the photon is absorbed and then emitted during the process, it is called *resonance fluorescence (RF)*. Although the conceptual difference between resonance Raman scattering and resonance fluorescence is subtle, there are several experimental differences which can be used to

*If the exciting line is close to but not inside an electronic absorption band, the process is called *preresonance Raman scattering*.

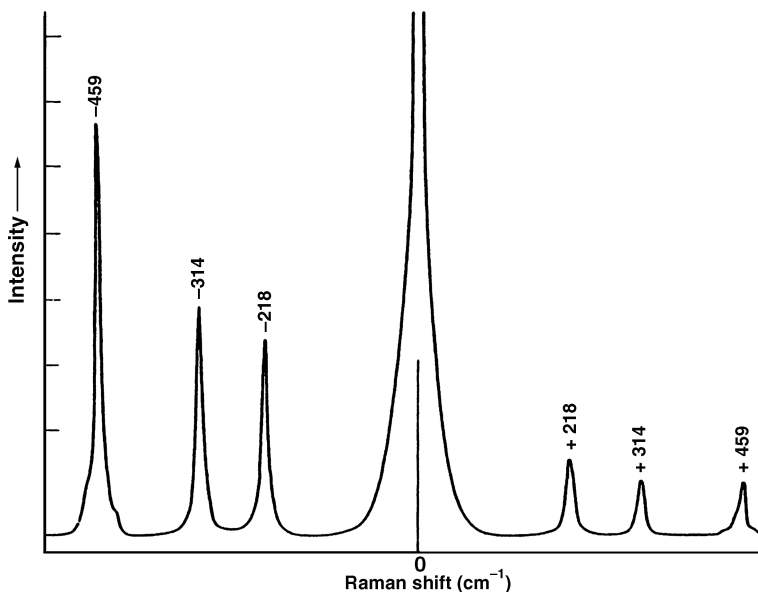


Fig. 1.6. Raman spectrum of CCl_4 (488.0 nm excitation).

distinguish between these two phenomena. For example, in RF spectra all lines are depolarized, whereas in RR spectra some are polarized and others are depolarized. Additionally, RR bands tend to be broad and weak compared with RF bands [66,67].

In the case of Stokes lines, the molecule at $v = 0$ is excited to the $v = 1$ state by scattering light of frequency $\nu - \nu_i$. Anti-Stokes lines arise when the molecule initially in the $v = 1$ state scatters radiation of frequency $\nu + \nu_i$ and reverts to the $v = 0$ state. Since the population of molecules is larger at $v = 0$ than at $v = 1$ (*Maxwell-Boltzmann distribution law*), the Stokes lines are always stronger than the anti-Stokes lines. Thus, it is customary to measure Stokes lines in Raman spectroscopy. Figure 1.6 illustrates the Raman spectrum (below 500 cm^{-1}) of CCl_4 excited by the blue line (488.0 nm) of an argon ion laser.

1.3. VIBRATION OF A DIATOMIC MOLECULE

Through quantum mechanical considerations [2,7], the vibration of two nuclei in a diatomic molecule can be reduced to the motion of a single particle of mass μ , whose displacement q from its equilibrium position is equal to the change of the internuclear distance. The mass μ is called the *reduced mass* and is represented by

$$\frac{1}{\mu} = \frac{1}{m_1} + \frac{1}{m_2} \quad (1.15)$$

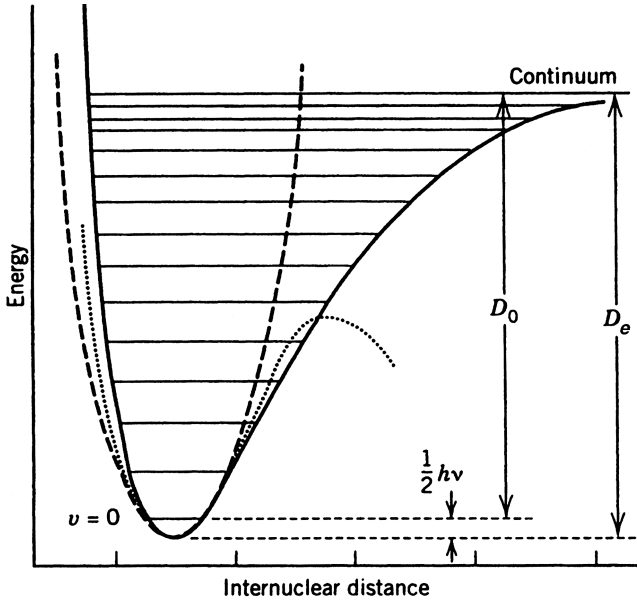


Fig. 1.7. Potential energy curves for a diatomic molecule: actual potential (solid line), parabolic potential (dashed line), and cubic potential (dotted line).

where m_1 and m_2 are the masses of the two nuclei. The kinetic energy is then

$$T = \frac{1}{2} \mu \dot{q}^2 = \frac{1}{2\mu} p^2 \quad (1.16)$$

where p is the conjugate momentum $\mu \dot{q}$. If a simple parabolic potential function such as that shown in Fig. 1.7 is assumed, the system represents a *harmonic oscillator*, and the potential energy is simply given by.

$$V = \frac{1}{2} K q^2 \quad (1.17)$$

Here K is the force constant for the vibration. Then the Schrödinger wave equation becomes

$$\frac{d^2 \psi}{dq^2} + \frac{8\pi^2 \mu}{h^2} \left(E - \frac{1}{2} K q^2 \right) \psi = 0 \quad (1.18)$$

If this equation is solved with the condition that ψ must be single-valued, finite, and continuous, the eigenvalues are

$$E_v = h\nu \left(v + \frac{1}{2} \right) = hc\tilde{\nu} \left(v + \frac{1}{2} \right) \quad (1.19)$$

with the frequency of vibration

$$v = \frac{1}{2\pi} \sqrt{\frac{K}{\mu}} \quad \text{or} \quad \tilde{\nu} = \frac{1}{2\pi c} \sqrt{\frac{K}{\mu}} \quad (1.20)$$

Here v is the vibrational quantum number, and it can have the values 0, 1, 2, 3, and so on.

The corresponding eigenfunctions are

$$\psi_v = \frac{(\alpha/\pi)^{1/4}}{\sqrt{2^v v!}} e^{-\alpha q^2/2} H_v(\sqrt{\alpha} q) \quad (1.21)$$

where $\alpha = 2\pi\sqrt{\mu K}/h = 4\pi^2\mu\nu/h$, and $H_v(\sqrt{\alpha} q)$ is a Hermite polynomial of the v th degree. Thus the eigenvalues and the corresponding eigenfunctions are

$$\begin{aligned} E_0 &= \frac{1}{2} h\nu, & \psi_0 &= (\alpha/\pi)^{1/4} e^{-\alpha q^2/2} \\ E_1 &= \frac{3}{2} h\nu, & \psi_1 &= (\alpha/\pi)^{1/4} 2^{1/2} q e^{-\alpha q^2/2} \\ & & \vdots & \\ & & \vdots & \end{aligned} \quad (1.22)$$

As Fig. 1.7 shows, actual potential curves can be approximated more exactly by adding a cubic term [2]:

$$V = \frac{1}{2} Kq^2 - Gq^3 \quad (K \gg G) \quad (1.23)$$

Then, the eigenvalues become

$$E_v = hc\omega_e \left(v + \frac{1}{2} \right) - hc x_e \omega_e \left(v + \frac{1}{2} \right)^2 + \cdots \quad (1.24)$$

where ω_e is the wavenumber corrected for *anharmonicity* and $x_e \omega_e$ indicates the magnitude of anharmonicity. Table 2.1a (in Chapter 2) lists ω_e and $x_e \omega_e$ for a number of diatomic molecules. Equation 1.24 shows that the energy levels of the anharmonic oscillator are not equidistant, and the separation decreases slowly as v increases. This anharmonicity is responsible for the appearance of overtones and combination vibrations, which are forbidden in the harmonic oscillator.

The values of x_e and $x_e \omega_e$ can be determined by observing a series of overtone bands in IR and Raman spectra. From Eq. 1.24, we obtain

$$\frac{E_v - E_0}{hc} = v\omega_e - x_e \omega_e (v^2 + v) + \cdots$$

Then

$$\begin{aligned} \text{Fundamental:} & \quad \tilde{\nu}_1 = \omega_e - 2x_e \omega_e \\ \text{First overtone:} & \quad \tilde{\nu}_2 = 2\omega_e - 6x_e \omega_e \\ \text{Second overtone:} & \quad \tilde{\nu}_3 = 3\omega_e - 12x_e \omega_e \end{aligned}$$

For H^{35}Cl , these transitions are observed at 2885.9 , 5668.1 , and 8347.0 cm^{-1} , respectively, in IR spectrum [2]. Using these values, we find that

$$\omega_e = 2988.9\text{ cm}^{-1} \quad \text{and} \quad x_e\omega_e = 52.05\text{ cm}^{-1}$$

As will be shown in Sec. 1.23, a long series of overtone bands can be observed when Raman spectra of small molecules such as I_2 and TiI_4 are measured under rigorous resonance conditions. Anharmonicity constants can also be determined from the analysis of rotational fine structures of vibrational transitions [2].

Since the anharmonicity correction has not been made for most polyatomic molecules, in large part because of the complexity of the calculation, the frequencies given in Chapter 2 are not corrected for anharmonicity (except those given in Table 2.1a).

According to Eq. 1.20, the wavenumber of the vibration in a diatomic molecule is given by

$$\tilde{\nu} = \frac{1}{2\pi c} \sqrt{\frac{K}{\mu}} \quad (1.20)$$

A more exact expression is given by using the wavenumber corrected for anharmonicity:

$$\omega_e = \frac{1}{2\pi c} \sqrt{\frac{K}{\mu}} \quad (1.25)$$

or

$$K = 4\pi^2 c^2 \omega_e^2 \mu \quad (1.26)$$

For HCl , $\omega_e = 2989\text{ cm}^{-1}$ and $\mu = 0.9799\text{ awu}$ (where awu is the atomic weight unit). Thus, we obtain*

$$\begin{aligned} K &= \frac{4(3.14)^2(3 \times 10^{10})^2}{6.025 \times 10^{23}} \omega_e^2 \mu \\ &= (5.8883 \times 10^{-2}) \omega_e^2 \mu \\ &= (5.8883 \times 10^{-2})(2989)^2(0.9799) \\ &= 5.16 \times 10^5 (\text{dyn/cm}) \\ &= 5.16 (\text{mdyn}/\text{\AA})^* \end{aligned}$$

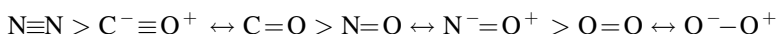
Table 1.2 lists the observed frequencies ($\tilde{\nu}$), wavenumbers corrected for anharmonicity (ω_e), reduced masses (μ), and force constants (K) for several series of diatomic

* $10^5 (\text{dynes/cm}) = 10^5 (10^3 \text{ millidynes}/10^8 \text{ \AA}) = 1 (\text{mdyn}/\text{\AA}) = 10^2 \text{ N/m (SI unit)}$.

TABLE 1.2. Relationships between Vibrational Frequency, Reduced Mass, and Force Constant

Molecule	Obs. $\tilde{\nu}$ (cm ⁻¹)	ω_e (cm ⁻¹)	μ (amu)	K (mdyn/Å)
H ₂	4160	4395	0.5041	5.73
HD	3632	3817	0.6719	5.77
D ₂	2994	3118	1.0074	5.77
HF	3962	4139	0.9573	9.65
HCl	2886	2989	0.9799	5.16
HBr	2558	2650	0.9956	4.12
HI	2233	2310	1.002	3.12
F ₂	892	—	9.5023	4.45
Cl ₂	564	565	17.4814	3.19
Br ₂	319	323	39.958	2.46
I ₂	213	215	63.466	1.76
N ₂	2331	2360	7.004	22.9
CO	2145	2170	6.8584	19.0
NO	1877	1904	7.4688	15.8
O ₂	1555	1580	8.000	11.8

molecules. In the first series, ω_e decreases in the order $\text{H}_2 > \text{HD} > \text{D}_2$, because μ increases in the same order, while K is almost constant (*mass effect*). In the second series, ω_e decreases in the order $\text{HF} > \text{HCl} > \text{HBr} > \text{HI}$, because K decreases in the same order, while μ shows little change (*force constant effect*). In the third series, ω_e decreases in the order $\text{F}_2 > \text{Cl}_2 > \text{Br}_2 > \text{I}_2$, because μ increases and K decreases in the same order. In this case, both mass effect and force constant effect are operative. In the last series, ω_e decreases in the order $\text{N}_2 > \text{CO} > \text{NO} > \text{O}_2$, mainly owing to the force constant effect. This may be attributed to the differences in bond order:



More examples of similar series in diatomic molecules are found in Sec. 2.1. These simple rules, obtained for a diatomic molecule, are helpful in understanding the vibrational spectra of polyatomic molecules.

Figure 1.8 indicates the relationship between the force constant and the dissociation energy for the three series listed in Table 1.2. In the series of hydrogen halides, the dissociation energy decreases almost linearly as the force constant decreases. Thus, the force constant may be used as a measure of the bond strength in this case. However, such a monotonic relationship does not hold for the other two series. This is not unexpected, because the force constant is a measure of the curvature of the potential well near the equilibrium position

$$K = \left(\frac{d^2V}{dq^2} \right)_{q \rightarrow 0} \quad (1.27)$$

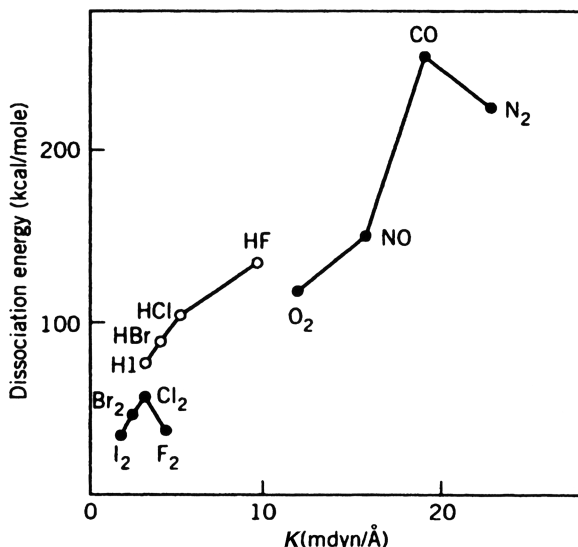


Fig. 1.8. Relationships between force constants and dissociation energies in diatomic molecules.

whereas the dissociation energy D_e is given by the depth of the potential energy curve (Fig. 1.7). Thus, a large force constant means sharp curvature of the potential well near the bottom, but does not necessarily indicate a deep potential well. Usually, however, a larger force constant is an indication of a stronger bond if the nature of the bond is similar in a series.

It is difficult to derive a general theoretical relationship between the force constant and the dissociation energy even for diatomic molecules.

In the case of small molecules, attempts have been made to calculate the force constants by quantum mechanical methods. The principle of the method is to express the total electronic energy of a molecule as a function of nuclear displacements near the equilibrium position and to calculate its second derivatives, $\partial^2 V / \partial q_i^2$, and so on for each displacement coordinate q_i . In the past, *ab initio* calculations of force constants were made for small molecules such as HF, H₂O, and NH₃. The force constants thus obtained are in good agreement with those calculated from the analysis of vibrational spectra. More recent progress in computer technology has made it possible to extend this approach to more complex molecules (Sec. 1.24).

There are several empirical relationships which relate the force constant to the bond distance. Badger's rule [68] is given by

$$K = 1.86(r - d_{ij})^{-3} \quad (1.28)$$

where r is the bond distance and d_{ij} has a fixed value for bonds between atoms of row i and j in the periodic table. Gordy's rule [69] is expressed as

$$K = aN \left(\frac{\chi_A \chi_B}{d^2} \right)^{3/4} + b \quad (1.29)$$

where χ_A and χ_B are the electronegativities of atoms A and B constituting the bond, d is the bond distance, N is the bond order, and a and b are constants for certain broad classes of compounds. Herschbach and Laurie [70] modified Badger's rule in the form

$$r = d_{ij} + (a_{ij} - d_{ij})K^{-1/3} \quad (1.30)$$

Here, a_{ij} and d_{ij} are constants for atoms of rows i and j in the periodic table.

Another empirical relationship is found by plotting stretching frequencies against bond distances for a series of compounds having common bonds. Such plots are highly important in estimating the bond distance from the observed frequency. Typical examples are found in the $\text{OH} \cdots \text{O}$ hydrogen-bonded compounds [71], carbon–oxygen and carbon–nitrogen bonded compounds [72], and molybdenum–oxygen [73] and vanadium–oxygen bonded compounds [74]. More examples are given in Sec. 2.2.

1.4. NORMAL COORDINATES AND NORMAL VIBRATIONS

In diatomic molecules, the vibration of the nuclei occurs only along the line connecting two nuclei. In polyatomic molecules, however, the situation is much more complicated because all the nuclei perform their own harmonic oscillations. It can be shown, however, that any of these extremely complicated vibrations of the molecule may be represented as a superposition of a number of *normal vibrations*.

Let the displacement of each nucleus be expressed in terms of rectangular coordinate systems with the origin of each system at the equilibrium position of each nucleus. Then the kinetic energy of an N -atom molecule would be expressed as

$$T = \frac{1}{2} \sum_N m_N \left[\left(\frac{d\Delta x_N}{dt} \right)^2 + \left(\frac{d\Delta y_N}{dt} \right)^2 + \left(\frac{d\Delta z_N}{dt} \right)^2 \right] \quad (1.31)$$

If generalized coordinates such as

$$q_1 = \sqrt{m_1} \Delta x_1, \quad q_2 = \sqrt{m_1} \Delta y_1, \quad q_3 = \sqrt{m_1} \Delta z_1 \quad q_4 = \sqrt{m_2} \Delta x_2, \dots \quad (1.32)$$

are used, the kinetic energy is simply written as

$$T = \frac{1}{2} \sum_i^{3N} \dot{q}_i^2 \quad (1.33)$$

The potential energy of the system is a complex function of all the coordinates involved. For small values of the displacements, it may be expanded in a Taylor's series as

$$V(q_1, q_2, \dots, q_{3N}) = V_0 + \sum_i^{3N} \left(\frac{\partial V}{\partial q_i} \right)_0 q_i + \frac{1}{2} \sum_{i,j}^{3N} \left(\frac{\partial^2 V}{\partial q_i \partial q_j} \right)_0 q_i q_j + \dots \quad (1.34)$$

where the derivatives are evaluated at $q_i = 0$, the equilibrium position. The constant term V_0 can be taken as zero if the potential energy at $q_i = 0$ is taken as a standard. The $(\partial V / \partial q_i)_0$ terms also become zero, since V must be a minimum at $q_i = 0$. Thus, V may be represented by

$$V = \frac{1}{2} \sum_{i,j}^{3N} \left(\frac{\partial^2 V}{\partial q_i \partial q_j} \right)_0 q_i q_j = \frac{1}{2} \sum_{i,j}^{3N} b_{ij} q_i q_j \quad (1.35)$$

neglecting higher-order terms.

If the potential energy given by Eq. 1.35 did not include any cross-products such as $q_i q_j$, the problem could be solved directly by using Lagrange's equation:

$$\frac{d}{dt} \left(\frac{\partial T}{\partial \dot{q}_i} \right) + \frac{\partial V}{\partial q_i} = 0, \quad i = 1, 2, \dots, 3N \quad (1.36)$$

From Eqs. 1.33 and 1.35, Eq. 1.36 is written as

$$\ddot{q}_i + \sum_j b_{ij} q_j = 0, \quad j = 1, 2, \dots, 3N \quad (1.37)$$

If $b_{ij} = 0$ for $i \neq j$, Eq. 1.37 becomes

$$\ddot{q}_i + b_{ii} q_i = 0 \quad (1.38)$$

and the solution is given by

$$q_i = q_i^0 \sin \left(\sqrt{b_{ii}} t + \delta_i \right) \quad (1.39)$$

where q_i^0 and δ_i are the amplitude and the phase constant, respectively.

Since, in general, this simplification is not applicable, the coordinates q_i must be transformed into a set of new coordinates Q_i through the relations

$$\begin{aligned} q_1 &= \sum_i B_{1i} Q_i \\ q_2 &= \sum_i B_{2i} Q_i \\ &\vdots \\ q_k &= \sum_i B_{ki} Q_i \end{aligned} \quad (1.40)$$

The Q_i are called *normal coordinates* for the system. By appropriate choice of the coefficients B_{ki} , both the potential and the kinetic energies can be written as

$$T = \frac{1}{2} \sum_i \dot{Q}_i^2 \quad (1.41)$$

$$V = \frac{1}{2} \sum_i \lambda_i Q_i^2 \quad (1.42)$$

without any cross-products.

If Eqs. 1.41 and 1.42 are combined with Lagrange's equation (Eq. 1.36), there results

$$\ddot{Q}_i + \lambda_i Q_i = 0 \quad (1.43)$$

The solution of this equation is given by

$$Q_i = Q_i^0 \sin(\sqrt{\lambda_i} t + \delta_i) \quad (1.44)$$

and the frequency is

$$\nu_i = \frac{1}{2\pi} \sqrt{\lambda_i} \quad (1.45)$$

Such a vibration is called a *normal vibration*.

For the general N -atom molecule, it is obvious that the number of the normal vibrations is only $3N - 6$, since six coordinates are required to describe the translational and rotational motion of the molecule as a whole. Linear molecules have $3N - 5$ normal vibrations, as no rotational freedom exists around the molecular axis. Thus, the general form of the molecular vibration is a superposition of the $3N - 6$ (or $3N - 5$) normal vibrations given by Eq. 1.44.

The physical meaning of the normal vibration may be demonstrated in the following way. As shown in Eq. 1.40, the original displacement coordinate is related to the normal coordinate by

$$q_k = \sum_i B_{ki} Q_i \quad (1.40)$$

Since all the normal vibrations are independent of each other, consideration may be limited to a special case in which only one normal vibration, subscripted by 1, is excited (i.e., $Q_1^0 \neq 0, Q_2^0 = Q_3^0 = \dots = 0$). Then, it follows from Eqs. 1.40 and 1.44 that

$$\begin{aligned} q_k &= B_{k1} Q_1 = B_{k1} Q_1^0 \sin(\sqrt{\lambda_1} t + \delta_1) \\ &= A_{k1} \sin(\sqrt{\lambda_1} t + \delta_1) \end{aligned} \quad (1.46)$$

This relation holds for all k . Thus, it is seen that the excitation of one normal vibration of the system causes vibrations, given by Eq. 1.46, of all the nuclei in the system. In other words, in the normal vibration, all the nuclei move with the same frequency and in phase.

This is true for any other normal vibration. Thus Eq. 1.46 may be written in the more general form

$$q_k = A_k \sin(\sqrt{\lambda}t + \delta) \quad (1.47)$$

If Eq. 1.47 is combined with Eq. 1.37, there results

$$-\lambda A_k + \sum_j b_{kj} A_j = 0 \quad (1.48)$$

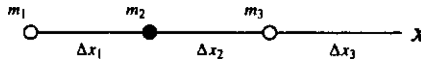
This is a system of first-order simultaneous equations with respect to A . In order for all the A s to be nonzero, we must solve

$$\begin{vmatrix} b_{11} - \lambda & b_{12} & b_{13} & \dots \\ b_{21} & b_{22} - \lambda & b_{23} & \dots \\ b_{31} & b_{32} & b_{33} - \lambda & \dots \\ \vdots & \vdots & \vdots & \ddots \end{vmatrix} = 0 \quad (1.49)$$

The order of this secular equation is equal to $3N$. Suppose that one root, λ_1 , is found for Eq. 1.49. If it is inserted in Eq. 1.48, A_{k1}, A_{k2}, \dots are obtained for all the nuclei. The same is true for the other roots of Eq. 1.49. Thus, the most general solution may be written as a superposition of all the normal vibrations:

$$q_k = \sum_l B_{kl} Q_l^0 \sin\left(\sqrt{\lambda_l}t + \delta_l\right) \quad (1.50)$$

The general discussion developed above may be understood more easily if we apply it to a simple molecule such as CO_2 , which is constrained to move in only one direction. If the mass and the displacement of each atom are defined as follows:



the potential energy is given by

$$V = \frac{1}{2} k \left[(\Delta x_1 - \Delta x_2)^2 + (\Delta x_2 - \Delta x_3)^2 \right] \quad (1.51)$$

Considering that $m_1 = m_3$, we find that the kinetic energy is written as

$$T = \frac{1}{2} m_1 (\dot{\Delta x}_1^2 + \dot{\Delta x}_3^2) + \frac{1}{2} m_2 \dot{\Delta x}_2^2 \quad (1.52)$$

Using the generalized coordinates defined by Eq. 1.32, we may rewrite these energies as

$$2V = k \left[\left(\frac{q_1}{\sqrt{m_1}} - \frac{q_2}{\sqrt{m_2}} \right)^2 + \left(\frac{q_2}{\sqrt{m_2}} - \frac{q_3}{\sqrt{m_1}} \right)^2 \right] \quad (1.53)$$

$$2T = \sum \dot{q}_i^2 \quad (1.54)$$

From comparison of Eq. 1.53 with Eq. 1.35, we obtain

$$\begin{aligned} b_{11} &= \frac{k}{m_1}, & b_{22} &= \frac{2k}{m_2} \\ b_{12} = b_{21} &= -\frac{k}{\sqrt{m_1 m_2}}, & b_{23} = b_{32} &= -\frac{k}{\sqrt{m_1 m_2}} \\ b_{13} = b_{31} &= 0, & b_{33} &= \frac{k}{m_1} \end{aligned}$$

If these terms are inserted in Eq. 1.49, we obtain the following result:

$$\begin{vmatrix} \frac{k}{m_1} - \lambda & -\frac{k}{\sqrt{m_1 m_2}} & 0 \\ -\frac{k}{\sqrt{m_1 m_2}} & \frac{2k}{m_2} - \lambda & -\frac{k}{\sqrt{m_1 m_2}} \\ 0 & -\frac{k}{\sqrt{m_1 m_2}} & \frac{k}{m_1} - \lambda \end{vmatrix} = 0 \quad (1.55)$$

By solving this secular equation, we obtain three roots:

$$\lambda_1 = \frac{k}{m_1}, \quad \lambda_2 = k\mu, \quad \lambda_3 = 0$$

where

$$\mu = \frac{2m_1 + m_2}{m_1 m_2}$$

Equation 1.48 gives the following three equations:

$$\begin{aligned} -\lambda A_1 + b_{11}A_1 + b_{12}A_2 + b_{13}A_3 &= 0 \\ -\lambda A_2 + b_{21}A_1 + b_{22}A_2 + b_{23}A_3 &= 0 \\ -\lambda A_3 + b_{31}A_1 + b_{32}A_2 + b_{33}A_3 &= 0 \end{aligned}$$

Using Eq. 1.47, we rewrite these as

$$(b_{11} - \lambda)q_1 + b_{12}q_2 + b_{13}q_3 = 0$$

$$b_{21}q_1 + (b_{22} - \lambda)q_2 + b_{23}q_3 = 0$$

$$b_{31}q_1 + b_{32}q_2 + (b_{33} - \lambda)q_3 = 0$$

If $\lambda_1 = k/m_1$ is inserted in the simultaneous equations above, we obtain

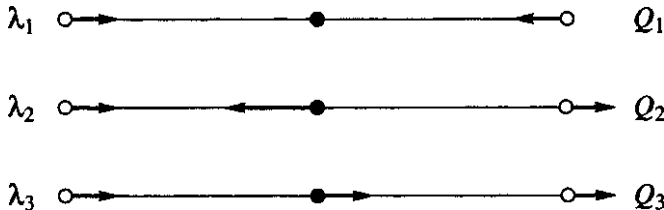
$$q_1 = -q_3, \quad q_2 = 0$$

Similar calculations give

$$q_1 = q_3, \quad q_2 = -2\sqrt{\frac{m_1}{m_2}}q_1 \quad \text{for } \lambda_2 = k\mu$$

$$q_1 = q_3, \quad q_2 = \sqrt{\frac{m_2}{m_1}}q_1 \quad \text{for } \lambda_3 = 0$$

The relative displacements are depicted in the following figure:



It is easy to see that λ_3 corresponds to the translational mode ($\Delta x_1 = \Delta x_2 = \Delta x_3$). The inclusion of λ_3 could be avoided if we consider the restriction that the center of gravity does not move; $m_1(\Delta x_1 + \Delta x_3) + m_2\Delta x_2 = 0$.

The relationships between the generalized coordinates and the normal coordinates are given by Eq. 1.40. In the present case, we have

$$q_1 = B_{11}Q_1 + B_{12}Q_2 + B_{13}Q_3$$

$$q_2 = B_{21}Q_1 + B_{22}Q_2 + B_{23}Q_3$$

$$q_3 = B_{31}Q_1 + B_{32}Q_2 + B_{33}Q_3$$

In the normal vibration whose normal coordinate is Q_1 , $B_{11} : B_{21} : B_{31}$ gives the ratio of the displacements. From the previous calculation, it is obvious that $B_{11} : B_{21} : B_{31} = 1 : 0 : -1$. Similarly, $B_{12} : B_{22} : B_{32} = 1 : -2\sqrt{m_1/m_2} : 1$ gives the ratio of the displacements in the normal vibration whose normal coordinate is Q_2 . Thus the mode

of a normal vibration can be drawn if the normal coordinate is translated into a set of rectangular coordinates, as is shown above.

So far, we have discussed only the vibrations whose displacements occur along the molecular axis. There are, however, two other normal vibrations in which the displacements occur in the direction perpendicular to the molecular axis. They are not treated here, since the calculation is not simple. It is clear that the method described above will become more complicated as a molecule becomes larger. In this respect, the **GF** matrix method described in Sec. 1.12 is important in the vibrational analysis of complex molecules.

By using the normal coordinates, the Schrödinger wave equation for the system can be written as

$$\sum_i \frac{\partial^2 \psi_n}{\partial Q_i^2} + \frac{8\pi^2}{h^2} \left(E - \frac{1}{2} \sum_i \lambda_i Q_i^2 \right) \psi_n = 0 \quad (1.56)$$

Since the normal coordinates are independent of each other, it is possible to write

$$\psi_n = \psi_1(Q_1) \psi_2(Q_2) \cdots \quad (1.57)$$

and solve the simpler one-dimensional problem.

If Eq. 1.57 is substituted in Eq. 1.56, there results

$$\frac{d^2 \psi_i}{dQ_i^2} + \frac{8\pi^2}{h^2} \left(E_i - \frac{1}{2} \lambda_i Q_i^2 \right) \psi_i = 0 \quad (1.58)$$

where

$$E = E_1 + E_2 + \cdots$$

with

$$\begin{aligned} E_i &= h\nu_i \left(v_i + \frac{1}{2} \right) \\ v_i &= \frac{1}{2\pi} \sqrt{\lambda_i} \end{aligned} \quad (1.59)$$

1.5. SYMMETRY ELEMENTS AND POINT GROUPS [9–14]

As noted before, polyatomic molecules have $3N-6$ or, if linear, $3N-5$ normal vibrations. For any given molecule, however, only vibrations that are permitted by

the selection rule for that molecule appear in the infrared and Raman spectra. Since the selection rule is determined by the symmetry of the molecule, this must first be studied.

The spatial geometric arrangement of the nuclei constituting the molecule determines its symmetry. If a coordinate transformation (a reflection or a rotation or a combination of both) produces a configuration of the nuclei indistinguishable from the original one, this transformation is called a *symmetry operation*, and the molecule is said to have a corresponding *symmetry element*. Molecules may have the following symmetry elements.

1.5.1. Identity I

This symmetry element is possessed by every molecule no matter how unsymmetric it is; the corresponding operation is to leave the molecule unchanged. The inclusion of this element is necessitated by mathematical reasons that will be discussed in Sec. 1.7.

1.5.2. A Plane of Symmetry σ

If reflection of a molecule with respect to some plane produces a configuration indistinguishable from the original one, the plane is called a *plane of symmetry*.

1.5.3. A Center of Symmetry i

If reflection at the center, that is, inversion, produces a configuration indistinguishable from the original one, the center is called a *center of symmetry*. This operation changes the signs of all the coordinates involved: $x_i \rightarrow -x_i$, $y_i \rightarrow -y_i$, $z_i \rightarrow -z_i$.

1.5.4. A p -Fold Axis of Symmetry C_p^*

If rotation through an angle $360^\circ/p$ about an axis produces a configuration indistinguishable from the original one, the axis is called a p -fold axis of symmetry C_p . For example, a twofold axis C_2 implies that a rotation of 180° about the axis reproduces the original configuration. A molecule may have a two-, three-, four-, five-, or sixfold, or higher axis. A linear molecule has an infinite-fold (denoted by ∞ -fold) axis of symmetry C_∞ since a rotation of $360^\circ/\infty$, that is, an infinitely small angle, transforms the molecule into one indistinguishable from the original.

1.5.5. A p -Fold Rotation–Reflection Axis S_p^*

If rotation by $360^\circ/p$ about the axis, followed by reflection at a plane perpendicular to the axis, produces a configuration indistinguishable from the original one, the axis is called a p -fold rotation–reflection axis. A molecule may have a two-, three-, four-,

* The notation C_p^n (or S_p^n) is used to indicate that the C_p (or S_p) operation is carried out successively n times.

five-, or sixfold, or higher, rotation–reflection axis. A symmetrical linear molecule has an S_∞ axis. It is easily seen that the presence of S_p always means the presence of C_p as well as σ when p is odd.

1.5.6. Point Group

A molecule may have more than one of these symmetry elements. Combination of more and more of these elements produces systems of higher and higher symmetry. Not all combinations of symmetry elements, however, are possible. For example, it is highly improbable that a molecule will have a C_3 and C_4 axis in the same direction because this requires the existence of a 12-fold axis in the molecule. It should also be noted that the presence of some symmetry elements often implies the presence of other elements. For example, if a molecule has two σ planes at right angles to each other, the line of intersection of these two planes must be a C_2 axis. A possible combination of symmetry operations whose axes intersect at a point is called a *point group*.*

Theoretically, an infinite number of point groups exist, since there is no restriction on the order (p) of rotation axes that may exist in an isolated molecule. Practically, however, there are few molecules and ions that possess a rotation axis higher than C_6 . Thus most of the compounds discussed in this book belong to the following point groups:

- (1) C_p . Molecules having only a C_p and no other elements of symmetry: C_1 , C_2 , C_3 , and so on.
- (2) C_{ph} . Molecules having a C_p and a σ_h perpendicular to it: $C_{1h} \equiv C_s$, C_{2h} , C_{3h} , and so on.
- (3) C_{pv} . Molecules having a C_p and $p\sigma_v$ through it: $C_{1v} \equiv C_s$, C_{2v} , C_{3v} , C_{4v} , \dots , $C_{\infty v}$.
- (4) D_p . Molecules having a C_p and pC_2 perpendicular to the C_p and at equal angles to one another: $D_1 \equiv C_2$, $D_2 \equiv V$, D_3 , D_4 , and so on.
- (5) D_{ph} . Molecules having a C_p , $p\sigma_v$ through it at angles of $360^\circ/2p$ to one another, and a σ_h perpendicular to the C_p : $D_{1h} \equiv C_{2v}$, $D_{2h} \equiv V_h$, D_{3h} , D_{4h} , D_{5h} , D_{6h} , \dots , $D_{\infty h}$.
- (6) D_{pd} . Molecules having a C_p , pC_2 perpendicular to it, and $p\sigma_d$ which go through the C_p and bisect the angles between two successive C_2 axes: $D_{2d} \equiv V_d$, D_{3d} , D_{4d} , D_{5d} , and so on.
- (7) S_p . Molecules having only a S_p (p even). For p odd, S_p is equivalent to $C_p \times \sigma_h$, for which other notations such as C_{3h} are used: $S_2 \equiv C_i$, S_4 , S_6 , and so on.
- (8) T_d . Molecules having three mutually perpendicular C_2 axes, four C_3 axes, and a σ_d through each pair of C_3 axes: regular tetrahedral molecules.

*In this respect, point groups differ from space groups, which involve translations and rotations about nonintersecting axes (see Sec. 1.27).

- (9) O_h . Molecules having three mutually perpendicular C_4 axes, four C_3 axes, and a center of symmetry, i : regular octahedral and cubic molecules.
- (10) I_h . Molecules having 6 C_5 axes, 10 C_3 axes, 15 C_2 axes, 15 σ planes, and a center of symmetry. In total, such molecules possess 120 symmetry elements. One example is an icosahedron having 20 equilateral triangular faces, which is found in the B_{12} skeleton of the $B_{12}H_{21}^{2-}$ ion (Sec. 2.13). Another example is a regular dodecahedron having 12 regular pentagonal faces. Buckminsterfullerene, C_{60} (Sec. 2.14), also belongs to the I_h point group. It is a truncated icosahedron with 20 hexagonal and 12 pentagonal faces.

Figure 1.9 illustrates the symmetry elements present in the point group, D_{4h} . Complete listings of the symmetry elements for common point groups are found in the character tables included in Appendix I. Figure 1.10 illustrates examples of molecules belonging to some of these point groups. From the symmetry perspective, molecules

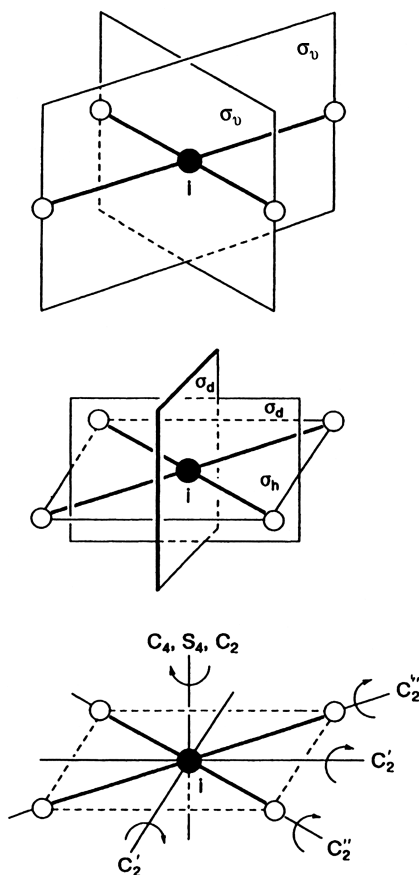


Fig. 1.9. Symmetry elements in D_{4h} point group.

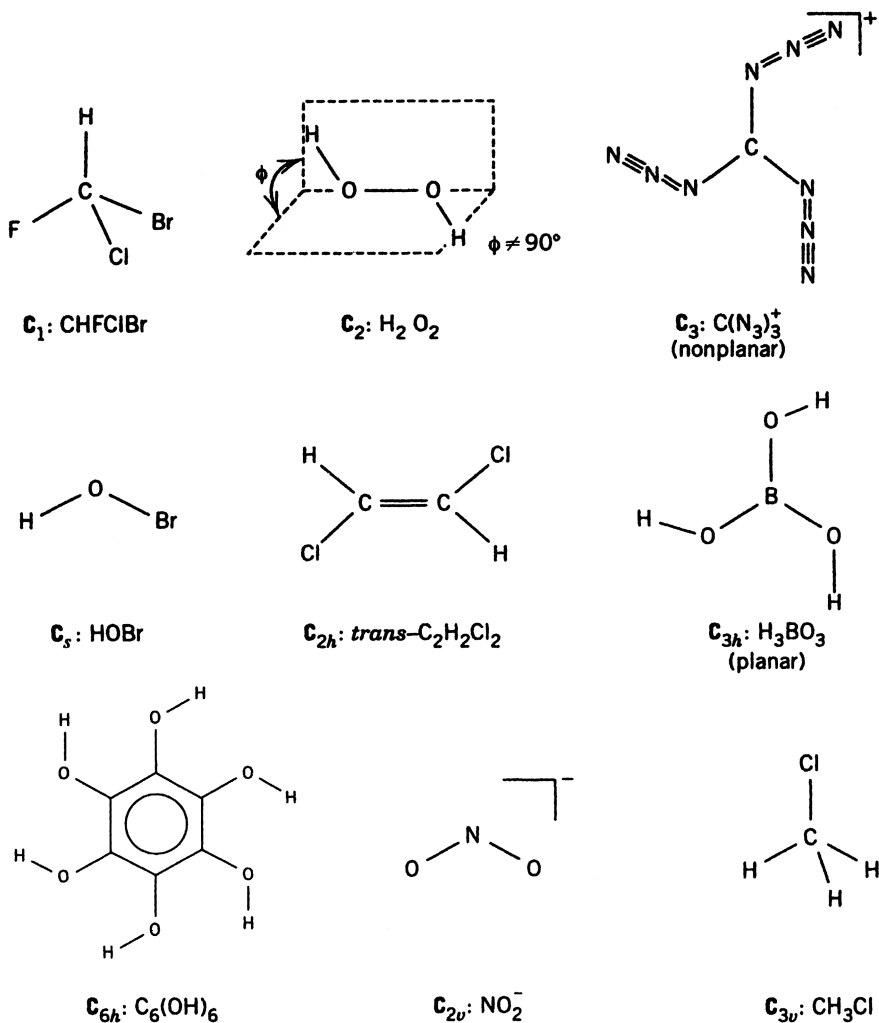


Fig. 1.10. Examples of molecules belonging to some point groups.

belonging to the C_1 , C_2 , C_3 , $D_2 \equiv V$, and D_3 groups possess only C_p axes, and are thus optically active.

1.6. SYMMETRY OF NORMAL VIBRATIONS AND SELECTION RULES

Figures 1.11 and 1.12 illustrate the normal modes of vibration of CO_2 and H_2O molecules, respectively. In each normal vibration, the individual nuclei carry out a simple harmonic motion in the direction indicated by the arrow, and all the nuclei have

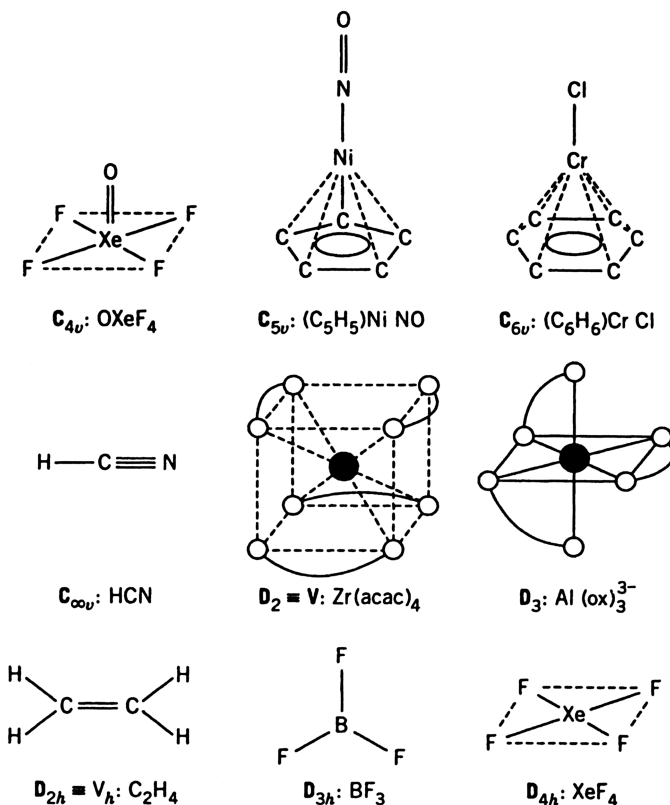


Fig. 1.10. (Continued)

the same frequency of oscillation (i.e., the frequency of the normal vibration) and are moving in the same phase. Furthermore, the relative lengths of the arrows indicate the relative velocities and the amplitudes for each nucleus.* The ν_2 vibrations in CO_2 are worth comment, since they differ from the others in that two vibrations (ν_{2a} and ν_{2b}) have exactly the same frequency. Apparently, there are an infinite number of normal vibrations of this type, which differ only in their directions perpendicular to the molecular axis. Any of them, however, can be resolved into two vibrations such as ν_{2a} and ν_{2b} , which are perpendicular to each other. In this respect, the ν_2 vibrations in CO_2 are called *doubly degenerate vibrations*. Doubly degenerate vibrations occur only when a molecule has an axis higher than twofold. *Triply degenerate vibrations* also occur in molecules having more than one C_3 axis.

To determine the symmetry of a normal vibration, it is necessary to begin by considering the kinetic and potential energies of the system. These were discussed in Sec. 1.4:

*In this respect, all the normal modes of vibration shown in this book are only approximate.

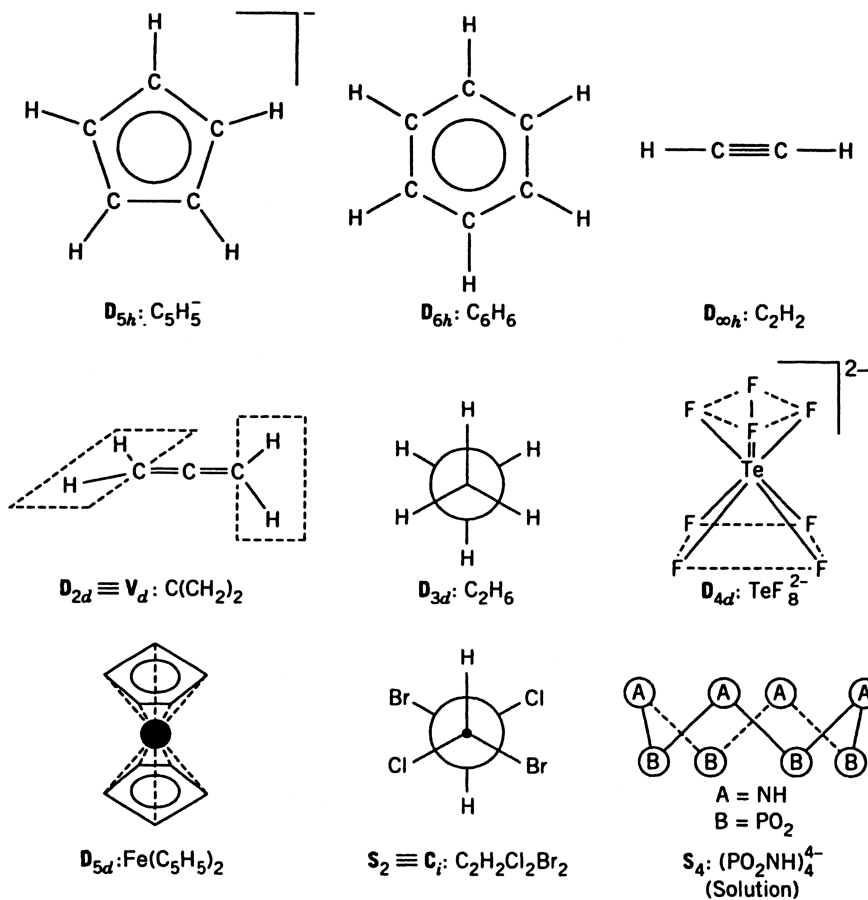


Fig. 1.10. (Continued)

$$T = \frac{1}{2} \sum_i \dot{Q}_i^2 \quad (1.60)$$

$$V = \frac{1}{2} \sum_i \lambda_i Q_i^2 \quad (1.61)$$

Consider a case in which a molecule performs only one normal vibration, Q_i . Then, $T = \frac{1}{2} \dot{Q}_i^2$ and $V = \frac{1}{2} \lambda_i Q_i^2$. These energies must be invariant when a symmetry operation, R , changes Q_i to RQ_i . Thus, we obtain

$$T = \frac{1}{2} \dot{Q}_i^2 = \frac{1}{2} (R\dot{Q}_i)^2$$

$$V = \frac{1}{2} \lambda_i Q_i^2 = \frac{1}{2} \lambda_i (RQ_i)^2$$

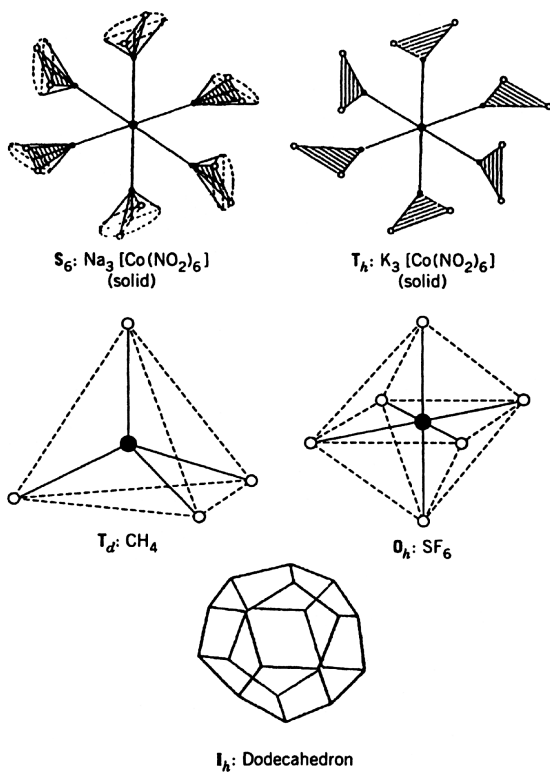


Fig. 1.10. (Continued)

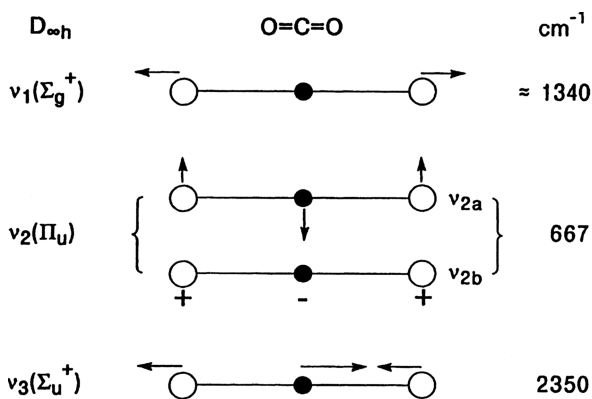


Fig. 1.11. Normal modes of vibration in CO_2 (+ and - denote vibrations going upward and downward, respectively, in the direction perpendicular to the paper plane).

For these relations to hold, it is necessary that

$$(RQ_i)^2 = Q_i^2 \quad \text{or} \quad RQ_i = \pm Q_i \quad (1.62)$$

Thus, the normal coordinate must change either into itself or into its negative. If $Q_i = RQ_i$, the vibration is said to be *symmetric*. If $Q_i = -RQ_i$, it is said to be *antisymmetric*.

If the vibration is doubly degenerate, we have

$$T = \frac{1}{2} \dot{Q}_{ia}^2 + \frac{1}{2} \dot{Q}_{ib}^2$$

$$V = \frac{1}{2} \lambda_i (Q_{ia})^2 + \frac{1}{2} \lambda_i (Q_{ib})^2$$

In this case, a relation such as

$$(RQ_{ia})^2 + (RQ_{ib})^2 = Q_{ia}^2 + Q_{ib}^2 \quad (1.63)$$

must hold. As will be shown later, such a relationship is expressed more conveniently by using a matrix form:*

$$R \begin{bmatrix} Q_{ia} \\ Q_{ib} \end{bmatrix} = \begin{bmatrix} A & B \\ C & D \end{bmatrix} \begin{bmatrix} Q_{ia} \\ Q_{ib} \end{bmatrix}$$

where the values of A , B , C , and D depend on the symmetry operation, R . In any case, the normal vibration must be either symmetric or antisymmetric or degenerate for each symmetry operation.

The symmetry properties of the normal vibrations of the H_2O molecule shown in Fig. 1.12 are classified as indicated in Table 1.3. Here, $+1$ and -1 denote symmetric and antisymmetric, respectively. In the ν_1 and ν_2 vibrations, all the symmetry properties are preserved during the vibration. Therefore they are *symmetric vibrations* and are called, in particular, *totally symmetric vibrations*. In the ν_3 vibration, however, symmetry elements such as C_2 and $\sigma_v(xz)$ are lost. Thus, it is called a *nonsymmetric vibration*. If a molecule has a number of symmetry elements, the normal vibrations are classified according to the number and the kind of symmetry elements preserved during the vibration.

To determine the activity of the vibrations in the infrared and Raman spectra, the selection rule must be applied to each normal vibration. As will be shown in Sec. 1.10, rigorous selection rules can be derived quantum mechanically, and applied to individual molecules using group theory.

For small molecules, however, the IR and Raman activities may be determined by simple inspection of their normal modes. First, we consider the general rule which states that *the vibration is IR-active if the dipole moment is changed during the vibration*. It is obvious that the vibration of a homopolar diatomic molecule is

*For matrix algebra, see Appendix II.

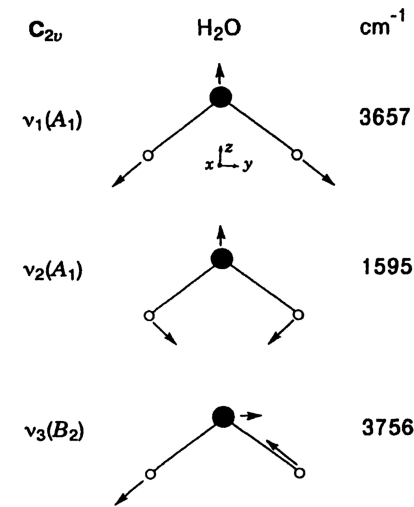


Fig. 1.12. Normal modes of vibration in H_2O .

TABLE 1.3.

C_{2v}	I	$C_2(z)$	$\sigma_v(xz)^a$	$\sigma_v(yz)^a$
Q_1, Q_2	+1	+1	+1	+1
Q_3	+1	-1	-1	+1

^a σ_v = vertical plane of symmetry.

not IR-active, whereas that of a heteropolar diatomic molecule is IR-active. In the case of CO_2 , shown in Fig. 1.11, it is readily seen that the ν_1 is not IR-active, whereas the ν_2 and ν_3 are IR-active. Figure 1.13 illustrates the changes in dipole moment during the three normal vibrations of H_2O . It is readily seen that all the vibrations are IR-active because the magnitude or direction of the dipole moment is changed as indicated.

To discuss Raman activity, we must consider the nature of polarizability introduced in Sec. 1.2. When a molecule interacts with the electric field of a laser beam, its electron cloud is distorted because the positively charged nuclei are attracted toward the negative pole, and the electrons toward the positive pole, as shown in Fig. 1.14. The charge separation produces an induced dipole moment (P) given by*

$$P = \alpha E^*$$

(1.64)

*A more complete form of this equation is $P = \alpha E + \frac{1}{2}\beta E^2 \dots$. Here, $\beta \ll \alpha$ and β is called the *hyperpolarizability*. The second term becomes significant only when E is large ($\sim 10^9$ V cm^{-1}). In this case, we observe novel spectroscopic phenomena such as the hyper Raman effect, stimulated Raman effect, inverse Raman effect, and coherent anti-Stokes Raman scattering (CARS). For a discussion of nonlinear Raman spectroscopy, see Refs. 25 and 26.

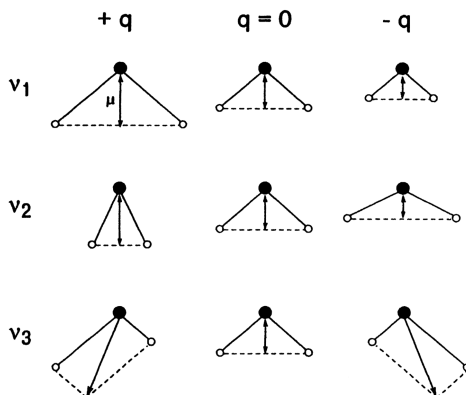


Fig. 1.13. Changes in dipole moment for H_2O during each normal vibration.

where E is the strength of the electric field and α is the polarizability. By resolving P , α , and E in the x , y , and z directions, we can write.

$$P_x = \alpha_x E_x, \quad P_y = \alpha_y E_y, \quad P_z = \alpha_z E_z \quad (1.65)$$

However, the actual relationship is more complicated since the direction of polarization may not coincide with the direction of the applied field. This is so because the direction of chemical bonds in the molecule also affects the direction of polarization. Thus, instead of Eq. 1.65, we have the relationship

$$\begin{aligned} P_x &= \alpha_{xx} E_x + \alpha_{xy} E_y + \alpha_{xz} E_z \\ P_y &= \alpha_{yx} E_x + \alpha_{yy} E_y + \alpha_{yz} E_z \\ P_z &= \alpha_{zx} E_x + \alpha_{zy} E_y + \alpha_{zz} E_z \end{aligned} \quad (1.66)$$

In matrix form, Eq. 1.66 is written as

$$\begin{bmatrix} P_x \\ P_y \\ P_z \end{bmatrix} = \begin{bmatrix} \alpha_{xx} & \alpha_{xy} & \alpha_{xz} \\ \alpha_{yx} & \alpha_{yy} & \alpha_{yz} \\ \alpha_{zx} & \alpha_{zy} & \alpha_{zz} \end{bmatrix} \begin{bmatrix} E_x \\ E_y \\ E_z \end{bmatrix} \quad (1.67)$$

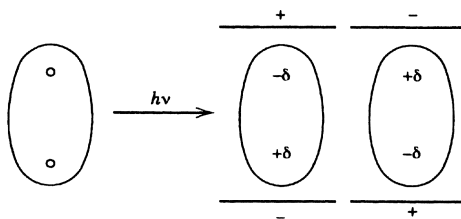
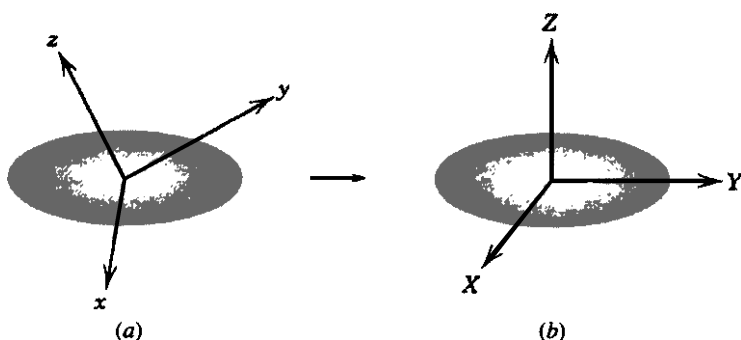


Fig. 1.14. Polarization of a diatomic molecule in an electric field.

and the first matrix on the right-hand side is called the *polarizability tensor*. In normal Raman scattering, the tensor is symmetric; $\alpha_{xy} = \alpha_{yx}$, $\alpha_{yz} = \alpha_{zy}$, and $\alpha_{xz} = \alpha_{zx}$. This is not so, however, in the case of resonance Raman scattering (Sec. 1.22).

According to quantum mechanics, *the vibration is Raman-active if one of these six components of the polarizability changes during the vibration*. Thus, it is obvious that the vibration of a homopolar diatomic molecule is Raman-active but not IR-active, whereas the vibration of a heteropolar diatomic molecule is both IR- and Raman-active.

Changes in the polarizability tensor can be visualized if we draw a *polarizability ellipsoid* by plotting $1/\sqrt{\alpha}$ in every direction from the origin. This gives a three-dimensional surface such as shown below:



If we rotate such an ellipsoid so that its principal axes coincide with the molecular axes (X , Y , and Z), Eq. 1.67 is simplified to

$$\begin{bmatrix} P_X \\ P_Y \\ P_Z \end{bmatrix} = \begin{bmatrix} \alpha_{XX} & 0 & 0 \\ 0 & \alpha_{YY} & 0 \\ 0 & 0 & \alpha_{ZZ} \end{bmatrix} \begin{bmatrix} E_X \\ E_Y \\ E_Z \end{bmatrix} \quad (1.68)$$

Such axes are called *principal axes of polarizability*. In terms of the polarizability ellipsoid, *the vibration is Raman-active if the polarizability ellipsoid changes in size, shape, or orientation during the vibration*.

As an example, Fig. 1.15 illustrates the polarizability ellipsoids for the three normal vibrations of H_2O at the equilibrium ($q = 0$) and two extreme configurations ($q = \pm q$). It is readily seen that both ν_1 and ν_2 are Raman-active because the size and the shape of the ellipsoid (α_{xx} , α_{yy} , and α_{zz}) change during these vibrations. The ν_3 is also Raman-active because the orientation of the ellipsoid (α_{yz}) changes during the vibration. Thus, all three normal vibrations of H_2O are Raman-active. Figure 1.16 illustrates the changes in polarizability ellipsoids during the normal vibrations of CO_2 . It is readily seen that ν_1 is Raman-active because the size of the ellipsoid

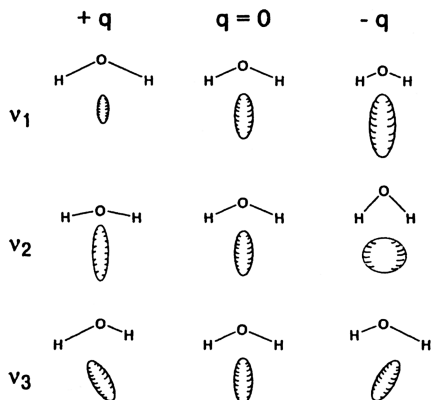


Fig. 1.15. Changes in polarizability ellipsoid during normal vibrations of H_2O .

changes during the vibration (α_{xx} , α_{yy} , and α_{zz} change proportionately). Although the size and/or shape of the ellipsoid change during the ν_2 and ν_3 vibrations, they are identical in two extreme positions, as seen in Fig. 1.16. If we consider a limiting case where the nuclei undergo very small displacements, there is effectively no change in the polarizability. This is illustrated in Fig. 1.17. Thus, these two vibrations are not Raman-active.

It should be noted that in CO_2 the vibration symmetric with respect to the center of symmetry (ν_1) is Raman-active and not IR-active, whereas the vibrations antisymmetric with respect to the center of symmetry (ν_2 and ν_3) are IR-active but not Raman-active. In a polyatomic molecule having a center of symmetry, the vibrations symmetric with respect to the center of symmetry (*g* vibrations*) are Raman-active

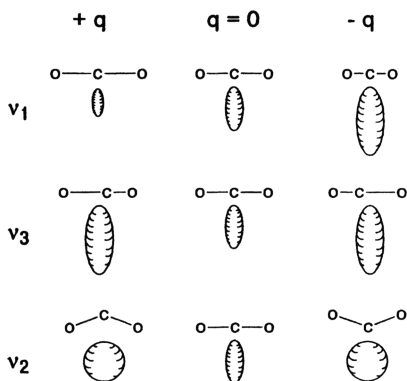


Fig. 1.16. Changes in polarizability ellipsoid during normal vibrations of CO_2 .

*The symbols *g* and *u* stand for *gerade* and *ungerade* (German), respectively.

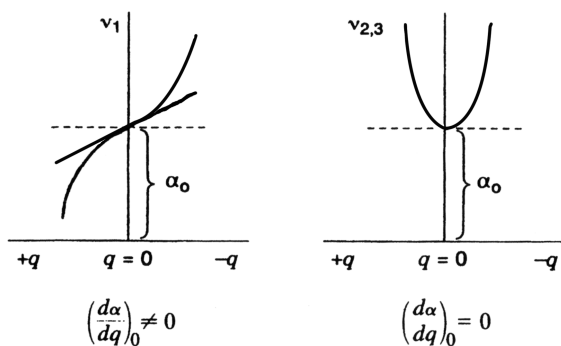


Fig. 1.17. Changes in polarizability with respect to displacement coordinate during the ν_1 and $\nu_{2,3}$ vibrations in CO_2 .

and not IR-active, but the vibrations antisymmetric with respect to the center of symmetry (u vibrations^{*}) are IR-active and not Raman-active. This rule is called the “mutual exclusion rule.” It should be noted, however, that in polyatomic molecules having several symmetry elements in addition to the center of symmetry, the vibrations that should be active according to this rule may not necessarily be active, because of the presence of other symmetry elements. An example is seen in a square-planar XY_4 -type molecule of D_{4h} symmetry, where the A_{2g} vibrations are not Raman-active and the A_{1u} , B_{1u} , and B_{2u} vibrations are not IR-active (see Sec. 2.6).

1.7. INTRODUCTION TO GROUP THEORY [9–14]

In Sec. 1.5, the symmetry and the point group allocation of a given molecule were discussed. To understand the symmetry and selection rules of normal vibrations in polyatomic molecules, however, a knowledge of group theory is required. The minimum amount of group theory needed for this purpose is given here.

Consider a pyramidal XY_3 molecule (Fig. 1.18) for which the symmetry operations I , C_3^+ , C_3^- , σ_1 , σ_2 , and σ_3 are applicable. Here, C_3^+ and C_3^- denote rotation through 120° in the clockwise and counterclockwise directions, respectively; and σ_1 , σ_2 , and σ_3 indicate the symmetry planes that pass through X and Y_1 , X and Y_2 , and X and Y_3 , respectively. For simplicity, let these symmetry operations be denoted by I , A , B , C , D , and E , respectively. Other symmetry operations are possible, but each is equivalent to some one of the operations mentioned. For instance, a clockwise rotation through 240° is identical with operation B . It may also be shown that two successive applications of any one of these operations is equivalent to some single operation of the group mentioned. Let operation C be applied to the original figure. This interchanges Y_2 and Y_3 . If operation A is applied to the resulting figure, the net result is the same as

^{*}The symbols g and u stand for *gerade* and *ungerade* (German), respectively.

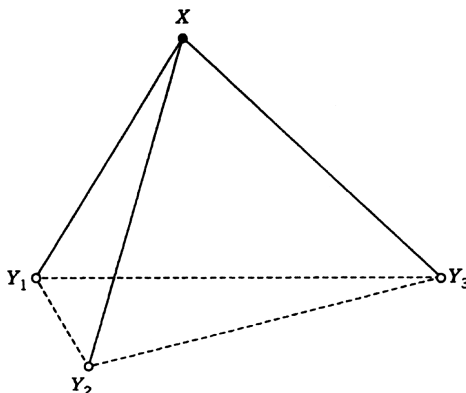


Fig. 1.18. Pyramidal XY_3 molecule.

application of the single operation D to the original figure. This is written as $CA = D$. If all the possible multiplicative combinations are made, then a tabular display such as Table 1.4, in which the operation applied first is written across the top, is obtained. This is called the *multiplication table* of the group.

It is seen that a group consisting of the mathematical elements (symmetry operations) I, A, B, C, D , and E satisfies the following conditions:

- (1) The product of any two elements in the set is another element in the set.
- (2) The set contains the identity operation that satisfies the relation $IP = PI = P$, where P is any element in the set.
- (3) The associative law holds for all the elements in the set, that is, $(CB)A = C(BA)$, for example.
- (4) Every element in the set has its reciprocal, X , which satisfies the relation $XP = PX = I$, where P is any element in the set. This reciprocal is usually denoted by P^{-1} .

These are necessary and sufficient conditions for a set of elements to form a *group*. It is evident that operations I, A, B, C, D , and E form a group in this sense. It should be noted

TABLE 1.4.

	I	A	B	C	D	E
I	I	A	B	C	D	E
A	A	B	I	D	E	C
B	B	I	A	E	C	D
C	C	E	D	I	B	A
D	D	C	E	A	I	B
E	E	D	C	B	A	I

that the commutative law of multiplication does not necessarily hold. For example, Table 1.4 shows that $CD \neq DC$.

The six elements can be classified into three types of operation: the identity operation I , the rotations C_3^+ and C_3^- , and the reflections σ_1 , σ_2 , and σ_3 . Each of these sets of operations is said to form a *class*. More precisely, two operations, P and Q , which satisfy the relation $X^{-1}PX = P$ or Q , where X is any operation of the group and X^{-1} is its reciprocal, are said to belong to the same class. It can easily be shown that C_3^+ and C_3^- , for example, satisfy the relation. Thus the six elements of the point group C_{3v} are usually abbreviated as I , $2C_3$, and $3\sigma_v$.

The relations between the elements of the group are shown in the multiplication table (Table 1.4). Such a tabulation of a group is, however, awkward to handle. The essential features of the table may be abstracted by replacing the elements by some analytical function that reproduces the multiplication table. Such an analytical expression may be composed of a simple integer, an exponential function, or a matrix. Any set of such expressions that satisfies the relations given by the multiplication table is called a *representation* of the group and is designated by Γ . The representations of the point group C_{3v} discussed above are indicated in Table 1.5. It can easily be proved that each representation in the table satisfies the multiplication table.

In addition to the three representations in Table 1.5, it is possible to write an infinite number of other representations of the group. If a set of six matrices of the type $S^{-1}R(K)S$ is chosen, where $R(K)$ is a representation of the element K given in Table 1.5, $S(|S| \neq 0)$ is any matrix of the same order as R , and S^{-1} is the reciprocal of S , this set also satisfies the relations given by the multiplication table. The reason is obvious from the relation

$$S^{-1}R(K)SS^{-1}R(L)S = S^{-1}R(K)R(L)S = S^{-1}R(KL)S$$

Such a transformation is called a *similarity transformation*. Thus, it is possible to make an infinite number of representations by means of similarity transformations.

On the other hand, this statement suggests that a given representation may possibly be broken into simpler ones. If each representation of the symmetry element K is

TABLE 1.5.

C_{3v}	I	A	B	C	D	E
$A_1(\Gamma_1)$	1	1	1	1	1	1
$A_2(\Gamma_2)$	1	1	1	-1	-1	-1
$E(\Gamma_3)$	$\begin{pmatrix} 1 & 0 \\ 0 & 1 \end{pmatrix}$	$\begin{pmatrix} -\frac{1}{2} & \frac{\sqrt{3}}{2} \\ -\frac{\sqrt{3}}{2} & -\frac{1}{2} \end{pmatrix}$	$\begin{pmatrix} -\frac{1}{2} & -\frac{\sqrt{3}}{2} \\ \frac{\sqrt{3}}{2} & -\frac{1}{2} \end{pmatrix}$	$\begin{pmatrix} -1 & 0 \\ 0 & 1 \end{pmatrix}$	$\begin{pmatrix} \frac{1}{2} & -\frac{\sqrt{3}}{2} \\ -\frac{\sqrt{3}}{2} & -\frac{1}{2} \end{pmatrix}$	$\begin{pmatrix} \frac{1}{2} & \frac{\sqrt{3}}{2} \\ \frac{\sqrt{3}}{2} & -\frac{1}{2} \end{pmatrix}$

transformed into the form

$$R(K) = \begin{vmatrix} Q_1(K) & 0 & 0 & 0 \\ 0 & Q_2(K) & 0 & 0 \\ 0 & 0 & Q_3(K) & 0 \\ 0 & 0 & 0 & Q_3(K) \end{vmatrix} \quad (1.69)$$

by a similarity transformation, $Q_1(K), Q_2(K), \dots$ are simpler representations. In such a case, $R(K)$ is called *reducible*. If a representation cannot be simplified any further, it is said to be *irreducible*. The representations Γ_1, Γ_2 , and Γ_3 in Table 1.5 are all irreducible representations. It can be shown generally that the number of irreducible representations is equal to the number of classes. Thus, only three irreducible representations exist for the point group C_{3v} . These representations are entirely independent of each other. Furthermore, the sum of the squares of the dimensions (l) of the irreducible representations of a group is always equal to the total number of the symmetry elements, namely, the *order of the group* (h). Thus

$$\sum l_i^2 = l_1^2 + l_2^2 + \dots = h \quad (1.70)$$

In the point group C_{3v} , it is seen that

$$1^2 + 1^2 + 2^2 = 6$$

A point group is classified into *species* according to its irreducible representations. In the point group C_{3v} , the species having the irreducible representations Γ_1, Γ_2 , and Γ_3 are called the A_1, A_2 , and E species, respectively.*

The sum of the diagonal elements of a matrix is called the *character* of the matrix and is denoted by χ . It is to be noted in Table 1.5 that the character of each of the elements belonging to the same class is the same. Thus, using the character, Table 1.5 can be simplified to Table 1.6. Such a table is called the *character table* of the point group C_{3v} .

That the *character* of a matrix is not changed by a similarity transformation can be proved as follows. If a similarity transformation is expressed by $T = S^{-1}RS$, then

$$\begin{aligned} \chi T &= \sum_i (S^{-1}RS)_{ii} = \sum_{i,j,k} (S^{-1})_{ij} R_{jk} S_{ki} = \sum_{j,k,i} S_{ki} (S^{-1})_{ij} R_{jk} \\ &= \sum_{j,k} \delta_{kj} R_{jk} = \sum_k R_{kk} = \chi R \end{aligned}$$

*For labeling of the irreducible representations (species), see Appendix I.

TABLE 1.6. Character Table of the Point Group C_{3v}

C_{3v}	I	$2C_3(z)$	$3\sigma_v$
$A_1 (\chi_1)$	1	1	1
$A_2 (\chi_2)$	1	1	-1
$E (\chi_3)$	2	-1	0

where δ_{kj} is Krönecker's delta (0 for $k \neq j$ and 1 for $k=j$). Thus, any reducible representation can be reduced to its irreducible representations by a similarity transformation that leaves the character unchanged. Therefore, the character of the reducible representation, $\chi(K)$, is written as

$$\chi(K) = \sum_m a_m \chi_m(K) \quad (1.71)$$

where $\chi_m(K)$ is the character of $Q_m(K)$, and a_m is a positive integer that indicates the number of times that $Q_m(K)$ appears in the matrix of Eq. 1.69. Hereafter the character will be used rather than the corresponding representation because a 1 : 1 correspondence exists between these two, and the former is sufficient for vibrational problems.

It is important to note that the following relation holds in Table 1.6:

$$\sum_K \chi_i(K) \chi_j(K) = h \delta_{ij} \quad (1.72)$$

If Eq. 1.71 is multiplied by $\chi_i(K)$ on both sides, and the summation is taken over all the symmetry operations, then

$$\begin{aligned} \sum_K \chi(K) \chi_i(K) &= \sum_K \sum_m a_m \chi_m(K) \chi_i(K) \\ &= \sum_m \sum_K a_m \chi_m(K) \chi_i(K) \end{aligned}$$

For a fixed m , we have

$$\sum_K a_m \chi_m(K) \chi_i(K) = a_m \sum_K \chi_m(K) \chi_i(K) = a_m h \delta_{im}$$

If we consider the sum of such a term over m , only the sum in which $m = i$ remains. Thus, we obtain

$$\sum_K \chi(K) \chi_m(K) = h a_m$$

or

$$a_m = \frac{1}{h} \sum_K \chi(K) \chi_m(K) \quad (1.73)$$

This formula is written more conveniently as

$$a_m = \frac{1}{h} \sum n \chi(K) \chi_m(K) \quad (1.74)$$

where n is the number of symmetry elements in any one class, and the summation is made over the different classes. As Sec. 1.8 will show, this formula is very useful in determining the number of normal vibrations belonging to each species.*

1.8. THE NUMBER OF NORMAL VIBRATIONS FOR EACH SPECIES

As shown in Sec. 1.6, the $3N - 6$ (or $3N - 5$) normal vibrations of an N -atom molecule can be classified into various species according to their symmetry properties. The number of normal vibrations in each species can be calculated by using the general equations given in Appendix III. These equations were derived from consideration of the vibrational degrees of freedom contributed by each set of identical nuclei for each symmetry species [1]. As an example, let us consider the NH_3 molecule belonging to the C_{3v} point group. The general equations are as follows:

$$\begin{aligned} A_1 \text{ species: } & 3m + 2m_v + m_0 - 1 \\ A_2 \text{ species: } & 3m + m_v - 1 \\ E \text{ species: } & 6m + 3m_v + m_0 - 2 \\ N(\text{total number of atoms}) &= 6m + 3m_v + m_0 \end{aligned}$$

From the definitions given in the footnotes of Appendix III, it is obvious that $m = 0$, $m_0 = 1$, and $m_v = 1$ in this case. To check these numbers, we calculate the total number of atoms from the equation for N given above. Since the result is 4, these assigned numbers are correct. Then, the number of normal vibrations in each species can be calculated by inserting these numbers in the general equations given above: 2, 0, and 2, respectively, for the A_1 , A_2 , and E species. Since the E species is doubly degenerate, the total number of vibrations is counted as 6, which is expected from the $3N - 6$ rule.

A more general method of finding the number of normal vibrations in each species can be developed by using group theory. The principle of the method is that all the

*Since this equation is not applicable to the infinite point groups ($C_{\infty v}$ and $D_{\infty h}$), several alternative approaches have been proposed (see Refs. 75 and 76).

representations are irreducible if normal coordinates are used as the basis for the representations. For example, the representations for the symmetry operations based on three normal coordinates, Q_1 , Q_2 , and Q_3 , which correspond to the ν_1 , ν_2 , and ν_3 vibrations in the H_2O molecule of Fig. 1.12, are as follows:

$$I \begin{bmatrix} Q_1 \\ Q_2 \\ Q_3 \end{bmatrix} = \begin{bmatrix} 1 & 0 & 0 \\ 0 & 1 & 0 \\ 0 & 0 & 1 \end{bmatrix} \begin{bmatrix} Q_1 \\ Q_2 \\ Q_3 \end{bmatrix}, \quad C_2(z) \begin{bmatrix} Q_1 \\ Q_2 \\ Q_3 \end{bmatrix} = \begin{bmatrix} 1 & 0 & 0 \\ 0 & 1 & 0 \\ 0 & 0 & -1 \end{bmatrix} \begin{bmatrix} Q_1 \\ Q_2 \\ Q_3 \end{bmatrix}$$

$$\sigma_v(xz) \begin{bmatrix} Q_1 \\ Q_2 \\ Q_3 \end{bmatrix} = \begin{bmatrix} 1 & 0 & 0 \\ 0 & 1 & 0 \\ 0 & 0 & -1 \end{bmatrix} \begin{bmatrix} Q_1 \\ Q_2 \\ Q_3 \end{bmatrix}, \quad \sigma_v(yz) \begin{bmatrix} Q_1 \\ Q_2 \\ Q_3 \end{bmatrix} = \begin{bmatrix} 1 & 0 & 0 \\ 0 & 1 & 0 \\ 0 & 0 & 1 \end{bmatrix} \begin{bmatrix} Q_1 \\ Q_2 \\ Q_3 \end{bmatrix}$$

Let a representation be written with the $3N$ rectangular coordinates of an N -atom molecule as its basis. If it is decomposed into its irreducible components, the basis for these irreducible representations must be the normal coordinates, and the number of appearances of the same irreducible representation must be equal to the number of normal vibrations belonging to the species represented by this irreducible representation. As stated previously, however, the $3N$ rectangular coordinates involve six (or five) coordinates, which correspond to the translational and rotational motions of the molecule as a whole. Therefore, the representations that have such coordinates as their basis must be subtracted from the result obtained above. Use of the character of the representation, rather than the representation itself, yields the same result.

For example, consider a pyramidal XY_3 molecule that has six normal vibrations. At first, the representations for the various symmetry operations must be written with the 12 rectangular coordinates in Fig. 1.19 as their basis. Consider pure rotation C_p^+ . If the

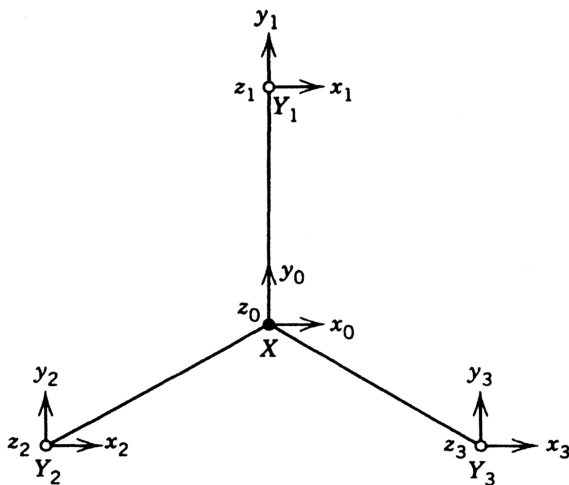


Fig. 1.19. Rectangular coordinates in a pyramidal XY_3 molecule (Z axis is perpendicular to the paper plane).

clockwise rotation of the point (x, y, z) around the z axis by the angle θ brings it to the point denoted by the coordinates (x', y', z') , the relations between these two sets of coordinates are given by.

$$\begin{aligned} x' &= x \cos\theta + y \sin\theta \\ y' &= -x \sin\theta + y \cos\theta \\ z' &= z \end{aligned} \quad (1.75)$$

By using matrix notation,* this can be written as

$$\begin{bmatrix} x' \\ y' \\ z' \end{bmatrix} = C_0^+ \begin{bmatrix} x \\ y \\ z \end{bmatrix} = \begin{bmatrix} \cos\theta & \sin\theta & 0 \\ -\sin\theta & \cos\theta & 0 \\ 0 & 0 & 1 \end{bmatrix} \begin{bmatrix} x \\ y \\ z \end{bmatrix} \quad (1.76)$$

Then the character of the matrix is given by

$$\chi(C_\theta^+) = 1 + 2\cos\theta \quad (1.77)$$

The same result is obtained for $\chi(C_\theta^-)$. If this symmetry operation is applied to all the coordinates of the XY_3 molecule, the result is

$$C_\theta \begin{bmatrix} x_0 \\ y_0 \\ z_0 \\ x_1 \\ y_1 \\ z_1 \\ x_2 \\ y_2 \\ z_2 \\ x_3 \\ y_3 \\ z_3 \end{bmatrix} = \begin{bmatrix} \mathbf{A} & 0 & 0 & 0 \\ \hline 0 & 0 & 0 & \mathbf{A} \\ \hline 0 & \mathbf{A} & 0 & 0 \\ \hline 0 & 0 & \mathbf{A} & 0 \end{bmatrix} \begin{bmatrix} x_0 \\ y_0 \\ z_0 \\ x_1 \\ y_1 \\ z_1 \\ x_2 \\ y_2 \\ z_2 \\ x_3 \\ y_3 \\ z_3 \end{bmatrix} \quad (1.78)$$

where \mathbf{A} denotes the small square matrix given by Eq. 1.76. Thus, the character of this representation is simply given by Eq. 1.77. It should be noted in Eq. 1.78 that only the small matrix \mathbf{A} , related to the nuclei unchanged by the symmetry operation, appears as a diagonal element. Thus, a more general form of the character of the representation for rotation around the axis by θ is

*For matrix algebra, see Appendix II.

$$\chi(R) = N_R(1 + 2 \cos \theta) \quad (1.79)$$

where N_R is the number of nuclei unchanged by the rotation. In the present case, $N_R = 1$ and $\theta = 120^\circ$. Therefore, we obtain

$$\chi(C_3) = 0 \quad (1.80)$$

Identity (I) can be regarded as a special case of Eq. 1.79 in which $N_R = 4$ and $\theta = 0^\circ$. The character of the representation is

$$\chi(I) = 12 \quad (1.81)$$

Pure rotation and identity are called *proper rotation*.

It is evident from Fig. 1.19 that a symmetry plane such as σ_1 changes the coordinates from (x_i, y_i, z_i) to $(-x_i, y_i, z_i)$. The corresponding representation is therefore written as

$$\sigma_1 \begin{bmatrix} x \\ y \\ z \end{bmatrix} = \begin{bmatrix} -1 & 0 & 0 \\ 0 & 1 & 0 \\ 0 & 0 & 1 \end{bmatrix} \begin{bmatrix} x \\ y \\ z \end{bmatrix} \quad (1.82)$$

The result of such an operation on all the coordinates is

$$\sigma_1 \begin{bmatrix} x_0 \\ y_0 \\ z_0 \\ x_1 \\ y_1 \\ z_1 \\ x_2 \\ y_2 \\ z_2 \\ x_3 \\ y_3 \\ z_3 \end{bmatrix} = \begin{bmatrix} \mathbf{B} & 0 & 0 & 0 \\ \hline 0 & \mathbf{B} & 0 & 0 \\ \hline 0 & 0 & 0 & \mathbf{B} \\ \hline 0 & 0 & \mathbf{B} & 0 \end{bmatrix} \begin{bmatrix} x_0 \\ y_0 \\ z_0 \\ x_1 \\ y_1 \\ z_1 \\ x_2 \\ y_2 \\ z_2 \\ x_3 \\ y_3 \\ z_3 \end{bmatrix} \quad (1.83)$$

where \mathbf{B} denotes the small square matrix of Eq. 1.82. Thus, the character of this representation is calculated as $2 \times 1 = 2$. It is noted again that the matrix on the diagonal is nonzero only for the nuclei unchanged by the operation.

More generally, a reflection at a plane (σ) is regarded as $\sigma = i \times C_2$. Thus, the general form of Eq. 1.82 may be written as

$$\begin{bmatrix} -1 & 0 & 0 \\ 0 & -1 & 0 \\ 0 & 0 & -1 \end{bmatrix} \begin{bmatrix} \cos\theta & \sin\theta & 0 \\ -\sin\theta & \cos\theta & 0 \\ 0 & 0 & 1 \end{bmatrix} = \begin{bmatrix} -\cos\theta & -\sin\theta & 0 \\ \sin\theta & -\cos\theta & 0 \\ 0 & 0 & -1 \end{bmatrix}$$

Then

$$\chi(\sigma) = -(1 + 2 \cos\theta)$$

As a result, the character of the large matrix shown in Eq. 1.83 is given by

$$\boxed{\chi(R) = -N_R(1 + 2 \cos\theta)} \quad (1.84)$$

In the present case, $N_R = 2$ and $\theta = 180^\circ$. This gives

$$\chi(\sigma_v) = 2 \quad (1.85)$$

Symmetry operations such as i and S_p are regarded as

$$\begin{aligned} i &= i \times I, & \theta &= 0^\circ \\ S_3 &= i \times C_6, & \theta &= 60^\circ \\ S_4 &= i \times C_4, & \theta &= 90^\circ \\ S_6 &= i \times C_3, & \theta &= 120^\circ \end{aligned}$$

Therefore, the characters of these symmetry operations can be calculated by Eq. 1.84 with the values of θ defined above. Operations such as σ , i , and S_p are called *improper rotations*. Thus, the character of the representation based on 12 rectangular coordinates is as follows:

I	$2C_3$	$3\sigma_v$
12	0	2

(1.86)

To determine the number of normal vibrations belonging to each species, the $\chi(R)$ thus obtained must be resolved into the $\chi_i(R)$ of the irreducible representations of each species in Table 1.6. First, however, the characters corresponding to the translational and rotational motions of the molecule must be subtracted from the result shown in Eq. 1.86.

The characters for the translational motion of the molecule in the x , y , and z directions (denoted by T_x , T_y , and T_z) are the same as those obtained in Eqs. 1.79 and 1.84. They are as follows:

$$\boxed{\chi_t(R) = \pm(1 + 2 \cos\theta)} \quad (1.87)$$

where the $+$ and $-$ signs are for proper and improper rotations, respectively. The characters for the rotations around the x , y , and z axes (denoted by R_x , R_y , and R_z) are

given by

$$\boxed{\chi_r(R) = + (1 + 2 \cos \theta)} \quad (1.88)$$

for both proper and improper rotations. This is due to the fact that a rotation of the vectors in the plane perpendicular to the x , y , and z axes can be regarded as a rotation of the components of angular momentum, M_x, M_y , and M_z , about the given axes. If p_x, p_y , and p_z are the components of linear momentum in the x , y , and z directions, the following relations hold:

$$M_x = yp_z - zp_y$$

$$M_y = zp_x - xp_z$$

$$M_z = xp_y - yp_x$$

Since (x, y, z) and (p_x, p_y, p_z) transform as shown in Eq. 1.76, it follows that

$$C_\theta \begin{bmatrix} M_x \\ M_y \\ M_z \end{bmatrix} = \begin{bmatrix} \cos \theta & \sin \theta & 0 \\ -\sin \theta & \cos \theta & 0 \\ 0 & 0 & 1 \end{bmatrix} \begin{bmatrix} M_x \\ M_y \\ M_z \end{bmatrix}$$

Then, a similar relation holds for R_x, R_y , and R_z :

$$C_\theta \begin{bmatrix} R_x \\ R_y \\ R_z \end{bmatrix} = \begin{bmatrix} \cos \theta & \sin \theta & 0 \\ -\sin \theta & \cos \theta & 0 \\ 0 & 0 & 1 \end{bmatrix} \begin{bmatrix} R_x \\ R_y \\ R_z \end{bmatrix}$$

Thus, the characters for the proper rotations are as given by Eq. 1.88. The same result is obtained for the improper rotation if the latter is regarded as $i \times$ (proper rotation). Therefore, the character for the vibration is obtained from

$$\boxed{\chi_v(R) = \chi(R) - \chi_t(R) - \chi_r(R)} \quad (1.89)$$

It is convenient to tabulate the foregoing calculations as in Table 1.7. By using the formula in Eq. 1.74 and the character of the irreducible representations in Table 1.6, a_m can be calculated as follows:

$$a_m(A_1) = \frac{1}{6}[(1)(6)(1) + (2)(0)(1) + (3)(2)(1)] = 2$$

$$a_m(A_2) = \frac{1}{6}[(1)(6)(1) + (2)(0)(1) + (3)(2)(-1)] = 0$$

$$a_m(E) = \frac{1}{6}[(1)(6)(2) + (2)(0)(-1) + (3)(2)(0)] = 2$$

TABLE 1.7.

Symmetry Operation:	I $2C_3$		$3\sigma_v$
Kind of Rotation:	Proper		Improper
θ :	0°	120°	180°
$\cos \theta$	1	$-\frac{1}{2}$	-1
$1 + 2 \cos \theta$	3	0	-1
N_R	4	1	2
$\chi, \pm N_R(1 + 2 \cos \theta)$	12	0	2
$\chi_t, \pm (1 + 2 \cos \theta)$	3	0	1
$\chi_r, \pm (1 + 2 \cos \theta)$	3	0	-1
$\chi_v, \chi - \chi_t - \chi_r$	6	0	2

and

$$\chi_v = 2\chi_{A_1} + 2\chi_E \quad (1.90)$$

In other words, the six normal vibrations of a pyramidal XY_3 molecule are classified into two A_1 and two E species.

This procedure is applicable to any molecule. As another example, a similar calculation is shown in Table 1.8 for an octahedral XY_6 molecule. By use of Eq. 1.74 and the character table in Appendix I, the a_m are obtained as

$$\begin{aligned}
 a_m(A_{1g}) &= \frac{1}{48}[(1)(15)(1) + (8)(0)(1) + (6)(1)(1) + (6)(1)(1) \\
 &\quad + (3)(-1)(1) + (1)(-3)(1) + (6)(-1)(1) + (8)(0)(1) \\
 &\quad + (3)(5)(1) + (6)(3)(1)] \\
 &= 1
 \end{aligned}$$

TABLE 1.8.

Symmetry Operation	I	$8C_3$	$6C_2$	$6C_4$	$3C_4^2 \equiv C_2''$	$S_2 \equiv i$	$6S_4$	$8S_6$	$3\sigma_h^a$	$6\sigma_d^a$
Kind of Rotation:	Proper					Improper				
θ :	0°	120°	180°	90°	180°	0°	90°	120°	180°	180°
$\cos \theta$	1	$-\frac{1}{2}$	-1	0	-1	1	0	$-\frac{1}{2}$	-1	-1
$1 + 2 \cos \theta$	3	0	-1	1	-1	3	1	0	-1	-1
N_R	7	1	1	3	3	1	1	1	5	3
$\chi, \pm N_R(1 + 2 \cos \theta)$	21	0	-1	3	-3	-3	-1	0	5	3
$\chi_b \pm (1 + 2 \cos \theta)$	3	0	-1	1	-1	-3	-1	0	1	1
$\chi_r \pm (1 + 2 \cos \theta)$	3	0	-1	1	-1	3	1	0	-1	-1
$\chi_v, \chi - \chi_t - \chi_r$	15	0	1	1	-1	-3	-1	0	5	3

^a σ_h = horizontal plane of symmetry; σ_d = diagonal plane of symmetry.

$$\begin{aligned}
a_m(A_{1u}) &= \frac{1}{48}[(1)(15)(1) + (8)(0)(1) + (6)(1)(1) + (6)(1)(1) \\
&\quad + (3)(-1)(1) + (1)(-3)(-1) + (6)(-1)(-1) \\
&\quad + (8)(0)(-1) + (3)(5)(-1) + (6)(3)(-1)] \\
&= 0 \\
&\vdots
\end{aligned}$$

and therefore

$$\chi_v = \chi_{A_{1g}} + \chi_{E_g} + 2\chi_{F_{1u}} + \chi_{F_{2g}} + \chi_{F_{2u}}$$

1.9. INTERNAL COORDINATES

In Sec. 1.4, the potential and the kinetic energies were expressed in terms of rectangular coordinates. If, instead, these energies are expressed in terms of *internal coordinates* such as increments of the bond length and bond angle, the corresponding force constants have clearer physical meanings than do those expressed in terms of rectangular coordinates, since these force constants are characteristic of the bond stretching and the angle deformation involved. The number of internal coordinates must be equal to, or greater than, $3N - 6$ (or $3N - 5$), the degrees of vibrational freedom of an N -atom molecule. If more than $3N - 6$ (or $3N - 5$) coordinates are selected as the internal coordinates, this means that these coordinates are not independent of each other. Figure 1.20 illustrates the internal coordinates for various types of molecules.

In linear XYZ (a), bent XY₂ (b), and pyramidal XY₃ (c) molecules, the number of internal coordinates is the same as the number of normal vibrations. In a nonplanar X₂Y₂ molecule (d) such as H₂O₂, the number of internal coordinates is the same as the number of vibrations if the twisting angle around the central bond ($\Delta\tau$) is considered. In a tetrahedral XY₄ molecule (e), however, the number of internal coordinates exceeds the number of normal vibrations by one. This is due to the fact that the six angle coordinates around the central atom are not independent of each other, that is, they must satisfy the relation

$$\Delta\alpha_{12} + \Delta\alpha_{23} + \Delta\alpha_{31} + \Delta\alpha_{14} + \Delta\alpha_{24} + \Delta\alpha_{34} = 0 \quad (1.91)$$

This is called a *redundant condition*. In a planar XY₃ molecule (f), the number of internal coordinates is seven when the coordinate $\Delta\theta$, which represents the deviation from planarity, is considered. Since the number of vibrations is six, one redundant

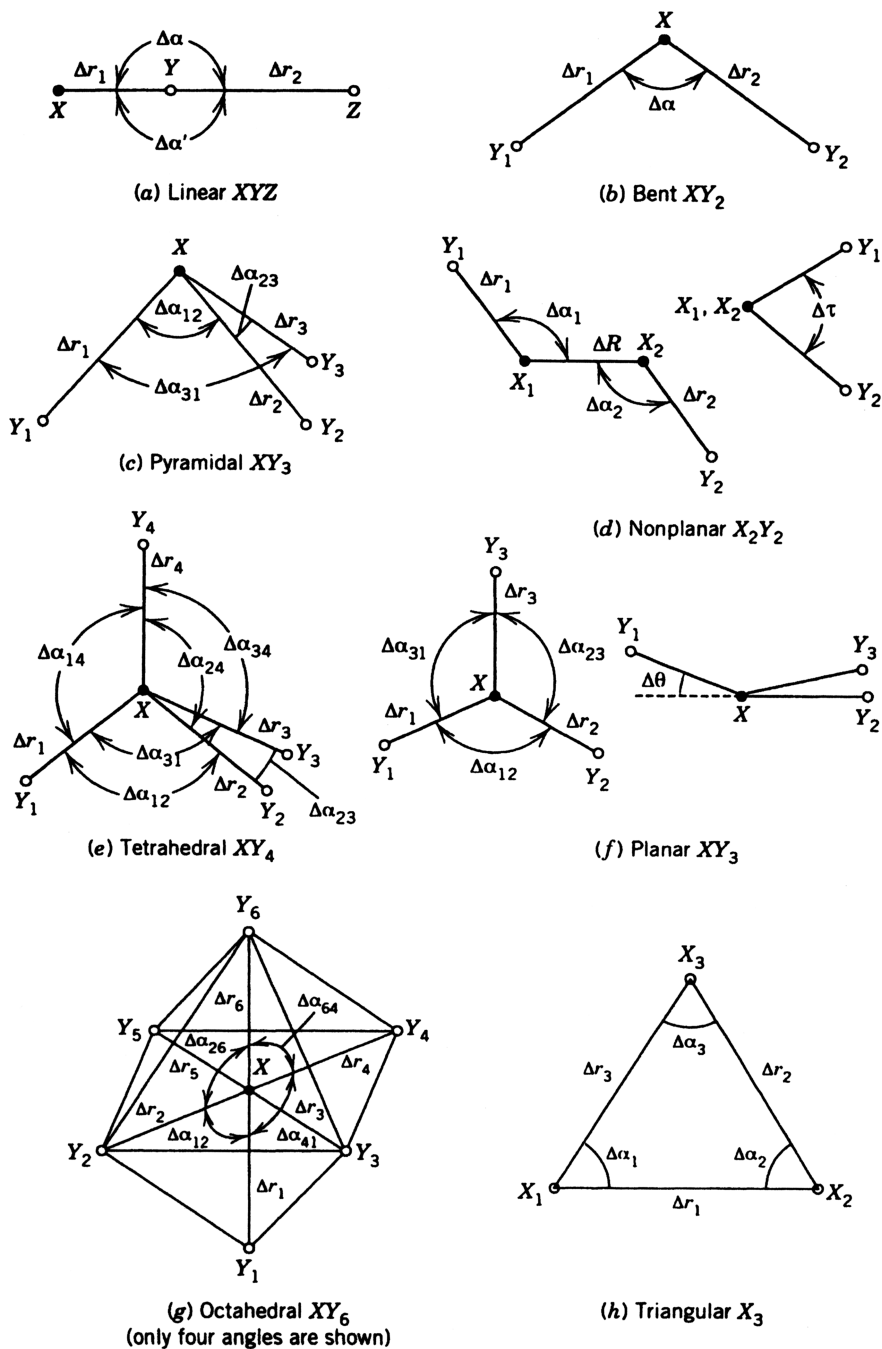


Fig. 1.20. Internal coordinates for various molecules.

condition such as

$$\Delta\alpha_{12} + \Delta\alpha_{23} + \Delta\alpha_{31} = 0 \quad (1.92)$$

must be involved. Such redundant conditions always exist for the angle coordinates around the central atom. In an octahedral XY_6 molecule (g), the number of internal coordinates exceeds the number of normal vibrations by three. This means that, of the 12 angle coordinates around the central atom, three redundant conditions are involved:

$$\begin{aligned} \Delta\alpha_{12} + \Delta\alpha_{26} + \Delta\alpha_{64} + \Delta\alpha_{41} &= 0 \\ \Delta\alpha_{15} + \Delta\alpha_{56} + \Delta\alpha_{63} + \Delta\alpha_{31} &= 0 \\ \Delta\alpha_{23} + \Delta\alpha_{34} + \Delta\alpha_{45} + \Delta\alpha_{52} &= 0 \end{aligned} \quad (1.93)$$

The redundant conditions are more complex in ring compounds. For example, the number of internal coordinates in a triangular X_3 molecule (h) exceeds the number of vibrations by three. One of these redundant conditions (A'_1 species) is

$$\Delta\alpha_1 + \Delta\alpha_2 + \Delta\alpha_3 = 0 \quad (1.94)$$

The other two redundant conditions (E' species) involve bond stretching and angle deformation coordinates such as

$$\begin{aligned} (2\Delta r_1 - \Delta r_2 - \Delta r_3) + \frac{r}{\sqrt{3}}(\Delta\alpha_1 + \Delta\alpha_2 - 2\Delta\alpha_3) &= 0 \\ (\Delta r_2 - \Delta r_3) - \frac{r}{\sqrt{3}}(\Delta\alpha_1 - \Delta\alpha_2) &= 0 \end{aligned} \quad (1.95)$$

where r is the equilibrium length of the X–X bond. The redundant conditions mentioned above can be derived by using the method described in Sec. 1.12.

The procedure for finding the number of normal vibrations in each species was described in Sec. 1.8. This procedure is, however, considerably simplified if internal coordinates are used. Again, consider a pyramidal XY_3 molecule. Using the internal coordinates shown in Fig. 1.20c, we can write the representation for the C_3^+ operation as

$$C_3^+ \begin{bmatrix} \Delta r_1 \\ \Delta r_2 \\ \Delta r_3 \\ \Delta\alpha_{12} \\ \Delta\alpha_{23} \\ \Delta\alpha_{31} \end{bmatrix} = \begin{bmatrix} 0 & 0 & 1 & 0 & 0 & 0 \\ 1 & 0 & 0 & 0 & 0 & 0 \\ 0 & 1 & 0 & 0 & 0 & 0 \\ 0 & 0 & 0 & 0 & 0 & 1 \\ 0 & 0 & 0 & 1 & 0 & 0 \\ 0 & 0 & 0 & 0 & 1 & 0 \end{bmatrix} \begin{bmatrix} \Delta r_1 \\ \Delta r_2 \\ \Delta r_3 \\ \Delta\alpha_{12} \\ \Delta\alpha_{23} \\ \Delta\alpha_{31} \end{bmatrix} \quad (1.96)$$

Thus $\chi(C_3^+) = 0$, as does $\chi(C_3^-)$. Similarly, $\chi(I) = 6$ and $\chi(\sigma_v) = 2$. This result is exactly the same as that obtained in Table 1.7 using rectangular coordinates. When

TABLE 1.9.

	I	$8C_3$	$6C_2$	$6C_4$	$3C_4^2 \equiv C''_2$	$S_2 \equiv i$	$6S_4$	$8S_6$	$3\sigma_h$	$6\sigma_d$
$\chi^r(R)$	6	0	0	2	2	0	0	0	4	2
$\chi^\alpha(R)$	12	0	2	0	0	0	0	0	4	2

using internal coordinates, however, the character of the representation is simply given by the number of internal coordinates unchanged by each symmetry operation.

If this procedure is made separately for stretching (Δr) and bending ($\Delta\alpha$) coordinates, it is readily seen that

$$\begin{aligned}\chi^r(R) &= \chi_{A_1} + \chi_E \\ \chi^\alpha(R) &= \chi_{A_1} + \chi_E\end{aligned}\tag{1.97}$$

Thus, it is found that both A_1 and E species have one stretching and one bending vibration, respectively. No consideration of the translational and rotational motions is necessary if the internal coordinates are taken as the basis for the representation.

Another example, for an octahedral XY_6 molecule, is given in Table 1.9. Using Eq. 1.74 and the character table in Appendix I, we find that these characters are resolved into.

$$\chi^r(R) = \chi_{A_{1g}} + \chi_{E_g} + \chi_{F_{1u}}\tag{1.98}$$

$$\chi^\alpha(R) = \chi_{A_{1g}} + \chi_{E_g} + \chi_{F_{1u}} + \chi_{F_{2g}} + \chi_{F_{2u}}\tag{1.99}$$

Comparison of this result with that obtained in Sec. 1.8 immediately suggests that three redundant conditions are included in these bending vibrations (one in A_{1g} and one in E_g). Therefore, $\chi^\alpha(R)$ for genuine vibrations becomes

$$\chi^\alpha(R) = \chi_{F_{1u}} + \chi_{F_{2g}} + \chi_{F_{2u}}\tag{1.100}$$

Thus, it is concluded that six stretching and nine bending vibrations are distributed as indicated in Eqs. 1.98 and 1.100, respectively. Although the method given above is simpler than that of Sec. 1.8, caution must be exercised with respect to the bending vibrations whenever redundancy is involved. In such a case, comparison of the results obtained from both methods is useful in finding the species of redundancy.

1.10. SELECTION RULES FOR INFRARED AND RAMAN SPECTRA

According to quantum mechanics [3], the selection rule for the infrared spectrum is determined by the following integral:

$$[\mu]_{v'v''} = \int \psi_{v'}^*(Q_a) \mu \psi_{v''}(Q_a) dQ_a \quad (1.101)$$

Here, μ is the dipole moment in the electronic ground state, ψ is the vibrational eigenfunction given by Eq. 1.21, and v' and v'' are the vibrational quantum numbers before and after the transition, respectively. The activity of the normal vibration whose normal coordinate is Q_a is being determined. By resolving the dipole moment into the three components in the x , y , and z directions, we obtain the result

$$\begin{aligned} [\mu_x]_{v'v''} &= \int \psi_{v'}^*(Q_a) \mu_x \psi_{v''}(Q_a) dQ_a \\ [\mu_y]_{v'v''} &= \int \psi_{v'}^*(Q_a) \mu_y \psi_{v''}(Q_a) dQ_a \\ [\mu_z]_{v'v''} &= \int \psi_{v'}^*(Q_a) \mu_z \psi_{v''}(Q_a) dQ_a \end{aligned} \quad (1.102)$$

If one of these integrals is not zero, the normal vibration associated with Q_a is infrared-active. If all the integrals are zero, the vibration is infrared-inactive.

Similar to the case of infrared spectrum, the selection rule for the Raman spectrum is determined by the integral

$$[\alpha]_{v'v''} = \int \psi_{v'}^*(Q_a) \alpha \psi_{v''}(Q_a) dQ_a \quad (1.103)$$

As shown in Sec. 1.6, α consists of six components, α_{xx} , α_{yy} , α_{zz} , α_{xy} , α_{yz} , and α_{xz} . Thus Eq. 1.103 may be resolved into six components:

$$\begin{aligned} [\alpha_{xx}]_{v'v''} &= \int \psi_{v'}^*(Q_a) \alpha_{xx} \psi_{v''}(Q_a) dQ_a \\ [\alpha_{yy}]_{v'v''} &= \int \psi_{v'}^*(Q_a) \alpha_{yy} \psi_{v''}(Q_a) dQ_a \\ &\dots\dots\dots \end{aligned} \quad (1.104)$$

If one of these integrals is not zero, the normal vibration associated with Q_a is Raman-active. If all the integrals are zero, the vibration is Raman-inactive. As shown below, it is possible to determine whether the integrals of Eqs. 1.102 and 1.104 are zero or nonzero from a consideration of symmetry:

1.10.1. Selection Rules for Fundamentals

Let us consider the fundamentals in which transitions occur from $v' = 0$ to $v'' = 1$. It is evident from the form of the vibrational eigenfunction (Eq. 1.22) that $\psi_0(Q_a)$ is invariant under any symmetry operation, whereas the symmetry of $\psi_1(Q_a)$ is the same as that of Q_a . Thus, the integral does not vanish when the symmetry of μ_x , for example, is the same as that of Q_a . If the symmetry properties of μ_x and Q_a differ in even one

symmetry element of the group, the integral becomes zero. In other words, for the integral to be nonzero, Q_a must belong to the same species as μ_x . *More generally, the normal vibration associated with Q_a becomes infrared-active when at least one of the components of the dipole moment belongs to the same species as Q_a .* Similar conclusions are obtained for the Raman spectrum. Namely, *the normal vibration associated with Q_a becomes Raman-active when at least one of the components of the polarizability belongs to the same species as Q_a .*

Since the species of the normal vibration can be determined by the methods described in Sections 1.8 and 1.9, it is necessary only to determine the species of the components of the dipole moment and polarizability of the molecule. This can be done as follows. The components of the dipole moment, μ_x , μ_y , and μ_z , transform as do those of translational motion, T_x , T_y , and T_z , respectively. These were discussed in Sec. 1.8. Thus, the character of the dipole moment is given by Eq. 1.87, which is

$$\chi_u(R) = \pm(1 + 2 \cos \theta) \quad (1.105)$$

where $+$ and $-$ have the same meaning as before. In a pyramidal XY_3 molecule, Eq. 1.105 gives

	I	$2C_3$	$3\sigma_v$
$\chi_\mu(R)$	3	0	1

Using Eq. 1.74, we resolve this into $A_1 + E$. It is obvious that μ_z belongs to A_1 . Then, μ_x and μ_y must belong to E . In fact, the pair, μ_x and μ_y , transforms as follows:

$$I \begin{bmatrix} \mu_x \\ \mu_y \end{bmatrix} = \begin{bmatrix} 1 & 0 \\ 0 & 1 \end{bmatrix} \begin{bmatrix} \mu_x \\ \mu_y \end{bmatrix}, \quad C_3^+ \begin{bmatrix} \mu_x \\ \mu_y \end{bmatrix} = \begin{bmatrix} -\frac{1}{2} & \frac{\sqrt{3}}{2} \\ -\frac{\sqrt{3}}{2} & -\frac{1}{2} \end{bmatrix} \begin{bmatrix} \mu_x \\ \mu_y \end{bmatrix}$$

$$\chi(I) = 2, \quad \chi(C_3^+) = -1$$

$$\sigma_1 \begin{bmatrix} \mu_x \\ \mu_y \end{bmatrix} = \begin{bmatrix} -1 & 0 \\ 0 & 1 \end{bmatrix} \begin{bmatrix} \mu_x \\ \mu_y \end{bmatrix}$$

$$\chi(\sigma_1) = 0$$

Thus, it is found that μ_z belongs to A_1 and (μ_x, μ_y) belongs to E .

The character of the representation of the polarizability is given by

$$\boxed{\chi_{\alpha}(R) = 2 \cos\theta(1 + 2 \cos\theta)} \quad (1.106)$$

for both proper and improper rotations. This can be derived as follows. The polarizability in the x , y , and z directions is related to that in X , Y , and Z coordinates by

$$\begin{bmatrix} \alpha_{XX} & \alpha_{XY} & \alpha_{XZ} \\ \alpha_{YX} & \alpha_{YY} & \alpha_{YZ} \\ \alpha_{ZX} & \alpha_{ZY} & \alpha_{ZZ} \end{bmatrix} = \begin{bmatrix} C_{Xx} & C_{Xy} & C_{Xz} \\ C_{Yx} & C_{Yy} & C_{Yz} \\ C_{Zx} & C_{Zy} & C_{Zz} \end{bmatrix} \begin{bmatrix} \alpha_{xx} & \alpha_{xy} & \alpha_{xz} \\ \alpha_{yx} & \alpha_{yy} & \alpha_{yz} \\ \alpha_{zx} & \alpha_{zy} & \alpha_{zz} \end{bmatrix} \begin{bmatrix} C_{Xx} & C_{Yx} & C_{Zx} \\ C_{Xy} & C_{Yy} & C_{Zy} \\ C_{Xz} & C_{Yz} & C_{Zz} \end{bmatrix}$$

where C_{Xx} , C_{Xy} , and so forth denote the direction cosines between the two axes subscripted. If a rotation through θ around the Z axis superimposes the X , Y , and Z axes on the x , y , and z axes, the preceding relation becomes

$$C_{\theta} \begin{bmatrix} \alpha_{xx} & \alpha_{xy} & \alpha_{xz} \\ \alpha_{yx} & \alpha_{yy} & \alpha_{yz} \\ \alpha_{zx} & \alpha_{zy} & \alpha_{zz} \end{bmatrix} = \begin{bmatrix} \cos\theta & \sin\theta & 0 \\ -\sin\theta & \cos\theta & 0 \\ 0 & 0 & 1 \end{bmatrix} \begin{bmatrix} \alpha_{xx} & \alpha_{xy} & \alpha_{xz} \\ \alpha_{yx} & \alpha_{yy} & \alpha_{yz} \\ \alpha_{zx} & \alpha_{zy} & \alpha_{zz} \end{bmatrix} \begin{bmatrix} \cos\theta & -\sin\theta & 0 \\ \sin\theta & \cos\theta & 0 \\ 0 & 0 & 1 \end{bmatrix}$$

This can be written as

$$C_{\theta} \begin{bmatrix} \alpha_{xx} \\ \alpha_{yy} \\ \alpha_{zz} \\ \alpha_{xy} \\ \alpha_{xz} \\ \alpha_{yz} \end{bmatrix} = \begin{bmatrix} \cos^2\theta & \sin^2\theta & 0 & 2\sin\theta\cos\theta & 0 & 0 \\ \sin^2\theta & \cos^2\theta & 0 & -2\sin\theta\cos\theta & 0 & 0 \\ 0 & 0 & 1 & 0 & 0 & 0 \\ -\sin\theta\cos\theta & \sin\theta\cos\theta & 0 & 2\cos^2\theta - 1 & 0 & 0 \\ 0 & 0 & 0 & 0 & \cos\theta & \sin\theta \\ 0 & 0 & 0 & 0 & -\sin\theta & \cos\theta \end{bmatrix} \cdot \begin{bmatrix} \alpha_{xx} \\ \alpha_{yy} \\ \alpha_{zz} \\ \alpha_{xy} \\ \alpha_{xz} \\ \alpha_{yz} \end{bmatrix}$$

Thus, the character of this representation is given by Eq. 1.106. The same results are obtained for improper rotations if they are regarded as the product $i \times$ (proper rotation). For a pyramidal XY_3 molecule, Eq. 1.106 gives

	I	$2C_3$	$3\sigma_v$
$\chi_{\alpha}(R)$	6	0	2

Using Eq. 1.74, this is resolved into $2A_1 + 2E$. Again, it is immediately seen that* the component α_{zz} belongs to A_1 , and the pair α_{zx} and α_{zy} belongs to E since

$$\begin{bmatrix} zx \\ zy \end{bmatrix} = z \begin{bmatrix} x \\ y \end{bmatrix} = A_1 \times E = E$$

It is more convenient to consider the components $\alpha_{xx} + \alpha_{yy}$ and $\alpha_{xx} - \alpha_{yy}$ than α_{xx} and α_{yy} . If a vector of unit length is considered, the relation

$$x^2 + y^2 + z^2 = 1$$

holds. Since α_{zz} belongs to A_1 , $\alpha_{xx} + \alpha_{yy}$ must belong to A_1 . Then, the pair $\alpha_{xx} - \alpha_{yy}$ and α_{xy} must belong to E . As a result, the character table of the point group C_{3v} , is completed as in Table 1.10. Thus, it is concluded that, in the point group C_{3v} both the A_1 and the E vibrations are infrared- as well as Raman-active, while the A_2 vibrations are inactive.

Complete character tables like Table 1.10 have already been worked out for all the point groups. Therefore, no elaborate treatment such as that described in this section is necessary in practice. Appendix I gives complete character tables for the point groups that appear frequently in this book. From these tables, the selection rules for the infrared and Raman spectra are obtained immediately: *The vibration is infrared- or Raman-active if it belongs to the same species as one of the components of the dipole moment or polarizability, respectively.* For example, the character table of the point group O_h signifies immediately that only the F_{1u} vibrations are infrared-active and only the A_{1g} , E_g , and F_{2g} vibrations are Raman-active, for the components of the dipole moment or the polarizability belong to these species in this point group. It is to be noted in these character tables that (1) a totally symmetric vibration is Raman-active in any

*The quantum mechanical expression of the polarizability [77] is

$$\alpha_{xx} = \frac{2}{3h} \sum_j \frac{(\mu_x)_{j0}^2 v_{j0}^2}{v_{j0}^2 - \nu^2}$$

$$\alpha_{xy} = \frac{2}{3h} \sum_j \frac{(\mu_x)_{j0} (\mu_y)_{j0} v_{j0}^2}{v_{j0}^2 - \nu^2} \quad \text{etc.}$$

Here, $(\mu_x)_{j0}$, for example, is the induced dipole moment along the x axis caused by the 0 (ground state) $\rightarrow j$ (excited state) electronic transition, v_{j0} is the frequency of the $0 \rightarrow j$ transition, and ν is the exciting frequency. Thus, it is readily seen that the character of the polarizability components such as α_{xx} and α_{xy} is determined by considering the product of the characters of dipole moments such as μ_x and μ_y .

TABLE 1.10. Character Table of the Point Group C_{3v}

C_{3v}	I	$2C_3$	$3\sigma_v$		
A_1	+1	+1	+1	μ_z	$\alpha_{xx} + \alpha_{yy}, \alpha_{zz}$
A_2	+1	+1	-1		
E	+2	-1	0	$(\mu_x, \mu_y)^a$	$(\alpha_{xz}, \alpha_{yz}),^a (\alpha_{xx} - \alpha_{yy}, \alpha_{xy})^a$

^aA doubly degenerate pair is represented by two terms in parentheses.

point group, and (2) the infrared- and Raman-active vibrations always belong to u and g types, respectively, in point groups having a center of symmetry.

1.10.2. Selection Rules for Combination and Overtone Bands

As stated in Sec. 1.3, some combination and overtone bands appear weakly because actual vibrations are not harmonic and some of these nonfundamentals are allowed by symmetry selection rules.

Selection rules for combination bands ($\nu_i \pm \nu_j$) can be derived from the characters of the *direct products* of those of individual vibrations. Thus, we obtain

$$\chi_{ij}(R) = \chi_i(R) \times \chi_j(R) \quad (1.107)$$

As an example, consider a molecule of C_{3v} symmetry. It is readily seen that

	I	$2C_3$	$3\sigma_v$
$\chi_{A_1}(R)$	1	1	1
$\times) \chi_E(R)$	2	-1	0
$\chi_{A_1 \times E}(R)$	2	-1	0

$$\chi_{A_1 \times E}(R) = \chi_E(R)$$

Thus, a combination band between the A_1 and E vibrations is IR- as well as Raman-active. The activity of a combination band between two E vibrations can be determined by considering the direct product of their characters:

	I	$2C_3$	$3\sigma_v$
$\chi_E(R)$	2	-1	0
$\times) \chi_E(R)$	2	-1	0
$\chi_{E \times E}(R)$	4	1	0

Using Eq. 1.74, this set of the characters can be resolved into

$$\chi_{E \times E}(R) = \chi_{A_1}(R) + \chi_{A_2}(R) + \chi_E(R)$$

Since both A_1 and E species are IR- and Raman-active, a combination band between two E vibrations is also IR- and Raman-active. It is convenient to apply the general rules of Appendix IV in determining the symmetry species of direct products.

Selection rules for overtones of nondegenerate vibrations can be obtained using the following relation:

$$\chi^n(\mathbf{R}) = [\chi(\mathbf{R})]^n \quad (1.108)$$

Here, $\chi^n(\mathbf{R})$ is the character of the $(n - 1)$ th overtone ($n = 2$ for the first overtone). As an example, consider a molecule of C_{3v} symmetry. The character of the first overtone of the A_2 fundamental is calculated as follows:

	I	$2C_3$	$3\sigma_v$
$\chi_{A_2}(\mathbf{R})$	1	1	-1
$\times) \chi_{A_2}(\mathbf{R})$	1	1	-1
$\chi_{A_2}^2(\mathbf{R})$	1	1	1

Namely, it is IR- as well as Raman-active because $\chi_{A_2}^2(\mathbf{R}) = \chi_{A_1}(\mathbf{R})$. However, the second overtone of the A_2 fundamental is IR- as well as Raman-inactive because $\chi_{A_2}^3(\mathbf{R}) = \chi_{A_2}^2(\mathbf{R}) \times \chi_{A_2}(\mathbf{R}) = \chi_{A_2}(\mathbf{R})$ (inactive). In general, odd overtones (A_1) are IR- and Raman-active, whereas even overtones (A_2) are inactive. It is obvious that all the overtones of the A_1 fundamental are IR- and Raman-active.

Selection rules for overtones of doubly degenerate vibrations (E species) are determined by

$$\chi_E^n(\mathbf{R}) = \frac{1}{2}[\chi_E^{n-1}(\mathbf{R}) \cdot \chi_E(\mathbf{R}) + \chi_E(\mathbf{R}^n)] \quad (1.109)$$

For the first overtone, this is written as

$$\chi_E^2(\mathbf{R}) = \frac{1}{2}[\{\chi_E(\mathbf{R})\}^2 + \chi_E(\mathbf{R}^2)]$$

Here, $\chi_E(\mathbf{R}^2)$ is the character that corresponds to the operation R performed twice successively. Thus, one obtains

$$\begin{aligned} \chi_E(I^2) &= \chi_E(I) = 2 \\ \chi_E[(C_3^+)^2] &= \chi_E(C_3^-) = -1 \\ \chi_E[(\sigma_v)^2] &= \chi_E(I) = 2 \end{aligned}$$

Therefore, $\chi_E^2(\mathbf{R})$ can be calculated as follows:

	I	$2C_3$	$3\sigma_v$
$\chi_E(\mathbf{R})$	2	-1	0
$\times) \chi_E(\mathbf{R})$	2	-1	0
$\{\chi_E(\mathbf{R})\}^2$	4	1	0
$+) \chi_E(\mathbf{R}^2)$	2	-1	2
$\{\chi_E(\mathbf{R})\}^2 + \chi_E(\mathbf{R}^2)$	6	0	2
$\div 2) \chi_E^2(\mathbf{R})$	3	0	1
$\chi_E^2(\mathbf{R}) = \chi_{A_1}(\mathbf{R}) + \chi_E(\mathbf{R})$			

Thus, the first overtone of the doubly degenerate vibration is IR- and Raman-active. The characters of overtones for triply degenerate vibrations are given by

$$\begin{aligned}\chi_F^n(\mathbf{R}) = & \frac{1}{3}\{2\chi_F(\mathbf{R})\chi_F^{n-1}(\mathbf{R}) - \frac{1}{2}\chi_F^{n-2}(\mathbf{R})[\chi_F(\mathbf{R})]^2 \\ & + \frac{1}{2}\chi_F(\mathbf{R}^2)\chi_F^{n-2}(\mathbf{R}) + \chi_F(\mathbf{R}^n)\}\end{aligned}\quad (1.110)$$

For more details, see Refs. [3,5], and [9].

1.11. STRUCTURE DETERMINATION

Suppose that a molecule has several probable structures, each of which belongs to a different point group. Then the number of infrared- and Raman-active fundamentals should be different for each structure. Therefore, the most probable model can be selected by comparing the observed number of infrared- and Raman-active fundamentals with that predicted theoretically for each model.

Consider the XeF_4 molecule as an example. It may be tetrahedral or square-planar. By use of the methods described in the preceding sections, the number of infrared- or Raman-active fundamentals can be found easily for each structure. Tables 1.11a and 1.11b summarize the results. It is seen that the distinction of these two structures can be made by comparing the number of IR- and Raman-active FXeF bending modes; the tetrahedral structure predicts one IR and two Raman bands, whereas the square-planar structure predicts two IR and one Raman bands. In general, the XeF stretching vibrations appear above 500 cm^{-1} , whereas the FXeF bending vibrations are observed below 300 cm^{-1} . The IR and Raman spectra of XeF_4 are shown in Fig. 2.17. The IR spectrum exhibits two bending bands at 291 and 123 cm^{-1} , whereas the Raman

TABLE 1.11a. Number of Fundamentals for Tetrahedral XeF_4

T_d	Activity ^a	Number of Fundamentals	XeF Stretching	FXeF Bending
A_1	R (p)	1	1	0
A_2	ia	0	0	0
E	R (dp)	1	0	1
F_1	ia	0	0	0
F_2	IR, R (dp)	2	1	1
<i>Total</i>	IR	2	1	1
	R	4	2	2

^a p , polarized; dp , depolarized (see Sec. 1.20).

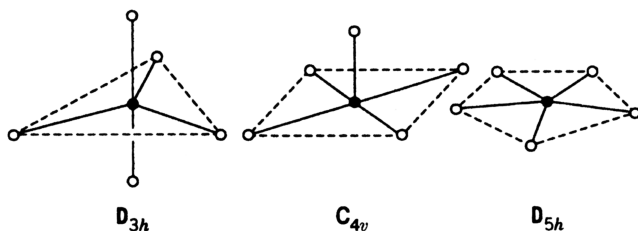
TABLE 1.11b. Number of Fundamentals for Square-Planar XeF₄

D_{4h}	Activity	Number of Fundamentals	XeF Stretching	FXeF Bending
A_{1g}	R (p)	1	1	0
A_{1u}	ia	0	0	0
A_{2g}	ia	0	0	0
A_{2u}	IR	1	0	1
B_{1g}	R (dp)	1	1	0
B_{1u}	ia	0	0	0
B_{2g}	R (dp)	1	0	1
B_{2u}	ia	1	0	1
E_g	R (dp)	0	0	0
E_u	IR	2	1	1
Total	IR	3	1	2
	R	3	2	1

spectrum shows one bending vibration at 218 cm^{-1} . Thus, the square-planar structure is preferable to the tetrahedral structure.*

Another example is given by the XeF_5^- ion, which has the three possible structures shown in Fig. 1.21. The results of vibrational analysis for each are summarized in Table 1.12. It is seen that the numbers of IR-active vibrations are 5, 6, and 3 and those of Raman-active vibrations are 6, 9, and 3, respectively, for the D_{3h} , C_{4v} , and D_{5h} structures. As discussed in Sec. 2.7.3, the XeF_5^- ion exhibits three IR bands ($550\text{--}400$, 290 , and 274 cm^{-1}) and three Raman bands (502 , 423 , and 377 cm^{-1}). Thus, a pentagonal planar structure is preferable to the other two structures. The somewhat unusual structures thus obtained for XeF_4 and XeF_5^- can be rationalized by the use of the valence shell electron-pair repulsion (VSEPR) theory (Sec. 2.6.3).

This rather simple method has been used widely for the elucidation of molecular structure of inorganic and coordination compounds. In Chapter 2, the number of IR- and Raman-active vibrations is compared for possible structures of XY_n and other

Fig. 1.21. Three possible structures for the XeF_5^- ion.

*This conclusion may be drawn directly from observation of the mutual exclusion rule, which holds for D_{4h} but not for T_d .

TABLE 1.12. Number of IR- and Raman-Active Fundamentals for Three Possible Structures of the XeF_5^- Anion

Type	D_{3h}	C_{4v}	D_{5h}
IR	$2A''_2 + 3E'$	$3A_1 + 3E$	$A''_2 + 2E'_1$
Raman	$2A'_1 + 3E' + E''$	$3A_1 + 2B_1 + B_2 + 3E$	$A'_1 + 2E'_2$

molecules. Appendix V lists the number of IR- and Raman-active vibrations of MX_nY_m -type molecules. It should be noted, however, that this method does not give a clear-cut answer if the predicted numbers of infrared- and Raman-active fundamentals are similar for various probable structures. Furthermore, a practical difficulty arises in determining the number of fundamentals from the observed spectrum, since the intensities of overtone and combination bands are sometimes comparable to those of fundamentals when they appear as satellite bands of the fundamental. This is particularly true when overtone and combination bands are enhanced anomalously by *Fermi resonance* (accidental degeneracy). For example, the frequency of the first overtone of the ν_2 vibration of CO_2 (667 cm^{-1}) is very close to that of the ν_1 vibration (1337 cm^{-1}). Since these two vibrations belong to the same symmetry species (\sum_g^+), they interact with each other and give rise to two strong Raman lines at 1388 and 1286 cm^{-1} . Fermi resonances similar to the resonance observed for CO_2 may occur for a number of other molecules. It is to be noted also that the number of observed bands depends on the resolving power of the instrument used. Finally, the molecular symmetry in the isolated state is not necessarily the same as that in the crystalline state (Sec. 1.27). Therefore, this method must be applied with caution to spectra obtained for compounds in the crystalline state.

1.12. PRINCIPLE OF THE GF MATRIX METHOD*

As described in Sec. 1.4, the frequency of the normal vibration is determined by the kinetic and potential energies of the system. The kinetic energy is determined by the masses of the individual atoms and their geometrical arrangement in the molecule. On the other hand, the potential energy arises from interaction between the individual atoms and is described in terms of the force constants. Since the potential energy provides valuable information about the nature of interatomic forces, it is highly desirable to obtain the force constants from the observed frequencies. This is usually done by calculating the frequencies, assuming a suitable set of force constants. If the agreement between the calculated and observed frequencies is satisfactory, this particular set of the force constants is adopted as a representation of the potential energy of the system.

* For details, see Ref. 3. The term "normal coordinate analysis" is almost synonymous with the **GF** matrix method, since most of the normal coordinate calculations are carried out by using this method.

To calculate the vibrational frequencies, it is necessary first to express both the potential and the kinetic energies in terms of some common coordinates (Sec. 1.4). Internal coordinates (Sec. 1.9) are more suitable for this purpose than rectangular coordinates, since (1) force constants expressed in terms of internal coordinates have clearer physical meanings than those expressed in terms of rectangular coordinates, and (2) a set of internal coordinates does not involve translational and rotational motion of the molecule as a whole.

Using the internal coordinates R_i we write the potential energy as

$$2V = \tilde{\mathbf{R}}\mathbf{F}\mathbf{R} \quad (1.111)$$

For a bent Y_1XY_2 molecule such as that in Fig. 1.20b, \mathbf{R} is a column matrix of the form

$$\mathbf{R} = \begin{bmatrix} \Delta r_1 \\ \Delta r_2 \\ \Delta \alpha \end{bmatrix}$$

$\tilde{\mathbf{R}}$ is its transpose:

$$\tilde{\mathbf{R}} = [\Delta r_1 \quad \Delta r_2 \quad \Delta \alpha]$$

and \mathbf{F} is a matrix whose components are the force constants

$$\mathbf{F} = \begin{bmatrix} f_{11} & f_{12} & r_1 f_{13} \\ f_{21} & f_{22} & r_2 f_{23} \\ r_1 f_{31} & r_2 f_{32} & r_1 r_2 f_{33} \end{bmatrix} \equiv \begin{bmatrix} F_{11} & F_{12} & F_{13} \\ F_{21} & F_{22} & F_{23} \\ F_{31} & F_{32} & F_{33} \end{bmatrix} \quad (1.112)^*$$

Here r_1 and r_2 are the equilibrium lengths of the $X-Y_1$ and $X-Y_2$ bonds, respectively.

The kinetic energy is not easily expressed in terms of the same internal coordinates. Wilson [78] has shown, however, that the kinetic energy can be written as

$$2T = \tilde{\mathbf{R}}\mathbf{G}^{-1}\dot{\mathbf{R}} \quad (1.113)^\dagger$$

where \mathbf{G}^{-1} is the reciprocal of the \mathbf{G} matrix, which will be defined later. If Eqs. 1.111 and 1.113 are combined with Lagrange's equation

$$\frac{d}{dt} \left(\frac{\partial T}{\partial \dot{R}_k} \right) + \frac{\partial V}{\partial R_k} = 0 \quad (1.36)$$

*Here f_{11} and f_{22} are the stretching force constants of the $X-Y_1$ and $X-Y_2$ bonds, respectively, and f_{33} is the bending force constant of the Y_1XY_2 angle. The other symbols represent interaction force constants between stretching and stretching or between stretching and bending vibrations. To make the dimensions of all the force constants the same, f_{13} (or f_{31}), f_{23} (or f_{32}), and f_{33} are multiplied by r_1 , r_2 , and $r_1 r_2$, respectively.

†Appendix VI gives the derivation of Eq. 1.113.

the following secular equation, which is similar to Eq. 1.49, is obtained:

$$\begin{vmatrix} F_{11} - (G^{-1})_{11}\lambda & F_{12} - (G^{-1})_{12}\lambda & \cdots \\ F_{21} - (G^{-1})_{21}\lambda & F_{22} - (G^{-1})_{22}\lambda & \cdots \\ \vdots & \vdots & \ddots \end{vmatrix} \equiv |\mathbf{F} - \mathbf{G}^{-1}\lambda| = 0 \quad (1.114)$$

By multiplying by the determinant of \mathbf{G}

$$\begin{vmatrix} G_{11} & G_{12} & \cdots \\ G_{21} & G_{22} & \cdots \\ \vdots & \vdots & \ddots \end{vmatrix} \equiv |\mathbf{G}| \quad (1.115)$$

from the left-hand side of Eq. 1.114, the following equation is obtained:

$$\begin{vmatrix} \sum G_{1i}F_{i1} - \lambda & \sum G_{1i}F_{i2} & \cdots \\ \sum G_{2i}F_{i1} & \sum G_{2i}F_{i2} - \lambda & \cdots \\ \vdots & \vdots & \ddots \end{vmatrix} \equiv |\mathbf{GF} - \mathbf{E}\lambda| = 0 \quad (1.116)$$

Here, \mathbf{E} is the unit matrix, and λ is related to the wavenumber $\tilde{\nu}$ by the relation $\lambda = 4\pi^2 c^2 \tilde{\nu}^2$.^{*} The order of the equation is equal to the number of internal coordinates used.

The \mathbf{F} matrix can be written by assuming a suitable set of force constants. If the \mathbf{G} matrix is constructed by the following method, the vibrational frequencies are obtained by solving Eq. 1.116. The \mathbf{G} matrix is defined as

$$\mathbf{G} = \mathbf{B}\mathbf{M}^{-1}\tilde{\mathbf{B}} \quad (1.117)$$

Here \mathbf{M}^{-1} is a diagonal matrix whose components are μ_i , where μ_i is the reciprocal of the mass of the i th atom. For a bent XY_2 molecule, we obtain

$$\mathbf{M}^{-1} = \begin{bmatrix} \mu_1 & & & 0 \\ & \mu_1 & & \\ & & \mu_1 & \\ 0 & & & \ddots \\ & & & & \mu_3 \end{bmatrix}$$

where μ_3 and μ_1 are the reciprocals of the masses of the X and Y atoms, respectively. The \mathbf{B} matrix is defined as

$$\mathbf{R} = \mathbf{B}\mathbf{X} \quad (1.118)$$

where \mathbf{R} and \mathbf{X} are column matrices whose components are the internal and rectangular coordinates, respectively.

^{*}Here λ should not be confused with λ_w (wavelength).

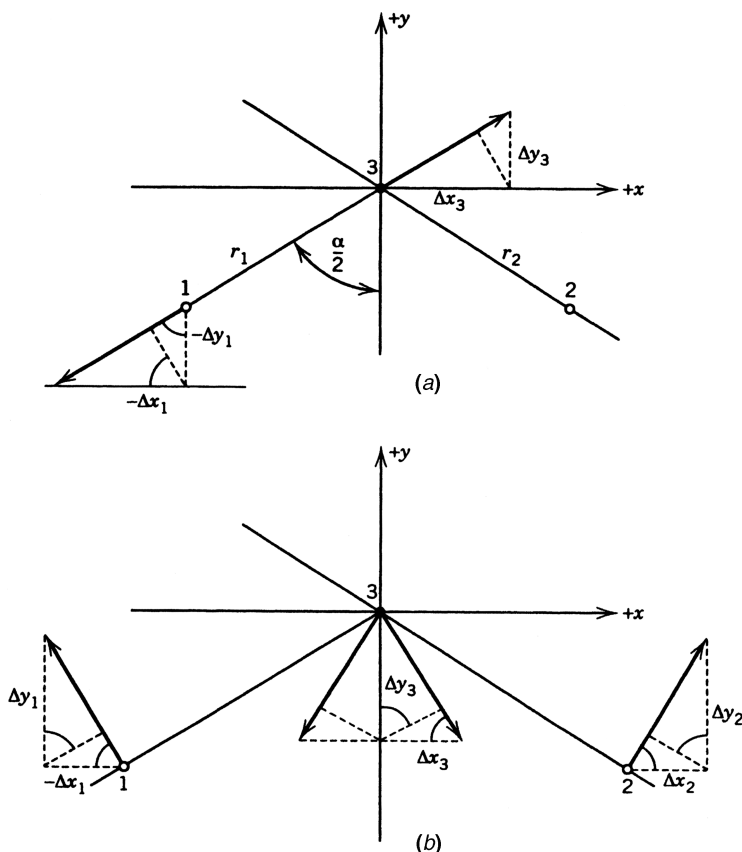


Fig. 1.22. Relationship between internal and rectangular coordinates in (a) stretching and (b) bending vibrations of a bent XY_2 molecule.

To write Eq. 1.118 for a bent XY_2 molecule, we express the bond stretching (Δr_1) in terms of the x and y coordinates shown in Fig. 1.22a. It is readily seen that

$$\Delta r_1 = -(\Delta x_1)(s) - (\Delta y_1)(c) + (\Delta x_3)(s) + (\Delta y_3)(c)$$

Here, $s = \sin(\alpha/2)$, $c = \cos(\alpha/2)$, and r is the equilibrium distance between the X and Y atoms. A similar expression is obtained for Δr_2 . Thus

$$\Delta r_2 = (\Delta x_2)(s) - (\Delta y_2)(c) - (\Delta x_3)(s) + (\Delta y_3)(c)$$

For the bond bending ($\Delta\alpha$), consider the relationships illustrated in Fig. 1.22b. It is readily seen that

$$r(\Delta\alpha) = -(\Delta x_1)(c) + (\Delta y_1)(s) + (\Delta x_2)(c) + (\Delta y_2)(s) - 2(\Delta y_3)(s)$$

If these equations are summarized in a matrix form, we obtain

$$\begin{bmatrix} \Delta r_1 \\ \Delta r_2 \\ \Delta \alpha \end{bmatrix} = \begin{bmatrix} -s & -c & 0 & | & 0 & 0 & 0 & | & s & c & 0 \\ 0 & 0 & 0 & | & s & -c & 0 & | & -s & c & 0 \\ -c/r & s/r & 0 & | & c/r & s/r & 0 & | & 0 & -2s/r & 0 \end{bmatrix} \begin{bmatrix} \Delta x_1 \\ \Delta y_1 \\ \Delta z_1 \\ \hline \Delta x_2 \\ \Delta y_2 \\ \Delta z_2 \\ \hline \Delta x_3 \\ \Delta y_3 \\ \Delta z_3 \end{bmatrix} \quad (1.119)$$

If unit vectors such as those in Fig. 1.23 are considered, Eq. 1.119 can be written in a more compact form using vector notation:

$$\begin{bmatrix} \Delta r_1 \\ \Delta r_2 \\ \Delta \alpha \end{bmatrix} = \begin{bmatrix} \mathbf{e}_{31} & 0 & -\mathbf{e}_{31} \\ 0 & \mathbf{e}_{32} & -\mathbf{e}_{32} \\ \mathbf{p}_{31}/r & \mathbf{p}_{32}/r & -(\mathbf{p}_{31} + \mathbf{p}_{32})/r \end{bmatrix} \begin{bmatrix} \boldsymbol{\rho}_1 \\ \boldsymbol{\rho}_2 \\ \boldsymbol{\rho}_3 \end{bmatrix} \quad (1.120)$$

Here $\boldsymbol{\rho}_1$, $\boldsymbol{\rho}_2$, and $\boldsymbol{\rho}_3$ are the displacement vectors of atoms 1, 2, and 3, respectively. Thus Eq. 1.120 can be written simply as

$$\mathbf{R} = \mathbf{S} \cdot \boldsymbol{\rho} \quad (1.121)$$

where the dot represents the scalar product of the two vectors. Here \mathbf{S} is called the \mathbf{S} matrix, and its components (\mathbf{S} vector) can be written according to the following formulas: (1) bond stretching

$$\Delta r_1 = \Delta_{31} = \mathbf{e}_{31} \cdot \boldsymbol{\rho}_1 - \mathbf{e}_{31} \cdot \boldsymbol{\rho}_3 \quad (1.122)$$

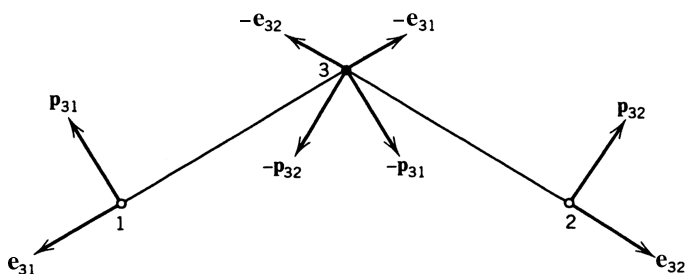


Fig. 1.23. Unit vectors in a bent XY_2 molecule.

and (2) angle bending:

$$\Delta\alpha = \Delta\alpha_{132} = \frac{\mathbf{p}_{31} \cdot \boldsymbol{\rho}_1 + \mathbf{p}_{32} \cdot \boldsymbol{\rho}_2 - (\mathbf{p}_{31} + \mathbf{p}_{32}) \cdot \boldsymbol{\rho}_3}{r} \quad (1.123)$$

It is seen that the \mathbf{S} vector is oriented in the direction in which a given displacement of the i th atom will produce the greatest increase in Δr or $\Delta\alpha$. Formulas for obtaining the \mathbf{S} vectors of other internal coordinates such as those of out-of-plane ($\Delta\theta$) and torsional ($\Delta\tau$) vibrations are also available [3].

By using the \mathbf{S} matrix, Eq. 1.117 is written as

$$\mathbf{G} = \mathbf{S} \mathbf{m}^{-1} \tilde{\mathbf{S}} \quad (1.124)$$

For a bent XY_2 molecule, this becomes

$$\begin{aligned} \mathbf{G} &= \begin{bmatrix} \mathbf{e}_{31} & 0 & -\mathbf{e}_{31} \\ 0 & \mathbf{e}_{32} & -\mathbf{e}_{32} \\ \mathbf{p}_{31}/r & \mathbf{p}_{32}/r & -(\mathbf{p}_{31} + \mathbf{p}_{32})/r \end{bmatrix} \begin{bmatrix} \mu_1 & 0 & 0 \\ 0 & \mu_1 & 0 \\ 0 & 0 & \mu_3 \end{bmatrix} \\ &\times \begin{bmatrix} \mathbf{e}_{31} & 0 & \mathbf{p}_{31}/r \\ 0 & \mathbf{e}_{32} & \mathbf{p}_{32}/r \\ -\mathbf{e}_{31} & -\mathbf{e}_{32} & -(\mathbf{p}_{31} + \mathbf{p}_{32})/r \end{bmatrix} \\ &= \begin{bmatrix} (\mu_3 + \mu_1)\mathbf{e}_{31}^2 & \mu_3\mathbf{e}_{31} \cdot \mathbf{e}_{32} & \frac{\mu_1}{r}\mathbf{e}_{31} \cdot \mathbf{p}_{31} + \frac{\mu_3}{r}\mathbf{e}_{31} \cdot (\mathbf{p}_{31} + \mathbf{p}_{32}) \\ & (\mu_3\mu_1)\mathbf{e}_{32}^2 & \frac{\mu_1}{r}\mathbf{e}_{32} \cdot \mathbf{p}_{32} + \frac{\mu_3}{r}\mathbf{e}_{32} \cdot (\mathbf{p}_{31} + \mathbf{p}_{32}) \\ & & \frac{\mu_1}{r^2}\mathbf{p}_{31}^2 + \frac{\mu_1}{r^2}\mathbf{p}_{32}^2 + \frac{\mu_3}{r^2}(\mathbf{p}_{31} + \mathbf{p}_{32})^2 \end{bmatrix} \end{aligned}$$

Considering

$$\begin{aligned} \mathbf{e}_{31} \cdot \mathbf{e}_{31} = \mathbf{e}_{32} \cdot \mathbf{e}_{32} = \mathbf{p}_{31} \cdot \mathbf{p}_{31} = \mathbf{p}_{32} \cdot \mathbf{p}_{32} &= 1, & \mathbf{e}_{31} \cdot \mathbf{p}_{31} = \mathbf{e}_{32} \cdot \mathbf{p}_{32} &= 0 \\ \mathbf{e}_{31} \cdot \mathbf{e}_{32} &= \cos \alpha, & \mathbf{e}_{31} \cdot \mathbf{p}_{32} = \mathbf{e}_{32} \cdot \mathbf{p}_{31} &= -\sin \alpha \\ (\mathbf{p}_{31} + \mathbf{p}_{32})^2 &= 2(1 - \cos \alpha) \end{aligned}$$

we find that the \mathbf{G} matrix is calculated as follows:

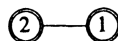
$$\mathbf{G} = \begin{bmatrix} \mu_3 + \mu_1 & \mu_3 \cos \alpha & -\frac{\mu_3}{r} \sin \alpha \\ & \mu_3 + \mu_1 & -\frac{\mu_3}{r} \sin \alpha \\ & & \frac{2\mu_1}{r^2} + \frac{2\mu_3}{r^2} (1 - \cos \alpha) \end{bmatrix} \quad (1.125)$$

If the **G**-matrix elements obtained are written for each combination of internal coordinates, there results

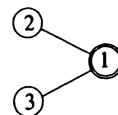
$$\begin{aligned}
 G(\Delta r_1, \Delta r_1) &= \mu_3 + \mu_1 \\
 G(\Delta r_2, \Delta r_2) &= \mu_3 + \mu_1 \\
 G(\Delta r_1, \Delta r_2) &= \mu_3 \cos \alpha \\
 G(\Delta \alpha, \Delta \alpha) &= \frac{2\mu_1}{r^2} + \frac{2\mu_3}{r^2} (1 - \cos \alpha) \\
 G(\Delta r_1, \Delta \alpha) &= -\frac{\mu_3}{r} \sin \alpha \\
 G(\Delta r_2, \Delta \alpha) &= -\frac{\mu_3}{r} \sin \alpha
 \end{aligned} \tag{1.126}$$

If such calculations are made for several types of molecules, it is immediately seen that the **G**-matrix elements themselves have many regularities. Decius [79] developed general formulas for writing **G**-matrix elements.* Some of them are as follows:

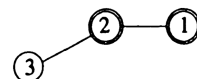
$$G_{rr}^2 = \mu_1 + \mu_2$$



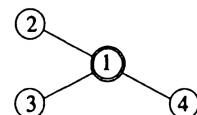
$$G_{rr}^1 = \mu_1 \cos \phi$$



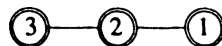
$$G_{r\phi}^2 = -\rho_{23} \mu_2 \sin \phi$$



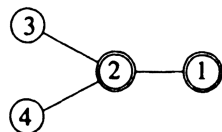
$$\begin{aligned}
 G_{r\phi}^1 \begin{pmatrix} 1 \\ 1 \end{pmatrix} &= -(\rho_{13} \sin \phi_{213} \cos \psi_{234} \\
 &\quad + \rho_{14} \sin \phi_{214} \cos \psi_{243}) \mu_1
 \end{aligned}$$



$$\begin{aligned}
 G_{\phi\phi}^3 &= \rho_{12}^2 \mu_1 + \rho_{23}^2 \mu_3 + (\rho_{12}^2 + \rho_{23}^2 \\
 &\quad - 2\rho_{12}\rho_{23} \cos \phi) \mu_2
 \end{aligned}$$



$$\begin{aligned}
 G_{\phi\phi}^2 \begin{pmatrix} 1 \\ 1 \end{pmatrix} &= (\rho_{12}^2 \cos \psi_{314}) \mu_1 + [\rho_{12} - \rho_{23} \cos \phi_{123} \\
 &\quad - \rho_{24} \cos \phi_{124}] \rho_{12} \cos \psi_{314} \\
 &\quad + (\sin \phi_{123} \sin \phi_{124} \sin^2 \psi_{314} \\
 &\quad + \cos \phi_{324} \cos \psi_{314}) \rho_{23} \rho_{24} \mu_2
 \end{aligned}$$



*See also Refs. 3 and 80.

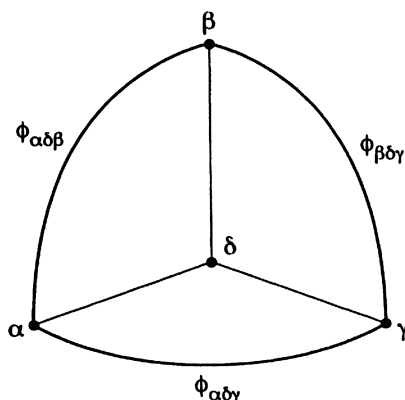


Fig. 1.24. Spherical angles involving atomic positions, α , β , γ , and δ .

Here, the atoms surrounded by a bold line circle are those common to both coordinates. The symbols μ and ρ denote the reciprocals of mass and bond distance, respectively. The spherical angle $\psi_{\alpha\beta\gamma}$ in Fig. 1.24 is defined as

$$\cos\psi_{\alpha\beta\gamma} = \frac{\cos\phi_{\alpha\delta\gamma} - \cos\phi_{\alpha\delta\beta}\cos\phi_{\beta\delta\gamma}}{\sin\phi_{\alpha\delta\beta}\sin\phi_{\beta\delta\gamma}} \quad (1.127)$$

The correspondence between the Decius formulas and the results obtained in Eq. 1.126 is evident.

With the Decius formulas, the **G**-matrix elements of a pyramidal XY_3 molecule have been calculated and are shown in Table 1.13.

1.13. UTILIZATION OF SYMMETRY PROPERTIES

In view of the equivalence of the two $X-Y$ bonds of a bent XY_2 molecule, the **F** and **G** matrices obtained in Eqs. 1.112 and 1.125 are written as

$$\mathbf{F} = \begin{bmatrix} f_{11} & f_{12} & rf_{13} \\ f_{12} & f_{11} & rf_{13} \\ rf_{13} & rf_{13} & r^2 f_{33} \end{bmatrix} \quad (1.128)$$

$$\mathbf{G} = \begin{bmatrix} \mu_3 + \mu_1 & \mu_3 \cos\alpha & -\frac{\mu_3}{r} \sin\alpha \\ \mu_3 \cos\alpha & \mu_3 + \mu_1 & -\frac{\mu_3}{r} \sin\alpha \\ -\frac{\mu_3}{r} \sin\alpha & -\frac{\mu_3}{r} \sin\alpha & \frac{2\mu_1}{r^2} + \frac{2\mu_3}{r^2} (1 - \cos\alpha) \end{bmatrix} \quad (1.129)$$

TABLE 1.13.

	Δr_1	Δr_2	Δr_3	$\Delta \alpha_{23}$	$\Delta \alpha_{31}$	$\Delta \alpha_{12}$
Δr_1	A	B	B	C	D	D
Δr_2	—	A	B	D	C	D
Δr_3	—	—	A	D	D	C
$\Delta \alpha_{23}$	—	—	—	E	F	F
$\Delta \alpha_{31}$	—	—	—	—	E	F
$\Delta \alpha_{12}$	—	—	—	—	—	E

$$A = G_{rr}^2 = \mu_x + \mu_y$$

$$B = G_{rr}^1 = \mu_x \cos \alpha$$

$$C = G_{r\phi}^1 \begin{pmatrix} 1 \\ 1 \end{pmatrix} = -\frac{2}{r} \frac{\cos \alpha (1 - \cos \alpha) \mu_x}{\sin \alpha}$$

$$D = G_{2\phi}^2 = -\frac{\mu_x}{r} \sin \alpha$$

$$E = G_{\phi\phi}^3 = \frac{2}{r^2} [\mu_y + \mu_x (1 - \cos \alpha)]$$

$$F = G_{\phi\phi}^2 \begin{pmatrix} 1 \\ 1 \end{pmatrix} = \frac{\mu_y}{r^2} \frac{\cos \alpha}{1 + \cos \alpha} + \frac{\mu_x}{r^2} \frac{(1 + 3 \cos \alpha)(1 - \cos \alpha)}{1 + \cos \alpha}$$

Both of these matrices are of the form

$$\begin{bmatrix} A & C & D \\ C & A & D \\ D & D & B \end{bmatrix} \quad (1.130)$$

The appearance of the same elements is evidently due to the equivalence of the two internal coordinates, Δr_1 and Δr_2 . Such symmetrically equivalent sets of internal coordinates are seen in many other molecules, such as those in Fig. 1.20. In these cases, it is possible to reduce the order of the \mathbf{F} and \mathbf{G} matrices (and hence the order of the secular equation resulting from them) by a coordinate transformation.

Let the internal coordinates R be transformed by

$$\mathbf{R}^s = \mathbf{U}\mathbf{R} \quad (1.131)$$

Then, we obtain

$$\begin{aligned} 2T &= \tilde{\mathbf{R}}\mathbf{G}^{-1}\dot{\mathbf{R}} = \tilde{\mathbf{R}}^s \tilde{\mathbf{U}}^{-1} \mathbf{G}^{-1} \mathbf{U}^{-1} \dot{\mathbf{R}}^s \\ &= \tilde{\mathbf{R}}^s \mathbf{G}_s^{-1} \dot{\mathbf{R}}^s \\ 2V &= \tilde{\mathbf{R}}\mathbf{F}\mathbf{R} = \tilde{\mathbf{R}}^s \tilde{\mathbf{U}}^{-1} \mathbf{F} \mathbf{U}^{-1} \mathbf{R}^s \\ &= \tilde{\mathbf{R}}^s \mathbf{F}_s \mathbf{R}^s \end{aligned}$$

where

$$\begin{aligned}\mathbf{G}_s^{-1} &= \tilde{\mathbf{U}}^{-1} \mathbf{G}^{-1} \mathbf{U}^{-1} \quad \text{or} \quad \mathbf{G}_s = \mathbf{U} \mathbf{G} \tilde{\mathbf{U}} \\ \mathbf{F}_s &= \tilde{\mathbf{U}}^{-1} \mathbf{F} \mathbf{U}^{-1}\end{aligned}\quad (1.132)$$

If \mathbf{U} is an orthogonal matrix ($\mathbf{U}^{-1} = \tilde{\mathbf{U}}$), Eq. 1.132 is written as

$$\mathbf{F}_s = \mathbf{U} \mathbf{F} \tilde{\mathbf{U}} \quad \text{and} \quad \mathbf{G}_s = \mathbf{U} \mathbf{G} \tilde{\mathbf{U}} \quad (1.133)$$

Both $\mathbf{G}\mathbf{F}$ and $\mathbf{G}_s\mathbf{F}_s$ give the same roots, since

$$\begin{aligned}|\mathbf{G}_s\mathbf{F}_s - \mathbf{E}\lambda| &= |\mathbf{U} \mathbf{G} \tilde{\mathbf{U}} \tilde{\mathbf{U}}^{-1} \mathbf{F} \mathbf{U}^{-1} - \mathbf{E}\lambda| \\ &= |\mathbf{U} \mathbf{G} \mathbf{F} \mathbf{U}^{-1} - \mathbf{E}\lambda| \\ &= |\mathbf{U}||\mathbf{G}\mathbf{F} - \mathbf{E}\lambda||\mathbf{U}^{-1}| \\ &= |\mathbf{G}\mathbf{F} - \mathbf{E}\lambda|\end{aligned}\quad (1.134)$$

If we choose a proper \mathbf{U} matrix from symmetry consideration, it is possible to factor the original \mathbf{G} and \mathbf{F} matrices into smaller ones. This, in turn, reduces the order of the secular equation to be solved, thus facilitating their solution. These new coordinates \mathbf{R}^s are called *symmetry coordinates*.

The \mathbf{U} matrix is constructed by using the equation

$$\mathbf{R}^s = N \sum_K \chi_i(K) K(\Delta r_1) \quad (1.135)$$

Here, K is a symmetry operation, and the summation is made over all symmetry operations. Also, $\chi_i(K)$ is the character of the representation to which \mathbf{R}^s belongs. Called a generator, Δr_1 is, by symmetry operation K , transformed into $K(\Delta r_1)$, which is another coordinate of the same symmetrically equivalent set. Finally, N is a normalizing factor.

As an example, consider a bent \mathbf{XY}_2 molecule in which Δr_1 and Δr_2 are equivalent. Using Δr_1 as a generator, we obtain

	I	$C_2(z)$	$\sigma(xz)$	$\sigma(yz)$
$K(\Delta r_1)$	Δr_1	Δr_2	Δr_2	Δr_1
$\chi_{A_1}(K)$	1	1	1	1
$\chi_{B_2}(K)$	1	-1	-1	1

Thus

$$R_{A_1}^s = N \sum \chi_{A_1}(K) K(\Delta r_1) = 2N(\Delta r_1 + \Delta r_2)$$

$$N = \frac{1}{2\sqrt{2}} \quad \text{since } (2N)^2 + (2N)^2 = 1$$

Then

$$R_{A_1}^s = \frac{1}{\sqrt{2}}(\Delta r_1 + \Delta r_2) \quad (1.136)$$

Similarly,

$$R_{B_2}^s = \frac{1}{\sqrt{2}}(\Delta r_1 - \Delta r_2) \quad (1.137)$$

The remaining internal coordinate, $\Delta\alpha$, belongs to the A_1 species. Thus, the complete \mathbf{U} matrix is written as

$$\begin{bmatrix} R_1^s(A_1) \\ R_2^s(A_1) \\ R_3^s(B_2) \end{bmatrix} = \begin{bmatrix} \frac{1}{\sqrt{2}} & \frac{1}{\sqrt{2}} & 0 \\ 0 & 0 & 1 \\ \frac{1}{\sqrt{2}} & \frac{-1}{\sqrt{2}} & 0 \end{bmatrix} \begin{bmatrix} \Delta r_1 \\ \Delta r_2 \\ \Delta\alpha \end{bmatrix} \quad (1.138)$$

If the \mathbf{G} and \mathbf{F} matrices of type 1.130 are transformed by relations 1.133, where \mathbf{U} is given by the matrix of Eq. 1.138, they become

$$\mathbf{F}_s, \mathbf{G}_s = \left[\begin{array}{cc|c} \mathbf{A} + \mathbf{C} & \sqrt{2}\mathbf{D} & 0 \\ \sqrt{2}\mathbf{D} & \mathbf{B} & 0 \\ \hline 0 & 0 & \mathbf{A} - \mathbf{C} \end{array} \right] \quad (1.139)$$

or, more explicitly

$$\mathbf{F}_s = \left[\begin{array}{cc|c} f_{11} + f_{12} & r\sqrt{2}f_{13} & 0 \\ r\sqrt{2}f_{13} & r^2f_{33} & 0 \\ \hline 0 & 0 & f_{11} - f_{12} \end{array} \right] \quad (1.140)$$

$$\mathbf{G}_S = \left[\begin{array}{cc|c} \mu_3(1 + \cos \alpha) + \mu_1 & -\frac{\sqrt{2}}{r} \mu_3 \sin \alpha & 0 \\ -\frac{\sqrt{2}}{r} \mu_3 \sin \alpha & \frac{2\mu_1}{r^2} + \frac{2\mu_3}{r^2} (1 - \cos \alpha) & 0 \\ \hline 0 & 0 & \mu_3(1 - \cos \alpha) + \mu_1 \end{array} \right] \quad (1.141)$$

In a pyramidal XY_3 molecule (Fig. 1.20c), Δr_1 , Δr_2 , and Δr_3 are the equivalent set; so are $\Delta\alpha_{23}$, $\Delta\alpha_{31}$, and $\Delta\alpha_{12}$. It is already known from Eq. 1.107 that one A_1 and one E vibration are involved both in the stretching and in the bending vibrations. Using Δr_1 as a generator, we obtain from Eq. 1.135

	I	C_3^+	C_3^-	σ_1	σ_2	σ_3
$K(\Delta r_1)$	Δr_1	Δr_2	Δr_3	Δr_1	Δr_3	Δr_2
$\chi_{A_1}(K)$	1	1	1	1	1	1
$\chi_E(K)$	2	-1	-1	0	0	0

Then, we obtain

$$R_{A_1}^s = \frac{1}{\sqrt{3}}(\Delta r_1 + \Delta r_2 + \Delta r_3) \quad (1.142)$$

$$R_{E_1}^s = \frac{1}{\sqrt{6}}(2\Delta r_1 - \Delta r_2 - \Delta r_3) \quad (1.143)$$

To find a coordinate that forms a degenerate pair with Eq. 1.143, we repeat the same procedure, using Δr_2 and Δr_3 as the generators. The results are

$$R_{E_2}^s = N(2\Delta r_2 - \Delta r_3 - \Delta r_1)$$

$$R_{E_3}^s = N(2\Delta r_3 - \Delta r_1 - \Delta r_2)$$

However, these coordinates are not orthogonal to $R_{E_1}^s$ (Eq. 1.143).

If we take a linear combination, $R_{E_2}^s + R_{E_3}^s$, we obtain Eq. 1.143. If we take $R_{E_2}^s - R_{E_3}^s$, we obtain

$$R_{E_4}^s = \frac{1}{\sqrt{2}}(\Delta r_2 - \Delta r_3) \quad (1.144)$$

Since Eqs. 1.143 and 1.144 are mutually orthogonal, these two coordinates are taken as a degenerate pair. Similar results are obtained for three angle-bending coordinates. Thus, the complete **U** matrix is written as

$$\begin{bmatrix} R_1^s(A_1) \\ R_2^s(A_1) \\ R_{3a}^s(E) \\ R_{4a}^s(E) \\ R_{3b}^s(E) \\ R_{4b}^s(E) \end{bmatrix} = \begin{bmatrix} 1/\sqrt{3} & 1/\sqrt{3} & 1/\sqrt{3} & 0 & 0 & 0 \\ 0 & 0 & 0 & 1/\sqrt{3} & 1/\sqrt{3} & 1/\sqrt{3} \\ 2/\sqrt{6} & -1/\sqrt{6} & -1/\sqrt{6} & 0 & 0 & 0 \\ 0 & 0 & 0 & 2/\sqrt{6} & -1/\sqrt{6} & -1/\sqrt{6} \\ 0 & 1/\sqrt{2} & -1/\sqrt{2} & 0 & 0 & 0 \\ 0 & 0 & 0 & 0 & 1/\sqrt{2} & -1/\sqrt{2} \end{bmatrix} \cdot \begin{bmatrix} \Delta r_1 \\ \Delta r_2 \\ \Delta r_3 \\ \Delta \alpha_{23} \\ \Delta \alpha_{31} \\ \Delta \alpha_{12} \end{bmatrix} \quad (1.145)$$

The **G** matrix of a pyramidal XY_3 molecule has already been calculated (see Table 1.14). By using Eq. 1.133, the new **G_s** matrix becomes

$$\mathbf{G}_s = \begin{bmatrix} A+2B & C+2D & & \\ C+2D & E+2F & 0 & 0 \\ \hline & 0 & A-B & C-D \\ & & C-D & E-F \\ \hline & 0 & & 0 \\ & & A-B & C-D \\ & & C-D & E-F \end{bmatrix} \quad (1.146)$$

Here *A*, *B*, and so forth denote the elements in Table 1.13. The **F** matrix transforms similarly. Therefore, it is necessary only to solve two quadratic equations for the A_1 and E species.

For the tetrahedral XY_4 molecule shown in Fig. 1.20e, group theory (Secs. 1.8 and 1.9) predicts one A_1 and one F_2 stretching, and one E and one F_2 bending, vibration. The **U** matrix for the four stretching coordinates is

$$\begin{bmatrix} R_1^s(A_1) \\ R_{2a}^s(F_2) \\ R_{2b}^s(F_2) \\ R_{2c}^s(F_2) \end{bmatrix} = \begin{bmatrix} 1/2 & 1/2 & 1/2 & 1/2 \\ 1/\sqrt{6} & 1/\sqrt{6} & -2/\sqrt{6} & 0 \\ 1/\sqrt{12} & 1/\sqrt{12} & 1/\sqrt{12} & -3/\sqrt{12} \\ -1/\sqrt{2} & 1/\sqrt{2} & 0 & 0 \end{bmatrix} \begin{bmatrix} \Delta r_1 \\ \Delta r_2 \\ \Delta r_3 \\ \Delta r_4 \end{bmatrix} \quad (1.147)$$

whereas the **U** matrix for the six bending coordinates becomes

$$\begin{bmatrix} R_1^s(A_1) \\ R_{2a}^s(E) \\ R_{2b}^s(E) \\ R_{3a}^s(F_2) \\ R_{3b}^s(F_2) \\ R_{3c}^s(F_2) \end{bmatrix} = \begin{bmatrix} 1/\sqrt{6} & 1/\sqrt{6} & 1/\sqrt{6} & 1/\sqrt{6} & 1/\sqrt{6} & 1/\sqrt{6} \\ 2/\sqrt{12} & -1/\sqrt{12} & -1/\sqrt{12} & -1/\sqrt{12} & -1/\sqrt{12} & 2/\sqrt{12} \\ 0 & 1/2 & -1/2 & 1/2 & -1/2 & 0 \\ 2/\sqrt{12} & -1/\sqrt{12} & -1/\sqrt{12} & 1/\sqrt{12} & 1/\sqrt{12} & -2/\sqrt{12} \\ 1/\sqrt{6} & 1/\sqrt{6} & 1/\sqrt{6} & -1/\sqrt{6} & -1/\sqrt{6} & -1/\sqrt{6} \\ 0 & 1/2 & -1/2 & -1/2 & 1/2 & 0 \end{bmatrix} \cdot \begin{bmatrix} \Delta\alpha_{12} \\ \Delta\alpha_{23} \\ \Delta\alpha_{31} \\ \Delta\alpha_{14} \\ \Delta\alpha_{24} \\ \Delta\alpha_{34} \end{bmatrix} \quad (1.148)$$

The symmetry coordinate $R_1^s(A_1)$ in Eq. 1.148 represents a *redundant coordinate* (see Eq. 1.91). In such a case, a coordinate transformation reduces the order of the matrix by one, since all the **G**-matrix elements related to this coordinate become zero. Conversely, this result provides a general method of finding redundant coordinates. Suppose that the elements of the **G** matrix are calculated in terms of internal coordinates such as those in Table 1.13. If a suitable combination of internal coordinates is made so that $\sum_j G_{ij} = 0$ (where j refers to all the equivalent internal coordinates), such a combination is a redundant coordinate. By using the **U** matrices in Eqs. 1.147 and 1.148, the problem of solving a tenth-order secular equation for a tetrahedral XY_4 molecule is reduced to that of solving two first-order (A_1 and E) and one quadratic (F_2) equation.

The normal modes of vibration of the tetrahedral XY_4 molecule are shown in Fig. 2.12 of Chapter 2. It can be seen that the normal modes, ν_1 and ν_3 , correspond to the symmetry coordinates $R_1^s(A_1)$ and $R_{2b}^s(F_2)$ of Eq. 1.147, respectively, and that the normal modes, ν_2 and ν_4 , correspond to the symmetry coordinates $R_{2a}^s(E)$ and $R_{3b}^s(F_2)$ of Eq. 1.148, respectively.

1.14. POTENTIAL FIELDS AND FORCE CONSTANTS

Using Eqs. 1.111 and 1.128, we write the potential energy of a bent XY_2 molecule as

$$\begin{aligned} 2V = & f_{11}(\Delta r_1)^2 + f_{11}(\Delta r_2)^2 + f_{33}r^2(\Delta\alpha)^2 + 2f_{12}(\Delta r_1)(\Delta r_2) \\ & + 2f_{13}r(\Delta r_1)(\Delta\alpha) + 2f_{13}r(\Delta r_2)(\Delta\alpha) \end{aligned} \quad (1.149)$$

This type of potential field is called a *generalized valence force* (GVF) field.* It consists of stretching and bending force constants, as well as the interaction force constants between them. When using such a potential field, four force constants are needed to describe the potential energy of a bent XY_2 molecule. Since only three vibrations are observed in practice, it is impossible to determine all four force constants simultaneously. One method used to circumvent this difficulty is to calculate the vibrational frequencies of isotopic molecules (e.g., D_2O and HDO for H_2O), assuming the same set of force constants.† This method is satisfactory, however, only for simple molecules. As molecules become more complex, the number of interaction force constants in the GVF field becomes too large to allow any reliable evaluation.

In another approach, Shimanouchi [82] introduced the *Urey-Bradley force* (UBF) field, which consists of stretching and bending force constants, as well as repulsive force constants between nonbonded atoms. The general form of the potential field is given by

$$\begin{aligned}
 V = & \sum_i \left(\frac{1}{2} K_i (\Delta r_i)^2 + K'_i r_i (\Delta r_i) \right) \\
 & + \sum_i \left(\frac{1}{2} H_i r_{i\alpha}^2 (\Delta \alpha_i)^2 + H'_i r_{i\alpha}^2 (\Delta \alpha_i) \right) \\
 & + \sum_i \left(\frac{1}{2} F_i (\Delta q_i)^2 + F'_i q_i (\Delta q_i) \right)
 \end{aligned} \tag{1.150}$$

Here Δr_i , $\Delta \alpha_i$, and Δq_i , are the changes in the bond lengths, bond angles, and distances between nonbonded atoms, respectively. The symbols K_i , K'_i , H_i , H'_i and F_i , F'_i represent the stretching, bending, and repulsive force constants, respectively. Furthermore, r_i , $r_{i\alpha}$, and q_i are the values of the distances at the equilibrium positions and are inserted to make the force constants dimensionally similar. Linear force constants (K'_i , H'_i and F'_i) must be included since Δr_i , $\Delta \alpha_i$, and Δq_i are not completely independent of each other.

Using the relation

$$q_{ij}^2 = r_i^2 + r_j^2 - 2r_i r_j \cos \alpha_{ij} \tag{1.151}$$

*A potential field consisting of stretching and bending force constants only is called a *simple valence force* field.

†In addition to isotope frequency shifts, mean amplitudes of vibration, Coriolis coupling constants, centrifugal distortion constants, and so forth may be used to refine the force constants of small molecules (see Ref. 81).

and considering that the first derivatives can be equated to zero in the equilibrium case, we can write the final form of the potential field as

$$\begin{aligned}
 V = & \frac{1}{2} \sum_i \left[K_i + \sum_{j(\neq i)} (t_{ij}^2 F'_{ij} + s_{ij}^2 F_{ij}) \right] (\Delta r_i)^2 \\
 & + \frac{1}{2} \sum_{i < j} (H_{ij} - s_{ij} s_{ji} F'_{ij} + t_{ij} t_{ji} F_{ij}) (\sqrt{r_i r_j} \Delta \alpha_{ij})^2 \\
 & + \sum_{i < j} (-t_{ij} t_{ji} F'_{ij} + s_{ij} s_{ji} F_{ij}) (\Delta r_i) (\Delta r_j) \\
 & + \sum_{i \neq j} (t_{ij} s_{ji} F'_{ij} + t_{ji} s_{ij} F_{ij}) \left(\frac{r_j}{r_i} \right)^{1/2} (\Delta r_i) (\sqrt{r_i r_j} \Delta \alpha_{ij})
 \end{aligned} \tag{1.152}*$$

Here

$$\begin{aligned}
 s_{ij} &= \frac{r_i - r_j \cos \alpha_{ij}}{q_{ij}} \\
 s_{ji} &= \frac{r_j - r_i \cos \alpha_{ij}}{q_{ij}} \\
 t_{ij} &= \frac{r_j \sin \alpha_{ij}}{q_{ij}} \\
 t_{ji} &= \frac{r_i \sin \alpha_{ij}}{q_{ij}}
 \end{aligned} \tag{1.153}$$

In a bent XY_2 molecule, Eq. 1.152 becomes

$$\begin{aligned}
 V = & \frac{1}{2} (K + t^2 F' + s^2 F) [(\Delta r_1)^2 + (\Delta r_2)^2] + \frac{1}{2} (H - s^2 F' + t^2 F) (r \Delta \alpha)^2 \\
 & + (-t^2 F' + s^2 F) (\Delta r_1) (\Delta r_2) + ts (F' + F) (\Delta r_1) (r \Delta \alpha) \\
 & + ts (F' + F) (\Delta r_2) (r \Delta \alpha)
 \end{aligned} \tag{1.154}$$

where

*In the case of tetrahedral molecules, a term

$$\sum_{i \neq j \neq k} \left(\frac{\kappa}{\sqrt{2}} \right) r_{ij} r_{ik} (r_{ij} \Delta \alpha_{ij}) (r_{ik} \Delta \alpha_{ik})$$

must be added, where κ is called the *internal tension*.

$$s = \frac{r(1 - \cos\alpha)}{q}$$

$$t = \frac{r\sin\alpha}{q}$$

Comparing Eqs. 1.154 and 1.149, we obtain the following relations between the force constants of the generalized valence force field and those of the Urey–Bradley force field:

$$\begin{aligned} f_{11} &= K + t^2 F' + s^2 F \\ r^2 f_{33} &= (H - s^2 F' + t^2 F) r^2 \\ f_{12} &= -t^2 F' + s^2 F \\ r f_{13} &= t s (F' + F) r \end{aligned} \tag{1.155}$$

Although the Urey–Bradley field has four force constants, F' is usually taken as $-\frac{1}{10}F$, on the assumption that the repulsive energy between nonbonded atoms is proportional to $1/r^9$.* Thus, only three force constants, K , H , and F , are needed to construct the \mathbf{F} matrix. The *orbital valence force* (OVF) field developed by Heath and Linnett [83] is similar to the UBF field. The OVF field uses the angle $(\Delta\beta)$, which represents the distortion of the bond from the axis of the bonding orbital instead of the angle between two bonds $(\Delta\alpha)$.

The number of force constants in the Urey–Bradley field is, in general, much smaller than that in the generalized valence force field. In addition, the UBF field has the advantage that (1) the force constants have clearer physical meanings than those of the GVF field, and (2) they are often transferable from molecule to molecule. For example, the force constants obtained for SiCl_4 and SiBr_4 can be used for SiCl_3Br , SiCl_2Br_2 , and SiClBr_3 . Mizushima, Shimanouchi, and their coworkers [81] and Overend and Scherer [84] have given many examples that demonstrate the transferability of the force constants in the UBF field. This property of the Urey–Bradley force constants is highly useful in calculations for complex molecules. It should be mentioned, however, that ignorance of the interactions between nonneighboring stretching vibrations and between bending vibrations in the Urey–Bradley field sometimes causes difficulties in adjusting the force constants to fit the observed frequencies. In such a case, it is possible to improve the results by introducing more force constants [84,85].

*This assumption does not cause serious error in final results, since F' is small in most cases.

Evidently, the values of force constants depend on the force field initially assumed. Thus, a comparison of force constants between molecules should not be made unless they are obtained by using the same force field. The normal coordinate analysis developed in Secs. 1.12–1.14 has already been applied to a number of molecules of various structures. Appendix VII lists the **G** and **F** matrix elements for typical molecules.

1.15. SOLUTION OF THE SECULAR EQUATION

Once the **G** and **F** matrices are obtained, the next step is to solve the matrix secular equation:

$$|\mathbf{GF} - \mathbf{E}\lambda| = 0 \quad (1.116)$$

In diatomic molecules, $\mathbf{G} = G_{11} = 1/\mu$ and $\mathbf{F} = F_{11} = K$. Then $\lambda = G_{11}F_{11}$ and $\tilde{\nu} = \sqrt{\lambda}/2\pi c = \sqrt{K/\mu}/2\pi c$ (Eq. 1.20). If the units of mass and force constant are atomic weight and mdyn/Å (or 10^5 dyn/cm), respectively,* λ is related to $\tilde{\nu}(\text{cm}^{-1})$ by

$$\tilde{\nu} = 1302.83\sqrt{\lambda}$$

or

$$\lambda = 0.58915 \left(\frac{\tilde{\nu}}{1000} \right)^2 \quad (1.156)$$

As an example, for the HF molecule $\mu = 0.9573$ and $K = 9.65$ in these units. Then, from Eqs. 1.20 and 1.156, $\tilde{\nu}$ is 4139 cm^{-1} .

The **F** and **G** matrix elements of a bent XY_2 molecule are given in Eqs. 1.140 and 1.141, respectively. The secular equation for the A_1 species is quadratic:

$$|\mathbf{GF} - \mathbf{E}\lambda| = \begin{vmatrix} G_{11}F_{11} + G_{12}F_{21} - \lambda & G_{11}F_{12} + G_{12}F_{22} \\ G_{21}F_{11} + G_{22}F_{21} & G_{21}F_{12} + G_{22}F_{22} - \lambda \end{vmatrix} = 0 \quad (1.157)$$

If this is expanded into an algebraic equation, the following result is obtained:

$$\lambda^2 - (G_{11}F_{11} + G_{22}F_{22} + 2G_{12}F_{12})\lambda + (G_{11}G_{22} - G_{12}^2)(F_{11}F_{22} - F_{12}^2) = 0 \quad (1.158)$$

* Although the bond distance is involved in both the **G** and **F** matrices, it is canceled during multiplication of the **G** and **F** matrix elements. Therefore, any unit can be used for the bond distance.

For the H₂O molecule, we obtain

$$\mu_1 = \mu_{\text{H}} = \frac{1}{1.008} = 0.99206$$

$$\mu_3 = \mu_{\text{O}} = \frac{1}{15.995} = 0.06252$$

$$r = 0.96(\text{\AA}), \quad \alpha = 105^\circ$$

$$\sin\alpha = \sin 105^\circ = 0.96593$$

$$\cos\alpha = \cos 105^\circ = -0.25882$$

Then, the **G** matrix elements of Eq. 1.141 are

$$G_{11} = \mu_1 + \mu_3(1 + \cos\alpha) = 1.03840$$

$$G_{12} = -\frac{\sqrt{2}}{r}\mu_3\sin\alpha = -0.08896$$

$$G_{22} = \frac{1}{r^2}[2\mu_1 + 2\mu_3(1 - \cos\alpha)] = 2.32370$$

If the force constants in terms of the generalized valence force field are selected as

$$f_{11} = 8.4280, \quad f_{12} = -0.1050$$

$$f_{13} = 0.2625, \quad f_{33} = 0.7680$$

the **F** matrix elements of Eq. 1.140 are

$$F_{11} = f_{11} + f_{12} = 8.32300$$

$$F_{12} = \sqrt{2}rf_{13} = 0.35638$$

$$F_{22} = r^2f_{33} = 0.70779$$

Using these values, we find that Eq. 1.158 becomes

$$\lambda^2 - 10.22389\lambda + 13.86234 = 0$$

The solution of this equation gives

$$\lambda_1 = 8.61475, \quad \lambda_2 = 1.60914$$

If these values are converted to $\tilde{\nu}$ through Eq. 1.156, we obtain

$$\tilde{\nu}_1 = 3824 \text{ cm}^{-1}, \quad \tilde{\nu}_2 = 1653 \text{ cm}^{-1}$$

With the same set of force constants, the frequency of the B_2 vibration is calculated as

$$\begin{aligned}\lambda_3 &= G_{33}F_{33} = [\mu_1 + \mu_3(1 - \cos \alpha)] (f_{11} - f_{12}) \\ &= 9.13681 \\ \tilde{\nu}_3 &= 3938 \text{ cm}^{-1}\end{aligned}$$

The observed frequencies corrected for anharmonicity are as follows: $\omega_1 = 3825 \text{ cm}^{-1}$, $\omega_2 = 1654 \text{ cm}^{-1}$, and $\omega_3 = 3936 \text{ cm}^{-1}$.

If the secular equation is third order, it gives rise to a cubic equation:

$$\begin{aligned}\lambda^3 - (G_{11}F_{11} + G_{22}F_{22} + G_{33}F_{33} + 2G_{12}F_{12} + 2G_{13}F_{13} + 2G_{23}F_{23})\lambda^2 \\ + \left\{ \begin{vmatrix} G_{11} & G_{12} \\ G_{21} & G_{22} \end{vmatrix} \begin{vmatrix} F_{11} & F_{12} \\ F_{21} & F_{22} \end{vmatrix} + \begin{vmatrix} G_{12} & G_{13} \\ G_{22} & G_{23} \end{vmatrix} \begin{vmatrix} F_{12} & F_{13} \\ F_{22} & F_{23} \end{vmatrix} + \begin{vmatrix} G_{11} & G_{13} \\ G_{21} & G_{23} \end{vmatrix} \begin{vmatrix} F_{11} & F_{13} \\ F_{21} & F_{23} \end{vmatrix} \right. \\ + \begin{vmatrix} G_{11} & G_{12} \\ G_{31} & G_{32} \end{vmatrix} \begin{vmatrix} F_{11} & F_{12} \\ F_{31} & F_{32} \end{vmatrix} + \begin{vmatrix} G_{12} & G_{13} \\ G_{32} & G_{33} \end{vmatrix} \begin{vmatrix} F_{12} & F_{13} \\ F_{32} & F_{33} \end{vmatrix} \\ + \begin{vmatrix} G_{11} & G_{13} \\ G_{31} & G_{33} \end{vmatrix} \begin{vmatrix} F_{11} & F_{13} \\ F_{31} & F_{33} \end{vmatrix} + \begin{vmatrix} G_{21} & G_{22} \\ G_{31} & G_{32} \end{vmatrix} \begin{vmatrix} F_{21} & F_{22} \\ F_{31} & F_{32} \end{vmatrix} + \begin{vmatrix} G_{22} & G_{23} \\ G_{32} & G_{33} \end{vmatrix} \begin{vmatrix} F_{22} & F_{23} \\ F_{32} & F_{33} \end{vmatrix} \\ \left. + \begin{vmatrix} G_{21} & G_{23} \\ G_{31} & G_{33} \end{vmatrix} \begin{vmatrix} F_{21} & F_{23} \\ F_{31} & F_{33} \end{vmatrix} \right\} \lambda - \begin{vmatrix} G_{11} & G_{12} & G_{13} \\ G_{21} & G_{22} & G_{23} \\ G_{31} & G_{32} & G_{33} \end{vmatrix} \begin{vmatrix} F_{11} & F_{12} & F_{13} \\ F_{21} & F_{23} & F_{33} \\ F_{31} & F_{32} & F_{33} \end{vmatrix} = 0 \quad (1.159)\end{aligned}$$

Thus, it is possible to solve the secular equation by expanding it into an algebraic equation. If the order of the secular equation is higher than three, however, direct expansion such as that just shown becomes too cumbersome. There are several methods of calculating the coefficients of an algebraic equation using indirect expansion [3]. The use of an electronic computer greatly reduces the burden of calculation. Excellent programs written by Schachtschneider [86] and other workers are available for the vibrational analysis of polyatomic molecules.

1.16. VIBRATIONAL FREQUENCIES OF ISOTOPIC MOLECULES

As stated in Sec. 1.14, the vibrational frequencies of isotopic molecules are very useful in refining a set of force constants in vibrational analysis. For large molecules, isotopic substitution is indispensable in making band assignments, since only vibrations involving the motion of the isotopic atom will be shifted by isotopic substitution.

Two important rules hold for the vibrational frequencies of isotopic molecules. The first, called the *product rule*, can be derived as follows.

Let $\lambda_1, \lambda_2, \dots, \lambda_n$ be the roots of the secular equation $|\mathbf{G}\mathbf{F} - \mathbf{E}\lambda| = 0$. Then

$$\lambda_1 \lambda_2 \cdots \lambda_n = |\mathbf{G}||\mathbf{F}| \quad (1.160)$$

holds for a given molecule. Since the isotopic molecule has exactly the same $|\mathbf{F}|$ as that in Eq. 1.160, a similar relation

$$\lambda'_1 \lambda'_2 \cdots \lambda'_n = |\mathbf{G}'| |\mathbf{F}|$$

holds for this molecule. It follows that

$$\frac{\lambda_1 \lambda_2 \cdots \lambda_n}{\lambda'_1 \lambda'_2 \cdots \lambda'_n} = \frac{|\mathbf{G}|}{|\mathbf{G}'|} \quad (1.161)$$

Since

$$\tilde{\nu} = \frac{1}{2\pi c} \sqrt{\lambda}$$

Equation 1.161 can be written as

$$\frac{\tilde{\nu}_1 \tilde{\nu}_2 \cdots \tilde{\nu}_n}{\tilde{\nu}'_1 \tilde{\nu}'_2 \cdots \tilde{\nu}'_n} = \sqrt{\frac{|\mathbf{G}|}{|\mathbf{G}'|}} \quad (1.162)$$

This rule has been confirmed by using pairs of molecules such as H_2O and D_2O and CH_4 and CD_4 . The rule is also applicable to the product of vibrational frequencies belonging to a single symmetry species.

A more general form of Eq. 1.162 is given by the *Redlich-Teller product rule* [1]:

$$\frac{\tilde{\nu}_1 \tilde{\nu}_2 \cdots \tilde{\nu}_n}{\tilde{\nu}'_1 \tilde{\nu}'_2 \cdots \tilde{\nu}'_n} = \sqrt{\left(\frac{m'_1}{m_1}\right)^\alpha \left(\frac{m'_2}{m_2}\right)^\beta \cdots \left(\frac{M}{M'}\right)^t \left(\frac{I_x}{I'_x}\right)^{\delta_x} \left(\frac{I_y}{I'_y}\right)^{\delta_y} \left(\frac{I_z}{I'_z}\right)^{\delta_z}} \quad (1.163)$$

Here m_1, m_2, \dots are the masses of the representative atoms of the various sets of equivalent nuclei (atoms represented by m, m_0, m_{xy}, \dots in the tables given in Appendix III); α, β, \dots are the coefficients of m, m_0, m_{xy}, \dots ; M is the total mass of the molecule; t is the number of T_x, T_y, T_z in the symmetry type considered; I_x, I_y, I_z are the moments of inertia about the x, y, z axes, respectively, which go through the center of the mass; and $\delta_x, \delta_y, \delta_z$ are 1 to 0, depending on whether R_x, R_y, R_z belong to the symmetry type considered. A degenerate vibration is counted only once on both sides of the equation.

Another useful rule in regard to the vibrational frequencies of isotopic molecules, called the *sum rule*, can be derived as follows. It is obvious from Eqs. 1.158 and 1.159 that

$$\lambda_1 + \lambda_2 + \cdots + \lambda_n = \sum_n \lambda = \sum_{i,j} G_{ij} F_{ij} \quad (1.164)$$

Let σ_k denote $\sum_{ij} G_{ij} F_{ij}$ for k different isotopic molecules, all of which have the same \mathbf{F} matrix. If a suitable combination of molecules is taken, so that

$$\begin{aligned}\sigma_1 + \sigma_2 + \cdots + \sigma_k &= \left(\sum G_{ij} F_{ij} \right)_1 + \left(\sum G_{ij} F_{ij} \right)_2 + \cdots + \left(\sum G_{ij} F_{ij} \right)_k \\ &= \left[\left(\sum G_{ij} \right)_1 + \left(\sum G_{ij} \right)_2 + \cdots + \left(\sum G_{ij} \right)_k \right] \left(\sum F_{ij} \right) \\ &= 0\end{aligned}$$

then it follows that

$$\left(\sum \lambda \right)_1 + \left(\sum \lambda \right)_2 + \cdots + \left(\sum \lambda \right)_k = 0 \quad (1.165)$$

This rule has been verified for such combinations as H_2O , D_2O , and HDO , where

$$2\sigma(\text{HDO}) - \sigma(\text{H}_2\text{O}) - \sigma(\text{D}_2\text{O}) = 0$$

Such relations between the frequencies of isotopic molecules are highly useful in making band assignments.

1.17. METAL-ISOTOPE SPECTROSCOPY [87,88]

As a first approximation, vibrational spectra of coordination compounds (Chapter 3, in Part B) can be classified into ligand vibrations that occur in the high-frequency region ($4000\text{--}600\text{ cm}^{-1}$) and metal-ligand vibrations that appear in the low-frequency region (below 600 cm^{-1}). The former provide information about the effect of coordination on the electronic structure of the ligand, while the latter provide direct information about the structure of the coordination sphere and the nature of the metal-ligand bond. Since the main interest of coordination chemistry is the coordinate bond, it is the metal-ligand vibrations that have held the interest of inorganic vibrational spectroscopists. It is difficult, however, to make unequivocal assignments of metal-ligand vibrations since the interpretation of the low-frequency spectrum is complicated by the appearance of ligand vibrations as well as lattice vibrations in the case of solid-state spectra.

Conventional methods that have been used to assign metal-ligand vibrations are

- (1) Comparison of spectra between a free ligand and its metal complex; the metal-ligand vibration should be absent in the spectrum of the free ligand. This method often fails to give a clear-cut assignment because some ligand vibrations activated by complex formation may appear in the same region as the metal-ligand vibrations.

- (2) The metal–ligand vibration should be metal sensitive and be shifted by changing the metal or its oxidation state. This method is applicable only when a series of metal complexes have exactly the same structure, where only the central metal is different. Also, it does not provide definitive assignments since some ligand vibrations (such as chelate ring deformations) are also metal-sensitive.
- (3) The metal–ligand stretching vibration should appear in the same frequency region if the metal is the same and the ligands are similar. For example, the $\nu(\text{Zn-N})$ (ν : stretching) of Zn(II) pyridine complexes are expected to be similar to those of Zn(II) α -picoline complexes. This method is applicable only when the metal–ligand vibration is known for one parent compound.
- (4) The metal–ligand vibration exhibits an isotope shift if the ligand is isotopically substituted. For example, the $\nu(\text{Ni-N})$ of $[\text{Ni}(\text{NH}_3)_6]\text{Cl}_2$ at 334 cm^{-1} is shifted to 318 cm^{-1} on deuteration of the ammonia ligands. The observed shift (16 cm^{-1}) is in good agreement with that predicted theoretically for this mode. This method was used to assign the metal–ligand vibrations of chelate compounds such as oxamido ($^{14}\text{N}/^{15}\text{N}$) and acetylacetonato($^{16}\text{O}/^{18}\text{O}$) complexes. However, isotopic substitution of the α -atom (atom directly bonded to the metal) causes shifts of not only metal–ligand vibrations but also of ligand vibrations involving the motion of the α -atom. Thus, this method alone cannot provide an unequivocal assignment of the metal–ligand vibration.
- (5) The frequency of a metal–ligand vibration may be predicted if the metal–ligand stretching and other force constants are known *a priori*. At present, this method is not practical since only a limited amount of information is available on the force constants of coordination compounds.

It is obvious that none of the above methods is perfect in assigning metal–ligand vibrations. Furthermore, these methods encounter more difficulties as the structure of the complex (and hence the spectrum) becomes more complicated. Fortunately, the “metal isotope technique” which was developed in 1969 may be used to obtain reliable metal–ligand assignments [89]. Isotope pairs such as (H/D) and ($^{16}\text{O}/^{18}\text{O}$) had been used routinely by many spectroscopists. However, isotopic pairs of heavy metals such as ($^{58}\text{Ni}/^{62}\text{Ni}$) and ($^{104}\text{Pd}/^{110}\text{Pd}$) were not employed until 1969 when the first report on the assignments of the Ni–P vibrations of *trans*-Ni(PEt₃)₂X₂ (X = Cl and Br) was made. The delay in their use was probably due to two reasons:

- (1) It was thought that the magnitude of isotope shifts arising from metal isotope substitution might be too small to be of practical value.
- (2) Pure metal isotopes were too expensive to use routinely in the laboratory. Nakamoto and coworkers [87,88] have shown, however, that the magnitudes of metal isotope shifts are generally of the order of $2\text{--}10\text{ cm}^{-1}$ for stretching modes and $0\text{--}2\text{ cm}^{-1}$ for bending modes, and that the experimental error in measuring the frequency could be as small as $\pm 0.2\text{ cm}^{-1}$ if proper precautions

are taken. They have also shown that this technique is financially feasible if the compounds are prepared on a milligram scale. Normally, the vibrational spectrum of a compound can be obtained with a sample less than 10 mg. Table 1.14 lists metal isotopes that are useful for vibrational studies of coordination compounds.

TABLE 1.14. Some Stable Metal Isotopes^a

Element	Inventory Form	Isotope	Natural Abundance (%)	Purity (%)
Magnesium	Oxide	Mg-24	78.99	99.9
		Mg-25	10.00	94
		Mg-26	11.01	97
Silicon	Oxide	Si-28	92.23	>99.8
		Si-30	3.10	>94
Titanium	Oxide	Ti-46	8.0	70–96
		Ti-48	73.8	>99
Chromium	Oxide	Cr-50	4.345	>95
		Cr-52	83.79	>99.7
		Cr-53	9.50	>96
Iron	Oxide	Fe-54	5.9	>96
		Fe-56	91.72	>99.9
		Fe-57	2.1	86–93
Nickel	Metal	Ni-58	68.27	>99.9
	Oxide	Ni-60	26.1	>99
	Oxide	Ni-62	3.59	>96
Copper	Oxide	Cu-63	69.17	>99.8
		Cu-65	30.83	>99.6
Zinc	Oxide	Zn-64	48.6	>99.8
		Zn-66	27.9	>98
		Zn-68	18.8	97–99
Germanium	Oxide	Ge-72	27.4	>97
		Ge-74	36.5	>98
Zirconium	Oxide	Zr-90	51.45	97–99
		Zr-94	17.38	>98
Molybdenum	Metal/oxide	Mo-92	14.84	>97
		Mo-95	15.92	>96
		Mo-97	9.55	>92
		Mo-100	9.63	>97
Ruthenium	Metal	Ru-99	12.7	>98
		Ru-102	31.6	>99
Palladium	Metal	Pd-104	11.4	>95
		Pd-108	26.46	>98
Tin	Oxide	Sn-116	14.53	>95
		Sn-120	32.59	>98
		Sn-124	5.79	>94
Barium	Carbonate	Ba-135	6.593	>93
		Ba-138	71.70	>99

^aAvailable at Oak Ridge National Laboratory.

It should be noted that the central atom of a highly symmetrical molecule (\mathbf{T}_d , \mathbf{O}_h , etc.) does not move during the totally symmetric vibration. Thus, no metal–isotope shifts are expected in these cases [90]. When the central atom is coordinated by several different donor atoms, multiple isotope labeling is necessary to distinguish different coordinate bond-stretching vibrations. For example, complete assignments of bis (glycino)nickel(II) require $^{14}\text{N}/^{15}\text{N}$ and/or $^{16}\text{O}/^{18}\text{O}$ isotope shift data as well as $^{58}\text{Ni}/^{62}\text{Ni}$ isotope shift data [91]. This book contains many other applications of metal–isotope techniques. These results show that metal–isotope data are indispensable not only in assigning the metal–ligand vibrations but also in refining metal–ligand stretching force constants in normal coordinate analysis [88]. The presence of vibrational coupling between metal–ligand and other vibrations can also be detected by combining metal–isotope data with normal coordinate calculations (Sec. 1.18) since both experimental and theoretical isotope shift values would be smaller when such couplings occur.

The metal–isotope techniques become more important as the molecules become larger and complex. In biological molecules such as heme proteins, structural and bonding information about the active site (iron porphyrin) can be obtained through definitive assignments of coordinate bond-stretching vibrations around the iron atom. Using resonance Raman techniques (Sec. 1.22), it is possible to observe iron porphyrin and iron-axial ligand vibrations without interference from peptide chain vibrations. Thus, these vibrations can be assigned by comparing resonance Raman spectra of a natural heme protein with that of a ^{54}Fe -reconstituted heme protein. Chapter 5 (in Part B) includes several examples of applications of metal-isotope techniques to bioinorganic compounds [hemoglobin (^{54}Fe , ^{57}Fe), oxy-hemocyanin (^{63}Cu , ^{65}Cu), etc.]. An example of a multiple labeling is seen in the case of cytochrome P450_{cam} having the axial Fe–S linkage in addition to four Fe–N (porphyrin) bonds; Champion et al. [92] were able to assign its Fe–S stretching vibration (351 cm^{-1}) by combining ^{32}S – ^{34}S and ^{54}Fe – ^{56}Fe isotope shift data.

1.18. GROUP FREQUENCIES AND BAND ASSIGNMENTS

From observation of the infrared spectra of a number of compounds having a common group of atoms, it is found that, regardless of the rest of the molecule, this common group absorbs over a narrow range of frequencies, called the *group frequency*. For example, the methyl group exhibits the antisymmetric stretching [$\nu_a(\text{CH}_3)$], symmetric stretching [$\nu_s(\text{CH}_3)$], degenerate bending [$\delta_d(\text{CH}_3)$], symmetric bending [$\delta_s(\text{CH}_3)$], and rocking [$\rho_s(\text{CH}_3)$] vibrations in the ranges 3050–2950, 2970–2860, 1480–1410, 1385–1250, and 1200–800 cm^{-1} , respectively. Figure 1.25 illustrates their vibrational modes together with the observed frequencies for CH_3Cl . The methylene group vibrations are also well known; the antisymmetric stretching [$\nu_a(\text{CH}_2)$], symmetric stretching [$\nu_s(\text{CH}_2)$], scissoring [$\delta(\text{CH}_2)$], wagging [$\rho_w(\text{CH}_2)$], twisting [$\rho_r(\text{CH}_2)$], and rocking [$\rho_r(\text{CH}_2)$] vibrations appear

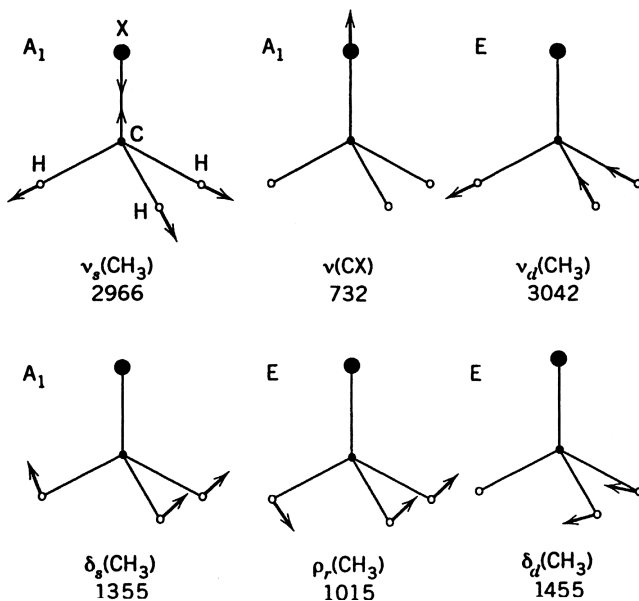


Fig. 1.25. Approximate normal modes of a CH_3X -type molecule (frequencies are given for $\text{X}=\text{Cl}$). The subscripts *s*, *d*, and *r* denote symmetric, degenerate, and rocking vibrations, respectively. Only the displacements of the H or X atoms are shown.

in the regions 3100–3000, 3060–2980, 1500–1350, 1400–1100, 1260–1030, and 1180–750 cm^{-1} , respectively. Figure 1.26 illustrates the normal modes of these vibrations together with the observed frequencies for CH_2Cl_2 . The normal modes illustrated for CH_3Cl and CH_2Cl_2 are applicable to vibrational assignments of coordination and organometallic compounds, which will be discussed in Chapters 3 and 4, respectively. Group frequencies have been found for a number of organic and inorganic groups, and they have been summarized as *group frequency charts* [39,40] which are highly useful in identifying the atomic groups from observed spectra. Group frequency charts for inorganic compounds are given in Appendix VIII as well as in Figs. 2.55 and 2.61.

The concept of group frequency rests on the assumption that the vibrations of a particular group are relatively independent of those of the rest of the molecule. As stated in Sec. 1.4, however, all the nuclei of the molecule perform their harmonic oscillations in a normal vibration. Thus, an *isolated vibration*, which the group frequency would have to be, cannot be expected in polyatomic molecules. If, however, a group includes relatively light atoms such as hydrogen (OH, NH, NH_2 , CH, CH_2 , CH_3 , etc.) or relatively heavy atoms such as the halogens (CCl, CBr, Cl, etc.), as compared to other atoms in the molecule, the idea of an isolated vibration may be justified, since the amplitudes (or velocities) of the harmonic oscillation of these atoms are relatively larger or smaller than those of the other atoms in the same molecule. Vibrations of groups having multiple bonds ($\text{C}\equiv\text{C}$, $\text{C}\equiv\text{N}$, $\text{C}=\text{C}$, $\text{C}=\text{N}$, $\text{C}=\text{O}$, etc.) may

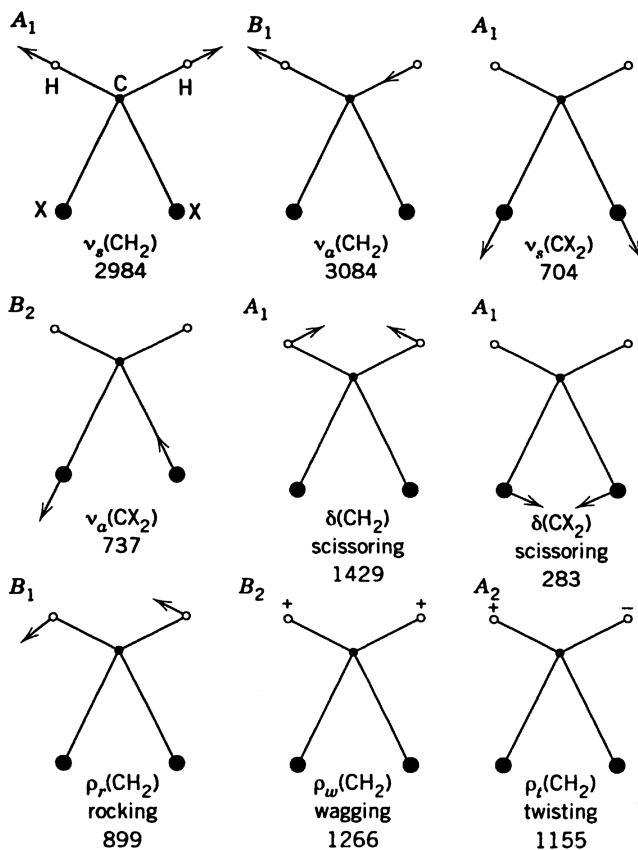
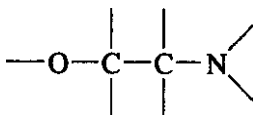


Fig. 1.26. Approximate normal modes of a CH_2X_2 -type molecule (frequencies are given for $\text{X}=\text{Cl}$). Only the displacements of the H or X atoms are shown.

also be relatively independent of the rest of the molecule if the groups do not belong to a conjugated system.

If atoms of similar mass are connected by bonds of similar strength (force constant), the amplitude of oscillation is similar for each atom of the whole system. Therefore, it is not possible to isolate the group frequencies in a system like the following:



A similar situation may occur in a system in which resonance effects average out the single and multiple bonds by conjugation. Examples of this effect are seen for

the metal chelate compounds discussed in Chapter 3. When the group frequency approximation is permissible, the mode of vibration corresponding to this frequency can be inferred empirically from the band assignments obtained theoretically for simple molecules. If *coupling* between various group vibrations is serious, it is necessary to make a theoretical analysis for each individual compound, using a method like the following one.

As stated in Sec. 1.4, the generalized coordinates are related to the normal coordinates by

$$q_k = \sum_i B_{ki} Q_i \quad (1.40)$$

In matrix form, this is written as

$$\mathbf{q} = \mathbf{B}_q \mathbf{Q} \quad (1.166)$$

It can be shown [3] that the internal coordinates are also related to the normal coordinates by

$$\mathbf{R} = \mathbf{LQ} \quad (1.167)$$

This is written more explicitly as

$$\begin{aligned} R_1 &= l_{11}Q_1 + l_{12}Q_2 + \cdots + l_{1N}Q_N \\ R_2 &= l_{21}Q_1 + l_{22}Q_2 + \cdots + l_{2N}Q_N \\ &\vdots \qquad \qquad \qquad \vdots \\ R_i &= l_{i1}Q_1 + l_{i2}Q_2 + \cdots + l_{iN}Q_N \end{aligned} \quad (1.168)$$

In a normal vibration in which the normal coordinate Q_N changes with frequency ν_N , all the internal coordinates, R_1, R_2, \dots, R_i , change with the same frequency. The amplitude of oscillation is, however, different for each internal coordinate. The relative ratio of the amplitudes of the internal coordinates in a normal vibration associated with Q_N is given by

$$l_{1N} : l_{2N} : \cdots : l_{iN} \quad (1.169)$$

If one of these elements is relatively large compared to the others, the normal vibration is said to be predominantly due to the vibration caused by the change of this coordinate.

The ratio of l 's given by Eq. 1.169 can be obtained as a column matrix (or eigenvector) l_N , which satisfies the relation [3]

$$\mathbf{G}\mathbf{F}l_N = l_N\lambda_N \quad (1.170)$$

It consists of i elements, $l_{1N}, l_{2N}, \dots, l_{iN}$, where i is the number of internal coordinates, and can be calculated if the \mathbf{G} and \mathbf{F} matrices are known. An assembly by columns of the l elements obtained for each λ gives the relation

$$\mathbf{G}\mathbf{F}\mathbf{L} = \mathbf{L}\mathbf{\Lambda} \quad (1.171)$$

where $\mathbf{\Lambda}$ is a diagonal matrix whose elements consist of λ values.

As an example, calculate the \mathbf{L} matrix of the H_2O molecule, using the results obtained in Sec. 1.15. The \mathbf{G} and \mathbf{F} matrices for the A_1 species are as follows:

$$\mathbf{G} = \begin{bmatrix} 1.03840 & -0.08896 \\ -0.08896 & 2.32370 \end{bmatrix}, \quad \mathbf{F} = \begin{bmatrix} 8.32300 & 0.35638 \\ 0.35638 & 0.70779 \end{bmatrix}$$

with $\lambda_1 = 8.61475$ and $\lambda_2 = 1.60914$. The $\mathbf{G}\mathbf{F}$ product becomes

$$\mathbf{G}\mathbf{F} = \begin{bmatrix} 8.61090 & 0.30710 \\ 0.08771 & 1.61299 \end{bmatrix}$$

The \mathbf{L} matrix can be calculated from Eq. 1.171:

$$\begin{bmatrix} 8.61090 & 0.30710 \\ 0.08771 & 1.61299 \end{bmatrix} \begin{bmatrix} l_{11} & l_{12} \\ l_{21} & l_{22} \end{bmatrix} = \begin{bmatrix} l_{11} & l_{12} \\ l_{21} & l_{22} \end{bmatrix} \begin{bmatrix} 8.61475 & 0 \\ 0 & 1.60914 \end{bmatrix}$$

However, this equation gives only the ratios $l_{11}:l_{21}$ and $l_{12}:l_{22}$. To determine their values, it is necessary to use the following normalization condition:

$$\mathbf{L}\tilde{\mathbf{L}} = \mathbf{G} \quad (1.172)^*$$

Then the final result is

$$\begin{bmatrix} l_{11} & l_{12} \\ l_{21} & l_{22} \end{bmatrix} = \begin{bmatrix} 1.01683 & -0.06686 \\ 0.01274 & 1.52432 \end{bmatrix}$$

*This equation can be derived as follows. According to Eq. 1.113, $2T = \tilde{\mathbf{R}}\mathbf{G}^{-1}\dot{\mathbf{R}}$. On the other hand, Eq. 1.167 gives $\dot{\mathbf{R}} = \mathbf{L}\dot{\mathbf{Q}}$ and $\tilde{\mathbf{R}} = \dot{\mathbf{Q}}\tilde{\mathbf{L}}$. Thus $2T = \dot{\mathbf{Q}}\tilde{\mathbf{L}}\mathbf{G}^{-1}\mathbf{L}\dot{\mathbf{Q}}$. Comparing this with $2T = \dot{\mathbf{Q}}\mathbf{E}\dot{\mathbf{Q}}$ (matrix form of Eq. 1.41), we obtain $\tilde{\mathbf{L}}\mathbf{G}^{-1}\mathbf{L} = \mathbf{E}$ or $\mathbf{L}\tilde{\mathbf{L}} = \mathbf{G}$.

This result indicates that, in the normal vibration Q_1 , the relative ratio of amplitudes of two internal coordinates, R_1 (symmetric OH stretching) and R_2 (HOH bending), is 1.0168: 0.0127. Therefore, this vibration (3824 cm^{-1}) is assigned to an almost pure OH stretching mode. The relative ratio of amplitudes for the Q_2 vibration is -0.0669 : 1.5243. Thus, this vibration is assigned to an almost pure HOH bending mode. In other cases, the l values do not provide the band assignments that are expected empirically. This occurs because the dimension of l for a stretching coordinate is different from that for a bending coordinate.

The potential energy due to a normal vibration, Q_N is written as

$$V(Q_N) = \frac{1}{2} Q_N^2 \sum_{ij} F_{ij} l_{iN} l_{jN} \quad (1.173)^*$$

Individual $F_{ij} l_{iN} l_{jN}$ terms in the summation represent the potential energy distribution (PED) in Q_N , which gives a better measure for making band assignments [93]. In general, the value of $F_{ij} l_{iN} l_{jN}$ is large when $i = j$. Therefore, the $F_{ii} l_{iN}^2$ terms are most important in determining the distribution of the potential energy. Thus, the ratios of the $F_{ii} l_{iN}^2$ terms provide a measure of the relative contribution of each internal coordinate R_i to the normal coordinate Q_N . If any $F_{ii} l_{iN}^2$ term is exceedingly large compared with the others, the vibration is assigned to the mode associated with R_i . If $F_{ii} l_{iN}^2$ and $F_{jj} l_{jN}^2$ are relatively large compared with the others, the vibration is assigned to a mode associated with both R_i and R_j (coupled vibration).

As an example, let us calculate the potential energy distribution for the H_2O molecule. Using the \mathbf{F} and \mathbf{L} matrices obtained previously, we find that the $\tilde{\mathbf{L}}\mathbf{F}\mathbf{L}$ matrix is calculated to be

$$\begin{bmatrix} \left(\begin{array}{ccc} l_{11}^2 F_{11} & + & l_{21}^2 F_{22} & + & 2l_{21} l_{11} F_{12} \\ 8.60551 & & 0.00011 & & 0.00923 \end{array} \right) & 0 \\ 0 & \left(\begin{array}{ccc} l_{12}^2 F_{11} & + & l_{22}^2 F_{22} & + & 2l_{12} l_{22} F_{12} \\ 0.03721 & & 1.644459 & & 0.07264 \end{array} \right) \end{bmatrix}$$

Then, the potential energy distribution in each normal vibration ($F_{ii} l_{iN}^2$) is given by

$$\begin{array}{cc} \lambda_1 & \lambda_2 \\ R_1 & \begin{bmatrix} 8.60551 & 0.03721 \\ 0.00011 & 1.64459 \end{bmatrix} \\ R_2 & \end{array}$$

* According to Eq. 1.111, the potential energy is written as $2V = \tilde{\mathbf{R}}\mathbf{F}\mathbf{R}$. Using Eq. 1.167, we can write this as $2V = \tilde{\mathbf{Q}}\tilde{\mathbf{L}}\mathbf{F}\mathbf{L}\mathbf{Q}$. On the other hand, Eq. 1.42 can be written as $2V = \mathbf{Q}\mathbf{\Lambda}\mathbf{Q}$. A comparison of these two expressions gives $\mathbf{\Lambda} = \tilde{\mathbf{L}}\mathbf{F}\mathbf{L}$. If this is written for one normal vibration whose frequency is λ_N , we have

$$\lambda_N = \sum_{ij} l_{Ni} F_{ij} l_{jN} = \sum_{ij} F_{ij} l_{iN} l_{jN}$$

Then the potential energy due to this vibration is expressed by Eq. 1.173.

More conveniently, PED is expressed by calculating $(F_{ii}l_{iN}^2/\Sigma F_{ii}l_{iN}^2) \times 100$ for each coordinate:

$$\begin{array}{cc} \lambda_1 & \lambda_2 \\ R_1 & \begin{bmatrix} 99.99 & 2.21 \\ 0.01 & 97.79 \end{bmatrix} \\ R_2 & \end{array}$$

In this case, the final results are the same whether the band assignments are based on the \mathbf{L} matrix or on the potential energy distribution: Q_1 is the symmetric OH stretching and Q_2 is the HOH bending. In other cases, different results may be obtained, depending on which criterion is used for band assignments.

In the example above, no serious coupling occurs between the OH stretching and HOH bending modes of H_2O in the A_1 species. This is because the vibrational frequencies of these two modes are far apart. In other cases, however, vibrational frequencies of two or more modes in the same symmetry species are relatively close to each other. Then, the l_{iN} values for these modes become comparable.

A more rigorous method of determining the vibrational mode involves drawing the displacements of individual atoms in terms of rectangular coordinates. As in Eq. 1.167, the relationship between the rectangular and normal coordinates is given by

$$\mathbf{X} = \mathbf{L}_x \mathbf{Q} \quad (1.174)$$

The \mathbf{L}_x matrix can be obtained from the relationship [94]

$$\mathbf{L}_x = \mathbf{M}^{-1} \tilde{\mathbf{B}} \mathbf{G}^{-1} \mathbf{L} \quad (1.75)^*$$

The matrices on the right-hand sides have already been defined.

Three-dimensional drawings of normal modes, such as those shown in Chapter 2, can be made from the Cartesian displacement calculations obtained above. However, hand plotting of these data is laborious and complicated. Use of computer plotting programs greatly facilitates this process [95].

1.19. INTENSITY OF INFRARED ABSORPTION [16]

The absorption of strictly monochromatic light (ν) is expressed by the Lambert–Beer law:

$$I_\nu = I_{0,\nu} e^{-\alpha_\nu p l} \quad (1.176)$$

*By combining Eqs. 1.118 and 1.174, we have $\mathbf{R} = \mathbf{B}\mathbf{X} = \mathbf{B}\mathbf{L}_x \mathbf{Q}$. Since $\mathbf{R} = \mathbf{L}\mathbf{Q}$ (Eq. 1.167), it follows that $\mathbf{L}\mathbf{Q} = \mathbf{B}\mathbf{L}_x \mathbf{Q}$ or $\mathbf{L}_x = \mathbf{B}\mathbf{L}_x$. The kinetic energy is written as $2T = \dot{\mathbf{X}}\mathbf{M}\dot{\mathbf{X}}$. In terms of internal coordinates, it is written as $2T = \dot{\mathbf{R}}\mathbf{G}^{-1}\dot{\mathbf{R}} = \dot{\mathbf{X}}\tilde{\mathbf{B}}\mathbf{G}^{-1}\dot{\mathbf{B}}\dot{\mathbf{X}}$. By comparing these two expressions, we have $\mathbf{M} = \tilde{\mathbf{B}}\mathbf{G}^{-1}\mathbf{B}$. Then we can write $\mathbf{L}_x = \mathbf{M}^{-1}\mathbf{M}\mathbf{L}_x = \mathbf{M}^{-1}\tilde{\mathbf{B}}\mathbf{G}^{-1}\mathbf{B}\mathbf{L}_x = \mathbf{M}^{-1}\tilde{\mathbf{B}}\mathbf{G}^{-1}\mathbf{L}$.

where I_v is the intensity of the light transmitted by a cell of length l containing a gas at pressure p , $I_{0,v}$ is the intensity of the incident light, and α_v is the absorption coefficient for unit pressure. The true integrated absorption coefficient A is defined by

$$A = \int_{\text{band}} \alpha_v dv = \frac{1}{pl} \int_{\text{band}} \ln \left(\frac{I_{0,v}}{I_v} \right) dv \quad (1.177)$$

where the integration is carried over the entire frequency region of a band.

In practice, I_v and $I_{0,v}$ cannot be measured accurately, since no spectrophotometers have infinite resolving power. Therefore we measure instead the apparent intensity T_v :

$$T_v = \int_{\text{slit}} I(v)g(v, v')dv \quad (1.178)$$

where $g(v, v')$ is a function indicating the amount of light of frequency v when the spectrophotometer reading is set at v' . Then the apparent integrated absorption coefficient B is defined by

$$B = \frac{1}{pl} \int_{\text{band}} \ln \frac{\int_{\text{slit}} I_0(v)g(v, v')dv}{\int_{\text{slit}} I(v)g(v, v')dv} dv' \quad (1.179)$$

It can be shown that

$$\lim_{pl \rightarrow 0} (A - B) = 0 \quad (1.180)$$

if I_0 and α_v are constant within the slit width used. (This condition is approximated by using a narrow slit.) In practice, we plot B/pl against pl , and extrapolate the curve to $pl \rightarrow 0$. To apply this method to gaseous molecules, it is necessary to broaden the vibrational-rotational bands by adding a high-pressure inert gas (pressure broadening).

For liquids and solutions, p and α in the preceding equations are replaced by M (molar concentration) and ε (molar absorption coefficient), respectively. However, the extrapolation method just described is not applicable, since experimental errors in determining B values become too large at low concentration or at small cell length. The true integrated absorption coefficient of a liquid can be calculated if we assume that the shape of an absorption band is represented by the Lorentz equation and that the slit function is triangular [96].

Theoretically, the true integrated absorption coefficient A_N of the N th normal vibration is given by [3]

$$A_N = \frac{n\pi}{3c} \left[\left(\frac{\partial \mu_x}{\partial Q_N} \right)_0^2 + \left(\frac{\partial \mu_y}{\partial Q_N} \right)_0^2 + \left(\frac{\partial \mu_z}{\partial Q_N} \right)_0^2 \right] \quad (1.181)$$

where n is the number of molecules per cubic centimeter, and c is the velocity of light. As shown by Eq. 1.167, an internal coordinate R_i is related to a set of normal

coordinates by

$$R_i = \sum_N L_{iN} Q_N \quad (1.182)$$

If the additivity of the bond dipole moment is assumed, it is possible to write

$$\begin{aligned} \frac{\partial \mu}{\partial Q_N} &= \sum_i \left(\frac{\partial \mu}{\partial R_i} \right) \left(\frac{\partial R_i}{\partial Q_N} \right) \\ &= \sum_i \left(\frac{\partial \mu}{\partial R_i} \right) L_{iN} \end{aligned} \quad (1.183)$$

Then Eq. 1.181 is written as

$$\begin{aligned} A_N &= \frac{n\pi}{3c} \left[\left(\sum_i \frac{\partial \mu_x}{\partial R_i} L_{iN} \right)_0^2 + \left(\sum_i \frac{\partial \mu_y}{\partial R_i} L_{iN} \right)_0^2 + \left(\sum_i \frac{\partial \mu_z}{\partial R_i} L_{iN} \right)_0^2 \right] \\ &= \frac{n\pi}{3c} \sum_i \left[\left(\frac{\partial \mu_x}{\partial R_i} \right)_0^2 + \left(\frac{\partial \mu_y}{\partial R_i} \right)_0^2 + \left(\frac{\partial \mu_z}{\partial R_i} \right)_0^2 \right] (L_{iN})^2 \end{aligned} \quad (1.184)$$

This equation shows that the intensity of an infrared band depends on the values of the $\partial \mu / \partial R$ terms as well as the L matrix elements.

Equation 1.184 has been applied to relatively small molecules to calculate the $\partial \mu / \partial R$ terms from the observed intensity and known L_{iN} values [7]. However, the additivity of the bond dipole moment does not strictly hold, and the results obtained are often inconsistent and conflicting. Thus far, very few studies have been made on infrared intensities of large molecules because of these difficulties.

As seen in Eq. 1.184, the IR band becomes stronger as the $\partial \mu / \partial R$ term becomes larger if the L_{iN} term does not vary significantly. In general, the more polar the bond, the larger the $\partial \mu / \partial R$ term. Thus, the IR intensities of the stretching vibrations follow the general trends:

$$\begin{aligned} \nu(\text{OH}) &> \nu(\text{NH}) > \nu(\text{CH}) \\ \nu(\text{C=O}) &> \nu(\text{C=N}) > \nu(\text{C=C}) \end{aligned}$$

It is also noted that the antisymmetric stretching vibration is always stronger than the symmetric stretching vibration because the $\partial \mu / \partial R$ term is larger for the former than for the latter. This can be seen for functional groups such as >CH_2 and >CCl_2 . These trends are entirely opposite to those found in Raman spectra (Sec. 1.21), and make both IR and Raman spectroscopy complementary.

1.20. DEPOLARIZATION OF RAMAN LINES

As stated in Secs. 1.8 and 1.9, it is possible, by using group theory, to classify the normal vibration into various symmetry species. Experimentally, measurements of the

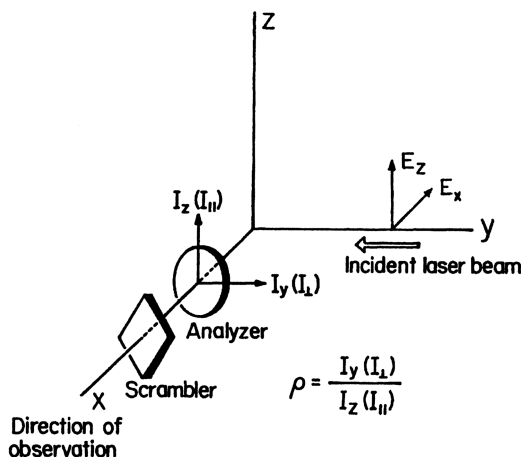


Fig. 1.27. Experimental configuration for measuring depolarization ratios. The scrambler is placed after the analyzer because the monochromator gratings show different efficiencies for \perp and \parallel directions.

infrared dichroism and polarization properties of Raman lines of an orientated crystal provide valuable information about the symmetry of normal vibrations (Sec. 1.31). Here, we consider the polarization properties of Raman lines in liquids and solutions in which molecules or ions take completely random orientations.*

Suppose that we irradiate a molecule fixed at the origin of a space-fixed coordinate system with natural light from the positive- y direction, and observe the Raman scattering in the x direction as shown in Fig. 1.27. The incident light vector E may be resolved into two components, E_x and E_z , of equal magnitude ($E_y = 0$). Both components give induced dipole moments, P_x , P_y , and P_z . However, only P_y and P_z contribute to the scattering along the x axis, since an oscillating dipole cannot radiate in its own direction. Then, from Eq. 1.66, we have.

$$P_y = \alpha_{yx}E_x + \alpha_{yz}E_z \quad (1.185)$$

$$P_z = \alpha_{zx}E_x + \alpha_{zz}E_z \quad (1.186)$$

The intensity of the scattered light is proportional to the sum of squares of the individual $\alpha_{ij}E_j$ terms. Thus, the ratio of the intensities in the y and z directions is

$$\rho_n = \frac{I_y}{I_z} = \frac{\alpha_{yx}^2 E_x^2 + \alpha_{yz}^2 E_z^2}{\alpha_{zx}^2 E_x^2 + \alpha_{zz}^2 E_z^2} \quad (1.187)$$

where ρ_n is called the *depolarization ratio for natural light* (n).

In a homogeneous liquid or gas, the molecules are randomly oriented, and we must consider the polarizability components averaged over all molecular

*It is possible to obtain approximate depolarization ratios of fine powders where the molecules or ions take pseudorandom orientations (see Ref. 97).

orientations. The results are expressed in terms of two quantities: $\bar{\alpha}$ (*mean value*) and γ (*anisotropy*):

$$\bar{\alpha} = \frac{1}{3}(\alpha_{xx} + \alpha_{yy} + \alpha_{zz}) \quad (1.188)$$

$$\gamma^2 = \frac{1}{2} [(\alpha_{xx} - \alpha_{yy})^2 + (\alpha_{yy} - \alpha_{zz})^2 + (\alpha_{zz} - \alpha_{xx})^2 + 6(\alpha_{xy}^2 + \alpha_{yz}^2 + \alpha_{zx}^2)] \quad (1.189)$$

These two quantities are invariant to any coordinate transformation. It can be shown [3] that the average values of the squares of α_{ij} are

$$\overline{(\alpha_{xx})^2} = \overline{(\alpha_{yy})^2} = \overline{(\alpha_{zz})^2} = \frac{1}{45} [45(\bar{\alpha})^2 + 4\gamma^2] \quad (1.190)$$

$$\overline{(\alpha_{xy})^2} = \overline{(\alpha_{yz})^2} = \overline{(\alpha_{zx})^2} = \frac{1}{15} \gamma^2 \quad (1.191)$$

Since $E_x = E_z = E$, Eq. 1.187 can be written as

$$\rho_n = \frac{I_y}{I_z} = \frac{6\gamma^2}{45(\bar{\alpha})^2 + 7\gamma^2} \quad (1.192)$$

The total intensity I_n is given by

$$I_n = I_y + I_z = \text{const} \left\{ \frac{1}{45} [45(\bar{\alpha})^2 + 13\gamma^2] \right\} E^2 \quad (1.193)$$

If the incident light is plane-polarized (e.g., a laser beam), with its electric vector in the z direction ($E_x = 0$), Eq. 1.192 becomes

$$\rho_p = \frac{I_y}{I_z} = \frac{3\gamma^2}{45(\bar{\alpha})^2 + 4\gamma^2} \quad (1.194)$$

where ρ_p is the *depolarization ratio for polarized light* (p). In this case, the total intensity is given by

$$I_p = I_y + I_z = \text{const} \left\{ \frac{1}{45} [45(\bar{\alpha})^2 + 7\gamma^2] \right\} E^2 \quad (1.195)$$

The symmetry property of a normal vibration can be determined by measuring the depolarization ratio. From an inspection of character tables (Appendix I), it is obvious that $\bar{\alpha}$ is nonzero only for totally symmetric vibrations. Then, Eq. 1.192 gives $0 \leq \rho_n < \frac{6}{7}$, and the Raman lines are said to be *polarized*. For all nontotally symmetric vibrations, $\bar{\alpha}$ is zero, and $\rho_n = \frac{6}{7}$. Then, the Raman lines are said to be *depolarized*. If the exciting line is plane polarized, these criteria must be changed according to

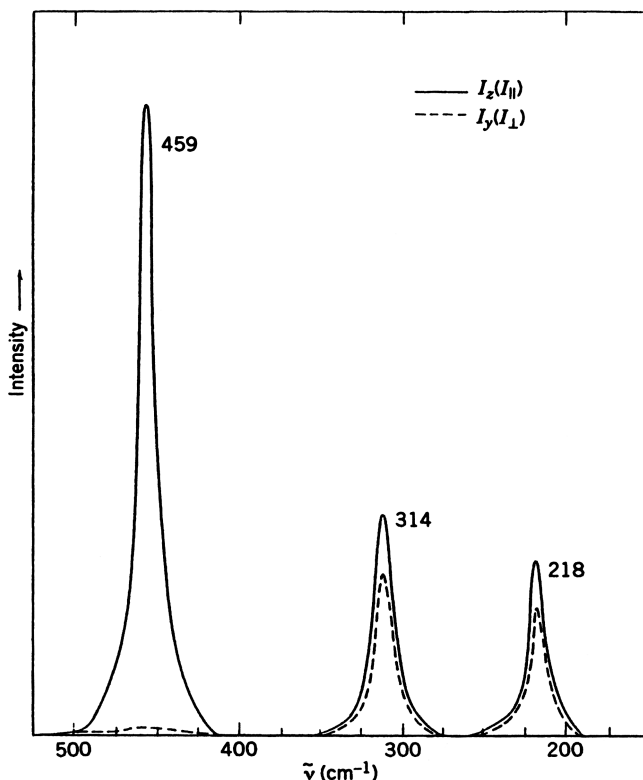


Fig. 1.28. Raman spectra of CCl_4 in two directions of polarization (488 nm excitation).

Eq. 1.194. Thus, $0 \leq \rho_p < \frac{3}{4}$ for totally symmetric vibrations, and $\rho_p = \frac{3}{4}$ for nontotally symmetric vibrations. Figure 1.28 shows the Raman spectra of CCl_4 ($500\text{--}150\text{ cm}^{-1}$) in two directions of polarization obtained with the 488 nm excitation. The three bands at 459 , 314 , and 218 cm^{-1} give ρ_p values of approximately 0.02, 0.75, and 0.75, respectively. Thus, it is concluded that the 459 cm^{-1} band is polarized (A_1), whereas the two bands at 314 (F_2) and 218 (E) cm^{-1} are depolarized.

As stated in Sec. 1.6, the polarizability tensors are symmetric in normal Raman scattering. If the exciting frequency approaches that of an electronic absorption, some scattering tensors become antisymmetric,* and resonance Raman scattering can occur (Sec. 1.22). In this case, Eq. 1.194 must be written in a more general form [98]

$$\rho_p = \frac{3g^s + 5g^a}{10g^o + 4g^s} \quad (1.196)$$

* A tensor is called antisymmetric if $\alpha_{xx} = \alpha_{yy} = \alpha_{zz} = 0$ and $\alpha_{xy} = -\alpha_{yx}$, $\alpha_{yz} = -\alpha_{zy}$, and $\alpha_{zx} = -\alpha_{xz}$.

where

$$\begin{aligned}
 g^o &= 3(\bar{\alpha})^2 \\
 g^s &= \frac{1}{3} \left[(\alpha_{xx} - \alpha_{yy})^2 + (\alpha_{yy} - \alpha_{zz})^2 + (\alpha_{zz} - \alpha_{xx})^2 \right] \\
 &\quad + \frac{1}{2} \left[(\alpha_{xy} + \alpha_{yx})^2 + (\alpha_{xz} + \alpha_{zx})^2 + (\alpha_{yz} + \alpha_{zy})^2 \right] \\
 g^a &= \frac{1}{2} \left[(\alpha_{xy} - \alpha_{yx})^2 + (\alpha_{xz} - \alpha_{zx})^2 + (\alpha_{yz} - \alpha_{zy})^2 \right]
 \end{aligned} \tag{1.197}$$

If we define

$$\gamma_s^2 = \frac{3}{2} g^s \quad \text{and} \quad \gamma_{as}^2 = \frac{3}{2} g^a \tag{1.198}$$

Eq. 1.196 can be written as

$$\rho_p = \frac{3\gamma_s^2 + 5\gamma_{as}^2}{45(\bar{\alpha})^2 + 4\gamma_s^2} \tag{1.199}$$

In normal Raman scattering, $\gamma_s^2 = \gamma^2$ and $\gamma_{as}^2 = 0$. Then Eq. 1.199 is reduced to Eq. 1.194.

The symmetry properties of resonance Raman lines can be predicted on the basis of Eq. 1.199. For totally symmetric vibrations, $\bar{\alpha} \neq 0$ and $\gamma_{as} = 0$. Then, Eq. 20.15 gives $0 \leq \rho_p < \frac{3}{4}$. Nontotally symmetric vibrations ($\bar{\alpha} = 0$) are classified into two types: those that have symmetric scattering tensors, and those that have antisymmetric scattering tensors. If the tensor is symmetric, $\gamma_{as} = 0$ and $\gamma_s \neq 0$. Then Eq. 1.199 gives $\rho_p = \frac{3}{4}$ (depolarized). If the tensor is antisymmetric, $\gamma_{as} \neq 0$ and $\gamma_s = 0$. Then, Eq. 1.199 gives $\rho_p = \infty$ (*inverse polarization*). In the case of the \mathbf{D}_{4h} point group, the B_{1g} and B_{2g} representations belong to the former type, whereas the A_{2g} representations belongs to the latter [99]. As will be shown in Sec. 1.22, Spiro and Strekas [98] observed for the first time A_{2g} vibrations which exhibit ρ_p values $\frac{3}{4} < \rho_p < \infty$. For these vibrations, the term “anomalous polarization (*ap*)” is used instead of “inverse polarization (*ip*)” [100].

1.21. INTENSITY OF RAMAN SCATTERING

According to the quantum mechanical theory of light scattering, the intensity per unit solid angle of scattered light arising from a transition between states m and n is given by

$$I_{n \leftarrow m} = \text{const} (v_0 \pm v_{mn})^4 \sum_{\rho\sigma} |(P_{\rho\sigma})_{mn}|^2 \tag{1.200}$$

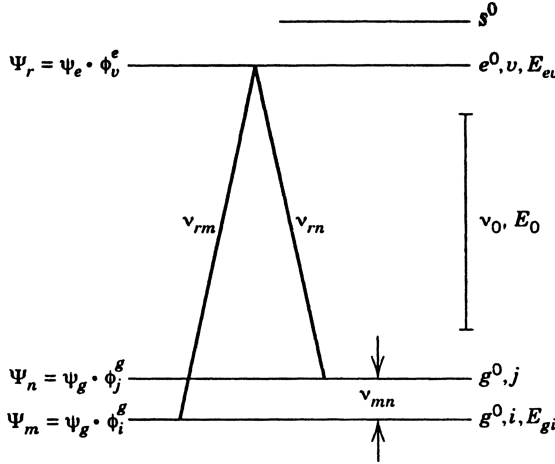


Fig. 1.29. Energy-level diagram for Raman scattering.

where

$$(P_{\rho\sigma})_{mn} = (\alpha_{\rho\sigma})_{mn} E = \frac{1}{h} \sum_r \left[\frac{(M_{\rho})_{rn} (M_{\sigma})_{mr}}{v_{rm} - v_0} + \frac{(M_{\rho})_{mr} (M_{\sigma})_{rn}}{v_{rm} + v_0} \right] E \quad (1.201)$$

Here v_0 is the frequency of the incident light: v_{rm} , v_{rn} , and v_{mn} are the frequencies corresponding to the energy differences between subscripted states; terms of the type $(M_{\sigma})_{mr}$ are the Cartesian components of transition moments such as $\int \Psi_r^* \mu_{\sigma} \Psi_m d\tau$; and E is the electric vector of the incident light. It should be noted here that the states denoted by m , n , and r represent vibronic states $\psi_g(\xi, Q) \phi_i^g(Q)$, $\psi_g(\xi, Q) \phi_j^g(Q)$ and $\psi_e(\xi, Q) \phi_v^e(Q)$, respectively, where ψ_g and ψ_e are electronic ground- and excited-state wavefunctions, respectively, and ϕ_i^g , ϕ_j^g , and ϕ_v^e vibrational functions. The symbols ξ and Q represent the electronic and nuclear coordinates, respectively. These notations are illustrated in Fig. 1.29. Finally, σ and ρ denote x , y , and z components.

Since the electric dipole operator acts only on the electronic wavefunctions, the $(\alpha_{\rho\sigma})_{mn}$ term in Eq. 1.201 can be written in the form

$$(\alpha_{\rho\sigma})_{mn} = \frac{1}{h} \int \phi_j^g (\alpha_{\rho\sigma})_{gs} \phi_i^g dQ \quad (1.202)$$

where

$$(\alpha_{\rho\sigma})_{gs} = \sum_e \left(\frac{\int \psi_g^* \mu_{\sigma} \psi_e d\tau \cdot \int \psi_e^* \mu_{\rho} \psi_g d\tau}{\bar{v}_{eg} - v_0} + \frac{\int \psi_g^* \mu_{\rho} \psi_e d\tau \cdot \int \psi_e^* \mu_{\sigma} \psi_g d\tau}{\bar{v}_{eg} + v_0} \right)$$

Here \bar{v}_{eg} corresponds to the energy of a pure electronic transition between the ground and excited states.

To discuss the Raman scattering, we expand the $(\alpha_{\rho\sigma})_{gg}$ term as a Taylor series with respect to the normal coordinate Q :

$$(\alpha_{\rho\sigma})_{gg} = (\alpha_{\rho\sigma})_{gg}^0 + \left[\frac{\partial(\alpha_{\rho\sigma})_{gg}}{\partial Q} \right]_0 Q + \dots \quad (1.203)$$

Then, we write Eq. 1.202 as

$$(\alpha_{\rho\sigma})_{mn} = \frac{1}{h} (\alpha_{\rho\sigma})_{gg}^0 \int \phi_j^g \phi_i^g dQ + \frac{1}{h} \left[\frac{\partial(\alpha_{\rho\sigma})_{gg}}{\partial Q} \right]_0 \int \phi_j^g Q \phi_i^g dQ \quad (1.204)$$

The first term on the right-hand side is zero unless $i=j$. This term is responsible for Rayleigh scattering. The second term determines the activity of fundamental vibrations in Raman scattering; it vanishes for a harmonic oscillator unless $j = i \pm 1$ (Sec. 1.10).

If we consider a Stokes transition, $v \rightarrow v+1$, Eq. 1.204 is written as [3]

$$(\alpha_{\rho\sigma})_{v,v+1} = \frac{1}{h} \left[\frac{\partial(\alpha_{\rho\sigma})_{gg}}{\partial Q} \right]_0 \sqrt{\frac{(v+1)h}{8\pi^2\mu\nu}} \quad (1.205)$$

where μ and ν are the reduced mass and the Stokes frequency. Then Eq. 1.200 is written as

$$I = \text{const}(v_0 - \nu)^4 \frac{E^2}{h^2} \left[\frac{\partial(\alpha_{\rho\sigma})_{gg}}{\partial Q} \right]_0^2 \frac{(v+1)h}{8\pi^2\mu\nu} \quad (1.206)$$

In Sec. 1.20, we derived a classical equation for Raman intensity:

$$\begin{aligned} I_n &= \text{const} \left(\frac{\partial\alpha}{\partial Q} \right)^2 E^2 \\ &= \text{const} \left\{ \frac{1}{45} [45(\bar{\alpha})^2 + 13\gamma^2] \right\} E^2 \end{aligned} \quad (1.193)$$

By replacing the $\partial\alpha/\partial Q$ term of Eq. 1.206 with the term enclosed in braces in Eq. 1.193, we obtain

$$I_n = \text{const}(v_0 - \nu)^4 \frac{(v+1)E^2}{8\pi^2\mu\nu h^2} \left\{ \frac{1}{45} [45(\bar{\alpha})^2 + 13\gamma^2] \right\} \quad (1.207)$$

At room temperature, most of the scattering molecules are in the $v=0$ state, but some are in higher vibrational states. Using the Maxwell-Boltzmann distribution

law, we find that the fraction of molecules f_v with vibrational quantum number v is given by

$$f_v = \frac{e^{-[v + (1/2)]hv/kT}}{\sum_v e^{-[v + (1/2)]hv/kT}} \quad (1.208)$$

Then the total intensity is proportional to $\sum_v f_v(v+1)$, which is equal to $(1 - e^{-hv/kT})^{-1}$ (see Ref. 23). Hence we can rewrite Eq. 1.207 in the form

$$I_n = KI_0 \frac{(v_0 - v)^4}{\mu v(1 - e^{-hv/kT})} [45(\bar{\alpha})^2 + 13\gamma^2] \quad (1.209)$$

Here I_0 is the incident light intensity which is proportional to E^2 , and K summarizes all other constant terms.

If the incident light is polarized, the form of Eq. 1.209 is slightly modified:

$$I_p = KI_0 \frac{(v_0 - v)^4}{\mu v(1 - e^{-hv/kT})} [45(\bar{\alpha})^2 + 7\gamma^2] \quad (1.210)$$

As shown in Sec. 1.20, the degree of depolarization ρ_p is

$$\rho_p = \frac{3\gamma^2}{45(\bar{\alpha})^2 + 4\gamma^2} \quad \text{or} \quad \gamma^2 = \frac{45(\bar{\alpha})^2 \rho_p}{3 - 4\rho_p} \quad (1.211)$$

Since $\rho_p = \frac{3}{4}$ for nontotally symmetric vibrations, Eq. 1.211 holds only for totally symmetric vibrations. Then Eq. 1.210 is written as

$$I_p = K' I_0 \frac{(v_0 - v)^4}{\mu v(1 - e^{-hv/kT})} \left(\frac{1 + \rho_p}{3 - 4\rho_p} \right) (\bar{\alpha})^2 \quad (1.212)$$

In the case of a solution, the intensity is proportional to the molar concentration C . Then Eq. 1.212 is written as

$$I_p = K'' I_0 \frac{C(v_0 - v)^4}{\mu v(1 - e^{-hv/kT})} \left(\frac{1 + \rho_p}{3 - 4\rho_p} \right) (\bar{\alpha})^2 \quad (1.213)$$

If we compare the intensities of totally symmetric vibrations (A_1 mode) of two tetrahedral XY_4 -type molecules, the intensity ratio is given by

$$\frac{I_1}{I_2} = \frac{C_1}{C_2} \left(\frac{\tilde{\nu}_0 - \tilde{\nu}_1}{\tilde{\nu}_0 - \tilde{\nu}_2} \right)^4 \frac{\tilde{\nu}_2 \mu_2 (1 - e^{-hc\tilde{\nu}_2/kT}) (\bar{\alpha}_1)^2}{\tilde{\nu}_1 \mu_1 (1 - e^{-hc\tilde{\nu}_1/kT}) (\bar{\alpha}_2)^2} \quad (1.214)$$

In this case, the ρ_p term drops out, since $\gamma^2 = 0$ for isotropic molecules such as tetrahedral XY_4 and octahedral XY_6 types. By using CCl_4 as the standard, it is possible to determine the relative value of the $\partial\alpha/\partial Q$ term, which provides information about the degree of covalency and the bond order [23].

As seen above, the intensity of Raman scattering increases as the $(\partial\alpha/\partial Q)_0$ term becomes larger. The following general rules may reflect the trends in the $(\partial\alpha/\partial Q)_0$ values: (1) stretching vibrations produce stronger Raman bands than do bending vibrations; (2) symmetric vibrations produce stronger Raman bands than do anti-symmetric vibrations, and totally symmetric “breathing” vibrations produce the most intense Raman bands; (3) stretching vibrations of covalent bonds produce Raman bands stronger than those of ionic bonds (among the covalent bonds, Raman intensities increase as the bond order increases; thus, the ratio of relative intensities of the $C\equiv C$, $C=C$, and $C-C$ stretching vibrations is approximately 3:2:1); and (4) bonds involving heavier atoms produce stronger Raman bands than do those involving lighter atoms. For example, the $\nu(S-S)$ is stronger than the $\nu(C-C)$. Coordination compounds containing heavy metals and sulfur ligands are ideal for Raman studies.

1.22. PRINCIPLE OF RESONANCE RAMAN SPECTROSCOPY

In normal Raman spectroscopy, the exciting frequency lies in the region where the compound has no electronic absorption band. In resonance Raman spectroscopy, the exciting frequency falls within the electronic band (Sec. 1.2). In the gaseous phase, this tends to cause resonance fluorescence since the rotational–vibrational levels are discrete. In the liquid and solid states, however, these levels are no longer discrete because of molecular collisions and/or intermolecular interactions. If such a broad vibronic bands is excited, it tends to give resonance Raman rather than resonance fluorescence spectra [101,102].

Resonance Raman spectroscopy is particularly suited to the study of biological macromolecules such as heme proteins because only a dilute solution (biological condition) is needed to observe the spectrum and only vibrations localized within the chromophoric group are enhanced when the exciting frequency approaches that of the relevant chromophore. This *selectivity* is highly important in studying the theoretical relationship between the electronic transition and the vibrations to be resonance-enhanced.

The origin of resonance Raman enhancement is explained in terms of Eq. 1.201. In normal Raman spectroscopy, ν_0 is chosen in the region that is far from the electronic absorption. Then, $\nu_{rm} \gg \nu_0$, and $\alpha_{p\sigma}$ is independent of the exciting frequency ν_0 . In resonance Raman spectroscopy, the denominator, $\nu_{rm} - \nu_0$, becomes very small as ν_0 approaches ν_{rm} . Thus, the first term in the square brackets of Eq. 1.201 dominates all other terms and results in striking enhancement of Raman lines. However, Eq. 1.201 cannot account for the selectivity of resonance Raman enhancement since it is not specific about the states of the molecule. Albrecht [103] derived a more specific equation for the initial and final states of resonance Raman scattering by

introducing the Herzberg–Teller expansion of electronic wave functions into the Kramers–Heisenberg dispersion formula. The results are as follows:

$$(\alpha_{\rho\sigma})_{gi,gj} = A + B + C \quad (1.215)$$

$$A = \sum_{e \neq g} \sum_v \left[\frac{(g^0 | R_\sigma | e^0)(e^0 | R_\rho | g^0)}{E_{ev} - E_{gi} - E_0} + (\text{nonresonance term}) \right] \langle i | v \rangle \langle v | j \rangle \quad (1.216)$$

$$\begin{aligned} B = & \sum_{e \neq g} \sum_v \sum_{s \neq e} \sum_a \left\{ \left[\frac{(g^0 | R_\sigma | e^0)(e^0 | h_a | s^0)(s^0 | R_\rho | g^0)}{E_{ev} - E_{gi} - E_0} + (\text{nonresonance term}) \right] \right. \\ & \times \frac{\langle i | v \rangle \langle v | Q_a | j \rangle}{E_e^0 - E_s^0} + \left[\frac{(g^0 | R_\sigma | s^0)(s^0 | h_a | e^0)(e^0 | R_\rho | g^0)}{E_{ev} - E_{gi} - E_0} + (\text{nonresonance term}) \right] \\ & \left. \times \frac{\langle i | Q_a | v \rangle \langle v | j \rangle}{E_e^0 - E_s^0} \right\} \quad (1.217) \end{aligned}$$

$$\begin{aligned} C = & \sum_{e \neq g} \sum_{t \neq g} \sum_v \sum_a \left\{ \left[\frac{(e^0 | R_\rho | g^0)(g^0 | h_a | t^0)(t^0 | R_\sigma | e^0)}{E_{ev} - E_{gi} - E_0} + (\text{nonresonance term}) \right] \right. \\ & \times \frac{\langle i | v \rangle \langle v | Q_a | j \rangle}{E_g^0 - E_t^0} + \left[\frac{(e^0 | R_\rho | t^0)(t^0 | h_a | g^0)(g^0 | R_\sigma | e^0)}{E_{ev} - E_{gi} - E_0} + (\text{nonresonance term}) \right] \\ & \left. \times \frac{\langle i | Q_a | v \rangle \langle v | j \rangle}{E_g^0 - E_t^0} \right\} \quad (1.218) \end{aligned}$$

The notations g, i, j, e , and v were explained in Sec. 1.21. Other notations are as follows: s , another excited electronic state; h_a , the vibronic coupling operator $\partial\mathcal{H}/\partial Q_a$, \mathcal{H} , and Q_a , the electronic Hamiltonian and the a th normal coordinate of the electronic ground state, respectively; E_{gi} and E_{ev} , the energies of states gi and ev , respectively; $|g^0\rangle$, $|e^0\rangle$, and $|s^0\rangle$, the electronic wavefunctions for the equilibrium nuclear positions of the ground and excited states; E_e^0 and E_s^0 , the corresponding energies of the electronic states, e^0 and s^0 , respectively; and E_0 , the energy of the exciting light. The nonresonance terms are similar to the preceding terms except that the denominator is $(E_{ev} - E_{gj} + E_0)$ instead of $(E_{ev} - E_{gj} - E_0)$ and that R_σ and R_ρ (Cartesian components of the transition moment) in the numerator are interchanged. These terms can be neglected under the strict resonance condition since the resonance terms become very large. The C term is usually neglected because its components are denominated by $E_g^0 - E_t^0$, where t refers to an excited state that is much higher in energy than the first excited state. These notations are shown on the right-hand side of Fig. 1.29. In more rigorous expressions, the damping factor $i\Gamma$ must be added to the

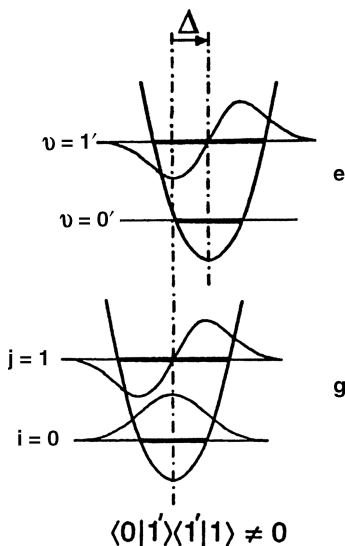


Fig. 1.30. Shift of equilibrium position caused by totally symmetric vibration.

denominators such as $E_{ev} - E_{gj} - E_0$ so that the resonance term does not become infinity under rigorous resonance conditions [103].

For the A term to be nonzero, the $g \leftrightarrow e$ electronic transition must be allowed, and the product of the integrals $\langle i | v \rangle \langle v | j \rangle$ (Franck–Condon factor) must be nonzero. The latter condition is satisfied if the equilibrium position is shifted by a transition ($\Delta \neq 0$ as shown in Fig. 1.30). Totally symmetric vibrations tend to be resonance-enhanced via the A term since they tend to shift the equilibrium position upon electronic excitation. If the equilibrium position is not shifted by the $g \leftrightarrow e$ transition, the A term becomes zero since either one of the integrals, $\langle i | v \rangle$ or $\langle v | j \rangle$, becomes zero. This situation tends to occur for nontotally symmetric vibrations.

In contrast to the A term, the B term resonance requires at least one more electronic excited state(s), which must be mixed with the e state via normal vibration, Q_a . Namely, the integral $\langle e^0 | h_a | s^0 \rangle$ must be nonzero. The B -term resonance is significant only when these two excited states are closely located so that the denominator, $E_e^0 - E_s^0$, is small. Other requirements are that the $g \leftrightarrow e$ and $g \leftrightarrow s$ transitions should be allowed and that the integrals $\langle i | v \rangle$ and $\langle v | Q_a | j \rangle$ should not be zero. The B term can cause resonance enhancement of nontotally symmetric as well as totally symmetric vibrations, although it is mainly responsible for resonance enhancement of the former.

As seen in Eqs. 1.216 and 1.217, both A and B terms involve summation over v , which is the vibrational quantum number at the electronic excited state. Since the harmonic oscillator selection rule ($\Delta v = \pm 1$) does not hold for a large v , overtones and combination bands may appear under resonance conditions. In fact, series of these nonfundamental vibrations have been observed in the case of A -term resonance (Sec. 1.23).

In Sec. 1.20, we have shown that the depolarization ratio for totally symmetric vibrations is in the range $0 \leq \rho_p < \frac{3}{4}$. For the A term to be nonzero, however, the term $(g^0 | R_\sigma | e^0)(e^0 | R_\rho | g^0)$ must be nonzero. Since g^0 is totally symmetric, this condition is realized only when both $\chi(R_\sigma)\chi(e^0)$ and $\chi(R_\rho)\chi(e^0)$ belong to the totally symmetric species. Thus, $\chi(R_\sigma) = \chi(R_\rho)$, and only one of the diagonal terms of the polarizability tensor (α_{xx} , α_{yy} , or α_{zz}) becomes nonzero. Then, it is readily seen from Eq. 1.199 that $\rho_p = \frac{1}{3}$. This rule has been confirmed by many observations. If the electronic excited state is degenerate, two of the diagonal terms must be nonzero. In this case, $\rho_p = \frac{1}{8}$. These rules hold for any point group with at least one C_3 or higher axis, with the exception of the cubic groups in which the Cartesian coordinates transform as a single irreducible degenerate representation.

1.23. RESONANCE RAMAN SPECTRA

Because of the advantages mentioned in the preceding section, resonance Raman (RR) spectroscopy has been applied to vibrational studies of a number of inorganic as well as organic compounds. It is currently possible to cover the whole range of electronic transitions continuously by using excitation lines from a variety of lasers and Raman shifters [26]. In particular, the availability of excitation lines in the UV region has made it possible to carry out UV resonance Raman (UVR) spectroscopy [104].

In RR spectroscopy, the excitation line is chosen inside the electronic absorption band. This condition may cause thermal decomposition of the sample by local heating. To minimize thermal decomposition, several techniques have been developed. These include the rotating sample technique, the rotating (or oscillating) laser beam technique, and their combinations with low-temperature techniques [21,26]. It is always desirable to keep low laser power so that thermal decomposition is minimal. This will also minimize photodecomposition, which occurs depending on laser lines in some compounds.

An example of the A -term resonance is given by I_2 , which has an absorption band near 500 nm and its fundamental at $\sim 210 \text{ cm}^{-1}$. Figure 1.31 shows the RR spectrum of I_2 in solution obtained by Kiefer and Bernstein [105] (excitation at 514.5 nm). It shows a series of overtones up to the seventeenth. The vibrational energy of an anharmonic oscillator including the cubic term is expressed as

$$E_v = hc\omega_e \left(v + \frac{1}{2} \right) - hc\chi_e\omega_e \left(v + \frac{1}{2} \right)^2 + hcy_e\omega_e \left(v + \frac{1}{2} \right)^3 \dots$$

The anharmonicity constants, $\chi_e\omega_e$ and $y_e\omega_e$ can be determined by plotting the $\tilde{\nu}(\text{obs})/v$ against the vibrational quantum number v , as shown in Fig. 1.32. The straight line gives $\chi_e\omega_e$ and the deviation from the straight line (at higher v) gives $y_e\omega_e$. The results (CCl_4 solution) in cm^{-1} are

$$\omega_e = 212.59 \pm 0.08, \quad \chi_e\omega_e = 0.62 \pm 0.03, \quad y_e\omega_e = -0.005 \pm 0.002$$

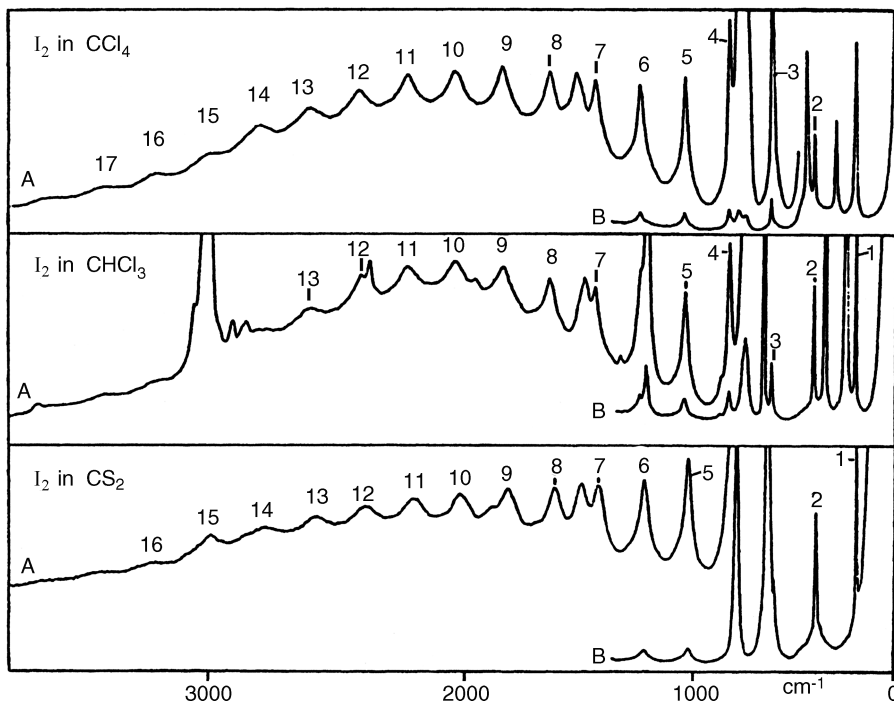


Fig. 1.31. Resonance Raman spectra of I_2 in CCl_4 , $CHCl_3$, and CS_2 (514.5 nm excitation) [105].

As stated in the preceding section, the depolarization ratio (ρ_p) is expected to be closed to $\frac{1}{3}$ for totally symmetric vibrations. However, this value increases as the change in vibrational quantum number (Δv) increases. For example, it is 0.48 for the tenth overtone of I_2 in CCl_4 [100].

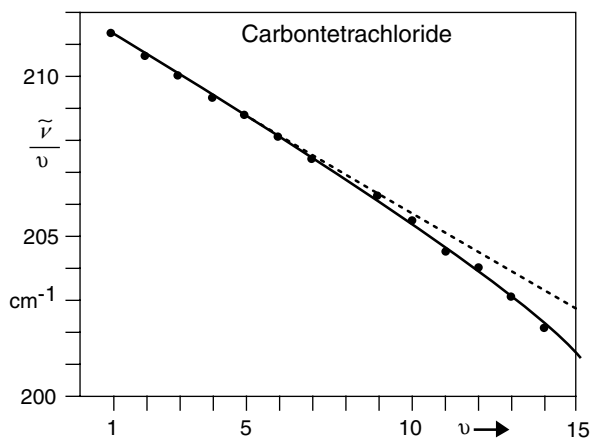


Fig. 1.32. Plot of $\tilde{\nu}/\nu$ vs. ν for I_2 in CCl_4 [105].

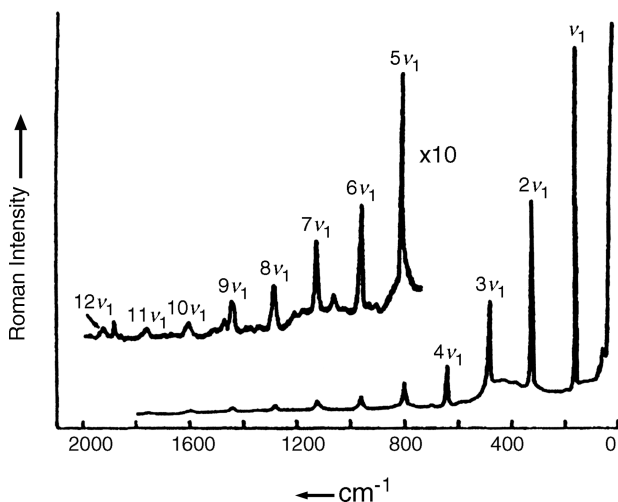


Fig. 1.33. Resonance Raman spectrum of solid TiI_4 (514.5 nm excitation) [106].

The second example is given by TiI_4 , which has the absorption maximum near 514 nm. Figure 1.33 shows the RR spectrum of solid TiI_4 obtained by Clark and Mitchell [106] with 514.5 nm excitation. In this case, a series of overtones up to the twelfth has been observed. Using these data, they obtained the following constants (cm^{-1}):

$$\omega_e = 161.0 \pm 0.2 \quad \text{and} \quad X_{11} = 0.11 \pm 0.03$$

Here, X_{11} is the anharmonicity constant corresponding to $\chi_e \omega_e$ of a diatomic molecule (Sec. 1.3).

Theoretical treatments of Raman intensities of these overtone series under rigorous resonance conditions have been made by Nafie et al. [107]. There are many other examples of RR spectra of small molecules and ions that exhibit *A*-term resonance. Section 2.6 includes references on RR spectra of the CrO_4^{2-} and MnO_4^- ions. Kiefer [101] reviewed RR studies of small molecules and ions.

Hirakawa and Tsuboi [108] noted that among the totally symmetric modes, the mode that leads to the excited-state configuration is most strongly resonance enhanced. For example, the NH_3 molecule is pyramidal in the ground state and planar in the excited state (216.8 nm above the ground state). Then, the symmetric bending mode near 950 cm^{-1} is enhanced 10 times more than the symmetric stretching mode near 3300 cm^{-1} when the excitation wavelength is changed from 514.5 to 351.1 nm.

A typical example of the *B*-term resonance is given by metalloporphyrins and heme proteins. As shown in Fig. 1.34, $\text{Ni}(\text{OEP})$ (OEP:octaethylporphyrin) exhibits two electronic transitions referred to as the Q_0 (or α) and **B** (or Soret) bands along with a vibronic side band (Q_1 or β) in the 350–600 nm region. According to MO (molecular orbital) calculations on the porphyrin core of D_{4h} , symmetry, Q_0 and **B** transitions

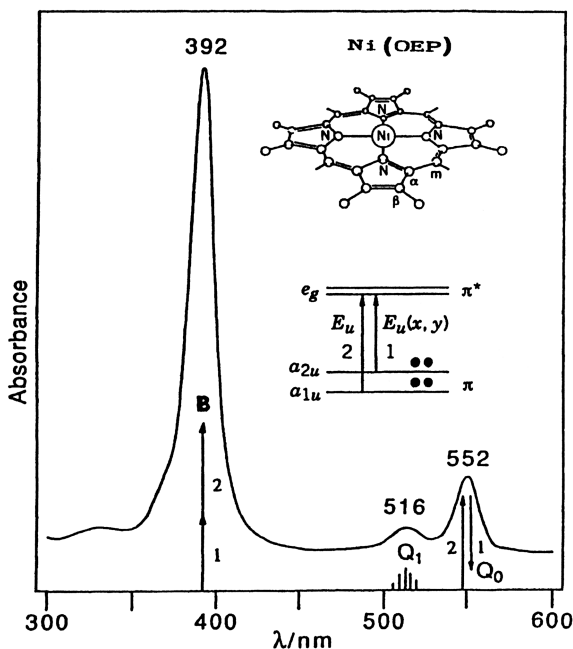


Fig. 1.34. Structure, energy-level diagram, and electronic spectrum of Ni(OEP) [109].

result from strong interaction between the $a_{1u}(\pi) \rightarrow e_g(\pi^*)$ and $a_{2u}(\pi) \rightarrow e_g(\pi^*)$ transitions which have similar energies and the same excited-state symmetry (E_u). The transition dipoles add up for the strong **B** transition and nearly cancel out for the weak Q_0 transition. This is an ideal situation for *B*-term resonance. According to Eq. 1.217, any normal modes which give nonzero values for the integral $(e^0 | h_a | s^0)$ are enhanced via the *B* term. These vibrations must belong to one of the symmetry species given by $E_u \times E_u$, that is, $A_{1g} + B_{1g} + B_{2g} + A_{2g}$.*

Figure 1.35 shows the RR spectra of Ni(OEP) with excitation near the **B**, Q_1 and Q_0 transitions as obtained by Spiro and coworkers [109]. As discussed in Sec. 1.20, polarization properties are expected to be A_{1g} (*p*, polarized), B_{1g} and B_{2g} (*dp*, depolarized), and A_{2g} (*ap*, anomalous polarization). These polarization properties, together with normal coordinate analysis, were used to make complete vibrational assignments of Ni(OEP) [110]. It is seen that the spectra obtained by excitation near the Q_0 band (bottom traces) are dominated by the *dp* bands (B_{1g} and B_{2g} species), while those obtained by excitation between the Q_0 and Q_1 bands (middle traces) are dominated by the *ap* bands (A_{2g} species). The spectra obtained by excitation near the **B** band (top traces) are dominated by the *p* bands (A_{1g} species). In this

*For symmetry species of the direct products, see Appendix IV. Also note that the A_{1g} vibrations are not effective in vibronic mixing.

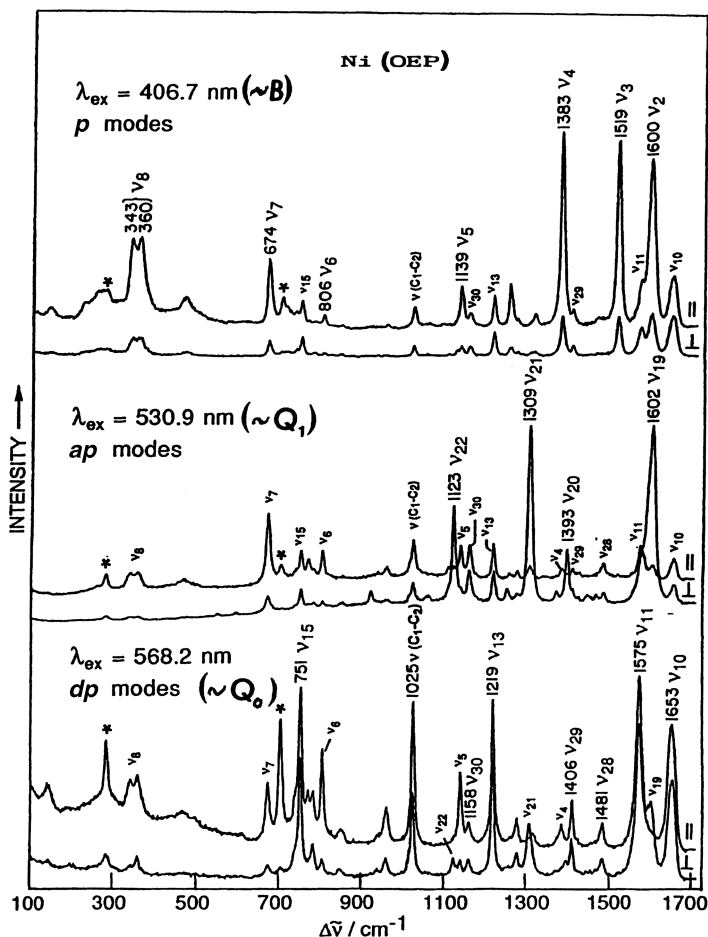


Fig. 1.35. Resonance Raman spectra of Ni(OEP) obtained by excitation near the B, Q_1 , and Q_0 bands [110].

case, the A-term resonance is much more important than the B-term resonance because of the very strong absorption strength of the **B** band. Mizutani and coworkers [110a] analyzed the resonance Raman spectra of Ni(OEP) obtained at the $d-d$ excited state.

As will be shown in Sec. 2.8, anomalously polarized bands have also been observed in the RR spectra of the IrCl_6^{2-} ion, although their origin is different from the vibronic coupling mentioned above [111,112].

The majority of compounds studied thus far exhibit the A-term rather than the B-term resonance. A more complete study of resonance Raman spectra involves the observation of *excitation profiles* (Raman intensity plotted as a function of the excitation frequency for each mode), and the simulation of observed excitation profiles based on theoretical treatments of resonance Raman scattering [113].

1.24. THEORETICAL CALCULATION OF VIBRATIONAL FREQUENCIES

The procedure for calculating harmonic vibrational frequencies and force constants by **GF** matrix method has been described in Sec. 1.12. In this method, both **G** (kinetic energy) and **F** (potential energy) matrices are expressed in terms of internal coordinates (**R**) such as increments of bond distances and bond angles. Then, the kinetic (*T*) and potential (*V*) energies are written as:

$$2T = \tilde{\mathbf{R}}\mathbf{G}^{-1}\dot{\mathbf{R}} \quad (1.113)$$

$$2V = \tilde{\mathbf{R}}\mathbf{F}\mathbf{R} \quad (1.111)$$

and the secular equation

$$|\mathbf{GF} - \mathbf{E}\lambda| = 0 \quad (1.116)$$

is solved to obtain vibrational frequencies. Here, **E** is a unit matrix, and λ is related to the wavenumber by the relation given by Eq. 1.156. The **G** matrix elements can be calculated from the known bond distances and angles, and the **F** matrix elements (force constants) are refined until the differences between the observed and calculated frequencies are minimized. Force constants thus obtained can be transferred to similar molecules to predict their vibrational frequencies.

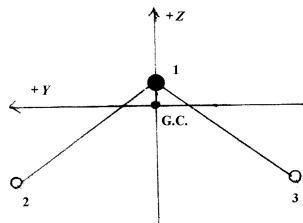
On the other hand, quantum mechanical methods utilize an entirely different approach to this problem. The principle of the method is to express the total electronic energy (*E*) of a molecule as a function of nuclear displacements near the equilibrium positions and to calculate its second derivatives with respect to nuclear displacements, namely, vibrational force constants. In the past, *ab initio* calculations of force constants were limited to small molecules [114] such as H₂O and C₂H₂ because computational time required for large molecules was prohibitive. This problem has been solved largely by more recent progress in density functional theory (DFT) [115] coupled with commercially available computer software. Currently, the DFT method is used almost routinely to calculate vibrational parameters of a variety of inorganic, organic, coordination, and organometallic compounds. The advent of high-speed personal computers further facilitated this trend.

Using a commercially available computer program such as “Gaussian 03,” DFT calculations of the H₂O molecule proceed in the following order: First, molecular parameters (masses of constituent atoms, approximate bond distances and angles) are used as input data. As an example, let us assume that the O–H distance is 0.96 Å and the HOH angle is 109.5°. Then, the program calculates the cartesian coordinates of the three atoms by placing the origin at the center of gravity (CG) of the molecule. It also determines the point group of the molecule as C_{2v} on the basis of the given geometry.

Since the total electronic energy (*E*) of the H₂O molecule is a function of the nine Cartesian coordinates (*x_i*, *i* where *i* = 1, 2, ..., 9), the equilibrium configuration that renders all the nine first derivatives ($\partial E/\partial x_i$) zero can be determined (energy optimization). Accuracy of the results depends on the level of the approximation method

TABLE 1.15. Calculated Cartesian Coordinates of H₂O

Center Number	Atomic Number	Coordinate (Å)		
		X	Y	Z
1	8	0.0000	0.0000	0.1110
2	1	0.0000	0.8010	-0.4440
3	1	0.0000	-0.8010	-0.4440



chosen in calculating E . Using 6-31G* basis set with B3LYP functional [116], for example, the optimal geometry was found to be: OH distance = 0.9745 Å and HOH angle = 110.5670°. These values were used to recalculate the Cartesian coordinates listed in Table 1.15

The next step is to calculate the second derivatives near the equilibrium positions $[(\partial^2 E / \partial x_i \partial x_j)_0, i, j = 1 \sim 9]$, namely, the force constants in terms of Cartesian coordinates ($f_{i,j}$), using analytical methods [116a]. The force constants thus obtained are converted to mass-weighted Cartesian coordinates ($X_{M,i}$) by

$$x_{M,1} = \sqrt{m_1}x_1, \quad x_{M,2} = \sqrt{m_1}x_2, \dots \quad (1.219)$$

$$f_{M,i,j} = \frac{f_{i,j}}{\sqrt{m_i m_j}} = \left(\frac{\partial^2 V}{\partial x_{M,i} \partial x_{M,j}} \right)_0 \quad (1.220)$$

These $f_{M,i,j}$ terms are the elements of the force constant (Hessian) matrix.

Using matrix expression, the relationship between mass-weighted Cartesian (\mathbf{X}_M) and Cartesian (\mathbf{X}) coordinates is written as follows:

$$\mathbf{X}_M = \mathbf{M}^{1/2} \mathbf{X} \quad (1.221)$$

Here, $\mathbf{M}^{1/2}$ is a diagonal matrix whose elements are $\sqrt{m_1}, \dots, \sqrt{m_9}$ and \mathbf{X} is a column matrix, $[x_1, \dots, x_9]$. The product, $\mathbf{M}^{1/2} \mathbf{X}$, gives a column matrix, \mathbf{X}_M , $[\sqrt{m_1}x_1, \dots, \sqrt{m_9}x_9]$. Equation (1.221) is rewritten as

$$\mathbf{X} = \mathbf{M}^{-(1/2)} \mathbf{X}_M \quad (1.222)$$

The relationship between the internal coordinate \mathbf{R} and \mathbf{X} (Eqs. 1.118 and 1.119) is now written as

$$\mathbf{R} = \mathbf{B} \mathbf{X} = \mathbf{B} \mathbf{M}^{-(1/2)} \mathbf{X}_M \quad (1.223)$$

and its transpose is

$$\tilde{\mathbf{R}} = \tilde{\mathbf{X}}_M \mathbf{M}^{-(1/2)} \tilde{\mathbf{B}} \quad (1.224)$$

where \mathbf{B} is a rectangular (3×9) matrix shown by Eq. 1.119.

The kinetic energy (Eq. 1.113) in terms of \mathbf{X}_M is written as

$$2T = \dot{\tilde{\mathbf{X}}}_M \dot{\mathbf{X}}_M \quad (1.225)$$

and the potential energy (Eq. 1.111) in terms of the same coordinate, \mathbf{X}_M , is

$$2V = \tilde{\mathbf{R}}\mathbf{F}_R\mathbf{R} = \tilde{\mathbf{X}}_M\mathbf{M}^{-(1/2)}\tilde{\mathbf{B}}\mathbf{F}_R\mathbf{B}\mathbf{M}^{-(1/2)}\mathbf{X}_M = \tilde{\mathbf{X}}_M\mathbf{F}_{XM}\mathbf{X}_M \quad (1.226)$$

where

$$\mathbf{F}_{XM} = \mathbf{M}^{-(1/2)}\tilde{\mathbf{B}}\mathbf{F}_R\mathbf{B}\mathbf{M}^{-(1/2)} \quad (1.227)$$

or

$$\tilde{\mathbf{B}}\mathbf{F}_R\mathbf{B} = \mathbf{M}^{1/2}\mathbf{F}_{XM}\mathbf{M}^{1/2} \quad (1.228)$$

Vibrational frequencies are calculated by solving the following equation:

$$|\mathbf{F}_{XM} - \mathbf{E}\lambda| = 0 \quad (1.229)$$

In the case of H_2O , we obtain nine frequencies, six of which are near zero. These six frequencies must be eliminated from the results because they correspond to the translational and rotational motions of the molecule as a whole ($3N-6$ rule). Thus, the remaining three frequencies correspond to the normal modes of the H_2O molecule. It should be noted that vibrational frequencies are intrinsic of individual molecules and do not depend on the coordinate system chosen (\mathbf{R} or \mathbf{X}_M).

The next step is to convert the force constants (\mathbf{F}_{XM}) in terms of \mathbf{X}_M coordinates to those of internal coordinates (\mathbf{F}_R), which have clearer physical meanings. For this purpose, Eq. 1.228 is rewritten as [117–119]

$$\mathbf{F}_R = \mathbf{U}\Gamma^{-1}\tilde{\mathbf{U}}\mathbf{B}\mathbf{M}^{1/2}\mathbf{F}_{XM}\mathbf{M}^{1/2}\tilde{\mathbf{B}}\mathbf{U}\Gamma^{-1}\tilde{\mathbf{U}} \quad (1.230)$$

Here, \mathbf{U} is an orthogonal matrix ($\mathbf{U} = \tilde{\mathbf{U}}^{-1}$) that diagonalizes $\tilde{\mathbf{B}}\mathbf{B}$, and Γ is a diagonal matrix that is defined as follows:

$$\tilde{\mathbf{B}}\mathbf{B}\mathbf{U} = \mathbf{U}\Gamma \quad (1.231)$$

In the case of H_2O , \mathbf{B} is a 3×9 matrix, whereas \mathbf{U} , Γ , and \mathbf{F}_R are 3×3 matrices. To take advantage of symmetry properties, internal coordinates are further transformed to internal symmetry coordinates (\mathbf{R}^S) by the relation

$$\mathbf{R}^S = \mathbf{U}^S\mathbf{R} \quad (1.131)$$

where \mathbf{U}^S is an orthogonal matrix chosen by symmetry consideration. Then, the force constants in terms of internal symmetry coordinates (\mathbf{F}_R^S) are given by

$$\mathbf{F}_R^S = \mathbf{U}^S\mathbf{F}_R\tilde{\mathbf{U}}^S \quad (1.232)$$

TABLE 1.16. Comparison of Observed and Calculated Frequencies (cm^{-1}) and Normal Modes of H_2O

Normal Vibration:	$\nu_1(A_1)$			$\nu_2(A_1)$			$\nu_3(B_2)$		
Observed frequencies ^a	1595			3657			3756		
Calculated frequencies	1565.5			3639.2			3804.7		
Normal modes ^b	X	Y	Z	X	Y	Z	X	Y	Z
O(1)	0.00	0.00	0.08	0.00	0.00	0.04	0.00	0.07	0.00
H(2)	0.00	-0.38	-0.60	0.00	0.62	-0.35	0.00	-0.58	0.40
H(3)	0.00	0.38	-0.60	0.00	-0.62	-0.35	0.00	-0.58	-0.40
Assignment	HOH bending			Symmetric OH stretch			Antisymmetric OH stretch		

^aIR spectrum (Table 2.2d of Chapter 2).^bThe normal modes shown in Fig. 1.12 are obtained by plotting these displacement coordinates.

Thus, $\mathbf{F}_{\mathbf{XM}}$ can be converted to $\mathbf{F}_{\mathbf{R}}^{\mathbf{S}}$ using Eqs. 1.230 and 1.232. Several computer programs are available for this conversion [118].

Table 1.16 summarizes the results of DFT calculation of H_2O . It is seen that the calculated frequencies are in good agreement with the observed values. In other cases, however, the former becomes higher than the latter because (1) the effect of anharmonicity is not included in the calculation and (2) systematic errors result from the use of finite basis sets and incomplete inclusion of electron correlation effects. In such cases, several empirical “scaling methods” are applied to the force constants [120] or frequencies [121] obtained by DFT calculations.

Computer programs such as “Gaussian 03” can simultaneously calculate several other parameters including normal modes (shown in Table 1.15), IR intensities, Raman scattering intensities, and depolarization ratios.

1.25. VIBRATIONAL SPECTRA IN GASEOUS PHASE [122] AND INERT GAS MATRICES [29,30]

As distinct from molecules in condensed phases, those in the gaseous phase are free from intermolecular interactions. If the molecules are relatively small, vibrational spectra of gases exhibit rotational fine structure (see Fig. 1.3) from which moments of inertia and hence internuclear distances and bond angles can be calculated [1,2]. Furthermore, detailed analysis of rotational fine structure provides information about the magnitude of rotation–vibration interaction (Coriolis coupling), centrifugal distortion, anharmonicity, and even nuclear spin statistics in some cases. In the past, infrared spectroscopy was the main tool in measuring gas-phase vibrational spectra. However, Raman spectroscopy is also playing a significant role because of the development of powerful laser sources and high-resolution spectrophotometers. For example, Clark and Rippon [123] measured gas-phase Raman spectra of Group IV tetrahalides, and calculated the Coriolis coupling constants from the observed band contours. For gas-phase Raman spectra of other inorganic compounds, see

Ref. [122]. Unfortunately, the majority of inorganic and coordination compounds exist as solids at room temperature. Although some of these compounds can be vaporized at high temperatures without decomposition, it is rather difficult to measure their spectra by the conventional method. Furthermore, high-temperature spectra are difficult to interpret because of the increased importance of rotational and vibrational hot bands.

In 1954, Pimentel and his colleagues [124] developed the *matrix isolation technique* to study the infrared spectra of unstable and stable species. In this method, solute molecules and inert gas molecules such as Ar and N₂ are mixed at a ratio of 1:500 or greater and deposited on an IR window such as a CsI crystal cooled to 10–15 K. Since the solute molecules trapped in an inert gas matrix are completely isolated from each other, the matrix isolation spectrum is similar to the gas-phase spectrum; no crystal field splittings and no lattice modes are observed. However, the former spectrum is simpler than the latter because, except for a few small hydride molecules, no rotational transitions are observed because of the rigidity of the matrix environment at low temperatures. The lack of rotational structure and intermolecular interactions results in a sharpening of the solute band so that even very closely located metal isotope peaks can be resolved in a matrix environment. This technique is also applicable to a compound which is not volatile at room temperature. For example, matrix isolation spectra of metal halides can be measured by vaporizing these compounds at high temperatures in a Knudsen cell and co-condensing their vapors with inert gas molecules on a cold window [125].

More recent developments of laser ablation techniques coupled with closed-cycle helium refrigerators greatly facilitated its application. Thus, matrix isolation technique has now been utilized to obtain structural and bonding information of a number of inorganic and coordination compounds. Some important features and applications are described in this and the following sections.

1.25.1. Vibrational Spectra of Radicals

Highly reactive radicals can be produced *in situ* in inert gas matrices by photolysis and other techniques. Since these radicals are stabilized in matrix environments, their spectra can be measured by routine spectroscopic techniques. For example, the spectrum of the HOO radical [126] was obtained by measuring the spectrum of the photolysis product of a mixture of HI and O₂ in an Ar matrix at ~4 K. Chapter 2 lists the vibrational frequencies of many other radicals, such as CN, OF, and HSi, obtained by similar methods.

1.25.2. Vibrational Spectra of High-Temperature Species

Alkali halide vapors produced at high temperatures consist mainly of monomers and dimers. The vibrational spectra of these salts at high temperatures are difficult to measure and difficult to interpret because of the presence of hot bands. The matrix isolation technique utilizing a Knudsen cell has solved this problem. The

vibrational frequencies of some of these high-temperature species are listed in Chapter 2.

1.25.3. Isotope Splittings

As stated before, it is possible to observe individual peaks due to heavy-metal isotopes in inert gas matrices since the bands are extremely sharp (half-band width, $1.5\text{--}1.0\text{ cm}^{-1}$) under these conditions. Figure 1.36a shows the infrared spectrum of the ν_7 band (coupled vibration between CrC stretching and CrCO bending modes) of $\text{Cr}(\text{CO})_6$ in a N_2 matrix [127]. The bottom curve shows a computer simulation using the measured isotope shift of 2.5 cm^{-1} per atomic mass unit, a 1.2 cm^{-1} half-band width, and the percentages of natural abundance of Cr isotopes: ^{50}Cr (4.31%), ^{52}Cr (83.76%), ^{53}Cr (9.55%), and ^{54}Cr (2.38%). The isotope splittings of SnCl_4 and GeCl_4 in Ar matrices are discussed in Sec. 2.6. These isotope frequencies are highly important in refining force constants in normal coordinate analysis.

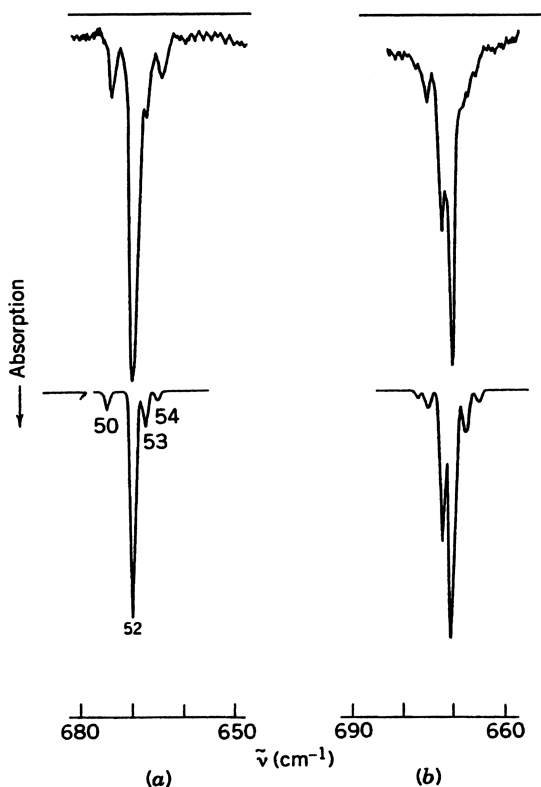


Fig. 1.36. Matrix isolation IR spectra of $\text{Cr}(\text{CO})_6$ in N_2 (a) and Ar (b) matrices. The bottom spectra were obtained by computer simulation [127].

1.25.4. Matrix Effect

The vibrational frequencies of matrix-isolated molecules give slight shifts when the matrix gas is changed. This result suggests the presence of weak interaction between the solute and matrix molecules. In some cases, the spectra are complicated by the presence of more than one trapping site. For example, the infrared spectrum of $\text{Cr}(\text{CO})_6$ in an Ar matrix (Fig. 1.36b) is markedly different from that in a N_2 matrix (Fig. 1.36a) [127]. The former spectrum can be interpreted by assuming two different sites in an Ar matrix. The computer-simulation spectrum (bottom curve) was obtained by assuming that these two sites are populated in a 2:1 ratio, the frequency separation of the corresponding peaks being 2 cm^{-1} . Thus, it is always desirable to obtain the matrix isolation spectra in several different environments.

1.26. MATRIX COCONDENSATION REACTIONS

A number of unstable and transient species have been synthesized via matrix cocondensation reactions, and their structure and bonding have been studied by vibrational spectroscopy. The principle of the method is to cocondense two solute vapors (atom, salt, or molecule) diluted by an inert gas on an IR window (IR spectroscopy) or a metal plate (Raman spectroscopy) that is cooled to low temperature by a cryocooler. Solid compounds can be vaporized by conventional heating (Knudsen cell), laser ablation, or other techniques, and mixed with inert gases at proper ratios [128]. In general, the spectra of the cocondensation products thus obtained exhibit many peaks as a result of the mixed species produced. In order to make band assignments, the effects of changing the temperature, concentration (dilution ratios), and isotope substitution on the spectra must be studied. In some cases, theoretical calculations (Sec. 1.24) must be carried out to determine the structure and to make band assignments. Vibrational frequencies of many molecules and ions obtained by matrix cocondensation reactions are listed in Chapter 2.

Matrix cocondensation reactions are classified into the following five types:

1. *Atom-Atom Reaction.* Liang et al. [129] studied the reaction: $\text{U} + \text{S} \rightarrow \text{US}_n (n = 1-3)$. Figure 1.37 shows the IR spectra of laser-ablated U atom vapor cocondensed with microwave-discharged S atom in Ar at 7 K. In (a) (^{32}S with higher concentration) and (b) (^{32}S with low concentration), the prominent band at 438.7 cm^{-1} and a weak band at 449.8 cm^{-1} show a consistent intensity ratio of 6 : 1, and are shifted to 427.8 and 437.4 cm^{-1} respectively, by $^{32}\text{S}/^{34}\text{S}$ substitution (c). In the mixed $^{32}\text{S} + ^{34}\text{S}$ experiments [traces] (d) and (e), both bands split into asymmetric triplets marked in (e). These results suggest that two equivalent S atoms are involved in this species. The bands at 438.7 and 449.8 cm^{-1} were assigned to the antisymmetric (ν_3) and symmetric (ν_1) stretching modes, respectively, of the nonlinear U^{32}S_2 molecule. Although the analogous UO_2 molecule is linear, the US_2 molecule is bent because of more favorable $\text{U}(6d)-\text{S}(3p)$ overlap. The weak band at 451.1 cm^{-1} , which is partly overlapped by the ν_1 mode of US_2 in (a), is shifted to 439.2 cm^{-1} by $^{32}\text{S}/^{34}\text{S}$ substitution (c), and was assigned to the diatomic US molecule. Another weak band at 458.2 cm^{-1} in (a) shows a

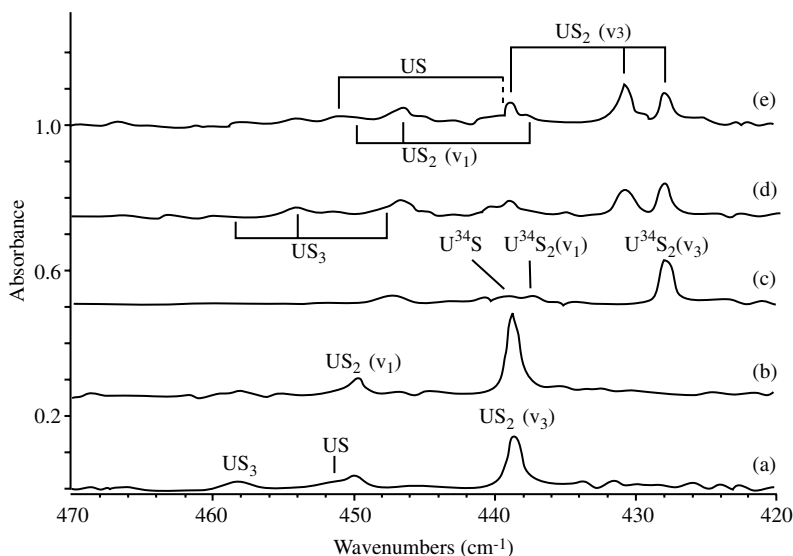


Fig. 1.37. Infrared spectra of laser-ablated U co-deposited with discharged isotopic S atoms in Ar at 7 K: (a) ^{32}S with higher concentration, (b) ^{32}S with lower concentration, (c) ^{34}S , (d) 35/65 $^{32}\text{S} + ^{34}\text{S}$ mixture, and (e) 50/50 $^{32}\text{S} + ^{34}\text{S}$ mixture [129].

triplet pattern in the mixed-isotope experiment shown in (d), and was assigned to the antisymmetric stretching vibration of the near-linear S—U—S unit of a T-shaped US_3 molecule similar to UO_3 . All these structures and band assignments are supported by DFT calculations.

2. Atom–Molecule Reaction. Zhou and Andrews [130] studied the reaction of $\text{Sc} + \text{CO} \rightarrow \text{Sc}(\text{CO})_n (n = 1-4)$ via cocondensation of laser-ablated Sc atoms with CO in excess Ar or Ne, and made band assignments based on the results of ^{13}CO and C^{18}O isotope shifts, matrix annealing, broadband photolysis, and DFT calculations. Figure 1.38a shows the IR spectrum of the cocondensation product after one hour deposition at 10 K in Ar. The strong and sharp band at 1834.2 cm^{-1} is shifted to 1792.9 and 1792.3 cm^{-1} by ^{13}CO and C^{18}O substitutions, respectively, and its intensity decreases upon annealing to 25 K (b) but increases on photolysis (c,d). Two weak bands near 1920 cm^{-1} in (a) are also isotope-sensitive and become stronger on annealing to 25 K (b). These bands were assigned to the $\text{Sc}(\text{CO})^+$ cation produced by the reaction of laser-ablated Sc^+ ion with CO. In a Ne matrix, a similar experiment exhibits a sharp band at 1732.0 cm^{-1} that was assigned to the $\text{Sc}(\text{CO})^-$ ion produced via electron capture by $\text{Sc}(\text{CO})$. The pair of bands at 1851.4 and 1716.3 cm^{-1} in (b) were assigned to the antisymmetric and symmetric stretching vibrations of the bent $\text{Sc}(\text{CO})_2$ molecule while the strong and sharp band at 1775.5 cm^{-1} in (c) was attributed to the linear $\text{Sc}(\text{CO})_2$ molecule. DFT calculations predict $\text{Sc}(\text{CO})_3$ to be trigonal pyramidal (C_{3v} symmetry) in the ground state. The bands at 1968.0 and 1822.2 cm^{-1} in (b) become weaker by photolysis (c,d) and stronger by annealing at 35 K (e). These bands were assigned to the nondegenerate symmetric and degenerate CO stretching

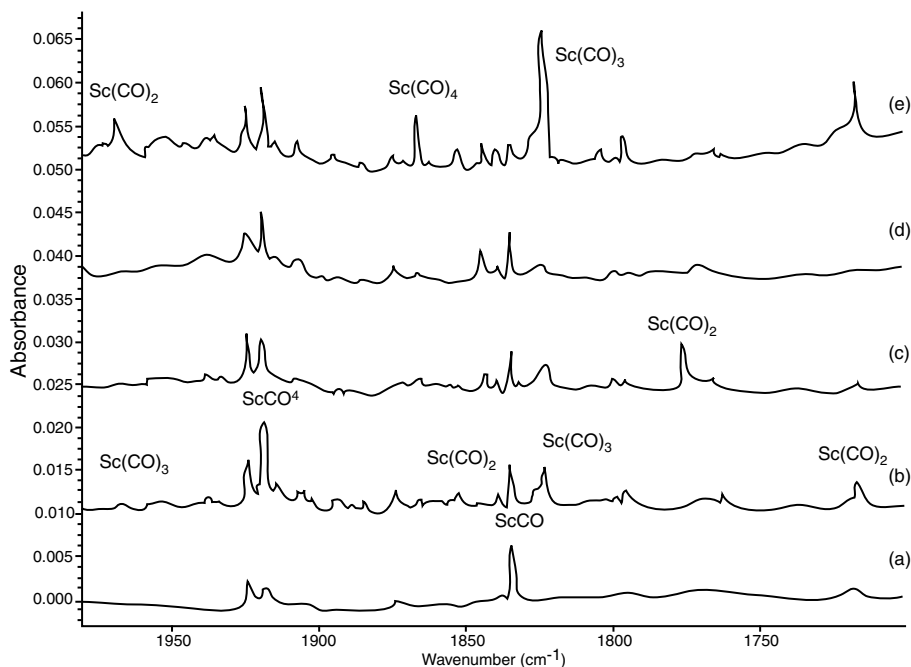


Fig. 1.38. Infrared spectra of laser-ablated Sc atoms co-deposited with 0.5 % CO in excess Ar.: (a) after 1 hr sample deposition at 10 K, (b) after annealing to 25 K, (c) after 20 min $\lambda > 470$ nm photolysis, (d) after 20 min full-arc photolysis, and (e) after annealing to 35 K [130].

vibrations, respectively, of the $\text{Sc}(\text{CO})_3$ molecule. The band at 1865.4 cm^{-1} appeared last when the matrix was annealed to 35 K (e), and was tentatively assigned to a degenerate vibration of $\text{Sc}(\text{CO})_4$. Matrix cocondensation reactions of this type have been studied most extensively as shown in Part B, Sec. 3.18.6.

3. Salt–Molecule Reaction. Tevault and Nakamoto [131] carried out matrix cocondensation reactions of metal salts such as PbF_2 with $\text{L}(\text{CO}, \text{NO}$ and $\text{N}_2)$ in Ar, and confirmed the formation of $\text{PbF}_2\text{--L}$ adducts by observing the shifts of IR bands of both components. These spectra are shown in Fig. 3.67 (of Sec. 3.18.6).

4. Salt–Salt Reaction. Ault [132] obtained the IR spectrum of the PbF_3^- ion via the reaction of the type, $\text{MF} + \text{PbF}_2 \rightarrow \text{M}[\text{PbF}_3]$ ($\text{M} = \text{Na}, \text{K}, \text{Rb}$, and Cs). Both salts were premixed, and the mixture was heated in a single Knudsen cell at $300\text{--}325^\circ\text{C}$, which is roughly 200°C below that is needed to vaporize either PbF_2 or MF. Figure 1.39 shows the IR spectra of PbF_2 and its cocondensation products with MF in Ar matrices. It is seen that, except for $\text{M} = \text{Na}$, the cocondensation products exhibit two prominent bands near 456 and 405 cm^{-1} with no bands due to PbF_2 . Thus, these two bands were assigned to the A_1 and E stretching vibrations, respectively, of the PbF_3^- ion of C_{3v} symmetry. The band at 242 cm^{-1} was observed weakly only in high-yield experiments, and tentatively assigned to a bending mode of the PbF_3^- ion.

5. Molecule–Molecule Reaction. The reaction $\text{Fe}(\text{TPP}) + \text{O}_2 \rightarrow (\text{TPP})\text{Fe--O}_2$ (TPP tetraphenylporphyrin) was carried out by Watanabe et al. [133] using $^{16}\text{O}_2$ and $^{18}\text{O}_2$

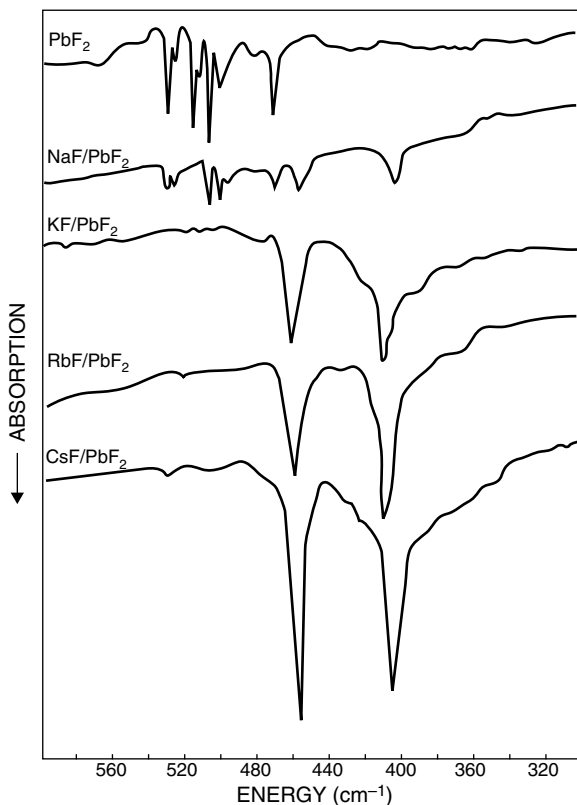


Fig. 1.39. Infrared spectra of the $M^+PbF_3^-$ isolated in Ar matrices. The top trace shows the spectrum of the parent PbF_2 salt, while the next four spectra show the bands attributable to the vaporization products from the solid mixtures of NaF/PbF_2 , KF/PbF_2 , RbF/PbF_2 , and CsF/PbF_2 in the $580 \sim 300 \text{ cm}^{-1}$ region [132].

diluted in Ar. The IR spectra shown in Fig. 3.76 (in Sec. 3.21.4) indicate that two new bands appear at 1195 and 1108 cm^{-1} which are due to the O_2 stretching vibrations of the end-on and side-on type $Fe(TPP)O_2$, respectively. Bajdor and Nakamoto [134] obtained a novel oxoferrylporphyrin $[O=Fe(IV)(TPP)]$ via laser photolysis of $Fe(TPP)O_2$ in pure O_2 matrices at $\sim 15 \text{ K}$. As seen in Fig. 1.82 (Sec. 1.22.4 of Part B), it exhibits the $Fe(IV)=O$ stretching vibration at 852 cm^{-1} .

1.27. SYMMETRY IN CRYSTALS

The symmetry elements and point groups of molecules and ions in the free state have been discussed in Sec. 1.5. For molecules and ions in crystals, however, it is necessary to consider some additional symmetry operations that characterize translational symmetries in the lattice. Addition of these translational operations results in the formation of the space groups that can be used to classify the symmetry of molecules and ions in crystals.

TABLE 1.17. Seven Crystallographic Systems and 32 Crystallographic Point Groups

System	Axes and Angles			32 Crystallographic Point Groups			
Triclinic	a α	b β	c γ	I C_1	\bar{I} C_i		
Monoclinic	a 90°	b β	c 90°	2 C_2	m or $\bar{2}$ C_s	$2/m$ C_{2h}	
Orthorhombic	a 90°	b 90°	c 90°			222 D_2	$mm2$ C_{2v} mmm D_{2h}
Tetragonal	a 90°	b 90°	c 90°	4 C_4	$\bar{4}$ S_4	$4/m$ C_{4h}	422 D_4 $4mm$ C_{4v} $42m$ D_{2d} $4/mmm$ D_{4h}
Trigonal (rhombohedral)	aaa $\alpha\alpha\alpha$	or	a 90° a 90° c 120°	3 C_3	$\bar{3}$ C_{3i}	32 D_3 $3m$ C_{3v} $\bar{3}m$ D_{3d}	
Hexagonal	a 90°	a 90°	c 120°	6 C_6	$\bar{6}$ C_{3h}	$6/m$ C_{6h}	622 D_6 $6mm$ C_{6v} $\bar{6}m2$ D_{3h} $6/mmm$ D_{6h}
Cubic	a 90°	a 90°	c 90°	23 T	$m\bar{3}$ T_h	432 O $\bar{4}3m$ T_d $m\bar{3}m$ O_h	

1.27.1. 32 Crystallographic Point Groups

As discussed in Sec. 1.5, molecular symmetry can be described by point groups that are derived from the combinations of symmetry operations, I (identity), C_p (p -fold axis of symmetry), σ (plane of symmetry), i (center of symmetry), and S_p (p -fold rotation–reflection axis), where p may range from 1 to ∞ . In the case of crystal symmetry, p is limited to 1, 2, 3, 4, and 6 because of space-filling requirement in a crystal lattice. As a result, only the 32 crystallographic point groups listed in Table 1.17 are possible. Here, Hermann–Mauguin (HM) as well as Schönflies (S) notations are shown. In the HM notation, 1, 2, 3, 4, and 6 denote the principal axis of rotation, C_p , where p is 1, 2, 3, 4, and 6, respectively, and $\bar{1}$, $\bar{2}$, $\bar{3}$, $\bar{4}$, and $\bar{6}$ denote a combination of respective rotation about an axis and inversion through a point on the axis. Thus, $\bar{1}$ means the center of inversion (i), $\bar{2}$ indicates σ on a mirror plane (m), and $\bar{3}$, $\bar{4}$, and $\bar{6}$ correspond to S_6 , S_4 , and S_3 , respectively. For example, the point group C_{2h} , (I , C_2 , σ , and i) can be written as $2m\bar{1}$, which can be simplified to $2/m$ where the slash means the C_2 axis is perpendicular to m . As shown in Table 1.17, these 32 crystallographic point groups which describe the symmetry of the unit cell can be classified into seven crystallographic systems according to the most simple choice of reference axes.

1.27.2. Symmetry of the Crystal Lattice

A crystal has a lattice structure that is a repetition of identical units. Bravais has shown that only the 14 different types of lattices shown in Fig. 1.40 are possible. These

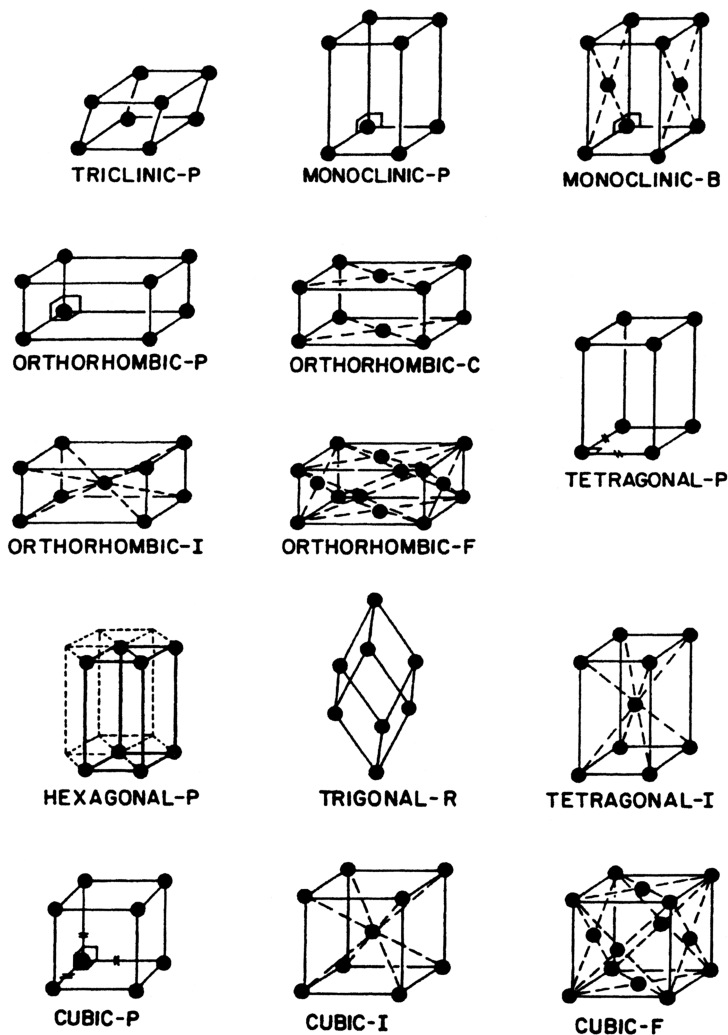


Fig. 1.40. The 14 Bravais lattices belonging to the seven crystallographic systems [135].

Bravais lattices are also classified into the seven crystallographic systems mentioned above. Here, the lattice points are regarded as “points” or “small, identical, perfect spheres,” thus representing the highest symmetry possible. In actual crystals, these points are occupied by unsymmetric but identical molecules or ions so that their high symmetry is lowered. In Fig. 1.40 P, C (or A or B), F, I, and R indicate primitive, base-centered, face-centered, body-centered, and rhombohedral lattices, respectively. The number of lattice points (LP) in each cell is summarized in Table 1.18. For crystal structures designated by P, crystallographic unit cells are identical with the Bravais unit cells. For those designated by other letters, crystallographic unit cells contain 2, 3, or 4 Bravais cells. In these cases, the number of molecules in the crystallographic unit

TABLE 1.18. Primitive and Centered Lattices

Type of Crystal Structure	Number of Lattice Points (LP)
Primitive (P)	1
Base-centered (A, B, or C)	2
Body-centered (I)	2
Rhombohedral (R)	3 or 1 ^a
Face-centered (F)	4

^aThe crystallographic unit cell may have been divided by 3.

cell must be divided by the corresponding LP since only the consideration of one Bravais cell is sufficient to interpret the vibrational spectra of crystals.

1.27.3. Space Groups

As stated above, the 32 point groups describe the symmetry of the unit cells, and the 14 Bravais lattices describe all possible arrangements of crystal lattices. To describe space symmetry, however, symmetry operations mentioned earlier are not enough. We must add three new symmetry operations:

Translation. A translational operation along one lattice direction gives an identical point.

Screw Axis. Rotation of a lattice point about an axis followed by translation gives an identical point. Namely, rotation by $2\pi/p$ followed by a translation of q/p ($q = 1, 2, \dots, n - 1$) in the direction of the axis is written as p_q . For example, 2_1 indicates twofold rotation followed by a translation of $\frac{1}{2}a$, $\frac{1}{2}b$, or $\frac{1}{2}c$, as shown in Fig. 1.41A. If the axis is threefold, the translation must be $\frac{1}{3}$ or $\frac{2}{3}$, and the symbols are 3_1 and 3_2 , respectively.

Glide Plane. Reflection in a plane followed by translation by $\frac{1}{2}a$, $\frac{1}{2}b$, $\frac{1}{2}c$, as shown in Fig. 1.41B. These planes are indicated by a , b , and c , respectively, n is used for diagonal translation of $(b + c)/2$, $(c + a)/2$, or $(a + b)/2$.

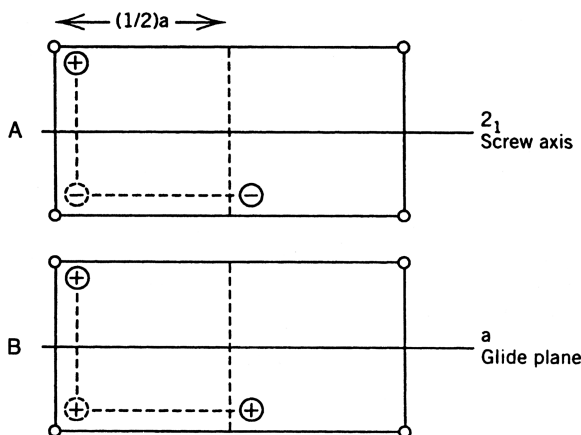


Fig. 1.41. Screw axis and glide plane.

Addition of these symmetry operations results in 230 different combinations which are called “space groups.” Table 1.19 shows the distribution of space groups among the seven crystal systems [136]. Some of these space groups are rarely found in actual crystals. About half of the crystals belong to 13 space groups of the monoclinic system. Space groups can be described by using either Hermann–Mauguin (HM) or Schönflies (S) notations. For example, $P2/m(\equiv C_{2h}^1)$ indicates a primitive lattice with m perpendicular to 2. The first symbol (capital letter) refers to the Bravais lattice (P, A, B, C, F, I, and R), and the next symbol indicates fundamental symmetry elements that lie along the special direction in the crystal. In the case of the monoclinic system, it is the twofold axis. Thus, $P2_1/m(\equiv C_{2h}^2)$ is a primitive cell with m perpendicular to 2_1 . These symbols indicate only the minimum symmetry elements that are necessary to distinguish the space groups. The differences among space groups can be found by comparing the “unit cell maps” given in the *International Tables for X-Ray Crystallography* [137].

1.28. VIBRATIONAL ANALYSIS OF CRYSTALS [48–52]

Because of intermolecular interactions, the symmetry of a molecule is generally lower in the crystalline state than in the gaseous (isolated) state. This change in symmetry may split the degenerate vibrations and activate infrared- (or Raman-) inactive vibrations. Additionally, intermolecular (interionic) interactions in the crystal lattice cause frequency shifts relative to the gaseous state. Finally, the spectra obtained in the crystalline state exhibit *lattice modes*—vibrations due to translatory and rotatory motions of a molecule in the crystalline lattice. Although their frequencies are usually lower than 300 cm^{-1} , they may appear in the high-frequency region as the combination bands with internal modes (see Fig. 2.18, for example). Thus, the vibrational spectra of crystals must be interpreted with caution, especially in the low-frequency region.

To analyze the spectra of crystals, it is necessary to carry out a site group or factor group analysis, as described in the following subsection.

1.28.1. Subgroups and Correlation Tables

For any point group, there are “subgroups” which consist of some, but not all, symmetry elements of the “parent group.” For example, the character table of the point group, C_{3v} (Table 1.6) contains I , C_3 , and σ_v as the symmetry elements. Then, the subgroups of C_{3v} are C_3 , consisting of I and C_3 , and C_s , consisting of I and σ_v only. The relationship between the symmetry species in the “parent group” and those in “subgroups” is given in a “correlation table.” Such correlation tables have already been worked out for all common point groups and are listed in Appendix IX. As an example, the correlation table for C_{3v} is shown below:

C_{3v}	C_3	C_s
A_1	A	A'
A_2	A	A''
E	E	$A' + A''$

TABLE 1.19. The 230 Space Groups

System	Point Groups		Space Group			
	S ^a	HM ^b				
Triclinic	C ₁	1	P1			
	C _i	$\bar{1}$	P $\bar{1}$			
Monoclinic	C ₂ ⁽¹⁻³⁾	2	P2			
	C _S ⁽¹⁻⁴⁾	m	Pm			
	C _{2h} ⁽¹⁻⁶⁾	2/m	P2/m			
	D ₂ ⁽¹⁻⁹⁾	222	P222			
Orthorhombic			I222			
	C _{2v} ⁽¹⁻²²⁾	mm2	Pmm2			
			Pba2			
			Abm2			
			Ima2			
			Pmmm			
			Pcca			
			Pbca			
			Ccca			
			P4			
Tetragonal	C ₄ ⁽¹⁻⁶⁾	4	P4			
	S ₈ ⁽¹⁻²⁾	$\bar{4}$	P $\bar{4}$			
	C _{4h} ⁽¹⁻⁶⁾	4/m	P4/m			
	D ₄ ⁽¹⁻¹⁰⁾	422	P422			
			P4 ₃ 2 ₁ 2			
	C _{4v} ⁽¹⁻¹²⁾	4mm	P4mm			
			P4 ₂ bc			
	D _{2d} ⁽¹⁻¹²⁾	$\bar{4}2m$	P42m			
			P4n2			
			P4/mmm			
			P4/ncc			
			P4 ₂ /ncm			
			P4 ₂ /nm			
			P4/mnc			
			P4 ₂ /mnc			
			P4 ₂ /nm			
			P4 ₂ /m			
			P4 ₂ c			
			P4 ₂ m			
			P4 ₂ n2			
			P4 ₂ bc			
			P4 ₂ m			
			P4 ₂ n2			
			P4 ₂ /nm			
			P4 ₂ /m			
			P4 ₂ c			
			P4 ₂ m			
			P4 ₂ n2			
			P4 ₂ /nm			
			P4 ₂ /m			
			P4 ₂ c			
			P4 ₂ m			
			P4 ₂ n2			
			P4 ₂ /nm			
			P4 ₂ /m			
			P4 ₂ c			
			P4 ₂ m			
			P4 ₂ n2			
			P4 ₂ /nm			
			P4 ₂ /m			
			P4 ₂ c			
			P4 ₂ m			
			P4 ₂ n2			
			P4 ₂ /nm			
			P4 ₂ /m			

Trigonal	$C_3^{(1-4)}$	3	P_3	$P_{3,1}$	$P_{3,2}$	R_3			
	$C_3^{(1-2)}$	$\bar{3}$	P_3	R_3					
	$D_3^{(1-7)}$	32	$P_{3,12}$	$P_{3,21}$	$P_{3,12}$	$P_{3,21}$	$P_{3,12}$	$P_{3,21}$	R_{32}
	$C_{3v}^{(1-6)}$	3m	$P_{3,1m}$	$P_{3,1c}$	$P_{3,1m}$	$P_{3,1c}$	R_{3m}	R_{3c}	
	$D_{3d}^{(1-6)}$	$\bar{3}m$	$P_{3,1m}$	$P_{3,1c}$	$P_{3,1m}$	$P_{3,1c}$	R_{3m}	R_{3c}	
Hexagonal	$C_6^{(1-6)}$	6	P_6	$P_{6,1}$	$P_{6,5}$	$P_{6,2}$	$P_{6,4}$	$P_{6,3}$	
	$C_{3h}^{(1)}$	$\bar{6}$	P_6						
	$C_6^{(1-2)}$	6/m	P_6/m	$P_{6,3/m}$					
	$D_6^{(1-6)}$	622	$P_{6,22}$	$P_{6,22}$	$P_{6,5,22}$	$P_{6,22}$	$P_{6,4,22}$	$P_{6,3,22}$	
	$C_{6v}^{(1-4)}$	6mm	$P_{6,mm}$	$P_{6,cc}$	$P_{6,3cm}$	$P_{6,3mc}$			
	$D_{3h}^{(1-4)}$	6m2	$P_{6,m2}$	$P_{6,c2}$	$P_{6,2m}$	$P_{6,2c}$			
	$D_{6h}^{(1-4)}$	6/mmm	$P_{6,mmm}$	$P_{6,mcc}$	$P_{6,3/mcm}$	$P_{6,3/mmc}$			
	$T^{(1-5)}$	23	P_{23}	F_{23}	I_{23}	$P_{2,13}$	$I_{2,3}$	P_{a3}	$Ia3$
	$T_h^{(1-7)}$	m3	$Pm3$	$Pm3$	$Fm3$	$Fd3$	$Im3$	P_{a3}	$Ia3$
	$O^{(1-8)}$	432	$P_{4,32}$	$P_{4,2,32}$	$F_{4,32}$	$F_{4,1,32}$	$I_{4,32}$	$P_{4,3,32}$	$P_{4,1,32}$
Cubic			$I_{4,32}$						
	$T_d^{(1-6)}$	$\bar{4}3m$	$P_{4,3m}$	$F_{4,3m}$	$I_{4,3m}$	$P_{4,3n}$	$F_{4,3c}$	$I_{4,3d}$	$Fd3m$
	$O_h^{(1-10)}$	m3m	$Pm3m$	$Pm3n$	$Pm3n$	$Pm3n$	$Fm3m$	$Fm3c$	
			$Fd3c$	$Im3m$	$Ia3d$	$Ph3m$			

^aSchönflies.

^bHermann-Mauguin.

Source: Ref. [136].

A pyramidal XY_3 molecule such as NH_3 belongs to the point group C_{3v} . If one of the Y atoms is replaced by a Z atom, the resulting XY_2Z molecule belongs to the point group C_s . As a result, the doubly degenerate vibration (E) splits into two vibrations ($A' + A''$). These correlation tables are highly important in predicting the effect of lowering of symmetry on molecular vibrations. Chapter 2 includes a number of examples of symmetry lowering by substitution of an atomic group by another group.

1.28.2. Site Group Analysis

According to Halford [138], the vibrations of a molecule in the crystalline state are governed by a new selection rule derived from *site symmetry*—a local symmetry around the center of gravity of a molecule in a unit cell. The site symmetry can be found by using the following two conditions: (1) the site group must be a subgroup of both the space group of the crystal and the molecular point group of the isolated molecule, and (2) the number of equivalent sites must be equal to the number of molecules in the unit cell. Halford derived a complete table that lists possible site symmetries and the number of equivalent sites for 230 space groups. Suppose that the space group of the crystal, the number of molecules in the unit cell (Z), and the point group of the isolated molecule are known. Then, the site symmetry can be found from the *Table of Site Symmetry for the 230 Space Groups*, which was originally derived by Halford. Appendix X gives its modified version by Ferraro and Ziomek [9]. In general, the site symmetry is lower than the molecular symmetry in an isolated state. In some cases, it may be difficult to make an unambiguous choice of site symmetry by the method cited above. Then, Wyckoff's tables on crystallographic data [139] must be consulted.

The vibrational spectra of calcite and aragonite crystals are markedly different, although both have the same composition (Sec. 2.4). This result can be explained if we consider the difference in site symmetry of the CO_3^{2-} ion between these crystals. According to X-ray analysis, the space group of calcite is D_{3d}^6 and Z is 2 Appendix X gives

$$D_3(2), \quad C_{3i}(2), \quad C_3(4), \quad C_i(6), \quad C_2(6), \quad C_1(12)$$

as possible site symmetries for space group D_{3d}^6 (the number in front of point group notation indicates the number of distinct sets of sites, and that in parentheses denotes the number of equivalent sites for each distinct set). Rule 2 eliminates all but $D_3(2)$ and $C_{3i}(2)$. Rule 1 eliminates the latter since C_{3i} is not a subgroup of D_{3h} . Thus, the site symmetry of the CO_3^{2-} ion in calcite must be D_3 . On the other hand, the space group of aragonite is D_{2h}^{16} and Z is 4. Appendix X gives

$$2C_i(4), \quad C_s(4), \quad C_1(8)$$

Since C_i is not a subgroup of D_{3h} , the site symmetry of the CO_3^{2-} ion in aragonite must be C_s . Thus, the D_{3h} symmetry of the CO_3^{2-} ion in an isolated state is lowered to D_3 in

TABLE 1.20. Correlation Table for D_{3h} , D_3 , C_{2v} , and C_s

Point Group	ν_1	ν_2	ν_3	ν_4
D_{3h}	$A'_1(R)$	$A''_2(I)$	$E'(I, R)$	$E'(I, R)$
D_3	$A_1(R)$	$A_2(I)$	$E(I, R)$	$E(I, R)$
C_{2v}	$A_1(I, R)$	$B_1(I, R)$	$A_1(I, R) + B_2(I, R)$	$A_1(I, R) + B_2(I, R)$
C_s	$A'(I, R)$	$A''(I, R)$	$A'(I, R) + A''(I, R)$	$A'(I, R) + A''(I, R)$

calcite and to C_s in aragonite. Then, the selection rules are changed as shown in Table 1.20.

There is no change in the selection rule in going from the free CO_3^{2-} ion to calcite. In aragonite, however, ν_1 becomes infrared active, and ν_3 and ν_4 each split into two bands. The observed spectra of calcite and aragonite are in good agreement with these predictions (see Table 2.4b).

1.28.3. Factor Group Analysis

A more complete analysis including lattice modes can be made by the method of factor group analysis developed by Bhagavantam and Venkatarayudu [140]. In this method, we consider all the normal vibrations for an entire Bravais cell. Figure 1.42 illustrates the Bravais cell of calcite, which consists of the following symmetry elements:

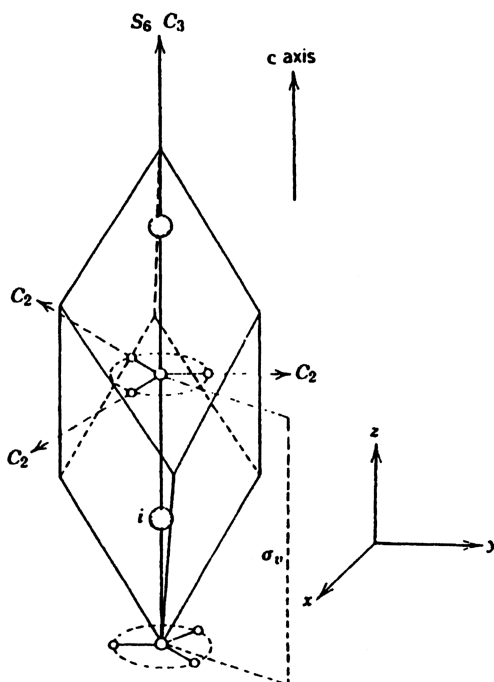


Fig. 1.42. The Bravais cell of calcite.

I , $2S_6$, $2S_6^2 \equiv 2C_3$, $S_6^3 \equiv i$, $3C_2$, and $3\sigma_v$ (glide plane). These elements are exactly the same as those of the point group \mathbf{D}_{3d} , although the last element is a glide plane rather than a plane of symmetry in a single molecule.

As mentioned in Sec. 1.27, it is possible to derive the 230 space groups by combining operations possessed by the 32 crystallographic point groups with operations such as pure translation, screw rotation (translation + rotation), and glide plane reflection (translation + reflection). If we regard the translations that carry a point in a unit cell into the equivalent point in another cell as identity, we define the 230 factor groups that are the subgroups of the corresponding space groups. In the case of calcite, the factor group consists of the symmetry elements described above, and is denoted by the same notation as that used for the space group (\mathbf{D}_{3d}^6). The site group discussed previously is a subgroup of a factor group.

Since the Bravais cell contains 10 atoms, it has $3 \times 10 - 3 = 27$ normal vibrations, excluding three translational motions of the cell as a whole.* These 27 vibrations can be classified into various symmetry species of the factor group \mathbf{D}_{3d}^6 , using a procedure similar to that described in Sec. 1.8 for internal vibrations. First, we calculate the characters of representations corresponding to the entire freedom possessed by the Bravais cell $[\chi_R(N)]$, translational motions of the whole cell $[\chi_R(T)]$, translatory lattice modes $[\chi_R(T')]$, rotatory lattice modes $[\chi_R(R')]$, and internal modes $[\chi_R(n)]$, using the equations given in Table 1.21. Then, each of these characters is resolved into the symmetry species of the point group, \mathbf{D}_{3d} . The final results show that three internal modes (A_{2u} and two E_u), three translatory modes (A_{2u} and two E_u), and two rotatory modes (A_{2u} and E_u) are infrared-active, and three internal modes (A_{1g} and two E_g), one translatory mode (E_g), and one rotatory mode (E_g) are Raman-active. As will be shown in the following sections, these predictions are in perfect agreement with the observed spectra.

1.29. THE CORRELATION METHOD

In the preceding section, we described the application of factor group analysis to the calcite crystal. However, the correlation method developed largely by Fateley et al. [15] is simpler and gives the same results. In this method, intramolecular and lattice vibrations are classified under point groups of molecular symmetry, site symmetry, and factor group symmetry, and correlations are made using the correlation tables given in Appendix IX. In the following, we demonstrate its utility using calcite as an example. For more detailed discussions and applications, the reader should consult the books by Fateley et al. [15] and Ferraro and Ziemeck [9].

1.29.1. The CO_3^{2-} Ion in the Free State

As mentioned in Sec. 1.4, normal vibrations of a molecule can be described in terms of translational motions of the individual atoms along the x , y , and z axes. Thus, the

*These three motions give acoustical modes (Sec. 1.30).

TABLE 1.21. Factor Group Analysis of Calcite Crystal

D_6^6 3_d	I	$2C_6$	$2C_3$	i	$3C_2$	$3C_6$	N	T	T'	R'	n		
			$ $ $2S_6^2$	$ $ S_6^3		$3\sigma_v$							
A_{1g}	1	1	1	1	1	1	1	0	0	0	1		$\alpha_{xx} + \alpha_{yy}, \alpha_{zz}$
A_{1u}	1	-1	1	-1	1	-1	2	0	1	0	1		
A_{2g}	1	1	1	1	-1	-1	3	0	1	1	1		
A_{2u}	1	-1	1	-1	-1	1	4	1	1	1	1		
E_g	2	-1	-1	2	0	0	4	0	1	1	2	T_z	$(\alpha_{xx} - \alpha_{yy}, \alpha_{xy}), (\alpha_{xz}, \alpha_{yx})$
E_u	2	1	-1	-2	0	0	6	1	2	1	2	(T_x, T_y)	
$N_R(p)$	10	2	4	2	4	0	\blacktriangle	\blacktriangle	\blacktriangle	\blacktriangle	\blacktriangle		
$N_R(s)$	4	2	4	2	2	0	\vdots	\vdots	\vdots	\vdots	\vdots		
$N_R(s-v)$	2	0	2	0	2	0	\vdots	\vdots	\vdots	\vdots	\vdots		
$\chi_R(N)$	30	0	0	-6	-4	0	\vdots	\vdots	\vdots	\vdots	\vdots		
$\chi_R(T)$	3	0	0	-3	-1	1	\vdots	\vdots	\vdots	\vdots	\vdots		
$\chi_R(T')$	9	0	0	-3	-1	-1	\vdots	\vdots	\vdots	\vdots	\vdots		
$\chi_R(R')$	6	0	0	0	-2	0	\vdots	\vdots	\vdots	\vdots	\vdots		
$\chi_R(n)$	12	0	0	0	0	0	\vdots	\vdots	\vdots	\vdots	\vdots		

Key:

- p , total number of atoms in the Bravais cell.
 - s , total number of molecules (ions) in the Bravais cell.
 - v , total number of monoatomic molecules (ions) in the Bravais cell.
 - $N_R(p)$, number of atoms unchanged by symmetry operation R .
 - $N_R(s)$, number of molecules (ions) whose center of gravity is unchanged by symmetry operation R .
 - $N_R(s-v)$, $N_R(s)$ minus number of monoatomic molecules (ions) unchanged by symmetry operation R .
 - $\chi_R(N) = N_R(p) \{ \pm (1 + 2 \cos \theta) \}$, character of representation for entire freedom possessed by the Bravais cell.
 - $\chi_R(T) = \pm (1 + 2 \cos \theta)$, character of representation for translation motions of the whole Bravais cell.
 - $\chi_R(T') = \pm (1 + 2 \cos \theta)$, character of representation for translation motions of the whole Bravais cell.
 - $\chi_R(R) = N_R(s-v) \{ \pm (1 + 2 \cos \theta) \}$, character of representation for rotary lattice modes.
 - $\chi_R(n) = \chi_R(N) - \chi_R(T) - \chi_R(T') - \chi_R(R)$, character of representation for internal modes.
- Note that + and - signs are for proper and improper rotations, respectively. The symbol θ should be taken as defined in Sec. 1.8.

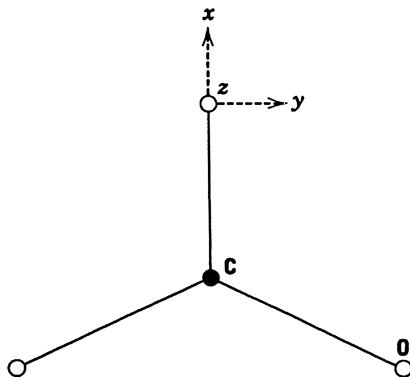


Fig. 1.43. The x , y , and z axes chosen for planar CO_3^{2-} ion.

normal modes of an N -atom molecule can be expressed by using $3N$ translational motions. Furthermore, the symmetry species of these normal modes must correlate with those of the translational motions of an atom located at a particular site within the molecule. Since the latter are known from the molecular structure, the former may be determined directly by using the correlation table.

As an example, consider a planar CO_3^{2-} ion for which the x , y , and z axes are chosen as shown in Fig. 1.43. It is readily seen that the C atom is situated at the \mathbf{D}_{3h} site, whereas the O atom is situated at a site where the local symmetry is only \mathbf{C}_{2v} (\mathbf{I} , \mathbf{C}_2 , σ_h , and σ_v). The translational motions of the C atom under \mathbf{D}_{3h} symmetry are: $T_z(A''_2)$ and $(T_x, T_y)(E')$. The translational motions of the O atom under \mathbf{C}_{2v} symmetry are: $T_x(A_1)$, $T_y(B_2)$ and $T_z(B_1)$. In Table 1.22, the symmetry species of these translational motions are connected by arrows to those of the whole ion using the correlation table. Then, the number of times a particular symmetry species occurs in the total representation is given by the number of arrows that terminate on that species. The number of normal vibrations of the CO_3^{2-} ion in each symmetry species is given by subtracting those of the translational and rotational motions of the whole ion from the total representation. The results are shown at the bottom of Table 1.22.

Thus, the CO_3^{2-} ion exhibits four normal vibrations; $\nu_1(A'_1)$ Raman-active), $\nu_2(A''_2)$ IR-active), $\nu_3(E')$, IR- and Raman-active), and $\nu_4(E')$, IR- and Raman-active). The normal modes of these four vibrations are shown in Fig. 2.8.

In Sec. 1.8, we derived the general method to classify normal vibrations into symmetry species based on group theory. As seen above, this procedure is greatly simplified if we use the correlation method.

1.29.2. Intramolecular Vibrations in the CO_3^{2-} Ion in Calcite

Applying the same principle as that used above, we can classify the normal vibrations of the CO_3^{2-} ion in the calcite lattice by using the correlation method. As discussed in

TABLE 1.22. Correlation Method for the CO_3^{2-} Ion in the Free State

C Atom D_{3h}	CO_3^{2-} Ion D_{3h}	O Atom C_{2v}
	A'_1 $A'_2(R_z)$ A''_1 $A''_2(T_z)$ $E'(T_x, T_y)$ $E''(R_x, R_y)$	$A_1(T_x)$ $B_2(T_y)$ $B_1(T_z)$
$\chi(\text{total}) = A'_1 + A'_2 + 2A''_2 + 3E' + E''$ $\chi(\text{trans}) = A''_2 + E'$ $\chi(\text{rot}) = A'_2 + E''$ $\chi(\text{vib}) = A'_1 + A''_2 + 2E'$		

Sec. 1.28, calcite belongs to the space group D_{3d}^6 , and Z is 2. From the Bravais cell shown in Fig. 1.42, it is readily seen that the CO_3^{2-} ion is at the D_3 site, whereas the Ca^{2+} ion is at the C_{3i} ($\equiv \text{S}_6$) site. Table 1.23 shows the correlations among the molecular symmetry (D_{3h}), site symmetry (D_3), and factor group symmetry (D_{3d}). Under the “Vib.” column, we list the number of vibrations belonging to each species of D_{3h} symmetry (Table 1.22). Throughout the present correlations, the number of degrees of vibrational freedom for all the doubly degenerate species must be multiplied by 2 since there are two E' modes (ν_3 and ν_4). Thus, it is 4 for the E' species. The number under “ f ” indicates “Vib.” times Z ($=2$), which is the number of vibrations of the unit cell. In going from D_{3h} to D_3 , no changes occur

TABLE 1.23. Correlation between Molecular Symmetry, Site Symmetry, and Factor Group Symmetry for Intramolecular Vibrations of CO_3^{2-} Ion in Calcite

f	Vib.	Molecular Symmetry (D_{3h})	Site Symmetry (D_3)	Factor Group Symmetry (D_{3d})	
				C a_m	C a_ζ
2	1	$A'_1 \longrightarrow (\nu_1)$	A_1	1×2	A_{1g} A_{1u} 1×1 1×1
8	4	$E' \longrightarrow (\nu_3, \nu_4)$	E	2×4	E_g E_u 2×2 2×2
2	1	$A''_2 \longrightarrow (\nu_2)$	A_2	1×2	A_{2g} A_{2u} 1×1 1×1

$$\chi(\text{intra}) = A_{1g} + A_{1u} + A_{2g} + A_{2u} + 2E_g + 2E_u.$$

TABLE 1.24. Correlation between Site Symmetry and Factor Group Symmetry for Lattice Vibrations of CO_3^{2-} Ion in Calcite

f	t	Site Symmetry (D_3)	Factor Group Symmetry (D_{3d})	C	a_f
4	2	$E(T_x, T_y)$ (R_x, R_y)	$\rightarrow E_g(R_x, R_y)$	2	1
			$\rightarrow E_u(T_x, T_y)$	2	1
2	1	$A_2(T_z)$ (R_z)	$\rightarrow A_{2g}(R_z)$	1	1
			$\rightarrow A_{2u}(T_z)$	1	1

$$\chi(\text{trans}, \text{CO}_3^{2-}) = E_g + E_u + A_{2g} + A_{2u}.$$

$$\chi(\text{rot}, \text{CO}_3^{2-}) = E_g + E_u + A_{2g} + A_{2u}.$$

except for changes in notations of symmetry species. Column C indicates the degeneracy, and column a_m shows the degree of vibrational freedom contributed by the corresponding molecular symmetry species. Finally, the species under D_3 symmetry are connected to those of the factor group by the arrows using the correlation table. The last column, “ a ”, is the degree of vibrational freedom contributed by the corresponding site symmetry species to the factor group species. It should be noted that the number of degrees of vibrational freedom must be 12 throughout the described correlations above. Such bookkeeping must be carried out for every correlation.

1.29.3. Lattice Vibrations in Calcite

Table 1.24 shows the correlation diagram for lattice vibrations of the CO_3^{2-} ion. The variables “ t ” and “ f ” denote the degrees of translational freedom of the CO_3^{2-} ion for each ion and for the Bravais cell, respectively. The same result is obtained for the rotatory lattice vibrations. Table 1.25 shows the correlation diagram for translatory

TABLE 1.25. Correlation between Site Symmetry and Factor Group Symmetry for Lattice Vibrations of the Ca^{2+} Ion in Calcite

f	t	Site Symmetry (C_{3i})	Factor Group Symmetry (D_{3d})	C	a_f
2	1	$A_u(T_z)$	$\rightarrow A_{1u}$	1	1
			$\rightarrow A_{2u}(T_z)$	1	1
4	2	$E_u(T_x, T_y)$	$\rightarrow E_u(T_x, T_y)$	2	2

$$\chi(\text{trans}, \text{Ca}^{2+}) = A_{1u} + A_{2u} + 2E_u.$$

$$\chi(\text{acoustical}) = A_{2u} + E_u.$$

$$\begin{aligned} \chi(\text{trans, total}) &= \chi(\text{trans}, \text{CO}_3^{2-}) + \chi(\text{trans}, \text{Ca}^{2+}) - \chi(\text{acoustical}) \\ &= A_{1u} + A_{2g} + A_{2u} + E_g + 2E_u. \end{aligned}$$

TABLE 1.26. Distribution of Normal Vibrations of Calcite as Obtained by Correlation Method

Symmetry Species of Factor Group (D_{3d})	Translatory Lattice	Acoustical	Rotatory Lattice	Intramolecular
A_{1g} (Raman)	0	0	0	1
A_{1u}	1	0	0	1
A_{2g}	1	0	1	1
A_{2u} (IR)	1	1	1	1
E_g (Raman)	1	0	1	2
E_u (IR)	2	1	1	2
<i>Total</i>	9	3	6	12

lattice vibrations of the Ca^{2+} ion. No rotatory lattice vibrations exist for single-atom ions such as the Ca^{2+} ion. The distribution of all the translatory lattice vibrations can be obtained by subtracting χ (acoustical) from χ (*trans*, CO_3^{2-}) + χ (*trans*, Ca^{2+}).

1.29.4. Summary

Table 1.26 summarizes the results obtained in Tables 1.23–1.25. The total number of vibrations including the acoustical modes should be 30 since the Bravais cell contains 10 atoms. These results are in complete agreement with that obtained by factor group analysis (Table 1.21).

1.30. LATTICE VIBRATIONS [48]

Consider a lattice consisting of two alternate layers of atoms; atoms 1 of mass M_1 lie on one set of planes and atoms 2 of mass M_2 lie on another set of planes, as shown in Fig. 1.44. For example, such an arrangement is found in the 111 plane of the

TABLE 1.27. Correlation between Site Symmetry (C_{2v}) and Factor Group Symmetry (D_{2h}) for Orthorhombic form of the 123 Conductor^a

f	t	Site Symmetry (C_{2v}), $C_2(z)$	Factor Group Symmetry (D_{2h})	a_f
2	1	$A_1(T_z)$	A_g	1
			$B_{1u}(T_z)$	1
			$B_{2g}(R_y)$	1
2	1	$B_1(T_x, R_y)$	$B_{3u}(T_x)$	1
			$B_{3g}(R_x)$	1
2	1	$B_2(T_y, R_x)$	$B_{2u}(T_y)$	1

^aFor f , t , and a , see Sec. 1.29. The complete correlation table is found in Appendix IX.

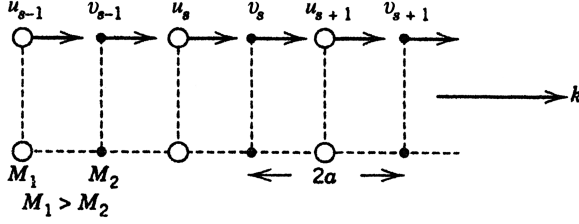


Fig. 1.44. Displacements of atoms 1 and 2 in a diatomic lattice.

NaCl crystal. Let a denote the distance between atoms 1 and 2. Then the length of the primitive cell is $2a$. We consider waves that propagate in the direction shown by the arrow, and assume that each plane interacts only with its neighboring planes. If the force constants (f) are identical between all these neighboring planes, we have

$$M_1 \frac{d^2 u_s}{dt^2} = f(v_s + v_{s-1} - 2u_s) \quad (1.233)$$

$$M_2 \frac{d^2 v_s}{dt^2} = f(u_{s+1} + u_s - 2v_s) \quad (1.234)$$

where u_s and v_s denote the displacements of atoms 1 and 2 in the cell indexed by s .

The solutions for these equations take the form of a traveling wave having different amplitudes u and v . Thus, we obtain

$$u_s = u \exp[i(\omega t + 2ska)] \quad (1.235)$$

$$v_s = v \exp[i(\omega t + 2ska)] \quad (1.236)$$

Here ω is angular frequency, $2\pi\nu$ [in reciprocal seconds (s^{-1})]. If these are substituted in Eqs. 1.233 and 1.234, respectively, we obtain

$$[M_1 \omega^2 - 2f]u + f[1 + \exp(-2ika)]v = 0 \quad (1.237)$$

$$f[1 + \exp(2ika)]u + [M_2 \omega^2 - 2f]v = 0 \quad (1.238)$$

These homogeneous linear equations have a nontrivial solution if the following determinant is zero:

$$\begin{vmatrix} M_1 \omega^2 - 2f & f[1 + \exp(-2ika)] \\ f[1 + \exp(2ika)] & M_2 \omega^2 - 2f \end{vmatrix} = 0 \quad (1.239)$$

By solving this equation, we obtain

$$\omega^2 = f \left(\frac{1}{M_1} + \frac{1}{M_2} \right) + f \left[\left(\frac{1}{M_1} + \frac{1}{M_2} \right)^2 - \frac{4 \sin^2 ka}{M_1 M_2} \right]^{1/2} \quad (1.240)$$

(optical branch)

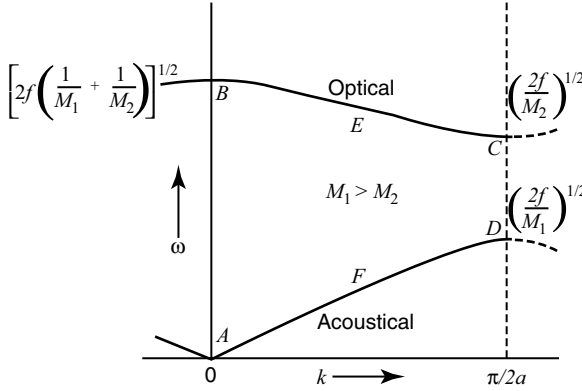


Fig. 1.45. Dispersion curves for lattice vibrations.

$$\omega^2 = f \left(\frac{1}{M_1} + \frac{1}{M_2} \right) - f \left[\left(\frac{1}{M_1} + \frac{1}{M_2} \right)^2 - \frac{4 \sin^2 ka}{M_1 M_2} \right]^{1/2} \quad (1.241)$$

(acoustical branch)

The term k in Eqs. 1.235–1.241 is called the *wavevector* and indicates the phase difference between equivalent atoms in each unit cell. In the case of a one-dimensional lattice, $|k| = k$. Thus, we use k rather than $|k|$ in this case, and k can take any value between $-\pi/2a$ and $+\pi/2a$. This region is called the *first Brillouin zone*. Figure 1.45 shows a plot of ω versus k for the positive half of the first Brillouin zone. There are two values for each ω that constitute the “optical” and “acoustical” branches in the dispersion curves.

At the center of the first Brillouin zone ($k = 0$), we have

$$\omega = 0 \quad \text{and} \quad u = v \quad (\text{acoustical}) \quad (1.242)$$

$$\omega = \sqrt{2f \left(\frac{1}{M_1} + \frac{1}{M_2} \right)} \quad (1.243)$$

$$\text{and} \quad \frac{u}{v} = -\frac{M_2}{M_1} \quad \text{or} \quad M_1 u + M_2 v = 0 \quad (\text{optical})$$

At the end of the first Brillouin zone ($k = \pi/2a$), we have

$$\omega = \sqrt{\frac{2f}{M_2}} \quad \text{and} \quad u = 0 \quad (\text{optical}) \quad (1.244)$$

$$\omega = \sqrt{\frac{2f}{M_1}} \quad \text{and} \quad v = 0 \quad (\text{acoustical}) \quad (1.245)$$

points A, B, C, and D in Fig. 1.45 correspond to Eqs. 1.242, 1.243, 1.244, and 1.245, respectively.

To observe lattice vibrations in IR spectra, the momentum of the IR photon must be equal to that of the phonon.* The momentum of the photon (P) is given by

$$P = \frac{h}{\lambda} = \frac{h/2\pi}{\lambda/2\pi} = \hbar Q \quad (1.246)$$

where $Q = 2\pi/\lambda$. On the other hand, the momentum of the phonon is given by $\hbar k$ [141]. Thus, the following relationship must hold:

$$\hbar Q = \hbar k \quad (1.247)$$

Since lattice vibrations are observed in the low-frequency region ($\lambda \cong 10^{-3}$ cm), $Q = 2\pi/\lambda \cong 10^3$ cm. The k value at the end of the Brillouin zone is $k = \pi/2a \cong 10^8$ cm $^{-1}$. Thus, the k value that corresponds to the IR photon for lattice vibration is much smaller than the k value at the end of the Brillouin zone. This result indicates that the optical transitions we observe in IR spectra occur practically at $k \cong 0$. A similar conclusion can be derived for Raman spectra of lattice vibrations.

Figure 1.46 shows the modes of lattice vibrations corresponding to various points on the dispersion curve shown in Fig. 1.45. At point *A* (acoustical mode), all atoms move in the same direction (translational motion of the whole lattice) and its frequency is zero. This is seen in Fig. 1.46a. In a three-dimensional lattice, there are three such modes. Thus, we subtract 3 from our calculations in factor group analysis (Sec. 1.28).

On the other hand, at point *B* (optical branch), the two atoms move in opposite directions, but the center of gravity of the unit cell remains unshifted (Fig. 1.46b). Furthermore, the equivalent atom in each lattice moves in phase. If the two atoms carry opposite electrical charges, such a motion produces an oscillating dipole moment that can interact with incident IR radiation. Thus, it is possible to observe it optically. It should be noted that the frequency of a diatomic molecule in the free state is $\omega = \sqrt{f/\mu}$, whereas that of a diatomic lattice is $\omega = \sqrt{2f/\mu}$ (μ = reduced mass).

At point *C* (optical branch), the lighter atoms are moving back and forth against each other while the heavier atoms are fixed (Fig. 1.46c). At point *D* (acoustical branch), the situation is opposite to that of point *C*. The vibrational modes in the middle of the Brillouin zone (points *E* and *F*) are shown in Figs. 1.46e and 1.46f, respectively.

Thus far, we have discussed the lattice vibrations of a one-dimensional chain. The treatment of the three-dimensional lattice is basically the same, although more complicated [48]. If the primitive cell contains σ molecules, each of which consists of N atoms, there are 3 acoustical modes and $3N\sigma - 3$ optical modes. The latter is grouped into $(3N - 6)\sigma$ internal modes and $6\sigma - 3$ lattice modes. The general forms of

*The lattice vibration causes elastic waves in crystals. The quantum of the lattice vibrational energy is called "phonon," in analogy with the photon of the electromagnetic wave.

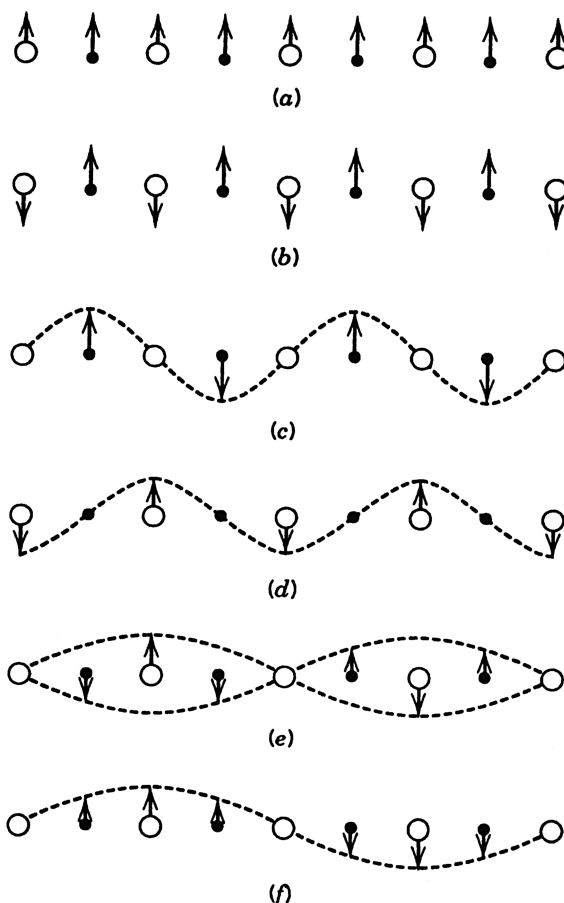


Fig. 1.46. Wave motions corresponding to various points on the dispersion curves.

the dispersion curves of such a crystal are shown in Fig. 1.47. In this book, our interest is focused on vibrational analysis of $3N\sigma-3$ optical modes at $k \cong 0$. Examples are found in diamond and graphite (Sec. 2.14.3) and quartz (Sec. 2.15.2).

1.31. POLARIZED SPECTRA OF SINGLE CRYSTALS

In the preceding section, the 30 normal vibrations of the Bravais cell of calcite crystal have been classified into symmetry species of the factor group \mathbf{D}_{3d} . The results (Table 1.26) show that three intramolecular ($A_{2u} + 2E_u$), three translatory lattice ($A_{2u} + 2E_u$) and two rotatory lattice ($A_{2u} + E_u$) vibrations are IR-active, whereas three intramolecular ($A_{1g} + 2E_g$), one translatory lattice (E_g), and one rotatory lattice (E_g) vibrations are Raman-active. In order to classify the observed bands into these symmetry species, it is desirable to measure infrared dichroism and polarized Raman spectra using single crystals of calcite.

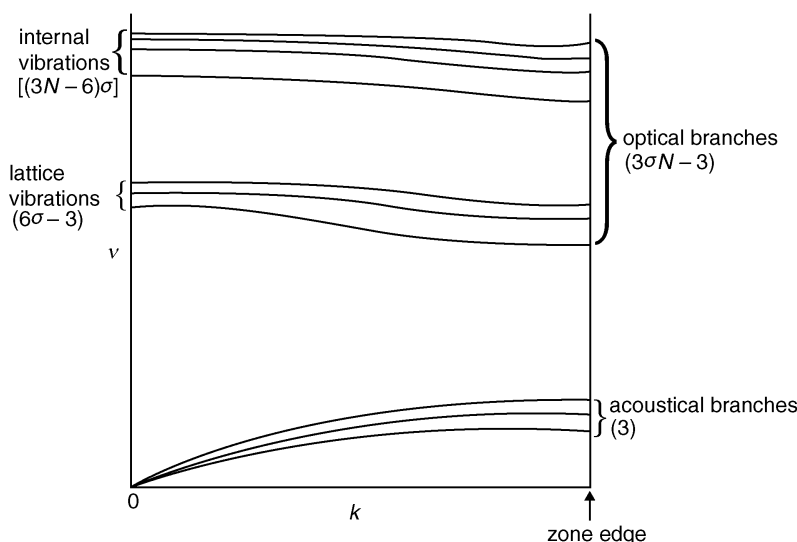


Fig. 1.47. General form of dispersion curves for a molecular crystal [48].

1.31.1. Infrared Dichroism

Suppose that we irradiate a single crystal of calcite with polarized infrared radiation whose electric vector vibrates along the c axis (z direction) in Fig. 1.42. Then the infrared spectrum shown by the solid curve of Fig. 1.48 is obtained [142]. According to Table 1.21, only the A_{2u} vibrations are activated under such conditions. Thus, the three bands observed at $885(\nu)$, $357(t)$, and $106(r)$ cm^{-1} are assigned to the A_{2u} species. The spectrum shown by the dotted curve is obtained if the direction of polarization is perpendicular to the c axis (x,y plane). In this case, only the E_u vibrations should be infrared-active. Therefore the five bands observed at $1484(\nu)$, $706(\nu)$, $330(t)$, $182(t)$, and $106(r)$ cm^{-1} are assigned to the E_u species. Here, ν , t , and r denote intramolecular, translatory lattice, and rotatory lattice modes, respectively.

1.31.2. Polarized Raman Spectra

Polarized Raman spectra provide more information about the symmetry properties of normal vibrations than do polarized infrared spectra [143]. Again consider a single

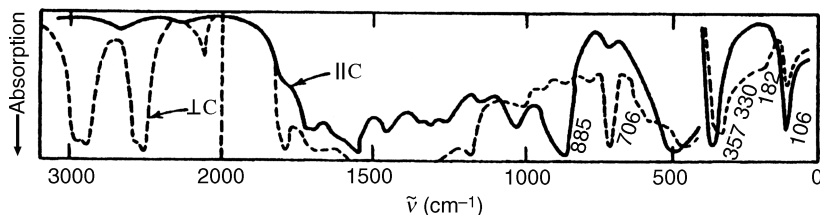


Fig. 1.48. Infrared dichroism of calcite [142].

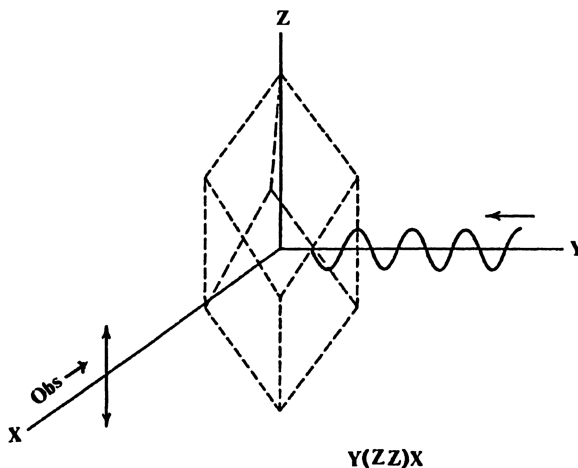


Fig. 1.49. Schematic representation of experimental condition $y(zz)x$.

crystal of calcite. According to Table 1.21, the A_{1g} vibrations become Raman-active if any one of the polarizability components, α_{xx} , α_{yy} , and α_{zz} , is changed. Suppose that we irradiate a calcite crystal from the y direction, using polarized radiation whose electric vector vibrates parallel to the z axis (see Fig. 1.49), and observe the Raman scattering in the x direction with its polarization in the z direction. This condition is abbreviated as $y(zz)x$. In this case, Eq. 1.66 is simplified to $P_z = \alpha_{zz}E_z$ because $E_x = E_y = 0$ and $P_x = P_y = 0$. Since α_{zz} belongs to the A_{1g} species, only the A_{1g} vibrations are observed under this condition. Figure 1.50c illustrates the Raman spectrum obtained with this condition. Thus, the strong Raman line at 1088 cm^{-1} (ν) is assigned to the A_{1g} species. Both the A_{1g} and E_g vibrations are observed if the $z(xx)y$ condition is used. The Raman spectrum (Fig. 1.50a) shows that five Raman lines [$1088(\nu)$, $714(\nu)$, $283(r)$, $156(t)$, and $1434(\nu)\text{ cm}^{-1}$ (not shown)] are observed under this condition. Since the 1088 cm^{-1} line belongs to the A_{1g} species, the remaining four must belong to the E_g species. These assignments can also be confirmed by measuring Raman spectra using the $y(xy)x$ and $x(zx)y$ conditions (Figs. 1.50b and 1.50d).

1.31.3. Normal Coordinate Analysis on the Bravais Cell

In the discussion above, we have assigned several bands in the same symmetry species to the ν , t , and r types. In general, the intramolecular (ν) vibrations appear above 400 cm^{-1} , whereas the lattice vibrations appear below 400 cm^{-1} . However, more complete assignments can be made only via normal coordinate analysis on the entire Bravais cell [144]. Such calculations have been made by Nakagawa and Walter [145] on crystals of alkali-metal nitrates that are isomorphous with calcite. These workers employed four intramolecular and seven intermolecular force constants. The latter are in the range of $0.12\text{--}0.00\text{ mdyne/\AA}$. Figure 1.51 illustrates the vibrational modes of the 18 (27 if E modes are counted as 2) optically active vibrations together with the corresponding frequencies of calcite.

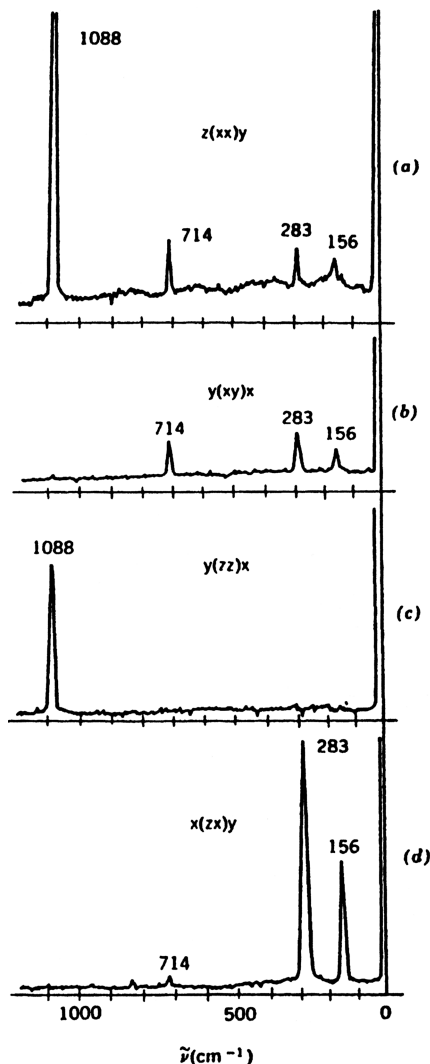


Fig. 1.50. Polarized Raman spectra of calcite [143].

1.32. VIBRATIONAL ANALYSIS OF CERAMIC SUPERCONDUCTORS

In 1987, Wu et al. [146] synthesized a ceramic superconductor of the composition, $\text{YBa}_2\text{Cu}_3\text{O}_{7-\delta}$, whose superconducting critical temperature (T_c) was above the boiling point of liquid nitrogen (77 K). Since then, IR and Raman spectra of this and related compounds have been studied extensively, and the results are reviewed by Ferraro and Maroni [147, 148]. Here, we limit our discussion to the Raman spectra of the superconductor mentioned above and their significance in studying oxygen deficiency and the structural changes resulting from it.

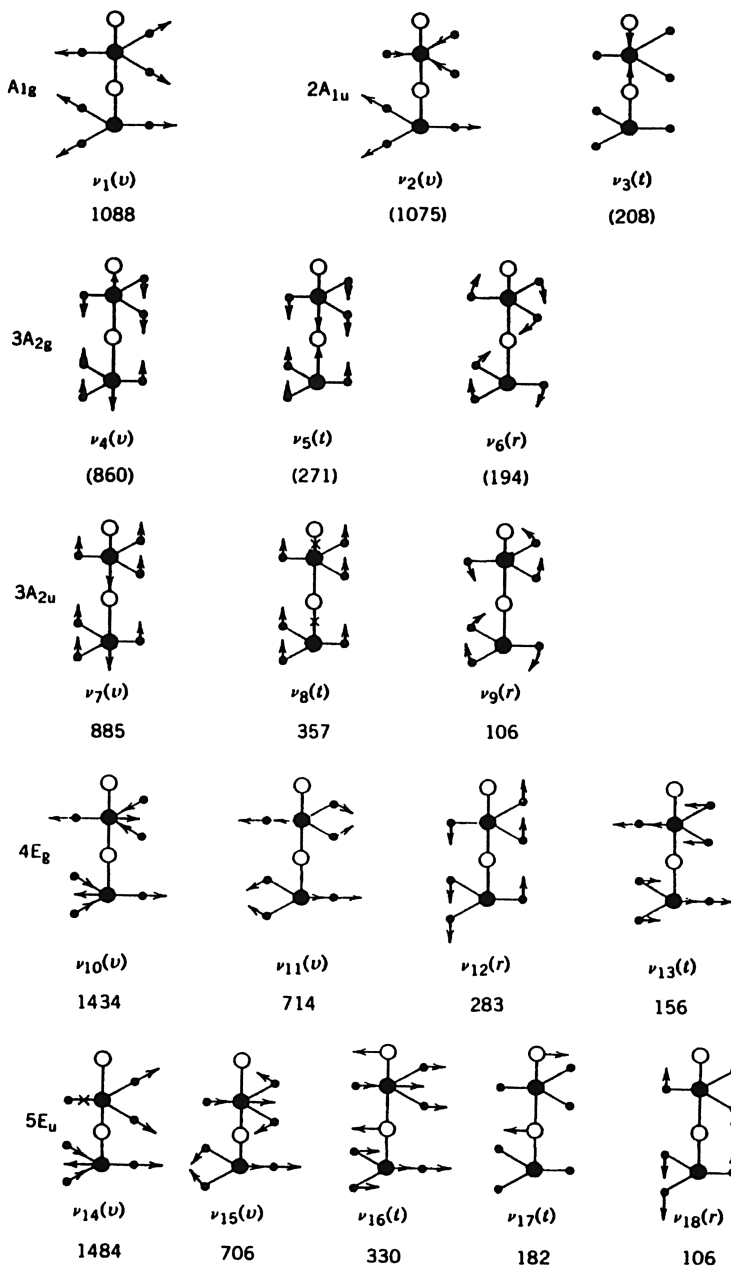


Fig. 1.51. Vibrational modes of calcite. The observed and calculated (in parentheses) are listed under each mode [145].

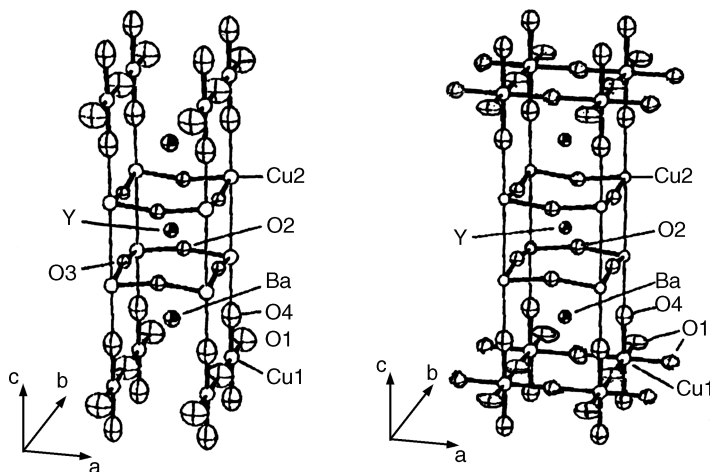


Fig. 1.52. The Bravais unit cells of the orthorhombic and tetragonal forms of $\text{YBa}_2\text{Cu}_3\text{O}_{7-\delta}$ [149].

The superconductor, $\text{YBa}_2\text{Cu}_3\text{O}_{7-\delta}$ (abbreviated as the 123 conductor), can be obtained by baking a mixture of Y_2O_3 , and BaCO_3 , and CuO in a proper ratio. The product is normally a mixture of an orthorhombic form ($0 < \delta < 1$) which is superconducting and a tetragonal form ($\delta = 1$) that is an insulator. The T_c increases as δ approaches 0.

Figure 1.52 shows the Bravais unit cells of the orthorhombic ($Pmmm = D_{2h}^1$) and tetragonal ($P4/mmm = D_{4h}^1$) forms. The former is a distorted, oxygen-deficient form of perovskite. The orthorhombic unit cell contains 13 atoms, and their possible site symmetries can be found from the tables of site symmetries (Appendix X) as follows:

$$8D_{2h}(1), \quad 12C_{2v}(2), \quad 6C_s(4), \quad C_1(8)$$

It is seen in Fig. 1.52 that the three atoms, Y, O(1), and Cu(1), are at the D_{2h} sites. These atoms contribute $3B_{1u} + 3B_{2u} + 3B_{3u}$ vibrations since T_x , T_y , and T_z belong to the B_{3u} , B_{2u} , and B_{1u} species, respectively, in the D_{2h} point group. On the other hand, the 10 atoms, 2Ba, 2Cu(2), 2O(2), 2O(3), and 2O(4) are at the C_{2v} sites. As shown in Table 1.27, each pair of these atoms possess six degrees of vibrational freedom ($2A_1 + 2B_1 + 2B_2$), which are split into $A_g + B_{2g} + B_{3g} + B_{1u} + B_{2u} + B_{3u}$ under D_{2h} symmetry. The number of optical modes at $k \cong 0$ in each species can be obtained by subtracting three acoustical modes ($B_{1u} + B_{2u} + B_{3u}$) from the above counting. Table 1.28 summarizes the results. It is seen that the orthorhombic unit cell has 15 Raman-active modes ($5A_g + 5B_{2g} + 5B_{3g}$) and 21 IR-active modes ($7B_{1u} + 7B_{2u} + 7B_{3u}$). It should be noted that the mutual exclusion rule holds in this case since the D_{2h} point group has a center of symmetry. Although the same results can be obtained by using factor group analysis [150], the correlation method is simpler and straightforward.

Similar calculations on the tetragonal unit cell ($\text{YBa}_2\text{Cu}_3\text{O}_6$) show that 10 vibrations ($4A_{1g} + B_{1g} + 5E_g$) are Raman-active while 11 vibrations ($5A_{2u} + 6E_u$) are IR-active under D_{4h} symmetry.

TABLE 1.28. Vibrational Analysis for Orthorhombic Form of $\text{YBa}_2\text{Cu}_3\text{O}_{7-\delta}$ Using the Correlation Method

D_{2h}	D_{2h} Y, O(1), Cu (1)	C_{2v} Ba, Cu(2), O(2), O(3), O(4)	Acoustical Vib.	Total Optical Vib.	Activity
A_g	0	5	0	5	Raman
B_{1g}	0	0	0	0	Raman
B_{2g}	0	5	0	5	Raman
B_{3g}	0	5	0	5	Raman
A_u	0	0	0	0	Inactive
B_{1u}	3	5	1	7	IR
B_{2u}	3	5	1	7	IR
B_{3u}	3	5	1	7	IR
Total	9	30	3	36	

Figure 1.53 shows the Raman spectrum of a polished sintered pellet of the 123 conductor ($\delta = 0.3$) obtained by Ferraro et al. [151]. The five A_g modes appear strongly, and the most probable assignments for these bands are [152,153].

492 cm^{-1}	Axial motion of the O(4) atoms
445 cm^{-1}	O(2)–Cu(2)–O(3) bending with the two O atoms moving in phase
336 cm^{-1}	O(2)–Cu(2)–O(3) bending with the two O atoms moving out of phase
145 cm^{-1}	Axial motion of the Cu(2) atoms
116 cm^{-1}	Axial motion of the Ba atoms

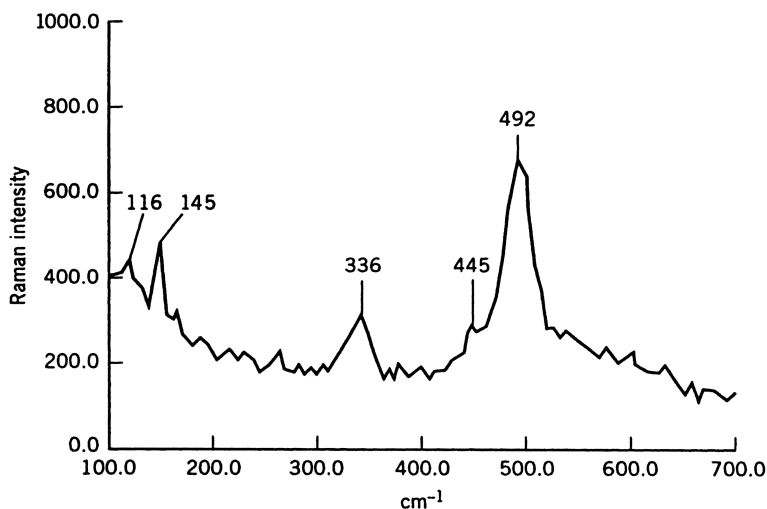


Fig. 1.53. Backscattered Raman spectrum of a polished sintered pellet of $\text{YBa}_2\text{Cu}_3\text{O}_{7-\delta}$ [151].

These values fluctuate within $\pm 10 \text{ cm}^{-1}$ depending on variations in oxygen stoichiometry and crystalline disorder. The results of normal coordinate analysis [154] indicate considerable mixing among the vibrations represented by the Cartesian coordinates of individual atoms.

If the 123 conductor is prepared in pure oxygen and the oxygen is removed quantitatively by heating the sample in argon, a series of samples having $\delta = 0, 0.2, 0.5$, and 0.7 can be obtained. The T_c values of these samples were found to be 94, 77, 50, and 20 K, respectively. Thomsen et al. [155] prepared a series of such samples, and measured their Raman spectra. Figure 1.54 shows a plot of vibrational frequencies of the four A_g modes mentioned above against δ values. It is seen that the two modes at 502 and 154 cm^{-1} are softened and the two modes at 438 and 334 cm^{-1} are hardened as the oxygen is removed from the sample. These results

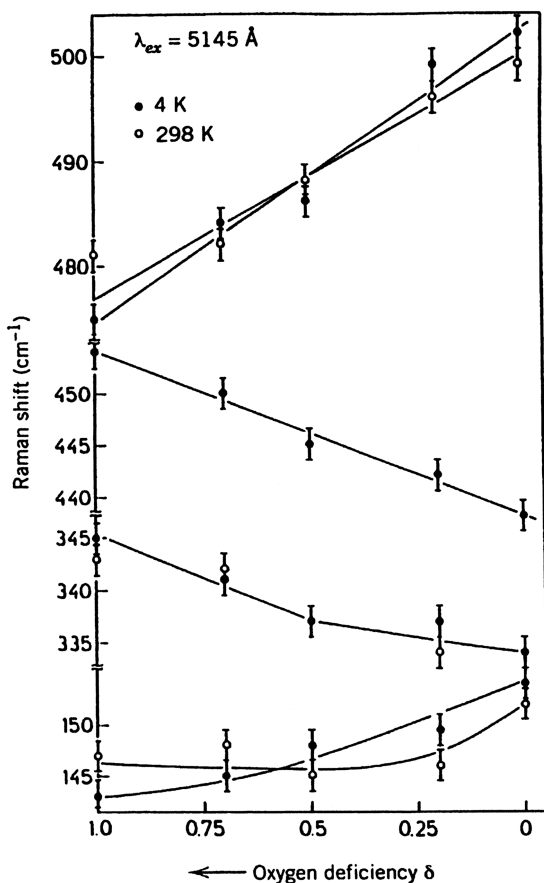


Fig. 1.54. Dependence of four Raman frequencies on oxygen concentration at 4 K and 298 K [155].

seem to suggest that the T_c of the 123 conductor is related to oxygen deficiency in the O(2)–Cu(2)–O(3) layer. The effect of changing the size of the cation (Y) [156] and isotopic substitution ($^{16}\text{O}/^{18}\text{O}$) [157] on these Raman bands has also been studied.

Thus far, IR studies on the 123 conductor have been hindered by the difficulties in obtaining IR spectra from highly opaque samples and in making reliable band assignments [147,148].

REFERENCES

Theory of Molecular Vibrations

1. G. Herzberg, *Molecular Spectra and Molecular Structure, Vol. II: Infrared and Raman Spectra of Polyatomic Molecules*, Van Nostrand, Princeton, NJ, 1945.
2. G. Herzberg, *Molecular Spectra and Molecular Structure, Vol. I: Spectra of Diatomic Molecules*, Van Nostrand, Princeton, NJ, 1950.
3. E. B. Wilson, J. C. Decius, and P. C. Cross, *Molecular Vibrations*, McGraw-Hill, New York, 1955.
4. C. J. H. Schutte, *The Theory of Molecular Spectroscopy, Vol. I: The Quantum Mechanics and Group Theory of Vibrating and Rotating Molecules*, North Holland, Amsterdam, 1976.
5. L. A. Woodward, *Introduction to the Theory of Molecular Vibrations and Vibrational Spectroscopy*, Oxford University Press, London, 1972.
6. J. D. Craybeal, *Molecular Spectroscopy*, McGraw-Hill, New York, 1988.
7. J. M. Hollas, *Modern Spectroscopy*, 2nd ed., Wiley, New York, 1992.
8. M. Diem, *Introduction to Modern Vibrational Spectroscopy*, Wiley, New York, 1993.

Symmetry and Group Theory

9. J. R. Ferraro and J. S. Ziomek, *Introductory Group Theory and Its Application to Molecular Structure*, 2nd ed., Plenum Press, New York, 1975.
10. D. C. Harris and M. D. Bertolucci, *Symmetry and Spectroscopy*, Oxford University Press, London, 1978.
11. P. R. Bunker, *Molecular Symmetry and Spectroscopy*, Academic Press, New York, 1979.
12. F. A. Cotton, *Chemical Application of Group Theory*, 3rd ed., Wiley-Interscience, New York, 1990.
13. R. L. Carter, *Molecular Symmetry and Group Theory*, Wiley, New York, 1992.
14. S. F. A. Kettle, *Symmetry and Structure*, 2nd ed., Wiley, New York, 2000.

Correlation Method

15. W. G. Fateley, F. R. Dollish, N. T. McDevitt, and F. F. Bentley, *Infrared and Raman Selection Rules for Molecular and Lattice Vibrations: The Correlation Method*, Wiley-Interscience, New York, 1972.

Vibrational Intensities

16. W. B. Person and G. Zerbi, eds., *Vibrational Intensities in Infrared and Raman Spectroscopy*, Elsevier, Amsterdam, 1982.

Fourier Transform Infrared Spectroscopy

17. J. R. Ferraro and L. J. Basile, eds., *Fourier Transform Infrared Spectroscopy*, Vol. I, Academic Press, New York, 1978 to present.
18. P. G. Griffiths, and J. A. de Haseth, *Fourier Transform Infrared Spectrometry*, Wiley, New York, 1986.
19. J. R. Ferraro and K. Krishnan, eds., *Practical Fourier Transform Infrared Spectroscopy*, Academic Press, San Diego, CA, 1990.
20. H. C. Smith, *Fundamentals of Fourier Transform Infrared Spectroscopy*, CRC Press, Boca Raton, FL, 1996.

Raman Spectroscopy

21. D. P. Strommen and K. Nakamoto, *Laboratory Raman Spectroscopy*, Wiley, New York, 1984.
22. J. G. Grasselli and B. J. Bulkin, eds., *Analytical Raman Spectroscopy*, Wiley, New York, 1991.
23. H. A. Szymanski, eds., *Raman Spectroscopy: Theory and Practice*, Vol. 1, Plenum Press, New York, 1967; Vol. 2 1970.
24. J. A. Koningstein, *Introduction to the Theory of the Raman Effect*, D. Reidel, Dordrecht (Holland), 1973.
25. D. A. Long, *Raman Spectroscopy*, McGraw-Hill, New York, 1977.
26. J. R. Ferraro, K. Nakamoto, and C. W. Brown, *Introductory Raman Spectroscopy*, 2nd ed., Academic Press, San Diego, CA, 2003.
27. E. Smith, *Modern Raman Spectroscopy*, Wiley, New York, 2004.

Low-Temperature and Matrix Isolation Spectroscopy

28. B. Meyer, *Low-Temperature Spectroscopy*, Elsevier, Amsterdam, 1971.
29. H. E. Hallarn, ed., *Vibrational Spectroscopy of Trapped Species*, Wiley, New York, 1973.
30. M. Moskovits and G. A. Ozin, eds., *Cryochemistry*, Wiley, New York, 1976.

Time-Resolved Spectroscopy

31. G. H. Atkinson, *Time-Resolved Vibrational Spectroscopy*, Academic Press, New York, 1983.
32. M. D. Fayer, ed., *Ultrafast Infrared and Raman Spectroscopy*, Marcel Dekker, New York, 2001.

High-Pressure Spectroscopy

33. J. R. Ferraro, *Vibrational Spectroscopy at High External Pressures—the Diamond Anvil Cell*, Academic Press, New York, 1984.

Vibrational Spectra of Inorganic, Coordination, and Organometallic Compounds

34. J. R. Ferraro, *Low-Frequency Vibrations of Inorganic and Coordination Compounds*, Plenum Press, New York, 1971.
35. L. H. Jones, *Inorganic Spectroscopy*, Vol. I, Marcel Dekker, New York, 1971.
36. R. A. Nyquist and R. O. Kagel, *Infrared Spectra of Inorganic Compounds*, Academic Press, New York, 1971.
37. S. D. Ross, *Inorganic Infrared and Raman Spectra*, McGraw-Hill, New York, 1972.
38. E. Maslowsky, Jr., *Vibrational Spectra of Organometallic Compounds*, Wiley, New York, 1977.

Vibrational Spectra of Organic Compounds

39. N. B. Colthup, L. H. Daly, and S. E. Wiberley, *Introduction to Infrared and Raman Spectroscopy*, 3rd ed., Academic Press, San Diego, CA, 1990.
40. D. Lin-Vien, N. B. Colthup, W. G. Fateley, and J. G. Grasselli, *The Handbook of Infrared and Raman Characteristic Frequencies of Organic Molecules*, Academic Press, San Diego, CA, 1991.

Vibrational Spectra of Biological Compounds

41. A. T. Tu, *Raman Spectroscopy in Biology*, Wiley, New York, 1982.
42. P. R. Carey, *Biochemical Applications of Raman and Resonance Raman Spectroscopies*, Academic Press, New York, 1982.
43. F. S. Parker, *Application of Infrared, Raman and Resonance Raman Spectroscopy in Biochemistry*, Plenum Press, New York, 1983.
44. T. G. Spiro, ed., *Biological Applications of Raman Spectroscopy*, Vols. 1–3, Wiley, New York, 1987–1988.
45. H.-U. Gremlich and B. Yan, eds., *Infrared and Raman Spectroscopy of Biological Materials*, Marcel Dekker, New York, 2001.

Vibrational Spectra of Adsorbed Species

46. A. T. Bell and M. L. Hair, eds., *Vibrational Spectroscopies for Adsorbed Species*, American Chemical Society, Washington, DC, 1980.
47. J. T. Yates, Jr. and T. E. Madey, eds., *Vibrational Spectroscopy of Molecules on Surfaces*, Plenum Press, New York, 1987.

Vibrational Spectra of Crystals and Minerals

48. G. Turrell, *Infrared and Raman Spectra of Crystals*, Academic Press, New York, 1972.
49. V. C. Farmer, *The Infrared Spectra of Minerals*, Mineralogical Society, London, 1974.
50. J. A. Gadsden, *Infrared Spectra of Minerals and Related Inorganic Compounds*, Butterworth, London, 1975.
51. C. Karr, ed., *Infrared and Raman Spectroscopy of Lunar and Terrestrial Minerals*, Academic Press, New York, 1975.

52. J. C. Decius and R. M. Hexter, *Molecular Vibrations in Crystals*, McGraw-Hill, New York, 1977.

Advances Series

53. *Spectroscopic Properties of Inorganic and Organometallic Compounds*, Vol. 1 to present, The Chemical Society, London.
54. *Molecular Spectroscopy—Specialist Periodical Reports*, Vol. 1 to present, The Chemical Society, London.
55. R. J. H. Clark and R. E. Hester, eds., *Advances in Infrared and Raman Spectroscopy*, Vol. 1 to present, Heyden, London.
56. J. Durig, ed., *Vibrational Spectra and Structure*, Vol. 1 to present, Elsevier, Amsterdam.
57. C. B. Moore, ed., *Chemical and Biochemical Applications of Lasers*, Vol. 1 to present, Academic Press, New York.
58. *Structure and Bonding*, Vol. 1 to present, Springer-Verlag, New York.

Index and Collection of Spectral Data

59. N. N. Greenwood, E. J. F. Ross, and B. P. Straughan, *Index of Vibrational Spectra of Inorganic and Organometallic Compounds*, Vols. 1–3, Butterworth, London, 1972–1977.
60. B. Schrader, *Raman/IR Atlas of Organic Compounds*, VCH, New York, 1989.
61. *Sadtler's IR Handbook of Inorganic Chemicals*, Bio-Rad Laboratories, Sadtler Division, Philadelphia, PA, 1996.

Handbooks and Encyclopedia

62. R. A. Ayquist, R. O. Kagel, C. I. Putzig, and M. A. Leugers, *The Handbook of Infrared and Raman Spectra of Inorganic Compounds and Organic Salts*, Vols. 1–4, Academic Press, San Diego, CA, 1996.
63. *Encyclopedia of Spectroscopy and Spectrometry*, 3-vol. set with online version Academic Press, San Diego, CA, 2000.
64. I. R. Lewis and H. G. M. Edwards, eds., *Handbook of Raman Spectroscopy*, Marcel Dekker, New York, 2001.
65. J. M. Chalmers and P. R. Griffiths, eds., *Handbook of Vibrational Spectroscopy*, Vols. 1–5, Wiley, Chichester, UK, 2002.

General

66. W. Holzer, W. F. Murphy, and H. J. Bernstein, *J. Chem. Phys.* **52**, 399 (1970).
67. C. F. Shaw, III, *J. Chem. Educ.* **58**, 343 (1981).
68. R. M. Badger, *J. Chem. Phys.* **2**, 128 (1934).
69. W. Gordy, *J. Chem. Phys.* **14**, 305 (1946).
70. D. R. Herschbach and V. W. Laurie, *J. Chem. Phys.* **35**, 458 (1961).
71. K. Nakamoto, M. Margoshes, and R. E. Rundle, *J. Am. Chem. Soc.* **77**, 6480 (1955).
72. E. M. Layton, Jr., R. D. Cross, and V. A. Fassel, *J. Chem. Phys.* **25**, 135 (1956).

73. F. D. Hardcastle and I. E. Wachs, *J. Raman Spectrosc.* **21**, 683 (1990).
74. F. D. Hardcastle and I. E. Wachs, *J. Phys. Chem.* **95**, 5031 (1991).
75. D. P. Strommen and E. R. Lippincott, *J. Chem. Educ.* **49**, 341 (1972).
76. G. C. Lie, *J. Chem. Educ.* **56**, 636 (1979).
77. H. Eyring, J. Walter, and G. E. Kimball, *Quantum Chemistry*, 5th ed., Wiley, New York, 1949, p. 121.
78. E. B. Wilson, *J. Chem. Phys.* **7**, 1047 (1939); **9**, 76 (1941).
79. J. C. Decius, *J. Chem. Phys.* **16**, 1025 (1948).
80. T. Shimanouchi, *J. Chem. Phys.* **25**, 660 (1956).
81. T. Shimanouchi, "The Molecular Force Field," in D. Henderson, ed., *Physical Chemistry: An Advanced Treatise*, Vol. 4, Academic Press, New York, 1970.
82. T. Shimanouchi, *J. Chem. Phys.* **17**, 245, 734, 848 (1949).
83. D. F. Heath and J. W. Linnett, *Trans. Faraday Soc.* **44**, 556, 873, 878, 884 (1948); **45**, 264 (1949).
84. J. Overend and J. R. Scherer, *J. Chem. Phys.* **32**, 1289, 1296, 1720 (1960); **33**, 446 (1960); **34**, 547 (1961); **36**, 3308 (1962).
85. T. Shimanouchi, *Pure Appl. Chem.* **7**, 131 (1963).
86. J. H. Schachtschneider, "Vibrational Analysis of Polyatomic Molecules," Pts. V and VI, Tech. Rept. 231-64 and 53-65, Shell Development Co., Emeryville, CA, 1964 and 1965.
87. K. Nakamoto, *Angew. Chem.* **11**, 666 (1972).
88. N. Mohan, K. Nakamoto, and A. Müller, "The Metal Isotope Effect on Molecular Vibrations," in R. J. H. Clark and R. E. Hester, eds., *Advances in Infrared and Raman Spectroscopy*, Vol. 1, Heyden, London, 1976.
89. K. Nakamoto, K. Shobatake, and B. Hutchinson, *Chem. Commun.* 1451 (1969).
90. J. Takemoto and K. Nakamoto, *Chem. Commun.* 1017 (1970).
91. J. R. Kincaid and K. Nakamoto, *Spectrochim. Acta.* **32A**, 277 (1976).
92. P. M. Champion, B. R. Stallard, G. C. Wagner, and I. C. Gunsalus, *J. Am. Chem. Soc.* **104**, 5469 (1982).
93. Y. Morino and K. Kuchitsu, *J. Chem. Phys.* **20**, 1809 (1952).
94. B. L. Crawford and W. H. Fletcher, *J. Chem. Phys.* **19**, 141 (1951).
95. P. LaBonville and J. M. Williams, *Appl. Spectrosc.* **25**, 672 (1971).
96. D. A. Ramsey, *J. Am. Chem. Soc.* **74**, 72 (1952).
97. D. P. Strommen and K. Nakamoto, *Appl. Spectrosc.* **37**, 436 (1983).
98. T. G. Spiro and T. C. Strekas, *Proc. Natl Acad. Sci. USA.* **69**, 2622 (1972).
99. W. M. McClain, *J. Chem. Phys.* **55**, 2789 (1971).
100. D. P. Strommen, *J. Chem. Educ.* **69**, 803 (1992).
101. W. Kiefer, *Appl. Spectrosc.* **28**, 115 (1974).
102. M. Mingardi and W. Siebrand, *J. Chem. Phys.* **62**, 1074 (1975).
103. A. C. Albrecht, *J. Chem. Phys.* **34**, 1476 (1961).
104. S. A. Asher, *Anal. Chem.* **65**, 59A, 201A (1993).
105. W. Kiefer and H. J. Bernstein, *J. Raman Spectrosc.* **1**, 417 (1973).
106. R. J. H. Clark and P. D. Mitchell, *J. Am. Chem. Soc.* **95**, 8300 (1973).

107. L. A. Nafie, P. Stein, and W. L. Peticolas, *Chem. Phys. Lett.* **12**, 131 (1971).
108. Y. Hirakawa and M. Tsuboi, *Science* **188**, 359 (1975).
109. T. G. Spiro, R. S. Czernuszewicz, and X.-Y. Li, *Coord. Chem. Rev.* **100**, 541 (1990).
110. X.-Y. Li, R. S. Czernuszewicz, J. R. Kincaid, P. Stein, and T. G. Spiro, *J. Phys. Chem.* **94**, 47 (1990).
- 110a. Y. Mizutani, Y. Uesugi, and T. Kitagawa, *J. Chem. Phys.* **111**, 8950 (1999).
111. H. Hamaguchi, I. Harada, and T. Shimanouchi, *Chem. Phys. Lett.* **32**, 103 (1975).
112. H. Hamaguchi, *J. Chem. Phys.* **69**, 569 (1978).
113. F. Inagaki, M. Tasunai, and T. Miyazawa, *J. Mol. Spectrosc.* **50**, 286 (1974).
114. P. Pulay, *Mol. Phys.* **17**, 192 (1969); **18**, 473 (1970); P. Pulay and W. Meyer, *J. Mol. Spectrosc.* **40**, 59 (1971).
115. R. G. Parr and W. Yang, *Density Functional Theory of Atoms and Molecules*, Oxford University Press, Oxford, 1989; J. K. Labanowski and J. W. Andzelm, eds., *Density Functional Methods in Chemistry*, Springer, Berlin, 1990. S. M. Clark, R. L. Gabriel, and D. Ben-Amotz, *J. Chem. Educ.* **27**, 654 (2000).
116. J. B. Foresman and A. Fisch, *Exploring Chemistry with Electronic Structure Method*, 2nd ed., Gaussian Inc., Pittsburgh, PA, 1996.
- 116a. B. G. Johnson and M. J. Fisch, *J. Chem. Phys.* **100**, 7429 (1994).
117. H. D. Stidham, A. C. Vlaservich, D. Y. Hsu, G. A. Guirgis, and J. R. Durig, *J. Raman Spectrosc.* **25**, 751 (1994).
118. W. B. Collier, *J. Chem. Phys.* **88**, 7295 (1988).
119. J. A. Boatz and M. S. Gordon, *J. Phys. Chem.* **93**, 1819 (1989).
120. P. Pulay, *J. Mol. Struct.* **147**, 293 (1995).
121. M. W. Wong, *Chem. Phys. Lett.* **256**, 391 (1996).
122. G. A. Ozin, "Single Crystal and Gas Phase Raman Spectroscopy in Inorganic Chemistry," in S. J. Lippard, ed., *Progress in Inorganic Chemistry*, Vol. 14, Wiley-Interscience, New York, 1971.
123. R. J. H. Clark and D. M. Rippon, *J. Mol. Spectrosc.* **44**, 479 (1972).
124. E. Whittle, D. A. Dows, and G. C. Pimentel, *J. Chem. Phys.* **22**, 1943 (1954).
125. M. J. Linevsky, *J. Chem. Phys.* **34**, 587 (1961).
126. D. E. Milligan and M. E. Jacox, *J. Chem. Phys.* **38**, 2627 (1963).
127. D. Tevault and K. Nakamoto, *Inorg. Chem.* **14**, 2371 (1975).
128. S. P. Willson and L. Andrews, "Matrix Isolation Infrared Spectroscopy," in J. M. Chalmers and P. R. Griffiths, eds., *Handbook of Vibrational Spectroscopy*, Vol. 2, Wiley, London, 2002, p. 1342.
129. B. Liang, L. Andrews, N. Ismail, and C. J. Marsden, *Inorg. Chem.* **41**, 2811 (2002).
130. M. Zhou and L. Andrews, *J. Phys. Chem. A* **103**, 2964 (1999).
131. D. Tevault and K. Nakamoto, *Inorg. Chem.* **15**, 1282 (1976).
132. B. S. Ault, *J. Phys. Chem.* **85**, 3083 (1981).
133. T. Watanabe, T. Ama, and K. Nakamoto, *J. Phys. Chem.* **88**, 440 (1984).
134. K. Bajdor and K. Nakamoto, *J. Am. Chem. Soc.* **106**, 3045 (1984).
135. G. Burns and A. M. Glazer, *Space Groups for Solid State Scientists*, Academic Press, New York, 1978, p. 81.

136. J. M. Robertson, *Organic Crystals and Molecules*, Cornell University Press, Ithaca, NY, 1953, p. 44.
137. *International Tables for X-Ray Crystallography*, Knoch Press, Birmingham, UK, 1952.
138. R. S. Halford, *J. Chem. Phys.* **14**, 8 (1946).
139. R. W. C. Wyckoff, *Crystal Structures*, Vols. I and II, Wiley-Interscience, New York, 1964.
140. S. Bhagavantam and T. Venkatarayudu, *Proc. Indian Acad. Sci.* **9A**, 224 (1939). *Theory of Groups and Its Application to Physical Problems*, Andhra University, Waltair, India, 1951.
141. C. Kittel, *Introduction to Solid State Physics*, 5th ed., Wiley, New York, 1976, p. 118.
142. M. Tsuboi, *Infrared Absorption Spectra*, Vol. 6, Nankodo, Tokyo, 1958, p. 41.
143. S. P. Porto, J. A. Giordmaine, and T. C. Damen, *Phys. Rev.* **147**, 608 (1966).
144. T. Shimanouchi, M. Tsuboi, and T. Miyazawa, *J. Chem. Phys.* **35**, 1597 (1961).
145. I. Nakagawa and J. L. Walter, *J. Chem. Phys.* **51**, 1389 (1969).
146. M. K. Wu, J. R. Ashburn, C. J. Torng, P. H. Hor, R. L. Meng, L. Gao, Z. J. Huang, Y. Q. Wang, and C. W. Chu, *Phys. Rev. Lett.* **55**, 908 (1987).
147. J. R. Ferraro and V. A. Maroni, *Appl Spectrosc.* **44**, 351 (1990).
148. V. A. Maroni and J. R. Ferraro, *Practical Fourier Transform Infrared Spectroscopy*, Academic Press, San Diego, CA, 1990, p. 1.
149. I. K. Schuller and J. D. Jorgensen, *Mater. Res. Soc. Bull.* **14**(1), 27 (1989).
150. J. Hanuza, J. Klamut, R. Horyń, and B. Jeżowska-Trzebiatowska, *J. Mol Struct.* **193**, 57 (1989).
151. J. R. Ferraro and V. A. Maroni, private communication.
152. M. Stavola, D. M. Krol, L. F. Schneemeyer, S. A. Sunshine, J. V. Waszczak, and S. G. Kosinski, *Phys. Rev. B: Condens. Matter [3]* **39**, 287 (1989).
153. Y. Morioka, A. Tokiwa, M. Kikuchi, and Y. Syono, *Solid State Commun.* **67**, 267 (1988).
154. F. E. Bates and J. E. Eldridge, *Solid State Commun.* **64**, 1435 (1987). F. E. Bates, *Phys. Rev.* **B39**, 322 (1989).
155. C. Thomsen, R. Liu, M. Bauer, A. Wittlin, L. Genzel, M. Cardona, E. Schönherr, W. Bauhofer, and W. König, *Solid State Commun.* **65**, 55 (1988).
156. M. Cardona, R. Liu, C. Thomsen, M. Bauer, L. Genzel, W. König, A. Wittlin, U. Amador, M. Barahona, F. Fernandez, C. Otero, and R. Saez, *Solid State Commun.* **65**, 71 (1988).
157. B. Batlogg, R. J. Cava, A. Jarayaman, R. B. van Dover, G. A. Kourouklis, S. Sunshine, D. W. Murphy, L. W. Rupp, H. S. Chen, A. White, K. T. Short, A. M. Majsce, and E. A. Rietman, *Phys. Rev. Lett.* **58**, 2333 (1987).

Chapter 2

Applications in Inorganic Chemistry

2.1. DIATOMIC MOLECULES*

As shown in Sec. 1.3, diatomic molecules have only one vibration along the chemical bond; its frequency in term of wavenumber ($\tilde{\nu}$) is given by

$$\tilde{\nu} = \frac{1}{2\pi c} \sqrt{\frac{K}{\mu}}$$

where K is the force constant, μ the reduced mass and c is the velocity of light. In homopolar XX molecules ($\mathbf{D}_{\infty h}$) the vibration is not infrared-active but is Raman-active, whereas it is both infrared- and Raman-active in heteropolar XY molecules ($\mathbf{C}_{\infty v}$).

2.1.1. Vibrational Frequencies with Anharmonicity Corrections

Tables 2.1a and 2.1b list a number of diatomic molecules and ions of the X_2 and XY types, for which frequencies corrected for anharmonicity (ω_e) and anharmonicity constants ($x_e\omega_e$) are known. The force constants can be calculated directly from these ω_e values.

In the X_2 series, the ω_e values cover a wide range of frequencies, the highest being that of H_2 (4395 cm^{-1}) and the lowest being that of Cs_2 (42 cm^{-1}). Correspondingly,

* Hereafter, the word *molecules* is also used to represent *ions* and *radicals*.

TABLE 2.1a. Harmonic Frequencies and Anharmonicity Constants of X₂-Type Molecules (cm⁻¹)^{a,b}

Molecule	ω_e	$x_e\omega_e$	Ref.	Molecule	ω_e	$x_e\omega_e$	Ref.
H ₂	4395.2	117.91	1	³¹ P ₂	780.4	2.80	1
H ₂ ⁺	4004.77	—	2	⁷⁵ As ₂	429.4	1.12	1
⁷ Li ₂	351.4	2.59	1	⁷⁵ As ₂ ⁺	(314.8)	(1.25)	1
²³ Na ₂	159.2	0.73	1	Sb ₂	269.9	0.59	1
³⁹ K ₂	92.6	0.35	1	²⁰⁹ Bi ₂	172.7	0.32	1,7
⁸⁵ Rb ₂	57.3	0.96	1	¹⁶ O ₂	1580.4	12.07	1
¹³³ Cs ₂	42.0	0.08	1	O ₂ ⁺	1876.4	16.53	1
¹¹ B ₂	1051.3	9.4	1	³² S ₂	725.68	2.85	1
Al ₂	297.5	1.69	3	⁸⁰ Se ₂	391.8	1.06	1
¹² C ₂	1641.4	11.67	1	Te ₂	251	0.55	1
Si ₂	548.0	2.2	4	¹⁹ F ₂	916.93	11.32	8
Ge ₂	287.95	0.32	4a,4	³⁵ Cl ₂	559.71	2.70	9
Sn ₂	204.3	0.2	4	³⁵ Cl ₂ ⁺	645.3	2.90	1
²⁰⁸ Pb ₂	110.20	0.34	5	⁷⁹ Br ₂	325.43	1.10	10
¹⁴ N ₂	2358.54	14.31	6	¹²⁷ I ₂	214.6	0.61	1
¹⁴ N ₂ ⁺	2207.2	16.14	1	Xe ₂ ⁺	124	0.5	11
¹⁵ N ₂	2278.79	13.35	6	Y ₂	184.4	0.30	12
La ₂	236.0	0.9	13	Hf ₂	176.2	>1	18
Ce ₂	245.4	—	14	Re ₂ (ex)	317.1	1.0	19
Pr ₂	244.9	—	14	Co ₂	296.8	2.2	20
Nd ₂	148.0	0.7	14	Rh ₂	283.9	1.83	21
Gd ₂	138.7	0.3	15	⁵⁸ Ni ₂	259.2	1.9	22
Tb ₂	137.6	0.31	16	Ag ₂	151.39	0.7	23
Lu ₂	121.6	0.16	17				

^aThe compounds are listed in the order of the periodic table beginning with the first atom: IA, IIA, . . . , IB, IIB, and so on.

^bValues in parentheses are uncertain. The ω_e and $x_e\omega_e$ values are rounded off two decimals.

the $x_e\omega_e$ value is largest for H₂ (117.91 cm⁻¹) and smallest for Cs₂ (0.08 cm⁻¹). Extensive studies on hydrides show that their frequencies span from 4395 cm⁻¹ (H₂) to 891 cm⁻¹ (HCs). These tables also contain many isotopic frequencies involving light as well as heavy atoms. The effects of changing the mass and/or force constant in a series of diatomic molecules have been discussed in Sec. 1.3. Similar series are found in these tables. For example, we find that (all in units of cm⁻¹)

$$\text{Li}_2 (351.4) > \text{Na}_2 (159.2) > \text{K}_2 (92.6) > \text{Rb}_2 (57.3) > \text{Cs}_2 (42.0)$$

$$\text{HBe} (2058.6) > \text{HMg} (1495.3) > \text{HCa} (1298.4) > \text{HSr} (1206.9) > \text{HBa} (1168.4)$$

Across the periodic table, we find that

$$\text{HB} (\sim 2366) < \text{HC} (2860.4) < \text{HN} (\sim 3300) < \text{HO} (3735.2) < \text{HF} (4138.6)$$

The frequency decreases on removal of bonding electrons:

$$\text{N}_2 (2358.5) > \text{N}_2^+ (2207.2), \quad \text{As}_2 (429.4) > \text{As}_2^+ (314.8)$$

TABLE 2.1b. Harmonic Frequencies and Anharmonicity Constants of XY-Type Molecules (cm⁻¹)^{a,b}

Molecule	ω_e	$x_e\omega_e$	Ref.	Molecule	ω_e	$x_e\omega_e$	Ref.
HD	3817.1	94.96	1	H ¹³⁸ Ba	1168.43	14.61	37,38
DD	3118.5	64.10	1	DBa	829.84	7.37	36
H ⁶ Li	1420.12	23.66	24–26	HSc	1546.97	—	39
H ⁷ Li	1405.51	23.18	24,25	DSc	1141.27	12.38	39
D ⁶ Li	1074.33	13.54	24,26	HMn	1546.85	27.60	40
D ⁷ Li	1054.94	13.05	24	HCo	1858.79	—	41
H ²³ Na	1171.76	19.52	27,28	HNi	2000	40	42
D ²³ Na	845.97	9.98	29	HCu	1940.4	37	42
H ³⁹ K	985.67	14.90	29,30	H ¹⁰⁷ Ag	1759.67	33.93	43
H ⁸⁵ Rb	937.10	14.28	31	D ¹⁰⁹ Ag	1250.68	17.21	44
D ⁸⁵ Rb	666.66	7.06	29	H ¹⁹⁷ Au	2305.0	43.12	1
H ⁸⁷ Rb	936.98	14.27	31	H ⁶⁴ Zn	1615.72	59.62	45
H Cs	891.25	12.82	32	D ⁶⁴ Zn	1147.36	28.72	36
D ¹³³ Cs	632.80	6.34	29	H ¹¹⁰ Cd	1461.13	61.99	1
H ⁹ Be	2058.6	35.5	1	D ¹¹⁶ Cd	1032.04	29.29	36
H ²⁴ Mg	1495.26	31.64	33	H Hg	1387.1	83.01	1
D ²⁴ Mg	1078.14	16.15	33	D Y	1089.12	9.85	46
H Ca	1298.40	19.18	34	D Cr	1183.20	15.60	47
H ⁸⁸ Sr	1206.89	17.03	35	H ¹¹ B	(2366)	(49)	1
D ⁸⁸ Sr	858.85	8.64	36	H ²⁷ Al	1682.4	29.11	48,49
D ²⁷ Al	1211.77	15.06	49	D ¹⁶ O	2720.9	44.2	1,70
H ⁶⁹ Ga	1603.96	28.42	50,51	(D O) ⁻	2723.5	49.72	70
D ⁷¹ Ga	1142.77	14.42	44,51	HS	2696,25	48.74	71
H ¹¹⁵ In	1475.43	25.16	52,53	(H ³² S) ⁻	2647.1	53.28	72
D ¹¹⁵ In	1048.60	12.70	44	H Se	2421.72	44.60	73
H ²⁰⁵ Tl	1391.27	23.10	54	H ¹⁹ F	4138.55	90.07	1
D ²⁰⁵ Tl	987.04	11.67	44	D ¹⁹ F	2998.3	45.71	1
H ¹² C	2860.4	64.11	55	H ³⁵ Cl	2991.0	52.85	74
D ¹² C	2101.0	34.7	1,56	D ³⁵ Cl	2145.2	27.18	74,75
H ²⁸ Si	2042.5	35.67	57	D ³⁷ Cl	2141.97	27.08	75
H Ge	1831.85	32.86	58,59	H Br	2649.7	45.21	1
H ¹²⁰ Sn	1655.49	28.83	60–62	H I	2309.5	39.73	1
H ²⁰⁸ Pb	1560.53	28.79	63	(H ¹³² Xe) ⁺	2270.0	41.33	76
H ¹⁴ N	(3300)	—	1	⁷ Li O	799.07	—	77
D N	2399.13	42.11	64	⁶ Li F	964.31	9.20	78
(H ¹⁴ N) ⁻	3191.5	85.6	65	⁷ Li F	906.2	7.90	79,78
H P	2363.77	43.91	64	⁷ Li Cl	641.1	4.2	79
H As	2076.93	39.22	66	⁷ Li Br	563.2	3.53	79
H ²⁰⁹ Bi	1699.52	31.93	67–69	⁷ Li I	498.2	3.39	79
H ¹⁶ O	3735.2	82.81	1	²³ Na K	123.3	0.40	1
²³ Na Rb	106.6	0.46	1	²⁴ Mg ³⁵ Cl	465.4	2.05	1
²³ Na ¹⁹ F	536.1	3.83	80,81	²⁴ Mg ⁷⁹ Br	373.8	1.34	1
²³ Na Cl	366	2.05	82,83	Mg ¹²⁷ I	[312]	—	1
²³ Na Br	302	1.50	82,84	²⁴ Mg ¹⁶ O	785.1	5.18	1,90,91
²³ Na I	258	1.08	82	Mg S	525.2	2.93	1
K F	426	2.4	85,86	⁴⁰ Ca ¹⁹ F	587.1	2.74	1,92
K Cl	281	1.30	82,83	Ca ³⁵ Cl	369.8	1.31	1
K Br	213	0.80	82	Ca ⁷⁹ Br	285.3	0.86	1
K I	212	0.70	1	Ca ¹²⁷ I	242.0	0.64	1

(continued)

TABLE 2.1b. (Continued)

Molecule	ω_e	$x_e\omega_e$	Ref.	Molecule	ω_e	$x_e\omega_e$	Ref.
Rb ^{133}Cs	49.4	—	1	Ca ^{16}O	732.03	4.83	93,94
^{85}Rb ^{19}F	373.44	1.90	87,85	Sr ^{19}F	500.1	2.21	1,95
Rb Cl	228	0.92	82	Sr ^{35}Cl	302.3	0.95	1
^{132}Cs ^{19}F	352.62	1.63	87	Sr ^{79}Br	216.5	0.51	1
Cs Cl	209	0.75	82	Sr ^{127}I	173.9	0.42	1
^{133}Cs Br	(194)	(2.0)	1	Sr ^{16}O	653.5	4.0	1,96
^{133}Cs ^{127}I	142	(1.2)	1,88	Ba ^{19}F	468.9	1.79	1,97
^9Be ^{19}F	1265.5	9.12	1	^{138}Ba ^{35}Cl	279.3	0.89	1
^9Be ^{35}Cl	846.65	5.11	1	Ba ^{79}Br	193.8	0.42	1
^9Be ^{16}O	1487.3	11.83	1	Ba I	152.16	0.27	98
^{24}Mg ^{19}F	717.6	3.84	1,89	^{138}Ba O	669.73	2.02	99,90
^{45}Sc ^{16}O	971.6	3.95	1	^{55}Mn ^{16}O	840.7	4.89	1
^{89}Y ^{16}O	852.5	2.45	1	Fe ^{35}Cl	406.6	1.2	1
^{129}La ^{16}O	811.6	2.23	1	Fe ^{16}O	880	5	1
Ce ^{16}O	865.0	2.99	1	Co F	678.18	2.74	103
^{141}Pr ^{16}O	818.9	1.20	1	Co Cl	421.2	0.74	1
Gd ^{16}O	841.0	3.70	1	^{193}Ir N	1126.18	6.29	104
Lu ^{16}O	841.7	4.07	1	Ni Cl	419.2	1.04	1
Yb Cl	293.6	1.23	1	^{63}Cu ^{19}F	622.7	3.95	1
^{48}Ti ^{35}Cl	456.4	6.3	1	^{63}Cu ^{35}Cl	416.9	1.57	1
^{48}Ti ^{16}O	1008.4	4.61	1	^{63}Cu ^{79}Br	314.1	0.87	1
^{90}Zr ^{16}O	936.6	3.45	1	^{63}Cu ^{127}I	264.8	0.71	1
^{180}Hf N	932.72	4.41	100	Cu ^{16}O	628	3	1
V ^{16}O	1012.7	4.9	1	^{107}Ag ^{35}Cl	343.6	1.16	1
Cr F	664.10	4.22	101	^{107}Ag ^{81}Br	247.7	0.68	1
Cr Cl	396.66	—	102	^{107}Ag I	206.2	0.43	1
Cr ^{16}O	898.8	6.5	1	Ag O	493.21	4.10	1
^{55}Mn F	618.8	3.01	1	^{197}Au ^{35}Cl	382.8	1.30	1
^{55}Mn ^{35}Cl	384.9	1.4	1	Zn ^{19}F	(630)	(3.5)	1
^{55}Mn Br	289.7	0.9	1	Zn ^{35}Cl	390.56	1.55	1
Zn Br	(220)	—	1	^{27}Al ^{16}O	978.23	7.12	1,111
^{64}Zn ^{127}I	223.40	0.75	1	Al S	623.13	6.22	112
Cd ^{19}F	(535)	—	1	^{69}Ga F	622.37	3.30	113
Cd ^{35}Cl	330.55	1.2	1	^{69}Ga ^{35}Cl	365.0	1.11	1
Cd Br	230.0	0.50	1	^{69}Ga ^{81}Br	263.0	0.81	1
Cd ^{127}I	178.56	0.63	1	^{69}Ga ^{127}I	216.4	0.5	1
Hg ^{19}F	490.8	4.05	1	Ga As (gr)	215	3	114
Hg ^{35}Cl	292.60	1.60	1	Ga As (ex)	152	2.89	114
^{202}Hg ^{81}Br	186.39	0.98	1	Ga O	767.7	6.34	1
Hg ^{127}I	125.65	1.09	1	In As	182.7	0.5	115
Hg Tl	26.9	0.69	1	^{115}In F	535.36	2.67	116
^{11}B ^{19}F	1402.16	11.82	105	^{115}In ^{35}Cl	317.41	1.01	1
^{11}B ^{35}Cl	839.1	5.11	1	^{115}In ^{81}Br	221.0	0.65	1
^{11}B ^{81}Br	684.15	3.73	106,107	^{115}In ^{127}I	177.1	0.4	1
^{11}B ^{14}N	1514.6	12.3	1,108	In ^{16}O	703.1	3.71	1
^{11}B ^{16}O	1885.4	11.77	1	Tl ^{19}F	475.0	1.89	1,117
Al F	802.32	4.85	105	Tl ^{35}Cl	287.5	1.24	1
^{27}Al ^{35}Cl	481.4	2.03	109	Tl ^{81}Br	192.18	0.39	1
^{27}Al ^{79}Br	378.02	1.28	1,110	Tl ^{127}I	150	—	1
^{27}Al ^{127}I	316.1	1.0	1	(CF) $^+$	1792.76	13.23	118

TABLE 2.1b. (Continued)

Molecule	ω_e	$x_e\omega_e$	Ref.	Molecule	ω_e	$x_e\omega_e$	Ref.
(C Cl) ⁺	1177.7	6.65	119	²⁸ Si Se	580.0	1.78	1
¹² C ³⁵ Cl	846	1.0	1	²⁸ Si Te	481.2	1.30	1
C Br	727.99	3.95	120	(⁷⁹ Ge F) ⁺	815.60	3.22	128
¹² C ¹⁴ N	2068.7	13.14	1	Ge F	666.5	3.15	129
¹² C ³¹ P	1239.75	6.86	1	⁷⁴ Ge ³⁵ Cl	407.6	1.36	1
¹² C ¹⁶ O (gr)	2170.23	13.46	1	Ge Br	296.6	0.9	1
C O (ex)	1743.76	14.57	121	⁷⁴ Ge ¹⁶ O	985.7	4.30	1,130
(¹² C ¹⁶ O) ⁺	2214.24	15.16	1	⁷⁴ Ge ³² S	575.8	1.80	1,131
¹² C ³² S	1285.1	6.5	1,122	⁷⁴ Ge	402.66	0.87	132
¹² C Se	1036.0	4.8	1	⁷⁴ Ge ¹³⁰ Te	323.4	1.0	1
Si C	964.77	5.60	123	Sn ¹⁹ F	582.9	2.69	1
(Si F) ⁺	1050.47	4.95	124	Sn ³⁵ Cl	352.9	1.06	1
²⁸ Si ¹⁹ F	856.7	4.7	1,125	Sn Br	247.7	0.62	1
²⁸ Si ³⁵ Cl	535.4	2.20	1	Sn ¹⁶ O	822.4	3.73	1
[²⁸ Si ³⁵ Cl] ⁺	678.24	—	126	¹²⁰ Sn ³² S	487.23	1.35	133
Si Br	425.4	1.52	1	Sn Se	331.2	0.74	1
²⁸ Si ¹⁴ N	1151.7	6.56	1	Sn Te	259.5	0.50	1
²⁸ Si ¹⁶ O	1242.0	6.05	1	Pb ¹⁹ F	507.2	2.30	1
(Si O) ⁺	1162.18	6.97	127	Pb ³⁵ Cl	303.8	0.88	1
²⁸ Si ³² S	749.5	2.56	1	Pb ⁷⁹ Br	207.55	0.50	1
Pb ¹²⁷ I	160.53	0.25	1	Sb ¹⁴ N	942.05	5.6	1
Pb ¹⁶ O	721.8	3.70	1	Sb ¹⁶ O	817.2	5.30	1
²⁰⁸ Pb ³² S	428.1	1.20	1	Bi N	736.57	4.83	142
Pb Se	277.6	0.51	1	Bi P	430.28	1.53	143
Pb Te	211.8	0.12	1	Bi As	283.30	0.73	143
¹⁴ N ¹⁶ O	1903.9	13.97	1,134	²⁰⁹ Bi ¹⁹ F	510.8	2.05	1,144
¹⁴ N S	1220.0	7.75	1	²⁰⁹ Bi ³⁵ Cl	308.0	0.96	1
¹⁴ N Br	693	5.0	1	²⁰⁹ Bi ⁷⁹ Br	209.3	0.47	1
¹⁴ N ³¹ P	1337.2	6.98	1,135	²⁰⁹ Bi ¹²⁷ I	163.9	0.31	1
¹⁴ N ⁷⁵ As	1068.0	5.36	1	Bi O	688.4	4.8	145
¹⁴ N Sb	942.0	5.6	1	O F	1053.45	10.23	146
P F	846.7	4.49	136	¹⁶ O Cl	(780)	—	1
P Cl	551.4	2.23	137	¹⁶ O Br	713	7	1,147
³¹ P ¹⁶ O	1230.66	6.52	1	¹⁶ O I	(687)	(5)	1
P S.	739.1	2.79	138	¹⁶ O ³² S	1123.7	6.12	1
(As ³⁵ Cl) ⁺	527.7	1.74	139	Se ¹⁶ O	907.1	4.61	1
⁷⁵ As ¹⁶ O	967.4	5.3	1,140	Te ¹⁶ O	796.0	3.50	1
Sb ²⁰⁹ Bi	220.0	0.50	1	¹⁹ F ³⁵ Cl	783.5	4.95	148
Sb ¹⁹ F	614.2	2.77	1,141	¹⁹ F Br	662.3	3.80	148
Sb ³⁵ Cl	369.0	0.92	1,141	Cl Br	442.5	1.5	149
I F	610.26	3.14	150,151	¹²⁷ I ⁷⁹ Br	268.68	0.82	152
¹²⁷ I ³⁵ Cl	384.2	1.47	1				

^a The compounds are listed in the order of the periodic table beginning with the first atom: IA, IIA, . . . , IB, IIB, and so on.

^b Values in parentheses are uncertain, and those in square brackets are observed frequencies without anharmonicity correction. The ω_e and $x_e\omega_e$ values are rounded off to two decimals; (gr) and (ex) indicate the ground and excited states, respectively.

while the opposite trend is found when antibonding electrons are removed:

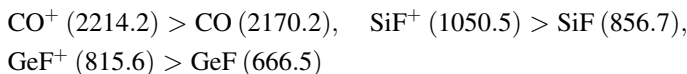
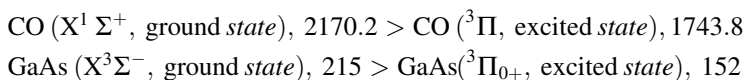


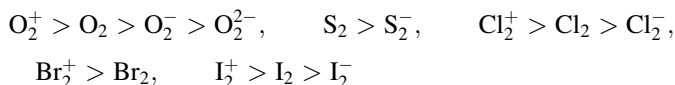
Table 2.1b also presents two examples for which vibrational frequencies were reported for both ground and excited electronic states:



Most of the ω_e and $x_e\omega_e$ values listed in Tables 2.1a and 2.1b were obtained mainly by analysis of rotational–vibrational fine structures of infrared or Raman spectra in the gaseous phase [1]. Their values can also be obtained by the analysis of overtone progression in resonance Raman spectra (Sec. 1.22). Vibrational spectra of unstable (or metastable) molecules were obtained in inert gas matrices (Sec. 1.25). Anharmonicity corrections are limited largely to diatomic molecules because nine parameters are required even for nonlinear triatomic molecules.

2.1.2. Vibrational Frequencies without Anharmonicity Corrections

Table 2.1c lists the observed frequencies of homopolar diatomic molecules, ions, and radicals. Combining these data with those given in Table 2.1a, the following frequency trends are immediately obvious:



As mentioned earlier, these orders can be explained in terms of simple molecular orbital theory. Table 2.1d shows the relationship among various molecular parameters in the $\text{O}_2^+ > \text{O}_2 > \text{O}_2^- > \text{O}_2^{2-}$ series. It is seen that, as the bond order decreases, the bond distance increases, the bond energy decreases, and the vibrational frequency decreases. Although the force constant is not rigorously related to the bond energy (Sec. 1.3), there is an approximate linear relationship between these parameters. Thus, these frequency trends provide valuable information about the nature of diatomic ligands in coordination compounds (see Chapter 3 in Part B). The O_2^+ ion was found in compounds such as $\text{O}_2^+ [\text{MF}_6]^-$ ($\text{M} = \text{As}, \text{Sb}, \text{etc.}$) and $\text{O}_2^+ [\text{M}_2\text{F}_{11}]^-$ ($\text{M} = \text{Nb}, \text{Ta}, \text{etc.}$) [171b], whereas the O_2^- ion was observed in a triangular MO_2 type complex formed by the reaction of alkali metals with O_2 in an Ar matrix [171c]. The $\nu(\text{O}_2)$ of simple metal superoxides ($\text{M}^+ \text{O}_2^-$) and peroxides ($\text{M}^{2+} \text{O}_2^{2-}$) have been measured [171d]. Linear relationships are noted between $\nu(\text{S}_2)$ and S–S bond distances for sulfur compounds [171e].

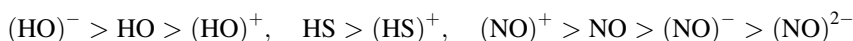
Table 2.1e lists vibrational frequencies of heteropolar diatomic molecules. It contains isotopic pairs such as (HO/DO), ($^6\text{Li}^{35}\text{Cl}/^7\text{Li}^{35}\text{Cl}$), and ($^{28}\text{Si}^{32}\text{S}/^{28}\text{Si}^{34}\text{S}$).

TABLE 2.1c. Observed Frequencies of X₂ Molecules (cm⁻¹)

Molecule	State ^a	$\tilde{\nu}$	Ref.	Molecule	State	$\tilde{\nu}$	Ref.
T ₂ ^b	Liquid	2458	153	Se ₂ ⁻	Solid ^e	349	162
C ₂ ⁻	Gas	1757,8	154	F ₂ ⁻	Mat	475	163
C ₂ ²⁻	Solid ^c	1845	155	³⁵ Cl ₂	Mat	546	164
Sn ₂	Mat	188	156	³⁵ Cl ₂ ⁻	Mat	247	165
Pb ₂	Mat	112	156	Br ₂ ⁺	Sol'n	360	166
P ₂	Gas	775	157	Br ₂	Gas	319	167
As ₂	Gas	421	157	I ₂ ⁺	Sol'n	238	168
¹⁶ O ₂ ^d	Mat	1555.6	158	I ₂	Gas	213	167
O ₂ ⁻	Mat	1097	159	I ₂ ⁻	Mat	115	169
O ₂ ²⁻	Solid	794, 738	160	K ₂	Mat	91.0	169
S ₂	Mat	718	161	Ag ₂	Mat	194	170
S ₂ ⁻	Solid ^e	623	162	Zn ₂	Mat	80	171
				Cd ₂	Mat	58	171

^aMat = inert gas matrix.^bT = ³H (tritium).^cNa salt.^d¹⁶O–¹⁷O, 1528.4 cm⁻¹; ¹⁶O–¹⁸O, 1508.3 cm⁻¹.^eDoped in KCl.

Charge effects on vibrational frequencies are seen for



Most of these frequencies were measured in inert gas matrices at low temperatures. For example, the SH radical was produced by photodecomposition of H₂S in Ar or Kr matrices [182], and the FeH radical was produced *via* the reaction of Fe metal vapor with H₂ in Ar matrices [187] (Sec. 3.26).

2.1.3. Dimers and Polymers

The N₄⁺ ion is linear and centrosymmetric in the ground state, and exhibits a strong IR absorption at 2237.6 cm⁻¹ in Ne matrices [252], and at 2234.51 cm⁻¹ in the gaseous state [253]. Surprisingly, stable AsF₆⁻ salt of the N₅⁺ ion was synthesized, and its

TABLE 2.1d. Relationship between Various Molecular Parameters in the O₂ and Its Ions

Species	Bond Order	Bond Distance (Å) ^a	Bond Energy (Kcal/mole)	$\tilde{\nu}$ (O ₂) (cm ⁻¹)	force Constant (mdyn/Å)
O ₂ ⁺	2.5	1.123	149.4	1876	16.59
O ₂	2.0	1.207	117.2	1580	11.76
O ₂ ⁻	1.5	1.280	—	1094	5.67
O ₂ ²⁻	1.0	1.49	48.8	791/736 ^{b,c}	2.76

^aRef. 171a.^bNa salt.^cSolid-state splitting.

TABLE 2.1e. Observed Frequencies of XY Molecules (cm⁻¹)

Molecule	State ^a	$\tilde{\nu}$	Ref.	Molecule	State	$\tilde{\nu}$	Ref.
H Al	Mat	1593	172	D Cr	Mat	1112	186
H Si	Mat	1967	173	H Fe	Mat	1767.0	187
	Gas	1971.04	174	H Rh	Mat	1920.6	187
H N	Mat	3131.6	175	⁷ Li O	Mat	745	188
H As	Gas	2077.00	176	Li F	Mat	885	189
H O	Mat	3548.2	177	⁶ Li ³⁵ Cl	Gas	686.1	190
D O	Mat	2616.1	177	⁷ Li ³⁵ Cl	Gas	643.0	190
(H O) ⁻	Solid	3637.4	178	⁶ Li ³⁷ Cl	Gas	683.3	190
	Gas	3555.59	179	⁷ Li ³⁷ Cl	Gas	640.1	190
(H O) ⁺	Gas	2956.37	180	Li Br	Mat	510	191
(T O) ⁻	Solid	2225	181	Li I	Mat	433	191
H S	Mat	2607	182	Na F	Mat	515	189
	Gas	2591	183	Na ³⁵ Cl	Gas	364.7	192
D S	Mat	1847.8	183	Mg F	Mat	738	193
(H ³² S) ⁺	Gas	2547.2	184	²⁶ Mg O	Mat	815.4	194
(D ³² S) ⁺	Gas	1829.1	184	Mg O	Gas	774.74	195
H F	Gas	3961.42	185	⁴⁰ Ca O	Mat	707.0	196
H Cr	Mat	1548	186	Ti O	Mat	1005	197
Ti N	Mat	1037	198	Al O	Mat	975	213
Zr O	Mat	975	197	Al F	Mat	793	214
Nb N	Mat	1002.5	199	Ti F	Mat	441	215
Nb O	Mat	968	199	²⁰⁵ Ti ³⁵ Cl	Mat	284.7	216
Ta O	Mat	1020	200	Ti Br	Mat	179	215
W O	Mat	1050.9	201	Ti I	Mat	143	215
Fe C	Gas	852.14	202	C F	Mat	1279	217
⁵⁶ Fe O	Mat	873.1	203		Gas	1286.13	218
Ru O	Mat	834.4	204	C O	Mat	2138.4	219
Co O	Mat	846.4	203	C S	Mat	1274	220
⁵⁸ Ni O	Mat	825.7	203	(C N) ⁻	Sol'n	2080	221
Th N	Mat	934.6	205	C N	Mat	2046	222
U N	Mat	995	206	²⁸ Si Ge	Mat	422.5	223
U O	Mat	820	207	²⁸ Si Sn	Mat	360	223
Pu N	Mat	855.7	208	²⁹ Si N	Gas	1972.80	224
Pu O	Mat	~ 820	209	²⁸ Si O	Mat	1225.9	225
Zn O	Mat	802	210	²⁸ Si ³² S	Gas	749.65	226
Cd O	Mat	719	210	²⁸ Si ³⁴ S	Gas	739.30	226
¹¹ B O	Gas	1861.92	211	⁷⁴ Ge O	Mat	973.4	227
BF	Gas	1378.7	212	⁷⁴ Ge S	Mat	566.6	228
⁷⁴ Ge ⁸⁰ Se	Mat	397.9	228	F O	Mat	1028.7	240
⁷⁴ Ge Te	Mat	317.67	228	Cl N	Mat	818.5	239
Sn O	Mat	816.1	229			825	
¹²⁰ Sn S	Mat	480.5	228	Cl O	Mat	850.7	241
¹²⁰ Sn ⁸⁰ Se	Mat	325.2	228	Br N	Mat	691	239
Pb O	Mat	718.4	230	Br O	Mat	729.9	242
Pb S	Mat	423.1	228	S Cl	Mat	617	243
²⁰⁸ Pb ³² S	Gas	426.6	231	S Br	Mat	518	243
Pb ⁸⁰ Se	Mat	275.1	228	S I	Mat	443	243
(N O) ⁺	Solid	2273	232	Se Te	Mat	313	244
N O	Mat	1880	233	(Cl F) ⁺	Sol'n	819	245
				⁷⁹ Br O	Gas	723.4	246

TABLE 2.1e. (Continued)

Molecule	State ^a	$\tilde{\nu}$	Ref.	Molecule	State	$\tilde{\nu}$	Ref.
(N O) ⁻	Mat	1358–1374	234	(Br O) ⁻	Sol'n	618	247
(N O) ²⁻	Mat	886	235	⁷⁹ Br F	Gas	669.9	248
P N	Mat	1323	236	⁷⁹ Br ³⁵ Cl	Gas	444.3	248
S O	Mat	1101.4	237	I N	Mat	590	249
(S Se) ⁻	Solid	464	238	I F	Gas	610.2	250
F N	Mat	1117	239	I Cl	Gas	381	251
				I Br	Gas	265	251

^aMat = inert gas matrix.

V-shaped (C_{2v}) structure was confirmed by X-ray analysis. Complete assignments of the IR and Raman spectra of the N_5^+ ion have been based on this structure [254,255]. Figure 2.1 shows the low-temperature Raman spectrum of solid $N_5^+AsF_6^-$. A new allotropic form of nitrogen in which all nitrogen atoms are connected by single covalent bonds was produced at temperatures of >2000 K and pressures of >110 GPa [256]. The Raman spectra shown in Fig. 2.2 were obtained at 110 GPa using a diamond anvil cell. At 300 K, a sharp $\nu(N\equiv N)$ peak is seen at 2400 cm^{-1} , which is replaced by a new peak at 840 cm^{-1} when the temperature is raised to 1990 K. The latter frequency is close to the $\nu(N-N)$ of N_2H_4 . The possibility of forming bicyclic N_{10} and fullerene-like N_{60} has been suggested on the basis of theoretical calculations [257].

In inert gas matrices, a variety of aggregates of diatomic molecules are produced, depending on the experimental conditions employed. For example, the Raman spectra of H_2 , HD, and D_2 in Ar matrices suggest the formation of aggregates of more than six molecules after annealing above 35 K [258].

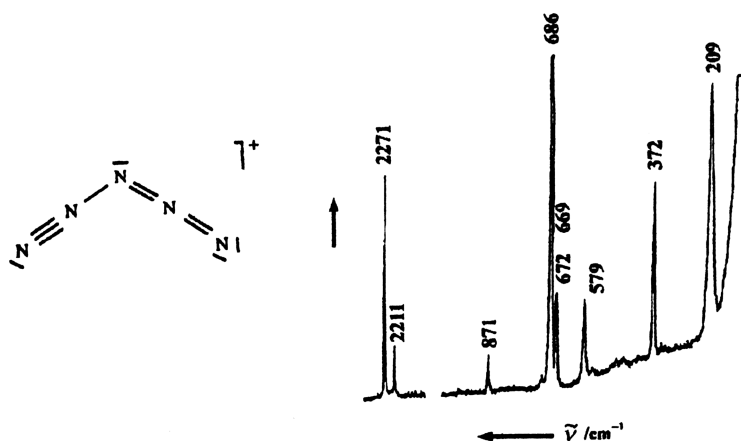


Fig. 2.1. Structure of the N_5^+ ion (a) and low-temperature Raman spectrum (b) of solid $N_5^+AsF_6^-$. The bands between 700 and 250 cm^{-1} are due to the AsF_6^- ion [254,255].

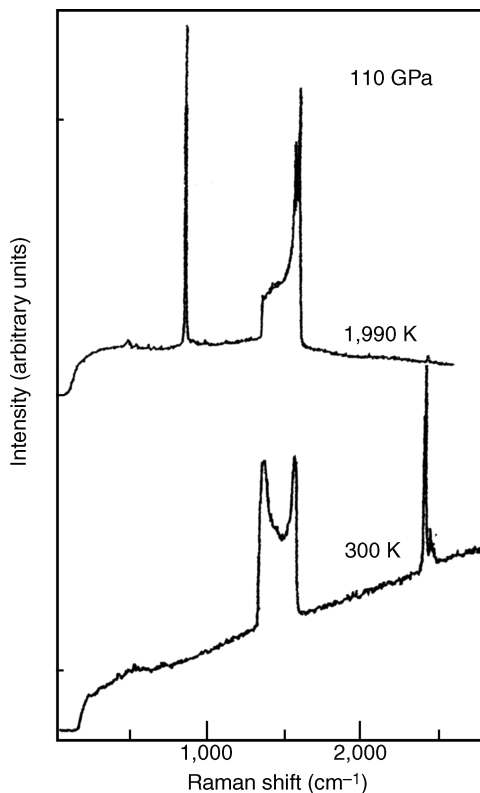
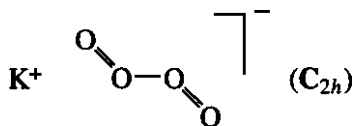


Fig. 2.2. Raman spectra of polymeric nitrogen (cubic gauche structure) before and after heating at 110 GPa. The starting sample (300 K, bottom) is in the molecular phase as indicated by the peak at 2400 cm^{-1} . The bands at $1550\text{--}1300\text{ cm}^{-1}$ are due to the stressed diamond adjacent to the sample. Laser heating to 1990 K (top) transforms it to the polymeric phase with a prominent peak at 840 cm^{-1} [256]. $1\text{ GPa} = 10^4\text{ atm}$.

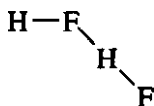
In an Ar matrix, $\text{K}^+(\text{O}_4)^-$ takes the *trans* structure:



and exhibits $\nu(\text{O}=\text{O})$ (A_g), $\nu(\text{O}=\text{O})$ (B_u), $\nu(\text{O}-\text{O})$ (A_g), and $\delta(\text{O}=\text{O}-\text{O})$ at 1291.5, 993, 305, and 131 cm^{-1} , respectively [259,260]. The structure of the O_4 molecule is predicted to be either quasisquare D_{4h} or triangular D_{3h} (similar to the CO_3^{2-} and NO_3^- ions) [262].

The IR spectra of the O_4^- ion in Ne matrices were interpreted as a mixture of a rectangular form (2949 and 1320 cm^{-1}) and a bent-*trans* form (2808 and 1164 cm^{-1}) [262a]. The $[\text{Cl}_4]^+$ ion in solid $[\text{Cl}_4]^+[\text{IrF}_6]^-$ salt assumes a rectangular structure with

two short Cl—Cl (1.94 Å) and two long Cl···Cl (2.93 Å) bonds. The Raman peaks at 578, 175, and 241 cm^{-1} were assigned to the $\nu(\text{Cl—Cl})$, $\nu(\text{Cl}\cdots\text{Cl})$ and $\delta((\text{Cl}\cdots\text{Cl}))$, respectively [262b]. The Raman spectra of $(\text{O}_2)_4$ (\mathbf{D}_{4h} symmetry) at pressure of 32.8 and 33.4 GPa exhibit 4 A_{1g} vibrations at 1600, 1380, 342, and 16 cm^{-1} [262c]. Assignments of the IR spectra of $(\text{HF})_2$ (HF)(DF), and $(\text{DF})_2$ in Ar matrices have been based on the structure [263]



This work has been extended to higher-molecular-weight polymers, $(\text{HF})_3$ and $(\text{HF})_4$ [264].

Matrix IR spectra of $(\text{LiF})_n$ (where $n = 2, 3, 4$) were interpreted in terms of ring structures (rhombic \mathbf{D}_{2h} , \mathbf{D}_{3h} , and \mathbf{D}_{4h} for $n = 2, 3$, and 4, respectively) [265]. The Raman spectrum of $(\text{NaI})_2$ in the gaseous state at 1084 K supports \mathbf{D}_{2h} structure [266]. The matrix IR spectra of $(\text{GeO})_2$ [267] and $(\text{KO})_2$ [268] suggest a rhombic structure (\mathbf{D}_{2h}) and a slightly out-of-plane rhombic structure (\mathbf{C}_{2v}), respectively.

The nitric oxide dimer, $(\text{NO})_2$, in Ar matrices exists as the *cis* form (1862 and 1768 cm^{-1}) or the *trans* form (1740 cm^{-1}), with the $\nu(\text{NO})$ shown in brackets [268a]. The IR spectrum of the *cis* dimer in the gaseous state has been assigned [268b].

IR spectra of *cis* and *trans* isomers of $(\text{NO})_2^+$ ion produced in Ne matrices exhibit the $\nu(\text{NO})$ at 1619 and 1424 cm^{-1} , respectively. The corresponding frequencies of the $(\text{NO})_2^-$ ion produced in Ne matrices are at 1225 (*cis*) and 1227 cm^{-1} (*trans*) [268c]. In the gaseous phase, NO forms a weakly bound “van der Waals” dimer, and the intermolecular vibrations are observed at 429 (δ_a), 239 (δ_s), 134 (intermolecular stretch) and $\sim 117 \text{ cm}^{-1}$ (out-of-plane torsion) [268d].

2.1.4. van der Waals Complexes

Inert gases and hydrogen halides form very weakly interacting van der Waals complexes. As expected, the $\nu(\text{HF})$ of Ne—HF [269] and $\nu(\text{HCl})$ of Ne—HCl [270] are shifted only slightly (+0.4722 and +3024 cm^{-1} , respectively) from their frequencies in the free state. Vibrational frequencies of analogous Ar complexes are also reported [271–275]. IR spectra of van der Waals complexes such as CO—CH_4 [276], CO—OCS [277] and CO—BF_3 [278] are available.

2.2. TRIATOMIC MOLECULES

The three normal modes of linear $\text{X}_3(\mathbf{D}_{\infty h})$ - and $\text{YXY}(\mathbf{D}_{\infty h})$ -type molecules were shown in Fig. 1.11; ν_1 is Raman-active but not infrared-active, whereas ν_2 and ν_3 are infrared-active but not Raman-active (mutual exclusion rule). However, all three

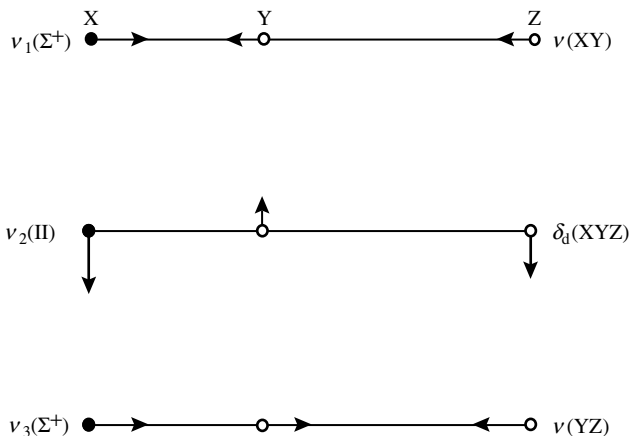


Fig. 2.3. Normal modes of vibration of linear XYZ molecules.

vibrations become infrared- as well as Raman-active in linear XYZ-type molecules ($C_{\infty v}$), shown in Fig. 2.3. The three normal modes of bent $X_3(C_{2v})$ and $YXY(C_{2v})$ -type molecules were also shown in Fig. 1.12. In this case, all three vibrations are both infrared- and Raman-active. The same holds for bent $XXY(C_s)$ - and $XYZ(C_s)$ -type molecules. Section 1.12 describes the procedure for normal coordinate analysis of the bent YXY -type molecule. In the following, vibrational frequencies of a number of triatomic molecules are listed for each class of compounds.

2.2.1. XY_2 -Type Halides

Table 2.2a lists the vibrational frequencies of XY_2 -type halides. Most of these data were obtained in inert gas matrices. It is seen that the majority of compounds follow the trend $\nu_3 > \nu_1$, and that exceptions occur for some bent molecules. Although the structures of these halides are classified either as linear or bent, it should be noted that the bond angles of the latter range from 95° to 170° [315]. Thus, some bent molecules are almost linear. In principle, the distinction between linear and bent structures can be made by IR/Raman selection rules. For example, the ν_1 is IR-active for the bent structure but IR-inactive for the linear structure. However, such a simple criterion may lead to conflicting results [319].

The bond angle (α) of the YXY molecule can be calculated if the ν'_3 of the $YX'Y$ molecule is available. Here, X' is an isotope of X. Using the G and F elements given in Appendix VII, the following equation can readily be derived:

$$\left(\frac{\tilde{\nu}'_3}{\tilde{\nu}_3}\right)^2 = \frac{M_X}{M_{X'}} \left[\frac{M_{X'} + M_Y(1 - \cos\alpha)}{M_X + M_Y(1 - \cos\alpha)} \right]$$

Here M denotes the mass of the atom subscripted. Figure 2.4 shows the spectra of NiF_2 in Ne and Ar matrices obtained by Hastie et al. [320]. Using the ν_3 values

TABLE 2.2a. Vibrational Frequencies of XY₂-Type Metal Halides (cm⁻¹)

Compound ^a	Structure	$\tilde{\nu}_1$	$\tilde{\nu}_2$	$\tilde{\nu}_3$	Ref.
BeF ₂	Linear	(680)	345	1555	279
BeCl ₂	Linear	(390)	250	1135	279
BeBr ₂	Linear	(230)	220	1010	279
BeI ₂	Linear	(160)	(175)	873	279
MgF ₂	Linear	550	249	842	280
MgCl ₂	Linear	327	93	601	280
MgBr ₂	Linear	198	82	497	280
MgI ₂	Linear	148	56	445	280
⁴⁰ CaF ₂	Bent	484.8	163.4	553.7	281
⁴⁰ Ca ³⁵ Cl ₂	Linear	—	63.6	402.3	282
CaI ₂ (g)	Linear	—	43.3	292.3	283
⁸⁶ SrF ₂	Bent	441.5	82.0	443.4	281
⁸⁸ Sr ³⁵ Cl ₂	Bent	269.3	43.7	299.5	282
BaF ₂	Bent	389.6	(64)	413.2	281
BaCl ₂	Bent	255.2	—	260.0	282
⁶⁹ GaCl ₂	Bent	373.0	—	415.1	284
InCl ₂ ⁻	Bent	328	177	291	285
CF ₂	Bent	1102	668	1222	286
C ³⁵ Cl ₂	Bent	719.5	—	745.7	287
CBr ₂	Bent	595.0	—	640.5	288
SiF ₂	Bent	851.5	(345)	864.6	289
²⁸ Si ³⁵ Cl ₂	Bent	513	—	502	290
²⁸ SiBr ₂	Bent	402.6	—	399.5	291
GeF ₂	Bent	692	263	663	292
GeCl ₂	Bent	398	—	373	293
SnF ₂	Bent	592.7	197	570.9	294
SnCl ₂	Bent	354	(120)	334	293
SnBr ₂	Bent	237	84	223	295
PbF ₂	Bent	531.2	165	507.2	294
PbCl ₂	Bent	297	—	321	293
PbBr ₂ (g)	Bent	200	64	—	296
NF ₂	Bent	1069.6	573.4	930.7	297
PF ₂	Bent	834.0	—	843.5	298
PCl ₂	Bent	452.0	—	524.8	299
PBr ₂	Bent	369.0	—	410	299
O ³⁵ Cl ₂	Bent	641.97	—	686.59	300
³² SF ₂	Bent	838	355	817	301
SCl ₂	Bent	518	208	526	302
SBr ₂	Bent	405	—	418	302
SiI ₂	Bent	368	—	376	302
⁷⁶ Se ¹⁹ F ₂	Bent	701.8	—	674.8	302a
SeCl ₂ (sol'n)	Bent	372	168	346	303
SeBr ₂ (sol'n)	Bent	261	110	221	303
TeCl ₂ (g)	Bent	377	125	—	304
KrF ₂ (g)	Linear	449	233	596,580	305
XeF ₂	Linear	497	213.2	555	306
Xe ³⁵ Cl ₂	Linear	—	—	314.1	307
⁶³ CuF ₂	Bent	—	183.0	743.9	308
[CuCl ₂] ⁻ (s)	Linear	302	108	407	308
[CuBr ₂] ⁻ (s)	Linear	194	81	326	308

(continued)

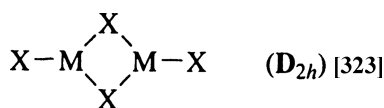
TABLE 2.2a. (Continued)

Compound ^a	Structure	$\tilde{\nu}_1$	$\tilde{\nu}_2$	$\tilde{\nu}_3$	Ref.
[CuI ₂] [−] (s)	Linear	148	65	279	309
[AgCl ₂] [−] (s)	Linear	268	88	333	309
[AgBr ₂] [−] (s)	Linear	170	61	253	309
[AgI ₂] [−] (s)	Linear	133	49	215	309
[AuCl ₂] [−] (s)	Linear	329	120, 112	350	310
[AuBr ₂] [−] (s)	Linear	209	79, 75	254	310
[AuI ₂] [−] (s)	Linear	158	67, 59	210	310
ZnF ₂	Linear	596	150	754	311
ZnCl ₂	Linear	352	103, 100	503	312
ZnBr ₂	Linear	223	71	404	312
ZnI ₂ (g)	Linear	163	67.6	337.5	283
CdF ₂	Linear	555	121	660	311
CdCl ₂	Linear	(327)	88	419	313
CdBr ₂	Linear	(205)	62	319	313
CdI ₂	Linear	(149)	(50)	269	313
HgF ₂	Linear	568	170	642	311
HgCl ₂	Linear	(348)	107	405	313
HgBr ₂	Linear	(219)	73	294	313
HgI ₂	Linear	(158)	63	237	313
TiF ₂	Bent	665	~180	766	314
VF ₂	Bent	—	—	733.2	315
CrF ₂	Linear	668	125	749	316
CrCl ₂	Linear	—	—	493.5	317
MnF ₂	Linear	—	124.8	700.1	315
MnCl ₂	Linear	—	83	476.8	317
MnI ₂ (g)	Linear	—	54.5	324.2	283
FeF ₂	Linear	—	141.0	731.3	315
FeCl ₂	Linear	—	88	493.2	317
CoF ₂	Bent	—	151.0	723.5	315
CoCl ₂	Linear	—	94.5	493.4	317
NiF ₂	Bent	—	139.7	779.6	315
NiCl ₂	Linear	(350)	85	520.6	317
NiBr ₂	Bent	—	—	331.9	318

^aAll data were obtained in inert gas matrices except those for which the physical state is indicated as g (gas), sol'n (solution), or s (solid).

obtained for isotopic NiF₂, the F–Ni–F angle was calculated to be 154–167°. The bond angle depends on the nature of the matrix gas employed. For example, NiCl₂ is linear in Ar matrices, but bent (~130°) in N₂ matrices [321]. Thus, structural data obtained in gas matrices must be interpreted with caution. As another example, the bond angle of CaF₂ increases from 139° to 143° to 156° on changing the matrix gas from Kr to Ne to N₂ [322].

The structure of the dimeric species (MX₂)₂ is known to be cyclic–planar:



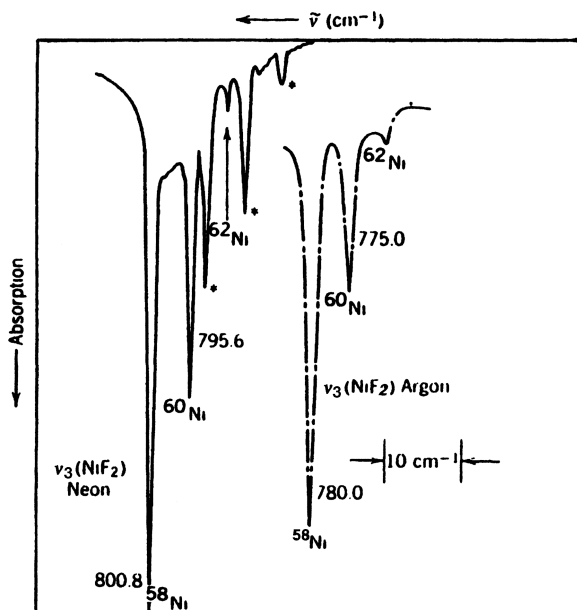
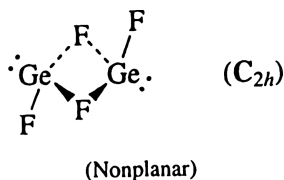
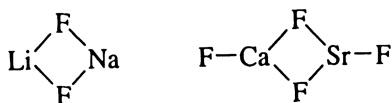


Fig. 2.4. IR spectra(ν_3) of NiF_2 in Ne and Ar matrices. Matrix splitting, indicated by asterisks, is present in the Ne matrix spectrum [320].

although an exception is reported for $(\text{GeF}_2)_2$ [324]:



Mixed fluorides such as LiNaF_2 and CaSrF_4 take planar ring structures in inert gas matrices [325]:



2.2.2. XY_2 -Type Oxides, Sulfide, and Related Compounds

Table 2.2b lists the vibrational frequencies of triatomic oxides, sulfides, selenides, and related compounds. Most of these data were obtained in inert gas matrices.

Although the NO_2^- (nitrite) ion is bent, the NO_2^+ (nitronium) ion is linear in most compounds. Solid N_2O_5 consists of the NO_2^+ and NO_3^- ions, and the former is slightly

TABLE 2.2b. Vibrational Frequencies of XY₂-Type Oxides and Related Compounds (cm⁻¹)

Compound ^a	Structure	$\tilde{\nu}_1$	$\tilde{\nu}_2$	$\tilde{\nu}_3$	Ref.
O Li O	Bent	—	243.4	730	188
O Na O	Bent	1080.0	390.7	332.8	326
O B O	Linear	—	—	1276	327
Al O Al	Bent	715	(120)	994	328
Ga O Ga	Bent	472	—	809.4	329
O C O (g)	Linear	(1337) ^b	667	2349	330
¹⁶ O ¹² C ¹⁷ O (g)	Linear	1333.37	670.12	2386.69	331
¹⁶ O ¹² C ¹⁸ O (g)	Linear	1314.49	667.69	2378.45	331
(O C O) ⁺	Linear	—	462.6	1421.7	332
(O C O) ⁻	Bent	1253.8	714.2	1658.3	332
(O C O) ²⁻	Bent	1187	745	1329	333
S C S (g)	Linear	658	397	1533	334
(S C S) ⁺	Linear	—	—	1207.1	335
(S C S) ⁻	Linear	—	—	1159.4	335
Se C Se	Linear	369.1	313.1	1301.9	336
O ¹²⁰ Sn O	Bent	—	—	863.1	337
(O N O) ⁻	Bent	1327	806	1286	338
O N O	Bent	1325	752	1610	339
(O N O) ⁺ (s)	Linear	1396	570	2360	340
O S O	Bent	1147	517	1351	341
(O S O) ⁻	Bent	985.1	495.5	1041.9	342
O ⁸⁰ Se O	Bent	992.0	372.5	965.6	343
O Te O	Bent	831.7	294	848.3	344
F O F	Bent	925/915	461	821	345
Cl O Cl (s)	Bent	630.7	296.4	670.8	346
(O Cl O) ⁻ (s)	Bent	790	400	840	347
O Cl O	Bent	944.8	448.7	1107.6	348
(O Cl O) ⁺ (s)	Bent	1055	520	1295/1230	349
¹⁶ O ⁷⁹ Br ¹⁶ O	Bent	795.7	317.0	845.2	350
Br O Br (s)	Bent	504	197	587	351
Br O Br	Bent	532.9	—	628.0	352
(O Br O) ⁺	Bent	865	375	932	353
(O Br O) ⁻	Bent	710	320	—	347
O I O	Bent	768.0	—	800.3	354
O Ce O	Bent	757.0	—	736.8	355
O Tb O	Bent	758.7	—	718.8	355
O Th O	Bent	787.4	—	735.3	355
O Ru O	Bent	926	—	902.2	356
O Pr O	Bent	—	—	730.4	355
O ⁴⁸ Tl O	Bent	—	—	934.8	357
O Ta O	Bent	971	—	912	358
¹⁶ O ¹⁸⁹ W ¹⁶ O	Bent	1030.2	~ 380	983.8	359
(ONiO) ²⁻ (s)	Linear	732.5	140	910	359a
O U O	Linear	(765.4)	—	776.1	360
(O U O) ²⁺ (s)	Linear	880	140	950	361
O Pu O	Linear	—	—	794.3	362
(N B N) ³⁻ (s)	Linear	1078	611	1702	363
¹⁴ N U ¹⁴ N	Linear	(1008.3)	—	1051.0	364
¹⁴ N U ¹⁵ N	Linear	987.2	—	1040.7	364

TABLE 2.2b. (Continued)

Compound ^a	Structure	$\tilde{\nu}_1$	$\tilde{\nu}_2$	$\tilde{\nu}_3$	Ref.
(P ¹¹ B P) ³⁻ (s)	Linear	490	379/385	1076	365
(P Be P) ⁴⁻ (s)	Linear	379	340	860	366
P Ga P	Bent	322	—	220.9	367
(P Zn P) ⁴⁻ (s)	Linear	344	47	415	368
(P Cd P) ⁴⁻ (s)	Linear	317	81	355	358
(P Hg P) ⁴⁻ (s)	Linear	335	71	341	368
(P Be P) ⁴⁻ (s)	Linear	379	340	860	366
(As Be As) ⁴⁻ (s)	Linear	222	310	775	366
(Sb Be Sb) ⁴⁻ (s)	Linear	—	255	700	366
S Ti S	Bent	533.5	—	577.8	369
S Zr S	Bent	502.9	—	504.6	369
S Hf S	Bent	492.2	—	483.2	369

^a All data were obtained in inert gas matrices except for those denoted as g (gas) or s (solid).

^b Fermi resonance with $2 \nu_2$ (Sec. 1.11).

bent, as indicated by the appearance of a strong $\delta(\text{ONO})$ band at 534 cm^{-1} in the Raman spectrum [370].

Metal dioxides produced by sputtering techniques [371] in inert gas matrices take linear or bent O—M—O structures. Metal dinitrides produced by the same technique also take linear N—M—N (M = U [372] and Pu [373]) or bent N—M—N (M = Th [374]) structures. These structures are markedly different from those of molecular oxygen and nitrogen complexes of various metals produced by the conventional matrix cocondensation technique (Chapter 3 in Part B).

The NpO_2^{2+} , PuO_2^{2+} , and AmO_2^{2+} ions are similar to the UO_2^{2+} ion in that they are linear and symmetric. They exhibit the ν_3 bands at 969, 962, and 939 cm^{-1} , respectively, in IR spectra [375]. The relationship between the U=O stretching force constant and the U=O distance was derived by Jones [376]. According to Bartlett and Cooney [377] the U=O distance R (in $\text{pm} = 10^{-2} \text{ \AA}$) is given by

$$R = 9141(\tilde{\nu}_3)^{-(2/3)} + 80.4$$

$$R = 10650(\tilde{\nu}_1)^{-(2/3)} + 57.5$$

where ν is in units of cm^{-1} .

Mizuoka and Ikeda [378] observed that the ν_3 of the $(\text{U}^{\text{IV}}\text{O}_2)^{2+}$ ion at 895 cm^{-1} in DMSO (dimethyl sulfoxide) solution is shifted to 770 cm^{-1} when reduced electrochemically to the $(\text{U}^{\text{V}}\text{O}_2)^+$ ion. Vibrational spectra of coordination compounds containing dioxo(O=M=O) groups are discussed in Chapter 3 (in Part B).

A T-shaped structure of C_{2v} symmetry was proposed for SiC_2 in an Ar matrix at 8K [379]. Assignments of IR spectra of BC_2 [380] and KO_2 [381] prepared in Ar matrices were based on triangular structures of C_{2v} symmetry. The linear CS_2 molecule in a N_2 matrix is converted to a cyclic structure [$881.3 \text{ cm}^{-1}(A_1)$ and $520.9 \text{ cm}^{-1}(B_2)$] on photo irradiation (193 nm) [382].

2.2.3. Triatomic Halogeno Compounds

Table 2.2c lists the vibrational frequencies of triatomic halogeno compounds. The resonance Raman spectrum of the I_3^- ion gives a series of overtones of the ν_1 vibration [408,409]. The resonance Raman spectra of the I_2Br^- and IBr_2^- ions and their complexes with amylose have been studied [410]. The same table also lists the vibrational frequencies of XHY-type (X,Y: halogens) compounds. All these species are linear except the $ClHCl^-$ ion, which was found to be bent by an inelastic neutron scattering (INS) and Raman spectral study [402].

TABLE 2.2c. Vibrational Frequencies of Triatomic Halogeno Compounds (cm^{-1})

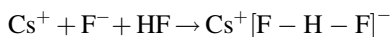
Compound ^a	Structure ^b	$\tilde{\nu}_1^c$	$\tilde{\nu}_2$	$\tilde{\nu}_3^c$	Ref.
FCIF ⁺	b	807	387	830	383
FCIF (m)	b	500	242	578/570	384
FCIF ⁻ (s)	l	510/478	—	636	385
FCICl ⁺ (s)	b	744	299/293	535/528	386
FBrF ⁺ (s)	b	706	362	702	387
FBrF ⁻ (s)	l	460	236	450	388
FIF ⁻ (s)	l	445	206	462	388a
ClFCI ⁺ (s)	b	~529	293/258	586/593	389
Cl ₃ ⁻ (m)	b	253	—	340	390
ClBrCl ⁻ (sl)	l	278	135	225	391
ClCl ⁺ (s)	b	371	147	364	392
ClCl ⁻ (sl)	l	269	127	226	391
ClI ⁺ (s)	b	360	(126)	197	393
Br ₃ ⁺ (s)	b	293	124	297	394
Br ₃ ⁻ (sl)	l	164	53	191	391
Br ₃ (m)	l	190	—	—	395
BrIBr ⁺ (s)	l	256	124	256	393
BrI ⁻ (s)	l	117	84	168	396
BrI ⁺ (s)	b	258	—	198	393
I ₃ ⁻ (c)	l	116	56/42	125	396a
HFH ⁺ (s)	b	2970	1680	3080	397
FHF ⁻ (s)	l	596/603	1233	1450	398
FHF ⁻ (m)	l	—	1217	1364	399
FHF ⁻ (g)	l	583.1	1286.0	1331.2	400
ClHF ⁻ (s)	l	275	863/823	2710	401
ClHCl ⁻ (s)	b	199	660/602	1670	402
ClHBr ⁻ (s)	l	—	508	1705	403
ClHI ⁻ (s)	l	—	485	2200	403
BrHF ⁻ (s)	l	220	740	2900	401
BrHBr ⁻ (s)	l	126	1038	1420	404
BrHBr ⁻ (m)	l	168	—	670	405
IHF ⁻ (s)	l	180	635	3145	401
IHI (m)	l	(120.7)	—	682.1	406
F ₃ ⁻ (m)	l	461	—	550	407

^am = insert gas matrix; sl = solution; s = solid.

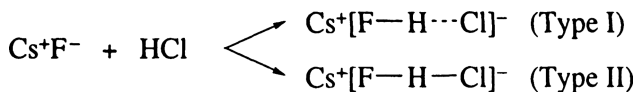
^bb = bent; l = linear.

^cFor XYZ type, ν_1 and ν_3 correspond to ν (XY) and ν (YZ), respectively.

Ault and coworkers have utilized salt-molecule reactions to produce a number of novel triatomic and other anions in isolated environments [411]. For example, the linear symmetric $[\text{FHF}]^-$ ion was produced in Ar matrices via codeposition of CsF vapor with HF gas diluted in Ar [399]:



The reaction of CsF vapor with HCl gas diluted in Ar yields a mixture of two types of the $[\text{FHC1}]^-$ anions; in type I, the H atom is not equidistant from the F and Cl atoms, and its ν_3 [mainly $\nu(\text{HF})$] is observed near 2500 cm^{-1} , whereas in type II, the H atom is symmetrically located and its ν_3 , is at 933 cm^{-1} [412].



The yield of each type is determined by the location of the cation in the ion pair, and the type I/type II ratio varies, depending on the cation used; smaller alkali metal cations favor type II, while larger cations prefer type I. These classifications were originally made by Evans and Lo, who observed crystalline HCl_2^- salts of types I and II depending on the cation employed [413].

2.2.4. Bent XH_2 Molecules

Table 2.2d lists the vibrational frequencies of bent XH_2 -type molecules. The XH stretching frequencies are lower and the XH_2 bending frequencies are higher in condensed phases than in the vapor phase because of hydrogen bonding in the former. This trend is also seen for H_2O and H_2S dissolved in organic solvents such as pyridine and dioxane [442,443].

In both liquid water and ice, H_2O molecules interact extensively via $\text{O}-\text{H}\cdots\text{O}$ bonds. However, there are marked differences between the two phases. In the latter, H_2O molecules are tetrahedrally hydrogen-bonded, and this local structure is repeated throughout the crystal. In liquid water, however, the $\text{O}-\text{H}\cdots\text{O}$ bond distance and angle vary locally, and the bond is sometimes broken. Thus, its vibrations cannot be described simply by using the three normal modes of the isolated H_2O molecule. According to Walrafen et al. [444] an isosbestic point exists at 3403 cm^{-1} in the Raman spectrum of liquid water obtained as a function of temperature, and the bands above and below this frequency are mainly due to non-hydrogen-bonded and hydrogen-bonded species, respectively. In addition, liquid water exhibits librational and restricted translational modes that correspond to rotational and translational motions of the isolated molecule, respectively. The librations yield a broad contour at $1000\text{--}330 \text{ cm}^{-1}$, while the restricted translations appear at 170 and 60 cm^{-1} [445]. For more details, see the review by Walrafen [446].

TABLE 2.2d. Vibrational Frequencies of Bent XH_2 -Type Molecules (cm^{-1})

Molecule	State	$\tilde{\nu}_1$	$\tilde{\nu}_2$	$\tilde{\nu}_3$	Ref.
CaH_2	Matrix	1267.0	—	1192.0	414
TiH_2	Matrix	1483.2	496	1435.5	415
ZrH_2	Matrix	—	625.03	1861.0	414
VH_2	Matrix	1532.4	529	1508.3	415
CrH_2	Matrix	1651.3	—	1614.9	416
MoH_2	Matrix	1752.7	—	1727.4	416
NiH_2	Matrix	2007	—	1969	417
AlH_2	Matrix	1766	760	1799	418
GaH_2	Matrix	1727.2	740.1	1799.5	419
InH_2	Matrix	1548.6	607.4	1615.5	419
SiH_2	Gas	1995.03	998.62	1992.82	420
GeH_2	Matrix	1887	920	1864	421
NH_2	Matrix	—	1499	3220	422
	Surface	3290	1610	3380	423
$[\text{NH}_2]^-$	Solid	3270	1556	3323	424
$[\text{PH}_2]^-$	Solid	2230	1080	2160	425
$[\text{OH}_2]^+$	Matrix	3182.7	1401.7	3219.5	426,427
$^{16}\text{OH}_2$	Gas	3657	1595	3756	428
	Liquid	3450	1640	3615	429
	Solid	3400	1620	3220	430
$^{16}\text{OHD}^a$	Gas	2727	1402	3707	428
	Solid	2416	1490	3275	430
$^{16}\text{OD}_2$	Gas	2671	1178	2788	428
	Solid	2495, 2336	1210	2432	430
$^{18}\text{OD}_2$	Gas	2657	1169	2764	431
OT_2^b	Gas	—	996	2370	432
	Solid	1988	1023	2104	433
SH_2	Gas	2615	1183	2627	434
	Matrix	2619.5	—	2632.6	435
	Solid	2532, 2523	1186, 1171	2544	436
SD_2	Gas	1892	934	2000	437
	Solid	1843, 1835	857, 847	1854	436
SeH_2	Gas	2345	1034	2358	438
SeD_2	Gas	1687	741	1697	438,439
$^{80}\text{SeHD}^a$	Gas	1692.14	—	2351.19	440
$^{130}\text{TeH}_2$	Gas	2065.27	—	2072.11	441

^aHere ν_1 and ν_3 denote ν (OD) and ν (OH), respectively.^bT = ^3H (tritium).

Hornig et al. [430] assigned the spectrum of ice I as shown in Table 2.2d. They also assigned some librational and translational modes. Bertie and Whalley [447] studied the vibrational spectra of ice in other phases, and found the spectra to be consistent with reported crystal structures in each phase. For crystal water and aquo complexes, see Sec. 3.8. The vibrational frequencies of H_2O , D_2O , HDO , and their dimers in argon matrices have been reported [448].

Infrared studies on $(\text{H}_2\text{O})_n$ ($^{16}\text{O}/^{18}\text{O}$) (where $n = 1, 2, >3$) in N_2 matrices [449] and $(\text{H}_2\text{O})_n$ ($n = 2-6$) formed in droplets of liquid helium have been reported [450]. Devlin et al. [451] measured the IR spectra of ice consisting of large $(\text{H}_2\text{O})_n$

($n = \sim 100\text{--}64,000$) clusters and studied the relationship between the frequency and intensity of the bending mode and the structure of the cluster.

2.2.5. X_3 -Type Molecules

X_3 -type halogeno molecules are listed in Table 2.2c. Table 2.2e lists vibrational frequencies of other X_3 -type molecules. The O_3 and O_3^- ion are bent (bond angle $120\text{--}110^\circ$), and the S_3 , S_3^- , and S_3^{2-} ions are all bent ($103\text{--}115^\circ$), with frequencies decreasing in this order. Detailed assignments of the IR spectra were made for six isotopomers of O_3 containing ^{16}O and ^{18}O in liquid oxygen solution at 77 K [454].

The $N_6^{\bullet -}$ radical anion was produced by the reaction of the N_3^- ion with N_3^\bullet . The most probable structure, on the basis of theoretical calculations is a rectangular cyclic structure of D_{2h} symmetry with two long N–N bonds that connect two azidyl monomeric units via the terminal nitrogen atoms. This is also supported by the observation of an IR band at 1842 cm^{-1} , which is intermediate between N_3^- and N_6^+ [469].

Figure 2.5 illustrates three normal modes of vibration of a triangular X_3 -type molecules of D_{3h} symmetry. The ν_1 is a symmetric stretch (A'_1 , Raman-active) while a degenerate pair of ν_{2a} and ν_{2b} (E' , IR/Raman-active) involves stretching as well as bending coordinates (Sec. 1.9).

TABLE 2.2e. Vibrational Frequencies of X_3 -Type Molecules (cm^{-1}) Bent (C_{2v}) and Linear ($D_{\infty h}$) Molecules

Molecule	State	Structure	$\tilde{\nu}_1$	$\tilde{\nu}_2$	$\tilde{\nu}_3$	Ref.
$(O_3)^-$	Solid	Bent	1020	620	816	452
$^{16}O_3$	Matrix	Bent	1104.3	699.8	1039.6	453,454
$(S_3)^{2-}$	Solid	Bent	458	229	479	455
S_3^-	Solution	Bent	535	235.5	571	456
S_3	Gas	Bent	581	281	~ 680	457,458
N_3^-	Solution	Linear	1343	637.5	2048	459
N_3^+	Matrix	Linear	1287	473.7	1657.5	460
Rh_3	Matrix	Bent	322.4	248	259	461
Mo_3	Matrix	Bent	386.8	224.5	236.2	462
Triangular (D_{3h}) Molecules						
Molecule	State		$\tilde{\nu}_1 (A'_1)$	$\tilde{\nu}_2 (E')$		Ref.
Rb_3	Matrix		53.9	38.3		463
Cs_3	Matrix		39.5	24.4		463
Cr_3	Matrix		432.2	302.0		464
Fe_3	Matrix		249	—		465
Ag_3	Matrix		119	—		465
Ru_3^a	Matrix		303.4	—		466
Ta_3^a	Matrix		251.2	—		466
Nb_3	Matrix		334.9	227.4		467
Au_3	Matrix		172	118		468

^a D_{3h} or C_{2v} .

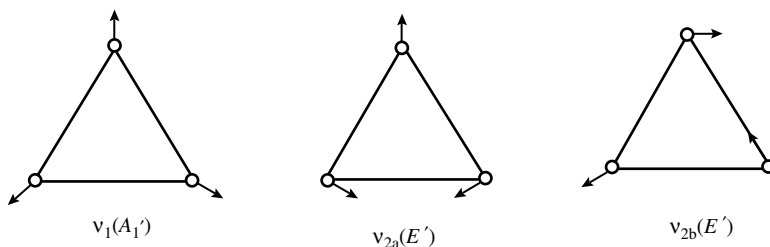


Fig. 2.5. Normal modes of vibration of triangular X_3 molecules.

2.2.6. XXY- and XYZ- Type Molecules

Table 2.2f lists vibrational frequencies of XXY-type molecules. Tables 2.2g and 2.2h list those of linear and bent XYZ-type molecules, respectively. It should be noted that the description of vibrational modes such as $\nu(\text{XX})$, $\nu(\text{XY})$, and $\nu(\text{YZ})$ is only qualitative. Most of these frequencies were measured in inert gas matrices. Some of these vibrations split into two because of Fermi resonance, matrix effect, or crystal, field effects.

The linear HArF molecule listed in Table 2.2g was obtained by photodissociation of HF in Ar matrices followed by annealing to increase the HArF concentration below 20 K. Figure 2.6 shows the IR spectra of H^{40}ArF , D^{40}ArF , and H^{36}ArF in Ar matrices

TABLE 2.2f. Vibrational Frequencies of XXY-Type Molecules (cm^{-1})

Molecule ^a	Structure	$\tilde{\nu}_1^b$	$\tilde{\nu}_2^c$	$\tilde{\nu}_3^d$	Ref.
${}^6\text{Li}{}^6\text{Li O}$	Linear	—	118	1028.5	470
C C O	Linear	1074	381	1978	471
(C C O) [−]	Linear	2082	656	1185	472
(N N H) ⁺ (g)	Linear	2257.9	686.8	3334.0	473
N N C	Linear	1235	394	2824	474
N N O (g)	Linear	2277	596.5	1300.3	475
(N N F) ⁺ (s)	Linear	2371	391	1057	475a
O O H (g)	Bent	1097.6	1391.8	3436.2	476
O O D (g)	Bent	1121.5	1020.2	2549.2	476
O O F	Bent	~1500	586.4	376.0	477
O O Cl	Bent	1477.8	432.4	214.9	478
O O Br	Bent	1484.0	—	—	479
O O S	Bent	~ 1005	—	739.9	480
S S H	Bent	595	903	2460/2463	481
S S O (g)	Bent	679.1	382	1166.5	482
${}^{35}\text{Cl}{}^{35}\text{Cl O}$	Bent	374.2	240.2	961.9	483

^aAll data were obtained in inert gas matrices except for those indicated as g (gas) or s (solid).

^b $\nu(\text{XX})$.

^c $\delta(\text{XXY})$.

^d $\nu(\text{XY})$.

TABLE 2.2g. Vibrational Frequencies of Linear XYZ-Type Molecules (cm⁻¹)

Molecule	State	$\tilde{\nu}_1$ (XY)	$\tilde{\nu}_2$ (δ)	$\tilde{\nu}_3$ (YZ)	Ref.
HCN	Gas	3311	712	2097	484
	Matrix	3306	721	—	485
D C N	Gas	2630	569	1925	484
T C N	Gas	2460	513	1724	485a
H N C	Matrix	3620	477	2029	486
	Gas	3813.4	448.5	2049.8	487
H ¹¹ B ⁷⁹ Br	Gas	2849.4	—	937.6	488
H ¹¹ B O	Matrix	(2849)	754	1817	489
D ¹¹ B O	Gas	2253.5	608.4	1647.7	490
(H C S) ⁺	Gas	3141.7	766.5	—	491
H Si N	Matrix	2152.2	—	1162.2	492
H ⁴⁰ Ar F	Matrix	1969.5	687.0	435.7	493, 493a
H Kr F	Matrix	1950	650	415	494
¹⁹ F ¹¹ B ³² S	Gas	—	(457)	1644.4	495
F C N	Gas	1077	449	2290	496
F P O	Gas	819.6	—	1297.5	497
F P ³² S	Gas	803.3	(313.6)	726.3	498
³⁵ Cl ¹² C ¹⁴ N	Gas	747.8 ^a	381.9 ^a	2249.3 ^a	499
Cl C N	Matrix	718	384/387 ^b	—	500
³⁵ Cl ¹¹ B ³² S	Gas	529.9	—	1407.6	501
³⁵ Cl ¹¹ B O	Gas	—	—	1972.2	502
(ClCO) ⁺	Solid	802.5	—	2256	503
Cl C S	Matrix	632.1	—	1189.3	504
³⁵ Cl C P	Gas	573.9	303.4	1477.3	505
Br C N	Gas	574	342.5	2200	506
	Matrix	575	349/351	—	500
I C N	Gas	485	304	2188	507
⁶ Li N C	Matrix	722.9	121.7	2080.5	508
Na C N	Matrix	382	170	2044	509
(C N O) ⁻	Solid	2096	471	1106	510
N C O	Matrix	1275	487	1922	511
(N C O) ⁻	Solution	2155	630	1282/1202 ^b	512
(N C ³² S) ⁻	Solid	2053	486/471	748	513
(N C Se) ⁻	Solid	2070	424/416	558	514
(N C Te) ⁻	Solid	2073	366	450	515
(N S O) ⁻	Solid	1283	528	999	516
(P C S) ⁻	Solid	1762	—	747	517
P N O	Matrix	865.2	—	1754.7	518
(O C S) ⁺	Matrix	2071.1	—	702.5	519
(O C S) ⁻	Matrix	1646.4	—	718.2	519
O C Te	Matrix	1965.3	—	—	520
S C O	Gas	859	520	2062	521
S C Se	Gas	1435	(355)	506	522
S C Te	Solution	1347	(377)	423	522
Al O Si	Matrix	534.9	—	1028.2	523
W C H	Gas	1006	660	—	524
Co C O	Matrix	579.2	424.9	1957.5	525

^aCorrected for anharmonicity.^bFermi resonance between ν_3 and $2\nu_2$.

TABLE 2.2h. Vibrational Frequencies of Bent XYZ-Type Molecules (cm⁻¹)

Molecule	State ^a	$\tilde{\nu}_1$ (XY)	$\tilde{\nu}_2$ (δ)	$\tilde{\nu}_3$ (YZ)	Ref.
HCO	Matrix	2483	1087	1863	526
H ¹² C F	Matrix	—	1405	1181.5	527
H N O	Matrix	3450	1110	1563	528
H ¹⁴ N F	Matrix	—	1432	1000	529
H O N	Matrix	3467.2	—	1095.6	530
H O F	Matrix	3537.1	1359.0	886.0	531
H O Cl	Matrix	3578	1239	728	532
H O Br	Matrix	3589	1164	626	532
H O I	Matrix	3597	1103	575	533
⁷ Li ¹⁶ O ²⁸ Si	Matrix	668.4	~ 249	998.5	534
N O F	Matrix	1886.2	734.9	492.2	535
N S F	Gas	1372	366	640	536
N S Cl	Gas	1325	273	414	537
O N F	Gas	1843.5	765.8	519.9	538
O N ³⁵ Cl	Gas	1799.7	595.8	331.9	539
O N Br	Gas	1799.0	542.0	266.4	540
O N I	Matrix	1809	470	216	541
O P F	Gas	1297.5	—	819.6	542
	Matrix	1292.2	416.0	811.4	543
O P Cl	Gas	1272.8	491.6	—	544
O C F	Matrix	1855	626	1018	545
O C Cl	Matrix	1880	281	570	546
O Cl F	Gas	1037.7	~ 310	596.9	547
S P F	Matrix	720.2	313.6	791.4	548
S P Br	Matrix	712	—	372	549
F N O	Gas	765.4	519.6	1844.1	550
F N Cl	Matrix	917	(341)	720	551
³⁵ Cl C F	Matrix	742	—	1146	552
³⁵ Cl ²⁸ Si ¹⁶ O	Matrix	509.4	—	1160.9	553
³⁵ Cl ³² S N	Matrix	1327.3	403.8	267.4	554
Cl Sn Br	Matrix	328	—	228	555
Cl Pb Br	Matrix	295	—	200	555
Br O N	Matrix	—	~ 350	1820.0	556
Br ³² S N	Matrix	1312.9	346.1	226.2	554
Br S F	Matrix	434	—	765	557
Pd ¹⁴ N ¹⁶ O	Matrix	229.8	522.1/510.3	1661.3	558

^aMatrix: inert gas matrix.

at 7.5 K obtained by Khriachtchev et al. [493, 493a]. Good agreement was obtained between the observed and theoretical. frequencies. This work was extended to HKrF [494].

Lapinski et al. [559] measured the IR spectra of 12 isotopomers of linear NNO involving ¹⁴N/¹⁵N and ¹⁶O/¹⁷O/¹⁸O in N₂ matrices, and assigned their fundamental, overtone, and combination bands on the basis of observed isotope shifts and DFT calculations. These 12 isotopomer bands in the ν_1 (N \equiv N stretch) region are marked by arrows in Fig. 2.7.

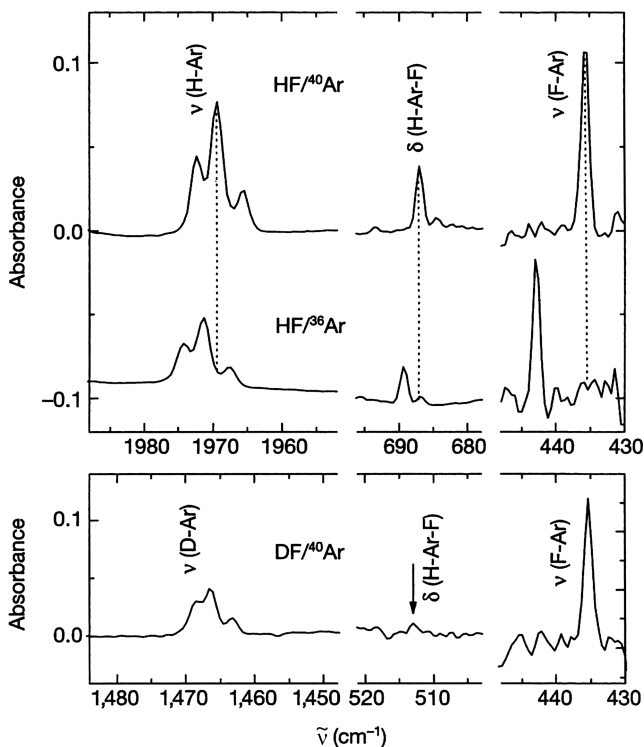


Fig. 2.6. IR spectra of HArF in solid Ar showing the effects of $^{40}\text{Ar}/^{36}\text{Ar}$ and H/D substitutions [493,493a].

2.3. PYRAMIDAL FOUR-ATOM MOLECULES

2.3.1. XY_3 Molecules (C_{3v})

The four normal modes of vibrations of a pyramidal XY_3 molecule are shown in Fig. 2.8. All four vibrations are both infrared- and Raman-active. The G and F matrix elements of the pyramidal XY_3 molecule are given in Appendix VII. Table 2.3a lists the fundamental frequencies of XH_3 -type molecules. Several bands marked by an asterisk are split into two by *inversion doubling*. As is shown in Fig. 2.9, two configurations of the XH_3 molecule are equally probable. If the potential barrier between them is small, the molecule may resonate between the two structures. As a result, each vibrational level splits into two levels (positive and negative) [560]. Transitions between levels of different signs are allowed in the infrared spectrum, whereas those between levels of the same sign are allowed in the Raman spectrum. The transition between the two levels at $\nu = 0$ is also observed in the microwave region ($\tilde{\nu} = 0.79 \text{ cm}^{-1}$).

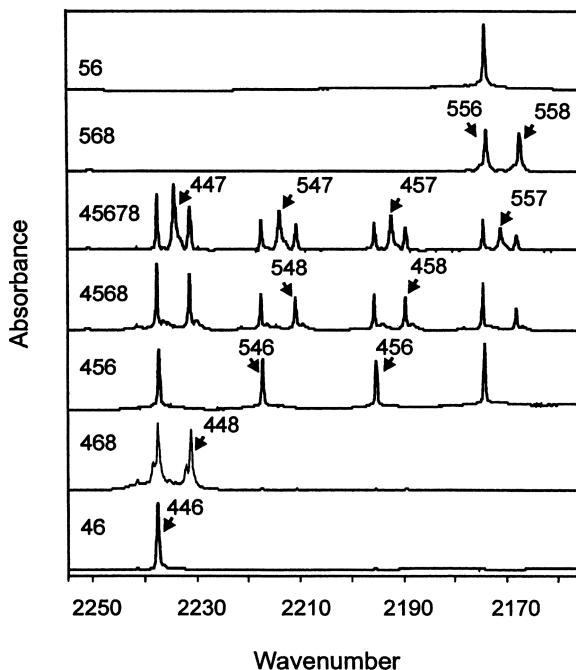


Fig. 2.7. IR spectra (ν_1 region) of NNO in N_2 matrices at 10 K. The labeling on the left indicates the isotopic composition of the mixture used in preparing the matrix. For example, 4568 denotes a mixture composed of equal fraction of $^{14}N, ^{15}N, ^{16}O$, and ^{18}O . Thus, the peak due to $^{14}N, ^{14}N, ^{16}O$ is indicated by the number 446 (bottom trace). This species exhibits the bands at 2235.6, 588.0, and 1291.2 cm^{-1} in N_2 matrices [559].

Splittings due to *inversion doubling* were also observed for the ν_4 of $^{14}NH_3$ [578], and ν_1 and ν_3 of ND_3 [579]. Optical isomers may be separated if the three Y groups are not identical and the inversion barrier is sufficiently high.

As is seen in Table 2.3a ν_1 and ν_3 overlap or are close in most compounds. The presence of the hydronium (H_3O^+) ion in hydrated acids has been confirmed by observing its characteristic frequencies. For example, it was shown from infrared spectra that $H_2PtCl_6 \cdot 2H_2O$ should be formulated as $(H_3O)_2 [PtCl_6]$ [580]. For normal

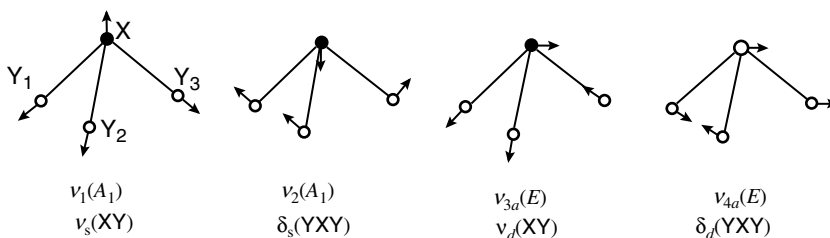


Fig. 2.8. Normal modes of vibration of pyramidal XY_3 molecules.

TABLE 2.3a. Vibrational Frequencies of Pyramidal XH_3 Molecules (cm^{-1})

Molecule	State	$\tilde{\nu}_1 (A_1)$	$\tilde{\nu}_2 (A_1)$	$\tilde{\nu}_3 (E)$	$\tilde{\nu}_4 (E)$	Ref.
NH_3	Gas	3335.9 } ^a 3337.5 }	931.6 } ^a 968.1 }	3414	1627.5	560
	Solid	3223	1060	3378	1646	561
ND_3	Gas	2419	748.6 } ^a 749.0 }	2555	1191.0	560
	Solid	2318	815	2500	1196	561
$^{15}\text{NH}_3$	Gas	3335	926 } ^a 961 }	3335	1625	562
NT_3	Gas	2016	647	2163	1000	563
PH_3	Gas	2327	990 } ^a 992 }	2421	1121	564
PD_3	Gas	1694	730	(1698)	806	564
AsH_3	Gas	2122	906	2185	1005	564,565
AsD_3	Gas	1534	660	—	714	564,566
SbH_3	Gas	1891	782	1894	831	567
SbD_3	Gas	1359	561	1362	593	567
BiH_3	Gas	1733.3	726.7	1734.5	751.2	568
$[\text{OH}_3]^+ \text{SbCl}_6^-$	Sol'n	3560	1095	3510	1600	569
$[\text{OH}_3]^+ \text{ClO}_4^-$	Solid	3285	1175	3100	1577	570
$[\text{OH}_3]^+ \text{NO}_3^-$	Solid	2780	1135	2780	1680	671
$[\text{OH}_3]^+$	Liquid SO_2	3385	—	3470	1700	572
$[\text{OD}_3]^+$	Liquid SO_2	2490	—	3400	1635	572
				2660	1255	
$[\text{SD}_3]^+$	Gas	1827.2	—	2580	—	573
$[\text{SeH}_3]^+$	Solid	2302	936	1838.6	1057	574
$[\text{CH}_3]^- \text{Na}^+$	Matrix	2760	1092	2320	1384	575
SiH_3	Gas	—	727.9	2805	—	576
$[\text{GeH}_3]^-$	Liquid NH_3	1740	809	—	886	577

^aInversion doubling.

coordinate analysis of pyramidal XH_3 molecules, see Refs. [581–583]. Infrared spectra of hydrated proton complexes $\text{H}^+(\text{H}_2\text{O})_n$ ($n = 2\text{--}11$), in water clusters were measured as Ar complexes at low temperatures, and band assignments were made based on their minimum-energy structures obtained by DFT calculation [583a].

Reaction of CH_3I with Na (or K) atoms in N_2 matrices at 20 K [575] produces an ion-pair complex $\text{CH}_3^- \text{Na}^+$ (or $\text{CH}_3^- \text{K}^+$), of C_{3v} symmetry. The $\nu(\text{Na}-\text{CH}_3)$ and $\nu(\text{K}-\text{CH}_3)$ vibrations were observed at 298 and 280 cm^{-1} , respectively. Vibrational spectra of the $(\text{NH}_3)_2$ dimer in Ar matrices show that two NH_3 molecules are bonded via a very weak hydrogen bond [584].

Table 2.3b lists the vibrational frequencies of pyramidal XY_3 halogeno compounds. Clark and Rippon [601] have measured the Raman spectra of a number of these compounds in the gaseous phase. The compounds show a $\nu_1 > \nu_3$ and $\nu_2 > \nu_4$ trend, whereas the opposite trend holds for the neutral XH_3 molecules listed in Table 2.3a. In some cases, the two stretching frequencies (ν_1 and ν_3) are too close to be distinguished empirically. This is also true for the two bending bands (ν_2 and ν_4).

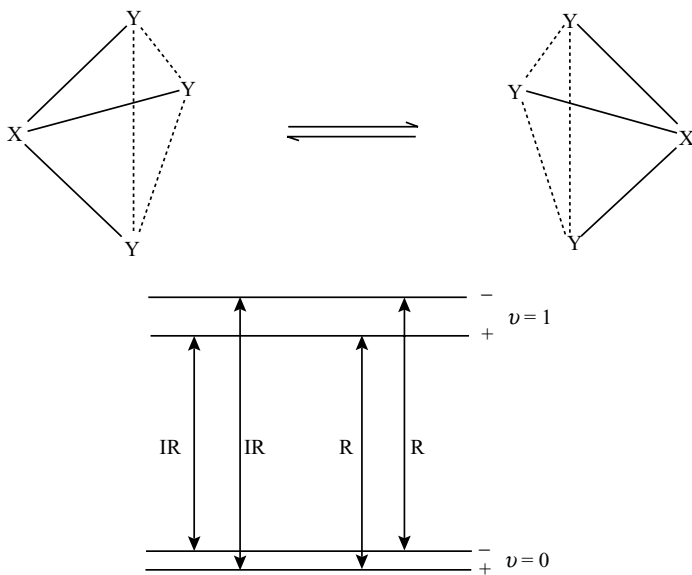


Fig. 2.9. Inversion doubling of pyramidal XY_3 molecules.

Figure 2.10 shows the Raman spectra of the SnX_3^- ions ($X = Cl, Br, \text{ and } I$) in solution obtained by Taylor [594]. In crystalline $[As(Ph)_4][SnX_3]$, the symmetry of the SnX_3^- ion is lowered to C_s so that ν_3 and ν_4 each split into two bands [592]. Normal coordinate analyses on the SnX_3^- ion ($X = F, Cl, Br, I$) [592] have been carried out.

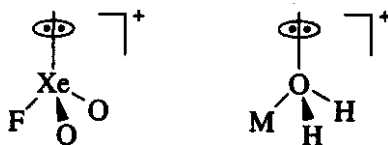
Table 2.3c lists the vibrational frequencies of pyramidal XO_3 -type compounds. Rocchiccioli [629] has measured the infrared spectra of a number of sulfites, selenites, chlorates, and bromates. Again, the ν_3 and ν_4 vibrations may split into two bands because of lowering of symmetry in the crystalline state. Although $\nu_2 > \nu_4$ holds in all cases, the order of two stretching frequencies (ν_1 and ν_3) depends on the nature of the central metal. It is to be noted that the SO_3^- and SO_3^{2-} anions are pyramidal, while the SO_3 molecule is planar (Table 2.4b).

Figure 2.11 shows the ER spectra of $KClO_3$ and KIO_3 obtained in the crystalline state.

2.3.2. ZXY_2 (C_s) and $ZXYW$ (C_1) Molecules

Substitution of one of the Y atoms of a pyramidal XY_3 molecule by a Z atom lowers the symmetry from C_{3v} to C_s . Then the degenerate vibrations split into two bands, and all six vibrations become infrared- and Raman-active. The relationship between C_{3v} and C_s is shown in Table 2.3d. Table 2.3e lists the vibrational frequencies of pyramidal ZXY_2 molecules.

Vibrational spectra of the $[SCl_nF_{3-n}]^+$ ions ($n = 0-3$) [663] and PH_nF_{3-n} ($n = 0-3$) [664] have been assigned. The $[XeO_2F]^+$ ion takes a pseudo-tetrahedral structure owing to the presence of a sterically active lone-pair electron of the Xe atom [661]:



Matrix cocondensation reactions of alkali halide molecules (M^+X^-) with H_2O diluted in Ar produce pyramidal $[MOH_2]^+$ ions that exhibit the $\nu(OH_2)$ and $\delta(OH_2)$ in the 3300–3100 and 700–400 cm^{-1} regions, respectively [665]. These ions may serve as simple models of aquo complexes.

TABLE 2.3b. Vibrational Frequencies of Pyramidal XY_3 Halogeno Compounds (cm^{-1})

Molecule	State	$\tilde{\nu}_1$	$\tilde{\nu}_2$	$\tilde{\nu}_3$	$\tilde{\nu}_4$	Ref.
$[InCl_3]^-$	Solid	252	102	185	97	585
$[InBr_3]^-$	Solid	177	74	149	46	585
$[InI_3]^-$	Solid	136	78	110	40	585
CF_3	Matrix	1084	703	1250	600,500	586
$^{28}SiF_3$	Matrix	832	406	954	290	587
$[SiF_3]^-$	Matrix	770.3	401	760.4	268	588
				757.0		
$^{28}SiCl_3$	Matrix	470.2	—	582.0	—	589
$GeCl_3$	Matrix	388	—	362	—	590
$[GeCl_3]^-$	Solid	303	—	285	—	591
$[SnF_3]^-$	Solid	520	280	477	224	592
	Matrix	509	256	454	—	593
$[SnCl_3]^-$	Sol'n	297	130	256	104	594
$[SnBr_3]^-$	Sol'n	205	82	180	65	594
$[SnI_3]^-$	Sol'n	162	61	148	48	594
$[PbF_3]^-$	Matrix	456	—	405	—	595
$[PbCl_3]^-$	Sol'n	249	—	—	—	596
$[PbBr_3]^-$	Sol'n	176	—	164	58	596
$[PbI_3]^-$	Sol'n	137	—	127	30~45	596
NF_3	Gas	1035	649	910	500	597
NCl_3	Sol'n	535	347	637	254	598
$^{14}NCl_3$	Matrix	554.2	365.2	644	263	599
NI_3	Solid	279	146	354	90	600
PF_3	Gas	893.2	486.5	858.4	345.6	601,602
PCl_3	Gas	515.0	258.3	504.0	186.0	601
PBr_3	Gas	390.0	159.9	384.4	112.8	601
PI_3	Solid	303	111	325	79	603
AsF_3	Gas	738.5	336.8	698.8	262.0	601,604
$AsCl_3$	Gas	416.5	192.5	391.0	150.2	601,605
$AsBr_3$	Melt	272	128	287	99	606
AsI_3	Gas	212.0	89.6	(201)	63.9	601
SbF_3	Matrix	654	259	624	—	607
$SbCl_3$	Gas	380.7	150.8	358.9	121.8	601
$SbBr_3$	Sol'n	254	101	245	81	606,608
SbI_3	Gas	186.5	74.0	(147)	54.3	601,609
$BiCl_3$	Gas	342	123	322	107	610
$BiBr_3$	Gas	220	77	214	63	611
BiI_3	Gas	(162)	59.7	163.5	47.0	609

(continued)

TABLE 2.3b. (Continued)

Molecule	State	$\tilde{\nu}_1$	$\tilde{\nu}_2$	$\tilde{\nu}_3$	$\tilde{\nu}_4$	Ref.
$[\text{SF}_3]^+$	Melt	943	690	922	356	612
$[\text{SCl}_3]^+$	Solid	498	276	533, 521	215, 208	613
$[\text{SBr}_3]^+$	Solid	375	175	429, 414	128	614
$[\text{SeF}_3]^+$	Melt	781	381	743	275	612
$[\text{SeCl}_3]^+$	Sol'n	430	206	415	172	615
$[\text{SeBr}_3]^+$	Sol'n	291	138	298	108	606
$[\text{TeCl}_3]^+$	Sol'n	362	186	347	(150)	616
$[\text{TeBr}_3]^+$	Sol'n	265	112	266	92	606
$[\text{MnBr}_3]^+$	Solid	280	110	150	80	617
FeCl_3	Matrix	363.0	68.7	460.2	113.8	618
YCl_3	Gas	378	78	359	58.6	619
CeCl_3	Gas	328	58	314	44	620
NdCl_3	Gas	333	60	320	45	620
SmCl_3	Gas	338	61	324	46	620
GdCl_3	Gas	343	64	330	46	620
DyCl_3	Gas	346	65	334	47	620

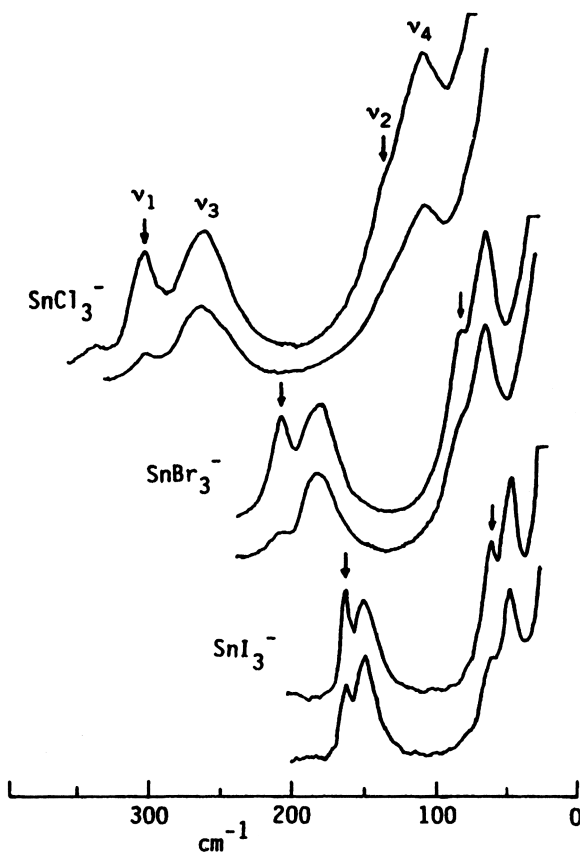


Fig. 2.10. Raman spectra of the SnX_3^- ions in diethyl ether extracts from SnX_2 in HX solutions. The arrows denote polarized bands [594].

TABLE 2.3c. Vibrational Frequencies of Pyramidal XO₃ Molecules (cm⁻¹)

Molecule	State	$\tilde{\nu}_1 (A_1)$	$\tilde{\nu}_2 (A_1)$	$\tilde{\nu}_3 (E)$	$\tilde{\nu}_4 (E)$	Ref.
[SO ₃] ²⁻	Sol'n	967	620	933	469	621
[SO ₃] ⁻	Matrix	1000	604	1175	511	622
[SeO ₃] ²⁻	Sol'n	807	432	737	374	623
[TeO ₃] ²⁻	Sol'n	758	364	703	326	623
[ClO ₃] ⁻	Sol'n	933	608	977	477	624
	Solid	939	614	971	489	625
³⁵ Cl ¹⁶ O ₃	Matrix	905	567	1081	476	626
[BrO ₃] ⁻	Sol'n	805	418	805	358	624,627
	Solid	810	428	790	361	625
[IO ₃] ⁻	Sol'n	805	358	775	320	624
	Solid	796	348	745	306	625
XeO ₃	Sol'n	780	344	833	317	628

The ZXYW-type molecule belongs to the C₁ point group, and all six vibrations are infrared- and Raman-active. The vibrational spectra of OSClBr [666] and [XSnYZ]⁻ (X,Y,Z: a halogen) have been reported [667]. For example, the Raman spectrum of the [ClSnBrI]⁻ ion in the solid state exhibits the $\nu(\text{SnCl})$, $\nu(\text{Sn-Br})$, and $\nu(\text{SnI})$ at 275, 193, and 155 cm⁻¹, respectively.

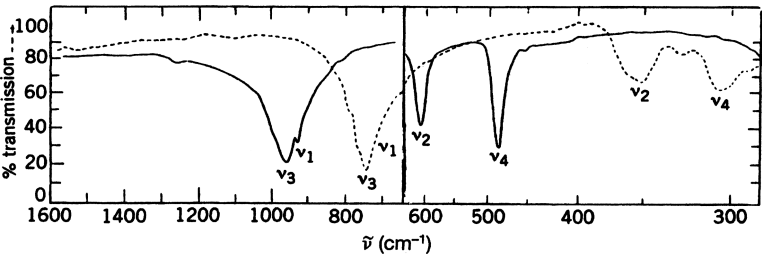


Fig. 2.11. IR spectra of KClO₃ (solid line) and KIO₃ (dotted line).

TABLE 2.3d. Relationship between C_{3v} and C_s

C _{3v}	$\nu_1(A_1)$	$\nu_2(A_1)$	$\nu_3(E)$		$\nu_4(E)$	
XY ₃	$\nu_s(XY)$	$\delta_s(YXY)$	$\nu_d(XY)$		$\delta_d(YXY)$	
	↓	↓	↙	↘	↙	↘
C _s	$\nu_1(A')$	$\nu_3(A')$	$\nu_2(A')$	$\nu_5(A'')$	$\nu_4(A')$	$\nu_6(A'')$
ZXY ₂	$\nu_s(XZ)$	$\delta_s(YXZ)$	$\nu_s(XY)$	$\nu_d(XY)$	$\delta_s(YXY)$	$\delta_d(YXZ)$

TABLE 2.3e. Vibrational Frequencies of Pyramidal ZXY_2 -Type Metal Halides (cm^{-1})

$Z-X \begin{matrix} \nearrow Y \\ \searrow Y \end{matrix}$	$\tilde{\nu}_1 (A')$ $\nu (XZ)$	$\tilde{\nu}_2 (A')$ $\nu_s (XY)$	$\tilde{\nu}_3 (A')$ $\delta_s (YXZ)$	$\tilde{\nu}_4 (A')$ $\delta (YXY)$	$\tilde{\nu}_5 (A'')$ $\nu_a (YX)$	$\tilde{\nu}_6 (A'')$ $\delta_a (YXZ)$	Ref.
HNF_2	3193	972	500	1307	888	1424	630
HNC1_2	3279	687	—	1002	695	1295	631
FNH_2	891	3234	1233	1564	3346	1241	632,633
CINH_2	679	3297	1056	1534	3374	1063	634
DPH_2	674		1092.6	892.9	—	969.5	635
FPH_2	795	2304	934	1090	2310	—	636,637
C1PH_2	511	2303	859	1096	2303	—	637
FAsH_2	649	2108	842	984	2117	—	638
ClPF_2	545	864	411	(302)	852	260	639
BrPF_2	459	858	244	391	849	215	639
FPCl_2	838	525	328	203	525	267	639
FPBr_2	824	398	258	123	423	221	639
IPF_2	375	851	198	413	846	204	640
$[\text{FOH}_2]^+$	865	3386	1067	1630	3225	1261	641
$[\text{BrOF}_2]^+$	1062	655	365	290	630	315	642
OSF_2	1323.5	799.9	531.9	381.5	736.6	397.3	643
OSCl_2	1251	492	194	344	455	284	644,645
OSBr_2	1121	405	120	267	379	223	646
$[\text{FSH}_2]$	853	2500	987	1181	2447	1020	647
$[\text{FSO}_2]^-$	594	1105	378	500	1169	367	648,649
			393		1183		
ClSO_2	288.2	1099.8	497.7	455.8	1131.0	260.1	650
		1098.2			1309.6		
$[\text{ClSO}_2]^-$	214	1120	172	526	1312	(103)	651
$[\text{BrSO}_2]^-$	203	1117	115	530	1308	—	651
$[\text{ISO}_2]$	184	1112	(55)	530	1300	—	651
$[\text{FSeO}_2]^-$	~430	903	283	324	888	238	652
OSeF_2	1049	667	362	282	637	253	653
OSeCl_2	995	388	161	279	347	255	654
$\text{OSe}(\text{OH})_2^a$	831	702	430	336	690	364	655,656
FC1O_2^b	1129.0	634.0	550.0	407.1	1292.2	360.1	657,658
FBrO_2	506	908	305	394	953	271	659
$[\text{OCIF}_2]^+$	1333	731	513	384	695	404	660
$[\text{FXeO}_2]^+$	594	873	281	321	931	249	661,662

^aThe OH group was assumed to be a single atom.^bEmpirical assignment.

2.4. PLANAR FOUR-ATOM MOLECULES

2.4.1. XY_3 Molecules (D_{3h})

The four normal modes of vibration of planar XY_3 molecules are shown in Fig. 2.12; ν_2 , ν_3 , and ν_4 , are infrared-active, and ν_1 , ν_3 , and ν_4 are Raman-active. This case should be contrasted with pyramidal XY_3 molecules, for which all four vibrations are both

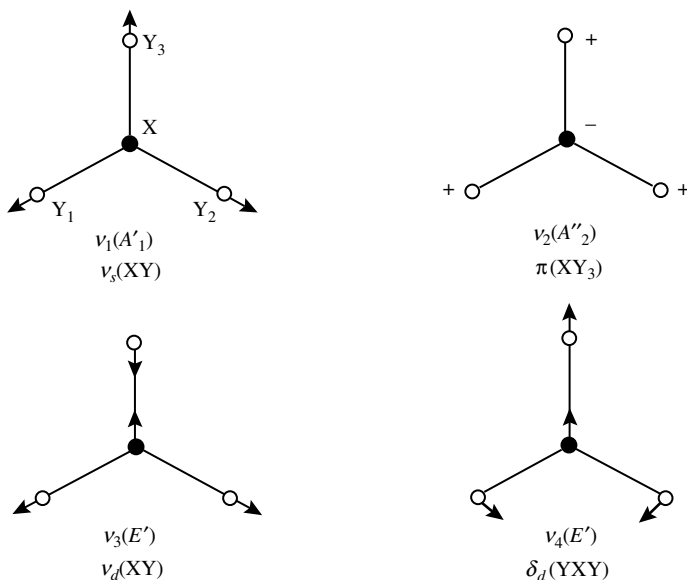


Fig. 2.12. Normal modes of vibration of planar XY_3 molecules.

infrared- and Raman-active. Appendix VII lists the **G** and **F** matrix elements of the planar XY_3 molecule.

Table 2.4a lists the vibrational frequencies of planar XY_3 molecules. As stated above, pyramidal and planar structures can be distinguished by the difference in selection rules. Thus, the pyramidal structure should exhibit two stretching bands (A_1 and E) while the planar structure should show only one stretching band (E') in IR spectra. The ν_3 and ν_4 frequencies are in the order $AlH_3 < GaH_3 < InH_3$ [680]. MnF_3 in the gaseous phase takes a planar structure of C_{2v} symmetry due to the Jahn–Teller effect, and exhibits three stretching [759 (B_2), 712 (A_1), and 644 (A_1)] and three bending [182 (B_1), 186 (A_1), and 180 (B_2 , calculated)] vibrations (all in cm^{-1}) [693].

Assignment of the IR spectrum of $AlCl_3 \cdot NH_3$ has been based on normal coordinate analysis (staggered conformation, C_{3v} symmetry) [694]. $^{11}BF_3$ in inert gas matrices takes a dimeric structure of C_{2h} symmetry via two B–F–B bridges as supported by IR spectra [695]. Other dimeric species such as Al_2F_6 and Al_2Cl_6 are discussed in Sec. 2.10. Normal coordinate calculations on planar XY_3 molecules have been carried out by many investigators [696,697].

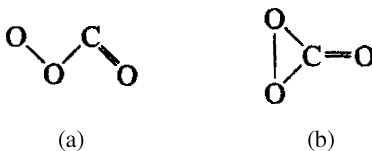
Table 2.4b lists the vibrational frequencies of planar XO_3 -type compounds. Figure 2.13 shows the Raman spectra of KNO_3 in the crystalline state and in aqueous solution. As discussed in Sec 1.26, the spectra of calcite and aragonite are markedly different because of the difference in crystal structure. More recent normal coordinate calculations [713] on the CO_3 radical indicate a *trans*- C_s

TABLE 2.4a. Vibrational Frequencies of Planar XY_3 Molecules (cm^{-1})

Molecule	State ^a	$\tilde{\nu}_1 (A'_1)$	$\tilde{\nu}_2 (A''_2)$	$\tilde{\nu}_3 (E')$	$\tilde{\nu}_4 (E')$	Ref.
$^{10}\text{BH}_3$	Mat	(2623)	1132	2820	1610	668
$^{10}\text{BF}_3$	Gas	888	719.3	1505.8	481.1	669,670
$^{11}\text{BCl}_3$	Liquid	472.7	—	950.7	253.7	671,672
$^{11}\text{BBr}_3$	Liquid	278	374	802	150	671,673
$^{11}\text{BI}_3$	Liquid	192	—	691.8	101.0	671,673
AlH_3	Mat	—	697.8	1882.8	783.4	674
AlD_3	Mat	—	513.9	1376.5	568.4	675
AlF_3	Mat	—	286.2	909.4	276.9	676
AlCl_3	Mat	393.5	—	618.8	150	677
AlBr_3	Gas	228	107	450–500	93	678
AlI_3	Gas	156	77	370–410	64	678
$[\text{AlSb}_3]^{6-}$	Solid	132	181	293,318	—	679
GaH_3	Mat	1923.2	717.4	—	758.7	680
GaCl_3	Mat	386.2	—	469.3	132	677
GaBr_3	Gas	219, 237	95	—	84	677,681
GaI_3	Gas	147	63	275	50	677,681
$[\text{GaSb}_3]^{6-}$	Solid	128	110	192, 210	—	679
InH_3	Mat	1754.5	613.2	—	607.8	680
InCl_3	Mat	359.0	—	400.5	119	677,682
InBr_3	Gas	212	74	280	62	678
InI_3	Gas	151	56	200–230	44	678
$[\text{InAs}_3]^{6-}$	Solid	171	99	197, 215	—	683
TlBr_3	Sol'n	190	125	220	51	684
CH_3	Mat	—	730.3	—	1383	685
$[\text{PS}_3]^-$	Melt	476	540	695	242	686
AuI_3	Solid	164	—	148	106	687
$[\text{CdCl}_3]^-$	Sol'n	265	—	287	90	688
$[\text{CdBr}_3]^-$	Sol'n	168	—	184	58	688
$[\text{CdI}_3]^-$	Sol'n	124	—	161	51	688
$[\text{HgCl}_3]^-$	Solid	273	113	263	100	689
PrF_3	Mat	526,542	86	458	99	690,691
VF_3	Mat	649	—	~732	—	692
CoF_3	Mat	663	—	732.2	162	692

^aMat: inert gas matrix.

structure (a) rather than a three-membered ring C_{2v} structure (b) suggested originally [714].



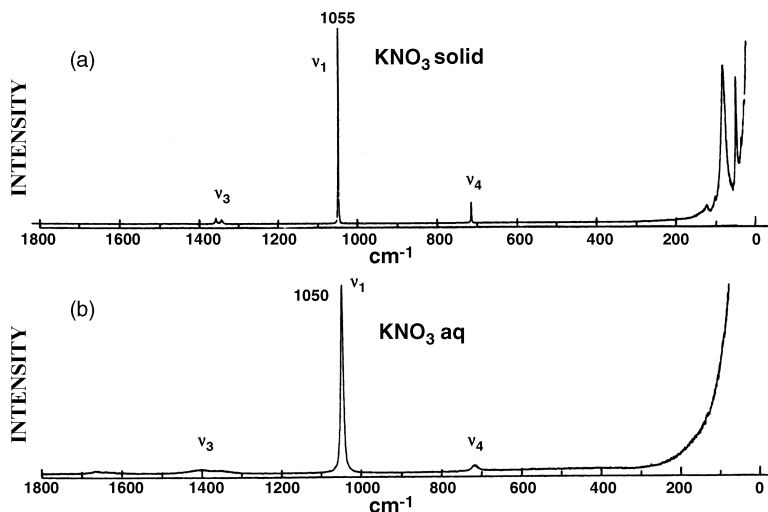
Crystals of LiNO_3 , NaNO_3 , and KNO_3 assume the calcite structure (Sec. 1.31). Nakagawa and Walter [705] carried out normal coordinate analyses on the whole Bravais lattices of these crystals.

TABLE 2.4b. Vibrational Frequencies of Planar XO₃ and Related Compounds in the Crystalline State (cm⁻¹)

Compound		$\tilde{\nu}_1$ (A' ₁)	$\tilde{\nu}_2$ (A'' ₂)	$\tilde{\nu}_3$ (E')	$\tilde{\nu}_4$ (E')	Ref.
La[¹⁰ BO ₃]	IR	939	740.5	1330.0	606.2	698,699
H ₃ [BO ₃]	IR	1060	668, 648	1490–1428	545	706
Ca[CO ₃] (calcite)	IR	—	879	1429–1492	706	701
	R	1087	—	1432	714	701
Ca[CO ₃] (aragonite)	IR	1080	866	1504,1492	711,706	701
	R	1084	852	1460	704	701
Ba[CS ₃]	R	510	516 ^b	920	314	702,703
Ba[CSe ₃]	IR	290	420	802	185	703,704
Na[NO ₃]	IR	—	831	1405	692	705
	R	1068	—	1385	724	705
K[NO ₃]	IR	—	828	1370	695	705
	R	1049	—	1390	716	705
NO ₃	IR	1060	762	1480	380	706–708
SO ₃ ^a	IR	(1068)	495	1391	529	709,710
	R	1065	497.5	1390	530.2	711
SeO ₃ ^a	R	923	—	1219	305	712

^a Gaseous state.^b Infrared.

Müller et al. [715] have shown that the half-width of the ν_3 band of the NO₃⁻ ion at 1384 cm⁻¹ in KBr pellets is decreased by a factor of >5 when the ion is trapped in the cavity of ionic carcerand compounds such as K₁₀[HV₁₂^{IV}V₆O₄₄(NO₃)₂].14.5H₂O. UV resonance Raman spectra of the NO₃⁻ ion in H₂O and ethylene glycol are dominated by the ν_1 , ν_3 , and their overtones and combination bands. The large splitting of the ν_3

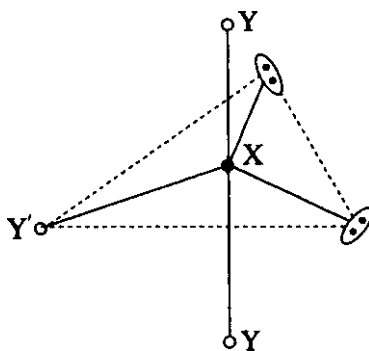
**Fig. 2.13.** Raman spectra of KNO₃ in (a) the solid state and (b) aqueous solution.

vibration ($\sim 60\text{ cm}^{-1}$) suggests the planar-to-pyramidal conversion by electronic excitation [716]. The IR spectrum of KNO_3 in Ar matrices suggest bidentate coordination of the K^+ ion to two oxygen atoms (C_{2v} symmetry) [717]. $^{28}\text{Si}^{16}\text{O}_3$ in Ar matrices also takes a C_{2v} structure with one shorter and two longer SiO bonds [718].

The spectra of anhydrous metal nitrates such as $\text{Zn}(\text{NO}_3)_2$ [719] and $\text{UO}_2(\text{NO}_3)_2$ [720] can be interpreted in terms of C_{2v} symmetry since the NO_3 group is covalently bonded to the metal. Raman spectra of metal nitrates in the molten state [721,722] indicate that the degeneracy of the ν_3 vibration is lost and the Raman-inactive ν_2 vibration appears. Apparently, the D_{3h} selection rule is violated because of cation-anion interaction.

Like CO_3^{2-} and NO_3^- ions, CS_3^{2-} and CSe_3^{2-} ions act as chelating ligands. For normal coordinate analyses of planar XO_3 molecules, see Refs. 723 and 724.

Some XY_3 -type halides take the unusual T-shaped structure of C_{2v} symmetry shown below. This geometry is derived from a trigonal-bipyramidal structure in which two equatorial positions are occupied by two lone-pair electrons. Typical examples are ClF_3 and BrF_3 . With the equatorial Y atom represented as Y' , the following assignments have been made for these molecules: $[\text{725}] \nu(\text{XY}'), A_1, 754 \text{ and } 672; \nu(\text{XY}), B_1, 683.2 \text{ and } 597; \nu(\text{XY}), A_1, 523 \text{ and } 547; \delta, A_1, 328 \text{ and } 235; \delta, B_1, 431 \text{ and } 347; \pi, B_2, 332 \text{ and } 251.5 \text{ cm}^{-1}$ (for each mode, the former value is for ClF_3 and the latter is for BrF_3). The Raman spectrum of XeF_4 in SbF_5 exhibits two strong polarized bands at 643 and 584 cm^{-1} , which were assigned to the T-shaped XeF_3^+ ion in $[\text{XeF}_3][\text{SbF}_6]$ [726]. XeOF_2 assumes a similar T structure [727]. In an inert gas matrix, UO_3 gives an infrared spectrum consistent with the T-shaped structure [728].



2.4.2. ZXY_2 (C_{2v} and $\text{ZXYW}(\text{C}_s)$ Molecules

If one of the Y atoms of a planar XY_3 molecule is replaced by a Z atom, the symmetry is lowered to C_{2v} . If two of the Y atoms are replaced by two different atoms, W and Z, the symmetry is lowered to C_s . As a result, the selection rules are changed, as already shown in Table 1.18. In both cases, all six vibrations become active in infrared and Raman spectra. Table 2.4c lists the vibrational frequencies of planar ZXY_2 and ZXYW molecules.

TABLE 2.4c. Vibrational Frequencies of Planar ZXY₂ and ZXYW Molecules (cm⁻¹)

XY ₃ (D _{3h})	$\tilde{\nu}_1 (A'_1)$	$\tilde{\nu}_2 (A''_2)$	$\tilde{\nu}_3 (\bar{E}')$		$\tilde{\nu}_4 (\bar{E}')$				Ref.
	$\nu_s (XY)$	$\pi (XY_3)$	$\tilde{\nu}_2 (A_1)$	$\nu_d (XY)$	$\tilde{\nu}_3 (A_1)$	$\tilde{\nu}_3 (A_1)$	$\tilde{\nu}_3 (A_1)$	$\tilde{\nu}_3 (A_1)$	
ZXY ₂ (C _{2v})	$\tilde{\nu}_1 (A_1)$	$\tilde{\nu}_6 (B_1)$	$\tilde{\nu}_2 (\bar{E})$		$\tilde{\nu}_3 (\bar{E})$				Ref.
	$\nu (XZ)$	$\pi (ZXY_2)$	$\tilde{\nu}_2 (A_1)$	$\nu_s (XY)$	$\tilde{\nu}_2 (B_2)$	$\tilde{\nu}_2 (B_2)$	$\tilde{\nu}_2 (B_2)$	$\tilde{\nu}_2 (B_2)$	
ZXYW (C _s)	$\tilde{\nu}_1 (A')$	$\tilde{\nu}_6 (A'')$	$\tilde{\nu}_1 (A)$	$\nu (XZ)$	$\tilde{\nu}_1 (A)$	$\tilde{\nu}_1 (A)$	$\tilde{\nu}_1 (A)$	$\tilde{\nu}_1 (A)$	Ref.
	$\nu (XZ)$	π	$\nu (XZ)$	$\nu (XZ)$	$\nu (XZ)$	$\nu (XZ)$	$\nu (XZ)$	$\nu (XZ)$	
H-BCl ₂	2616	786	735	1091	—	—	—	895	729
H-AlCl ₂	1966	473	482	580	—	—	—	655	730
H-AlBr ₂	1953	454	366	574	—	—	—	635	730
Cl-GaH ₂	406.9	620	1964.6	1978.1	731.4	731.4	731.4	510.1	731
H-GaCl ₂	2015.3	464.3	414.3	437.3	130	130	130	607.5	732,733
H-GaBr ₂	1991.5	445.5	287.5	333.0	—	—	—	597.0	733
Cl-InH ₂	343.4	415.7	1804.0	1820.3	575.8	575.8	575.8	541.4	734,735
H-InCl ₂	1846.9	469.7	369.1	358.5	—	—	—	402.6	734
[F-CO ₂] ^{-a}	883	—	1316	1749	—	—	—	—	736,737
[(HO)-CO ₂] ^{-a}	960	835	1338	1697	712	712	712	579	738
[H-CO ₂]	2803	1069	1351	1585	760	760	760	1383	739
[(CH ₃)-CO ₂] ^{-a}	926	621	1413	1556	650	650	650	471	739
Si=CH ₂	933	687	2947	—	1273	1273	1273	263	740
Si=CD ₂	808	539	2185	—	1054	1054	1054	216	740
O=CF ₂	1930	767.4	965.6	1243.7	582.9	582.9	582.9	619.9	741,742
O=CCl ₂	1815.6	581.2	568.3	837.4	368.0	368.0	368.0	441.8	743
O=CHF	1837	—	2981	1065	1343	1343	1343	663	744,745
O=CHI	1776.3	—	2930	(561)	1247.9	1247.9	1247.9	—	746
O=CBr ₂	1828	512	425	757	181	181	181	350	747
O=CClF	1868	667	776	1095	501	501	501	415	747,747a
O=CBrCl	1828	547	517	806	240	240	240	372	747

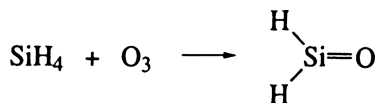
(continued)

TABLE 2.4c. (Continued)

$\text{XY}_3\ (\mathbf{D}_{3h})$	$\tilde{\nu}_1\ (\text{A}'_1)$ $\nu_s\ (\text{XY})$	$\tilde{\nu}_2\ (\text{A}''_2)$ $\pi\ (\text{XY}_3)$	$\underbrace{\tilde{\nu}_3\ (\text{E}')}_{\nu_d\ (\text{XY})}$	$\underbrace{\tilde{\nu}_4\ (\text{E}')}_{\delta_d\ (\text{YXY})}$	Ref.	
			$\underbrace{\tilde{\nu}_2\ (\text{A}_1)}_{\nu_s\ (\text{XY})}$	$\underbrace{\tilde{\nu}_3\ (\text{A}_1)}_{\delta_s\ (\text{ZXY})}$		
$\text{ZXY}_2\ (\mathbf{C}_{2v})$	$\tilde{\nu}_1\ (\text{A}_1)$ $\nu\ (\text{XZ})$	$\tilde{\nu}_6\ (\text{B}_1)$ $\pi\ (\text{ZXY}_2)$	$\underbrace{\tilde{\nu}_4\ (\text{B}_2)}_{\nu_d\ (\text{XY})}$	$\underbrace{\tilde{\nu}_5\ (\text{B}_2)}_{\delta_a\ (\text{ZXY})}$		
	$\tilde{\nu}_1\ (\text{A}')$ $\nu\ (\text{XZ})$	$\tilde{\nu}_6\ (\text{A}'')$ π	$\underbrace{\tilde{\nu}_4\ (\text{A}')}_{\nu\ (\text{XZ})}$	$\underbrace{\tilde{\nu}_5\ (\text{A}')}_{\delta\ (\text{ZXW})}$		
$\text{ZXYW}\ (\mathbf{C}_s)$						
$\text{O}=\text{CBrF}$	1874	620	721	398	335	747
$\text{S}=\text{CH}_2$	1063	993	2970	1550	1437	748
$\text{S}=\text{CF}_2$	1368	622	787	526	417	749,750
$\text{Se}=\text{CCl}_2$	1120	472	~500	296	~302	751
$\text{Se}=\text{CF}_2$	1280	560	710	432	352	752
$[\text{Se}-\text{CS}_2]^-$	442	485	433	284	265	753
$\text{O}=\text{SiCl}_2$	1240	—	501.1	—	—	754
$\text{S}=\text{SiF}_2$	638	296	996	337	247	755
$\text{S}=\text{SiCl}_2$	739.1	—	—	—	186	756
$\text{S}=\text{GeCl}_2$	580	—	404	—	—	757
$(\text{HO})=\text{NO}_2^a$	902	767	1311	660	597	758
$\text{F}-\text{NO}_2$	~555	740	1308	810	~555	759,760
$\text{Cl}-\text{NO}_2$	370	652	1318	787	411	754,760
$\text{O}=\text{NF}_2$	1573	(440)	813	705	553	761
$[\text{O}=\text{NF}_2]^+$	1862	715	897	569	347	762,763
$[\text{O}=\text{NCl}_2]^+$	1648	—	628	220	420	764
$\text{Br}-\text{PO}_2$	363.2	—	1146.5	513.5	230	765

^a Only the ZXY_2 skeletal vibrations are listed.

Silanone produced by the silane–ozone photochemical reaction in Ar matrices gives rise to a band at 1202 cm^{-1} in the IR spectrum that is assigned to the $\nu(\text{Si}=\text{O})$ [766]:



The frequencies listed for the formate and acetate ions were obtained in aqueous solution. Vibrational spectra of metal salts of these ions are discussed in Sec. 3.8. Although not listed in this table, the IR spectra of binary mixed halides of boron [767] and aluminum [768] have also been reported.

2.5. OTHER FOUR-ATOM MOLECULES

2.5.1. X_4 Molecules

Tetrahedral X_4 -type molecules of T_d symmetry exhibit three normal vibrations as shown in Fig. 2.14, and $\nu_1(A_1)$ and $\nu_2(E)$ are Raman-active whereas $\nu_3(F_2)$ is IR as well as Raman-active. Table 2.5a lists observed frequencies of tetrahedral X_4 molecules. Comparison of vibrational frequencies of the X_4^{4-} ($\text{X} = \text{Si}, \text{Ge}, \text{Sn}$) series and the corresponding isoelectronic Y_4 ($\text{Y} = \text{P}, \text{As}, \text{Sb}$) series shows that the ratio, $\nu(\text{X}_4^{4-})/\nu(\text{Y}_4)$ is approximately 0.77. On the basis of this criterion, Kliche et al. [770] predicted that the vibrational frequencies of the Pb_4^{4-} ion are $115 (A_1)$, $69 (E)$, and $93 (F_2) \text{ cm}^{-1}$.

On the other hand, the X_4 -type cation such as S_4^{2+} assumes a square–planar ring structure of D_{4h} symmetry, and its 6 ($3 \times 4 - 6$) vibrations are classified into $A_{1g}(\text{R}) + B_{1g}(\text{R}) + B_{2g}(\text{R}) + B_{2u}(\text{inactive}) + E_u(\text{IR})$. Assignments of these vibrations have been based on normal coordinate analysis [776a–776c]. Table 2.5b shows the normal modes and vibrational frequencies of square–planar X_4 cations.

2.5.2. X_2Y_2 Molecules

Molecules like O_2H_2 take the nonplanar C_2 structure (twisted about the O–O bond by $\sim 90^\circ$), whereas N_2F_2 and $[\text{N}_2\text{O}_2]^{2-}$ exist in two forms: *trans*-planar (C_{2h}) and

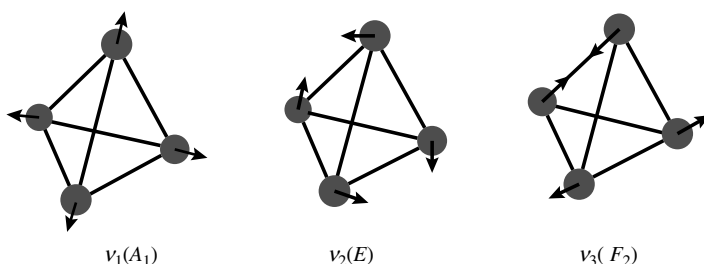


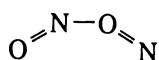
Fig. 2.14. Normal modes of vibration of tetrahedral X_4 molecules.

TABLE 2.5a. Vibrational Frequencies of X_4 Molecules (cm^{-1})

Molecule	$\tilde{\nu}_1 (A_1)$	$\tilde{\nu}_2 (E)$	$\tilde{\nu}_3 (F_2)$	Ref.
Si_4^{4-}	486	282 305	338 356 376	769,770
Ge_4^{4-}	276	154 165	197 206 216	769
Sn_4^{4-}	182	102	140	770
P_4	613.6	371.8	467.3	771,772
As_4	353	207.5	265.5	773
Sb_4	241.5	137.1	178.5	774
Bi_4	149.5	89.8	120.4	775
Ta_4	270.2	130.6	185.1	776





cis-planar (C_{2v}). Figure 2.15 shows the six normal modes of vibration for these three structures. The selection rules for the C_{2v} and C_2 structures are different only in the ν_6 vibration, which is infrared-inactive and Raman depolarized in the planar model but infrared-active and Raman polarized in the nonplanar model.

Table 2.5c lists the vibrational frequencies of X_2Y_2 -type molecules. In N_2 matrices, $(\text{NO})_2$ exists in three forms; *cis*, *trans*, and another form of uncertain structure. The *cis* form is most stable, and its ν_s and ν_a are at 1870 and 1776 cm^{-1} respectively [791]. The NO reacts with Lewis acids such as BF_3 to form a red species at 77 K . Ohlsen and Laane [792] measured its resonance Raman spectrum and concluded that it is an asymmetric $(\text{NO})_2$ dimer having a *cis*-planar structure:



A possible mechanism for the formation of such a dimer in the presence of Lewis acids has been proposed. Although the $\text{N}_2\text{O}_2^{2-}$ ion takes a *cis* or *trans* structure in the solid state, the $\text{N}_2\text{O}_2^{2-}$ ion produced in Ar matrices exhibits an IR band at

TABLE 2.5b. Vibrational Frequencies of Square-Planar X_4 -Type Ions (cm^{-1})

Ion		S_4^{2+}	Se_4^{2+}	Te_4^{2+}
$\tilde{\nu}_1 (A_{1g})$		583.6	321.3	219
$\tilde{\nu}_2 (B_{1g})$		371.2	182.3	109
$\tilde{\nu}_3 (B_{2g})$		598.1	312.3	219
$\tilde{\nu}_5 (E_u)$		542	302	187

Source: Taken from Ref. 776b.

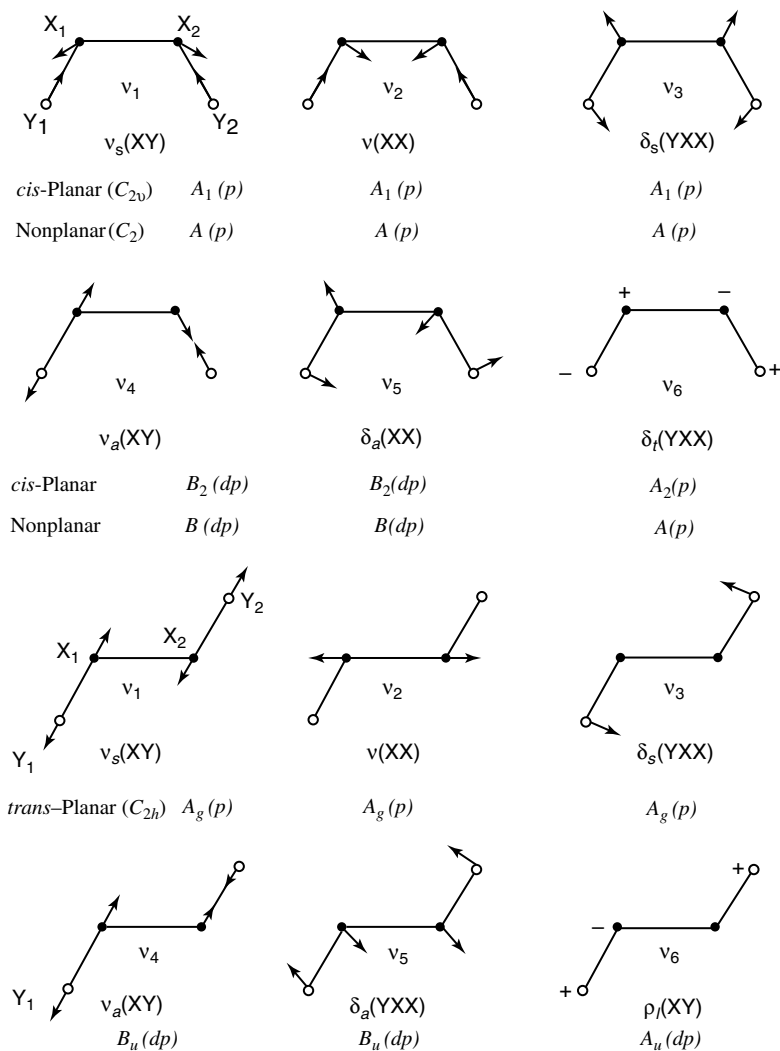
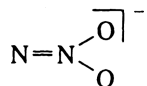


Fig. 2.15. Normal modes of vibration of nonlinear X_2Y_2 molecules (p —polarized; dp —depolarized) [749].

1205 cm^{-1} , and its structure was suggested to be [793]



Diazene (N_2H_2) exists in both *cis* and *trans* forms:

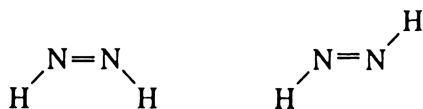


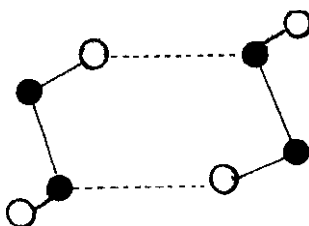
TABLE 2.5c. Vibrational Frequencies of X_2Y_2 Molecules (cm^{-1})^a

		ν_1	ν_2	ν_3	ν_4	ν_5	ν_6	
<i>trans</i> - X_2Y_2 :	C_{2h}	A_g	A_g	A_g	B_u	B_u	A_u	
<i>cis</i> - X_2Y_2 :	C_{2v}	A_1	A_1	A_1	B_2	B_2	A_2	
Twisted X_2Y_2 :	C_2	A	A	A	B	B	A	
Assignment		ν_s (XY)	ν (XY)	δ_s (YXX)	ν_a (XY)	δ_a (YXX)	π	Ref.
<i>cis</i> - $[N_2O_2]^{2-}$	Solid	830	1314	584	1047	330	—	777,778
<i>trans</i> - $[N_2O_2]^{2-}$	Soild	(1419)	(1121)	(396)	1031	371	492	779,780
<i>cis</i> - N_2F_2	Liquid	896	1525	341	952	737	(550)	781
<i>trans</i> - N_2F_2	Liquid	1010	1522	600	990	423	364	782
O_2H_2	Gas	3607	1394	864	3608	1266	317	783,784
O_2D_2	Gas	2669	1029	867	2661	947	230	783
O_2F_2	Matrix	611	1290	366	624	459	(202)	785
S_2H_2	Liquid	2509	509	(868) ^b	2557 ^c	882	—	786
S_2F_2	Gas	717	615	320	681	301	183	787
S_2Cl_2	Gas	466	546	202	457	240	92	788,789
S_2Br_2	Liquid	365	529	172	351	200	66	790
Se_2Cl_2	Liquid	367	288	130	367	146	87	789,790
Se_2Br_2	Liquid	265	292	107	265	118	50	790

^aExcept for N_2F_2 and $[N_2O_2]^{2-}$, all the molecules listed take the C_2 or C_{2v} structure.^bSolid.^cGas.

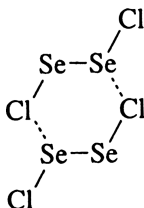
and the observed frequencies are 3116, 3025, 1347, and 1304 cm^{-1} for the *cis* form, and 3109 and 1333 cm^{-1} for the *trans* form [794].

The IR spectra of $(H_2O_2)_2$ dimer and its deuterated analogs have been measured in Ar matrices. Both experimental and theoretical studies suggest the cyclic structure shown below [794a]:



A strong vibrational coupling was observed between the two bonded OH stretching modes, and a relatively strong coupling was noted between the two HOO bending modes.

The Raman spectra of Se_2Cl_2 and Se_2Br_2 in CS_2 and CCl_4 solutions indicate that the former takes the C_2 structure, whereas the latter takes the C_{2v} structure [795]. Although S_2Cl_2 does not dimerize at low temperatures, Se_2Cl_2 forms a dimer below -50°C . A new Raman band observed at 215 cm^{-1} was attributed to the dimer for which the following ring structure was proposed [796]:



Ketelaar et al. [797] found that the liquid mixture of CS_2 and S_2Br_2 , for example, exhibits IR spectra that show combination bands between the ν_3 of CS_2 (1515 cm^{-1}) and a series of S_2Br_2 vibrations. Such “simultaneous transitions” seem to suggest the formation of an intermolecular complex, at least on the vibrational time scale.

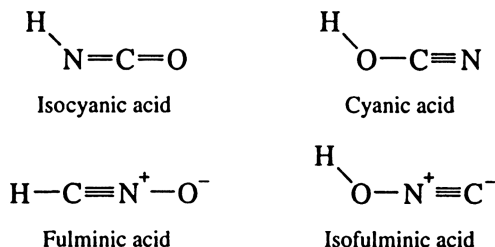
The Raman spectra of the $[\text{Te}_2\text{X}_2]^{2-}$ ion ($\text{X} = \text{Se}$ or Te), which takes an almost planar diamond-shaped ring structure (C_{2v}), have been assigned [798]. Si_2H_2 prepared in inert gas matrices assumes butterfly-like structure with the Si–Si bond located along the fold of the two Si–H–Si wing planes, and its IR spectrum was assigned on the basis of C_{2v} symmetry [799]. The $[\text{Cl}_2\text{O}_2]^+$ ion formed by the $\pi-\pi^*$ charge transfer interaction of Cl_2^+ and O_2 takes a planar trapezoid structure of C_{2v} symmetry, and the $\nu(\text{OO})$ and $\nu(\text{ClCl})$ are at $1534\text{ (A}_1)$ and $593\text{ (A}_1)$, respectively, and $\nu(\text{ClO})$ are at $414\text{ (B}_2)$ and $263\text{ (A}_1)$ (all in cm^{-1}) [800].

Normal coordinate analyses of H_2O_2 [801] and S_2X_2 (X : a halogen) [802,790] have been carried out. Other $(\text{XY})_2$ -type compounds include dimeric metal halides such as $(\text{LiF})_2$, which takes a planar ring structure (Sec. 2.1).

2.5.3. Planar WXYZ, XYZY, and XYYY Molecules (C_s)

Planar four-atom molecules of the WXYZ, XYZY, and XYYY types have six normal modes of vibration, as shown in Fig. 2.16. All these vibrations are both infrared- and Raman-active. In HXYZ and HYZY molecules, the XYZ and YZY skeletons may be linear (HNCO , HSCN) or nonlinear (HONO , HNSO). In the latter case, the molecule may take a *cis* or *trans* structure. Table 2.5d lists the vibrational frequencies of molecules and ions belonging to these types. Normal coordinate analyses have been carried out for HN_3 [831] and HONO [832].

Teles et al. [804] measured the IR spectra of all four possible isomers of HNCO in Ar matrices at 13 K, and compared the observed frequencies with those obtained by *ab initio* calculation:



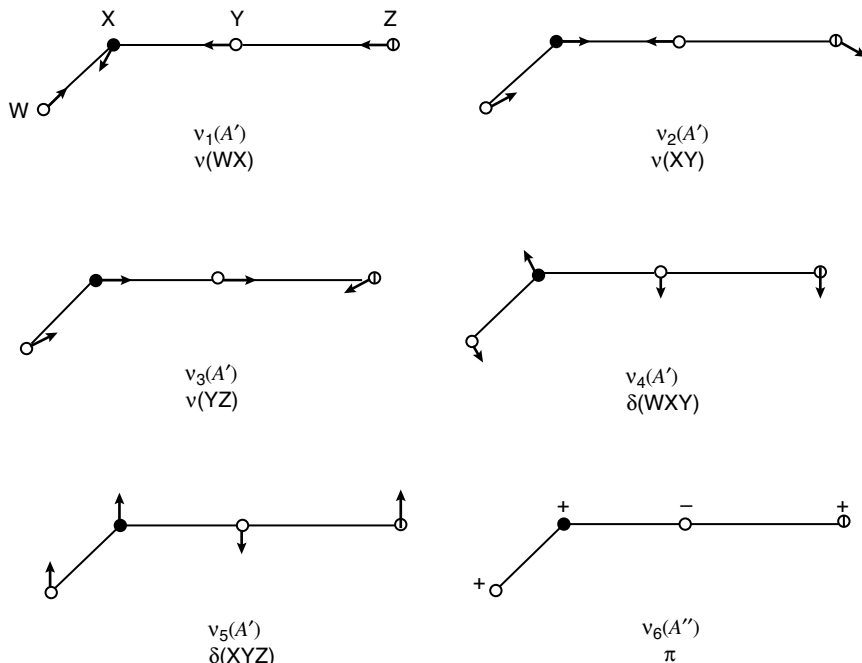


Fig. 2.16. Normal modes of vibration of nonlinear WXYZ molecules.

As shown above, fulminic acid is linear, while the remaining three acids assume bent structures. For a detailed discussion on the structures and IR spectra of these acids, see the review by Teles et al. [804].

Vibrational frequencies are reported for other four-atom molecules such as *cis*-OSOO, which was produced by laser irradiation (193 nm) of the planar SO_3 in Ar matrices at 12 K [833], and the HOOO radical, which is probably in *cis*-conformation in inert gas matrices [834]. Vibrational assignments have also been made for linear four-atom molecules containing CN groups; CNCN (isocyanogen) [835]. HCCN radical (cyanomethylene), [836] [FCNF] [837], and a pair of HBeCN and HBeNC that were formed by reacting Be atom with HCN in Ar matrices at 6–7 [838].

2.6. TETRAHEDRAL AND SQUARE-PLANAR FIVE-ATOM MOLECULES

2.6.1. Tetrahedral XY_4 Molecules (T_d)

Figure 2.17 illustrates the four normal modes of vibration of a tetrahedral XY_4 molecule. All four vibrations are Raman-active, whereas only ν_3 and ν_4 are infrared-active. Appendix VII lists the **G** and **F** matrix elements for such a molecule.

Fundamental frequencies of XH_4 -type molecules are listed in Table 2.6a. The trends $\nu_3 > \nu_1$ and $\nu_2 > \nu_4$ hold for the majority of the compounds. The XH stretching frequencies are lowered whenever the XH_4 ions form hydrogen bonds with counter-

TABLE 2.5d. Vibrational Frequencies of WXYZ and Related Molecules (cm⁻¹)

Molecule ^{a,b}	$\tilde{\nu}_1, \nu(\text{WX})$	$\tilde{\nu}_2, \nu(\text{XY})$	$\tilde{\nu}_3, \nu(\text{YZ})$	$\tilde{\nu}_4, \delta(\text{WXY})$	$\tilde{\nu}_5, \delta(\text{XYZ})$	$\tilde{\nu}_6, \pi$	Ref.
(HNCN) ⁻ (s)	3235	2085	1092	1190	570	538	803
HNCO	3516.8 3505.7	2259.0	—	769.8	573.7	—	804,805
DNCO	2606.9	2231.0	—	578.6	475.4	—	804
H N O O	3165.5	1092.3	1054.5	1485.5	—	764.0	806
HOCN	3569.6	1081.3	2286.3	1227.9	—	—	804,807
DOCN	2635.0	949.4	2284.6	1077.8	—	—	804,807
HCNO	3317.2	2192.7	1244.1	566.6	536.9 538.2	—	804
CICNO (g)	—	2219	1350 1336	—	—	—	808
DCNO	2612.7	2063.2	1218.5	418.7	—	—	804
HONC	3443.7	628.4	2190.1	1232.4	361.2	379.3	804
DONC	2545.2	623.1	2190.3	902.6	357.3	362.1	804
HNCO (film)	3203	2254	1325~1194	937~793	612	649	809
FNCO	861	2172	(2160)	529	695	646	810
CINCO (g)	607.7	2212.2	1306.6	—	707.7	559.0	811
BrNCO	505	2196.0	1290.9	137.4	691.1	572.2	812
INCO (g)	462.3	2201.1	1298.1	—	667.7	583.3	811
HNNN (g)	3324	2150	1168	1273	527	588	813
FNNN (g)	873	2037	1090	658	241	504	813
CINNN (g)	545	2075	1145	719	223	522	813
BrNNN (g)	452	2058	1150	682	—	—	813
INNN (g)	360	2055	1170	648	—	578	813
<i>cis</i> -HONO	~3397	~847	1630	~1317	616	~637	814,815
<i>trans</i> -HONO	~3553	~796	1685	1265	608	550	814
HOCIO	3527.1	591.5	973.9	1176.9	—	—	816
HNCS	3565	1979	988	577	461	—	817
DNCS	2623	1938	—	548	366	—	817
HCNS (g)	3539	1989	857	615	469	539	818
DCNS (g)	2645	1944	851	549	366	481	818
<i>trans</i> -HSCN	2580.9	—	2182.3	965.9	—	—	819
CISCN (sol'n)	520	678	2162	—	353	—	820,811
BrSCN (sol'n)	451	676	2157	—	369	—	820,811
I SCN (sol'n)	372	700	2130	—	362	—	820,811
<i>cis</i> -HNSO	3309	1083	1249	900	447	755	821,822
<i>trans</i> -HNSO	3308	982	1381	878	496	651	823
<i>trans</i> -HNNO	3254.0	1628.9	1296.2	1214.7	—	746.5	824
<i>cis</i> -CIONO	640.0	—	1710.5	—	—	—	825
<i>trans</i> -CIONO	658.0	—	1754.9	—	~850	—	825
<i>cis</i> -BrONO	862.6	573.5	1650.7	420	—	368.3	826
<i>trans</i> -BrONO	835.9	586.9	1723.4	391.2	197	299.3	826
<i>trans</i> -HONS	3528.0	642.1	969.5	1363.3	476.5	531	827
FNSO (liquid)	825	995	1230	228	600	395	828
CINSO (liquid)	526	989	1221	187	672	359	828
BrNSO (liquid)	451	1000	1214	161	624	342	828
INSO (liquid)	372	1928	1247	154	602	330	828
<i>cis</i> -OSNO	1156.1	—	1454.4	—	—	—	829
<i>trans</i> -OSNO	1178.0	—	1459.0	—	—	—	829

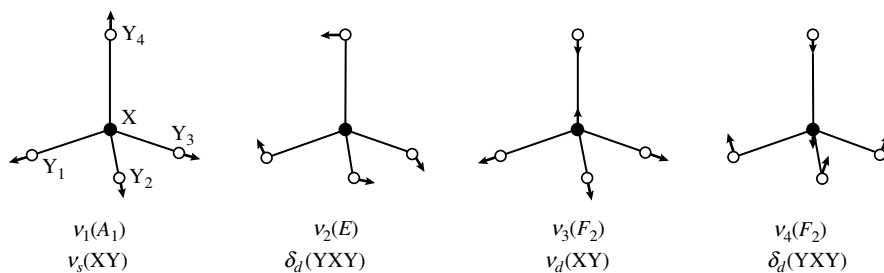
(continued)

TABLE 2.5d. (Continued)

Molecule ^{a,b}	$\tilde{\nu}_1$, $\nu(\text{WX})$	$\tilde{\nu}_2$, $\nu(\text{XY})$	$\tilde{\nu}_3$, $\nu(\text{YZ})$	$\tilde{\nu}_4$, $\delta(\text{WXY})$	$\tilde{\nu}_5$, $\delta(\text{XYZ})$	$\tilde{\nu}_6$, π	Ref.
<i>cis</i> -HOSO	3544	776	1166	—	—	—	830

^aVibrational frequencies were measured in inert gas matrices except for those marked by s (solid), g (gas), sol'n (solution), liquid, and film.

^bSome assignments listed are only empirical.

Fig. 2.17. Normal modes of vibration of tetrahedral XY_4 molecules.TABLE 2.6a. Vibrational Frequencies of Tetrahedral XH_4 Molecules (cm^{-1})

Molecule	$\tilde{\nu}_1$	$\tilde{\nu}_2$	$\tilde{\nu}_3$	$\tilde{\nu}_4$	Ref.
$[\text{}^{10}\text{BH}_4]^-$	2270	1208	2250	1093	839,840
$[\text{}^{10}\text{BD}_4]^-$	1604	856	1707	827	839,840
$[\text{AlH}_4]^-$	1757	772	1678	760 or 766	841,842
$[\text{AlD}_4]^-$	1256	549	1220	560 or 556	841,842
$[\text{GaH}_4]^-$	1807	—	—	—	841,842
CH_4	2917	1534	3019	1306	843
CD_4	2085	1092	2259	996	844,845
SiH_4	2180	970	2183	910	843,846
SiH_4	—	—	2192	913	847
SiD_4	(1545)	(689)	1597	681	846,848
GeH_4	2106	931	2114	819	843,849
GeD_4	1504	665	1522	596	843
SnH_4	—	758	1901	677	850
SnD_4	—	539	1368	487	850
PbH_4	—	—	1823	602	851
$[\text{}^{14}\text{NH}_4]^+$	3040	1680	3145	1400	843
$[\text{}^{15}\text{NH}_4]^+$	—	(1646)	3137	1399	852
$[\text{ND}_4]^+$	2214	1215	2346	1065	843
$[\text{NT}_4]^+$	—	976	2022	913	852
$[\text{PH}_4]^+$	2295	1086, 1026	2366, 2272	974, 919	853
$[\text{PD}_4]^+$	1654	772, 725	1732	677	853
$\{\text{AsH}_4\}^+$	2321	1024	2341	941	854
$[\text{AsD}_4]^+$	1664	732	1676	688	854
$[\text{SbH}_4]^+$	2051	842	2061	795	854
$[\text{SbD}_4]^+$	1462	600	1470	575	854

ions. In the same family of the periodic table, the XH stretching frequency decreases as the mass of the X atom increases. Shirk and Shriver [841] noted, however, that the ν_1 frequency and the corresponding force constant show an unusual trend in group IIIB:

	$[\text{BH}_4]^-$	$[\text{GaH}_4]^-$	$[\text{AlH}_4]^-$
$\tilde{\nu}_1$ (cm^{-1})	2270	1807	1757
F_{11} ($\text{mdyn}/\text{\AA}$)	3.07	1.94	1.84

In a series of ammonium halide crystals, the $\nu(\text{NH}_4^+)$ becomes lower and the $\delta(\text{NH}_4^+)$ becomes higher as the $\text{N}-\text{H}\cdots\text{X}$ hydrogen bond becomes weaker in the order $\text{X} = \text{F} > \text{Cl} > \text{Br} > \text{I}$.

Figure 2.18 shows the infrared spectrum of NH_4Cl , measured by Hornig and others [855], who noted that the combination band between ν_4 (F_2) and ν_6 (rotatory lattice mode) is observed for NH_4F , NH_4Cl , and NH_4Br because the NH_4^+ ion does not rotate freely in these crystals. In NH_4I (phase I), however, this band is not observed because the NH_4^+ ion rotates freely.

Table 2.6b lists the vibrational frequencies of a number of tetrahalogeno compounds. The trends $\nu_3 > \nu_x$ and $\nu_4 > \nu_2$ hold for most of the compounds. The latter trend is opposite to that found for MH_4 compounds. The same table also shows the effect of changing the halogen. First, the MX stretching frequency decreases as the halogen is changed in the order $\text{F} > \text{Cl} > \text{Br} > \text{I}$. The average values, of $\nu(\text{MBr})/\nu(\text{MCl})$ and $\nu(\text{MI})/\nu(\text{MCl})$ calculated from all the compounds listed in Table 2.6b are approximately 0.76 and 0.62, respectively, for ν_3 , and approximately 0.61 and 0.42, respectively, for ν_1 . These values are useful when we assign the MX stretching bands of halogeno complexes (Sec. 3.23 in Part B). Also, the effect of changing the oxidation state on the MX stretching frequency is seen in pairs such as $[\text{FeX}_4]^-$ and $[\text{FeX}_4]^{2-}$ ($\text{X} = \text{Cl}, \text{Br}$) [894], the MX stretching frequency increases as the oxidation state of the metal becomes higher. The ratio $\nu_3(\text{FeX}_4^-)/\nu_3(\text{FeX}_4^{2-})$ is 1.32 in this case.

In the solid state, ν_3 and ν_4 may split into two or three bands because of the site effect. In some cases, the MX_4 ions are distorted to a flattened tetrahedron (D_{2d}) or a structure of lower symmetry (C_s) [892,912]. According to an X-ray analysis [913] the unit cell of $[(\text{CH}_3)_2\text{CHNH}_3]_2[\text{CuCl}_4]$ contains two square-planar and four distorted tetrahedral $[\text{CuCl}_4]^{2-}$ ions.

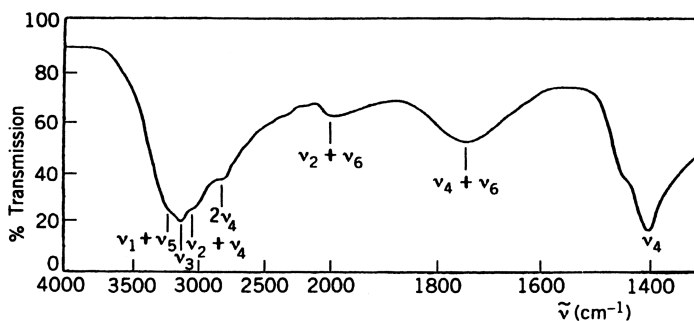


Fig. 2.18. IR spectrum of crystalline NH_4Cl (ν_5, ν_6 —lattice modes).

TABLE 2.6b. Vibrational Frequencies of Tetrahedral Halogeno Compounds (cm⁻¹)

Molecule	$\tilde{\nu}_1$	$\tilde{\nu}_2$	$\tilde{\nu}_3$	$\tilde{\nu}_4$	Ref.
[BcF ₄] ²⁻	547	255	800	385	856
[MgCl ₄] ²⁻	252	100	330	142	857
[MgBr ₄] ²⁻	150	60	290	90	857
[MgI ₄] ²⁻	107	42	259	60	857
[BF ₄] ⁻	777	360	1070	533	858
[BCl ₄] ⁻	406	192	722	278	859,860
[BBr ₄] ⁻	243	118	620	166	859,861
[BI ₄] ⁻	170	83	533	117	862
[AlF ₄] ⁻	622	210	760	322	863
[AlCl ₄] ⁻	348	119	498	182	864
[AlBr ₄] ⁻	212	98	394	114	865
[AlI ₄] ⁻	146	51	336	82	866
[GaCl ₄] ⁻	343	120	370	153	867
[GaBr ₄] ⁻	210	71	278	102	868
[GaI ₄] ⁻	145	52	222	73	869
[InCl ₄] ⁻	321	89	337	112	870
[InBr ₄] ⁻	197	55	239	79	871
[InI ₄] ⁻	139	42	185	58	869
[TlCl ₄] ⁻	303	83	296	104	872
[TlBr ₄] ⁻	186	54	199	64	872
[TlI ₄] ⁻	130	—	146	60	873
CF ₄	908.4	434.5	1283.0	631.2	874
CCl ₄	460.0	214.2	792,765 ^a	313.5	874
CBr ₄	267	123	672	183	875
Cl ₄	178	90	555	123	876
SiF ₄	800.8	264.2	1029.6	388.7	874
SiCl ₄	423.1	145.2	616.5	220.3	874
SiBr ₄	246.7	84.8	494.0	133.6	874
SiI ₄	168.1	62	405.5	90.6	877
⁷⁰ GeF ₄	735.0	202.9	806.9	273.7	878
GeCl ₄	396.9	125.0	459.1	171.0	874
GeBr ₄	235.7	74.7	332.0	111.1	874
GeI ₄	158.7	~60	264.1	79.0	877
SnCl ₄	369.1	95.2	408.2	126.1	874
SnBr ₄	222.1	59.4	284.0	85.9	874
SnI ₄	147.7	42.4	210	63.0	874
PbCl ₄	331	90	352	103	879
[NF ₄] ⁺	848	443	1159	611	880,882
[NCl ₄] ⁺	635	430.3	283.3	233.3	881
[PF ₄] ⁺	906	275	1167	358	882
[PCl ₄] ⁺	458	178	662	255	883
[PBr ₄] ⁺	266	106	512	153	884
[PI ₄] ⁺	193.5	71.0	410	89.0	885
[AsF ₄] ⁺	745	213	829	272	886
[AsCl ₄] ⁺	422	156	500	187	887,888
[AsBr ₄] ⁺	244	88	349	115	889
[AsI ₄] ⁺	183	72	319	87	890
[SbCl ₄] ⁺	395.6	121.5	450.7	139.4	891
[SbBr ₄] ⁺	234.4	76.2	304.9	92.1	891
[CuCl ₄] ²⁻	—	77	267, 248	136, 118	892,893

TABLE 2.6b. (Continued)

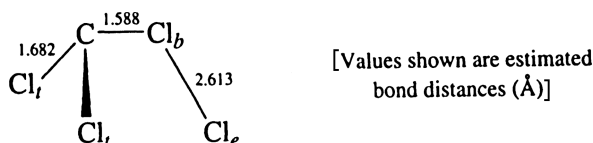
Molecule	$\tilde{\nu}_1$	$\tilde{\nu}_2$	$\tilde{\nu}_3$	$\tilde{\nu}_4$	Ref.
[CuBr ₄] ²⁻	—	—	216, 174	85	892
[ZnCl ₄] ²⁻	276	80	277	126	894
[ZnBr ₄] ²⁻	171	—	204	91	894
[ZnI ₄] ²⁻	118	—	164	—	894
[CdCl ₄] ²⁻	261	84	249, 240	98	895
[CdBr ₄] ²⁻	161	49	177	75, 61	895
[CdI ₄] ²⁻	116	39	—	50	895
[HgCl ₄] ²⁻	267	180	276	192	896
[HgI ₄] ²⁻	126	35	140	41	897
[Scl ₄] ⁻	129	37	—	54	898
TiF ₄	712	185	793	209	899
TiCl ₄	389	114	498	136	900
TiBr ₄	231.5	68.5	393	88	900
TiI ₄	162	51	323	67	900
ZrF ₄	(725–600)	(200–150)	668	190	901
ZrCl ₄	377	98	418	113	900
ZrBr ₄	225.5	60	315	72	900
ZrI ₄	158	43	254	55	900
HfCl ₄	382	101.5	390	112	900
HfBr ₄	235.5	63	273	71	900
HfI ₄	158	55	224	63	900
VCl ₄	383	128	475	128, 150	902
CrF ₄	717	—	790	201	903
CrCl ₄	373	116	486	126	904
CrBr ₄	224	60	368	71	904
[MnCl ₄] ²⁻	256	—	278, 301	120	894,905
[MnBr ₄] ²⁻	195	65	209, 221	89	894,905
[MnI ₄] ²⁻	108	46	188, 193	56	894,905
[FeCl ₄] ⁻	330	114	~378	~136	894
[FeBr ₄] ⁻	211	74	307/292	94	906,894
[FeCl ₄] ²⁻	266	82	286	119	894
[FeBr ₄] ²⁻	162	—	219	84	894
[Fe I ₄] ⁻	142	60	252/235	73	907
[NiCl ₄] ²⁻	264	—	294/280	119	892,908
[Ni Br ₄] ²⁻	—	—	228	81	892,908
[Ni I ₄] ²⁻	105	—	191	—	892
[CoCl ₄] ²⁻	287	92	320	143/126	909
[CoBr ₄] ²⁻	179	74	243/249	101/90	909
[Co I ₄] ²⁻	118	—	202/194	56	892
U F ₄	—	(123)	537	114	910
U Cl ₄	—	—	337.4	71.7	911

^a Fermi resonance with ($\nu_1 + \nu_4$).

Willett et al. [914] demonstrated by using IR spectroscopy that distorted tetrahedral ions can be pressed to square-planar ions under high pressure. In nitromethane, (Et₄N)₂[CuCl₄] exhibits two bands at 278 and 237 cm⁻¹, indicating the distortion in solution [915]. A solution of (Et₃NH) [GaCl₄] in 1,2-dichloroethylene exhibits three bands at 390, 383, and 359 cm⁻¹ due to lowering of symmetry caused by NH...Cl hydrogen bonding [916]. The IR spectra of long-chain tertiary and quaternary

ammonium salts of $[\text{GaCl}_4]^-$ and $[\text{GaBr}_4]^-$ ions in benzene solution show that the degree of distortion of these ions depends on the nature of the cation and the concentration [917]. Distortion of $[\text{MCl}_4]^{2-}$ ions ($\text{M} = \text{Fe}, \text{Co}, \text{Ni}, \text{Zn}$) is also reported for their cesium and rubidium salts [918].

Matrix isolation spectroscopy has provided structural information that is unique to XY_4 -type molecules in inert gas environments. For example, the symmetry of the anions in Cs^+BF_4^- and Cs^+PF_4^- formed via salt–molecule reactions in Ar matrices are lowered to C_{3v} in the former, and to a Symmetry no higher than C_{2v} , in the latter [920]. In inert gas matrices, the symmetry of UF_4 is distorted to D_{2d} [921]. Irradiation of CCl_4 , in Ar matrices at 12 K produced a new species, “isotetrachloromethane,” for which Maier et al. [922] proposed the following structure:



The $\nu(\text{C}-\text{Cl}_t)$ are observed at 1019.7 and 929.1 cm^{-1} , whereas the $\nu(\text{C}-\text{Cl}_b)$ and $\nu(\text{Cl}_b-\text{Cl}_e)$ are assigned at 501.9 and 246.4 cm^{-1} respectively. Jacox and Thompson [923], presented IR evidence for the formation of the CO_4^- ion resulting from the reaction of CO_2 , O_2 , and excited Ne atoms in Ne matrices. The planar structure of C_s symmetry has been proposed:

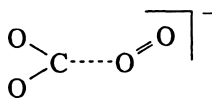


Table 2.6b includes a number of data obtained by Clark et al. from their gas-phase Raman studies [874,900]. Some halides such as TiI_4 [924], SnI_4 [877,925] and TiBr_4 [900], and VCl_4 [926] have strong electronic absorptions in the visible region, and their resonance Raman spectra have been measured in solution. As discussed in Sec. 1.23, these compounds exhibit a series of ν_1 overtones under rigorous resonance conditions.

A tetrahedral MCl_4 molecule in which M is isotopically pure and Cl is in natural abundance consists of five isotopic species because of mixing of the ^{35}Cl (75.4%) and ^{37}Cl (24.6%) isotopes. Table 2.6c lists their symmetries, percentages of natural abundance, and symmetry species of infrared-active modes corresponding to the ν_3 vibration of the T_d molecule. It has been established [927] that these nine bands overlap partially to give a “five-peak chlorine isotope pattern” whose relative intensity is indicated by the vertical lines shown in Fig. 2.19b. If M is isotopically mixed, the spectrum is too complicated to assign by the conventional method. For example, tin is a mixture of 10 isotopes, none of which is predominant. Thus 50 bands are expected to appear in the ν_3 region of SnCl_4 . It is almost impossible to resolve all these peaks, even

TABLE 2.6c. Infrared-Active Vibrations of $M^{35}\text{Cl}_n^{37}\text{Cl}_{4-n}$ Type Molecules

Species	Symmetry	Abundance (%)	IR-Active Modes
$M^{35}\text{Cl}_4$	T_d	32.5	F_2
$M^{35}\text{Cl}_3^{37}\text{Cl}$	C_{3v}	42.5	A_1, E
$M^{35}\text{Cl}_2^{37}\text{Cl}_2$	C_{2v}	20.5	A_1, B_1, B_2
$M^{35}\text{Cl}^{37}\text{Cl}_3$	C_{3v}	4.4	A_1, E
$M^{35}\text{Cl}_4$	T_d	0.4	F_2

in an inert gas matrix at 10 K. Königer and Müller [928] therefore, prepared $^{116}\text{SnCl}_4$ and $^{116}\text{Sn}^{35}\text{Cl}_4$ on a milligram scale and measured their infrared spectra in Ar matrices. As expected, the former gave a “five-peak chlorine isotope pattern,” whereas the latter showed a single peak at 409.8 cm^{-1} . This work was extended to GeCl_4 , which consists of two Cl and five Ge isotopes. In this case, 25 peaks are expected to appear in the ν_3 region. However, the observed spectrum (Fig. 2.19a) shows about 10 bands; Königer et al. [929], therefore, prepared $^{74}\text{GeCl}_4$ and $\text{Ge}^{35}\text{Cl}_4$ and measured their spectra in Ar

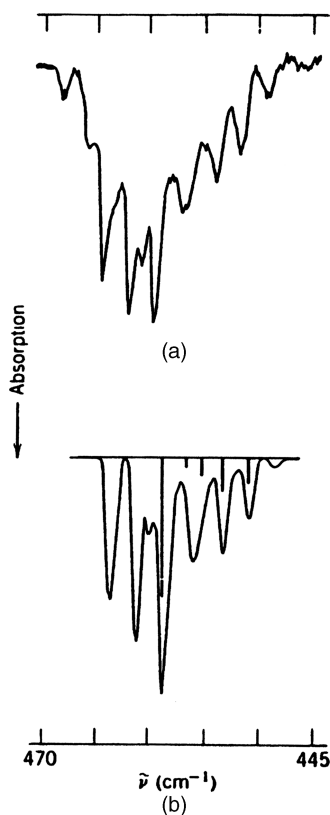
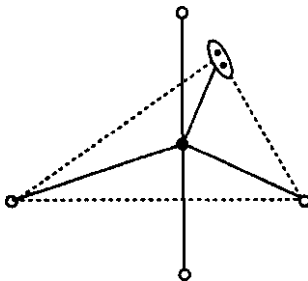


Fig. 2.19. Matrix isolation IR (a) and computer simulation spectra (b) of GeCl_4 . Vertical lines in (b) show the five-peak chlorine isotope pattern of $^{74}\text{GeCl}_4$.

matrices. As expected, both compounds showed a “five-peak” spectrum. The *ism* (isotope shift per unit mass difference) values for Cl and Ge were found to be 3.8 and 1.2 cm^{-1} , respectively. Using these values, it was then possible to calculate the frequencies of all other isotopic molecules. Furthermore, the relative intensity of individual peaks is known from the relative concentration of each isotopic molecule. On the basis of this information, Tevault et al. [930] obtained a computer-simulation infrared spectrum of GeCl_4 in natural abundance (Fig. 2.19).

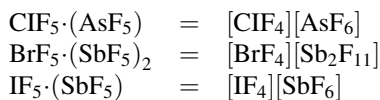
Normal coordinate analyses of tetrahedral XY_4 molecules have been carried out by a number of investigators [931]. Thus far, Basile et al. [932] have made the most complete study. They calculated the force constants of 146 compounds by using GVF, UBF, and OVF fields (Sec. 1.14), and discussed several factors that influence the values of the XY stretching force constants.

It has long been known that molecules such as SF_4 , SeF_4 , and TeF_4 assume a distorted tetrahedral structure (C_{2v}) derived from a trigonal-bipyramidal geometry with a lone-pair of electrons occupying an equatorial position:



These molecules exhibit nine normal vibrations that are classified into $4A_1 + A_2 + 2B_1 + 2B_2$. Here, all the vibrations are IR- as well as Raman-active except for A_2 which is only Raman-active. Table 2.6d lists the vibrational frequencies of distorted XY_4 molecules of this type. It should be noted that these molecules exhibit four stretching modes, two of which ($2A_1$) are polarized in the Raman. Adams and Downs [939] carried out normal coordinate analyses on SeF_4 and TeF_4 , and found that the axial bonds are weaker than the equatorial bonds. The vibrational spectra of tetraalkylammonium salts of $[\text{AsX}_4]^-$ ($\text{X} = \text{Cl}, \text{Br}$), $[\text{BiX}_4]^-$ ($\text{X} = \text{Cl}, \text{Br}, \text{I}$), and $[\text{SbX}_4]^-$ ($\text{X} = \text{Cl}, \text{Br}, \text{I}$) have been studied in the solid state and in solution [936]. Except for solid $(\text{Et}_4\text{N})[\text{AsCl}_4]$ and $[(n\text{-Bu})_4\text{N}][\text{SbI}_4]$, all these ions assume the distorted tetrahedral structure shown above.

The $[\text{ClF}_4]^+$, $[\text{BrF}_4]^+$, and $[\text{IF}_4]^+$ ions were found in the following adducts [941]:



It should be noted that SeCl_4 , SeBr_4 , TeCl_4 , and TeBr_4 consist of the pyramidal XY_3^+ cation and the Y^- anion in the solid [615,616].

TABLE 2.6d. Vibrational Frequencies^a of Distorted Tetrahedral XY₄ Molecules (cm⁻¹)

C _{2v}	$\tilde{\nu}_1, A_1$	$\tilde{\nu}_2, A_1$	$\tilde{\nu}_3, A_1$	$\tilde{\nu}_4, A_1$	$\tilde{\nu}_5, A_1$	$\tilde{\nu}_6, A_1$	$\tilde{\nu}_7, A_1$	$\tilde{\nu}_8, A_1$	$\tilde{\nu}_9, A_1$	Ref.
[PF ₄] ⁻	798	422	446	210	—	515	446	745	290	933,920
[SbF ₄] ⁻	584	404	305	161	—	480	247	541	220	934,935
[SbCl ₄] ⁻	339	296	147	—	—	321	199	246	—	935
[SbBr ₄] ⁻	228	190	—	—	—	201	140	169	—	935,936
[SbI ₄] ⁻	169	—	114	—	—	162	85	148	—	935,936
SF ₄	892	558	532	228	(437)	730	475	867	353	937
SeF ₄	739	551	362	200	—	585	254	717	403	938
TeF ₄	695	572	333.2	151.5	—	586.9	293.2	682.2	184.8	934,939
TeCl ₄	—	—	—	—	—	312	165	378	104	940
[ClF ₄] ⁺	800	571	385	250	475	795	515	829	385	937
[BrF ₄] ⁺	723	606	385	219	—	704	419	736	369	941
[IF ₄] ⁺	728	614	345	263	—	—	388	719	311	941

^aWhereas ν_1 and ν_8 are stretching modes of equatorial bonds, ν_2 and ν_6 are stretching modes of axial bonds. For the normal modes of bending vibrations, see Ref. 942.

Table 2.6e lists the vibrational frequencies of tetrahedral MO₄²⁻, MS₄²⁻, and MSe²⁻-type compounds. The rule $\nu_3 > \nu_1$ and $\nu_4 > \nu_2$ hold for the majority of the compounds. Figure 2.20 shows the Raman spectra of K₂SO₄ in the solid state as well as in aqueous solution. It should be noted that ν_2 and ν_4 are often too close to be observed as separate bands in Raman spectra. Weinstock et al. [960] showed that, in Raman spectra, ν_2 should be stronger than ν_4 , and that ν_4 is hidden by ν_2 in [MoO₄]²⁻ and [ReO₄]⁻ ions.

Baran et al. [974,975] have found several relationships between the ν_1/ν_3 ratio and the negative charge of the anion or the mass of the central atom in a series of oxoanions listed in Table 2.6e:

- (1) For a given central atom, the ν_1/ν_3 ratio increases as the negative charge of the anion increases (e.g., [MnO₄]⁻ < [MnO₄]²⁻ < [MnO₄]³⁻).
- (2) For anions of the same negative charge with the central atom belonging same group of the periodic table, the ν_1/ν_3 ratio increases with the mass of the central atom (e.g., [PO₄]³⁻ < [AsO₄]³⁻).
- (3) For isoelectronic ions in which the mass of the central atom remains approximately constant, the ν_1/ν_3 ratio increases with the increasingly negative charge of the anion (e.g., [ReO₄]⁻ < [WO₄]²⁻).

These trends are very useful in making correct assignments of the ν_1 and ν_3 vibrations of tetraoxoanions [975].

The IR spectra of matrix-isolated M₂(SO₄) (M = K, Rb, Cs) can be interpreted in terms of D_{2d} symmetry and their $\nu(\text{M}\cdots\text{O})$ vibrations are observed at 262–220, 215–190, and 195–148 cm⁻¹, respectively, for the K, Rb, and Cs salts [976].

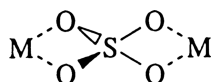


TABLE 2.6e. Vibrational Frequencies of Tetrahedral MO₄[−], MS₄[−], and MSe₄-Type Compounds (cm^{−1})

Compound	$\tilde{\nu}_1$	$\tilde{\nu}_2$	$\tilde{\nu}_3$	$\tilde{\nu}_4$	Ref.
[BO ₄] ^{5−}	880	372	886	627	943,944
[CS ₄] [−]	495	353	1000 } ^a 805 }	—	945
[SiO ₄] ^{4−}	819	340	956	527	946,947
[PO ₄] ^{3−}	938	420	1017	567	948,949
[PS ₄] ^{3−}	391	282	535 } ^a 512 }	317 } ^a 296 }	950
[PSe ₄] ^{3−}	416	215	548	270	951
[NO ₄] ^{3−}	843	540 } 500 }	1012 } ^a 988 }	669 } ^a 651 }	952 ^b
[AsO ₄] ^{3−}	837	349	878	463	953
[AsS ₄] ^{3−}	386	171	419	216	953
[SbS ₄] ^{3−}	366	156	380	178	953
[SO ₄] ^{2−}	983	450	1105	611	946
[SeO ₄] ^{2−}	822	328	856	411	954,946
[ClO ₄] [−]	928	459	1119	625	953
[BrO ₄] [−]	801	331	878	410	955,956
[IO ₄] [−]	791	256	853	325	957
XeO ₄	775.7	267	879.2	305.9	958
[TiO ₄] ^{4−}	761	306	770	371	959
[ZrO ₄] ^{4−}	792	332	846	387	959
[HfO ₄] ^{4−}	796	325	800	379	959
[VO ₄] ^{3−}	826	336	804	(336)	960
[VO ₄] ^{4−}	818	319	780	368	959
[VS ₄] ^{3−}	404.5	193.5	470	(193.5)	961
[VSe ₄] ^{3−}	(232)	121	365	(121)	961
[NbS ₄] ^{3−}	408	163	421	(163)	961
[NbSe ₄] ^{3−}	239	100	316	(100)	961
[TaS ₄] ^{3−}	424	170	399	(170)	961
[TaSe ₄] ^{4−}	249	103	277	(103)	961
[CrO ₄] ^{2−}	833	339	863	375	954
[CrO ₄] ^{3−}	844.0	240.3	775.8	363.9	955
[MoO ₄] ^{2−}	897	317	837	(317)	960
[MoS ₄] ^{2−}	458	184	472	(184)	962
[MoSe ₄] ^{2−}	255	120	340	120	963
[WO ₄] ^{2−}	931	325	838	(325)	960
[WS ₄] ^{2−}	479	182	455	(182)	962
[WSe ₄] ^{2−}	281	107	309	(107)	961
[MnO ₄] ^{2−}	834	346	902	386	964,965
[MnO ₄] ^{2−}	812	325	820	332	959
[MnO ₄] ^{3−}	789	308	778	332	966
[TcO ₄] [−]	912	325	912	336	960
[ReO ₄] [−]	971	331	920	(331)	960
[ReS ₄] [−]	501	200	486	(200)	967
[FeO ₄] ^{2−}	832	340	790	322	959
RuO ₄	885.3	~319	921	336	968
[RuO ₄] [−]	830	339	845	312	959
[RuO ₄] ^{2−}	840	331	804	336	959

TABLE 2.6e. (Continued)

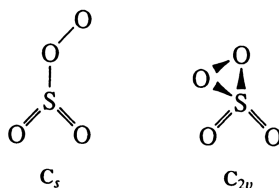
Compound	$\tilde{\nu}_1$	$\tilde{\nu}_2$	$\tilde{\nu}_3$	$\tilde{\nu}_4$	Ref.
OsO ₄	965.2	333.1	960.1	322.7	969
XeO ₄	776	267	878	305	969a
[CoO ₄] ⁴⁻	670	320	633	320	970
{B(OH) ₄ } ^{-c}	754	379	945	533	971,972
[Al(OH) ₄] ^{-c}	615	310	(720)	(310)	973
[Zn(OH) ₄] ^{-c}	470	300	(570)	(300)	973

^aSplitting may suggest D_{2d} symmetry in the crystalline state.

^bNa₃[NO₄]³⁻ was obtained by the reaction of NaNO₃ and Na₂O.

^cOnly MO₄ skeletal vibrations are listed for this ion.

The IR spectrum and normal coordinate analysis of the SO₄ radical produced by the reaction of SO₃ with atomic oxygen in inert gas matrices are suggestive of the C_s structure rather than the C_{2v} structure [977]:



The IR spectra of H₂SO₄ and its deuterated derivatives in Ar matrices have been assigned on the basis of C_2 symmetry ((HO)₂SO₂) [978]. The IR spectrum of the ClO₄

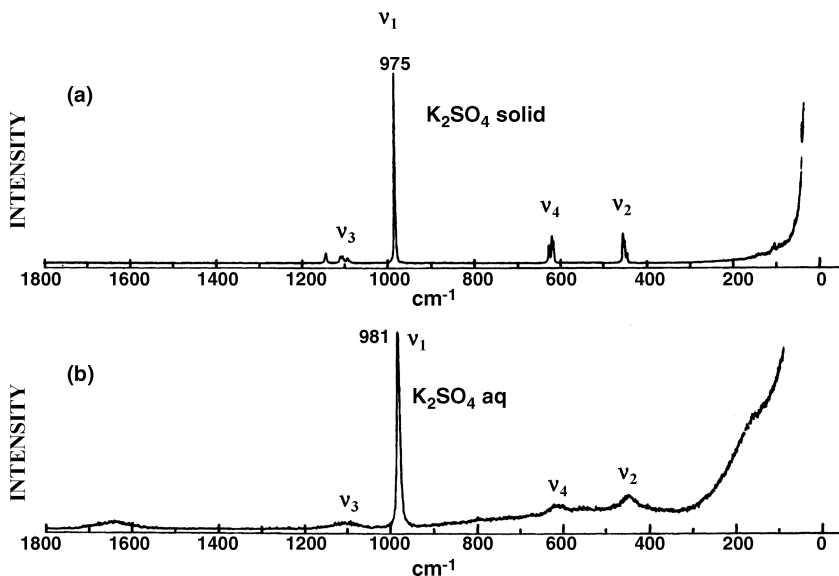


Fig. 2.20. Raman spectra of K₂SO₄ in (a) the solid state and (b) aqueous solution.

radical in inert gas matrices indicates a C_{3v} structure with one long Cl—O bond as the C_3 axis. The $\nu(\text{ClO})$ of this bond is at 874 cm^{-1} , which is much lower than those of the other three bonds (1234 and 1161 cm^{-1}) [979]. The IR/Raman spectra of $M^+\text{ClO}_4^-$ salts in nonaqueous solvents suggest the formation of a unidentate ion pair for $M = \text{Li}^+$, and a bidentate ion pair for $M = \text{Na}^+$ [980].

The RR spectra of highly colored ions such as CrO_4^{2-} [981], MoS_4^{2-} [982], VS_4^{3-} [983], and MnO_4^- [964,981] have been measured. The $\nu_3(\text{IR})$ bands of gaseous RuO_4 [968] and XeO_4 [984] exhibit complicated band contours consisting of individual isotope peaks of the central atoms. Müller and coworkers [974,985,986] reviewed the vibrational spectra of transition-metal chalcogen compounds. Basile et al. [932] carried out normal coordinate analysis on more than 60 compounds of these types.

2.6.2. Tetrahedral ZXY_3 , Z_2XY_2 , and ZWXY_2 Molecules

If one of the Y atoms of an XY_4 molecule is replaced by a Z atom, the symmetry of the molecule is lowered to C_{3v} . If two Y atoms are replaced, the symmetry becomes C_{2v} . In ZWXY_2 and ZWXYU types, the symmetry is further lowered to C_s and C_1 , respectively. As a result, the selection rules are changed as shown in Table 2.6f. The number of infrared-active vibrations is six for ZXY_3 and eight for Z_2XY_2 . Table 2.6g lists the vibrational frequencies of ZXY_3 -type molecules. The SO stretching frequency of the $[\text{OSF}_3]^+$ ion in $[\text{OSF}_3]\text{SbF}_6$ (1536 cm^{-1}) is the highest that has been observed, and corresponds to a force constant of 14.7 mdyn/\AA [1006]. It is also interesting to note that the structure the $[\text{OXeF}_3]^+$ ion is C_s [726] whereas that of the $[\text{OXeF}_3]^-$ ion is C_{2v} [727] as shown below:

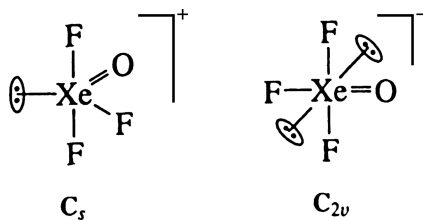


TABLE 2.6f. Correlation Table^a for T_d , C_{3v} , C_{2v} , and C_1

Point Group	ν_1	ν_2	ν_3	ν_4
T_d	A_1 (R)	E (R)	F_2 (IR, R)	F_2 (IR, R)
C_{3v}	A_1 (IR, R)	E (IR, R)	A_1 (IR, R)+ E (IR, R)	A_1 (IR, R)+ E (IR, R)
C_{2v}	A_1 (IR, R)	A_1 (IR, R)+ A_2 (R)	A_1 (IR, R)+ B_1 (IR, R)	A_1 (IR, R)+ B_1 (IR, R)+ B_2 (IR, R)
C_1	A (IR, R)	$2A$ (IR, R)	$3A$ (IR, R)	$3A$ (IR, R)

^a See Appendix IX.

TABLE 2.6g. Vibrational Spectra of ZXY_3 Molecules (cm^{-1})

C_{3v} ZXY_3	$\tilde{\nu}_1 (A_1)$ $\nu (XY_3)$	$\tilde{\nu}_2 (A_1)$ $\nu (XZ)$	$\tilde{\nu}_3 (A_1)$ $\delta (XY_3)$	$\tilde{\nu}_4 (E)$ $\nu (XY_3)$	$\tilde{\nu}_5 (E)$ $\delta (XY_3)$	$\tilde{\nu}_6 (E)$ $\rho_r (XY_3)$	Ref.
$[\text{HGaCl}_3]^-$	349.5	1960.4	167.9	320.6	609.3	—	987
$[\text{OCF}_3]^-$	813	1560	595	960	422	576	988,989
FCCl_3	537.6	1080.4	351.3	847.8	242.8	395.3	990
BrCC_3	419.9	730.7	246.5	785.2	290.2	188.0	990
ICCl_3	390	684	224	755	284	188	991
FSiH_3	—	990.9	875.0	—	962.2	730.0	992
$\text{H}^{28}\text{SiF}_3$	855.8	2315.6	425.3	997.8	843.6	306.2	993
FSiCl_3	465	948	239	640	282	167	994
FSiBr_3	318	912	163	520	226	110	994
FSiI_3	242	894	115	424	194	71	994
BrSiF_3	858	505	288	940	338	200	994
$^{79}\text{BrSiH}_3$	2198.8	929.8	430.8	2209.3	996.4	632.4	995
$[\text{SSiCl}_3]^-$	395	685	220	492	—	225	996
$[\text{SGeCl}_3]^-$	356	505	163	360	—	178	996
HGeCl_3	418.4	2155.7	181.8	708.6	454	145.0	997
ONF_3	743	1691	528	883	558	400	998
$[\text{HPCl}_3]^+$	528	2481	208	634	280	653	999
$[\text{ClPBr}_3]^+$	285	587	149	500	172	120	1000
$[\text{BrPCl}_3]^+$	399	582	217	657	235	159	1000
$[\text{HPF}_3]^+$	948	2544	480	1090	989	380	1001,1001a
OPF_3	873	1415	473	990	485	345	1002
OPCl_3	486	1290	267	581	337	193	1002
OPBr_3	340	1261	173	488	267	118	764,1003
$[\text{FPO}_3]^-$	1001	794	534	1125	—	382	1004
SPF_3	—	985	696	947	442	405	1005
$[\text{OSF}_3]^+$	909	1540, 1532	535	1063	508	387	1006
NSF_3	772.6	1522.9	524.6	814.6	432.3	346.2	1007
ISCl_3	482	293	242	493	140	255	1008
$[\text{HSO}_3]^-$	1038	2588	629	1200	509	1123	1009
$[\text{FSO}_3]^-$	1142	862	571	1302	619	424	1010
$[\text{ClSO}_3]^-$	1042	381	601	1300	553	312	1011
$[\text{SSO}_3]^-$	995	446	669	1123	541	335	1012
$[\text{SeSO}_3]^{2-}$	995	310	645	1120	530	—	1013
$[\text{FSeO}_3]$	896	580,603	392	968,974	409	301	1014
FCIO_3	1062.6	716.3	549.7	1317.9	589.8	403.9	1015,1016
FBrO_3	875.2	605.0	(354)	974	(376)	(296)	1017,1018
$[\text{NClO}_3]^{2-}$	815	1256	594	870	623	457	1019
OVF_3	721.5	1057.8	257.8	806	204.3	308	1020
OVC1_3	408	1035	165	504	129	249	1020
OVBr_3	271	1025	120	400	83	212	1020
NVCl_3	352	1033	—	430	—	—	1021
ONbCl_3	395	997	106	448	225	110	1021a
$[\text{FCrO}_3]^-$	911	635	338	955	370	261	1022
$[\text{ClCrO}_3]^-$	907	438	295	954	365	209	1023
$[\text{BrCrO}_3]^-$	895	260	230	950	350	(175)	1024
$[\text{OMoS}_3]^{2-}$	461	862	183	470	183	263	1023
$[\text{OMoSe}_3]^{2-}$	293	858	120	355	120	188	1025
$[\text{SMoO}_3]^{2-}$	900	472	318	846	318	239	1026
$[\text{SMoSe}_3]^{2-}$	—	471	121	342	121	—	985

(continued)

TABLE 2.6g. (Continued)

C_{3v} ZXY_3	$\tilde{\nu}_1 (A_1)$ $\nu (XY_3)$	$\tilde{\nu}_2 (A_1)$ $\nu (XZ)$	$\tilde{\nu}_3 (A_1)$ $\delta (XY_3)$	$\tilde{\nu}_4 (E)$ $\nu (XY_3)$	$\tilde{\nu}_5 (E)$ $\delta (XY_3)$	$\tilde{\nu}_6 (E)$ $\rho_r (XY_3)$	Ref.
$[\text{SeMoS}_3]^{2-}$	349	458	—	473	150	183	1027
$[\text{OWS}_3]^{2-}$	474	878	182	451	182	264	1023
$[\text{OWSe}_3]^{2-}$	292	878	(120)	312	(120)	194	1025
$[\text{SWSe}_3]^{2-}$	468	281	108	311	150	108	1027
FMnO_3	903.6	715.5	339.0	950.6	380.0	264.0	1028,1029
ClMnO_3	889.9	458.9	305	951.6	365	~200	1026,1029
FTcO_3	962	696	317	951	347	231	1030
ClTcO_3	948	451	300	932	342	197	1031
FReO_3	1013.2	701	305.5	978.3	346.9	234.2	1032
ClReO_3	994	436,427	291	963	337	192	1032
BrReO_3	997	350	195	963	332	168	1022
$[\text{NReO}_3]^{2-}$	878	1022	315	830	273	380	1033
$[\text{SReO}_3]^-$	948	528	322	906	322	(240)	1022
$[\text{NOsO}_3]^-$	892.5	1026.2	310.0	872.0	299.7	371.5	1034
$[\text{FOsO}_3]^+$	1002	745	333	992	372	238	1035

The first example of the trifluorosulfite anion (OSF_3^-) was obtained as the Me_4N^+ salt, and its IR and Raman spectra assignments based on a theoretically predicted pseudo-trigonal-bipyramidal structure with two long S—F bonds in the axial direction and one F, one O atom and a sterically active lone-pair electrons at the triangular corners of the equatorial plane [1036]. The Raman spectrum of the $[\text{NVO}_3]^{4-}$ ion has been assigned as a pseudo-tetrahedral anion of C_s symmetry [1037].

Vibrational spectra have been reported for a number of mixed halogeno complexes. Some references are as follows: $[\text{AlCl}_n\text{Br}_{4-n}]^-$ [1038], $\text{SiF}_n\text{Cl}_{4-n}$ [1039], $\text{SiCl}_n\text{Br}_{4-n}$ [1040], and $[\text{FeCl}_n\text{Br}_{4-n}]^-$ [1041]. It is interesting to note that the SiFClBrI molecule exhibits the SiF, SiCl, SiBr, and SiI stretching bands at 910, 587, 486, and 333 cm^{-1} , respectively [1042]. The vibrational spectrum of OCIF_3 suggests a trigonal-bipyramidal structure similar to that of the $[\text{OXeF}_3]^+$ ion shown above [1043].

Table 2.6h lists the vibrational frequencies of tetrahedral Z_2XY_2 molecules. The vibrational spectrum of O_2XeF_2 can be interpreted on the basis of a trigonal-bipyramidal structure in which two F atoms are axial, and two O atoms and a pair of electrons are equatorial [1059]. The structures of $[\text{O}_2\text{ClF}_2]^-$ [1057] and $[\text{O}_2\text{BrF}_2]^-$ [1058] are similar to that of O_2XeF_2 , but that of $[\text{O}_2\text{ClF}_2]^+$ [1067] is pseudo-tetrahedral. The gas-phase Raman spectrum of Cl_2TeBr_2 at 310°C is indicative of the C_1 symmetry shown below [1068]. Table 2.6i lists the vibrational frequencies of tetrahedral ZWXY_2 molecules. Other references are as follows: SFPCl_2 [1075], FOPCl_2 [1076], FOPBr_2 [1077], ClOPBr_2 and BrOPCl_2 [1003], FBrSO_2 [1078], and FCIClO_2 [1079].

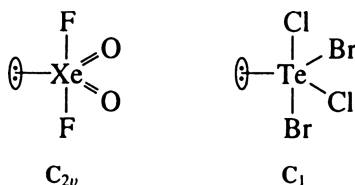


TABLE 2.6h. Vibrational Frequencies of Z₂XY₂ Molecules (cm⁻¹)

Z ₂ XY ₂	$\tilde{\nu}_1 (A_1)$ $\nu (XY_2)$	$\tilde{\nu}_2 (A_1)$ $\nu (XZ_2)$	$\tilde{\nu}_3 (A_1)$ $\delta (XY_2)$	$\tilde{\nu}_4 (A_1)$ $\delta (XZ_2)$	$\tilde{\nu}_5 (A_2)$ $\rho_r (XY_2)$	$\tilde{\nu}_6 (B_1)$ $\nu (XY_2)$	$\tilde{\nu}_7 (B_1)$ $\rho_w (XY_2)$	$\tilde{\nu}_8 (B_2)$ $\nu (XZ_2)$	$\tilde{\nu}_9 (B_2)$ $\rho_r (XY_2)$	Ref.
[F ₂ NH ₂] ⁺	2637	~1060	1543	528	—	2790	1176	1036	1487	1044
[O ₂ PH ₂] ⁻	2365	1046	1160	470	930	2308	820	1180	1093	1045
F ₂ Cl ₂	605	1064	272	112	251	740	200	1110	278	1046
H ₂ SiCl ₂	942	2221	514	188	710	868	566	2221	602	1047
H ₂ SiBr ₂	925	2206	393	122	688	828	456	2232	—	1048
F ₂ SiBr ₂	414	891	270	115	187	540	241	974	257	1049
H ₂ GeF ₂	860	2155	720	(270)	(664)	814	720	2174	596	1050
H ₂ GeCl ₂	840	2132	404	163	648	772	420	2155	533	1087
H ₂ GeBr ₂	848	2122	298	104	105	757	324	2138	492	1050
H ₂ GeI ₂	821	2090	220	96	628	706	294	2110	451	1050
[Cl ₂ PBr ₂] ⁺	326	584	191	132	150	518	173	616	201	1022
[O ₂ PF ₂] ⁺	910	1179	269	567	—	962	492	1269	528	1051
O ₂ SF ₂	847.4	1265.5	388.7	552.0	390.8	884.1	545.0	1497.0	538.2	1052, 1053
O ₂ SCl ₂	405	1182	218	560	388	362	380	1414	282	1054
F ₂ SCl ₂	527	592	—	—	—	533	—	770	—	1055
[O ₂ SeF ₂] ⁻	396	859	241	445	—	—	—	833	304	1056
[O ₂ ClF ₂] ⁻	363	1070	198	559	480	510	337	1221	337	1057
[O ₂ BrF ₂] ⁻	374	885	201	429	405	448	339	912	314	1058
O ₂ XeF ₂	490	845	198	333	—	578	~313	902	~313	1059
[O ₂ VF ₂] ⁻	631	969	199	365	—	664	285	960	265	1060
[O ₂ VOI ₂] ⁻	431	968	128	323	200	436	277	958	194	1060
[O ₂ NbS ₂] ³⁻	464	897	246	356	—	514	(297)	872	(271)	1061

(continued)

TABLE 2.6h. (Continued)

Z_2XY_2	$\tilde{\nu}_1 (A_1)$ $\nu (XY_2)$	$\tilde{\nu}_2 (A_1)$ $\nu (XZ_2)$	$\tilde{\nu}_3 (A_1)$ $\delta (XY_2)$	$\tilde{\nu}_4 (A_1)$ $\delta (XZ_2)$	$\tilde{\nu}_5 (A_2)$ $\rho_r (XY_2)$	$\tilde{\nu}_6 (B_1)$ $\nu (XY_2)$	$\tilde{\nu}_7 (B_1)$ $\rho_w (XY_2)$	$\tilde{\nu}_8 (B_2)$ $\nu (XZ_2)$	$\tilde{\nu}_9 (B_2)$ $\rho_r (XY_2)$	Ref.
O_2CrF_2	727	1006	208	364	(259)	789	304	1016	274	1062
O_2CrCl_2	475	995	140	356	(224)	500	257	1002	215	1063
O_2CrBr_2	399.0	982.6	—	(305)	—	403.5	—	995.4	—	1064
O_2MoBr_2	262	995	147	373	—	338	161	970	184	1065
$[O_2^{2-}MoS_2]^{2-}$	473	819	200	307	267	506	267	801	246	1066
$[O_2MoSe_2]^{2-}$	283	864	114	339	251	353	251	834	—	1061
$[O_2WS_2]^{2-}$	454	886	196	310	280	442	280	848	235	1061
$[O_2WSe_2]^{2-}$	282	888	116	319	235	329	235	845	156	1061

TABLE 2.6i. Vibrational Frequencies of ZWXY₂ Molecules (cm⁻¹)

ZWXY ₂ ^a	$\tilde{\nu}_1$ (A') ν_s (XY ₂)	$\tilde{\nu}_2$ (A') ν (XW)	$\tilde{\nu}_3$ (A') ν (XZ)	$\tilde{\nu}_4$ (A') δ_s (XY ₂)	$\tilde{\nu}_5$ (A') δ_s (WXY)	$\tilde{\nu}_6$ (A') δ_s (ZXY ₂)	$\tilde{\nu}_7$ (A'') ν_a (XY ₂)	$\tilde{\nu}_8$ (A'') δ (ZXW)	$\tilde{\nu}_9$ (A'') δ_a (XY ₂)	Ref.
OCiPF ₂	900	623	1384	(419)	(274)	412	960	274	419	639,1069
SCiPF ₂	949	549	735	394	363	209	925	252	613	639,1069
OBiPF ₂	884	561	1380	(413)	(240)	316	947	240	413	639,1069
SBrPF ₂	938	477	719	389	288	175	911	231	297	639,1069
OFPCl ₂	546	907	1358	205	330	382	626	253	374	639,1069
SFPCl ₂	479	915	750	193	328	268	574	193	317	639,1069
OFPBBr ₂	472	888	1337	133	273	304	536	220	290	639,1069
SFPBr ₂	377	887	713	129	274	218	470	162	254	639,1069
OBiPCl ₂	545	432	1285	242	172	285	580	161	327	1070
SBrPCl ₂	493	372	743	(230)	150	206	536	150	230	1070
OCiPBBr ₂	391	552	1275	130	209	291	492	157	271	1070
SCiOBBr ₂	333	500	729	121	196	190	436	136	205	1070
[OSeMoS ₂] ²⁻	478 ^b	355	869	190	—	273	467 ^b	—	273	1071,1072
[OSeWS ₂] ²⁻	473	320	879	190	—	265 ^b	458	—	255 ^b	1072,1073
[OSMoSe ₂] ²⁻	360 ^b	461	865	—	—	—	320 ^b	—	—	1074
[OSWSe ₂] ²⁻	317 ^b	459	882	—	—	—	312 ^b	—	—	1074

^a X denotes the central atom.

^b These assignments may be interchanged.

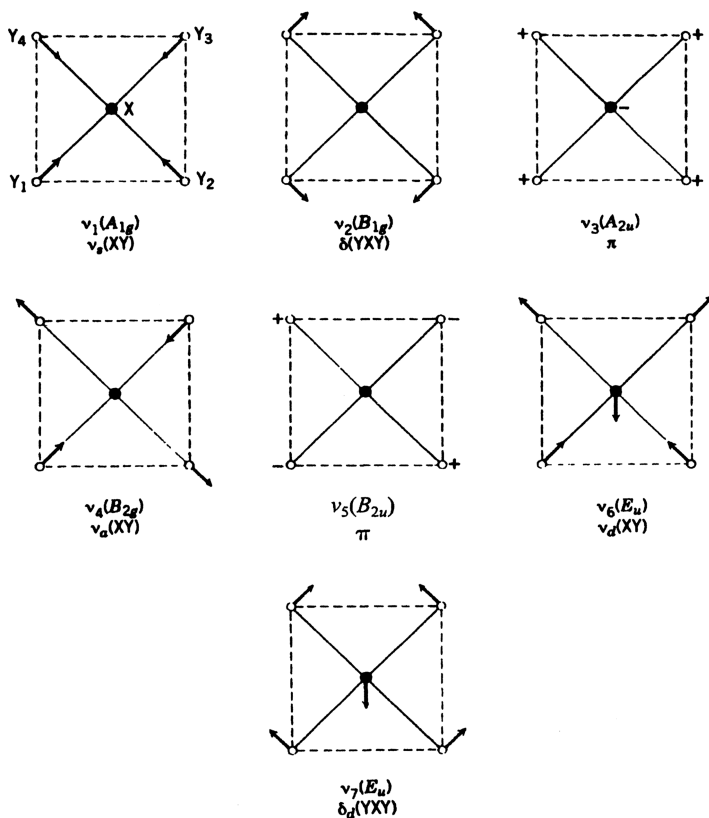


Fig. 2.21. Normal modes of vibration of square-planar XY_4 molecules.

2.6.3. Square-Planar XY_4 Molecules (D_{4h})

Figure 2.21 shows the seven normal modes of vibration of square-planar XY_4 molecules. Vibrations ν_3 , ν_6 , and ν_7 are infrared-active, whereas ν_1 , ν_2 , and ν_4 are Raman-active. However, ν_5 is inactive both in infrared and Raman spectra. In the case of the $[\text{PdCl}_4]^{2-}$ ion, the ν_5 was observed at 136 cm^{-1} by inelastic neutron scattering (INS) spectroscopy [1088]. Table 2.6j lists the vibrational frequencies of some ions belonging to this group. Chen et al. [1088a] also reported the IR and Raman spectra of $\text{K}_2[\text{MX}_4]$ ($\text{M} = \text{Pt}$ or Pd and $\text{X} = \text{Cl}$ or Br) and band assignments on the basis of normal coordinate analysis.

XeF_4 (Sec. 1.11) is an unusual example of a neutral molecule that takes a square-planar structure. This structure is predicted by the valence shell electron pair repulsion (VSEPR) theory [1089] which states that two lone-pairs in the valence shell occupy the axial positions because they exert greater mutual repulsion than

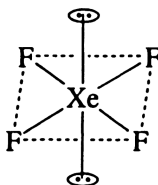
TABLE 2.6j. Vibrational Frequencies of Square-Planar XY_4 Molecules (cm^{-1})^a

XY_4	$\tilde{\nu}_1 (A_{1g})$ $\nu_s (XY)$	$\tilde{\nu}_2 (B_{1g})$ $\delta (XY_2)$	$\tilde{\nu}_3 (A_{2u})$ π	$\tilde{\nu}_4 (B_{2g})$ $\nu_a (XY)$	$\tilde{\nu}_6 (E_g)$ $\nu_d (XY)$	$\tilde{\nu}_7 (E_g)$ $\delta_d (XY_2)$	Ref.
$[\text{ClF}_4]^-$	505	288	425	417	680–500	—	1080
$[\text{BrF}_4]^-$	523	246	317	449	580–410	(194)	1080
$[\text{ICl}_4]^-$	288	128	—	261	266	—	1081
XeF_4	554.3	218	291	524	586	(161)	1082, 1083
$[\text{AuCl}_4]^-$	347	171	—	324	350	179	1084, 1085
$[\text{AuBr}_4]^-$	212	102	—	196	252 ^b	$\sim 110^b$	1084, 1085
$[\text{AuI}_4]^-$	148	75	—	110	192	113	1084
$[\text{PdCl}_4]^{2-}$	303	164	150	275	321	161	1085, 1086
$[\text{PdBr}_4]^{2-}$	188	102	114	172	243	104	1084, 1086
$[\text{PtCl}_4]^{2-}$	330	171	147	312	313	165	1085, 1086
$[\text{PtBr}_4]^{2-}$	208	106	105	194	227	112	1085, 1086
$[\text{PtI}_4]^{2-}$	155	85	105	142	180	127	1084, 1086

^a For these molecules ν_5 is inactive. The designations B_{1g} and B_{2g} may be interchanged, depending on the definition of symmetry axes involved.

^b From Ref. 1087.

single-bond pairs:



The structures of fluorides, oxides, and oxyfluorides of xenon discussed in other sections can also be rationalized on the basis of VSEPR theory. Figure 2.22

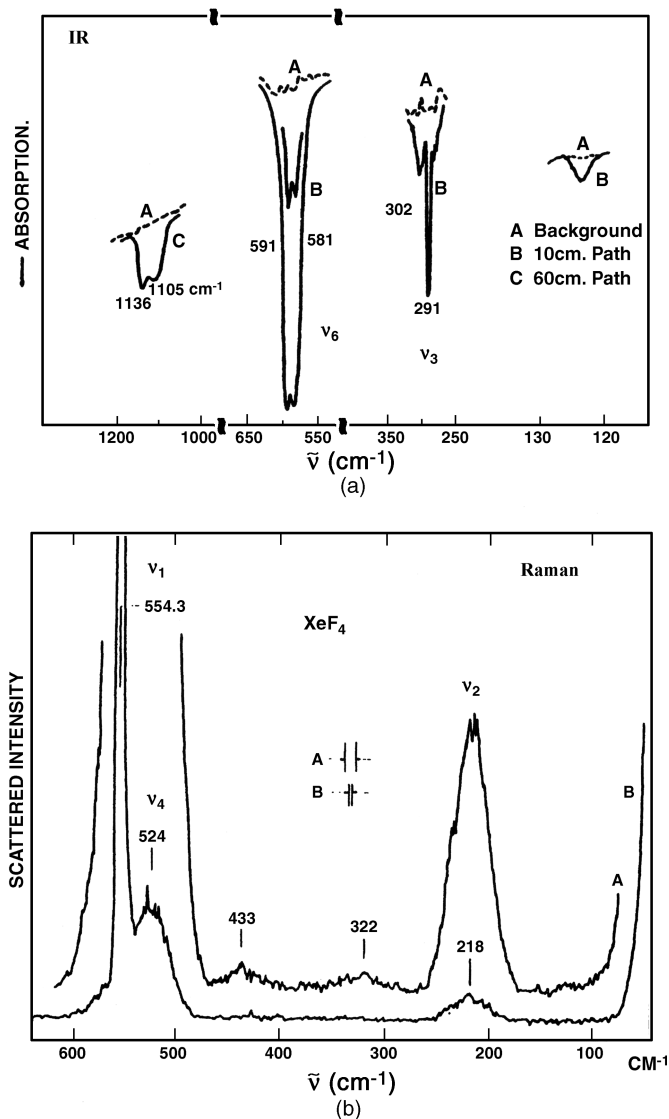


Fig. 2.22. (a) IR [1090] and (b) Raman [1082] spectra of XeF_4 vapor.

shows the IR and Raman spectra of gaseous XeF_4 obtained by Claassen et al. [1082,1090].

Bosworth and Clark [1091] measured the relative intensities of Raman-active fundamentals of some of these ions, and calculated their bond polarizability derivatives and bond anisotropies. They [1087] also measured the resonance Raman spectra of several $[AuBr_4]^-$ salts in the solid state, and observed progressions such as $n\nu_1$ ($n = 1-9$) and $\nu_2 + n\nu_1$ ($n = 1-5$). For normal coordinate analyses of square-planar XY_4 molecules, see Refs. [1081], [1092], and [1093]. An empirical relationship between the antisymmetric M-Cl stretching frequency $[\nu_a(M-Cl), \text{cm}^{-1}]$ and the M-Cl distance (R_{M-Cl} , Å) has been derived using IR and structural data for a large number of planar Pt(II) and Pd(II) complexes of MCl_2L_2 , $MC1_2LL'$, and $MC1L_3$ types (L: unidentate ligand)

$$[\nu_a(M-Cl)]^2 = \frac{P}{(R_{M-Cl} - 1.6)^3}$$

where P is 38988 for Pt(II) and 41440 for Pd(II) complexes [1094].

The IR and Raman spectra of the $[AuCl_{4-n}Br_n]^-$ ions ($n = 1-3$) [1095] and Raman spectra of the square-planar tetrahydrido $[PtH_4]^{2-}$ and related ions [[1095]a] are reported.

2.7. TRIGONAL-BIPYRAMIDAL AND TETRAGONAL-PYRAMIDAL XY_5 AND RELATED MOLECULES

An XY_5 molecule may be a trigonal bipyramid (D_{3h}) or a tetragonal pyramid (C_{4v}). If it is trigonal-bipyramidal, only two stretching vibrations (A_2'' and E') are infrared-active. If it is tetragonal-pyramidal, three stretching vibrations (two A_1 and E) are infrared-active. As discussed in Sec. 1.11, however, it is not always possible to make clear-cut distinctions of these structures based on the selection rules since practical difficulties arise in counting the number of fundamental vibrations in infrared and Raman spectra.

2.7.1. Trigonal-Bipyramidal XY_5 Molecules (D_{3h})

Figure 2.23 shows the eight normal vibrations of a trigonal-bipyramidal XY_5 molecule. Six of these eight (A_1' , E' , E'') are Raman-active, and five (A_2'' and E') are infrared-active. Three stretching vibrations (ν_1 , ν_2 , and ν_5) are allowed in the Raman, whereas two (ν_3 and ν_5) are allowed in the infrared. Table 2.7a lists the observed frequencies and band assignments of trigonal-bipyramidal XY_5 molecules. The IR spectrum of the ion-paired complex, $Cs^+[GeF_5]^-$, in inert gas matrices has been reported [1116]. It takes a trigonal-bipyramidal structure perturbed by the presence of the Cs^+ ion in its vicinity.

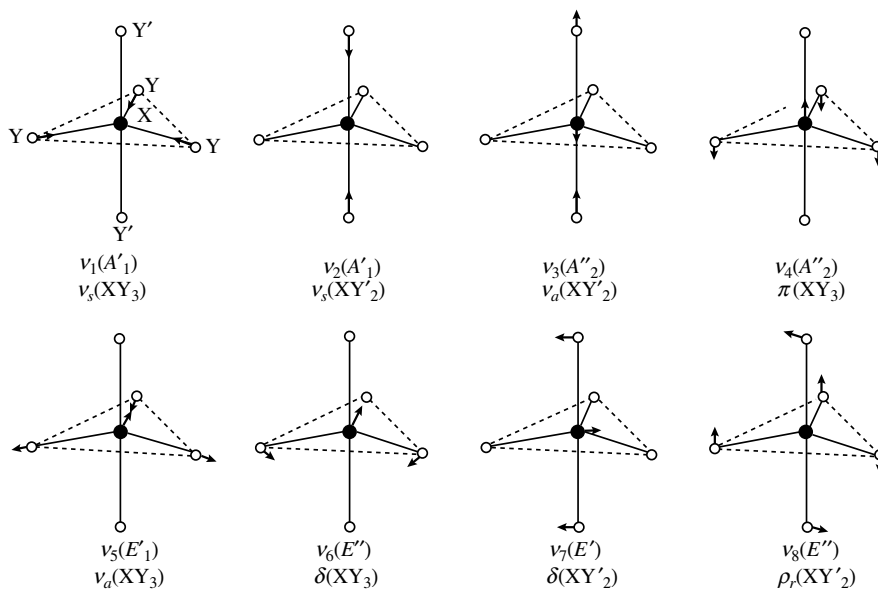
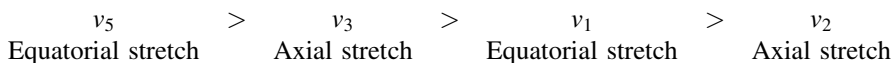


Fig. 2.23. Normal modes of vibration of trigonal-bipyramidal XY_5 molecules.

The majority of trigonal-bipyramidal compounds show the following frequency trend:



Although the IR spectrum of MoCl_5 in the gaseous phase has been assigned based on a trigonal-bipyramidal structure [1107] the corresponding spectrum in N_2 matrices suggests a tetragonal-pyramidal structure of C_{4v} symmetry [1117]. This is supported by the observation that it shows only two prominent IR bands at $473 \text{ (A}_1\text{)}$ and $408 \text{ cm}^{-1} \text{ (E)}$ in the $\nu(\text{Mo}-\text{Cl})$ region. Normal coordinate analyses on trigonal-bipyramidal XY_5 molecules have been carried out by several investigators [1118–1121]. These calculations show that equatorial bonds are stronger than axial bonds.

Most neutral XY_5 molecules are dimerized or polymerized in the condensed phases. The molecules MoCl_5 , [1122], NbCl_5 [1113,1123], TaCl_5 [1124], and WCl_5 [1125] are dimeric in the liquid and solid states (D_{2h}), whereas NbF_5 and TaF_5 are known to be tetrameric in the crystalline state [1126]. Some of these molecules are polymerized even in the gaseous phase. For example, SbF_5 is monomeric (D_{3h}) at 350°C but polymeric at 140°C in the gaseous phase [1127], and NbF_5 and TaF_5 are polymeric in the gaseous phase if the temperature is below 350°C . [1128]. Although PCl_5 exists as a D_{3h} molecule in the gaseous and liquid states, it has an ionic structure consisting of $[\text{PCl}_4]^+[\text{PCl}_6]^-$ units in the crystalline state, as

TABLE 2.7a. Vibrational Frequencies of Trigonal-Bipyramidal XY₅ Molecules (cm⁻¹)

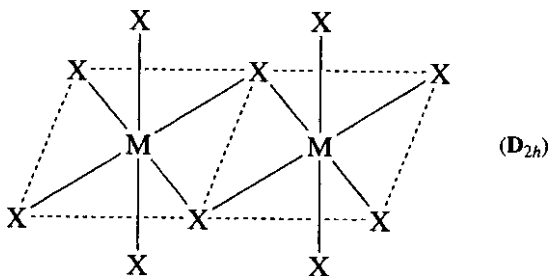
Molecule	Phase	$\tilde{\nu}_1$	$\tilde{\nu}_2$	$\tilde{\nu}_3$	$\tilde{\nu}_4$	$\tilde{\nu}_5$	$\tilde{\nu}_6$	$\tilde{\nu}_7$	$\tilde{\nu}_8$	Ref.
[SiF ₅] ⁻	Sol'n ^a	708	519	785	481	874	449	—	—	1096
[SiCl ₅] ⁻	Sol'n ^a	372	—	395	271	550	250	—	—	1097
[GeCl ₅] ⁻	Solid	348	236	310	200	395	200	—	—	1098
[SnCl ₅] ⁻	Solid	340	—	314	160	350	150	66	169	1099
[SnBr ₅] ⁻	Solid	—	—	208	106	256	111	—	—	1100
PF ₅	Gas	817	640	944	575	1026	532	300	514	1101
PCl ₅	Sol'n ^a	392	281	443	300	580	272	102	261	1102,1103
AsF ₅	Gas	733	642	784	400	809	366	123	388	1104
AsCl ₅	Sol'n ^a	369	295	385	184	437	220	83	213	1105
SbF ₅	Gas	667	264	—	—	716	498	90	228	1106
						710				
SbCl ₅	Gas	355	309	—	—	400	173	58	120	1107
[SeO ₅] ⁴⁻	Solid	756	736	775	674	344	806	—	355	1108
[CuCl ₅] ³⁻	Solid	260	—	268	—	170 ^b	95 ^c	—	—	1109
[CdCl ₅] ³⁻	Solid	251	—	236	—	157 ^b	98 ^c	—	—	1109
[TiCl ₅] ⁻	Sol'n ^a	348	302	355	178	411	190	66	166	1110
[TiCl ₅] ⁻	Solid	—	—	346	170	385	212	(83)	—	1100
VF ₅	Gas	719	608	784	331	810	282	(200)	350	1111,1112
NbCl ₅	Matrix	(349)	(349)	396	126	444	159	99	(139)	1113
NbBr ₅	Gas	234	178	288	(93)	315	119	67	101	1107,1114
TaCl ₅	Gas	406	324	—	—	—	181	54	127	1107
TaBr ₅	Gas	240	182	—	—	—	110	70	93	1107
MoF ₅	Matrix	—	—	683	—	713	261	112	—	1115
MoCl ₅	Gas	390	313	—	—	418	200	100	175	1107

^a Nonaqueous solution.

^b May be assigned to $\tilde{\nu}_7$.

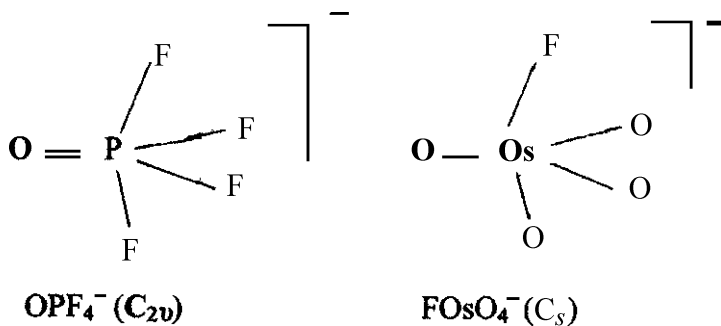
^c May be assigned to $\tilde{\nu}_8$.

proved by Raman spectroscopy [1129]. The importance of the ν_7 vibration in the intramolecular conversion of pentacoordinate molecules has been discussed by Holmes [1130].



Vibrational spectra of mixed halogeno compounds such as $\text{PF}_n\text{Cl}_{5-n}$, [1131,1132] PF_3X_2 ($\text{X} = \text{Cl}, \text{Br}$), [1133], $\text{PH}_n\text{F}_{5-n}$, [1134,1135], PH_3F_2 , [1136,1137] AsCl_3F_2 [1138] and AsCl_4F [1139] have been assigned.

The structure of OSF_4 is pseudo-trigonal-bipyramidal with two fluorines and one oxygen occupying the three equatorial positions. Thus, the IR and Raman spectra were assigned on the basis of C_{2v} symmetry [1140]. Since the OPF_4^- ion is isoelectronic with OSF_4 , the structure is similar to that of OSF_4 , and assignment of its Raman spectrum is based on the same symmetry [1141]. The FOsO_4^- ion assumes a distorted trigonal-bipyramidal structure with three oxygen atoms occupying the equatorial positions, and the IR and Raman spectra were assigned under C_s symmetry [1142]:



Although the Raman spectrum of $\text{C}_s^+ [\text{trans-XeO}_2\text{F}_3]^-$ was reported previously [1143], a later study showed that its structure is $\text{C}_s^+ [\text{XeO}_2\text{F}_3 \cdot n\text{XeF}_2]^-$, in which the two oxygen atoms are *cis* to each other [1144]. In the $[\text{F}(\text{cis-OsO}_2\text{F}_3)_2]^+$ ion, a fluorine bridge connects two trigonal bipyramidal cations in which two oxygen atoms and one fluorine atom occupy the equatorial plane and two fluorine atoms are in axial positions. The Raman spectra of its AsF_6^- and $\text{Sb}_2\text{F}_{11}^-$ salts have been assigned on the basis of

such a dimeric structure [1145]. $MO_2F_3 \cdot SbF_5$ ($M = Te, Re$) consists of infinite chains of alternating MO_2F_4 and SbF_6 units in which the bridging fluorine atoms on the antimony are *trans* to each other. The Raman spectra of these and related compounds have been reported [1146].

2.7.2. Tetragonal-Pyramidal XY_5 and ZXY_4 Molecules (C_{4v})

Figure 2.24 shows the nine normal modes of vibration of a tetragonal-pyramidal ZXY_4 molecule. Only A_1 and E vibrations are infrared-active, whereas all nine vibrations belonging to the A_1 , B_1 , B_2 , and E species are Raman-active. Table 2.7b lists the vibrational frequencies of tetragonal-pyramidal XY_5 and ZXY_4 molecules. In the majority of XY_5 molecules, the axial stretching frequency (ν_1) is higher than the equatorial stretching frequencies (ν_2 , ν_4 , and ν_7). This is opposite to the trend found for trigonal-bipyramidal XY_5 molecules, discussed in the preceding section. For normal coordinate analyses on these compounds, see Refs. [1150], [1153], [1170], and [1173].

An adduct, $XeF_6 \cdot BiF_5$, is formulated as $[XeF_5]^+[BiF_6]^-$ in the solid state; its $[XeF_5]^+$ cation is tetragonal-pyramidal [1157]. This should be contrasted to the $[XeF_5]^-$ anion which is pentagonal planar, as shown in the following section. In the $OCrF_4 - KrF_2$ adduct, KrF_2 coordinates to the vacant axial position of $OCrF_4$ through a

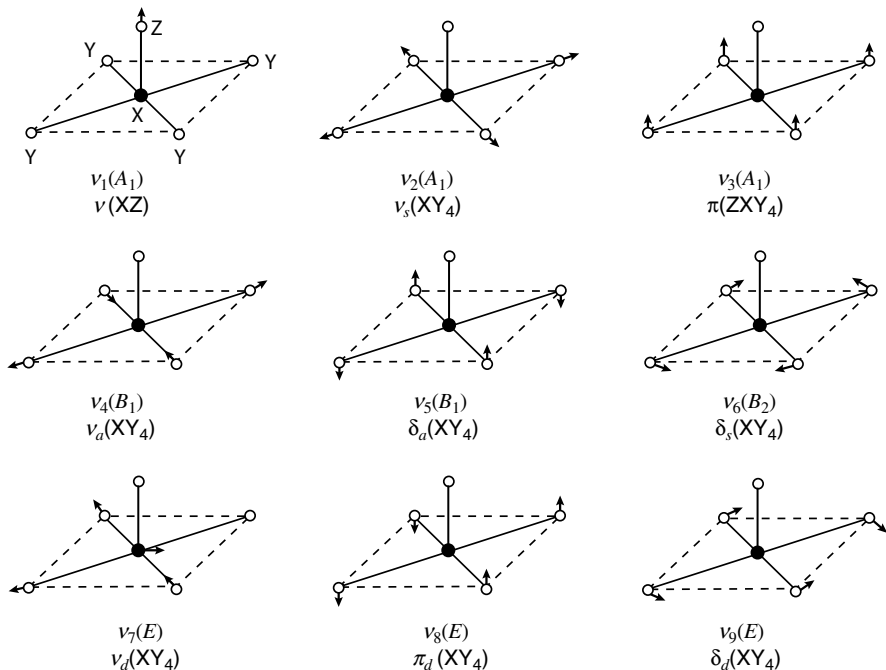


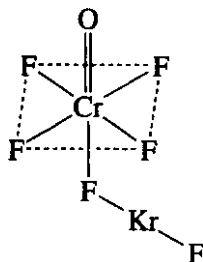
Fig. 2.24. Normal modes of vibration of tetragonal-pyramidal ZXY_4 molecules.

TABLE 2.7b. Vibrational Frequencies of Trigonal-Pyramidal XY_5 and ZXY_4 Molecules (cm^{-1})

XY_5 or ZXY_4	A_1 $\bar{\nu}_1$	A_1 $\bar{\nu}_2$	A_1 $\bar{\nu}_3$	B_1 $\bar{\nu}_4$	B_1 $\bar{\nu}_5$	B_2 $\bar{\nu}_6$	E $\bar{\nu}_7$	E $\bar{\nu}_8$	E $\bar{\nu}_9$	Ref.
$[\text{InCl}_6]^{2-}$	294	283	140	287	193	165	274	108	143	1147
$[\text{SbF}_6]^{2-}$	557	427	278	388	—	220	375,347	307	142	1148
$[\text{SbCl}_6]^-$	445	285	180	420	—	117	300	255	90	1149
$[\text{SF}_6]^-$	796	522	469	(435)	269	342	590	(435)	241	1150
$[\text{SeF}_6]^-$	666	515	332	460	236	282	480	399	202	1150
$[\text{TeF}_6]^-$	616	483	280	505	231	183	452	162	342	1148,1151
$[\text{TeCl}_6]^-$	363	254	136	270	98	82	246	90	169	1151
ClF_5	723	545	487	498	317	385	732	500	301	1152–1154
BrF_5	682	570	365	535	(281)	312	644	414	237	1153,1155
IF_5	698	593	315	575	(257)	273	640	374	189	1148,1153
NbF_5	740	686	513	—	—	—	729	261	103	1156
$[\text{XeF}_5]^+$	660	598	355	635	242	291	650	415	218	1157
				628				395		
$[\text{OTeF}_4]^{2-}$	837	461	—	390	—	190	335	—	129	1158
$[\text{OCIF}_4]^-$	1216	462	339	350	—	283	600,550	415,394	213	1159
								421		
$[\text{OBrF}_4]^-$	932	525	312	459	236	248	506 } 483 }	407 } 398 }	194 } 164 }	1160,1161

[OIF ₄] ⁻	888	533	273	475	—	214	485	365	124	1162
OXeF ₄	920	567	285	527	(230)	233	608	365	161	1153
OCrF ₄	1028	686	277	—	—	—	744	320	271	1163,1164
OMoF ₄	1050	714	267	—	—	—	708	306	238	1165–1167
OMoCl ₄	1015	450	143	400	148	220	396	256	172	1168,1169
[OMoCl ₄] ⁻	1008	354	184	327	158	167	364	240	114	1170
OWF ₄	1055	733	248	631	328	291	698	298	236	1166,1167
OReF ₄	1082	685	—	—	—	—	710	302	245	1171
[ORel ₄] ⁻	1014	169	85	183	—	—	240	181	—	1172
[NRuCl ₄] ⁻	1092	346	197	304	154	172	378	267	163	1170
[NRuBr ₄] ⁻	1088	224	156	187	103	128	304	211	98	1170
[NOSCl ₄] ⁻	1123	358	184	352	149	174	365	271	132	1170
[NOSBr ₄] ⁻	1119	162	122	156	110	120	220	273	98	1170
ORuF ₄	1060	685	—	—	—	—	713/710	310	—	1171
OOSF ₄	1080	695	—	—	—	—	685	319	—	1171

predominantly covalent bond [1174]:



As a result, the KrF_2 vibrations are markedly shifted in frequency relative to those of free KrF_2 [305]:

	ν_1	ν_2	ν_3
Free KrF_2	449	233	596, 580 cm^{-1}
Bound KrF_2	487	176	550, 542 cm^{-1}

2.7.3. Pentagonal–Planar XY_5 Molecules (D_{5h})

The first example of a pentagonal–planar XY_5 type molecule was the XeF_5^- anion [1175]. This anion was obtained as the 1:1 adduct of XeF_4 with $\text{N}(\text{CH}_3)_4\text{F}$, CsF or other alkali fluorides, and its structure was confirmed by X-ray analysis, IR/Raman, and NMR spectroscopy. Figure 2.25 shows the structure of the XeF_5^- anion, which can be derived by replacing the two axial fluorine ligands of the pentagonal–bipyramidal IF_7 molecule with two sterically active lone-pair electrons. The difference in structure between this anion and the XeF_5^+ cation discussed in the preceding section may be understood based on the VSEPR theory [1089].

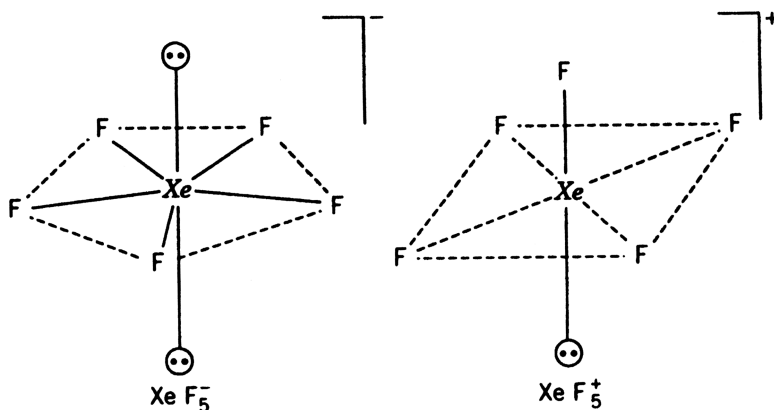


Fig. 2.25. Structures of the XeF_5^- and XeF_3^+ ions.

The XeF_5^- anion has 12 normal vibrations, which are classified into $A'_1(\text{R}) + A''_2(\text{IR}) + 2E'_1(\text{IR}) + 2E'_2(\text{R}) + E''_2$ (inactive) under D_{5h} symmetry. Thus, only three vibrations (A'_2 and $2E'_1$) are IR-active and only three vibrations ($A'_1 + 2E'_2$) are Raman-active. In agreement with this prediction, the observed Raman spectrum of $(\text{CH}_3)_4\text{N}[\text{XeF}_5]$ exhibits three bands at 502 (symmetric stretch, A'_1), 423 (asymmetric stretch, E'_2), and 377 cm^{-1} (in-plane bending, E'_2). As discussed in Sec. 1.11, the trigonal-bipyramidal and tetragonal-pyramidal structures can be ruled out since many more IR- and Raman-active bands are expected for these structures.

The second example of a pentagonal planar XY_5 -type molecule is the IF_5^{2-} ion, which is isoelectronic with the XeF_5^- ion. It was obtained as the $\text{N}(\text{CH}_3)_4^+$ salt from the reaction of $\text{N}(\text{CH}_3)_4\text{IF}_4$ and $\text{N}(\text{CH}_3)_4\text{F}$ in CH_3CN solution, and the IR and Raman spectra were assigned under D_{5h} symmetry [1176].

2.8. OCTAHEDRAL MOLECULES

2.8.1. Octahedral XY_6 Molecules (O_h)

Figure 2.26 illustrates the six normal modes of vibration of an octahedral XY_6 molecule. Vibrations ν_1 , ν_2 , and ν_5 are Raman-active, whereas only ν_3 and ν_4 are infrared-active. Since ν_6 is inactive in both, its frequency is estimated by several

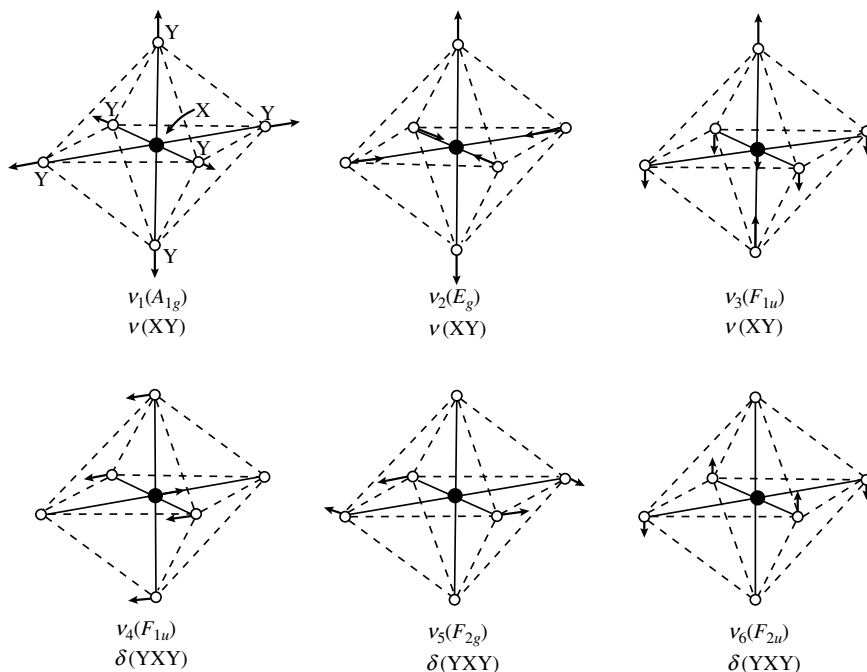


Fig. 2.26. Normal modes of vibration of octahedral XY_6 molecules.

methods including the analysis of nonfundamental frequencies and rotational fine structures of vibration spectra. The **G** and **F** matrix elements of the octahedral XY_6 molecule are listed in Appendix VII.

Table 2.8a lists the vibrational frequencies of a number of hexahalogeno compounds. In general, the order of the stretching frequencies is $\nu_1 > \nu_3$ (ν_2 or $\nu_1 < \nu_3$ (ν_2 , depending on the compound. The order of the bending frequencies is $\nu_4 > \nu_5 > \nu_6$ in most cases.

Parker et al. [1263] measured the IR, Raman, and INS (inelastic neutron scattering) spectra of the $[\text{FeH}_6]^{4-}$ ion and its deuterated analog listed at the end of Table 2.8a. These hexahydrido complexes are unusual in that the $\nu_1(A_{1g})$ and $\nu_2(E_g)$ frequencies are very close, although they are well separated in other XY_6 molecules. This result indicates that the stretching–stretching interaction force constant (f_{rr} in Appendix VII.6 is very small in the case of Fe–H(D) bonds. The ν_6 frequencies of these compounds listed in Table 2.8a were obtained by INS spectroscopy.

Several trends are noted in the octahedral XY_6 molecules listed in Table 2.8a, as described in Secs. 2.8.1.1–2.8.1.12.

2.8.1.1. Mass of Central Atom Within the same family of the periodic table, the stretching frequencies decrease as the mass of the central atom increases, for example

	$[\text{AlF}_6]^{3-}$		$[\text{GaF}_6]^{3-}$		$[\text{InF}_6]^{3-}$		$[\text{TiF}_6]^{3-}$
$\tilde{\nu}_1(\text{cm}^{-1})$	541	>	535	>	497	>	478
$\tilde{\nu}_3(\text{cm}^{-1})$	568	>	481	>	447	>	412

The trend in ν_1 directly reflects the trend in the stretching force constant (and bond strength) since the central atom is not moving in this mode. In ν_3 , however, both X and Y atoms are moving, and the mass effect of the X atom cannot be ignored completely.

2.8.1.2. Oxidation State of Central Atom Across the periodic table, the stretching frequencies increase as the oxidation state of the central atom becomes higher. Thus we have

	$[\text{AlF}_6]^{3-}$		$[\text{SiF}_6]^{2-}$		$[\text{PF}_6]^-$		SF_6
$\tilde{\nu}_1(\text{cm}^{-1})$	541	<	663	<	745	<	775
$\tilde{\nu}_3(\text{cm}^{-1})$	568	<	741	<	840	<	939

The effect of lowering the oxidation state of the same central atom is clearly seen in a series such as $[\text{VF}_6]^{n-}$ ($n = 1, 2, 3$) and $[\text{WC1}_6]^{n-}$ ($n = 0, 1, 2$):

	$[\text{VF}_6]^-$		$[\text{VF}_6]^{2-}$		$[\text{VF}_6]^{3-}$
$\tilde{\nu}_1(\text{cm}^{-1})$	676	>	584	>	533
$\tilde{\nu}_3(\text{cm}^{-1})$	646	>	578	>	511

As in many other cases, the higher the oxidation state, the higher the frequency. The bending frequencies do not exhibit clear-cut trends.

TABLE 2.8a. Vibrational Frequencies of Octahedral XY_6 Molecules (cm^{-1})

Molecule	$\tilde{\nu}_1$	$\tilde{\nu}_2$	$\tilde{\nu}_3$	$\tilde{\nu}_4$	$\tilde{\nu}_5$	$\tilde{\nu}_6^a$	Ref.
$[\text{AlF}_6]^{3-}$	541	(400)	568	387	322	(228)	1177,1178
$[\text{GaF}_6]^{3-}$	535	(398)	481	298	281	(198)	1178,1179
$[\text{InF}_6]^{3-}$	497	(395)	447	226	229	(162)	1177,1178
$[\text{InCl}_6]^{3-}$	277	193	250	157	(149)	—	1180
$[\text{TlF}_6]^{3-}$	478	387	412	202	209	(148)	1177,1178
$[\text{TlCl}_6]^{3-}$	280	262	294	222,246	155	(136)	1181
$[\text{TlBr}_6]^{3-}$	161	153	190,195	134,156	95	(80)	1181
$[\text{SiF}_6]^{2-}$	663	477	741	483	408	—	1182
$[\text{GeF}_6]^{2-}$	671	478	624	365,355	333/325	—	1183
$[\text{GeCl}_6]^{2-}$	318	213	310	213	191	—	1184
$[\text{SnF}_6]^{2-}$	592	477	559	300	252	—	1182
$[\text{SnCl}_6]^{2-}$	311	229	303	166	158	—	1185
$[\text{SnBr}_6]^{2-}$	190	144	224	118	109	—	1186
$[\text{SnI}_6]^{2-}$	122	93	161	84	78	—	1187
$[\text{PbCl}_6]^{2-}$	281	209	262	142	139	—	1185
$[\text{PF}_6]^{-}$	756	585,570	865,835	559,530	480 ~ 468	—	1188
$[\text{PCl}_6]^{-}$	360	283	444	285	238	—	1184,1189
$[\text{AsF}_6]^{-}$	689	573	700	385	375	(252)	1182
$[\text{AsCl}_6]^{-}$	337	289	333	220	202	—	1184
$[\text{SbF}_6]^{-}$	668	558	669	350	294	—	1182,1190
$[\text{SbCl}_6]^{-}$	330	282	353	180	175	—	1191
$[\text{SbCl}_6]^{3-}$	327	274	—	—	137	—	1192
$[\text{SbBr}_6]^{-}$	192	169	239,224	119	103,78	—	1193
$[\text{SbBr}_6]^{3-}$	180	153	180	107	73	—	1194,1195
$[\text{Sbl}_6]^{3-}$	107	96	108	82	54	—	1194,1195
$[\text{BIF}_6]^{-}$	590	547	585	—	231/247	—	1190,1196
$[\text{BiCl}_6]^{3-}$	259	215	172	130	115	—	1194,1195
$[\text{BiBr}_6]^{3-}$	156	130	128	75	62	—	1194,1195
$[\text{BI}_6]^{3-}$	114	103	96	(59)	54	—	1194,1195

(continued)

TABLE 2.8a. (Continued)

Molecule	$\tilde{\nu}_1$	$\tilde{\nu}_2$	$\tilde{\nu}_3$	$\tilde{\nu}_4$	$\tilde{\nu}_5$	$\tilde{\nu}_6^a$	Ref.
SF ₆	775	643	939	614	524	(347)	1197–1199
SeF ₆	708	658	780	437	403	(264)	1197, 1198
[SeCl ₆] ²⁻	299	255	280	160–140	165	—	1180
[SeBr ₆] ²⁻	176	155	221	129	138	—	1200
TeF ₆	698	672	752	325	312	(197)	1197, 1198
[TeCl ₆] ²⁻	298	250	250	136	140	—	1201
[TeCl ₆] ³⁻	264	192	230	146	(135)	—	1170
[TeBr ₆] ²⁻	174	153	198	—	75	—	1201, 1202
[ClF ₆] ⁻	525	384	—	—	289	—	1203
[ClF ₆] ⁺	679	630	890	582	513	—	1204
[BrF ₆] ⁺	658	660	—	—	405	—	1205
[BrF ₆] ⁻	568	454	400	204, 184	250	(138)	1206
[AuF ₆] ⁻	595	530	—	—	225	—	1207
[ScF ₆] ³⁻	495	375	458	257	235	—	1208
[ScI ₆] ³⁻	119	67	—	—	80	—	898
[XF ₆] ³⁻	476	382	160	74	194	—	1209
[LaF ₆] ³⁻	443	334	130	63	171	—	1209
[GaF ₆] ³⁻	473	380	140	72	185	—	1209
[YbF ₆] ³⁻	491	370	156	70	196	—	1209
[CeCl ₆] ²⁻	295	265	268	117	120	(86)	1210
[TiF ₆] ²⁻	618	(440)	615, 660	315, 281	308, 300	—	1211
[TiCl ₆] ²⁻	320	271	316	183	173	—	1212
[TiCl ₆] ³⁻	322	278	304, 290	—	175	—	1213
[TiBr ₆] ²⁻	192	—	244	119	115	—	1212
[ZrF ₆] ²⁻	589	(416)	537, 522	241, 192	258, 244	—	1214
[ZrCl ₆] ²⁻	327	237	290	150	153	—	1215
[ZrBr ₆] ²⁻	194	144	223	106	99	—	1216
[HfF ₆] ²⁻	572	(389)	448, 490	217, 184	259, 247	—	1211
[HfCl ₆] ²⁻	325	257	275	145	156	(80)	1185
[HfBr ₆] ²⁻	197	142	189	102	101	—	1216

$[\text{VF}_6]^{2-}$	584	—	578	273	—	—	1217
$[\text{VF}_6]^{3-}$	533	—	511	292	—	—	1217
$[\text{VCl}_6]^{2-}$	—	—	355,305	—	—	—	1218
$[\text{NbF}_6]^-$	683	562	602	244	280	—	1219,1220
$[\text{NbCl}_6]^-$	368	288	333	162	183	—	1185
$[\text{NbCl}_6]^{2-}$	—	—	314	165	—	—	1220,1221
$[\text{NbBr}_6]^-$	—	—	240 ~ 216	—	—	—	1222
$[\text{NbBr}_6]^{2-}$	—	—	236	112	—	—	1220,1221
$[\text{NbI}_6]^-$	—	—	180	70,66	—	—	1220,1223
$[\text{TaF}_6]^-$	692	581	560	240	272	(192)	1224
$[\text{TaCl}_6]^-$	378	298	330	158	180	—	1185
$[\text{TaCl}_6]^{2-}$	—	—	297	160	—	—	1185
$[\text{TaBr}_6]^-$	—	—	234 ~ 223	—	—	—	1222
$[\text{TaBr}_6]^{2-}$	—	—	217	109	—	—	1221
$[\text{TaI}_6]^-$	—	—	160	80	—	—	1223
CrF_6	(720)	(650)	790	(266)	(309)	(110)	1225,1226
$[\text{CrCl}_6]^{3-}$	286	237	315	199	162	182	1227
$^{92}\text{MoF}_6$	741.8	652.0	749.5	265.7	317	117	1228
$[\text{MoF}_6]^{2-}$	685	598	653	250	274	—	1229
$[\text{MoCl}_6]^-$	356	—	327	162	—	—	1230
$[\text{MoCl}_6]^{2-}$	329	—	308	168	154	—	1230
$[\text{MoCl}_6]^{3-}$	305	—	268 } 286 } 302 }	167 } 187 }	150	—	1230
WF_6	770	676	711	258	321	(127)	1197,1198
WCl_6	437	331	373	160	182	—	1185
$[\text{WCl}_6]^-$	382	—	332 } 312 }	157	168	—	1230
$[\text{WCl}_6]^{2-}$	341	—	293	166 } 150 }	—	—	1230

(continued)

TABLE 2.8a. (Continued)

Molecule	$\tilde{\nu}_1$	$\tilde{\nu}_2$	$\tilde{\nu}_3$	$\tilde{\nu}_4$	$\tilde{\nu}_5$	$\tilde{\nu}_6^a$	Ref.
$[\text{MnF}_6]^{2-}$	592	508	620	335	308	—	1231
TcF_6	713	(639)	748	275	(297)	(145)	1198
$[\text{ReF}_6]^+$	797	734	783	353	359	—	1232
ReF_6	754	(671)	715	257	(295)	(147)	1198
$[\text{ReF}_6]^{2-}$	611	530	535	249	221	(181)	1233
$[\text{ReCl}_6]^-$	—	—	318	161	—	—	1234
$[\text{ReCl}_6]^{2-}$	346	(275)	313	172	159	—	1185, 1235
$[\text{ReBr}_6]^{2-}$	213	(174)	217	118	104	—	1236
$[\text{FeF}_6]^{3-}$	507	—	456	—	273	—	1179
$[\text{NiF}_6]^{2-}$	555	512	648	332	307/298	—	1237
$[\text{PdF}_6]^{2-}$	558	276	615	—	212	—	1238
$[\text{PdCl}_6]^{2-}$	318	289	346	200	178	—	1239
$[\text{PdBr}_6]^{2-}$	198	176	253	130	100	—	1240
PtF_6	656	(601)	705	273	(242)	(211)	1198
$[\text{PtF}_6]^{2-}$	611	576	571	281	210	(143)	1241
$[\text{PtCl}_6]^{2-}$	348	318	342	183	171	(88)	1186
$[\text{PtBr}_6]^{2-}$	213	190	243	146	137	—	1239
$[\text{PtI}_6]^{2-}$	—	—	186	46	—	—	1242
$[\text{FeF}_6]^{3-}$	538	374	—	—	253	—	1243
RuF_6	(675)	(624)	735	275	(283)	(186)	1198, 1244
$[\text{RuCl}_6]^{2-}$	—	—	346	188	—	—	1244
OsF_6	731	(668)	720	268	(276)	(205)	1198
$[\text{OsCl}_6]^-$	375	302	325	168	183	—	1245
$[\text{OsCl}_6]^{2-}$	345.3	245.2	326	176	160	—	1246, 1247
$[\text{OsBr}_6]^{2-}$	210.6	169.2	227	122	100	—	1246, 1248
$[\text{Osl}_6]^{2-}$	152	121	170	91	80	—	1249
RhF_6	(634)	(595)	724	283	(269)	(192)	1198, 1244
$[\text{RhCl}_6]^{2-}$	—	320	335	—	253	—	1250
IrF_6	701.1	647.3	715.6	267.5	265.2	208.3 ^c	1251, 1252
$[\text{IrCl}_6]^{2-}$	341.3	289.4	—	—	159.6	—	1253

$[\text{IrCl}_6]^{3-}$	—	—	296	200	—	—	1242
$[\text{IrBr}_6]^{2-}$	209.6	175.1	—	—	103.2	—	1253
$[\text{IrI}_6]^{3-}$	149	133	175	87	88	—	1254
$[\text{ThCl}_6]^{2-}$	294	255	259	—	114	—	1255
UF_6	666	530	619	184	200	—	1256
$[\text{UF}_6]^-$	—	—	525	173	—	—	1257
$[\text{UCl}_6]^-$	343	273	310	122	136	—	1257, 1258
$[\text{UCl}_6]^{2-}$	299	237	262	114	121	(80)	1255
$[\text{Ubr}_6]^-$	—	—	214	87	—	—	1257
NpF_6^b	646	525	618	198	208	169	1259
NpF_6^c	643	574	604	191	—	138/149	1259
$[\text{NpCl}_6]^{2-}$	310	—	265	117	128	—	1260
PuF_6^b	625	519	612	200	209	177	1261
PuF_6^c	615	—	—	202	198	172	1262
$[\text{FeH}_6]^{4-}$	1873	1878	1746	899 ^d	1019	836 ^d	1263
$[\text{FeD}_6]^{4-}$	1342	1363	1260	655 ^d	1057	549 ^d	1263

^a The value of ν_6 can also be estimated by the relation, $\nu_6 = \nu_5/\sqrt{2}$ [1264, 1265].

^b Ground state.

^c Excited state.

^d INS frequency.

2.8.1.3. Halogen Series The effect of changing the halogen is seen in a number of series, for example

	[SnF ₆] ²⁻		[SnCl ₆] ²⁻		[SnBr ₆] ²⁻		[SnI ₆] ²⁻	
$\tilde{\nu}_1(\text{cm}^{-1})$	592	>	311	>	190	>	122	
$\tilde{\nu}_3(\text{cm}^{-1})$	559	>	303	>	224	>	161	

The stretching force constants also follow the same order. The ratios $\nu(\text{MBr})/\nu(\text{MCl})$ and $\nu(\text{MI})/\nu(\text{MCl})$ are about 0.61 and 0.42, respectively, for ν_1 , and about 0.76 and 0.62, respectively, for ν_3 .

2.8.1.4. Electronic Structure In the $[\text{MCl}_6]^{3-}$ series, ν_3 and ν_4 change as follows:

	Cr ³⁺ (d^3)	Mn ³⁺ (d^4)	Fe ³⁺ (d^5)	In ³⁺
$\tilde{\nu}_3(\text{cm}^{-1})$	315	342	248	248
$\tilde{\nu}_3(\text{cm}^{-1})$	200	183	184	161

All these metal ions are in the high-spin state. For $\text{Fe}^{3+}(t_{2g}^3 e_g^2)$, occupation of the antibonding orbitals lowers ν_3 drastically in comparison to the Cr^{3+} complex; its ν_3 is comparable to that of the In^{3+} complex, whose ν_3 is lowered because of the increased mass of the metal. On the other hand, the ν_3 of $[\text{MnCl}_6]^{3-}$ is higher than that of $[\text{CrCl}_6]^{3-}$ because the static Jahn–Teller effect of the Mn^{3+} ion causes a tetragonal distortion [1210].

2.8.1.5. Electronic Excited States Table 2.8a includes PuF_6 and NpF_6 , for which vibrational frequencies have been determined both for the ground and excited states. The excited frequencies were obtained from the analysis of vibrational fine structure of electronic spectra.

2.8.1.6. Raman Intensities The Raman intensity of an XY_6 molecule normally follows the order $I(\nu_1) > I(\nu_2) > I(\nu_5)$. Adams and Downs [1266] noted that $I(\nu_2)/I(\nu_1)$ is 0.5 to 1 for $[\text{TeCl}_6]^{2-}$ and $[\text{TeBr}_6]^{2-}$, although it normally ranges from 0.05 to 0.1. Furthermore, they observed ν_3 , which is not allowed in Raman spectra. From these and other items of evidence, they proposed that the O_h selection rule breaks down in $[\text{TeX}_6]^{2-}$ because less symmetric electronic excited states perturb the O_h ground state. They also noted the distortion of $[\text{SbX}_6]^{3-}$ ions to C_{3v} symmetry from their Raman spectra in solution. Woodward and Creighton [1267] noted that $I(\nu_2) > I(\nu_1)$ holds in the aqueous Raman spectra of Na_2PtX_6 ($\text{X} = \text{Cl}, \text{Br}$) and Na_2PdCl_6 , and attributed this unusual trend to the presence of six nonbonding d electrons in the valence shell.

2.8.1.7. Symmetry Lowering Table 2.8a contains XY_6 -type ions that exhibit splitting of degenerate vibrations due to lowering of symmetry in the crystalline state. For example, the ν_3 vibration of the ReF_6^{2-} ion in $\text{K}_2[\text{ReF}_6]$ splits into two bands (565 and 543 cm^{-1}) due to trigonal distortion in the crystalline state. Similar splitting is observed for the ν_4 vibration (222 and 257 cm^{-1}) [1268,1269].

More examples are found in the $[\text{ReCl}_6]^- (\text{C}_{4v})$ [1270] and $[\text{CuCl}_6]^{4-} (\text{D}_{2h})$ [1271] ions in the crystalline state.

2.8.1.8. Adduct Formation Hunt et al. [1272] obtained two types of 1:1 adducts by codepositing UF_6 with HF in excess Ar at 12 K; $\text{UF}_6\text{--HF}$ exhibits a strong band at 3848 cm^{-1} , while the anti-hydrogen-bonded complex, $\text{UF}_6\text{--FH}$, shows a weak, broad band at 3903 cm^{-1} in IR spectra. Similar experiments show, however, $\text{WF}_6\text{--HF}$ exhibits a weak band at 3911 cm^{-1} , while $\text{WF}_6\text{--FH}$ shows a strong band at 3884 cm^{-1} . These results indicate that, in hydrogen-bonded complexes, the order of proton affinity is $\text{WF}_6 < \text{UF}_6$, with HF serving as a proton donor and that, in anti-hydrogen-bonded complexes, the order of acidity is $\text{UF}_6 < \text{WF}_6$, with HF serving as a Lewis base. Relative yields of these two types are determined by the acidity/basicity of these fluorides.

2.8.1.9. Anomalous Polarization Preresonance Raman spectra of 17 XY_6 -type metal halides have been measured by Bosworth and Clark [1192]. Hamaguchi et al. [1273] observed anomalous polarization (Sec. 1.23) for all the Raman bands of the IrCl_6^{2-} ion measured under resonance condition. Figure 2.27 shows the polarized Raman spectra (488.0 nm excitation) of this ion in aqueous solution together with band assignments and depolarization ratios for each band. Since the Raman tensor for the ν_1 , ν_2 , and ν_5 vibrations cannot have an antisymmetric part, group theoretical arguments such as those used for heme proteins (Sec. 1.23) are not applicable to octahedral XY_6 ions. A more detailed study by Hamaguchi [1274] shows that electronic degeneracy in the $\text{IrCl}_6^{2-} (5d^5)$ ion induces an antisymmetric part of vibrational Raman tensors. Anomalous polarization was also observed for the $[\text{IrBr}_6]^{2-}$ ion [1275].

2.8.1.10. Jahn–Teller Effect Weinstock et al. [1276] noted that the combination bands ($\nu_1 + \nu_3$) and ($\nu_2 + \nu_3$) appear with similar frequencies, intensities, and shapes in the infrared Spectra of $\text{MoF}_6(d^0)$ and $\text{RhF}_6(d^3)$. As shown in Fig. 2.28 however, ($\nu_2 + \nu_3$) was very broad and weak in $\text{TcF}_6(d^1)$, $\text{ReF}_6(d^1)$, and $\text{RuF}_6(d^2)$, and $\text{OsF}_6(d^2)$. This anomaly was attributed to a dynamic Jahn–Teller effect. The static Jahn–Teller effect does not seem to operate in these compounds since no splittings of the triply degenerate fundamentals were observed.

Perhaps the most fascinating XY_6 -type molecule is XeF_6 . In their earlier work, Claassen et al. [1277] suggested the distortion of XeF_6 from O_h symmetry since they observed two stretching bands in infrared and three stretching bands in Raman spectra. It was not possible, however to determine the precise structure of XeF_6 until they [1278] carried out a detailed IR, Raman, and electronic spectral study of XeF_6 vapor as a function of temperature. They were then able to show that XeF_6 consists of the three electronic isomers shown in Fig. 2.29 and to explain subtle differences in spectra at different temperatures as a shift of equilibrium among these three isomers.

2.8.1.11. $^{235}\text{U}/^{238}\text{U}$ Isotope Shift UF_6 in natural abundance consists of 99.3% $^{238}\text{UF}_6$ and 0.7 % $^{235}\text{UF}_6$. Since the isotope shifts between them is extremely small, it

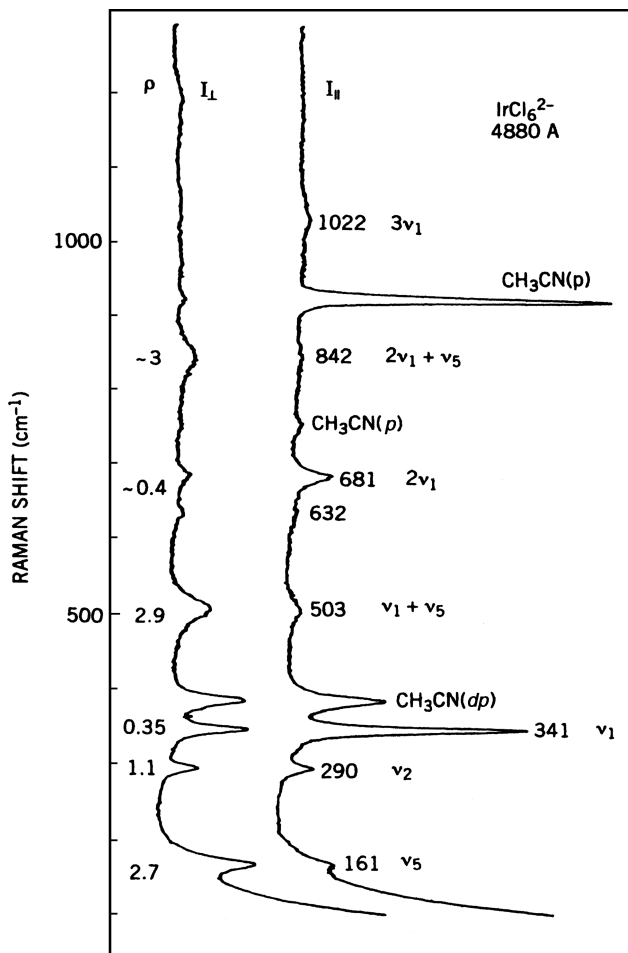


Fig. 2.27. Polarized Raman spectra of $[(n\text{-C}_4\text{H}_9)_4\text{N}]_2 [\text{IrCl}_6]$ in acetonitrile (488 nm excitation) [1273].

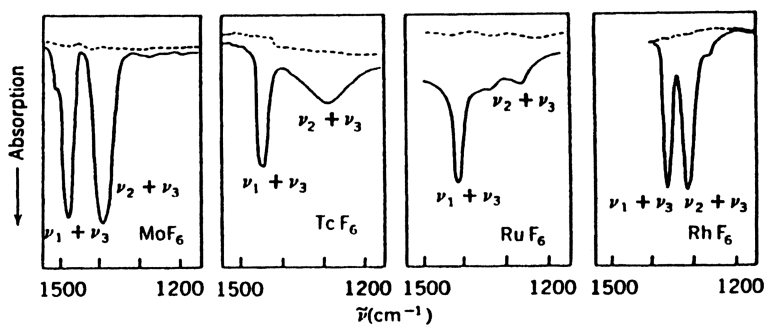


Fig. 2.28. Band profiles for $(\nu_1 + \nu_3)$ and $(\nu_2 + \nu_3)$ for the 4d transition series hexafluorides [1276].

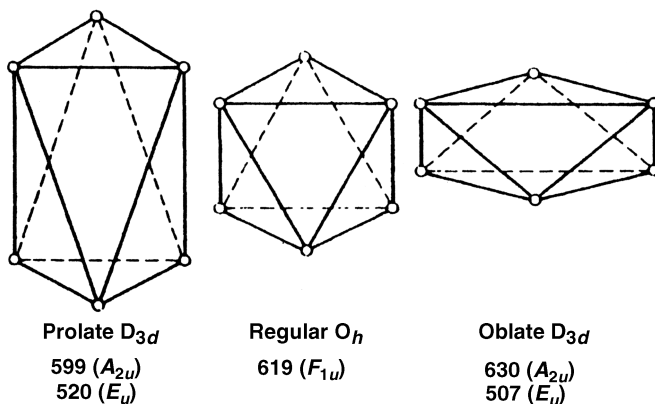


Fig. 2.29. Structures of three isomers of XeF_6 and their IR-active stretching frequencies (cm^{-1}). The Xe atom at the center is not shown.

is difficult to observe the vibrational spectrum of the latter without serious overlapping of the former. Takami et al. [1279] have overcome this difficulty by measuring the spectrum of a UF_6 (natural abundance)/Ar mixture as a supercooled vapor (below 100 K) using the cold-jet technique [1280]. Figure 2.30 shows the high-resolution IR spectrum of UF_6 in the ν_3 region thus obtained [1279]. It exhibits sharp rotational fine structures [1281] without hot band contributions, and the rotational components of $^{238}\text{UF}_6$ and $^{235}\text{UF}_6$ are well separated; the former shows the Q-branch as well as R(0)–R(6) branches whereas the latter exhibits the Q-branch between R(5) and R(6) of the former. Although the isotope shift is estimated to be only 0.6040 cm^{-1} , Takeuchi et al. [1282] have found that UF_6 gas in the supercooled state ($<100\text{ K}$) preferentially decomposes $^{235}\text{UF}_6$ to $^{235}\text{UF}_5$, when irradiated by a laser line at 625 cm^{-1} ($16\text{ }\mu$). This photolysis reaction was utilized to increase the relative concentration of ^{235}UF to the level sufficient for commercial generation of atomic energy.

2.8.1.12. Normal Coordinate Analysis Normal coordinate analyses on octahedral hexahalogeno compounds have been made by a number of investigators. Kim et al. [1283] calculated the force constants of 15 metal fluorides using the UBF and OVF fields (see Sec. 1.14), and found that the latter is better than the former. LaBonville et al. [1284] calculated the force constants of 62 metal halides by using the UBF, OVF, GVF, modified UBF, and modified OVF fields, and found that the modified OVF field gives the best overall agreement with the observed frequencies. They also discussed the dependence of force constants on the mass of the halogen, the oxidation state of the metal, the number of nonbonding electrons in the valence shell, and the crystal field stabilization energy.

2.8.1.13. Other Spectral Properties The ^{35}Cl NQR spectra provide information about the σ and π contributions to the covalent $\text{M}–\text{Cl}$ bonding in $[\text{MCl}_6]^{n-}$

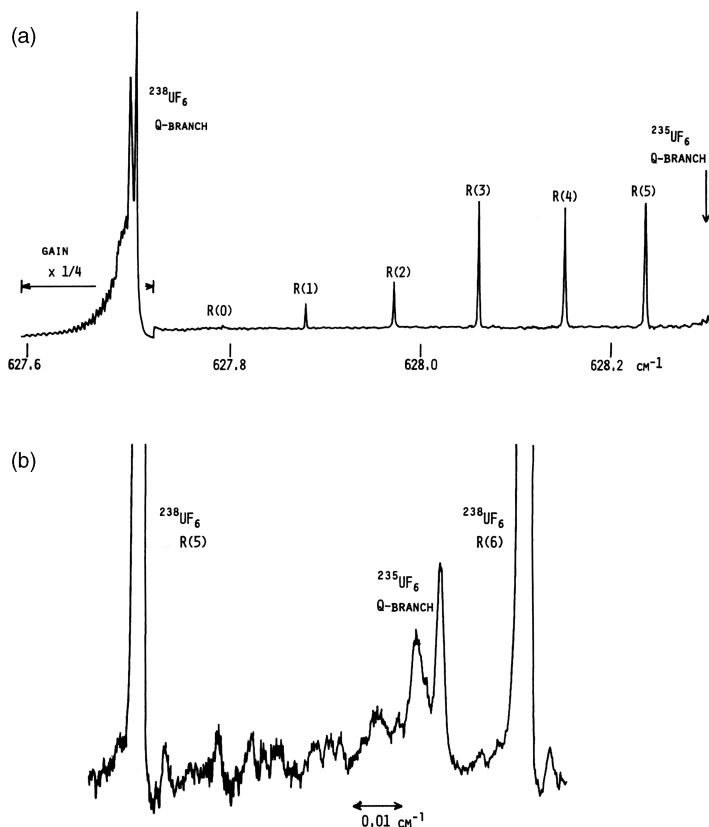


Fig. 2.30. (a) IR spectrum of UF_6 (ν_3 region) in the cold jet; (b) the $^{235}\text{UF}_6$ Q-branch spectrum recorded by expanded scale [1276].

type ions, and these can be correlated with the force constants obtained from infrared and Raman studies [1185]. Both infrared and NQR spectra suggest low-site symmetry of the $[\text{MCl}_6]^{3-}$ ion in $\text{K}_3[\text{MCl}_6] \cdot \text{H}_2\text{O}$ ($\text{M} = \text{Ir}, \text{Rh}$) crystals [1285].

Coriolis coupling constants have been calculated from the vapor-phase Raman spectra of some XY_6 -type molecules [1197].

Table 2.8b lists the vibrational frequencies of MO_6 -type ions. Hauck and Fadini calculated the force constants of these ions [1286,1287].

2.8.2. Octahedral $\text{XY}_n\text{Z}_{6-n}$ Molecules

The XY_5Z molecule belongs to the C_{4v} point group, and its 11 normal vibrations are classified into $4A_1$, $2B_1$, B_2 , and $4E$ modes, of which only A_1 and E are infrared-active; all are Raman-active.

The XY_4Z_2 molecule may be *cis* (C_{2v}) or *trans* (D_{4h}). The *cis* isomer is expected to give four XY stretching ($2A_1 + B_1 + B_2$) and two XZ stretching ($A_1 + B_1$) modes, all of which are infrared- as well as Raman-active. The *trans* isomer is expected to give three

TABLE 2.8b. Vibrational Frequencies of Octahedral MO₆ Molecules (cm⁻¹)

Compound	$\tilde{\nu}_1$	$\tilde{\nu}_2$	$\tilde{\nu}_3$	$\tilde{\nu}_4$	$\tilde{\nu}_5$	Ref.
Li ₆ [TeO ₆]	700	540	640	470	355	1286
Li ₆ [WO ₆]	740	450	620	425	360	1286
α -Li ₆ [ReO ₆]	680	505	620	425	360	1286
Ca ₄ [PtO ₆]	—	530	575	425	345	1287
α -Li[TeO ₆]	700	540	640	470	355	1287
Ca ₅ [O ₆] ₂	771	490,538	765,695	451,435	—	1287
[NbO ₆] ^a	620	542	600	350	269	1288

^aIn Sb[NbO₆] crystal.

XY stretching ($A_{1g} + B_{1g} + E_u$) and two XZ stretching ($A_{1g} + A_{2u}$) modes, of which E_u and A_{2u} are infrared-active and A_{1g} and B_{1g} are Raman-active. The selection rules for other XY_nZ_{6-n} molecules tabulated in Appendix V can be used to distinguish the structures of stereoisomers on the basis of their vibrational spectra. Table 2.8c lists the observed frequencies of XY_5Z and XY_4WZ -type molecules.

Preetz and co-workers carried out an extensive study on the preparation; isolation, and vibrational spectra of a number of mixed-halogeno complexes: $[MC1_nBr_{6-n}]^{2-}$ ($n = 0-6$, M = Ru [1311], Os [1312]), $[TeClnBr_{6-n}]^{2-}$ ($n = 0-6$) [1313], $[OsF_nCl_{6-n}]^{2-}$ ($n = 1-5$) [1314], $[MC1_nBr_{6-n}]^{3-}$ ($n = 1-5$, M = Rh, [1315], Ir [1316]), $[IrF_nCl_{6-n}]^{2-}$ ($n = 1-5$), [1317,1318] $[PtF_nCl_{6-n}]^{2-}$ ($n = 1-5$) [1319,1320], and $[PtCl_nBr_{6-n}]^{2-}$ ($n = 1-5$) [1321]. These workers assigned the IR Raman spectra and carried out normal coordinate analysis for these complexes [1322]. For example, the following stereoisomers were isolated for the $[OsF_nCl_{6-n}]^{2-}$ ions:

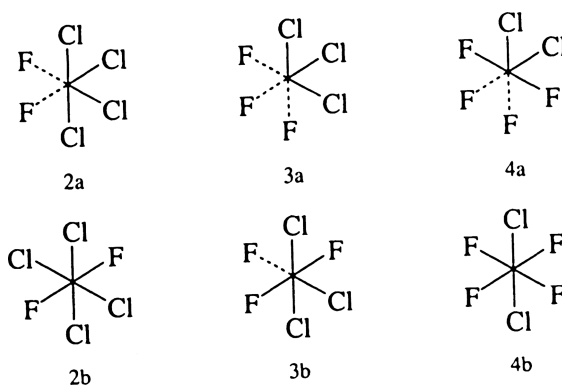


Figure 2.31 shows the IR and Raman spectra of these stereoisomers. In the Os—Cl stretching region ($350-300\text{ cm}^{-1}$), the *trans* isomer (2b, D_{4h}) exhibits one IR (E_u) and two Raman (A_{1g} and B_{1g}) bands, as expected from the selection rules. For the *cis* isomer (2a, C_{2v}), the selection rules predict four ($2A_1$, B_1 , and B_2) bands both in IR and Raman spectra. However, only three IR and two Raman bands are apparent in Fig. 2.24. Such

TABLE 2.8c. Vibrational Frequencies of Octahedral XY_6Z and XY_4WZ Molecules (cm^{-1})

XY_6Z or XY_4WZ	$\tilde{\nu}_1 (A_1)$ $\nu (XZ)$	$\tilde{\nu}_2 (A_1)$ $\nu (XW)^a$	$\tilde{\nu}_3 (A_1)$ $\nu (XY_4)$	$\tilde{\nu}_4 (A_1)$ $\pi (XY_4)$	$\tilde{\nu}_5 (B_1)$ $\nu (XY_4)$	$\tilde{\nu}_6 (B_1)$ $\pi (XY_4)$	$\tilde{\nu}_7 (B_2)$ $\delta (XY_4)$	$\tilde{\nu}_8 (E)$ $\nu (XY_4)$	$\tilde{\nu}_9 (E)$ $\rho W (XW)^a$	$\tilde{\nu}_{10} (E)$ $\rho W (XZ)$	$\tilde{\nu}_{11} (E)$ $\delta (XY_4)$	Ref.
$[PF_6H]^-$	2375	762	602	558	542	—	440	800	812	1238	333	1289
$[SbCl_6Br]^-$	219	308	334	151	287	—	—	344	—	—	—	1390, 1291
$[SbBr_5Cl]^-$	305	206	192	—	186	—	—	239	—	—	—	1290
SF_5Cl	402	855	707	602	625	271	505	909	597	399	441	1292
SF_5Br	272	848	691	586	620	—	500	898	575	222	419	1293
$[SF_5O]^-$	1153	722	697	506	541	472	452	780	607	530	325	1294, 1295
SeF_5Cl	729	654	440	384	636	—	380	745	421	334	213	1296
$[SeF_5O]^-$	919	559	649	—	556	—	—	639	—	—	—	1297
TeF_5Cl	708	662	312	410.5 404.0	651	—	302	726	324.6	259	167	1298
$[TeF_5O]^-$	867	576	643	345	—	260	—	635	331	320	279	1299
$[TiF_5O]^{3-}$	920	379	520	290	—	—	—	520	138	335	235	1300
$[VF_5O]^{3-}$	943	383	525	317	—	—	—	525	139	342	237	1300
$[NbCl_6Br]^-$	210	310	365	181	285	120	134	352	161	153	75	1301
$[TaCl_6Br]^-$	204	318	368	183	300	(120)	168	325	151	143	73	1301
TcF_5O	937	702	598	329	624	199	289	729	346	217	135	1302
$[TaBr_5Cl]^-$	323	613	187	110	180	(73)	96	214	123	144	76	1031
$[CrF_5O]^-$	993	231	530	302	577	—	—	586	346	277	—	1174
$[MoCl_5O]^{2-}$	998	318	331	168	336	159	164	321	233	137	147	1303
$[MoF_5O]^-$	973	662	492	300	580	—	—	580	324	252	—	1304

$[\text{WF}_5\text{O}]^-$	987	686	507	286	594	—	—	608	329	242	—	1304
WF_5Cl	407	744	703	257	644	182	377	661	290	227	307	1305
ReF_5O	990	739	643	309	652	234	334	713	260	365	125	1306
$[\text{RuCl}_5\text{N}]^-$	1048	284	318	192	307	168	184	337	233	154	174	1303
$[\text{RuBr}_5\text{N}]^-$	1046	201	207	156	181	136	147	204	257	110	144	1303
OsF_5O	963	716	644	281	644	210	332	701	263	367	164	1306, 1307
$[\text{OsF}_5\text{Cl}]^-$	381/374	654	614	227	635	—	253	627	256	265	170	1308
$[\text{OsCl}_5\text{N}]^2-$	1084	324	348	189	334	169	181	336	264	146	172	1303
$[\text{OsBr}_5\text{N}]^2-$	1085	192	198	156	172	136	149	234	217	115	144	1303
$[\text{UF}_5\text{O}]^-$	820	593	602	182	445	(161)	(283)	480	248	209	201	1309
$[\text{MoCl}_4\text{OBr}]^2-$	235	964	301	149	288	—	—	320	229	92	162	1310
$[\text{WCl}_4\text{OBr}]^2-$	233	960	326	149	—	—	187	298	230	92	162	1310

^a For XY_5Z , W is regarded as Y *trans* to Z.

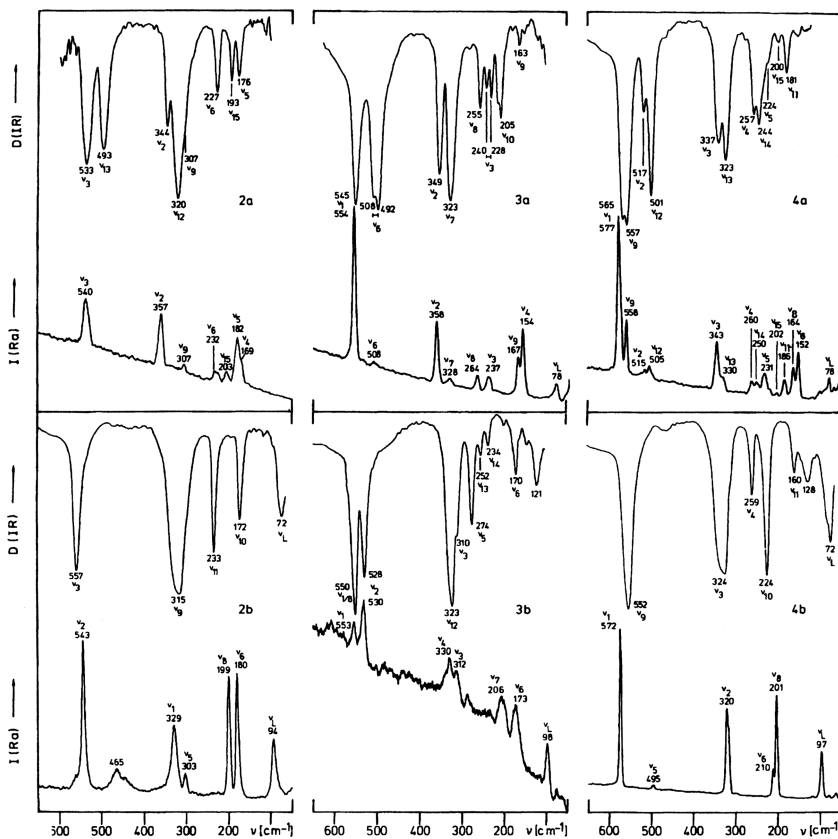


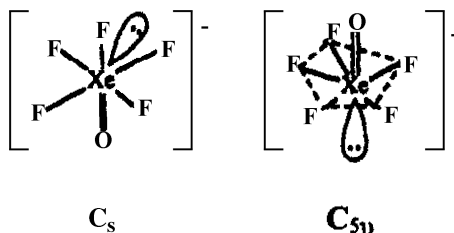
Fig. 2.31. IR and Raman spectra of $\text{Cs}_2[\text{OsF}_n\text{Cl}_{6-n}]^{2-}$ ($n=2-4$) (where $a = \text{cis}$, $b = \text{trans}$). Exciting lines used are 488 nm (2a, 2b, and 3a), 647.1 nm (3b), and 514.5 nm (4a and 4b) [1313].

discrepancies occur because bands are overlapped and IR/Raman-active fundamentals are weak in some cases. Preetz and coworkers [1323] reviewed the results of their extensive investigations on preparation and spectroscopic properties of mixed octahedral complexes and clusters. The Raman spectrum of crystalline $\text{Rb}_2[\text{TeBr}_{3.5}\text{Cl}_{2.5}]$ shows it to be a 1:1 mixture of $\text{Rb}_2[\text{TeBr}_3\text{Cl}_3]$ and $\text{Rb}_2[\text{TeBr}_4\text{Cl}_2]$ [1324].

The Raman spectra of *cis*- $[\text{MF}_4\text{O}_2]^-$ ions ($\text{M} = \text{Tc}$ [1325] and Re [1326]) have been assigned based on the basis of C_{2v} symmetry.

2.8.3. Pseudo-Pentagonal-Bipyramidal ZXY_5

Previously, the Raman spectrum of the $[\text{OXeF}_5]^-$ ion was assigned on the basis of an octahedral structure that is distorted to C_s symmetry because of the presence of a sterically active lone-pair on the octahedral faces adjacent to the axial fluorine [1327,1328]:



Later studies [1329] found that the vibrational spectra of the solid salts of the $[OXeF_5]^-$ ion agree with that predicted from the C_{5v} model in which the oxygen and the sterically active lone-pair occupy the two axial positions of a pseudopentagonal-bipyramid. The $[OIF_5]^{2-}$ ion is isoelectronic with $[OXeF_5]^-$, and its vibrational spectra were also assigned on the basis of the same C_{5v} symmetry [1330]. These C_{5v} structures are derived from the pentagonal-planar XY_5 molecules such as the XeF_5^- ion (Sec. 2.7.3) by replacing one of the axial lone-pair electrons by an oxygen atom.

2.9. XY₇ AND XY₈ MOLECULES

The XY₇-type molecules are very rare. Both IF₇ and ReF₇ are known to be pentagonal-bipyramidal (D_{5h}), and their vibrational spectra have been assigned completely, as shown in Table 2.9. The A'_1 , E'_1 , and E'_2 vibrations are Raman-active, and the A'_2 and E'_1 vibrations are infrared-active. According to Eysel and Seppelt [1334], IF₇ undergoes minor dynamic distortions from D_{5h} symmetry that cause violation of the D_{5h} selection rules for combination bands but not for the fundamentals. Normal coordinate analysis [1334] shows that the axial bonds are definitely stronger and shorter than the equatorial ones. Table 2.9 also lists the frequencies and assignments of the $[UO_2F_5]^{2-}$ ions of D_{5h} symmetry [1336]. The vibrational spectra of the $[IF_6O]^-$ [1330, 1332, 1337] and $[TeF_6O]^{2-}$ [1338] ions in which the axial positions of a pentagonal bipyramidal structure are occupied by a fluorine and an oxygen atom (C_{5v} symmetry) have been assigned.

The XY₈-type molecule may take the form of (I) a cube (O_h), (II) an archimedean antiprism (D_{4d}), (III) a dodecahedron (D_{2d}), or (IV) a face-centered trigonal prism (C_{2v}). Although XY₈ molecules are rare, X-ray analysis indicates that $[TaF_8]^{3-}$ and $[CrO_8]^{3-}$ ions take structures II and III, respectively [1339, 1340]. The infrared and Raman spectra of crystalline $Na_3[TaF_8]$ are in accord with structure II, proposed by X-ray analysis [1341]. However, the vibrational spectra of the $[IF_8]^-$ and $[TeF_8]^{2-}$ ions support the archimedean antiprism structures [1332] shown below:

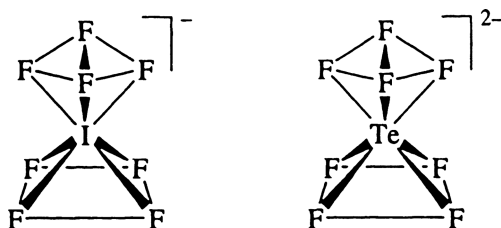


TABLE 2.9. Vibrational Frequencies^a of XY₇ and XY₅Z₂ Molecules (cm⁻¹)

D _{5h}	ReF ₇ [1331]	TeF ₇ ⁻ [1332, 1333]	IF ₇ [1332, 1334]	SbF ₇ ²⁻ [1335]	BeF ₇ ²⁻ [1335]	UF ₅ O ₂ ²⁻ [1336]	Assignment ^{b, c}
ν ₁ (A' ₁)	736	597	675	596	545	(668)	ν _s (MF _a)
ν ₂ (A' ₁)	645	640	629	512	510	816	ν _s (MF _a)
ν ₃ (A'' ₂)	703	695	746	627	—	873	ν _a (MF _a)
ν ₄ (A'' ₂)	299	332	363	—	—	380	δ (F _e MF _a)
ν ₅ (E' ₁)	703	625	672	574	520	740	ν _d (MF _a)
ν ₆ (E' ₁)	353	384	425	335	284	425	δ _d (F _e MF _e)
ν ₇ (E' ₁)	217	—	257	—	—	240	δ _d (F _a MF _a)
ν ₈ (E' ₁)	597	299	308	289	260	—	δ _d (F _a MF _a)
ν ₉ (E ₂)	489	458	509	490	460	—	ν _d (MF _e)
ν ₁₀ (E' ₂)	352	326	342	392	330	—	δ _d (F _e MF _e)

^a In these molecules ν₁₁ (E'₂) is inactive.
^b F_a and F_e denote the axial and equatorial F atoms, respectively.
^c For UF₅ O₂²⁻, F_a corresponds to the axial O atom.

For normal coordinate analyses of a cubic and an Archimedean antiprism XY₈ molecule, see Refs. 1342 and 1343, respectively.

2.10. X₂Y₄ AND X₂Y₆ MOLECULES

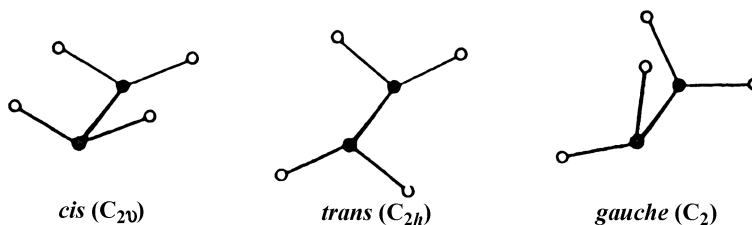
2.10.1. X₂Y₄ Molecules

Depending upon the twisting angle (τ) between the two XY₂ planes, the symmetry of the Y₂X–XY₂ molecule may be **D**_{2h} ($\tau = 0^\circ$, planar), **D**_{2d} ($\tau = 90^\circ$, staggered), or **D**₂ ($0^\circ < \tau < 90^\circ$, intermediate).

The **D**_{2h} structure may be confirmed if the infrared and Raman mutual exclusion rule holds. The **D**_{2d} and **D**₂ structures can be distinguished by comparing the number of fundamentals with that predicted for each structure: 8 for **D**₂ and 5 for **D**_{2d} in the infrared, and 12 for **D**₂ and 9 for **D**_{2d} in the Raman.

B₂F₄ [1344] and B₂Cl₄ [1345] are staggered in the gaseous and liquid phases and planar in the solid state, whereas B₂Br₄ [1346] is staggered in all phases. Apparently, steric hindrance plays a main role in determining the conformation. Both B₂F₄ and B₂Cl₄ are also staggered in Ar matrices [1347]. The vibrational spectra of gaseous and crystalline N₂O₄ have been assigned on the basis of **D**_{2h} symmetry [1348,1349]. In a N₂ matrix, N₂O₄ is a mixture of the **D**_{2h}, **D**_{2d}, and ONO–NO₂ isomers [1350]. The vibrational spectra of the oxalato ion (C₂O₄²⁻) have been assigned on the basis of **D**_{2d}, **D**_{2h}, and **D**₂ symmetry [1351~1353].

Molecules like N₂H₄ and N₂F₄ take the *trans* (**C**_{2h}), *gauche* (**C**₂), or *cis* (**C**_{2v}) structure depending on the angle of internal rotation. Evidently, the presence of lone-pair electrons on the X atom is responsible for the deviation of the X–XY₂ plane from the planarity. Most of these compounds exist as the *trans* or *gauche* isomer or as a mixture of both. The *trans* isomer shows 6, whereas the *gauche* isomer shows 12 fundamentals in the infrared.



In the gaseous, liquid, and solid states, N₂F₄ is a mixture of the *trans* and *gauche* isomers, and complete vibrational assignments have been made on each isomer [1354]. N₂H₄ is pure *gauche* in all physical states [1355], and its IR spectrum in Ar matrices has been assigned [1356]. The IR spectrum of P₂H₄ in the gaseous state has been assigned on the basis of the *gauche* structure. [1357]. However, it is *trans* in the solid state [1358]. The *trans* structure has been deduced from the vibrational spectra of P₂F₄ (all states) [1359], P₂Cl₄ (all states) [1360], and P₂I₄ (solid and solution) [1361].

The dithionite ion, $[\text{S}_2\text{O}_4]^{2-}$, assumes a structure of C_{2h} symmetry in both solution and the solid state, and its IR/Raman spectra have been assigned [1362].

X_2Y_4 -type molecules also take a planar-cyclic structure of D_{2h} symmetry as seen in dimeric metal halides (Sec. 2.2). Then, the 12 normal vibrations are grouped into $3A_g(\text{R}) + 2B_{1u}(\text{IR}) + B_{2g}(\text{R}) + 2B_{2u}(\text{IR}) + 2B_{3g}(\text{R}) + 2B_{3u}(\text{IR})$. Somer et al. [1363] assigned the six IR-active vibrations of the $[\text{M}_2\text{X}_4]^{6-}$ ions ($\text{M} = \text{Al}, \text{Ga}; \text{X} = \text{P}, \text{As}$). The structure of the $[\text{B}_2\text{S}_4]^{2-}$ ion is similar, and its infrared spectrum is assigned empirically [1364]. Durig and co-workers reviewed the vibrational spectra of X_2Y_4 -type molecules [1365].

2.10.2. Bridged X_2Y_6 Molecules (D_{2h})

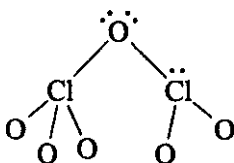
Figure 2.32 illustrates the 18 normal modes of vibration [1366] and band assignments for nonplanar bridging X_2Y_6 -type molecules. The A_g , B_{1g} , B_{2g} , and B_{3g} vibrations are Raman-active, whereas the B_{1u} , B_{2u} , and B_{3u} vibrations are infrared-active. Table 2.10a lists the vibrational frequencies of molecules belonging to this type. In most compounds, the ν_1 , ν_8 , ν_{11} , and ν_{16} vibrations are largely due to the terminal XY_2 stretching motions, and their frequencies are higher than those of ν_2 , ν_6 , ν_{13} , and ν_{17} , which are due mainly to the vibrations of the bridging $\text{X}_2\text{Y}'_2$ group. As shown in Table 2.10a, the ratios of the average terminal and bridging frequencies range from 0.74 to 0.61. Normal coordinate analyses of these compounds have been made by several investigators [1372,1375,1378,1379].

It should be noted that In_2Cl_6 and In_2Br_6 are polymeric, and In_2I_6 is dimeric in the crystalline state, as shown by their spectral [1380].

Table 2.10b lists eight stretching frequencies of planar X_2Y_6 ions and molecules. In the $[\text{M}_2\text{X}_6]^{2-}$ ($\text{M} = \text{Pd}, \text{Pt}; \text{X} = \text{Cl}, \text{Br}, \text{I}$) series, Goggin [1381] showed that the distinction between terminal and bridging vibrations is meaningless except for $\text{X} = \text{Cl}$, since these vibrations couple so strongly with each other. According to Forneris et al. [1383], the terminal and bridging stretching force constants of Au_2Cl_6 are 2.22 and 1.15 $\text{mdyn}/\text{\AA}$, respectively, and those of I_2Cl_6 are 1.70 and 0.40 $\text{mdyn}/\text{\AA}$, respectively (modified UBF). On the other hand, Adams and Churchill [1372] report values of 2.419 and 1.482 $\text{mdyn}/\text{\AA}$, respectively, for the terminal and bridging force constants of Au_2Cl_6 (GVF).

2.10.3. Singly Bridged X_2Y_6 Molecules

In the solid state, dichlorine hexaoxide, Cl_2O_6 , exists as an ionic salt, $[\text{ClO}_2]^+[\text{ClO}_4]^-$, and the vibrational frequencies of these ions have been listed in Tables 2.2b and 2.6e, respectively. In the gaseous state, Cl_2O_6 takes a singly bridged structure of C_s symmetry and its IR spectrum in inert gas matrices has been assigned [1384].



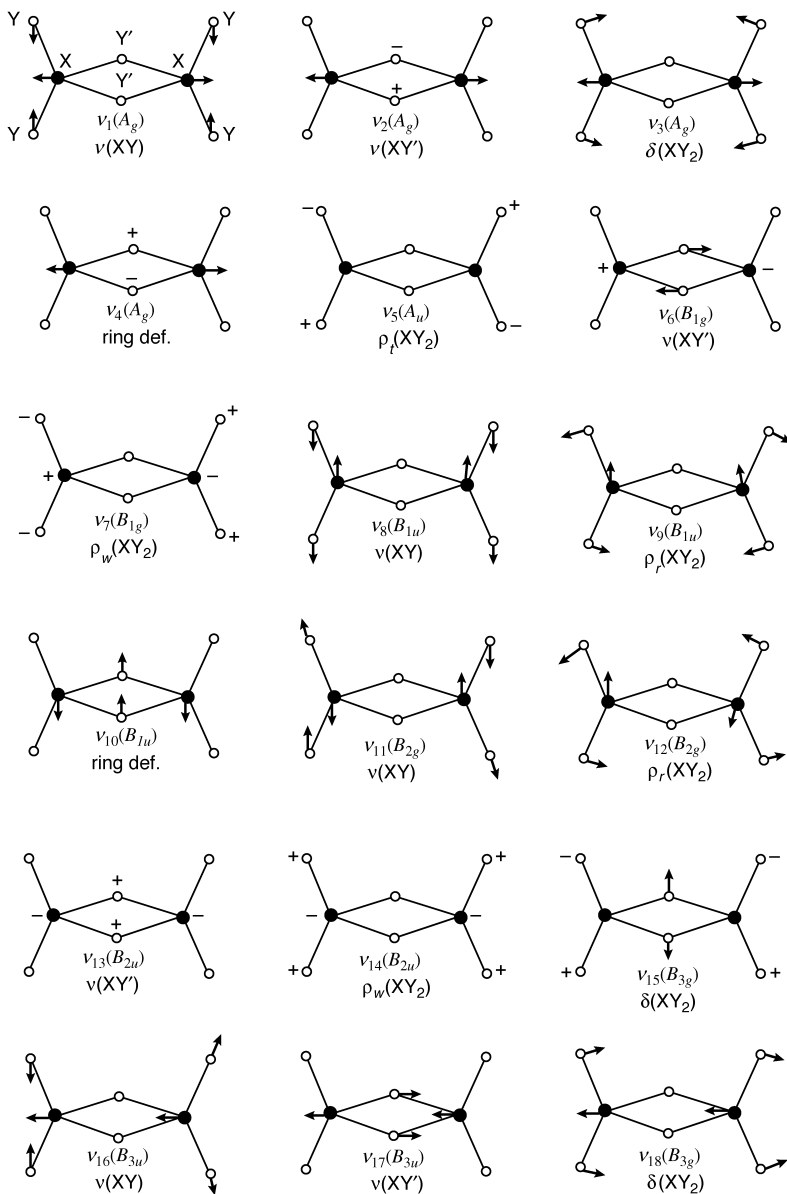


Fig. 2.32. Normal modes of vibration of bridged X_2Y_6 molecules [1366].

2.10.4. Ethane-Type X_2Y_6 Molecules (D_{3d})

The ethane-type X_2Y_6 molecule may be staggered (D_{3d}), eclipsed (D_{3h}), or *gauche* (D_3). Figure 2.33 shows the 12 normal modes of vibration of the staggered X_2Y_6

TABLE 2.10a. Vibrational Frequencies of Nonplanar Bridging X_2Y_6 Molecules (cm^{-1})

	B_2H_6	Al_2H_6	Al_2F_6	Al_2Cl_6	Al_2Br_6	Al_2I_6	Ga_2H_6	Ga_2Cl_6	Ga_2Br_6	Ga_2I_6	In_2I_6	Fe_2Cl_6
A_g	2526	2059	—	523	410	348	2082	413	291	229	187	422
	2096	1652	—	342	212	148	1571	318	204	143	134	305
	1187	816	—	219	142	95	792	167	119	85	69	150
	788	398	—	107	70	56	238	100	64	50	40	78
A_u	833	451	—	—	—	—	473	—	—	—	—	—
B_{1g}	1756	1492	—	284	354	—	1321	243	241	195	114	225
	860	532	—	166	82	82	374	125	85	64	55	112
B_{1u}	2613	2062	995	622	500	415	2075	464	347	273	228	467
	951	997	340	174	—	—	872	—	102	—	—	118
	367	249	—	—	—	—	239	—	—	—	—	24
B_{2g}	2597	2055	—	612	491	405	2068	462	339	265	232	450
	918	497	—	121	116	63	498	117	74	55	49	82
B_{2u}	1924	1350	600	422	341	291	1249	318	232	189	158	328
	974	694	—	135	90	64	693	114	82	61	49	99
B_{3g}	1023	844	—	—	—	54	821	215	158	68	44	80
B_{3u}	2518	2051	805	485	373	320	2074	390	269	213	178	406
	1615	1603	575	320	198	140	1400	282	188	134	125	280
	1175	766	300	144	110	81	729	156	90	77	59	116
ν_t/ν_b	0.72	0.74	—	0.61	0.62	—	0.67	0.67	0.69	0.67	0.65	0.65
Ref.	1367	1367	1370	1371	1372	1372	1367	1372	1372	1372	1372	618
	1368						1373	1375	1376	1376		1377
	1369						1374					1378

TABLE 2.10b. Vibrational Frequencies^a of Planar Bridging X_2Y_6 Molecules (cm^{-1})

	$[\text{Pd}_2\text{Cl}_6]^{2-}$	$[\text{Pd}_2\text{Br}_6]^{2-}$	$[\text{Pd}_2\text{I}_6]^{2-}$	$[\text{Pt}_2\text{Cl}_6]^{2-}$	$[\text{Pt}_2\text{Br}_6]^{2-}$	$[\text{Pt}_2\text{I}_6]^{2-}$	I_2Cl_6	Au_2Cl_6
A_g								
ν_1, ν (XY_t)	346	262	219	349	241	196	344	379
ν_2, ν (XY_b)	302	194	143	316	211	160	198	328
B_{1g}								
ν_6, ν (XY_t)	328	253	—	333	238	196	314	366
ν_7, ν (XY_b)	265	173	130	294	193	145	142	289
B_{2u}								
ν_{12}, ν (XY_t)	335	257	218	330	236	196	327	364
ν_{13}, ν (XY_b)	262	178	—	300	192	147	170	309
B_{3u}								
ν_{16}, ν (XY_t)	343	264	218	341	239	196	340	374
ν_{17}, ν (XY_b)	297	192	140	312	210	157	205	309
Ref.	1381	1381	1381	1381	1381	1381	1382	1382
	1382							1383 ^a

^a XY_t and XY_b denote terminal and bridging XY stretching modes, respectively. When these two modes couple strongly, distinction between them is not clear (see Ref. 1381).

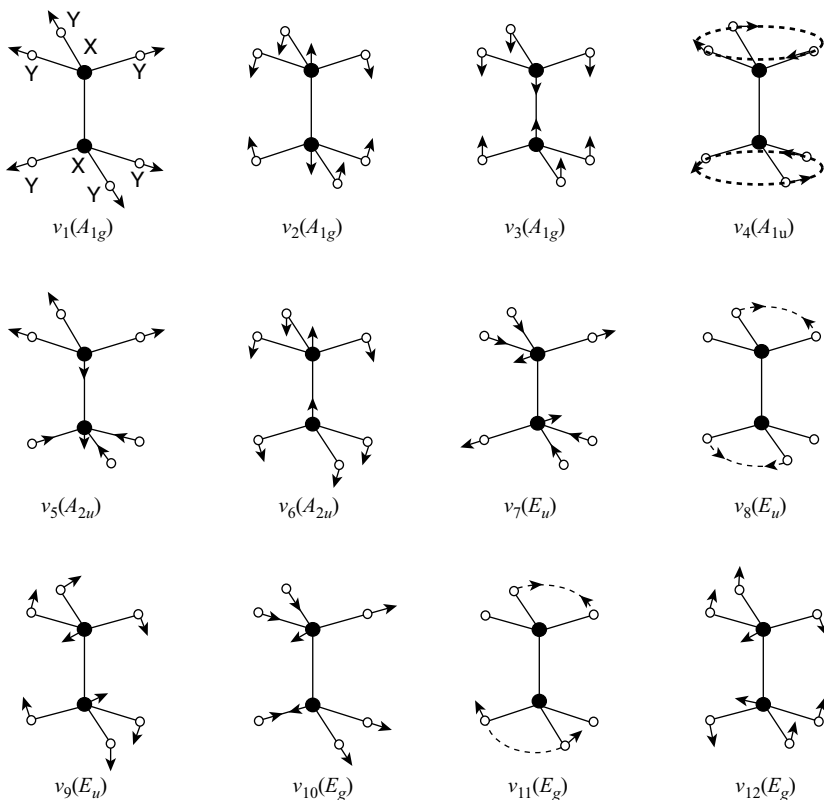


Fig. 2.33. Normal modes of vibration of ethane-type X_2Y_6 molecules.

molecule. The A_{1g} and E_g vibrations are Raman-active, and the A_{2u} and E_u vibrations are infrared-active. Table 2.10c lists the observed frequencies and band assignments on the basis of D_{3d} symmetry. It should be noted that neutral Ga_2X_6 (X: a halogen) molecules take the bridging D_{2h} structure (Table 2.10a), whereas $[\text{Ga}_2\text{X}_6]^{2-}$ ions assume the ethane-like D_{3d} structure.

The structure of Si_2Cl_6 has been controversial; Griffiths [1398] prefers the D_{3h} or D_{3h}' structure* for liquid Si_2Cl_6 , whereas Ozin [1399] favors the D_{3d} model for all phases. The D_{3h} and D_{3d} selection rules are similar except that the E_u modes of D_{3d} that are infrared-active become both infrared- and Raman-active (E') in D_{3h} . The SiSi stretching mode was assigned at 354 cm^{-1} by Griffiths and at 627 cm^{-1} by Ozin. According to Höfler et al., [1397] the SiSi stretching force constant increases in the order $\text{Si}_2\text{H}_6 < \text{Si}_2\text{H}_6 < \text{Si}_2\text{Br}_6 < \text{Si}_2\text{Cl}_6$.

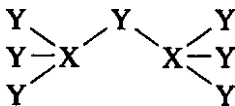
Takeuchi and coworkers [1395,1396] measured the IR and Raman spectra of gaseous Si_2F_6 in the low-frequency region, and noted that the symmetry selection rules of D_{3d} point group are not strictly obeyed; the ν_8 and ν_9 modes, which should be IR-active only under D_{3d} symmetry were observed very weakly at 308 and 104 cm^{-1} , respectively, in Raman spectra. They, therefore, proposed G_{36} (free internal rotation) dynamic group [1400] or its subgroup, D_{3h}' (internal rotation with low or zero barrier*), which allows these vibrations to appear in both IR and Raman spectra. They also observed the first overtone of the torsional mode [ν_4 (A_{1u}), inactive] at $\sim 78\text{ cm}^{-1}$ in the Raman spectrum. The barrier of the internal rotation was estimated to be $510\text{--}550\text{ cm}^{-1}$ on the basis of the torsional frequency (38 cm^{-1}).

Normal coordinate analyses were carried out on Si_2Cl_6 [1399] and $[\text{Ga}_2\text{Cl}_6]^{2-}$ [1394]. The stretching frequencies of the $[\text{In}_2\text{X}_6]^{2-}$ ions ($\text{X}=\text{Cl}, \text{Br}, \text{I}$) (1401), and vibrational spectra of the adducts such as $\text{H}_3\text{Si}-\text{GeD}_3$ [1402] and $\text{X}_3\text{P}-\text{BY}_3$ ($\text{X}=\text{Cl}, \text{Br}, \text{I}; \text{Y}=\text{Br}, \text{I}$) [1403] have been reported.

2.11. X_2Y_7 , X_2Y_8 , X_2Y_9 , AND X_2Y_{10} MOLECULES

2.11.1. X_2Y_7 Molecules

The X_2Y_7 ($\text{XY}_3-\text{Y}-\text{XY}_3$) type molecule belongs to the C_s , C_{2v} , or C_1 point group, depending on the relative orientation of the two XY_3 groups:



While 17 vibrations are infrared-active in C_{2v} , all 21 vibrations are infrared-active in C_s and C_1 symmetry. The 21 normal vibrations of the X_2Y_7 molecule may be

* When the rotation around the Si—Si bond occurs, the horizontal symmetry plane is lost, and the molecule belongs to D_{3h}' point group.

Molecule (D_{3d})														
C_2H_6	Si_2H_6	Ge_2H_6	$N_2H_6^{2+}$	$P_2O_6^{4-}$	$P_2S_6^{4-}$	$P_2Se_6^{4-}$	$S_2O_6^{2-}$	$Ga_2Cl_6^{2-}$	$Ga_2Br_6^{2-}$	$Ga_2I_6^{2-}$	Si_2F_6	Si_2Cl_6	Si_2Br_6	Si_2I_6
A_{1g}	2899 (1375)	2152 (2070)	2650 1524 1027	1062 670 275	557 197 374	452 116 217	1102 710 293	375 106 233	316 70 164	285 42, 48 118	915 218 541.5	351 127 624	223 80 562	154 (51) 510
A_{1u}	275	—	144	455	—	—	—	—	—	—	(3B)	—	—	—
A_{2u}	2954 1379	2154 844	2078 755	2600 1485	942 562	444 302	1000 577	302 151	201 110	155 88	823.8 406	460 241	329 168	255 116
E_u	2994 1486 821	2179 940 379	2114 898 407	2739 1613 1096	1085 494 200	585/606 243 87	478 173 132	1240 516 204	237, 228 92 64	200 74 (50)	992.3 308 104	603 178 74	479 114 50	388 81 (31)
E_g	2963 1460 (1155)	2155 929 625	2150 875 417	2745 1599 1105	1168 508 323	578 259 169	474 213 150	1216 556 320	314 116 146	228 84 102	979 340 203	590 211 132	473 139 89	398 94 (53)
Ref.	1385	1386 1387	1388	1389	1390	1391	1392	1393	1394	1394	1395 1396	1397	1397	1397

TABLE 2.11. YXY Bridging Frequencies of X_2Y_7 Molecules (cm^{-1})

Compound	ν_a (YX_2)	ν_s (YX_2)	δ (YX_2)	Ref.
$\text{Na}_4[\text{P}_2\text{O}_7]$	915	730	94	1404,1405
$\text{Na}_4[\text{As}_2\text{O}_7]$	735	550	245	1406
$\text{Na}_2[\text{S}_2\text{O}_7]$	825	725	182 or 116	1407
$\text{Na}_2[\text{Se}_2\text{O}_7]$	738	542	88	1404
$\text{Na}_4[\text{V}_2\text{O}_7]$	710	533	200	1407
$\text{Na}_2[\text{Cr}_2\text{O}_7]$	758	555	89	1404
Re_2O_7	868	480	50	1408
Cl_2O_7	785	700	(165)	1409
$[\text{Ga}_2\text{Cl}_7]^-$	286	276	—	1410
$[\text{Ga}_2\text{Br}_7]^-$	222	195	—	1410
$[\text{Si}_2\text{O}_7]^{6-}$	1014	669	415	1411
$[\text{Ge}_2\text{O}_7]^{6-}$	825	525	—	1411
				1412,1413

classified into in-phase and out-of-phase coupling motions of terminal XY_3 group vibrations and the skeletal vibrations of the XYX bridge. Table 2.11 lists the observed frequencies of these bridging vibrations.

On the basis of normal coordinate analyses, Brown and Ross [1407] have made complete assignments of the vibrational spectra of the $\text{S}_2\text{O}_7^{2-}$, $\text{Se}_2\text{O}_7^{2-}$, $\text{V}_2\text{O}_7^{4-}$, and $\text{Cr}_2\text{O}_7^{2-}$ ions (C_{2v} symmetry).

According to Wing and Callahan [1414], the MOM bridge angle is always larger than 115° , and $\nu_a(\text{MO})$ is at least 215 cm^{-1} higher than $\nu_s(\text{MO})$. This separation increases as the MOM angle increases. In a series of M_2^{2+} (V_2O_7) where M is Mg^{2+} , Ba^{2+} , Ni^{2+} , Co^{2+} , and so on, a linear relationship has been found between the $\text{V}-\text{O}-\text{V}$ angle (α) and the Δ value defined below [1418]:

$$\Delta = -38.79 + 0.39\alpha$$

where

$$\Delta = [(\nu_a - \nu_s)(\nu_a + \nu_s)] \times 100$$

The molecule Re_2O_7 is monomeric in the gaseous and liquid states and polymeric in the solid state. Beattie and Ozin [1416] assigned the spectra of gaseous Re_2O_7 on the basis of C_{2v} symmetry. Vibrational analysis of Cl_2O_7 has been made by assuming C_2 [1417] or C_{2v} [1409] symmetry. On the assumption of a linear OPO bridge, the vibrational assignments of divalent metal pyrophosphates ($\text{M}_2\text{P}_2\text{O}_7$) have been made in terms of D_{3h} or D_{3d} symmetry [1418,1419]. The vibrational spectra of the $\text{Si}_2\text{O}_7^{6-}$ and $\text{Ge}_2\text{O}_7^{6-}$ ions have also been assigned on the basis of D_{3d} symmetry [1411]. In contrast to the $[\text{Ga}_2\text{Cl}_7]^-$ ion, the $\text{Ga}-\text{I}-\text{Ga}$ bond of the $[\text{Ga}_2\text{I}_7]^-$ ion in the molten and crystalline phases is linear [1420].

In $[\text{Mn}_2(\text{Cr}_2\text{O}_7)_2(\text{bipy})_4]$ (bipy: 2,2'-bipyridine), the $\text{Cr}_2\text{O}_7^{2-}$ ion forms a bridge between two $\text{Mn}(\text{bipy})_2$ moieties via two terminal oxygen atoms. Since two such

bridges are formed, each Mn(bipy)₂ moiety is six-coordinate. The Raman spectrum exhibits the ν_s and δ vibrations of the Cr—O—Cr bridge at 527 and 230 cm⁻¹, respectively [1421]. The crystal structure of Mn₂As₂O₇·2H₂O has been determined, and its IR and Raman spectra have been reported by Stock et al. [1422]. The IR/Raman spectra of X₂HSi—SiHX₂ (X = F, Cl) have been assigned [1423].

2.11.2. X₂Y₈ Molecules

The symmetry of the X₂Y₈ (Y₃X—Y—Y—XY₃) molecule may be low enough to activate all 24 normal vibrations in both infrared and Raman spectra. Thus far, the YYYX bridging frequencies have been assigned at 988 [ν_a (YYYX)], 784 [ν_s (YYYX)], 890 [ν (YY)], and 397 and 328 [δ (YYYX)] for the [P₂O₈]⁴⁻ ion, and at 1062, 834, 854, and 328 and 236 cm⁻¹, respectively, for the [S₂O₈]⁴⁻ ion [1424].

In another type of X₂Y₈ ion, short, multiple M—M (metal–metal) bonds link two MX₄ units so that the overall symmetry becomes **D**_{4h} (eclipsed form) 1425.

Then, the 24 normal vibrations are grouped into

$$3A_{1g} + A_{1u} + 2A_{2u} + 2B_{1g} + B_{1u} + B_{2g} + 2B_{2u} + 3E_g + 3E_u$$

and A_{1g} , B_{1g} , B_{2g} , and E_g are Raman-active and A_{2u} and E_u are IR-active whereas A_{1u} , B_{1u} , and B_{2u} are inactive

In Raman spectra, these metal–metal bonded compounds exhibit strong ν (M—M) vibrations in the low-frequency region because displacements of heavy metal ions that are linked by strong, covalent bonds produce large changes in polarizability. Furthermore, these compounds, under resonance conditions, exhibit a series of overtones of ν (M—M), ν (M—X) (X: a halogen) and combination bands from which one can calculate frequencies corrected for anharmonicity (ω_e) and anharmonicity constants (X_{11}) (Sec. 1.23). Thus, RR spectra of the M₂X₈-type ions were studied extensively: [Mo₂Cl₈]⁴⁻ [1426,1427], [Re₂F₈]²⁻ [1428,1429], [Re₂Cl₈]²⁻ [1430,1429], [Re₂Br₈]²⁻ [1430,1429], [Re₂I₈]²⁻ [1431], [Te₂Cl₈]²⁻ [1432], [Te₂Cl₈]³⁻ [1432], and [Te₂Br₈]²⁻ [1432]. As an example, Fig. 2.34 shows the RR spectra of the [Re₂F₈]²⁻ ion obtained by Peters and Preetz [1428]. This ion exhibits an electronic absorption near 558 nm that is due to a transition from the $(\sigma)^2(\pi)^4(\delta)^2$ to the $(\sigma)^2(\pi)^4(\delta)(\delta^*)$ state. Thus, the RR spectrum was measured using the 530.9 nm line of a Kr ion laser. It is seen that the ν (Re—Re) at 320 cm⁻¹ is markedly enhanced, and a series of overtones ($n\nu_1$, up to $n=6$) and combination bands [ν_2 is the ν (Re—F) and the 182 cm⁻¹ band is a skeletal bending] are observed. Using these data, the ω_e and X_{11} values were calculated to be 319.6 ± 0.6 cm⁻¹ and 0.45 ± 0.05 cm⁻¹, respectively. In the [Re₂X₈]²⁻ series, the ν (Re—Re) frequency shifts somewhat irregularly when the halogen (X) is changed; F (320 cm⁻¹), Cl (272 cm⁻¹), Br (277 cm⁻¹), and I (258 cm⁻¹). It is interesting to note that, under extremely high pressure (15 GPa), the ν (Re—Re) of the [Re₂Cl₈]²⁻ ion is shifted to 357 cm⁻¹ owing to shortening of the Re—Re bond [1433].

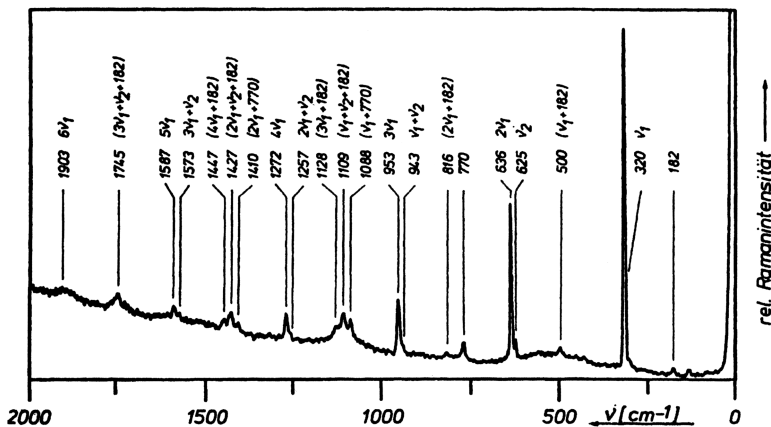


Fig. 2.34. Resonance Raman spectrum of $[(n\text{-C}_4\text{H}_9)_4\text{N}]_2[\text{Re}_2\text{F}_8]\cdot 4\text{H}_2\text{O}$ (530.9 nm excitation) [1428].

The $(n\text{-Bu}_4\text{N})^+$ salts of the $[\text{Os}_2\text{Y}_8]^{2-}$ ions ($\text{Y} = \text{Cl}, \text{Br}, \text{I}$) take a sterically favored staggered conformation of D_{4d} symmetry. Then, their normal vibrations are classified as

$$3A_1 + B_1 + 2B_2 + 3E_1 + 3E_2 + 3E_3$$

where A_1 , E_2 , and E_3 are Raman-active and B_2 and E_1 are IR-active. In this case, the $\nu(\text{Os}-\text{Os})$ frequencies are nearly constant, and observed at 285, 287, and 270 cm^{-1} for $\text{X} = \text{Cl}$, Br , and I , respectively [1434]. Normal coordinate calculations on X_2Y_8 molecules were carried out by Preetz et al. [1435].

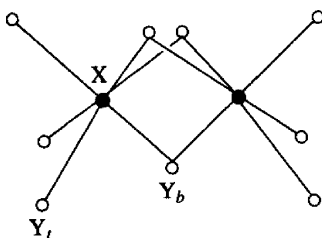
Finally, it is possible to measure the $\nu(\text{M}-\text{M})$ in the electronic excited state by using time-resolved resonance Raman (TR^3) spectroscopy (Ref. [31], Chapter 1). For example, the absorption maximum of the $\delta \rightarrow \delta^*$ transition of the $[\text{Re}_2\text{Cl}_8]^{2-}$ ion in CH_2Cl_2 is at 685 nm. Dallinger [1436] and co-workers [1437] saturated the $\delta\delta^*$ ($^1A_{2u}$) state (lifetime, $\sim 75\text{ ns}$) by using a pump laser at 640 nm (5-ns pulses). The $\nu(\text{Re}-\text{Re})$ of this electronic excited state was probed by using delayed 416 nm excitation. Three bands observed at 366, 204, and 138 cm^{-1} were assigned to $\nu(\text{Re}-\text{Cl})$, $\nu(\text{Re}-\text{Re})$, and $\delta(\text{Cl}-\text{Re}-\text{Re})$, respectively. This result indicates that $\nu(\text{Re}-\text{Re})$ decreases in going from the ground (δ^2 , 1A_g , 272 cm^{-1}) to the excited state ($\delta\delta^*$, $^1A_{2u}$, 204 cm^{-1}) because an electron is promoted from a bonding (δ) to an antibonding (δ^*) orbital. In other cases, the $\nu(\text{M}-\text{M})$ band is shifted to a higher frequency by electronic excitation because an electron is promoted from an antibonding to a bonding orbital. Examples of the latter are discussed in Chapter 1 of Part B.

2.11.3. X_2Y_9 Molecules

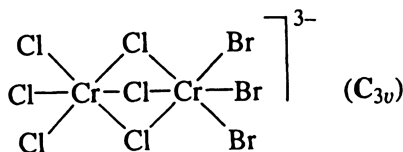
The X_2Y_9 molecule shown below belongs to the point group D_{3h} , and its 27 normal vibrations are classified into $4A'_1(\text{R})$, $A'_2(1a)$, $A'_2(1a)$, $3A'_2(\text{IR})$, $5E'(\text{IR}, \text{R})$, and $4E''(\text{R})$.

TABLE 2.12. Terminal and Bridging Frequencies of X_2Y_9 -Type Ions (cm^{-1})

Ion	$\text{Ti}_2\text{Cl}_9^{3-}$	$\text{Cr}_2\text{Cl}_9^{3-}$	$\text{W}_2\text{Cl}_9^{3-}$	Tc_2Br_9^-	$\text{Ir}_2\text{Cl}_9^{3-}$	$\text{Ir}_2\text{Br}_9^{3-}$	Pt_2Br_9^-
Terminal stretch							
$\nu_1, A'_1 (\text{R})$	417	375	332	266	340	232	253
$\nu_7, A''_2 (\text{IR})$	431	360	313	367	318	220	249
$\nu_{10}, E' (\text{IR, R})$	378	342	281	245	317	215	(219)
$\nu_{15}, E'' (\text{R})$	399 390	320	294	—	198	—	—
Bridging stretch							
$\nu_2, A'_1 (\text{R})$	321	280	257	201	280	211	211
$\nu_8, A''_2 (\text{IR})$	270	261	—	182	287	186	183
$\nu_{11}, E' (\text{IR, R})$	236	234	209	173	266	189	190
$\nu_{18}, E'' (\text{R})$	305	222	226	—	247	—	—
Ref.	1438	1439 1440	1439	1441	1442	1442	1443

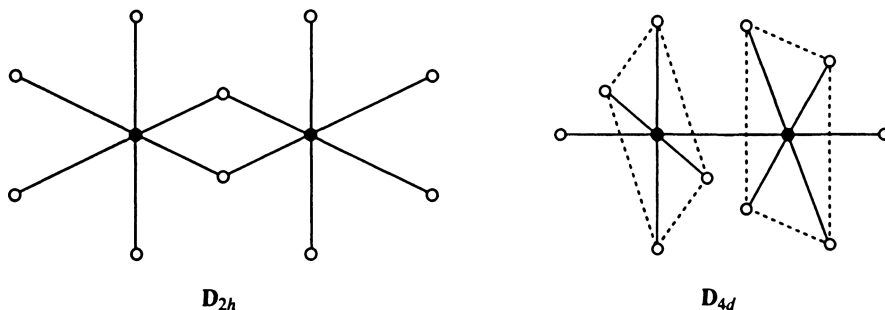


Two XY_t stretching (A'_2 and E') and two XY_b stretching (A''_2 and E') vibrations are infrared-active. Similarly, two XY_t stretching (A'_1 and E'') and two XY_b stretching (A'_1 and E'') are Raman-active. Table 2.12 lists observed frequencies of these terminal and bridging stretching vibrations. Normal coordinate treatments have been made on this type of compound by several groups of investigators [1439–1444]. The results show that there is mixing of terminal and bridging, as well as stretching and bending, modes. Thus, the assignments given in the table are only approximate. The strength of the terminal and bridging bonds may be compared in terms of their stretching force constants. In the case of the $[\text{Pt}_2\text{Br}_9]^-$ ion, the $\text{Pt}-\text{Br}_t$ and $\text{Pt}-\text{Br}_b$ stretching force constants are 1.55 and 0.93 $\text{mdyn}/\text{\AA}$, respectively [1443]. The IR and Raman spectra of the mixed-halogeno complex, $[\text{Cr}_2\text{Cl}_6\text{Br}_3]^{3-}$, can be assigned in terms of those of the $[\text{Cr}_2\text{Cl}_9]^{3-}$ and $[\text{Cr}_2\text{Br}_9]^{3-}$ ions [1445]:



2.11.4. X_2Y_{10} Molecules

The X_2Y_{10} molecule may take either one of the following structures:



The 30 normal vibrations of the D_{2h} molecule are classified into $6A_g$, $2A_u$, $4B_{1g}$, $4B_{1u}$, $3B_{2g}$, $4B_{2u}$, $2B_{3g}$, and $5B_{3u}$, of which 13 vibrations (B_{1u} , B_{2u} , and B_{3u}) are infrared-active, and 15 vibrations ($6A_g + 4B_{1g} + 3B_{2g} + 2B_{3g}$) are Raman-active. These include four terminal ($B_{1u} + B_{2u} + 2B_{3u}$) and two bridging ($B_{2u} + B_{3u}$) vibrations that are IR-active, and five terminal ($2A_g + 2B_{1g} + B_{2g}$) and one bridging (A_g) vibrations that are Raman-active. Vibrational assignments have been reported for: Nb_2Cl_{10} [1446], Re_2Cl_{10} [1446], Os_2Cl_{10} [1447], $[Ti_2Cl_{10}]^{2-}$ [1438], $[Re_2X_{10}]^{2-}$ ($X = Cl, Br$) [1448], $[Te_2X_{10}]^{2-}$ ($X = Cl, Br$) [1449], and $[Ir_2Cl_{10}]^{2-}$ [1450]. For example, the terminal and bridging vibrations of the $[Re_2Cl_{10}]^{2-}$ ion are found in the 367–321 and 278–250 cm^{-1} regions, respectively, although these modes may be mixed to some extent. Beattie et al. [1444] carried out normal coordinate analyses to assign the vibrational spectra of Nb_2X_{10} and Ta_2X_{10} ($X = Cl, Br$) the basis of D_{2h} symmetry.

The symmetry of the single-bridge XY_5-XY_5 -type molecule may be D_{4d} (staggered) or D_{4h} (eclipsed), and these two structures cannot be distinguished by the selection rules. Under D_{4d} symmetry, the 30 normal vibrations are classified into $4A_1$, B_1 , $3B_2$, $4E_1$, $3E_2$, and $4E_3$ species, of which B_2 and E_1 are infrared-active and A_1 , E_2 , and E_3 are Raman-active. Jones and Ekberg [1451] made complete assignments of infrared and Raman spectra of S_2F_{10} vapor on the basis of D_{4d} symmetry.

2.12. METAL CLUSTER COMPOUNDS

Heavy metals such as Mo, W, Nb, and Ta form octahedral metal clusters. Figure 2.35a shows the structure of the $[(M_6X_8)Y_6]^{2-}$ ion where M is Mo or W, X is a bridging halogen (Cl, Br), and Y is a terminal halogen (Cl, Br, I). Under O_h symmetry, the 54 ($3 \times 20 - 6$) normal vibrations of this ion are classified into $3A_{1g} + 3E_g + 2F_{lg} + 4F_{2g} + A_{2u} + E_u + 5F_{1u} + 3F_{2u}$, of which 10 vibrations (A_{1g} , E_g , and F_{2g}) are Raman-active and 5 vibrations (F_{1u}) are IR-active. As to the M_6 skeleton, two $\nu(M-M)$ are Raman-active (A_{1g} and E_g) and one $\nu(M-M)$ is IR-active (F_{1u}). It is rather difficult to assign the $\nu(M-M)$ empirically since strong coupling is

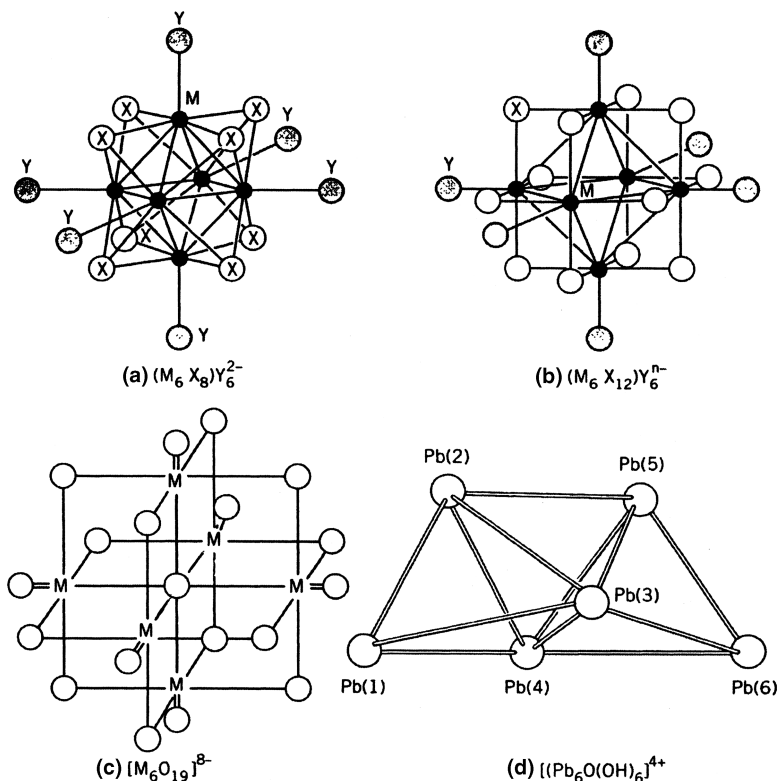


Fig. 2.35. Structures of metal cluster compounds.

expected among $\nu(M-M)$, $\nu(M-X)$, and $\nu(M-Y)$, which have the same symmetry and similar frequencies [1452].

Preetz and coworkers measured the IR and Raman spectra of metal clusters of this type, and carried out normal coordinate analysis; $[(Mo_6X_8)Y_6]^{2-}$ ($X = Cl, Br$; $Y = F, Cl, Br, I$) [1453], $[(Mo_6I_8)Y_6]^{2-}$ ($Y = F, Cl, Br, I$) [1454], $[(Mo_6X_8)(N_3)_6]^{2-}$ ($X = Cl, Br$) [1455]. The $\nu(Mo-Mo)$ force constants of these clusters are in the range of 1.2–1.5 mdyn/Å, and the Raman-active $\nu(Mo-Mo)$ vibrations are observed below 300 cm^{-1} . Their work was extended to $[(W_6Cl_8)Y_6]^{2-}$ ($Y = F, Cl, I, NCS$) [1456].

Figure 2.35b shows the structure of the $[(M_6X_{12})Y_6]^{n-}$ ion where M is Nb and Ta and X and Y are bridging and terminal halogens, respectively. Under O_h symmetry, the 66 ($3 \times 24 - 6$) normal vibrations of such an ion are grouped into $3A_{1g} + A_{2g} + 4E_g + 3F_{1g} + 4F_{2g} + A_{2u} + E_u + 6F_{1u} + 4F_{2u}$. Again, two $\nu(M-M)$, are Raman-active (A_{1g} and E_g) and one $\nu(M-M)$ is IR-active (F_{1u}) for the M_6 skeleton. The IR spectra of these and similar metal clusters have been reported by several investigators. [1457–1461]. The $\nu(Nb-Nb)$ of the Nb_6Cl_{12} cluster has been assigned empirically at 140 cm^{-1} [1458]. However, it may be mixed with other modes [1459]. Mattes [1460] carried out normal coordinate analysis on the $(M_6X_{12})Y_n$ system ($M = Nb, Ta$; $n = 2 \sim 4$), and

found their M–M stretching force constants to be less than $0.3 \text{ mdyn}/\text{\AA}$. These $\nu(\text{M}–\text{M})$ vibrations may be too low to be observed.

Figure 2.35c shows the structure of the $[\text{M}_6\text{O}_{19}]^{8-}$ ion ($\text{M} = \text{Nb}, \text{Ta}$). Under O_h symmetry, this ion has 7 IR-active vibrations of F_{1u} symmetry and 11 Raman-active vibrations, which are grouped into $3A_{1g}$, $4E_g$, and $4F_{2g}$. According to the results of normal coordinate analysis by Farrell et al. [1462], the stretching force constants associated with three types of the Nb–O bonds are

$K(\text{Nb}–\text{O})$			$K(\text{Nb}–\text{Nb})$
5.66	2.92	0.91	
terminal	bridging	central	$1.01 \text{ mdyn}/\text{\AA}$

The ratio of the first three force constants is about 6:3:1. Although the NbNb stretching constant was estimated to be $\sim 1 \text{ mdyn}/\text{\AA}$, this value does not represent the strength of this bond, since such a value can be obtained without any M–M interaction. Rather, these workers suggest the absence of Nb–Nb interactions for d_0 [Nb(V)] ions because the M–M bond breathing mode, which normally appears strongly in Raman spectra, is weak. Mattes et al. [1463] also carried out normal coordinate analysis on the same system and obtained a ratio of 8:4:1 for the three M–O stretching force constants mentioned above.

The Raman spectra of the $[\text{Ta}_6\text{O}_{19}]^{8-}$ ion [1464] and derivatives of the $[\text{Mo}_6\text{O}_{19}]^{2-}$ ion such as $(\text{Mo}_6\text{O}_{18})(\text{NPh})^{2-}$ [1465] have been reported.

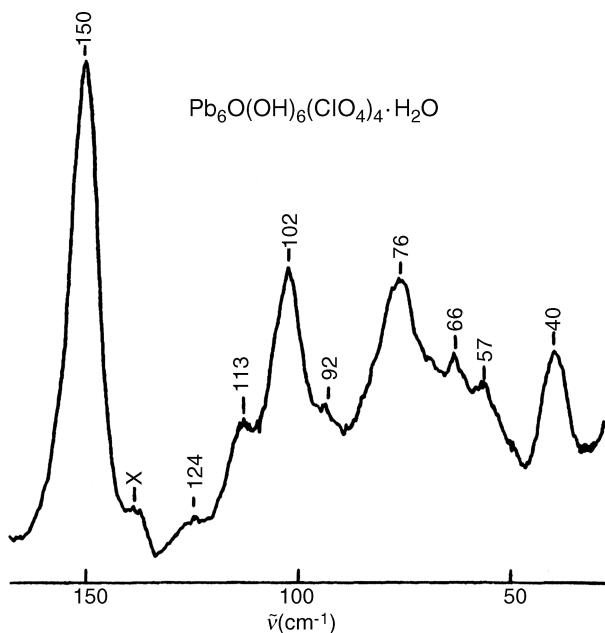


Fig. 2.36. Low-frequency Raman spectrum of a single crystal of $\text{Pb}_6\text{O}(\text{OH})_6(\text{ClO}_4)_4 \cdot \text{H}_2\text{O}$ at -110°C (632.8 nm excitation) [1468].

The Raman spectrum of crystals having the composition $\text{Pb}_3(\text{OH})_4(\text{ClO}_4)_2$ was originally interpreted in terms of an octahedral Pb_6 cluster [1466]. However, later X-ray analysis revealed the presence of the $[\text{Pb}_6\text{O}(\text{OH})_6]^{4+}$ ion having the very unusual structure shown in Fig. 2.35d [1467]. In this structure, three tetrahedra of Pb atoms share faces and the middle tetrahedron has an O atom (oxide) near the center, while the OH groups lie on the faces of the two end tetrahedra. There are 12 Pb–Pb interactions, and their Pb–Pb distances range from 3.44 to 4.00 Å. Figure 2.36 shows the low-frequency Raman spectrum in the region where the Pb–Pb vibrations appear [1468]. Under the idealized symmetry of C_2 , 12 cluster modes are expected. The strongest band at 150 cm^{-1} was assigned to the $\nu(\text{Pb}_3\text{--Pb}_4)$ since it is the shortest bond (3.44 Å). The remaining cluster modes were assigned using crude normal coordinate calculations. This spectrum is unique because it shows an unusually large number of cluster vibrations.

Figure 2.37a shows the bowl-like structure (near- C_3 symmetry) of the $[\text{Ni}_3\text{P}_3\text{S}_{12}]^{3-}$ ion, which exhibits $\nu(\text{Ni--S})$ vibrations at $\sim 310\text{ cm}^{-1}$ [1469]. The $[\text{Mo}_6\text{O}_6\text{S}_{14}]^{4-}$ ion

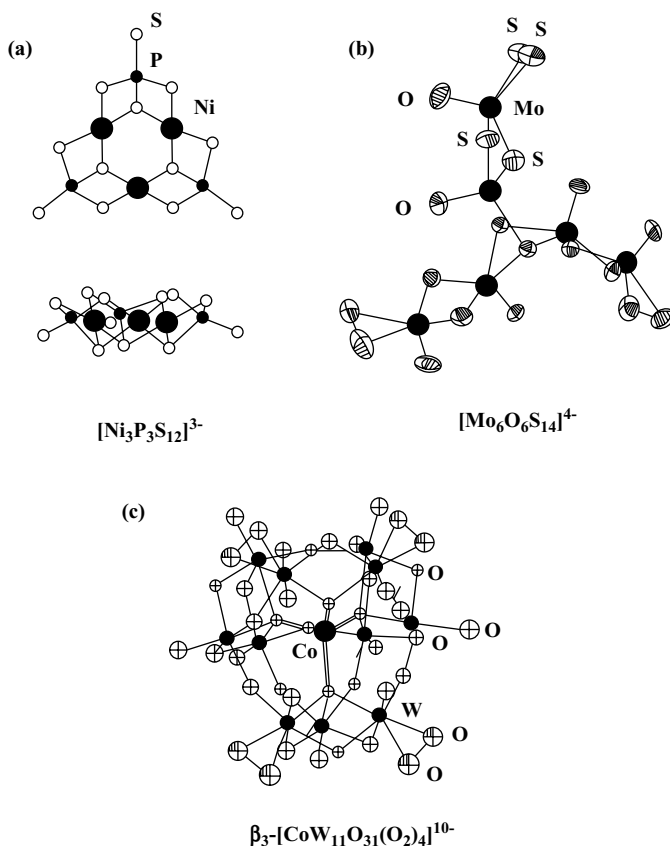


Fig. 2.37. Structures of metal cluster compounds.

shown in Fig. 2.37b exhibits the $\nu(\text{Mo}=\text{O})$ and $\nu(\text{Mo}-\text{Mo})$, vibration at 940–930 and 200–150 cm^{-1} , respectively [1470]. Figure 2.37c shows the structure of the tetraperoxide anion, $\beta_3-[(\text{Co}^{\text{II}}\text{O}_4) \text{W}_{11}\text{O}_{31}(\text{O}_2)_4]^{10-}$. The IR bands at 885 and 550 cm^{-1} were assigned to the $\nu(\text{O}-\text{O})$ and $\nu(\text{W}-\text{O}_2)$ of the side-on peroxides, respectively [1471]. Müller and coworkers [1472] prepared a giant metal cluster, $[\text{Mo}_{72}^{\text{VI}} \text{Mo}_{60}^{\text{V}} \text{O}_{372} (\text{CH}_3\text{COO})_{30} (\text{H}_2\text{O})_{72}]^{42-} (\text{NH}_4^+)_{42}$. It is interesting to note that the $\text{Mo}_{60}^{\text{V}}$ fragment assumes an icosahedral structure of I_h symmetry similar to C_{60} (Sec. 2.14.2). The $\nu(\text{M}=\text{O})$ are observed at 969 and 936 cm^{-1} in IR and at 953 and 875 cm^{-1} in Raman spectra. Vibrational spectra of large metal polycarbonyls such as $[\text{Pd}_{13}\text{N}_{13}(\text{CO})_{34}]^{4-}$ are discussed in Sec. 1.18 of Part B.

2.13. COMPOUNDS OF BORON

Boron compounds assume a wide variety of structures whose symmetries range from C_s to I_h . Some examples are shown in Fig. 2.38. Because of this, vibrational spectra of boron compounds have been studied extensively. The complications introduced by the natural abundances of ^{10}B (19.8%) and ^{11}B (80.2%) find use in making band assignments and in refining force constants for normal coordinate calculations. In the following, we list references for each group of compounds that have not been discussed in the preceding sections, and discuss band assignments for several selected compounds.

- (1) *Boron Oxides and Sulfides*. B_2O_2 and B_2O_3 [1473], B_2S_3 [1474], $(\text{HBS}_2)_3$ [1475], $\text{B}_3\text{H}_3\text{O}_3$ (boroxine) [1476], H_3BO_3 (boric acid) [1477], $\text{B}_3\text{O}_3 (\text{OH})_3$ (metaboric acid) [1478], $\text{H}_2\text{B}_2\text{O}_3$ [1479], H_2BSH [1480], CsBO_2 [1481], $\text{B}_3\text{O}_6^{3-}$ [1482,1483], $\text{B}_2\text{O}_5^{4-}$, and $\text{B}_3\text{O}_7^{5-}$ [1484].
- (2) *Boron Halides*. B_4Cl_4 [1485], $\text{B}_6\text{X}_6^{2-}$ [1486–1488], and $\text{B}_6\text{X}_n\text{Y}_{6-n}$ [1489,1490] and $\text{B}_{12}\text{X}_{12}^{2-}$ [1491,1492] ($\text{X}, \text{Y} = \text{a halogen}$). Figure 2.39 illustrates the IR and Raman spectra of the $\text{B}_6\text{X}_6^{2-}$ ions ($\text{X} = \text{Cl}, \text{Br}, \text{I}$) obtained by Preetz and Fritze [1487]. Under O_h symmetry, the 30 ($3 \times 12 - 6$) normal vibrations expected for these ions are classified into $2A_{1g} + 2E_g + F_{1g} + 2F_{2g} + 3F_{1u} + 2F_{2u}$. These vibrations can be subdivided into

$$\text{B}-\text{B vibrations} : A_{1g}(\nu_1) + E_g(\nu_3) + F_{2g}(\nu_5) + F_{1u}(\nu_7) + F_{2u}$$

$$\text{B}-\text{X vibrations} : A_{1g}(\nu_2) + E_g(\nu_4) + F_{1g} + F_{2g}(\nu_6) + 2F_{1u}(\nu_8, \nu_9) + F_{2u}$$

The A_{1g} , E_g , and F_{2g} vibrations are Raman-active, whereas the F_{1u} vibrations are IR-active. As seen in Fig. 2.39, the B–B vibrations are relatively insensitive, whereas the B–X vibrations are sensitive to halogen substitution. The $\text{B}_{12}\text{X}_{12}^{2-}$ ($\text{X} = \text{Cl}, \text{Br}, \text{I}$) ion (Fig. 2.38) belongs to the highest symmetry (I_h) point group, which consists of 120 symmetry operations. The 66 ($3 \times 24 - 6$) normal vibrations are classified into $2A_g + F_{1g} + 2G_g + 4H_g + 3F_{1u} + 2F_{2u} + 2G_u + 2H_u$. Here, G and H represent the four- and fivefold degenerate species, respectively.

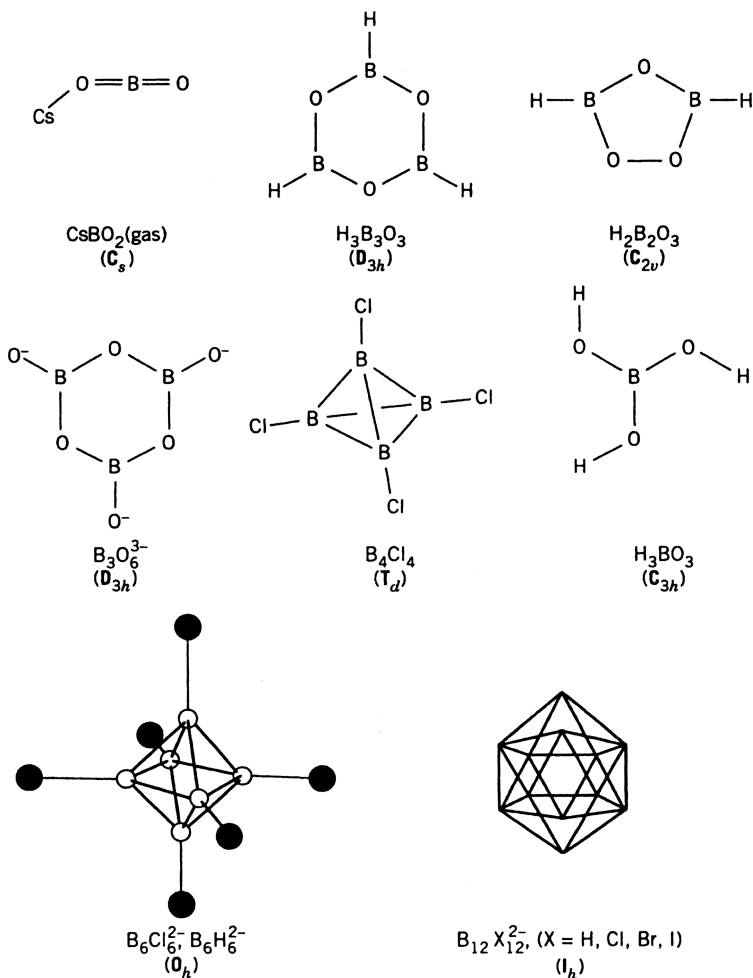


Fig. 2.38. Structures of some boron oxides and halides.

Owing to the high symmetry, its IR and Raman spectra are surprisingly simple; only three F_{1u} vibrations are IR-active, and only two A_g (polarized) and four H_g (depolarized) vibrations are Raman-active. Leites et al. [1491] reported the IR and Raman spectra together with empirical assignments, and Cyvin et al. [1492] carried out normal coordinate calculations on these ions.

- (3) *Boron hydrides (Boranes) and their ions.* B_5H_9 [1493], $\text{B}_{10}\text{H}_{14}$ [1494], B_2H_7^- [1495], $\text{B}_6\text{H}_6^{2-}$ [1496,1497] $\text{B}_6\text{X}_n\text{H}_{6-n}^{2-}$ [1498], and $\text{B}_{12}\text{H}_{12}^{2-}$ [1491,1492]. As is shown in Fig. 2.40 five boron atoms of B_5H_9 , form a square-pyramidal skeleton, with four hydrogen atoms bridging four base boron atoms while five hydrogen atoms are bonded terminally to each boron atom, so that the symmetry of the whole molecule is C_{4v} . Complete band assignments

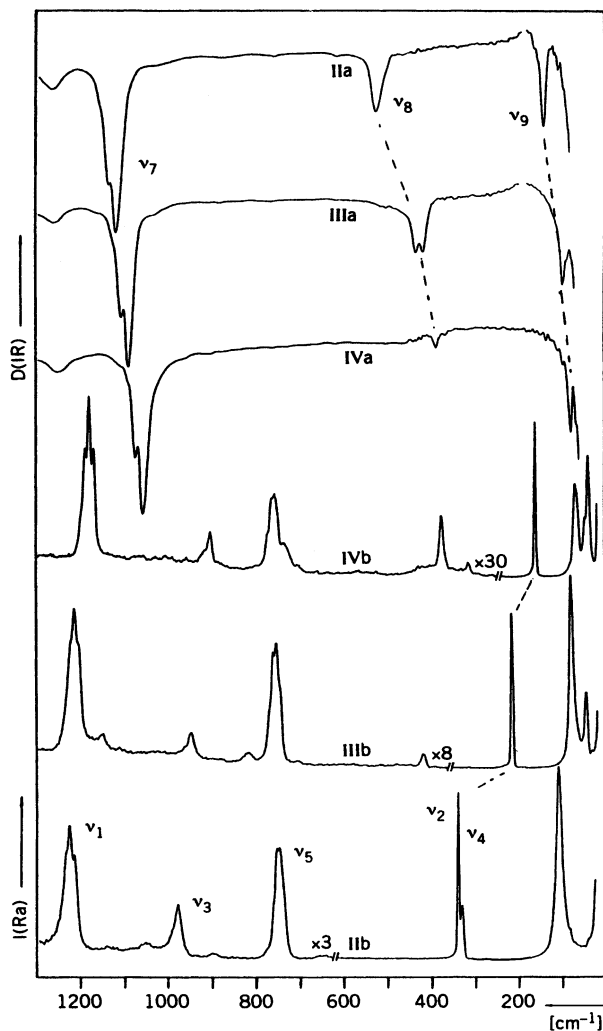


Fig. 2.39. (a) IR and (b) Raman spectra of solid $\text{Cs}_2\text{B}_6\text{Cl}_6$ (II), $\text{Cs}_2\text{B}_6\text{Br}_6$ (III), and $\text{Cs}_2\text{B}_6\text{I}_6$ (IV) [1487].

have been made by Kalasinsky [1493]. The structure of the $\text{B}_{12}\text{H}(\text{D})_{12}^{2-}$ ion is the same as that of the $\text{B}_{12}\text{X}_{12}^{2-}$ ion discussed previously. For the spectra and band assignments, see Refs. [1491, 1492] Gallaborane, $\text{H}_2\text{Ga}(\mu\text{-H})_2\text{BH}_2$, takes a diborane-like structure of C_{2v} symmetry, and exhibits the $\nu(\text{B-H})$ vibration at 2558 and 2482 cm^{-1} and the $\nu(\text{Ga-H})$ vibration at 2005 and 1982 cm^{-1} . The bridging stretchings coupled with ring deformation are at 2007 and 1937 cm^{-1} for $\nu(\text{B-H}_b)$ and at 1435 and 1315 cm^{-1} for $\nu(\text{Ga-H}_b)$ [1498a].

- (4) *Borazines*. $\text{B}_3\text{N}_3\text{H}_6$ [1476, 1499] and $\text{B}_3\text{N}_3\text{H}_3\text{Cl}_3$ [1500]. Both molecules assume planar ring structures of D_{3h} symmetry (Fig. 2.40) and their

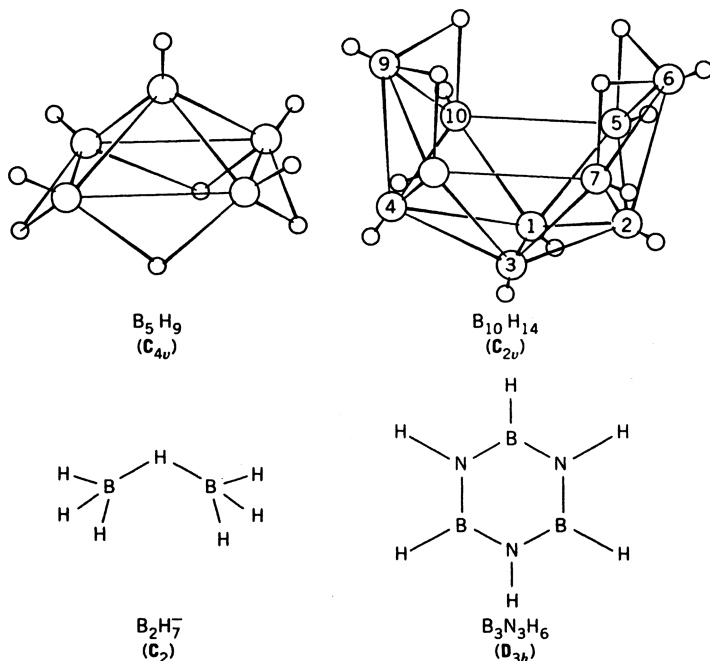


Fig. 2.40. Structures of some boranes and borazine.

30 ($3 \times 12 - 6$) vibrations are classified into $4A'_1(R) + 3A'_2$ (inactive) + $7E'$ (IR, R) + $3E''(R) + 3A''_2$ (IR). Figure 2.41 shows the IR spectra of matrix-isolated borazine obtained by Kaldor and Porter [1476]. Complete assignments based on normal coordinate calculations are found in the references cited above.

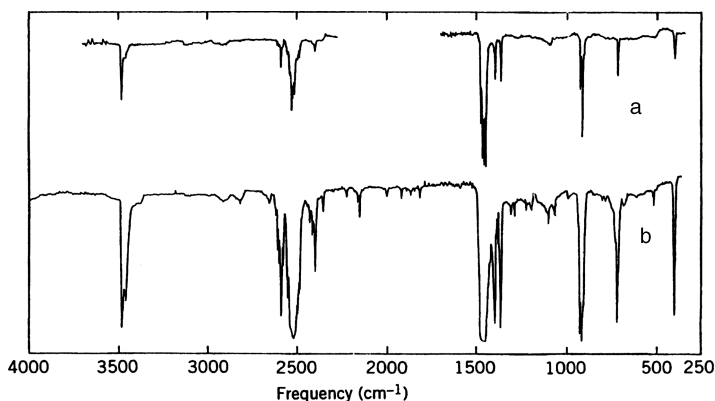


Fig. 2.41. IR spectra of borazine in Ar matrices (Ar/borazine = 1000) near 5 K: (a) 3-min deposition; (b) 30-min deposition [1476].

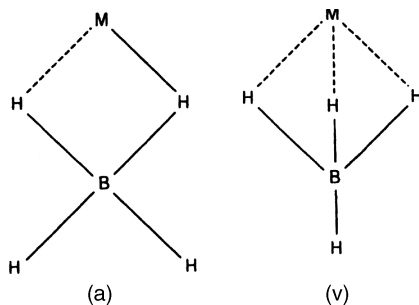


Fig. 2.42. Modes of coordination of the BH_4^- ion: (a) doubly bridging; (b) triply bridging.

- (5) *Borohydride Ion as a Ligand.* As shown in Fig. 2.42, the BH_4^- ion may coordinate to a metal, as either a bidentate or a tridentate via hydrogen bonding. For example, the Zr atom in $\text{Zr}(\text{BH}_4)_4$ is 12-coordinate because all of the BH_4^- ions are triply bridging [1501], whereas the U atom in polymeric $\text{U}(\text{BH}_4)_4$ in the solid state is 14-coordinate because it is coordinated by two triply bridging (*cis*) and four doubly bridging BH_4^- ions [1502]. In these cases, the terminal and bridging $\nu(\text{BH})$ bands are located in the 2600–2500 and 2200–2100 cm^{-1} regions, respectively [1501–1504].

Several review articles are available on the vibrational spectra of boron compounds. Lehmann and Shapiro [1505] reviewed $\nu(\text{BH})$, $\delta(\text{BH}_2)$, $\nu(\text{BC})$, $\nu(\text{BB})$, etc. of alkylboranes, and Bellamy et al. [1506] discussed $\nu(\text{BN})$, $\nu(\text{BH})$, $\nu(\text{BX})$, $\nu(\text{BC})$, and so on. Meller [1507] lists $\nu(\text{BN})$, $\nu(\text{BH})$, $\nu(\text{BX})$, and $\nu(\text{BC})$ of a number of organoboron–nitrogen compounds. For vibrational spectra of boron compounds containing the B–P bond, see a review by Verkade [1508]. The group frequency charts shown in Appendix VIII include $\nu(\text{BH})$, $\nu(\text{BO})$, and $\nu(\text{BX})$.

2.14. COMPOUNDS OF CARBON

2.14.1. Small Carbon Clusters

Vibrational studies on carbon clusters are highly important in interstellar and combustion research. An extensive review article on small carbon clusters (C_n , $n = 2\text{--}10$) is available [1509]. Table 2.13 lists the structures and IR (antisymmetric stretching) frequencies observed in the gaseous phase and/or in inert gas matrices.

For C_3 , the ν_1 , ν_2 , and ν_3 vibrations of the ground and two excited states are reported [1511]. It is seen that all neutral C_n ($n = 3\text{--}13$) molecules are linear except C_6 , which can also assume a cyclic structure of D_{3h} symmetry [1521,1522]. The linear C_{13} molecule exhibits the antisymmetric stretching vibration at 1809 cm^{-1} in the ground state [1527]. This result contradicts theoretical calculations, which predict the $\text{C}_{10}\text{--}\text{C}_{20}$ clusters are planar monocyclic. It was speculated that at high temperature

TABLE 2.13. Structures and IR Frequencies of Small Carbon Clusters

C_n	Structure	State	IR Frequencies (cm^{-1})	Ref.
C_3	Linear	Ar matrix	2038.9 (ν_3) 1216.4 (ν_1)	1510,1511
$^{13}C_3$		Gas	1938.7 (ν_3)	1512
C_4	Linear	Ar matrix	1543.4 (ν_3)	1513,1514
		Gas	1548.6 (ν_3)	1515
C_5	Linear	Ar matrix	2164 (ν_3)	1516,1517
		Gas	2169.4 (ν_3)	1518,1519
$^{13}C_5$		Gas	2085.8	1520
C_6	Linear	Ar matrix	1952.5 (ν_4) 1197.3 (ν_5)	1520
	Cyclic	Ar matrix	1694.9 (ν_4 , E')	1521,1522
C_7	Linear	Ar matrix	2127.8 (ν_4) 1894.3 (ν_5)	1523
C_8	Linear	Ar matrix	2071.5, 1710.5	1524
C_9	Linear	Ar matrix	2014.3, 1998, 1601	1524,1525
C_{11}	Linear	N_2 matrix	1942.6, 1854.8, 1357.0	1526
C_{13}	Linear	Gas	1809	1527

of graphite vaporization (~ 4000 K), the entropy factor strongly favors the formation of linear over cyclic structure.

Vala et al. [1516] confirmed the linear structure of the C_5 cluster by using isotope scrambling techniques. These workers trapped the C_5 cluster in Ar matrices (12 K) by evaporating graphite. As is seen in Fig. 2.43 (lower part), a single IR peak is observed at 2164 cm^{-1} when a ^{12}C graphite is used (the 2128 cm^{-1} peak is due to $^{12}C_9$ contamination). However, this peak splits into 20 peaks (upper part) when a graphite sample consisting of a 1:1 mixture of ^{12}C and ^{13}C is used. This result provides definitive evidence for the linear structure since the number of possible isotopomers are 20, 12, and 8 for the linear, trigonal-bipyramidal, and cyclic structures, respectively. On the other hand, the C_5^+ ion takes a planar, cyclic structure (D_{5h}) because its IR peak at 2052 cm^{-1} splits into 8 peaks when similar isotope scrambling experiments are carried out [1528].

The Raman spectra of C_{14} [1529], C_{16} [1530], C_{18} [1530], and C_{20} [1530] in N_2 matrices are also consistent with linear geometry. IR spectra of linear carbon cluster anions C_n^- ($n = 3, 4, 5, 6, 7, 9$) in Ar matrices are reported [1531~1534]. In general, their frequencies are markedly lower than those of the corresponding neutral clusters. For example, the stretching frequencies of the C_5^- and C_7^- ions are lower by 332 and 394 cm^{-1} respectively, than those of the corresponding neutral molecules.

2.14.2. C_{60} and Its Derivatives

Since C_{60} (Buckminster Fullerene) was discovered in 1985 [1535], the IR and Raman spectra of C_{60} and a large number of its analogs and derivatives (fullerenes) have been studied extensively. Among them, C_{60} has attracted considerable attention because of

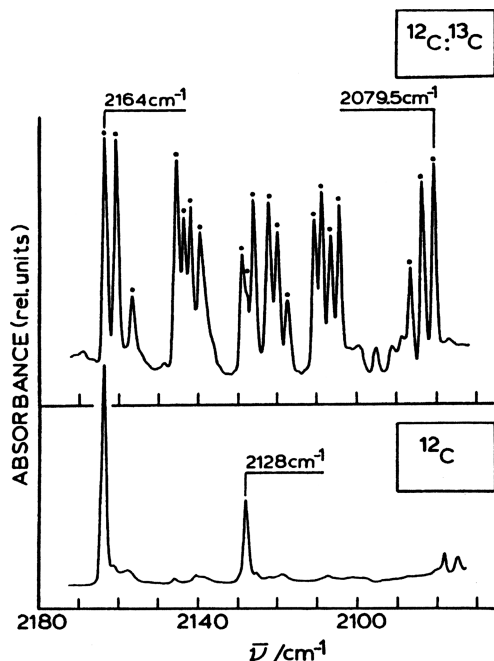


Fig. 2.43. Fourier transform IR spectra of 2180–2070 cm^{-1} region of the laser vaporized graphite in an Ar matrix (12 K). Upper trace: a 1 : 1 mixture of $^{12}\text{C}^{13}\text{C}$; black dots indicate bands due to isotopomers of linear C_5 ; the bands at 2164 and 2079.5 cm^{-1} are due to $^{12}\text{C}_5$ and $^{13}\text{C}_5$, respectively. Lower trace: pure ^{12}C graphite (the band at 2128 cm^{-1} is due to $^{12}\text{C}_9$ [1516]).

its highly symmetric “soccerball” structure [1536–1538]. It has 20 hexagonal faces and 12 pentagonal faces, with the 60 carbon atoms located at the vertices of a regular truncated icosahedron. The molecule belongs to the icosahedral point group I_h , consisting of 120 symmetry elements (Appendix I), some of which are shown in Fig. 2.44. The 174 ($3 \times 60 - 6$) normal vibrations of C_{60} are classified [1539] into $2A_g + A_u + 3F_{1g} + 4F_{1u} + 4F_{2g} + 5F_{2u} + 6G_g + 6G_u + 8H_g + 7H_u$. Because of its extremely high symmetry, only the four F_{1u} vibrations are IR-active and only the two A_g and eight H_g vibrations are Raman-active. Furthermore, the mutual exclusion rule holds because of the presence of a center of symmetry.

Figure 2.45 shows the IR and Raman spectra, respectively, of C_{60} [1539]. As predicted, the IR spectrum shows four bands at 1428, 1182, 577, and 527 cm^{-1} , and the Raman spectrum exhibits 10 bands at 1575, 1469, 1427, 1250, 1100, 774, 711, 496, 436, and 273 cm^{-1} . In general, the vibrations above $\sim 1000 \text{ cm}^{-1}$ are predominantly due to displacements tangential to the C_{60} surface, whereas those below 800 cm^{-1} are predominantly due to radial displacements [1540]. The two polarized (A_g) bands at 1470 and 496 cm^{-1} are assigned to the totally symmetric tangential stretching (or pentagonal pinching) and radial breathing modes, respectively. The lowest frequency band (depolarized) at 273 cm^{-1} is described as the cage-squashing mode (H_g) (Fig. 2.46) [1538].

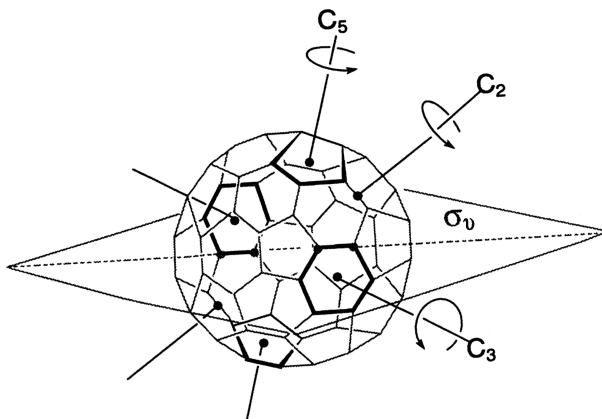


Fig. 2.44. Illustration of some symmetry elements in C_{60} [1539].

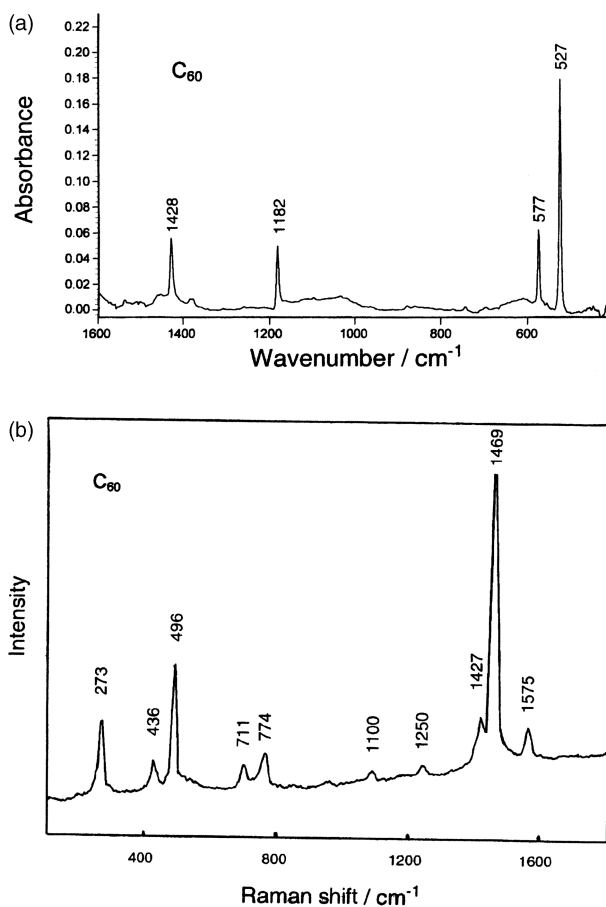


Fig. 2.45. IR (a) [in KBr pellet] and Raman (b) [thin film] (514.5 nm excitation) spectra of C_{60} [1539].

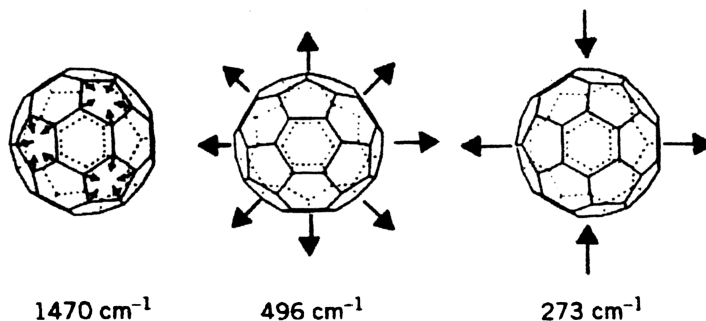


Fig. 2.46. Vibrational modes of three prominent Raman bands [1538].

The IR (film[1541], gas[1542]) and Raman spectra (single-crystal [1543], solution [1544], surface-enhanced Raman [1545]) have been measured by many investigators, and band assignments have been based on normal coordinate analysis [1546] and DFT calculations [1547].

Figure 2.47 shows a high-resolution Raman spectrum of the pentagonal pinching mode [$A_g(2)$] of C_{60} in a frozen solution in CS_2 at 30 K obtained by Guha et al. [1548].

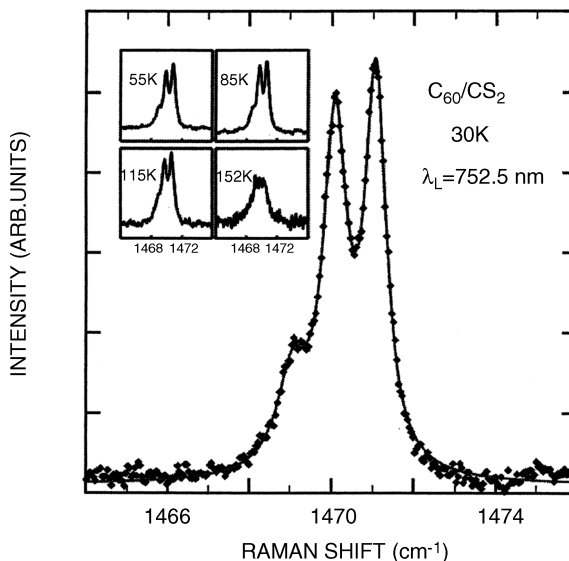


Fig. 2.47. Unpolarized Raman spectrum of a frozen solution of C_{60} in CS_2 at 30 K. The solid line is a 3-Lorentzian fit to the experimental data. The highest frequency is assigned to the totally symmetric pentagonal-pinch A_g mode in $^{12}C_{60}$. The other two lines are assigned to the pentagonal-pinch mode in molecules containing one and two ^{13}C isotopes, respectively. The inset shows the evolution of these peaks as the solution is warmed [1548].

Since the natural abundance of ^{13}C is 1.11%, C_{60} molecules prepared from natural graphite contain 51% of $^{12}\text{C}_{60}$, 35% of $^{12}\text{C}_{59}^{13}\text{C}$, and 11% of $^{12}\text{C}_{58}^{13}\text{C}_2$. Considering their relative concentrations in the mixture, the vibrations due to these isotopic species have been assigned to the peaks observed at 1471, 1470, and 1469 cm^{-1} (shoulder), respectively. The four-panel inset to Fig. 2.47 shows the effect of raising the temperature; it is seen that these peaks are no longer apparent when the solution is melted above 150 K.

Doping of alkali metals ($\text{M} = \text{K}, \text{Rb}, \text{Cs}$) in C_{60} produces a variety of exohedral fullerenes, M_xC_{60} , in which metals are *intercalated* between C_{60} molecules. Simple molecular orbital theory [1549] predicts that M_3C_{60} is electron-conducting whereas M_4C_{60} and M_6C_{60} are insulating. In fact, K_3C_{60} and Rb_3C_{60} are known to be superconducting at 18 and 28 K, respectively. Spectroscopic studies on these compounds provide information about the perturbation of the C_{60} structure resulting from the metal to C_{60} cage charge-transfer and the strength of the metal-cage interaction. For example, the Raman spectra obtained by Zhou et al. [1550] show that the A_g mode at 1469 cm^{-1} is shifted to 1452 and 1448 cm^{-1} , respectively, in the K- and Rb-doped compounds, and that all the H_g bands are broadened considerably. The magnitude of the shift of the 1469 cm^{-1} band has been used to determine the stoichiometry of x in K_xC_{60} [1551]. These results indicate that, on doping, electrons are transferred from the metal to the π -orbitals of the C_{60} surface, thus lengthening the CC bonds and that the C_{60} ion thus obtained undergoes symmetry lowering, which results in band splitting and/or broadening. Vibrational frequencies of C_{60}^{6-} were calculated by DFT and compared with the observed frequencies [1552].

In $\text{C}_{60}\text{Br}_{24}$, the overall symmetry is lowered to T_h because the 24 Br atoms are bonded to the C_1 , and C_4 atoms of the fused pairs of hexagons in the C_{60} framework. Under T_h symmetry, the $\nu(\text{C}=\text{C})$ vibrations are grouped into $2A_g + 2E_g + 3F_u + F_g$, of which the three (F_u) vibrations are IR-active, and the five ($2A_g$, $2E_g$, and F_g) vibrations are Raman-active. In agreement with these predictions, the IR spectrum shows three bands at 1688, 1641, and 1610 cm^{-1} , while the Raman spectrum shows five bands at 1690, 1675, 1654, 1631, and 1607 cm^{-1} [1553]. This work was extended to the $\nu(\text{C}-\text{Br})$ vibrations of $\text{C}_{60}\text{Br}_{24}$ (T_h), C_{60}Br_8 (C_{2v}), and C_{60}Br_6 (C_s), for which the numbers of IR-active modes are predicted to be 3(3), 6(5), and 6(6), respectively. The numbers in parentheses indicate those of the observed. However, such good agreement was not obtained in the case of Raman spectra [1554].

Of more than five possible structures of the photopolymerized C_{60} dimer, Takeuchi and coworkers [1555,1556] proposed a [2+2] cycloadditional ("dumbbell") structure of D_{2h} symmetry, shown in Fig. 2.48a. They reached this conclusion by comparing the observed IR spectrum with those calculated for each structure. Previously, Adams et al. [1557] obtained the same structure using theoretical calculations. Vibrational spectra are reported for C_{60} derivatives containing various η^2 -bridging ligands. In the case of $(\text{PPh}_3)_2\text{Pt}(\eta^2\text{-C}_{60})$, shown in Fig. 2.48b [1558], the Raman spectrum confirms the reduction of symmetry by exhibiting vibrational modes that are not allowed under I_h symmetry, and high-frequency modes are slightly shifted to lower frequencies as a result of slight weakening of the CC bonds [1558a].

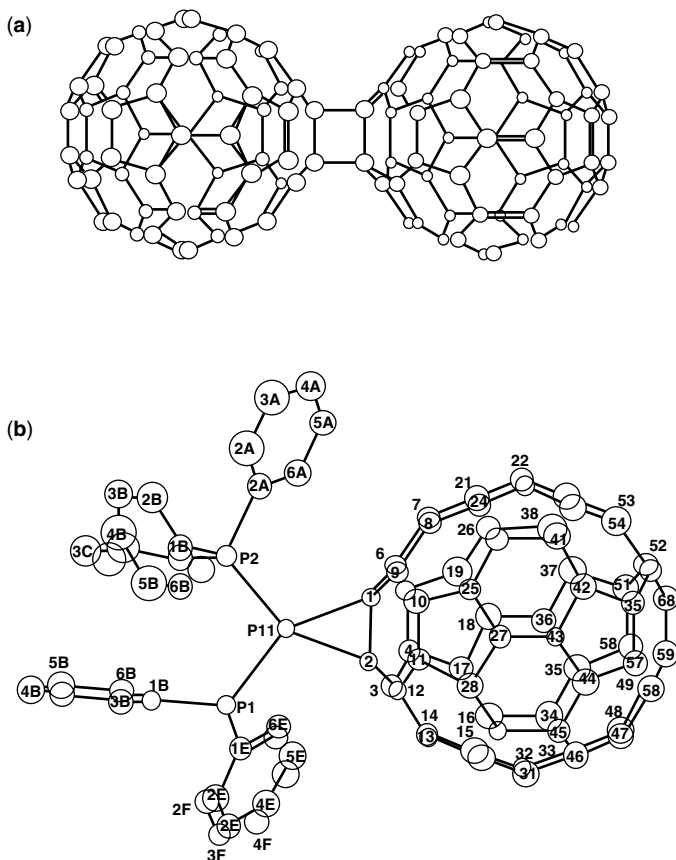


Fig. 2.48. Structures of (a) C₆₀ dimer [1556] and (b) Pt(PPh₃)₂(η²-C₆₀) [1558].

2.14.3. C₇₀ and Other Fullerenes

Laser ablation of graphite produces a mixture of many fullerenes, among which C₆₀ is most abundant and C₇₀ is next. As shown in Fig. 2.49, C₇₀ is a cage of D_{5h} symmetry with 25 hexagons and 12 pentagons. All closed cage structures of fullerenes consisting of h hexagonal and p pentagonal faces must obey Euler's rule, which states:

$$f + v = e + 2$$

Here, f , v , and e are the numbers of the faces, vertices, and edges, respectively, and f is equal to $p + h$. Since each edge shares two polygons, we have the relationship $2e = 5p + 6h$. We also have the relationship $3v = 5p + 6h$ because each vertex shares three polygons. Thus, we obtain the relationship $p = 6(f + v - e)$, which gives $p = 12$, and $v = 20 + 2h$ from Euler's rule. Namely, p must always be 12, and fullerenes must have "even" numbers of carbon atoms. If $h = 0$, v is 20. This is the smallest fullerene

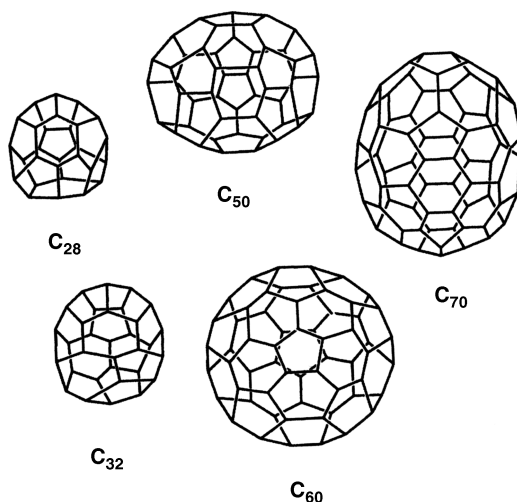


Fig. 2.49. Proposed and confirmed structures of fullerenes [1539].

that is a dodecahedron consisting of 12 pentagons without hexagons. However, such a structure is energetically not favorable because two pentagons adjacent to each other result in larger local curvature and more strain on the cage. Any fullerenes containing two adjacent pentagons are not stable. This is called the *isolated pentagon rule* (IPR). For $h = 4, 6, 15, 20$, and 25 , we obtain C_{28} , C_{32} , C_{50} , C_{60} , and C_{70} , respectively. Figure 2.49 illustrates IPR structures of these fullerenes (the former three are not confirmed)

The $204(3 \times 70 - 6)$ normal vibrations of C_{70} under D_{5h} symmetry are classified into $12A'_1 + 9A'_2 + 9A''_1 + 10A''_2 + 21E'_1 + 22E'_2 + 19E''_1 + 20E''_2$, of which 31 (A'_2 and E'_1) vibrations are IR-active and 53 (A'_1 , E'_2 , and E''_1) vibrations are Raman-active. Figure 2.50a and 2.50b show the IR and Raman spectra, respectively, of C_{70} obtained by Bethune et al. [1559]. The numbers of the observed bands (16 IR and 21 Raman) were much less than those predicted for the D_{5h} symmetry.

Similar results are reported by Jishi et al. (11 IR and 16 Raman) [1560] and Gallagher et al. (25 Raman) [1561]. These observations may suggest that some vibrations are inherently weak and/or that serious band overlaps occur in these spectra. Vibrational frequencies of C_{60} and C_{70} were calculated by the quantum mechanical method (AMI) [1562]. The IR spectra of M_3C_{70} and M_4C_{70} ($M = K, Rb$) salts show that the 1430 cm^{-1} band of C_{70} is, downshifted by 13 cm^{-1} per electron added to the carbon cage [1563]. Similar to dimeric C_{60} , C_{70} forms a $[2+2]$ cycloaddition dimer of C_{2h} symmetry, and its IR and Raman spectra are reported [1564]. Table 2.14 summarizes structural and spectroscopic data of C_{28} , C_{32} , C_{50} , C_{60} , and C_{70} [1539].

Carbon cages larger than C_{70} are known for C_{72} , C_{74} , C_{78} , C_{80} , C_{82} , C_{84} , and so on. In most cases, vibrational spectra are reported only for their endohedral forms since their carbon cages are unstable without electron transfer from the encapsulated species. However, C_{84} was obtained without encapsulation. Although there are 24 isomeric IPR structures for C_{84} [1565], Dennis et al. [1566] were able to isolate D_2

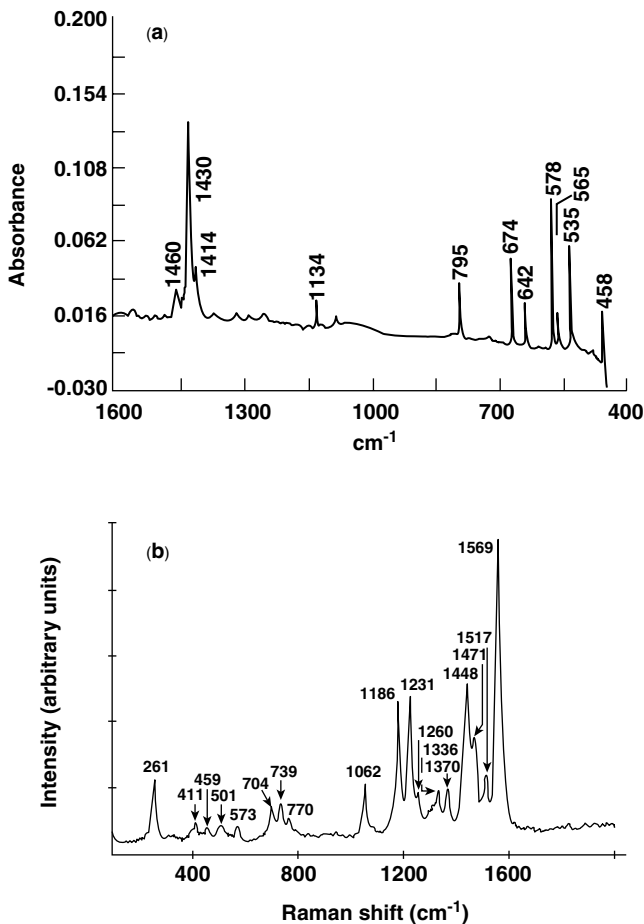


Fig. 2.50. (a) IR (film on a KBr substrate) and (b) Raman (film on a suprasil substrate) spectra of C_{70} [1559].

TABLE 2.14. Structures and Spectra of Fullerenes

	C_{28}	C_{32}	C_{50}	C_{60}	C_{70}
Number of hexagons	4	6	15	20	25
Number of pentagons	12	12	12	12	12
Point group	T_d	D_3^a	D_{5h}	I_h	D_{5h}
^{13}C NMR	3	6	4	1	5
IR-active bands	11	44	22	4	31
Raman-active bands	23	46	38	10	53

^aMolecules belonging to the D_3 point group are optically active.

(form IV) and D_{2d} (form II) isomers and measured their IR spectra. For the former, the 246 normal vibrations ($3 \times 84 - 6$) are grouped into $63A + 61B_1 + 61B_2 + 61B_3$, and 183 vibrations (B_1 , B_2 and B_3) are IR-active. For the latter, they are classified into $32A_1 + 30A_2 + 31B_1 + 31B_2 + 61E$, and 92 vibrations (B_2 and E) are IR-active. As seen in Fig. 2.51, however, their IR spectra are surprisingly similar. This result was attributed to the similarity of these two forms, which can be transformed into each other by a small perturbation, resulting in many degenerate modes for the former.

2.14.4. Endohedral Fullerenes

Endohedral fullerenes, which contain metal atoms or small molecules inside the carbon cages, hold great promise for application in optoelectronic devices because of their fullerene-like and metallic properties. However, their investigations are limited by extremely low yields of these fullerenes (mg~ μ g range). IR and Raman studies of endohedral fullerenes are important in elucidating the nature of interaction between the carbon cage and encapsulated species. Electronic structures and spectroscopic properties of endohedral fullerenes have been reviewed by Guha and Nakamoto [1549].

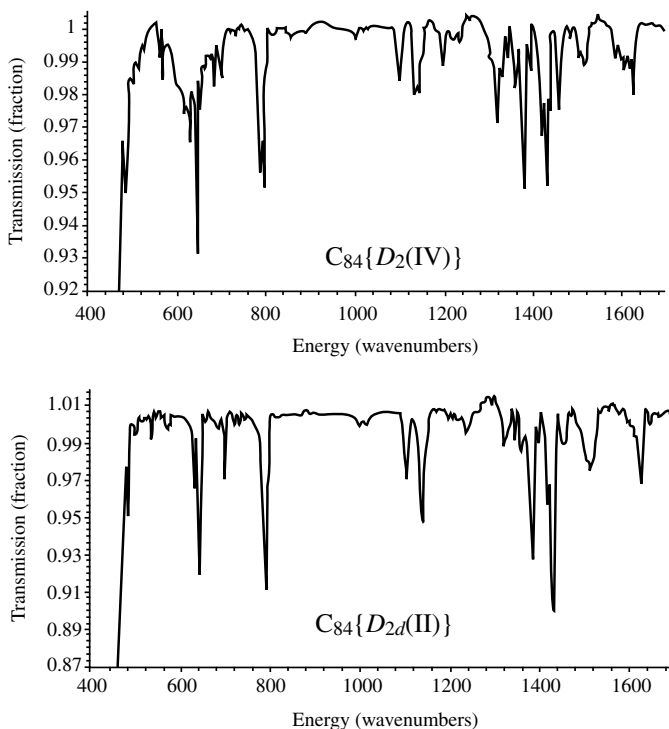


Fig. 2.51. IR spectra of C_{84} (D_2 , form IV and D_{2d} , form II) [1566].

The IR spectrum of $\text{Kr}@\text{C}_{60}$ (where @ denotes encapsulated species) shows that the bands near 1429 , 1182 , and 527 cm^{-1} of C_{60} are shifted to higher frequencies by 8.2 , 10.6 , and 15.4 cm^{-1} , respectively, and that the latter two bands are broadened on encapsulation of the Kr atom. [1567]. This result, together with those obtained by the UV-visible spectral studies, suggests that there is a weak electronic interaction between the Kr atom and C_{60} , although I_h symmetry is still retained. The Raman spectrum of $\text{Li}@\text{C}_{60}$ shows that the pentagonal pinching mode near 1470 cm^{-1} is shifted to a lower frequency by 4.3 cm^{-1} on encapsulation [1568]. Since this mode is known to be downshifted by $\sim 7\text{ cm}^{-1}$ per one electron transfer, the result was interpreted as indicating that one electron transfer occurs on average in every second C_{60} cage.

Figure 2.52 shows the IR and Raman spectra of $\text{Eu}@\text{C}_{74}$ (formulated as $\text{Eu}^{2+}\text{C}_{74}^{2-}$) obtained by Kuran et al. [1569]. Both spectra exhibit about 50 bands in the

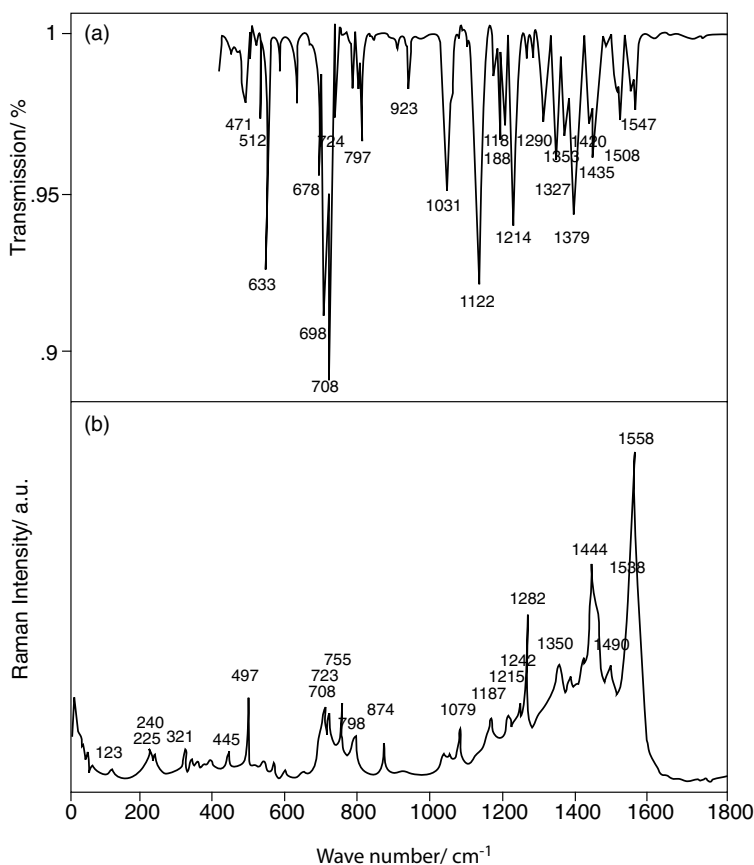


Fig. 2.52. IR (a) and Raman (b) spectra of solid $\text{Eu}@\text{C}_{74}$ (where @ denotes encapsulated species) [1569].

1600–200 cm^{-1} region, where the carbon cage vibrations are expected. These numbers are more than those predicted from the \mathbf{D}_{3h} structure of the C_{74} cage. Thus, the symmetry of Eu@C_{74} must be lower than \mathbf{D}_{3h} . The 123 cm^{-1} band in the Raman spectrum was assigned to the Eu-C_{74} interaction mode.

There are seven possible IPR structures for the C_{80} cage, which consists of 12 pentagons and 30 hexagons. Although the \mathbf{I}_h structure is most unstable, it becomes stable by accepting six electrons from the encapsulated species. For example, $\text{La}_2\text{@C}_{80}$ is stable as formulated as $(\text{La}^{3+})_2(\text{C}_{80})^{6-}$ [1570]. Similar charge transfer stabilization was noted for a series of $\text{A}_{3-n}\text{B}_n\text{N@C}_{80}$ ($n = 0-3$; A, B = rare-earth metal such as Sc and Y)-type compounds prepared by Stevenson et al. [1571]. After studying the results of X-ray analysis and electronic and ^{13}C NMR spectroscopy, these workers concluded that the dynamic motion of the trimetallic nitride cluster inside the cage yields a time-averaged electronic environment of \mathbf{I}_h symmetry, and that the encaged species is not located at any specific bonding site, at least on the NMR timescale at 295 K.

On the other hand, Krause et al. [1572] measured the IR and Raman spectra of $\text{Sc}_3\text{N@C}_{80}$ to determine the nature of the C_{80} cage– Sc_3N interaction. Under \mathbf{I}_h symmetry, the 234 ($3 \times 80 - 6$) vibrations of the C_{60}^{6-} cage are classified into $3A_g + A_u + 4F_{1g} + 6F_{1u} + 5F_{2g} + 7F_{2u} + 8G_g + 8G_u + 11H_g + 9H_u$, and only $6(F_{1u})$ are IR-active and $14(A_g + H_g)$ are Raman-active. The trigonal planar Sc_3N moiety of \mathbf{D}_{3h} symmetry exhibits two IR and three Raman bands. If there is no interaction between them, one expects 8 IR and 17 Raman fundamentals for $\text{Sc}_3\text{N@C}_{80}$. However, these workers observed 37 IR and 59 Raman bands excluding very weak bands, and also noted a violation of the mutual exclusion rule. Thus, their results clearly indicated that, on the vibrational timescale, the \mathbf{I}_h symmetry is significantly lowered as a result of the $\text{Sc}_3\text{N-C}_{80}$ interaction. The vibrations originated in the Sc_3N moiety were assigned by comparing the IR and Raman spectra of $\text{Sc}_3\text{N@C}_{80}$ and its Y_3N analog in the 800–200 cm^{-1} region. As seen in Fig. 2.53, only three Raman bands at 599 (weak), 411 (very strong), and 210 cm^{-1} (medium) are metal-sensitive, and shifted to 707 (weak), 429 (medium), and 194 cm^{-1} (strong), respectively, by Sc/Y substitution. These bands were assigned to the $\nu_a(E', \text{IR/Raman})$, $\nu_s(A'_1, \text{Raman})$ and $\delta(E', \text{IR/Raman})$ of the Sc_3N moiety, respectively. In IR spectra, the ν_a band at 597 (very strong) cm^{-1} is shifted to 724/712 cm^{-1} on the substitution. The upshifts of the two stretching vibrations by Sc/Y substitution are somewhat unexpected since the atomic weight of Y (88.91) is about two times larger than that of Sc (44.96). This was attributed to the particular bonding properties of the encaged Y_3N moiety. Figure 2.54 shows the optimized structure of $\text{Sc}_3\text{N@C}_{80}$ predicted by DFT calculations [1572]. Although the structure of the Sc_3N moiety remains intact, the symmetry of the whole molecule is only \mathbf{C}_3 , because the Sc atoms are not located ideally below the center of the pentagon and the Sc–N bond length varies within ~ 0.2 Å. According to these workers, there are 20 equivalent configurations of \mathbf{C}_3 symmetry, and the transition barriers between them is ~ 0.5 eV. They also assigned the Raman bands at 133, 108, 78, and 48 cm^{-1} to the translational and rotational vibrations of the $\text{Sc}_3\text{N-C}_{80}$ bonds. Theoretical calculations by other workers [1573, 1574] predict that the symmetry of the whole molecule remains to be \mathbf{I}_h since the Sc_3N moiety can rotate freely inside the cage.

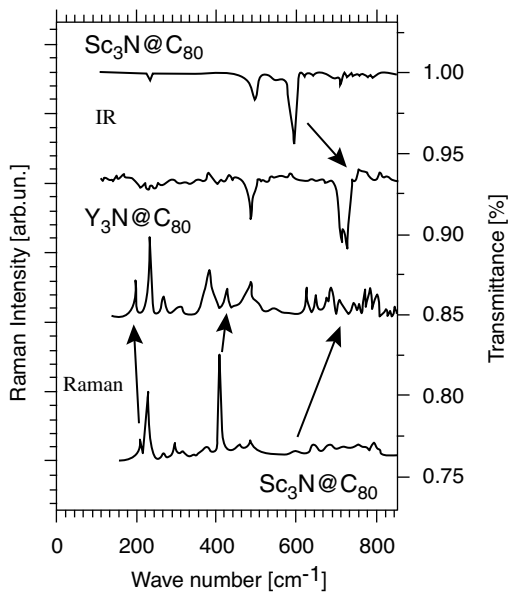


Fig. 2.53. Low-frequency IR and Raman (647 nm excitation) spectra of $\text{Sc}_3\text{N}@C_{80}$ and $\text{Y}_3\text{N}@C_{80}$ at 300 K [1572].

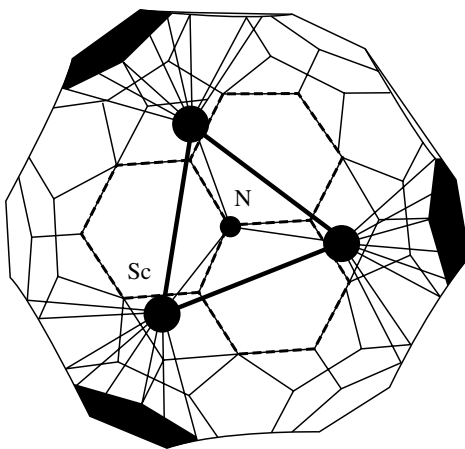


Fig. 2.54. Calculated optimized structure of $\text{Sc}_3\text{N}@C_{80}$. The C_{80} pentagons closest to the Sc atoms are blackened, and the shortest Sc–C distances are shown by solid lines [1572].

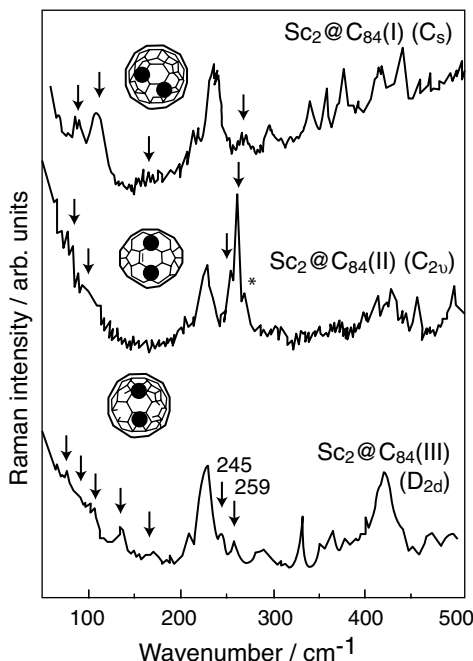


Fig. 2.55. Structures and Raman spectra of three isomers of $\text{Sc}_2\text{@C}_{84}$ at room temperature. The metal cage modes are indicated by arrows, and the band marked by the asterisk is due to C_{60} contamination [1575].

There are 24 isomeric structures for C_{84} [1565]. Inakuma et al. [1575] isolated three isomers of $\text{Sc}_2\text{@C}_{84}$ and determined their symmetries (C_s , C_{2v} , and D_{2d} for isomers I, II, and III, respectively) by ^{13}C NMR spectroscopy. Figure 2.55 shows the structures and Raman spectra of these three isomers. Assignments of the metal–cage vibrations were based on a simple linear three-mass oscillator model. In the case of isomer III, the $\text{Sc}-\text{C}_{84}$ vibrations were assigned at $\sim 250\text{ cm}^{-1}$ (ν_s), $\sim 170\text{ cm}^{-1}$ (ν_a) and $140\text{--}70\text{ cm}^{-1}$ (δ), and the calculated $\text{Sc}-\text{C}_{84}$ stretching force constant was 1.19 dyn/cm [1575a].

2.14.5. Nanotubes

Carbon nanotubes prepared by several methods are mixed with nanoparticles, amorphous carbon, fullerenes, and other contaminants [1576]. Nanotubes isolated from the mixture contain single-walled (SWNT) as well as multiwalled (MWNT) nanotubes. In general, the diameter of a SWNT is on the order of several nanometers, but the length can be several microns. Thus far, spectroscopic (mainly Raman) studies have been focused on SWNTs of small diameters ($<2\text{ nm}$) that become metallic or semiconducting depending on their diameter and chirality. Chemical and physical

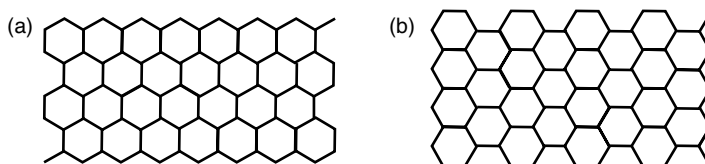


Fig. 2.56. (a) "Armchair" form and (b) "zigzag" form.

properties of carbon nanotubes have been reviewed by Dresselhaus et al. [1537] and Saito et al. [1576].

The structure of a SWNT is derived by rolling a graphite sheet into the shape of a cylindrical tube. The atomic coordinates of a one-dimensional unit cell of a nanotube are defined by using indices n, m [1537]. Depending on the direction of rolling along the long axis, two types of nanotubes of different symmetry are obtained. In Fig. 2.56, the long axis is in the horizontal direction; panels (a) and (b) show "armchair" (n, n) and "zigzag" ($n, 0$) configurations, respectively. Although not shown, the chiral form ($m \neq n$) is also known.

Rao et al. [1577] measured the Raman spectra of a bundle of SWNTs (mostly of the armchair configuration with different diameters) by changing the exciting laser wavelength. As seen in Fig. 2.57, the intensity ratio of the peak at $\sim 186\text{ cm}^{-1}$ (totally symmetric tube breathing mode, ν_b) relative to that at $\sim 1592\text{ cm}^{-1}$ (a composite of nontotally symmetric tube breathing modes) varies from 1: 2.3 at 514.5 nm excitation, to ~ 2 : 1 at 1064 nm excitation and to 1: 20 at 1320 nm excitation. This dramatic dependence of Raman intensity on the exciting wavelength clearly indicates the "resonance Raman scattering" discussed earlier for metalloporphyrins (Sec. 1.22). Furthermore, the ν_b band observed at 186 cm^{-1} by 514.5 nm excitation is shifted to 180 cm^{-1} by 1064 nm excitation. The dependence of this and other frequencies on the laser wavelength suggests that nanotubes of different diameters can be selectively resonance-enhanced by choosing proper exciting lines. Theoretical calculations predict that, as the tube diameter (d) decreases, the ν_b frequency increases and the electronic absorption maximum of a tube shifts to a higher energy. Figure 2.58 is a theoretical plot of the calculated ν_b versus $1/d$, which yields a straight line regardless of the symmetry type of the tube [1577a]. Thus, the frequency of the ν_b mode that can be resonance-enhanced is useful in estimating the diameter of a carbon nanotube.

2.14.6. Diamond and Graphite

Diamond and graphite are two crystalline forms of C_{∞} . In the former, carbon atoms are tetrahedrally bonded to four equivalent neighbors with a C—C bond distance of 1.54 \AA throughout the crystal (Fig. 2.59a). The primitive unit cell of diamond belongs to the factor group O_h^7 and contains two carbon atoms [1578]. Then, at $k = 0$ (Sec. I-30), only three ($3 \times 2 - 3$) vibrations are expected. These vibrations belong to a triply degenerate F_{2g} species that is Raman-active. In agreement with this prediction, the Raman

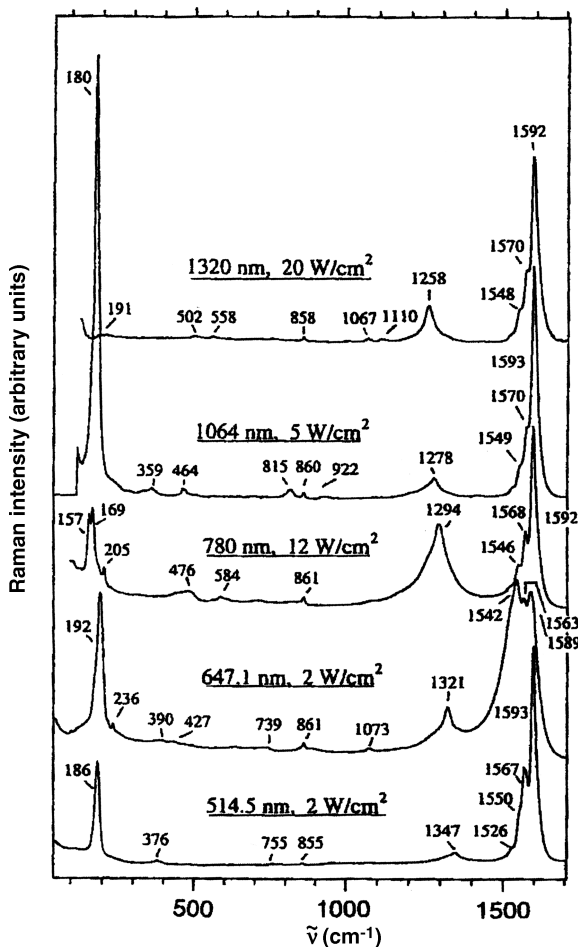


Fig. 2.57. Raman spectra of a bundle of SWNTs excited by different laser wavelength (room temperature). Laser wavelength and power density used for each spectrum are indicated [1577].

spectrum of diamond exhibits only one sharp band at 1332 cm^{-1} [1579]. In high-pressure Raman spectroscopy, this band has practical utility as a pressure sensor for a diamond anvil cell [1580]; its frequency has been measured as a function of pressure and temperature up to 15 GPa and 400°C , respectively [1581]. Thick crystals used for diamond anvil cells [1580] show IR absorptions: type I diamond at ~ 2000 and $\sim 1200\text{ cm}^{-1}$; type II diamond only at $\sim 2000\text{ cm}^{-1}$ [1582]. Thus, the latter is preferred for high-pressure IR studies. The absorptions at ~ 2000 and $\sim 1200\text{ cm}^{-1}$ are attributed to N_2 -induced defects and multiphonon effects, respectively [1583].

A hydrogen-doped diamond single crystal exhibits a $\nu(\text{C-H})$ band at 2834.1 cm^{-1} in IR spectra, indicating the formation of C-H bonds on the diamond surface [1584].

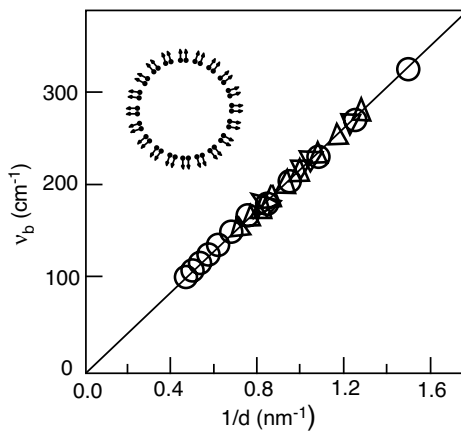
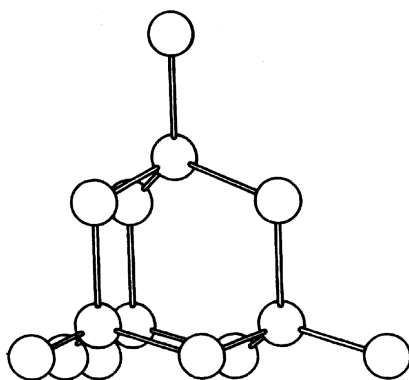
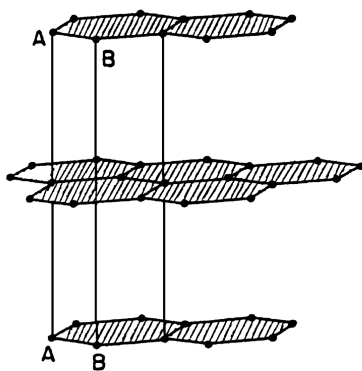


Fig. 2.58. A plot of calculated ν_b versus tube diameter for “armchair” (σ), “zigzag” (Δ), and “chiral” (∇) tubes. The normal mode of ν_b vibration is shown in upper left corner [1577a].



(a)



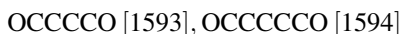
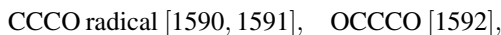
(b)

Fig. 2.59. Structures of diamond (a) and graphite (b).

In graphite, sheet structures are formed by linking each carbon atom to three equivalent neighbors in a trigonal planar fashion (C–C distance, 1.42 Å), and all sheets are parallel to each other with a distance of 3.35 Å, as shown in Fig. 2.59b. If we consider the isolated sheet of D_{6h} symmetry, there are two carbon atoms in the repeat unit. Then, three ($3 \times 2 - 3$) vibrations are grouped into the B_{2g} (inactive) and E_{2g} (Raman) species [1585]. In fact, the Raman spectrum of graphite exhibits only one band at 1575 cm^{-1} [1586]. This observation suggests that the intersheet interaction can be ignored for vibrational analysis. As expected, graphite shows no IR absorption bands [1587].

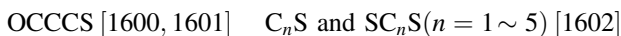
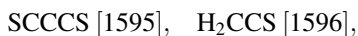
2.14.7. Inorganic Carbon Compounds

Carbon hydride radicals such as HCCC [1588] and HCCCC [1589] are of great interest in astronomy. The IR spectra of these radicals have been measured in Ar matrices. Their structures may be linear or cyclic. Boron carbides such as BC_3 and B_2C_2 are linear, and their IR spectra in Ar matrices have been assigned [1589a]. The IR spectra of carbon oxides are reported for the following compounds:



The structures of these oxides may be linear or pseudolinear. The C_4O_2 molecule may be linear or bent, depending on the electronic state.

The IR spectra and band assignments of several carbon sulfides have also been reported:



The structures of these molecules are linear.

The three carbon oxide anions, $C_3O_3^{2-}$ [1603], $C_4O_4^{2-}$ [1604], and $C_5O_5^{2-}$ [1604], take the planar ring structures shown in Fig. 2.60. Because of aromaticity of these rings, their IR spectra exhibit the C=O stretching vibrations below 1600 cm^{-1} , which are much lower than those of normal ketones ($\sim 1700\text{ cm}^{-1}$).

Complete band assignments are also available for the $C_4S_4^{2-}$ ion, which assumes a structure similar to that of the $C_4O_4^{2-}$ ion shown above [1605]. The vibrational spectra of the $C_3X_3^+$ ion ($X = \text{Cl}, \text{Br}, \text{I}$) have been assigned in terms of a D_{3h} structure similar to that of the $C_3O_3^{2-}$ ion [1606]. The $C(\text{CN})_3^-$ ion takes a planar D_{3h} structure, and its vibrational spectra have been assigned completely [1607].

Vibrational spectra are reported for $F_3C-C\equiv SF_3$ [$\nu(C\equiv S)$ 1800 cm^{-1}] [1608], $(CF_3)_2(SF)^+$ [1609], and $(Cl_3C)-SCl$ [1610].

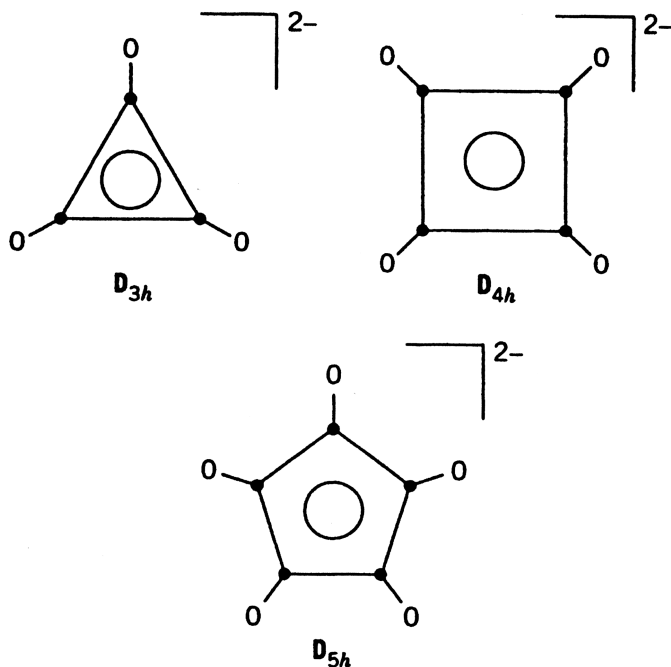


Fig. 2.60. Structures of carbon oxide anions.

2.15. COMPOUNDS OF SILICON, GERMANIUM, AND OTHER GROUP IVB ELEMENTS

2.15.1. Small Silicon Compounds

Recently, small silicon clusters such as Si_4 , Si_6 and Si_7 have been isolated and their structures determined by comparing Raman spectra predicted from *ab initio* quantum mechanical calculations with those observed in N_2 matrices [1611]. The numbers of Raman-active fundamentals should be three, five, and five for the predicted structures of a planar Si_4 rhombus (D_{2h}), a distorted Si_6 octahedron (D_{4h}), and a pentagonal bipyramidal Si_7 (D_{5h}), respectively. Figure 2.61 shows the Raman spectra of these clusters as obtained by Honea et al. [1611]. It is seen that the observed spectra are in excellent agreement with the theoretical spectra, except for the B_{3g} mode of Si_4 (which may be hidden under the strong A_g band). The matrix IR spectra of these Si_n clusters have been reported [1612]. In contrast to Si_4 , the Si_4^{4-} ion is tetrahedral (T_d), as its Raman spectrum shows the $\nu_1(A_1)$, $\nu_2(E)$, and $\nu_3(F_2)$ vibrations at 482, 285, and 356 cm^{-1} , respectively [1613].

The IR spectra of SiC_4 (linear) [1614], Si_2C_2 (rhombic) [1615], Si_2C_3 (linear) [1616], Si_3C (rhomboidal) [1617], and Si_3C_2 (pentagonal) [1618] have been assigned.

Silanes, such as Si_5H_{10} and Si_6H_{12} , take nonplanar ring structures consisting of the SiH_2 units. The vibrational spectra of these silanes have been assigned on the basis of

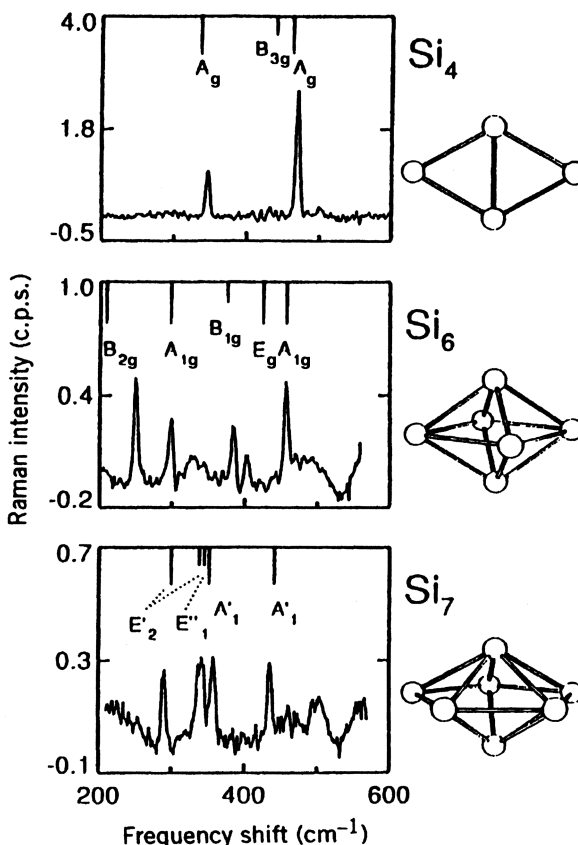


Fig. 2.61. Raman spectra of Si_4 , Si_6 , and Si_7 deposited in a N_2 matrix, along with their predicted structures and Raman-allowed vibrational frequencies and intensities [1611].

normal coordinate analysis assuming D_{5h} and D_{3d} symmetries, respectively [1619,1620]. Figure 2.62 shows the IR and Raman spectra of Si_6H_{12} obtained by Hassler et al. [1620]. Vibrational spectra and band assignments are reported for many other compounds: Si_3H_8 [1621], $\text{H}_2\text{Si}=\text{CH}_2$ [$\nu(\text{Si}=\text{C})$, 985 cm^{-1}] [1622], *trans*- $\text{RClSi}=\text{SiClR}$ [$\nu(\text{Si}=\text{Si})$, 589 cm^{-1} , $\text{R}=[^t\text{Bu}_3\text{Si}]_2\text{MeSi}$] [1623], *n*- $\text{Si}_4\text{Cl}_{10}$ [1624], $(\text{Cl}_2\text{H Si})_2\text{NH}$ [1625], $[(\text{CH}_3)_2\text{his}]_2\text{O}$ [1626], $(\text{H}_3\text{Si})_3\text{N}$ [1627], $(\text{H}_3\text{Si})_2\text{O}$ [1628], $(\text{H}_3\text{Si})_2\text{S}$ [1629], $(\text{H}_3\text{Si})\text{PH}_2$ [1630], $(\text{H}_3\text{Si})_4\text{N}_2$ [1631], $(\text{Cl}_3\text{Si})_2\text{NH}$ [1632], and $\text{Si}_2(\text{NCO})_6$ [1633]. It should be noted that trisilylamine is trigonal-planar while tetrasilylhydrazine takes a twisted D_{2d} structure (the dihedral angle is $\sim 90^\circ$).

2.15.2. Silicon–Oxygen Compounds, Silicates, and Silica

Vibrational spectra of relatively small silicon–oxygen compounds are reported for $(\text{SiO})_n$ ($n = 2,3,4$) [1634], $(\text{SiO}_3)_n$ ($n = 3,4,6$) [1635], $\text{H}_8(\text{Si}_8\text{O}_{12})$ (O_h in solution)

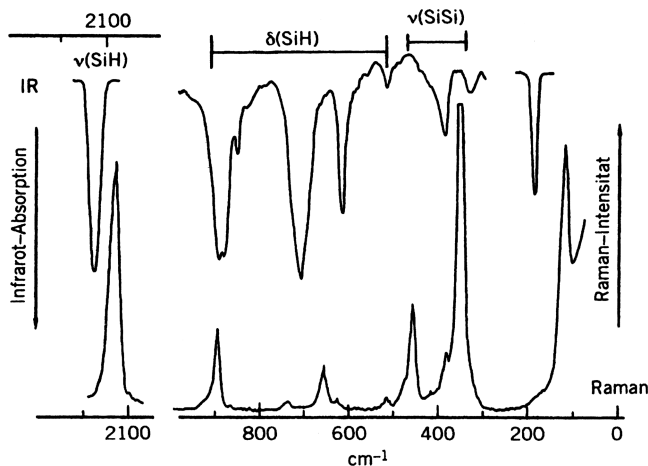
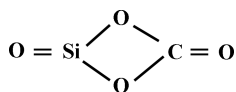


Fig. 2.62. IR and Raman spectra of Si_6H_{12} [1620].

[1636], $\text{Si}(\text{OCH}_3)_4$ [1637], $\text{Si}(\text{OC}_2\text{H}_5)_4$ [1638], and SiCO_4 [1639]. The IR spectrum of the last compound is consistent with the structure of C_{2v} symmetry:



Vibrational spectra of orthosilicates (SiO_4^{4-}) and pyrosilicates ($\text{Si}_2\text{O}_7^{6-}$) have been discussed in preceding sections. Higher silicates assume the variety of structures as shown in Fig. 2.63. Etchepare [1640] has assigned the vibrational spectra of these silicates using normal coordinate calculations. In general, the tetrahedral SiO_4 unit in these silicates exhibits the four fundamentals in the following regions: $\nu_1(A_1)$, $750\text{--}830\text{ cm}^{-1}$; $\nu_2(E)$, $300\text{--}400\text{ cm}^{-1}$; $\nu_3(F_2)$, $800\text{--}1000\text{ cm}^{-1}$; $\nu_4(F_2)$, $450\text{--}600\text{ cm}^{-1}$. According to McMillan [1641], the structural units in silicate glasses can be distinguished by Si—O stretching frequencies in Raman spectra:

Four terminal oxygens (SiO_4^{4-})	$\sim 850\text{ cm}^{-1}$
Three terminal oxygens ($\text{Si}_2\text{O}_7^{6-}$)	$\sim 900\text{ cm}^{-1}$
Two terminal oxygens ($\text{Si}_3\text{O}_9^{6-}$, chains)	$950\text{--}1000\text{ cm}^{-1}$
One terminal oxygen (sheets)	$1050\text{--}1100\text{ cm}^{-1}$

Aluminosilicates $[(\text{Al}, \text{Si})\text{O}_2]_n$, such as zeolites, exhibit AlO vibrations ($750\text{--}650\text{ cm}^{-1}$) in addition to SiO vibrations [1642]. Their vibrational spectra and structure have been reviewed by Lazarev [1643]. Condrate [1644,1645] reviewed the vibrational spectra of a variety of glasses.

Quartz— $(\text{SiO}_2)_\infty$ —is a three-dimensional polymer in which the SiO_4 units are linked throughout the crystal. The vibrational spectra of α -quartz (including the ^{30}Si

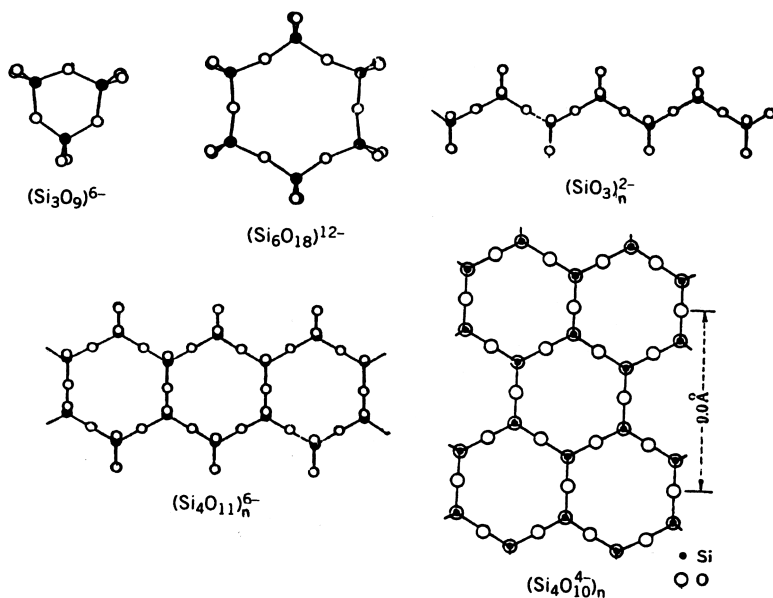


Fig. 2.63. Structures of silicates.

and ^{18}O derivatives) [1646] and β -quartz [1647] have been assigned according to their factor groups (\mathbf{D}_3 and \mathbf{D}_6 , respectively). Figure 2.64 shows the IR and Raman spectra of α -quartz obtained by Sato and McMillan [1646].

Vibrational spectra of silicon compounds have been reviewed by Smith [1648], Aylett (silicon hydrides) [1649], and Campbell-Ferguson and Ebsworth (halogenosilane-amine adducts) [1650].

2.15.3. Compounds of Germanium and Tin

Vibrational spectra of Ge_4^{4-} (\mathbf{T}_d) [1651], Ge_5^{2-} (\mathbf{D}_{3h}) [1652], Ge_9^{4-} (\mathbf{C}_{4v}) [1653] ($\text{H}_3\text{Ge})_3\text{M}$ ($\text{M} = \text{As}, \text{Sb}$) [1654] and $(\text{Ge}_4\text{Si}_{10})^{4-}$ (cage structure, \mathbf{T}_d) [1655] have been measured to confirm their structures. Vibrational spectra of small tin compounds such as Sn_5^{2-} (trigonal-bipyramidal, \mathbf{D}_{3h}) [1656], and $\text{Sn}_2\text{Se}_3^{2-}$ (\mathbf{D}_{3h}) [1657] are also available. Schumann [1658] reviewed the $\nu(\text{Ge}-\text{P})$ vibrations of a number of germanium compounds.

2.16. COMPOUNDS OF NITROGEN

2.16.1. Oxides

References on vibrational spectra of NO , NO_2 , NO_3 , N_2O , and N_2O_2 are given in preceding sections. The compound N_2O_3 takes the asymmetric form in the gaseous

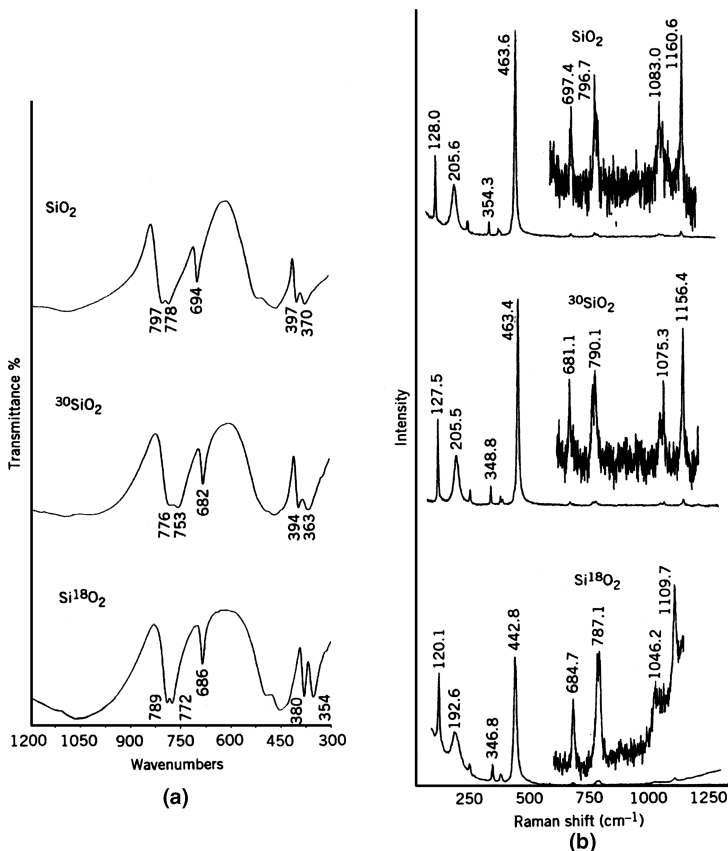
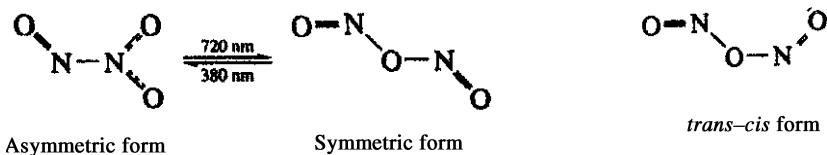


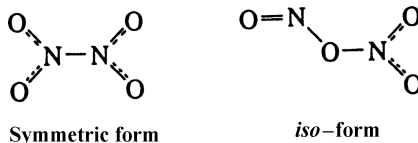
Fig. 2.64. IR (a) and Raman (b) spectra of α -quartz, SiO_2 , $^{30}\text{SiO}_2$, and Si^{18}O_2 [1646].

state, and its IR spectrum has been assigned on the basis of C_s symmetry [1659]:



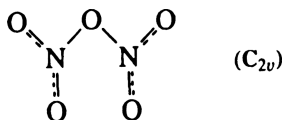
In N_2 matrices, however, the asymmetric form can be converted to the symmetric form by irradiation near 720 nm, and this form is reconverted to the asymmetric form by irradiation near 380 nm. The IR frequencies of both forms have been reported by Varette and Pimentel [1660]. Later, a new *trans-cis* form was found in an Ar matrix [1661], and the vibrational frequencies of the three forms were compared [1662].

As stated in Sec. 2.10, N_2O_4 is a mixture of the three isomers: a planar (D_{2h}) and its twisted ($\sim 90^\circ$, D_{2d}) forms and the *iso* form:



The IR spectrum of the latter has been assigned [1663]. The IR spectra of well-ordered [1664] and amorphous N_2O_4 (D_{2h}) films [1665] have been reported.

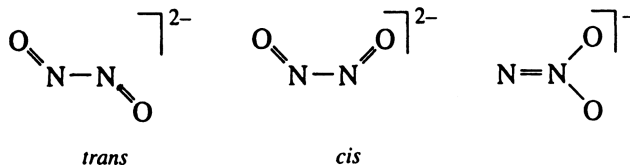
Although N_2O_5 assumes a planar structure in the gaseous state, it becomes an ionic crystal consisting of the NO_2^+ (nitronium) and NO_3^- ions:



Assignment of the IR spectrum of N_2O_5 in an Ar matrix has been based on a nonplanar form of C_2 symmetry [1666]. According to Raman studies, N_4O_2 obtained by the reaction of NaN_3 and $(\text{NO}_2)\text{SbF}_6$ is $\text{O}_2\text{N}-\text{N}_3$. It exhibits the $\nu_a(\text{NO}_2)$ and $\nu_s(\text{NO}_2)$ vibrations at 1556 and 1151 cm^{-1} , respectively, and the $\nu_a(\text{N}_3)$ and $\nu_s(\text{N}_3)$ vibrations at 2107 and 1060 cm^{-1} , respectively [1667]. The IR spectra of NO in liquid Ar ($84\text{--}105\text{ K}$) show the vibrations due to all the oxides mentioned above [1668]. DFT calculations were made on a variety of nitrogen oxides [1669], and possible isomeric structures of covalently bound N_3O_2 were suggested [1670].

2.16.2. Oxo Ions

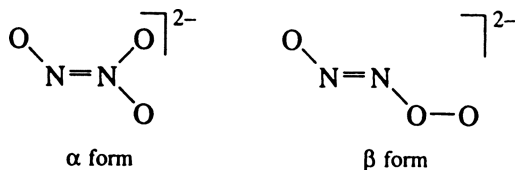
References on NO^+ , NO^- , NO_2^+ , NO_2^- , and NO_3^- ions are cited in preceding sections. The NO_4^{3-} ion is tetrahedral, and its IR and Raman spectra have been reported [1671]. As stated in Sec. 2.5, the $\text{N}_2\text{O}_2^{2-}$ ion takes the *cis* and *trans* forms while the N_2O_2^- ion obtained in Ar matrices may take a structure containing a terminal $\text{N}=\text{N}$ bond:



In the $\text{X}[\text{N}(\text{O})\text{NO}]^-$ ($\text{X} = \text{SO}_3^-, \text{O}^-, \text{Ph}, \dots$) series, all their $\text{O}-\text{N}-\text{N}-\text{O}$ systems are essentially planar with *cis* oxygens and show considerable double-bond character of the

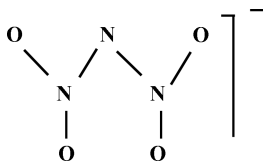
N—N linkages. Their IR and Raman spectra were assigned on the basis of $^{14/15}\text{N}$ isotope shifts and DFT calculations [1672].

The $\text{N}_2\text{O}_3^{2-}$ ion in $\text{Na}_2(\text{N}_2\text{O}_3)$ takes two forms:



The IR and Raman spectra of the former have been reported [1673].

The Raman spectrum of the dinitramide ion, $[\text{N}(\text{NO}_2)_2]^-$, is consistent with the twisted, nonplanar structure of C_1 symmetry shown below [1674]:



Vibrational spectra of nitrogen oxides and oxo ions have been reviewed extensively by Laane and Ohlsen [1675].

2.16.3. Halogeno Compounds

Figure 2.65 shows the structures of halogeno compounds for which complete vibrational assignments are found in the references cited. Other halogeno compounds

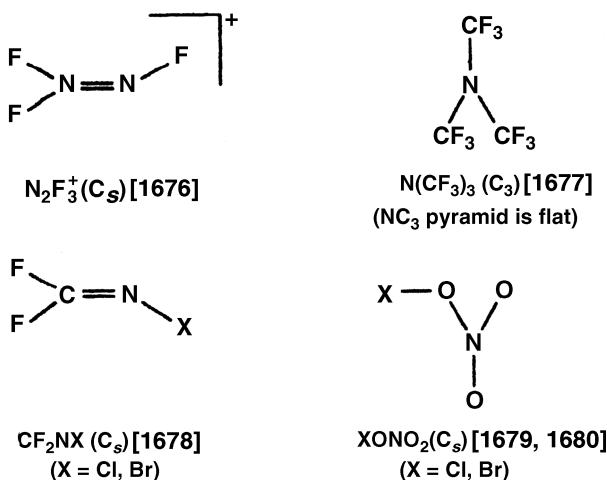


Fig. 2.65. Structures of halogeno compounds of nitrogen.

include $\text{CF}_3\text{C}(\text{O})\text{NCO}$ [1681], $\text{CF}_3\text{O}(\text{ONO}_2)$ [1682], $\text{F}_2\text{C}=\text{NH}$ [1683], $[\text{Cl}_2\text{C}=\text{NHCl}]^+$ [1684], $\text{O}_2\text{Cl}(\text{ONO}_2)$ [1685], and $\text{BrC}(\text{O})\text{NCO}$ [1686].

2.16.4. Amino Compounds

Figure 2.66 shows the structures of nitrogen compounds containing amino groups.

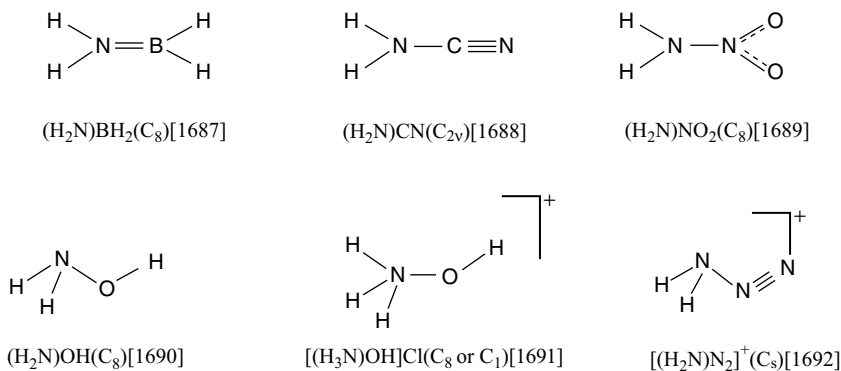


Fig. 2.66. Structures of nitrogen compounds containing amino groups.

Complete band assignments are found in the references cited. Figure 2.67 shows the IR spectrum of the heated vapor of cyanamide (H_2NCN) obtained by Birk and Winnewisser [1688]. It also shows some bands due to the tautomer, carbodiimide (HNCNH), which is more stable at lower temperatures.

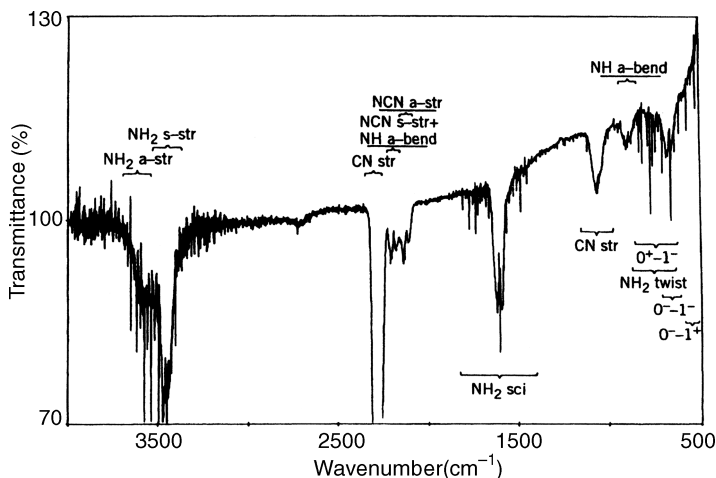
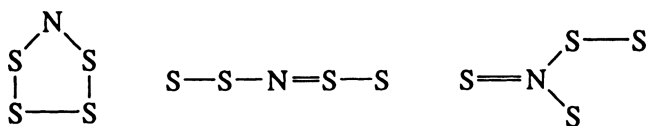


Fig. 2.67. IR spectrum of heated cyanamide vapor. The underlined approximate descriptions refer to absorptions due to the HNCNH tautomer [1688].

2.16.5. Sulfides and Selenides

The NS_4^- ion may be a cyclic ring, a linear chain, or a branched chain:



The IR/Raman spectra suggest the last structure [1693]. Figure 2.68 shows the ring structures of six compounds containing nitrogen and sulfur or selenium atoms for which vibrational frequencies and band assignments are available. It is possible to produce several isomers by replacing their sulfur atoms partly with selenium atoms. For example, $\text{N}_2\text{S}_3\text{Se}$ takes a half-chair conformation, and can have three isomers of

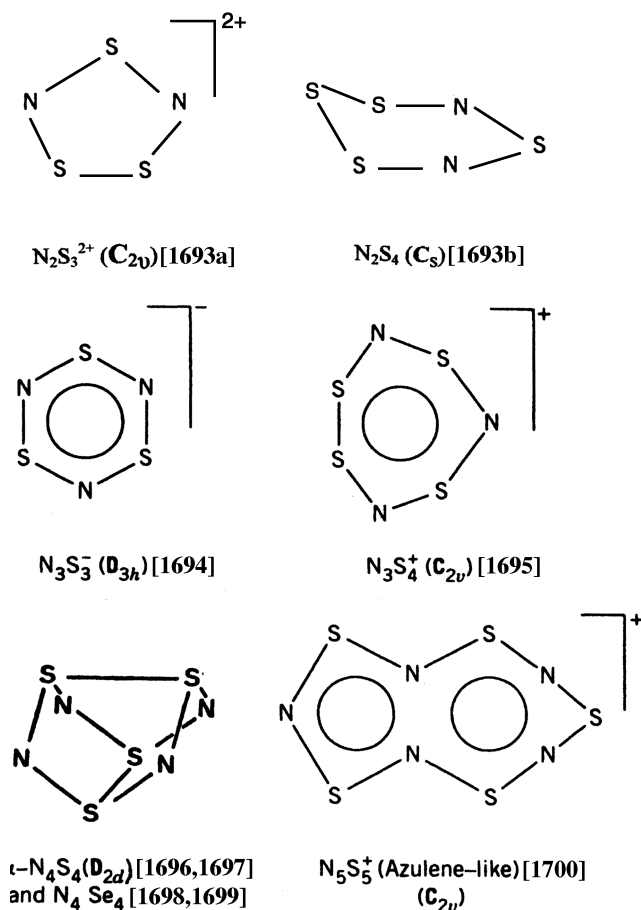


Fig. 2.68. Structures of nitrogen sulfides and selenides.

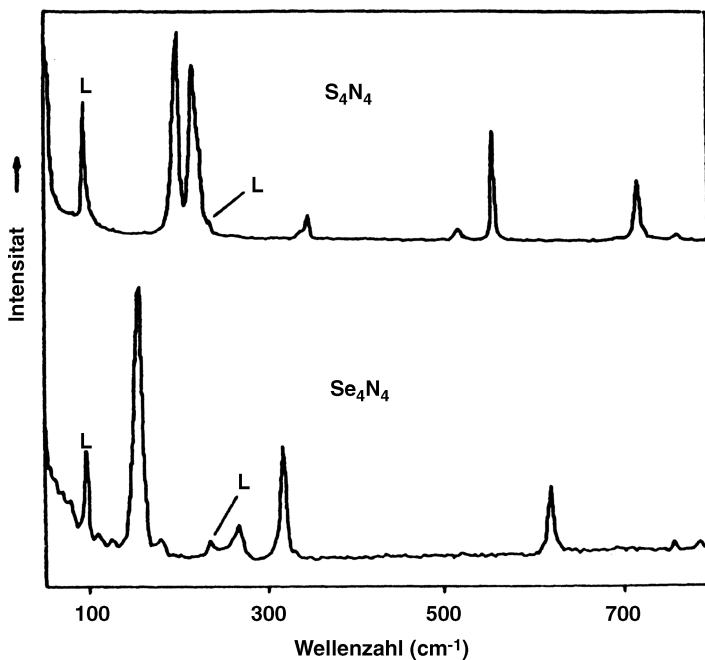


Fig. 2.69. Raman spectra (647 nm excitation) of N_4S_4 (crystal) and N_4Se_4 (powder) (L indicates laser lines) [1699].

C_1 , C_s , and C_2 symmetry depending on the position of a selenium atom in the ring, and their distinction has been made by theoretical calculations of vibrational frequencies [1693b]. N_4S_4 and N_4Se_4 assume a cage structure of D_{2d} symmetry, and their 18 ($3 \times 8 - 6$) normal vibrations are classified into $3A_1$ (R) + $2A_2$ (inactive) + $2B_1$ (R) $3B_2$ (IR, R) + $4E$ (IR, R). These vibrations have been assigned completely on the basis of normal coordinate calculations [1696]. Figure 2.69 shows the Raman spectra of N_4S_4 and N_4Se_4 obtained by Gowik and Klapötke [1699]. A highly unusual azulene-like structure of the $N_5S_5^+$ ion has been determined by X-ray analysis and characterized by IR spectroscopy [1700].

According to the electron diffraction study, *N*-cyanoimidosulfurous difluoride, (NC)–N=SF₂, takes a *syn* conformation in which the C≡N group is *syn* with respect to the bisector of the SF₂ angle (C_s symmetry). The IR and Raman spectra were assigned on the basis of normal coordinate analysis and DFT calculations [1701].

2.17. COMPOUNDS OF PHOSPHORUS AND OTHER GROUP VB ELEMENTS

Vibrational spectra of phosphorus compounds have been reviewed extensively [1702–1705]. Figure 2.70 shows a group frequency chart based on these review articles.

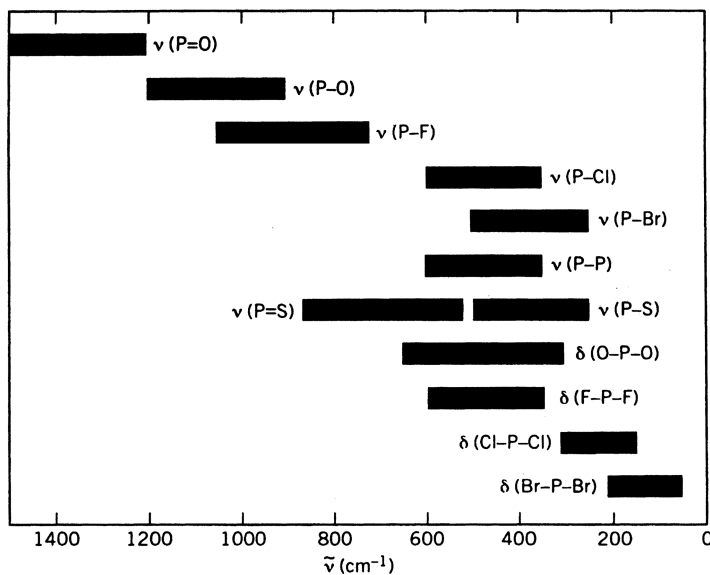


Fig. 2.70. Group frequency chart of phosphorus compounds.

Group frequency charts in Appendix VIII indicate the regions for $\nu(\text{PH})$, $\nu(\text{PO})$, and $\nu(\text{PX})$ (X: a halogen).

2.17.1. Phosphorus Clusters

Figure 2.71 shows the structures of phosphorus clusters for which vibrational assignments are available.

The Raman frequencies of the tetrahedral P_4 cluster are given in Sec. 2.5.1. The Raman spectrum of the $\text{Ag}(\text{P}_4)_2^+$ ion indicates that two $\eta^2\text{-P}_4$ ligands coordinate to the Ag^+ ion in D_{2h} symmetry [1706]. The P_5^- ion takes a planar ring structure of D_{5h} symmetry, and the medium-intensity Raman (polarized) band at 463 cm^{-1} and the strong IR band at 815 cm^{-1} have been assigned to the A'_1 and E'_1 species, respectively [1707]. The P_6^{4-} ion takes a planar ring structure of D_{6h} symmetry, and exhibits three Raman bands at $356 (A_{1g})$, $507 (E_{2g})$, and $202 (E_{2g}) \text{ cm}^{-1}$ [1708]. In the crystalline state, its symmetry is lowered to D_{2h} . The IR and Raman spectra of the P_8^{10-} ion in $\text{Ca}_5[\text{P}_8]$ were assigned on the basis of C_{2h} symmetry [1709]. The P_{11}^{3-} ion takes a cage structure of D_3 symmetry, and its 27 ($3 \times 11 - 6$) vibrations are classified into $5A_1 (\text{R}) + 4A_2 (\text{IR}) + 9E (\text{IR, R})$. Complete band assignments have been based on normal coordinate analysis of this ion [1710].

2.17.2. Oxides and Oxo Ions of Phosphorus

Reactions of P_2 and O_3 in inert gas matrices yield a variety of oxides, PO , PO_2 , P_2O , P_2O_2 , P_2O_3 , P_2O_4 , P_2O_5 , and PO_2^- for which the key bands of each species have been

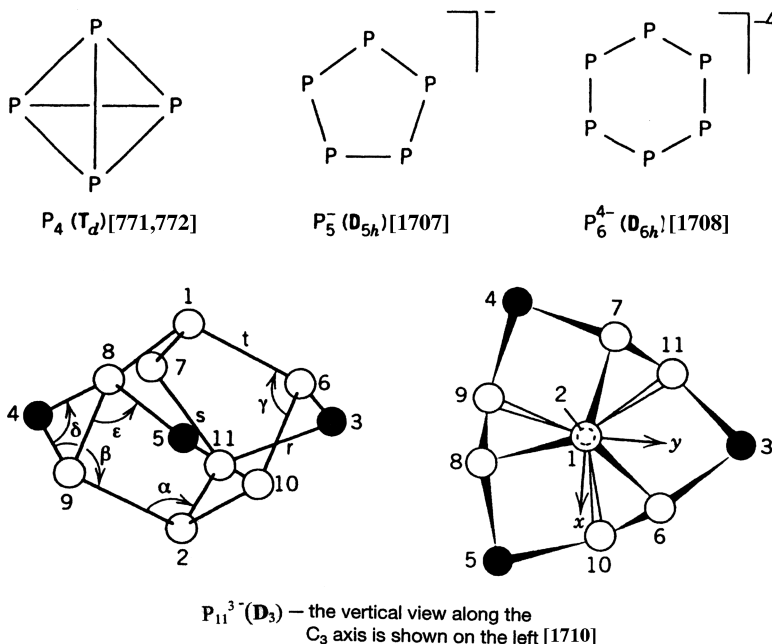


Fig. 2.71. Structures of phosphorus clusters.

identified in IR spectra [1711]. The IR spectrum of P_4O_{10} has been assigned on the basis of the cage structure of T_d symmetry [1712]. The higher oxo-ions take the ring structures shown in Fig. 2.72.

The vibrational frequencies of the $P_2O_7^{4-}$ ion are given in Sec. 2.11.1. The vibrational spectra of the $P_3O_9^{3-}$ ion have been assigned on the basis of D_{3h} symmetry [1713]. Although the highest symmetry expected for the $P_4O_{12}^{4-}$ ring is D_{4h} , the spectra obtained in the crystalline state suggest lowering of symmetry to S_4 , C_{2h} , C_{2v} , and so on [1714–1716]. For example, it is S_4 in the aluminium salt, and C_{2h} in the ammonium salt [1715]. The IR/Raman spectra are reported for the $P_{10}O_{30}^{10-}$ ion, which takes a “cradle” structure of C_2 symmetry [1717,1718]. Vibrational assignments of $P_4O_6X_2$ ($X = O, S, Se$) based on C_{2v} symmetry are reported [1719].

2.17.3. Sulfides and Selenides of Phosphorus

Phosphorus sulfides and selenides assume a variety of cage structures, as shown in Fig. 2.73. The compound α - P_4S_3 belongs to the point group C_{3v} , and its 15 ($3 \times 7 - 6$) vibrations are grouped into $4A_1$ (IR, R) + A_2 (inactive) + $5E$ (IR, Raman). These vibrations have been assigned completely based on normal coordinate analysis [1720]. Raman spectra are reported and assigned for α - P_4S_4 [1721], which takes the same structure as that of N_4S_4 , discussed in the preceding section [1696]. Gardner [1722] measured the IR and Raman spectra of P_4S_3 , P_4S_5 , P_4S_7 , and P_4S_{10} in solids, melts, and vapors. Except for P_4S_3 , these compounds decompose in melts and vapors. The

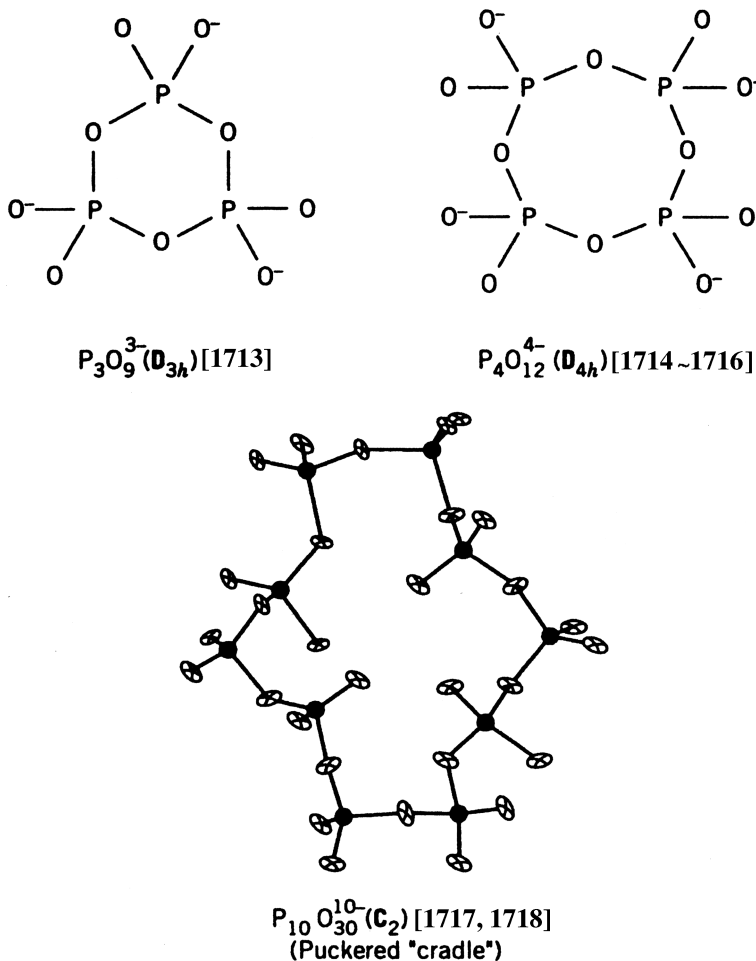


Fig. 2.72. Structures of phosphorus oxide anions.

compound P_4S_5 has no symmetry, and its 21 ($3 \times 9 - 6$) vibrations are all IR/Raman-active; P_4S_7 also has no symmetry. In the free state, P_4S_{10} belongs to the point group T_d , for which vibrational assignments have been made [1722].

Raman spectra and vibrational assignments are available for α - P_4S_3 [1723], which takes the same structure as α - P_4S_3 as well as for a series of $P_4S_xSe_{3-x}$ compounds ($x = 0, 1, 2$, and 3) [1724].

2.17.4. Phosphorus Compounds Containing Nitrogen

Figure 2.74 shows the structures of four nitrogen-containing phosphorus compounds for which complete vibrational assignments are available. The P_4N_4 skeleton of $P_4N_4Cl_8$ takes a skew-tub form at low temperatures and a skew-chair form at high

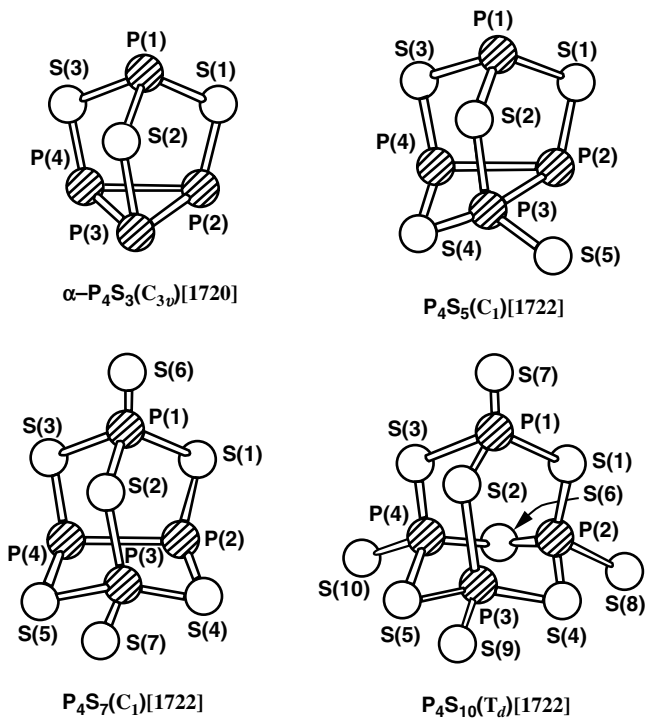
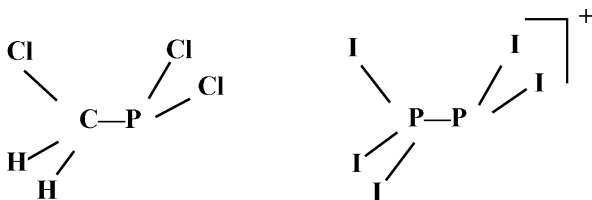


Fig. 2.73. Structures of phosphorus sulfides [1722].

temperatures. Varma et al. [1725] obtained the IR and Raman spectra of both forms (Fig. 2.75) and made complete assignments. Both $(\text{PNCl}_2)_3$ [1726] and $(\text{PNBr}_2)_3$ [1727] take a planar ring structure of D_{3h} symmetry. Although the highest symmetry expected for the $(\text{PO}_2\text{NH})_4^{4-}$ ion is D_{4h} , it is lowered to S_4 in solution and to C_{2h} , or S_4 in the solid state [1728]. $\text{P}(\text{CN})_3$ takes a pyramidal structure of C_{3v} symmetry [1729].

2.17.5. Halogeno Compounds

In the $[\text{Au}(\text{PF}_3)_2]^+$ ion (D_{3h}), the $\text{P}-\text{Au}-\text{P}$ bond is linear, and the $\nu(\text{Au}-\text{P})$ vibrations are at 227 (IR) and 231 cm^{-1} (Raman) [1730]. The vibrational spectra of $(\text{H}_2\text{Cl})\text{C}-\text{PCl}_2$ [1731] and the $[\text{P}_2\text{I}_5]^+$ ion [1732] have been assigned based on the C_s structures:



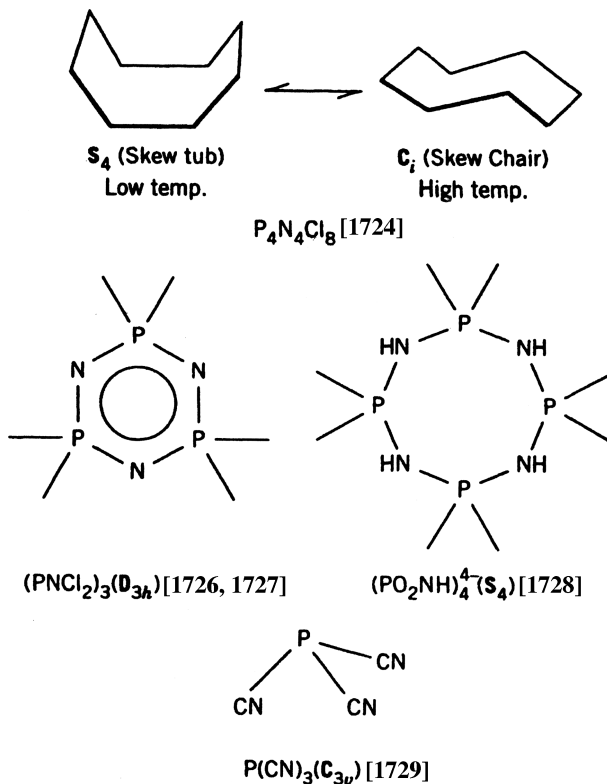


Fig. 2.74. Structures of phosphorus compounds containing nitrogen.

2.17.6. Phosphines and Other Phosphorus Compounds

Vibrational spectra of biphosphine (P_2H_4) [1733] (see also Sec. 2.10.1) and *n*-propylphosphine (${}^nPr-PH_2$) [1734] have been assigned. Metallophosphines, MPH_3 , $HMPH_2$, and H_2MPH ($M = Al, Ga, In$) were synthesized in Ar matrices and their IR spectra assigned [1735]. The IR and Raman spectra of a novel *trans*- $H_2PO_4^-$ ion were assigned by normal coordinate analysis based on a pseudo-octahedral model of D_{4h} symmetry [1736]. The $\nu(C\equiv P)$ vibrations of $H_3C-C\equiv P$ [1737] and $H_5C_6-C\equiv P$ [1738] are at 1543 and 1565 cm^{-1} , respectively.

2.17.7. Compounds of Arsenic, Antimony, and Bismuth

The vibrational frequencies of tetrahedral As_4 , Sb_4 , and Bi_4 molecules are tabulated in Sec. 2.5.1. The vibrational spectrum of the As_7^{3-} ion (cage structure of C_{3v} symmetry) has been assigned [1739]. The As_3^{3-} ion assumes a cage structure of D_3 symmetry similar to that shown previously for the P_{11}^{3-} ion, and its vibrational spectra have been

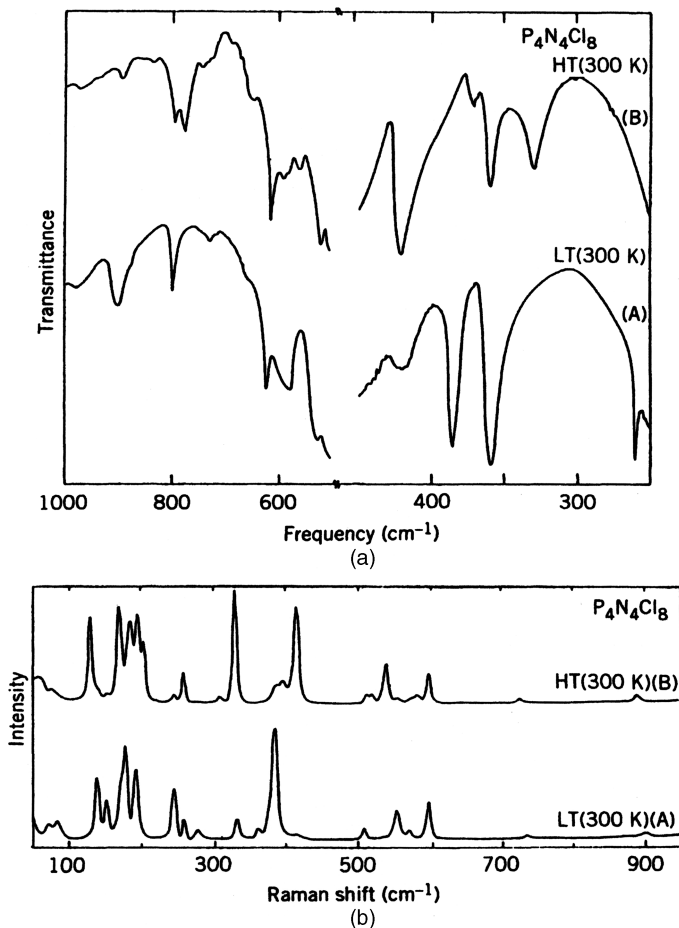


Fig. 2.75. IR (a) and Raman (b) spectra of the low- and high-temperature forms of solid $P_4N_4Cl_8$ measured at 300 K [1725].

assigned [1710]. The gas-phase Raman spectrum of As_4O_6 can be interpreted in terms of T_d symmetry [1740]. Factor group analysis on crystalline $(As_2O_3)_n$ has been carried out to give complete assignments of its IR/Raman spectra [1741]. Vibrational assignments are available for $As_3O_9^{3-}$ [1742] and $As(CN)_3$ [1729], which take the same structures as $P_3O_9^{3-}$ and $P(CN)_3$, respectively.

Gas-phase Raman spectra are reported for mixed As/P compounds such as As_3P (C_{3v}), As_2P_2 (C_{2v}), and AsP_3 (C_{3v}) [1743]. Far-IR spectra of the BiX_4^- , BiX_5^{2-} , and $Bi_2X_9^{3-}$ ions ($X = Cl, Br$) have been assigned empirically [1744]. Their structures in nonaqueous solutions may be C_{3v} or lower for BiX_4^- , a square-pyramid of C_{4v} symmetry for BiX_5^{2-} and a structure lower than D_{3h} for $Bi_2X_9^{3-}$.

2.18. COMPOUNDS OF SULFUR AND SELENIUM

Compounds of sulfur and selenium are of great interest for spectroscopists because of their unusual structures and strong Raman bands involving S—S or Se—Se bonds. Steudel and co-workers have made an extensive study on vibrational spectra of these compounds. Figure 2.76 shows a group frequency chart for sulfur compounds.

2.18.1. Sulfur Clusters

Vibrational frequencies of diatomic S_2 and S_2^{2-} and triatomic S_3 , S_3^{2-} , and S_3^{2-} are listed in Secs. 2.1 and 2.2, respectively. The IR spectra of the S_4 molecule produced in Ar matrices suggest the formation of two open-chain isomers [1745]. S_4 vapor consists of green-absorbing (λ_{\max} , 530 nm) and red-absorbing (560–660 nm) molecules. Raman spectra show that the former is a chain-like *trans*-planar molecule of C_{2h} symmetry whereas the latter is a branched-ring molecule [1746].

As is shown in Fig. 2.77 larger cluster molecules such as S_6 [1747], S_7 [1748], S_8 [1749], S_9 [1750], and S_{12} [1749] take puckered ring structures and their vibrational spectra have been reported. In general, the neutral molecules S_n ($n = 6-12$) take ring structures, while the anions S_n^{2-} ($n = 4-6$) take open-chain structures.

The S_4^{2-} ion assumes a nonplanar C_2 structure similar to that of H_2O_2 (dihedral angle, 98°), and its Raman spectrum has been assigned [1751]. In $(NH_4)_2S_5$, the S_5^{2-} ion assumes a helical chain of C_2 symmetry, while in Na_2S_5 , it takes a *cis* conformation of C_s symmetry. The Raman spectrum of the former has been assigned using normal coordinate analysis [1752]. The influence of the cation on the structures and spectra of these anions have been investigated [1753].

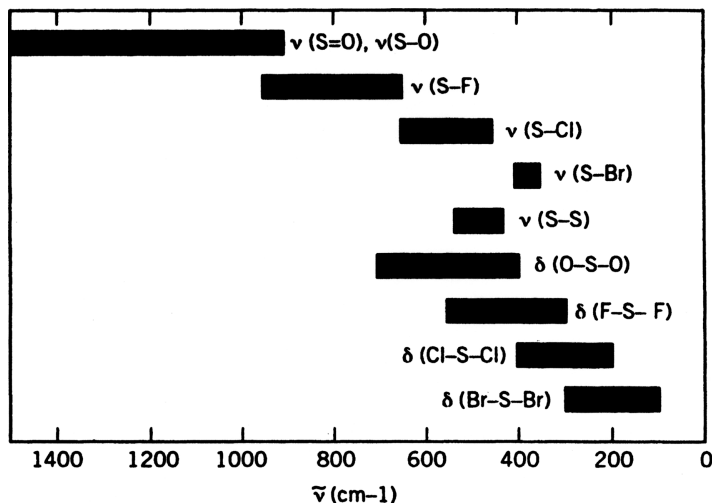


Fig. 2.76. Group frequency chart of sulfur compounds.

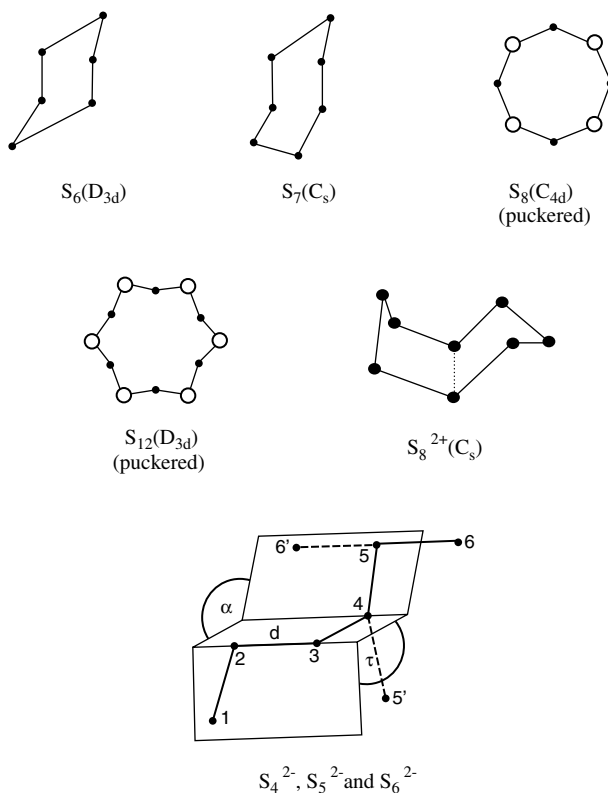


Fig. 2.77. Structures of sulfur clusters.

As shown in Sec. 2.5.1, cations such as S_4^{2+} assume a square-planar structure of D_{4h} symmetry. The Raman spectrum of the S_8^{2+} ion exhibits a cross-ring stretching vibration at 282 cm^{-1} reflecting a long *trans* annular S—S bond (dotted line in Fig. 2.77) [1754]. Table 2.2b (in Sec. 2.2.2) lists vibrational frequencies of bent SMS-type molecules that were produced by the reactions of laser-ablated metal atoms ($M = \text{Ti, Zr, Hf}$) [369] with sulfur vapor. Similar work was reported for other metals [1755]. The $[\text{In}(\text{S}_4)(\text{S}_6)\text{Cl}]^{2-}$ ion containing two chelating sulfur ligands exhibits the $\nu(\text{S—S})$ vibrations at 492 and 460 cm^{-1} [1756].

2.18.2. Sulfur Oxides

As is shown in Fig. 2.78, the $S_8\text{O}$ molecule is an eight-membered crown-shaped S_8 ring to which an oxygen atom is bonded (C_s symmetry). Steudel and coworkers have measured the IR/Raman spectra of $S_8\text{O}$ and made complete assignments based on normal coordinate analysis [1757,1758]. These workers also reported the Raman spectra of $S_9\text{O}$ and $S_{10}\text{O}$, which may acquire similar ring structures [1750]. The Raman

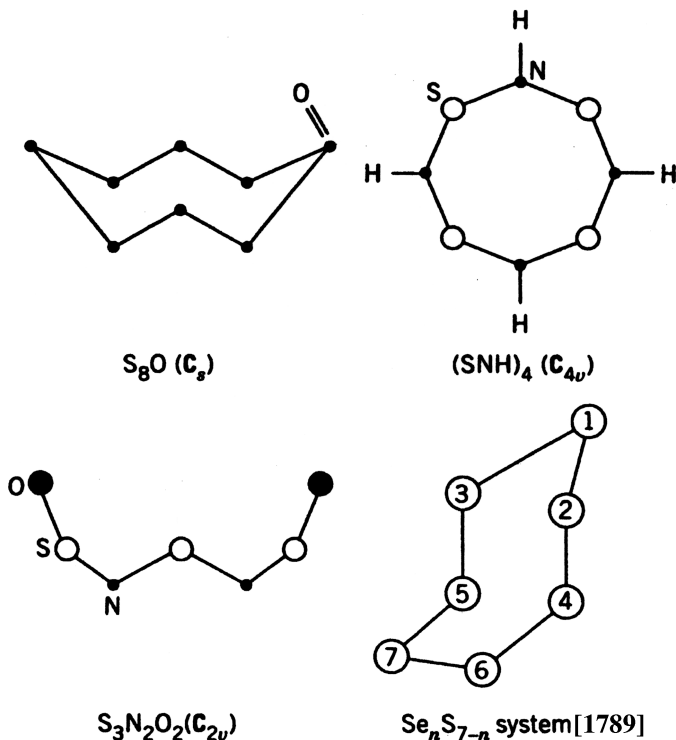


Fig. 2.78. Structures of sulfur compounds containing oxygen, nitrogen, and selenium.

spectrum of the disulfite ion, $S_2O_5^{2-}$, namely, $(O_3S-SO_2)^{2-}$, has been assigned in terms of C_s symmetry [1759].

2.18.3. Sulfur Acids

The IR and/or Raman spectra of $H_3S_2^+$, [1759a], H_2S_3 [1760], H_2S_4 [1760], $H_2SO_4(\text{gas})$ [1761], HSO_5^- (peroxymonosulfate ion) [1762], and $HOSO_2$ [1763] have been assigned empirically or theoretically. The last compound was obtained by the gaseous reaction of OH and SO_2 , and trapped in Ar matrices. Complete band assignments are reported for sulfur acids such as $H_3SO_4^+$ [1764], fluorosulfonic acid (FSO_2OH) [1765], $CF_3SO_3^-$ [1766], and $CCl_3SO_3^-$ [1767].

2.18.4. Sulfur Compounds Containing Nitrogen and Halogen

Heptasulfur imide (S_7NH) takes an eight-membered crown-shaped ring structure with the S_2NH group almost planar. Steudel has made complete assignments of the IR/Raman spectra of S_7NH and its D and ^{15}N analogs using normal coordinate analysis [1768]. The IR/Raman spectra of S_nNH ($n = 8, 9, 11$) are also reported [1769].

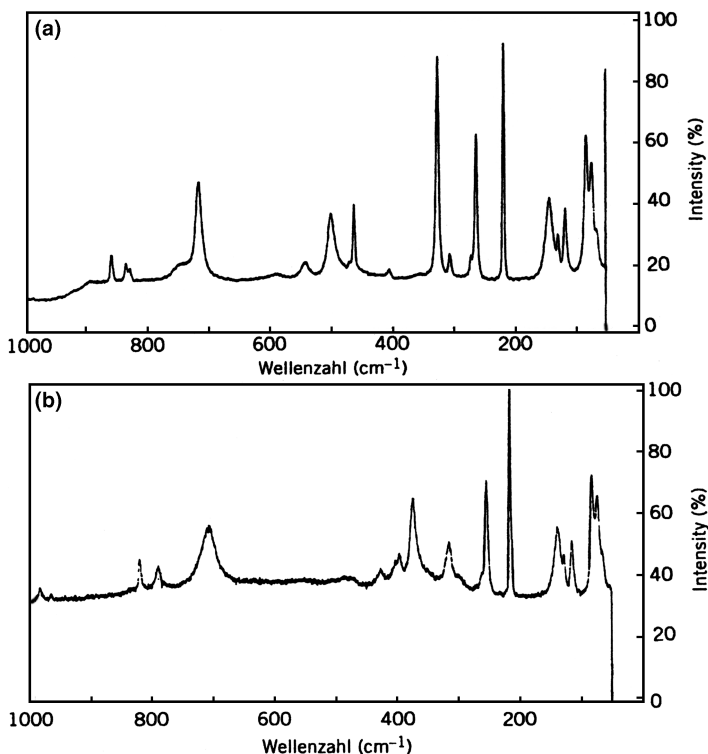


Fig. 2.79. Raman spectra of (a) $(\text{SNH})_4$ and (b) $(\text{SND})_4$ [1770].

The $(\text{SNH})_4$ molecule forms the eight-membered crown-shaped of C_{4v} symmetry shown in Fig. 2.78. Figure 2.79 shows the Raman spectra of $(\text{SNH})_4$ and $(\text{SND})_4$ obtained by Steudel and Rose [1770], who have made complete band assignments based on normal coordinate analysis. Later, Steudel further confirmed their assignments by $^{14}\text{N}/^{15}\text{N}$ substitution [1771]. Trisulfurdinitrogen dioxide ($\text{S}_3\text{N}_2\text{O}_2$) takes the zigzag chain structure of C_{2v} symmetry shown in Fig. 2.78, and its IR/Raman spectra have been assigned theoretically [1772]. Vibrational assignments are available for $\text{ClO}(\text{SO}_2\text{F})$ [1773] and $\text{XN}(\text{SF}_2)$ ($\text{X} = \text{F}, \text{Cl}, \text{Br}$) [1774], both of which belong to the C_s point group.

2.18.5. Sulfur Compounds Containing Halogen

Low-temperature Raman spectra of SCl_2 , SCl_4 , and S_2Cl_2 have been reported [1775]. The $\text{S}_2\text{I}_4^{2+}$ ion assumes a butterfly structure of C_2 (AsF_6^- salt) or C_{2v} (SbF_6^- salt) symmetry, and the $\nu(\text{S}-\text{S})$ and $\nu(\text{I}-\text{I})$ vibrations are at 734 and 227 cm^{-1} , respectively. The IR/Raman spectra of the S_7X^+ ion (X : a halogen) containing the S_7 ring are reported [1777]. Other halogen-containing sulfur compounds include $(\text{FO}_2\text{S})\text{CHF}(\text{COOH})$ [1778] and $\text{FC}(\text{O})\text{NSF}_2$ [1779].

2.18.6. Other Sulfur Compounds

There are many other sulfur compounds for which vibrational spectra and band assignments are available. Some examples are $\text{CH}_3\text{--S--S--CH}_3$ [1780], $\text{H}_2\text{C}(\eta\text{-S}_2)$ [1781], $\text{H}_2\text{C--S=O}$ [1782], *syn*- ClC(O)SBr [1783], $\text{F}_3\text{C--C(O)--NCS}$ [1784] and $\text{Cl}_3\text{C--SCN}$ [1785].

2.18.7. Compounds of Selenium and Tellurium

Infrared spectra of Se_n clusters in Ar matrices exhibit the $\nu(\text{Se--Se})$ vibration at 513 ($n = 2$), 350 ($n = 3$, bent), 345 ($n = 4$, *trans*-planar), and 370 cm^{-1} (*cis*-planar) [1786]. Vibrational frequencies of the square-planar Se_4^{2+} ion are given in Sec. 2.5.1.

Similar to S_8 , the Se_8 molecule takes a crown-shaped ring structure of D_{4d} symmetry, and its IR/Raman spectra have been assigned via normal coordinate analysis [1787]. According to X-ray analysis, the Se_9^{2-} ion in $[\text{Sr}(15\text{-crown-5})_2]$ (Se_9) takes a zigzag chain structure. Four stretching ($300\text{--}200\text{ cm}^{-1}$ region) and three bending ($170\text{--}120\text{ cm}^{-1}$ region) vibrations have been reported for this ion [1788].

Using the UBF field, Laitinen et al. [1789] calculated vibrational frequencies of six-membered $\text{Se}_n\text{S}_{6-n}$ ($n = 1\sim 5$) rings for 11 possible isomers, and seven-membered 1,2- Se_2S_5 , and 1,2- Se_5S_2 rings for four possible isomers. All these compounds assume chair conformations. Figure 2.78 shows the conformation and numbering of atoms of the seven-membered ring system. The results of their calculations indicate that the stretching frequencies of various isomers are sufficiently different so that Raman spectroscopy can be used to distinguish these isomers. The IR spectrum of 1,2- Se_2S_6 [1790] and the Raman spectrum of 1,2-5,6- Se_4S_4 [1791] have been assigned empirically. Simon and Paetzold [1792] conducted extensive vibrational studies on selenium compounds.

Figure 2.80 shows the structures of $\text{Se}_3\text{N}_2\text{Cl}^+$ [1793], $\text{Sn}_4\text{Se}_{10}^{4-}$ [1794], and $\text{Pb}_2\text{Se}_3^{2-}$ [1795] ions for which vibrational assignments are available. The Raman spectrum of N_4Se_4 (cage structure shown in Fig. 2.53) has been assigned [1698,1699].

Telluroketone (Te=CF_2) exhibits the $\nu(\text{Te=C})$ vibration at 1240 cm^{-1} [1796]. The Raman spectrum of the Te_2^{2-} ion (butterfly structure of C_{2v} symmetry) has been assigned [1797]. The Te_7^{2+} ion in $\{[\text{Te}_7][\text{AsF}_6]_2\}_\infty$ forms an infinite chain of the six-membered tellurium rings of the chair conformation that are connected by bridging tellurium atoms at the 1 and 4 positions as shown in Fig. 2.80, and exhibits IR bands at 396, 126, and 65 cm^{-1} [1298].

2.19. COMPOUNDS OF HALOGEN

Vibrational spectra of many halogeno compounds are listed in the preceding sections. There are other halogeno compounds that do not belong to these types. Figure 2.81 illustrates the structures of six halogeno compounds that have been determined by X-ray or electron diffraction techniques. Complete vibrational assignments have been made on the basis of these structures.

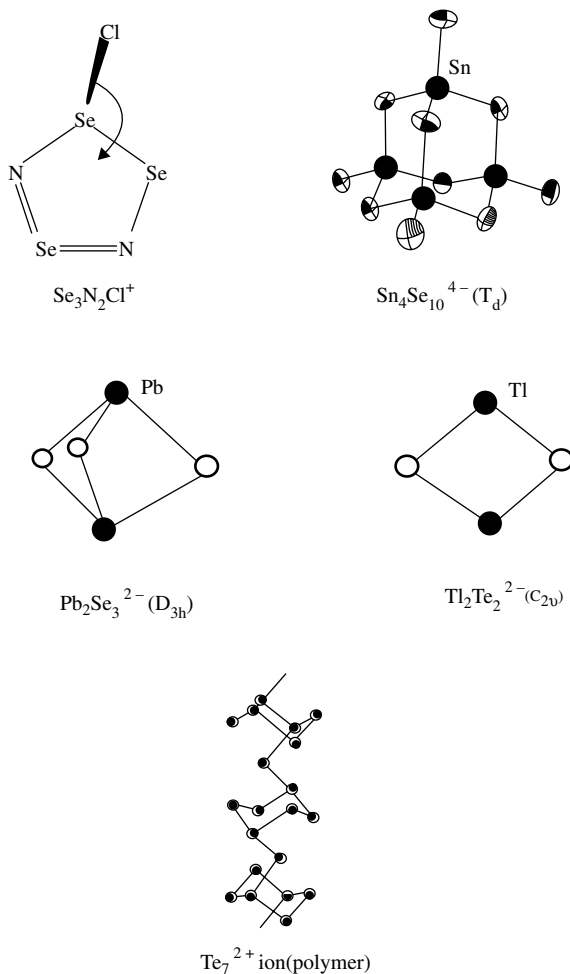


Fig. 2.80. Structures of selenium and tellurium compounds.

In difluorodioxirane, CF_2O_2 (C_{2v} symmetry), the CF_2 vibrations are at 917.9 [$\nu_s(\text{CF}_2)$], 511.1 [$\delta(\text{CF}_2)$], and 1259.6 [$\nu_a(\text{CF}_2)$], while the $\nu_s(\text{CO})$, $\nu(\text{OO})$, and $\nu_a(\text{CO})$ vibrations are at 1466.6, 658, and 1062.1 cm^{-1} , respectively [1799]. (Trifluoromethyl) iodine dichloride (CF_3ICl_2) assumes a T-shaped structure in which the Cl-I-Cl moiety is nearly linear with the CF_3 group coordinated to the central I atom in the direction perpendicular to the Cl-I-Cl bond (C_s symmetry). Examples of such an unusual T-shaped molecules are listed in Sec. 2.4.1. The CF_3 group vibrations are at 1277–1024 (ν), 750–739 (δ_s), 546 (δ_a) and 247 cm^{-1} (ρ_r), while the ICl_2 group vibrations are at 292 (ν_s), 265 (ν_a), and 160–145 (δ) cm^{-1} . The $\nu(\text{C-I})$ vibration was located at 279 cm^{-1} [1800].

In $[\text{C}_3\text{Cl}_3][\text{AlCl}_4]$, the C_3Cl_3^+ ion assumes a triangular ring geometry of D_{3h} symmetry. The $\nu(\text{C-C})$ are assigned at 1790 and 1315 cm^{-1} , whereas the $\nu(\text{C-Cl})$ are

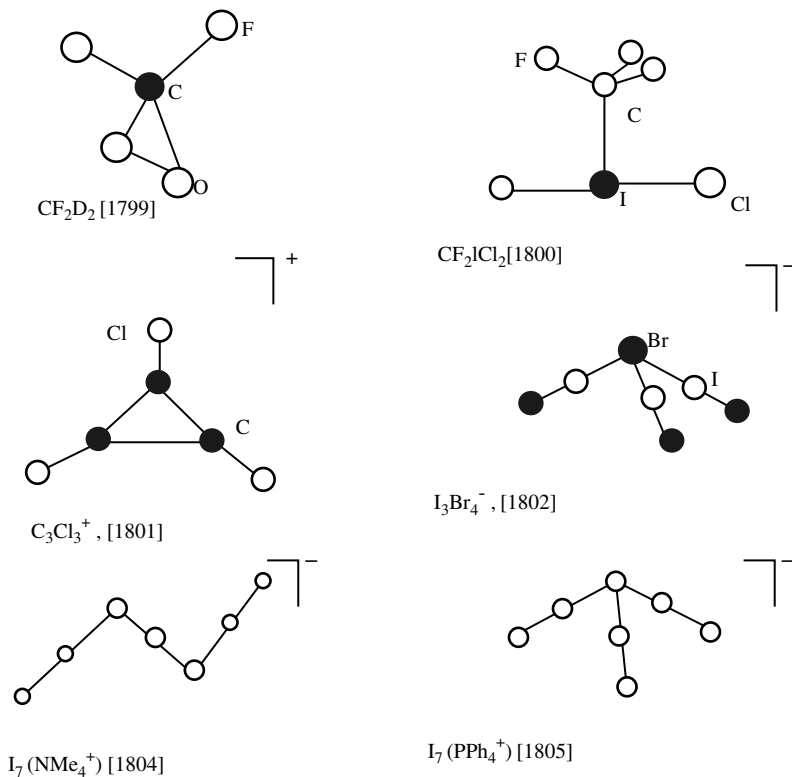


Fig. 2.81. Structures of halogeno compounds.

assigned at 733 and 458 cm⁻¹. In-plane (600 and 160 cm⁻¹) and out-of-plane bending (524 and 190 cm⁻¹) were also assigned [1801]. In [PPh₄][I₃Br₄], the I₃Br₄⁻ ion assumes a distorted pyramidal structure of nearly C_{3v} symmetry. The central BrI₃ unit exhibits ν_a and ν_s at 163 and 193 cm⁻¹, respectively, whereas the three terminal I–Br bonds exhibit the ν(I–Br) vibration at 231 and 215 cm⁻¹. Their δ(BrIBr) vibrations are observed between 97 and 72 cm⁻¹ [1802].

The structures and spectra of polyiodide anions depend not only on the physical state (gas, solid, matrix, and solution) but also on the cation and, in some cases, the method of preparation. As shown in the preceding sections, the I₃⁻ ion obtained as the crown-ether salt is linear and only slightly asymmetric (I–I distances 2.926 and 2.940 Å), and exhibits the ν_a, ν_s, and δ vibrations at 125, 116, and 56/42 cm⁻¹, respectively [396a]. The I₅⁻ ion in the [(CH₃)₄N]⁺ salt takes a symmetric, rectangular (L-shaped) structure of C_{2v} symmetry with the I⁻ ion at the center, and is formulated as (I⁻)(I₂)₂ [1803]. On the other hand, the I₅⁻ ion in the crown-ether salt [396a] was regarded as an I₂ unit coordinating to an asymmetric I₃⁻ ion to form a L-shaped structure. In this case, the ν(I₂), ν_a(I₃⁻), and ν_s(I₃⁻) vibrations were assigned at 168, 143, and 112 cm⁻¹, respectively (all in Raman). The I₇⁻ ion in the N(Et)₄⁺ salt takes a zigzag structure in which two I₂ units coordinate perpendicularly to the I₃⁻ ion

[i.e., $(\text{I}_3^-)(\text{I}_2)_2$]. The $\nu(\text{I}_2)$ vibration was at $\sim 182\text{ cm}^{-1}$, and $\nu(\text{I}_3^-)$ vibrations were located near 136 and 110 cm^{-1} [1804]. In the $\text{P}(\text{Ph}_4)^+$ salt, however, the I_7^- ion is formed via coordination of three I_2 units to the central I^- ion to form a pyramidal structure, and is formulated as $[(\text{I}^-)(\text{I}_2)_3]$. Its Raman spectrum exhibits the $\nu_a(\text{I} \cdots \text{I}_2)$ [mainly $\nu(\text{I}_2)$] at 178 and 166 cm^{-1} , and the ν_a and ν_s vibrations of the I_3^- units at 152 and 118 cm^{-1} , respectively [1805].

REFERENCES

1. The original references are found in G Herzberg, *Molecular Spectra and Molecular Structure*, Vol 1: *Spectra of Diatomic Molecules*, and K P Huber and G Herzberg, *Molecular Spectra and Molecular Structure*, Vol IV: *Constants of Diatomic Molecules*, Van Nostrand, Princeton, NJ, 1950 and 1977 resp.
2. D. A. Wild, R. L. Wilson, P. S. Weisler, and E. J. Bieske, *J. Chem. Phys.* **113**, 10154 (2000).
3. L. Fang, B. L. Davis, H. Lu, and J. R. Lombardi, *Spectrochim. Acta* **57A**, 2809 (2001).
4. S. Li, R. J. van Zee, and W. Weltner, *J. Chem. Phys.* **100**, 7079 (1994).
- 4a. D. A. Hostutler, H. Li, D. J. Clouthier, and G. Wannous, *J. Chem. Phys.* **116**, 4135 (2002).
5. K. D. Setzer, J. Borkowska-Burnecka, W. Zyrnicki, and E. H. Fink, *J. Mol. Spectrosc.* **203**, 244 (2000).
6. M. L. Orlov, J. F. Ogilvie, and J. W. Nibler, *J. Mol. Spectrosc.* **185**, 128 (1997).
7. R. F. Barrow, J. Chevalayre, C. Effantin, M. A. Lesbaut-Dorget, A. J. Ross, G. Wannous, and J. Vergès, *Chem. Phys. Lett.* **214**, 293 (1993).
8. R. Z. Martinez, D. Bermejo, J. Santos, and P. Cancio, *J. Mol. Spectrosc.* **168**, 343 (1994).
9. D. Bermejo, J. J. Jiménez, and R. Z. Martinez, *J. Mol. Spectrosc.* **212**, 186 (2002).
10. J. A. Horsley and R. F. Barrow, *Trans. Faraday. Soc.* **63**, 32 (1967).
11. D. R. Brown, M. J. Clegg, A. J. Downs, R. C. Fowler, A. R. Minihan, J. R. Norris, and L. Stein, *Inorg. Chem.* **31**, 5041 (1992).
12. L. Fang, X. Chen, X. Shen, Y. Liu, D. M. Lindsay, and J. R. Lombardi, *Low Temp. Phys.* **26**, 752 (2000).
13. Y. Liu, L. Fang, X. Shen, X. Chen, J. R. Lombardi, and D. M. Lindsay, *Chem. Phys.* **262**, 25 (2000).
14. X. Shen, L. Fang, X. Chen, and J. R. Lombardi, *J. Chem. Phys.* **113**, 2233 (2000).
15. X. Chen, L. Fang, X. Shen, and J. R. Lombardi, *J. Chem. Phys.* **112**, 9780 (2000).
16. L. Fang, X. Chen, X. Shen, and J. R. Lombardi, *J. Phys. Chem. A* **104**, 9153 (2000).
17. L. Fang, X. Chen, X. Shen, and J. R. Lombardi, *J. Chem. Phys.* **113**, 10202 (2000).
18. F. Azough, R. Freer, and J. Petzelt, *J. Mater. Sci.* **28**, 2273 (1993).
19. Z. Hu, J. G. Dong, J. R. Lombardi, D. M. Lindsay, and W. Harbrich, *J. Chem. Phys.* **101**, 95 (1994).

20. J. G. Dong, Z. Hu, R. Craig, J. R. Lombardi, and D. M. Lindsay, *J. Chem. Phys.* **101**, 9280 (1994).
21. H. Wang, H. Haouari, R. Craig, Y. Liu, J. R. Lombardi, and D. M. Lindsay, *J. Chem. Phys.* **106**, 2101 (1997).
22. H. Wang, H. Haouari, R. Craig, J. R. Lombardi, and D. M. Lindsay, *J. Chem. Phys.* **104**, 3420 (1996).
23. V. Beutel, M. Kuhn, and W. Demtröder, *J. Mol. Spectrosc.* **155**, 343 (1992).
24. A. G. Maki, W. B. Olson, and G. Thompson, *J. Mol. Spectrosc.* **144**, 257 (1990).
25. C. Yamada and E. Hirota, *J. Chem. Phys.* **88**, 6702 (1988).
26. M. Dulick, K.-Q. Zhang, B. Guo, and P. F. Bernath, *J. Mol. Spectrosc.* **188**, 14 (1998).
27. A. G. Maki and W. B. Olson, *J. Chem. Phys.* **90**, 6887 (1989).
28. U. Magg and H. Jones, *Chem. Phys. Lett.* **146**, 415 (1988).
29. K. Essig, R. D. Urban, H. Birk, and H. Jones, *Z. Naturforsch.* **48a**, 1111 (1993).
30. H. Uehara, K. Horiai, and T. Konno, *J. Mol. Struct.* **413/414**, 457 (1997).
31. U. Magg, H. Birk, and H. Jones, *Chem. Phys. Lett.* **151**, 503 (1988).
32. U. Magg and H. Jones, *Chem. Phys. Lett.* **148**, 6 (1988).
33. B. Lemoine, C. Demuynck, J. L. Destombes, and P. B. Davies, *J. Chem. Phys.* **89**, 673 (1988).
34. D. Petitprez, B. Lemoine, C. Demuynck, J. L. Destombes, and B. Macke, *J. Chem. Phys.* **91**, 4462 (1989).
35. U. Magg, H. Birk, and H. Jones, *Chem. Phys. Lett.* **151**, 263 (1988).
36. H. Birk, R. D. Urban, P. Polomsky, and H. Jones, *J. Chem. Phys.* **94**, 5435 (1991).
37. U. Magg, H. Birk, and H. Jones, *Chem. Phys. Lett.* **149**, 321 (1988).
38. K. A. Walker, H. G. Hedderich, and P. F. Bernath, *Mol. Phys.* **78**, 577 (1993).
39. P. S. Ram and P. F. Bernath, *J. Chem. Phys.* **105**, 2668 (1996).
40. R. D. Urban and H. Jones, *Chem. Phys. Lett.* **163**, 34 (1989).
41. R. S. Ram, P. F. Bernath, and S. P. Davis, *J. Mol. Spectrosc.* **175**, 1 (1996).
42. R. B. Wright, J. K. Bates, and D. M. Gruen, *Inorg. Chem.* **17**, 2275 (1978).
43. H. Birk and H. Jones, *Chem. Phys. Lett.* **161**, 27 (1989).
44. R. D. Urban, H. Birk, P. Polomsky, and H. Jones, *J. Chem. Phys.* **94**, 2523 (1991).
45. R. D. Urban, U. Magg, H. Birk, and H. Jones, *J. Chem. Phys.* **92**, 14 (1990).
46. R. S. Ram and P. F. Bernath, *J. Mol. Spectrosc.* **171**, 169 (1995).
47. R. S. Ram and P. F. Bernath, *J. Mol. Spectrosc.* **172**, 91 (1995).
48. J. L. Deutsch, W. S. Neil, and D. A. Ramsay, *J. Mol. Spectrosc.* **125**, 115 (1987).
49. J. B. White, M. Dulick, and P. F. Bernath, *J. Chem. Phys.* **99**, 8371 (1993).
50. R. D. Urban, U. Magg, and H. Jones, *Chem. Phys. Lett.* **154**, 135 (1989).
51. J. M. Campbell, M. Dulick, D. Klapstein, J. B. White, and P. F. Bernath, *J. Chem. Phys.* **99**, 8379 (1993).
52. A. H. Bahnmaier, R. D. Urban, and H. Jones, *Chem. Phys. Lett.* **155**, 269 (1989).

53. F. Itoh, T. Nakanaga, H. Takeo, K. Essig, and H. Jones, *J. Mol. Spectrosc.* **169**, 421 (1995).
54. R. D. Urban, A. H. Bahnmaier, U. Magg, and H. Jones, *Chem. Phys. Lett.* **158**, 443 (1989).
55. P. F. Bernath, *J. Chem. Phys.* **86**, 4838 (1987).
56. I. Morino, K. Matsumura, and K. Kawaguchi, *J. Mol. Spectrosc.* **174**, 123 (1995).
57. A. E. Douglas, *Can. J. Phys.* **35**, 71 (1957).
58. M. Petri, U. Simon, W. Zimmermann, W. Urban, J. P. Towle, and M. Brown, *Mol. Phys.* **72**, 315 (1991).
59. J. P. Towle and J. M. Brown, *Mol. Phys.* **78**, 249 (1993).
60. U. Simon, M. Petri, W. Zimmermann, and W. Urban, *Mol. Phys.* **71**, 1163 (1990).
61. W. Zimmermann, T. Neils, E. Bachem, R. Pahnke, and W. Urban, *Mol. Phys.* **68**, 199 (1989).
62. W. Zimmermann, U. Simon, M. Petri, and W. Urban, *Mol. Phys.* **74**, 1287 (1991).
63. U. Magg and H. Jones, *Chem. Phys. Lett.* **166**, 253 (1990).
64. R. S. Ram and P. F. Bernath, *J. Mol. Spectrosc.* **176**, 329 (1996).
65. H. C. Miller and J. W. Farley, *J. Chem. Phys.* **86**, 1167 (1987).
66. K. D. Hensel, R. A. Hughes, and J. M. Brown, *J. Chem. Soc., Faraday Trans.* **91**, 2999 (1995).
67. R. D. Urban, P. Polomsky, and H. Jones, *Chem. Phys. Lett.* **181**, 485 (1991).
68. A. M. R. P. Bopegedra, C. R. Brazier, and P. F. Bernath, *Chem. Phys. Lett.* **162**, 301 (1989).
69. H. G. Hedderich and P. F. Bernath, *J. Mol. Spectrosc.* **158**, 170 (1993).
70. B. D. Rehfuss, M. W. Crofton, and T. Oka, *J. Chem. Phys.* **85**, 1785 (1986).
71. R. S. Ram, P. F. Bernath, R. Engleman, and J. W. Brault, *J. Mol. Spectrosc.* **172**, 34 (1995).
72. M. Gruebele, M. Polak, and R. J. Saykally, *J. Chem. Phys.* **86**, 1698 (1987).
73. R. S. Ram and P. F. Bernath, *J. Mol. Spectrosc.* **203**, 9 (2000).
74. D. H. Rank, D. P. Eastman, B. S. Rao, and T. A. Wiggins, *J. Opt. Soc. Am.* **52**, 1 (1962).
75. T. Parekunnel, T. Hirao, R. J. Le Roy, and P. F. Bernath, *J. Mol. Spectrosc.* **195**, 185 (1999).
76. S. A. Rogers, C. R. Brazier, and P. F. Bernath, *J. Chem. Phys.* **87**, 159 (1987).
77. C. Yamada and E. Hirota, *J. Chem. Phys.* **99**, 8489 (1993).
78. H. G. Hedderich, C. I. Frum, R. Engleman, and P. F. Bernath, *Can. J. Chem.* **69**, 1659 (1991).
79. W. Klemperer, W. G. Norris, A. Büchler, and A. G. Emslie, *J. Chem. Phys.* **33**, 1534 (1960).
80. S. E. Veazey and W. Gordy, *Phys. Rev.* **138A**, 1303 (1965).
81. A. Muntianu, B. Guo, and P. F. Bernath, *J. Mol. Spectrosc.* **176**, 274 (1996).
82. S. A. Rice and W. Klemperer, *J. Chem. Phys.* **27**, 573 (1957).
83. R. S. Ram, M. Dulick, B. Guo, K.-Q. Zhang, and P. F. Bernath, *J. Mol. Spectrosc.* **183**, 360 (1997).

84. H. Uehara, K. Horiai, Y. Ozaki, and T. Konno, *Spectrochim. Acta* **50A**, 1389 (1994).
85. V. I. Baikov and K. P. Vasilevskii, *Opt. Spectrosc.* **22**, 198 (1967).
86. M.-C. Liu, A. Muntianu, K.-Q. Zhang, P. Colarusso, and P. F. Bernath, *J. Mol. Spectrosc.* **180**, 188 (1996).
87. A. G. Maki and W. B. Olson, *J. Mol. Spectrosc.* **140**, 185 (1990).
88. V. Braun, B. Guo, K.-Q. Zhang, M. Dulick, P. F. Bernath, and G. A. McRae, *Chem. Phys. Lett.* **228**, 633 (1994).
89. B. E. Barber, K.-Q. Zhang, B. Guo, and P. F. Bernath, *J. Mol. Spectrosc.* **169**, 583 (1995).
90. C. E. Blom, H. G. Hedderich, F. J. Lovas, R. D. Suenram, and A. G. Maki, *J. Mol. Spectrosc.* **152**, 109 (1992).
91. E. Kagi, T. Hirano, S. Takano, and K. Kawaguchi, *J. Mol. Spectrosc.* **168**, 109 (1994).
92. F. Charron, B. Guo, K.-Q. Zhang, Z. Morbi, and P. F. Bernath, *J. Mol. Spectrosc.* **171**, 160 (1995).
93. H. G. Hedderich and C. E. Blom, *J. Chem. Phys.* **90**, 4660 (1989).
94. C. Focsa, A. Poclet, B. Pinchemel, R. J. Le Roy, and P. F. Bernath, *J. Mol. Spectrosc.* **203**, 330 (2000).
95. P. Colarusso, B. Guo, K.-Q. Zhang, and P. F. Bernath, *J. Mol. Spectrosc.* **175**, 158 (1996).
96. H. Li, R. Skelton, C. Focsa, B. Pinchemel, and P. F. Bernath, *J. Mol. Spectrosc.* **203**, 188 (2000).
97. B. Guo, K.-Q. Zhang, and P. F. Bernath, *J. Mol. Spectrosc.* **170**, 59 (1995).
98. R. F. Guterrus, J. Vergès, and C. Amiot, *J. Mol. Spectrosc.* **196**, 29 (1999).
99. H. G. Hedderich and C. E. Blom, *J. Mol. Spectrosc.* **140**, 103 (1990).
100. R. S. Ram and P. F. Bernath, *J. Mol. Spectrosc.* **184**, 401 (1997).
101. R. Konisto, S. Wallin, and O. Launila, *J. Mol. Spectrosc.* **172**, 464 (1995).
102. M. Bencheiki, R. Koivisto, O. Launila, and J. P. Flament, *J. Chem. Phys.* **196**, 6231 (1997).
103. R. S. Ram, P. F. Bernath, and S. P. Davis, *J. Mol. Spectrosc.* **173**, 158 (1995).
104. R. S. Ram and P. F. Bernath, *J. Mol. Spectrosc.* **193**, 363 (1999).
105. K.-Q. Zhang, B. Guo, V. Braun, M. Dulick, and P. F. Bernath, *J. Mol. Spectrosc.* **170**, 82 (1995).
106. N. T. Hunt, W. Y. Fan, Z. Liu, and P. B. Davies, *J. Mol. Spectrosc.* **191**, 326 (1998).
107. C. Destoky, I. Dubois, and H. Bredohl, *J. Mol. Spectrosc.* **136**, 216 (1989).
108. R. S. Ram and P. F. Bernath, *J. Mol. Spectrosc.* **180**, 414 (1996).
109. E. Mahieu, I. Dubois, and H. Bredohl, *J. Mol. Spectrosc.* **134**, 317 (1989).
110. H. Uehara, K. Horiai, Y. Ozaki, and T. Konno, *Chem. Phys. Lett.* **214**, 527 (1993).
111. O. Launila and J. Jonsson, *J. Mol. Spectrosc.* **168**, 1 (1994).
112. O. Launila and J. Jonsson, *J. Mol. Spectrosc.* **168**, 483 (1994).
113. H. Uehara, K. Horiai, K. Nakagawa, and H. Suguro, *Chem. Phys. Lett.* **178**, 553 (1991).
114. G. W. Lemire, G. A. Bishea, S. A. Heidecke, and M. D. Morse, *J. Chem. Phys.* **92**, 121 (1990).
115. S. Li, R. J. van Zee, and W. Weltner, *J. Phys. Chem.* **98**, 2275 (1994).

116. H. Uehara, K. Horiiai, T. Mitani, and H. Suguro, *Chem. Phys. Lett.* **162**, 137 (1989).
117. H. Uehara, K. Horiiai, A. Kerim, and N. Aota, *Chem. Phys. Lett.* **189**, 217 (1992).
118. M. Gruebele, M. Polak, and R. J. Saykally, *Chem. Phys. Lett.* **125**, 165 (1986).
119. M. Gruebele, M. Polak, G. A. Blake, and R. J. Saykally, *J. Chem. Phys.* **85**, 6276 (1986).
120. A. J. Marr, T. J. Sears, and P. B. Davies, *J. Mol. Spectrosc.* **184**, 413 (1997).
121. P. B. Davies and P. A. Martin, *Mol. Phys.* **70**, 89 (1990).
122. R. S. Ram, P. F. Bernath, and S. P. Davis, *J. Mol. Spectrosc.* **173**, 146 (1995).
123. M. Wienkoop, P. Mürtz, P.-C. Schumann, M. Havenith, and W. Urban, *Chem. Phys.* **225**, 17 (1997).
124. Y. Akiyama, K. Tanaka, and T. Tanaka, *Chem. Phys. Lett.* **155**, 15 (1989).
125. T. Tanaka, M. Tamura, and K. Tanaka, *J. Mol. Struct.* **413/414**, 153 (1997).
126. W. Y. Fan, Z. Liu, and P. B. Davies, *J. Mol. Spectrosc.* **191**, 98 (1998).
127. S. D. Rosner, R. Cameron, T. J. Scholl, and R. A. Holt, *J. Mol. Spectrosc.* **189**, 83 (1998).
128. Y. Akiyama, K. Tanaka, and T. Tanaka, *Chem. Phys. Lett.* **165**, 335 (1990).
129. R. W. Martin and A. J. Merer, *Can. J. Phys.* **51**, 125 (1973).
130. E. G. Lee, J. Y. Seto, T. Hirao, P. F. Bernath, and R. J. Le Roy, *J. Mol. Spectrosc.* **194**, 197 (1999).
131. H. Uehara, K. Horiiai, Y. Ozaki, and T. Konno, *J. Mol. Struct.* **352/353**, 395 (1995).
132. T. Konno and H. Uehara, *Chem. Phys. Lett.* **247**, 529 (1995).
133. H. Birk and H. Jones, *Chem. Phys. Lett.* **181**, 245 (1991).
134. L. H. Coudert, V. Dana, J.-Y. Mandin, M. Morillon-Chapey, R. Farrenq, and G. Guelachvili, *J. Mol. Spectrosc.* **172**, 435 (1995).
135. I. K. Ahmad and P. A. Hamilton, *J. Mol. Spectrosc.* **169**, 286 (1995).
136. C. Yamada, M. C. Chang, and E. Hirota, *J. Chem. Phys.* **86**, 3804 (1987).
137. H. Kanamori, C. Yamada, J. E. Butler, K. Kawaguchi, and E. Hirota, *J. Chem. Phys.* **83**, 4945 (1985).
138. K. Kawaguchi, E. Hirota, M. Ohishi, H. Suzuki, S. Takano, S. Yamamoto, and S. Saito, *J. Mol. Spectrosc.* **130**, 81 (1988).
139. J. A. Coxon, S. Naxakis, and A. B. Yamashita, *Spectrochim. Acta* **41A**, 1409 (1985).
140. F. Ito, T. Nakanaga, H. Takeo, K. Essig, and H. Jones, *J. Mol. Spectrosc.* **174**, 417 (1995).
141. M. Beutel, K. D. Setzer, and E. H. Fink, *J. Mol. Spectrosc.* **195**, 147 (1999).
142. R. Breidohr, K. D. Setzer, O. Shestakov, E. H. Fink, and U. Zyrnicki, *J. Mol. Spectrosc.* **166**, 471 (1994).
143. R. Breidohr, O. Shestakov, K. D. Setzer, and E. H. Fink, *J. Mol. Spectrosc.* **172**, 369 (1995).
144. E. H. Fink, K. D. Setzer, D. A. Ramsay, J. P. Towle, and J. M. Brown, *J. Mol. Spectrosc.* **178**, 143 (1996).
145. E. H. Fink, K. D. Setzer, D. A. Ramsay, and M. Vervloet, *Chem. Phys. Lett.* **179**, 103 (1991).
146. J. B. Burkholder, P. D. Hammer, C. J. Howard, and A. R. W. McKellar, *J. Mol. Spectrosc.* **118**, 471 (1986).
147. B. J. Drouin, C. E. Miller, H. S. P. Müller, and E. A. Cohen, *J. Mol. Spectrosc.* **205**, 128 (2001).
148. H. Burger, P. Schulz, E. Jacob, and M. Föhnle, *Z. Naturforsch.* **41A**, 1015 (1986).

149. W. V. F. Brooks and B. Crawford, *J. Chem. Phys.* **23**, 363 (1955).
150. C. I. Frum, R. Engelman, and P. F. Bernath, *Chem. Phys. Lett.* **167**, 356 (1990).
151. F. Ito, K. Sugawara, T. Nakanaga, H. Takeo, and C. Matsumura, *J. Mol. Spectrosc.* **142**, 191 (1990).
152. B. Nelander, V. Sablinskas, M. Dulick, V. Braun, and P. F. Bernath, *Mol. Phys.* **93**, 137 (1998).
153. P. C. Souers, D. Fearon, R. Garza, E. M. Kelly, P. E. Roberts, R. H. Sanborn, R. T. Taugawa, J. L. Hunt, and J. D. Poll, *J. Chem. Phys.* **70**, 1581 (1979).
154. M. R. Furlanetto, N. I. Pivonka, T. Lenzer, and D. M. Newmark, *Chem. Phys. Lett.* **326**, 439 (2000).
155. S. Hammersbach, B. Zibrowius, and U. Ruschewitz, *Z. Anorg. Allg. Chem.* **625**, 1440 (1999).
156. R. A. Teichman, III, M. Epting, and E. R. Nixon, *J. Chem. Phys.* **68**, 336 (1978).
157. G. A. Ozin, *Chem. Commun.* 1325 (1969).
158. A. Kornath and I. Koper, *J. Raman. Spectrosc.* **28**, 829 (1997).
159. L. Andrews and R. R. Smardzewski, *J. Chem. Phys.* **58**, 2258 (1973).
160. J. C. Evans, *Chem. Commun.* 682 (1969).
161. A. G. Hopkins and C. W. Brown, *J. Chem. Phys.* **62**, 1598 (1975).
162. H. Fabian and F. Fisch, *J. Raman. Spectrosc.* **20**, 639 (1989).
163. W. F. Howard, Jr. and L. Andrews, *J. Am. Chem. Soc.* **95**, 3045 (1973).
164. M. R. Clarke and G. Mamantov, *Inorg. Nucl. Chem. Lett.* **7**, 993 (1971).
165. W. F. Howard, Jr. and L. Andrews, *J. Am. Chem. Soc.* **95**, 2056 (1973).
166. R. J. Gillespie and M. J. Morton, *Chem. Commun.* 1565 (1968).
167. W. Holzer, W. F. Murphy, and H. J. Bernstein, *J. Chem. Phys.* **52**, 399 (1970).
168. R. J. Gillespie and M. J. Morton, *J. Mol. Spectrosc.* **30**, 178 (1969).
169. W. F. Howard, Jr. and L. Andrews, *J. Am. Chem. Soc.* **97**, 2956 (1975).
- 169a. A. Kornath, R. Ludwig, and A. Zoerner, *Angew. Chem. Int. Ed.* **37**, 1575 (1998).
170. W. Schulze, H. U. Becker, R. Minkwitz, and K. Manzel, *Chem. Phys. Lett.* **55**, 59 (1978).
171. A. Givan and A. Loewenschuss, *Chem. Phys. Lett.* **62**, 592 (1979).
- 171a. R. D. Jones, D. A. Summerville, and F. Basolo, *Chem. Rev.* **79**, 139 (1979).
- 171b. A. J. Edwards, W. E. Falconer, J. E. Griffiths, W. A. Sunder, and M. J. Vasile, *J. Chem. Soc., Dalton Trans.* 1129 (1974).
- 171c. L. Andrews, and R. R. Smardzewski, *J. Chem. Phys.* **58**, 2258 (1973).
- 171d. H. H. Eysel, and S. Thym, *Z. Anorg. Allg. Chem.* **411**, 97 (1975).
- 171e. R. Steudel, *Z. Naturforsch.* **30B**, 281 (1975).
172. R. B. Wright, J. K. Bates, and D. M. Gruen, *Inorg. Chem.* **17**, 2275 (1978).
173. D. E. Milligan and M. E. Jacox, *J. Chem. Phys.* **52**, 2594 (1970).
174. W. Seebass, J. Werner, W. Urban, E. R. Comben, and J. M. Brown, *Mol. Phys.* **62**, 161 (1987).
175. K. Rosengren and G. C. Pimentel, *J. Chem. Phys.* **43**, 507 (1965).
176. J. R. Anaconda, P. B. Davies, and S. A. Johnson, *Mol. Phys.* **56**, 989 (1985).
177. B.-M. Cheng, Y.-P. Lee, and J. F. Ogilvie, *Chem. Phys. Lett.* **151**, 109 (1988).

178. W. R. Busing, *J. Chem. Phys.* **23**, 933 (1955).
179. J. C. Owruksy, N. H. Rosenbaum, L. M. Tack, and R. J. Saykally, *J. Chem. Phys.* **83**, 5338 (1985).
180. M. W. Crofton, R. S. Altman, M. F. Jagod, and T. Oka, *J. Phys. Chem.* **89**, 3614 (1985).
181. Y. Aratono, M. Nakashima, M. Saeki, and E. Tachikawa, *J. Phys. Chem.* **90**, 1528 (1986).
182. E. Isoniemi, M. Patterson, L. Khriachtchev, J. Lundell, and M. Räsänen, *J. Phys. Chem. A* **103**, 679 (1999).
183. N. Acquista and L. J. Schoen, *J. Chem. Phys.* **53**, 1290 (1970).
184. S. Civiš, C. E. Blom, and P. Jensen, *J. Mol. Spectrosc.* **138**, 69 (1989).
185. D. Goddon, A. Groh, H. J. Hansen, M. Schneider, and W. Urban, *J. Mol. Spectrosc.* **147**, 392 (1991).
186. R. J. Van Zee, T. C. DeVore, and W. Weltner, Jr. *J. Chem. Phys.* **71**, 2051 (1979).
187. G. V. Chertihin and L. Andrews, *J. Phys. Chem.* **99**, 12131 (1995).
- 187a. X. Wang, and L. Andrews, *J. Phys. Chem. A* **106**, 3706 (2002).
188. K. S. Seshadri, D. White, and D. E. Mann, *J. Chem. Phys.* **45**, 4697 (1966).
189. A. Snelson and K. S. Pitzer, *J. Phys. Chem.* **67**, 882 (1963).
190. G. A. Thompson, A. G. Maki, W. B. Olson, and A. Weber, *J. Mol. Spectrosc.* **124**, 130 (1987).
191. S. Schlick and O. Schnepf, *J. Chem. Phys.* **41**, 463 (1964).
192. H. Uehara, K. Horiai, K. Nakagawa, and T. Fujimoto, *J. Mol. Spectrosc.* **134**, 98 (1989).
193. D. E. Mann, G. V. Calder, K. S. Seshadri, D. White, and M. J. Linevsky, *J. Chem. Phys.* **46**, 1138 (1967).
194. L. Andrews, E. S. Prochaska, and B. S. Ault, *J. Chem. Phys.* **69**, 556 (1978).
195. S. Civiš, H. G. Hedderich, and C. E. Blom, *Chem. Phys. Lett.* **176**, 489 (1991).
196. L. Andrews and B. S. Ault, *J. Mol. Spectrosc.* **68**, 114 (1977).
197. W. Welter, Jr. and D. McLeod, Jr. *J. Phys. Chem.* **69**, 3488 (1965).
198. F. W. Froben and F. Rogge, *Chem. Phys. Lett.* **78**, 264 (1981).
199. D. W. Green, W. Korfmacher, and D. M. Gruen, *J. Chem. Phys.* **58**, 404 (1973).
200. W. Weltner, Jr. and D. McLeod, Jr. *J. Chem. Phys.* **42**, 882 (1965).
201. D. W. Green and K. M. Ervin, *J. Mol. Spectrosc.* **89**, 145 (1981).
202. J. W.-H. Leung, W. S. Tam, Q. Ran, and A. S.-C. Cheung, *Chem. Phys. Lett.* **343**, 64 (2001).
203. D. W. Green, G. T. Reedy, and J. G. Kay, *J. Mol. Spectrosc.* **78**, 257 (1979).
204. J. G. Kay, D. W. Green, K. Duca, and G. L. Zimmerman, *J. Mol. Spectrosc.* **138**, 49 (1989).
205. D. W. Green and G. T. Reedy, *J. Mol. Spectrosc.* **74**, 423 (1979).
206. D. W. Green and G. T. Reedy, *J. Chem. Phys.* **65**, 2921 (1976).
207. S. D. Gabelnick, G. T. Reedy, and M. G. Chasanov, *J. Chem. Phys.* **58**, 4468 (1973).
208. D. M. Green and G. T. Reedy, *J. Chem. Phys.* **69**, 552 (1978).
209. D. M. Green and G. T. Reedy, *J. Chem. Phys.* **69**, 544 (1978).
210. E. S. Prochaska and L. Andrews, *J. Chem. Phys.* **72**, 6782 (1980).
211. M. Osiac, J. Röpcke, and P. B. Davies, *Chem. Phys. Lett.* **344**, 92 (2001).

212. T. Nakanaga, H. Takeo, S. Kondo, and C. Matsumura, *Chem. Phys. Lett.* **114**, 88 (1985).
213. S. J. Bares, M. Haak, and J. W. Nibler, *J. Chem. Phys.* **82**, 670 (1985).
214. A. Snelson, *J. Phys. Chem.* **71**, 3202 (1967).
215. J. M. Brom, Jr. and H. F. Franzen, *J. Chem. Phys.* **54**, 2874 (1971).
216. A. G. Maki, *J. Mol. Spectrosc.* **137**, 147 (1989).
217. M. E. Jacox and D. E. Milligan, *J. Chem. Phys.* **50**, 3252 (1969).
218. T. Nakanaga, F. Ito, and H. Takeo, *J. Mol. Spectrosc.* **165**, 88 (1994).
219. H. Dubost and A. Abouaf-Marguin, *Chem. Phys. Lett.* **17**, 269 (1972).
220. R. R. Steudel, *Z. Anorg. Allg. Chem.* **361**, 180 (1968).
221. R. A. Penneman and L. H. Jones, *J. Chem. Phys.* **24**, 293 (1956).
222. D. E. Milligan and M. E. Jacox, *J. Chem. Phys.* **47**, 278 (1971).
223. S. Li, R. J. van Zee, and W. Weltzner, *Chem. Phys. Lett.* **229**, 531 (1994).
224. C. Yamada, E. Hirota, S. Yamamoto, and S. Saito, *J. Chem. Phys.* **88**, 46 (1988).
225. J. S. Anderson and J. S. Ogden, *J. Chem. Phys.* **51**, 4189 (1969).
226. C. I. Frum, R. Engleman, and P. F. Bernath, *J. Chem. Phys.* **93**, 5457 (1990).
227. J. S. Ogden and M. J. Ricks, *J. Chem. Phys.* **52**, 352 (1970).
228. C. P. Marino, J. D. Guérin, and E. R. Nixon, *J. Mol. Spectrosc.* **51**, 160 (1974).
229. J. S. Ogden and M. J. Ricks, *J. Chem. Phys.* **53**, 896 (1970).
230. J. S. Ogden and M. J. Ricks, *J. Chem. Phys.* **56**, 1658 (1972).
231. A. G. Maki and F. J. Lovas, *J. Mol. Spectrosc.* **125**, 188 (1987).
232. V. P. Babaeva and V. Y. Rosolovskii, *Russ. J. Inorg. Chem (Engl. transl.)* **16**, 471 (1971).
233. W. A. Guillory and C. E. Hunter, *J. Chem. Phys.* **50**, 3516 (1969).
234. D. E. Tevault and L. Andrews, *J. Phys. Chem.* **77**, 1646 (1973).
235. D. E. Tevault and L. Andrews, *J. Phys. Chem.* **77**, 1640 (1973).
236. R. M. Atkins and P. L. Timms, *Spectrochim. Acta.* **33A**, 853 (1977).
237. H. Kanamori, E. Tiemann, and E. Hirota, *J. Chem. Phys.* **89**, 621 (1988).
238. W. Holzer, W. F. Murphy, and H. J. Bernstein, *J. Mol. Spectrosc.* **32**, 13 (1969).
239. D. E. Milligan and M. E. Jacox, *J. Chem. Phys.* **40**, 2461 (1964).
240. L. Andrews and J. I. Raymond, *J. Chem. Phys.* **55**, 3078 (1971).
241. F. K. Chi and L. Andrews, *J. Phys. Chem.* **77**, 3062 (1973).
242. D. E. Tevault, N. Walker, R. R. Smardzewski, and W. B. Fox, *J. Phys. Chem.* **82**, 2733 (1978).
243. M. Feuerhahn, R. Minkwitz, and G. Vahl, *Spectrochim. Acta* **36A**, 183 (1980).
244. R. J. van Zee and W. Weltner, *J. Chem. Phys.* **99**, 762 (1993).
245. G. A. Olah and M. B. Comisarow, *J. Am. Chem. Soc.* **91**, 2172 (1969).
246. J. J. Orlando, J. B. Burkholder, A. M. R. P. Bopegedera, and C. J. Howard, *J. Mol. Spectrosc.* **145**, 278 (1991).
247. W. Levason, J. S. Ogden, M. D. Spicer, and N. A. Young, *J. Chem. Soc., Dalton Trans.* 349 (1990).
248. K. Nakagawa, K. Horiai, T. Konno, and H. Uehara, *J. Mol. Spectrosc.* **131**, 233 (1988).
249. R. Minkwitz and F. W. Froben, *Chem. Phys. Lett.* **39**, 473 (1976).
250. U. Magg, H. Birk, K. P. R. Nair, and H. Jones, *Z. Naturforsch.* **44A**, 313 (1989).

251. W. Holzer, W. F. Murphy, and H. J. Bernstein, *J. Chem. Phys.* **52**, 399 (1970).
252. W. E. Thompson and M. E. Jacox, *J. Chem. Phys.* **93**, 3856 (1990).
253. T. Ruchti, T. Speck, J. P. Connelly, E. J. Bieske, H. Linnartz, and J. P. Maier, *J. Chem. Phys.* **105**, 2591 (1996).
254. K. O. Christe, W. W. Wilson, J. A. Sheehy, and J. A. Boatz, *Angew. Chem. Int. Ed.* **38**, 2004 (1999).
255. A. Vij, W. W. Wilson, V. Vij, F. S. Tham, J. A. Sheehy, and K. O. Christe, *J. Am. Chem. Soc.* **123**, 6308 (2001).
256. M. I. Eremets, A. G. Gavriluk, I. A. Trojan, D. A. Dzivenko, and R. Boehler, *Nature Mater.* **3**, 558 (2004).
257. M. Riad Manaa, *Chem. Phys. Lett.* **331**(2–4), 262 (2000).
258. M. E. Alikhani, L. Manceron, and J.-P. Perchard, *J. Chem. Phys.* **92**, 22 (1990).
259. L. Manceron, A. M. LeQuere, and J. P. Perchard, *J. Phys. Chem.* **93**, 2960 (1989).
260. W. E. Thompson and M. E. Jacox, *J. Chem. Phys.* **91**, 3826 (1989).
261. V. Adamantides, D. Neisius, and G. Verhaegen, *Chem. Phys.* **48**, 215 (1980).
262. A. H. Jubert and E. L. Varetti, *An. Quim.* **82**, 227 (1986).
- 262a. M. E. Jacox and W. E. Thompson, *J. Chem. Phys.* **100**, 750 (1994).
- 262b. S. Seidel and K. Seppelt, *Angew. Chem. Int. Ed.* **39**, 3923 (2000).
- 262c. L. F. Lundegaard, G. Week, M. I. McMahon, S. Desgreniers, and P. Loubeyre, *Nature* **443**, 201 (2006).
263. R. D. Hunt and L. Andrews, *J. Chem. Phys.* **82**, 4442 (1985).
264. L. Andrews, S. R. Davis, and R. D. Hunt, *Mol. Phys.* **77**, 993 (1992).
265. R. L. Redington, *J. Chem. Phys.* **102**, 7325 (1995).
266. M. Fields, R. Devonshire, H. G. M. Edwards, and V. Fawcett, *Chem. Phys. Lett.* **240**, 334 (1995).
267. A. Zumbusch and H. Schnockel, *J. Chem. Phys.* **108**, 8092 (1998).
268. B. Tremblay, P. Roy, L. Manceron, P. Pullumbi, Y. Bouteiller, and D. Roy, *J. Chem. Phys.* **103**, 1284 (1995).
- 268a. W. G. Fateley, H. A. Bent, and B. Crawford, Jr. *J. Chem. Phys.* **31**, 204 (1959).
- 268b. P. Brechignac, S. De Benedictis, N. Halberstadt, B. J. Whittaker, and S. Avrillier, *J. Chem. Phys.* **83**, 2064 (1985).
- 268c. L. Andrews and M. Zhou, *J. Chem. Phys.* **111**, 6036 (1999).
- 268d. A. L. L. East, A. R. W. McKellar and J. K. G. Watson, *J. Chem. Phys.* **109**, 4378 (1998).
269. D. C. Clary, C. M. Lovejoy, S. V. O’Neil, and D. J. Nesbitt, *Phys. Rev. Lett.* **61**, 1576 (1988).
270. C. M. Lovejoy and D. J. Nesbitt, *Chem. Phys. Lett.* **147**, 490 (1988).
271. R. L. Robinson, D. Ray, D. H. Gwo, and R. J. Saykally, *J. Chem. Phys.* **87**, 5149 (1987).
272. R. L. Robinson, D. H. Gwo, and R. J. Saykally, *J. Chem. Phys.* **87**, 5156 (1987).
273. C. M. Lovejoy and D. J. Nesbitt, *Chem. Phys. Lett.* **146**, 582 (1988).
274. R. L. Robinson, D. H. Gwo, and R. J. Saykally, *Mol. Phys.* **63**, 1021 (1988).
275. C. M. Lovejoy, M. D. Schuder, and D. J. Nesbitt, *J. Chem. Phys.* **85**, 4890 (1986).
276. K. A. Walker, C. Xia, and A. R. McKellar, *J. Chem. Phys.* **114**, 4824 (2001).

277. C. Xia and A. R. McKellar, *Mol. Phys.* **98**, 1669 (2000).
278. B. J. van der Veken and E. J. Shuyts, *J. Mol. Struct.* **349**, 461 (1995).
279. A. Snelson, *J. Phys. Chem.* **72**, 250 (1968).
280. M. L. Lesiecki and J. W. Nibler, *J. Chem. Phys.* **64**, 871 (1976).
281. G. V. Calder, D. E. Mann, K. S. Seshadri, M. Allavena, and D. White, *J. Chem. Phys.* **51**, 2093 (1969).
282. D. White, G. V. Calder, S. Hemple, and D. E. Mann, *J. Chem. Phys.* **59**, 6645 (1973).
283. R. J. Konings and J. E. Fearon, *Chem. Phys. Lett.* **206**, 57 (1993).
284. E. D. Samsonova, S. B. Osin, and V. F. Shevel'kov, *Russ. J. Inorg. Chem. (Engl. transl.)* **33**, 1598 (1988).
285. J. J. Habeeb and D. G. Tuck, *J. Chem. Soc., Dalton Trans.* 866 (1976).
286. D. E. Milligan and M. E. Jacox, *J. Chem. Phys.* **48**, 2265 (1968).
287. L. Andrews, *J. Chem. Phys.* **48**, 979 (1968).
288. L. Andrews and T. G. Carver, *J. Chem. Phys.* **49**, 896 (1968).
289. J. W. Hastie, R. H. Hauge, and J. L. Margrave, *J. Am. Chem. Soc.* **91**, 2536 (1969).
290. D. E. Milligan and M. E. Jacox, *J. Chem. Phys.* **49**, 1938 (1968).
291. G. Maass, R. H. Hauge, and J. L. Margrave, *Z. Anorg. Allg. Chem.* **392**, 295 (1972).
292. J. W. Hastie, R. H. Hauge, and J. L. Margrave, *J. Phys. Chem.* **72**, 4492 (1968).
293. L. Andrews and D. L. Frederick, *J. Am. Chem. Soc.* **92**, 775 (1970).
294. R. H. Hauge, J. W. Hastie, and J. L. Margrave, *J. Mol. Spectrosc.* **45**, 420 (1973).
295. G. A. Ozin and A. Vender Voet, *J. Chem. Phys.* **56**, 4768 (1972).
296. I. R. Beattie and R. O. Perry, *J. Chem. Soc. A* 2429 (1970).
297. M. D. Harmony and R. J. Myers, *J. Chem. Phys.* **37**, 636 (1962).
298. J. K. Burdett, L. Hodges, V. Dunning, and J. H. Current, *J. Phys. Chem.* **74**, 4053 (1970).
299. L. Andrews and D. L. Frederick, *J. Phys. Chem.* **73**, 2774 (1969).
300. Y. Xu, A. R. W. McKellar, J. B. Burkholder, and J. J. Orlando, *J. Mol. Spectrosc.* **175**, 68 (1996).
301. P. Hassanzadeh and L. Andrews, *J. Phys. Chem.* **96**, 79 (1992).
302. M. Feuerhahn and G. Vahl, *Inorg. Nucl. Chem. Lett.* **16**, 5 (1980).
- 302a. G. D. Brabson, J. C. Dillon, and L. Andrews, *Chem. Phys. Lett.* **254**, 94 (1996).
303. A. Maaninen, T. Chivers, M. Parvez, J. Pietikäinen, and R. S. Laitinen, *Inorg. Chem.* **38**, 4093 (1999).
304. G. A. Ozin and A. Vander Voet, *Chem. Commun.* 896 (1970).
305. H. H. Claassen, G. L. Goodman, J. G. Malm, and F. Schreiner, *J. Chem. Phys.* **42**, 1229 (1965).
306. P. A. Agron, G. M. Begun, H. A. Levy, A. A. Mason, C. G. Jones, and D. F. Smith, *Science* **139**, 842 (1963).
307. L. Y. Nelson and G. C. Pimentel, *Inorg. Chem.* **6**, 1758 (1967).
308. I. Person, M. Sandström, A. T. Steel, M. J. Zapetero, and R. Aakesson, *Inorg. Chem.* **30**, 4075 (1991).
309. D. N. Waters and B. Basak, *J. Chem. Soc. A* 2733 (1971).

310. P. Braunstein and R. J. H. Clark, *J. Chem. Soc., Dalton Trans.* 1845 (1973).
311. A. Givan and A. Loewenschuss, *J. Chem. Phys.* **72**, 3809 (1980).
312. A. Givan and A. Loewenschuss, *J. Chem. Phys.* **68**, 2228 (1978).
313. A. Loewenschuss, A. Ron, and O. Schnepp, *J. Chem. Phys.* **50**, 2502 (1969).
314. J. W. Hastie, R. Hauge, and J. L. Margrave, *J. Chem. Phys.* **51**, 2648 (1969).
315. J. W. Hastie, R. H. Hauge, and J. L. Margrave, *Chem. Commun.* 1452 (1969).
316. O. V. Blinova, V. G. Shklyarik, and L. D. Shcherbe, *Zh. Fiz. Khim.* **62**, 1640 (1988).
317. M. E. Jacox and D. E. Milligan, *J. Chem. Phys.* **51**, 4143 (1969).
318. N. A. Young, *J. Chem. Soc., Dalton Trans.* 249 (1996).
319. I. Eliezer and A. Reger, *Coord. Chem. Rev.* **9**, 189 (1972/1973).
320. J. W. Hastie, R. H. Hauge, and J. L. Margrave, *High. Temp. Sci.* **1**, 76 (1969).
321. I. R. Beattie, P. J. Jones, and N. A. Young, *Mol. Phys.* **72**, 1309 (1991).
322. I. R. Beattie, P. J. Jones, and N. A. Young, *Inorg. Chem.* **30**, 2250 (1991).
323. D. L. Cocke, C. A. Chang, and K. A. Gingerich, *Appl. Spectrosc.* **27**, 260 (1973).
324. H. Huber, E. P. Kündig, G. A. Ozin, and A. Vander Voet, *Can. J. Chem.* **52**, 95 (1974).
325. F. Ramondo, L. Bencivenni, and V. Rossi, *Chem. Phys.* **124**, 291 (1988).
326. L. Andrews, *J. Phys. Chem.* **73**, 3922 (1969).
327. A. Sommer, D. White, M. J. Linevsky, and D. E. Mann, *J. Chem. Phys.* **38**, 87 (1963).
328. A. Snelson, *J. Phys. Chem.* **74**, 2574 (1970).
329. A. J. Hinchcliffe and J. S. Ogden, *J. Phys. Chem.* **77**, 2537 (1973); *Chem. Commun.* 1053 (1969).
330. A. H. Nielsen and R. J. Lagemann, *J. Chem. Phys.* **22**, 36 (1954).
331. S. A. Tashkun, V. I. Perevalov, and J.-L. Teffo, *J. Mol. Spectrosc.* **210**, 137 (2001).
332. W. E. Thompson and M. E. Jacox, *J. Chem. Phys.* **111**, 4487 (1999).
333. Z. Kafafi, R. Hauge, W. Billups, and J. Margrave, *Inorg. Chem.* **23**, 177 (1984).
334. T. Wentink, Jr., *J. Chem. Phys.* **29**, 188 (1958).
335. T. M. Halasinski, J. T. Godbout, J. Allison, and G. E. Leroi, *J. Phys. Chem.* **100**, 14865 (1996).
336. H. Bürger and H. Willner, *J. Mol. Spectrosc.* **128**, 221 (1988).
337. J. S. Anderson, A. Bos, and J. S. Ogden, *Chem. Commun.* 1381 (1971).
338. A. R. Evans and D. B. Fitchen, *Phys. Rev.* **B2**, 1074 (1970).
339. D. E. Tevault and L. Andrews, *Spectrochim. Acta* **30A**, 969 (1974).
340. J. W. Nebgen, A. D. McElroy, and H. F. Klodowski, *Inorg. Chem.* **4**, 1796 (1965).
341. D. Maillard, M. Allavena, and J. P. Perchard, *Spectrochim. Acta* **31A**, 1523 (1975).
342. L. Bencivenni, F. Ramondo, R. Teghil, and M. Pelino, *Inorg. Chim. Acta* **121**, 207 (1986).
343. S. N. Cesaro, M. Spoliti, A. J. Hinchcliffe, and J. S. Ogden, *J. Chem. Phys.* **55**, 5834 (1971).
344. M. Spoliti, S. N. Cesaro, and E. Ciffari, *J. Chem. Thermodyn.* **4**, 507 (1972).
345. J. S. Ogden and J. J. Turner, *J. Chem. Soc. A* 1483 (1967).
346. M. M. Rochkind and G. C. Pimentel, *J. Chem. Phys.* **42**, 1361 (1965).
347. W. Levason, J. S. Ogden, M. D. Spicer, and N. A. Young, *J. Chem. Soc., Dalton Trans.* 349 (1990).

348. H. S. P. Müller and H. Willner, *J. Phys. Chem.* **97**, 10589 (1993).
349. K. M. Tobias and M. Jansen, *Z. Anorg. Allg. Chem.* **550**, 16 (1987).
350. J. Kölm, A. Engdahl, O. Schrems, and B. Nelander, *Chem. Phys.* **214**, 313 (1997).
351. W. Levason, J. S. Ogden, M. D. Spicer, and N. A. Young, *J. Am. Chem. Soc.* **112**, 1019 (1990).
352. L. J. Chu and Z. Li, *Chem. Phys. Lett.* **330**, 68 (2000).
353. E. Jacob, *Angew. Chem. Int. Ed.* **15**, 158 (1976).
354. G. Maier and A. Bothur, *Chem. Ber./Recl.* **130**, 179 (1997).
355. S. D. Gabelnick, G. T. Reedy, and M. G. Chasanov, *J. Chem. Phys.* **60**, 1167 (1974).
356. J. G. Kay, D. W. Green, K. Duca, and G. L. Zimmerman, *J. Mol. Spectrosc.* **138**, 49 (1989).
357. N. S. McIntyre, K. R. Thompson, and W. Weltner, *J. Phys. Chem.* **75**, 3243 (1971).
358. W. Weltner and D. McLeod, *J. Chem. Phys.* **42**, 882 (1965).
359. M. Lorenz and V. E. Bondybey, *Chem. Phys.* **241**, 127 (1999).
- 359a. Möller, *Z. Anorg. Allg. Chem.* **628**, 77 (2002).
360. S. D. Gabelnick, G. T. Reedy, and M. G. Chasanov, *J. Chem. Phys.* **58**, 4468 (1973).
361. J. R. Ferraro and A. Walker, *J. Chem. Phys.* **45**, 550 (1966).
362. D. W. Green and G. T. Reedy, *J. Chem. Phys.* **69**, 544 (1978).
363. M. Somer, U. Herterich, J. Čurda, W. Carillo-Cabrera, A. Zürn, K. Peters, and H. G. von Schnering, *Z. Anorg. Allg. Chem.* **626**, 625 (2000).
364. R. D. Hunt, J. T. Yustein, and L. Andrews, *J. Chem. Phys.* **98**, 6070 (1993).
365. M. Somer, W. Carrillo-Cabrera, K. Peters, and H. G. von Schnering, *Z. Anorg. Allg. Chem.* **626**, 897 (2000).
366. M. Somer, M. Hartweg, K. Peters, T. Popp, and H. G. von Schnering, *Z. Anorg. Allg. Chem.* **595**, 217 (1991).
367. S. Li, R. J. van Zee, and W. Weltner, *J. Phys. Chem.* **97**, 11393 (1993).
368. M. Somer, *Z. Naturforsch.* **49B**, 1203 (1994).
369. B. Liang and L. Andrews, *J. Phys. Chem. A* **106**, 6295 (2002).
370. W. W. Wilson and K. O. Christe, *Inorg. Chem.* **26**, 1631 (1987).
371. D. W. Green and G. T. Reedy, in J. R. Ferraro and L. J. Basile, eds., *Fourier Transform Infrared Spectroscopy: Applications to Chemical Systems*, Vol. 1, Academic Press, New York, 1978.
372. D. W. Green and G. T. Reedy, *J. Chem. Phys.* **65**, 2921 (1976).
373. D. W. Green and G. T. Reedy, *J. Chem. Phys.* **69**, 552 (1978).
374. D. W. Green and G. T. Reedy, *J. Chem. Phys.* **74**, 423 (1979).
375. L. H. Jones and R. A. Penneman, *J. Chem. Phys.* **21**, 542 (1953).
376. L. H. Jones, *Spectrochim. Acta* **11**, 409 (1959).
377. J. R. Bartlett and R. P. Cooney, *J. Mol. Struct.* **193**, 295 (1989).
378. K. Mizuoka and Y. Ikeda, *Inorg. Chem.* **42**, 3396 (2003).
379. R. A. Shepherd and W. R. M. Graham, *J. Chem. Phys.* **88**, 3399 (1988).
380. J. M. L. Martin, P. R. Taylor, J. T. Yustein, T. R. Burkholder, and L. Andrews, *J. Chem. Phys.* **99**, 12 (1993).

381. B. Tremblay, L. Manceron, P. Roy, A. M. LeQuere, and D. Roy, *Chem. Phys. Lett.* **228**, 410 (1994).
382. M. Bahou, Y.-C. Lee, and Y.-P. Lee, *J. Am. Chem. Soc.* **122**, 661 (2000).
383. E. S. Prochaska and L. Andrews, *Inorg. Chem.* **16**, 339 (1977).
384. K. O. Christe, W. Sawodny, and J. P. Guertin, *Inorg. Chem.* **6**, 1159 (1967).
385. R. J. Gillespie and M. J. Morton, *Inorg. Chem.* **9**, 811 (1970).
386. K. O. Christe and C. J. Schack, *Inorg. Chem.* **9**, 2296 (1970).
387. T. Surles, L. A. Quaterman, and H. H. Hyman, *J. Inorg. Nucl. Chem.* **35**, 668 (1973).
388. R. Minkwitz, R. Bröchler, and R. Ludwig, *Inorg. Chem.* **36**, 4280 (1997).
- 388a. D. Naumann and A. Meurer, *J. Fluorine. Chem.* **70**, 83 (1995).
389. R. Minkwitz, J. Nowicki, H. Härtner, and W. Sawodny, *Spectrochim. Acta* **47A**, 1673 (1991).
390. B. S. Ault and L. Andrews, *J. Chem. Phys.* **64**, 4853 (1976).
391. W. Gabes and H. Gerding, *J. Mol. Struct.* **14**, 267 (1972).
392. R. Forneris and Y. Tavares-Forneris, *J. Mol. Struct.* **23**, 241 (1974).
393. W. W. Wilson and F. Aubke, *Inorg. Chem.* **13**, 326 (1974).
394. K. O. Christe, R. Bau, and D. Zhao, *Z. Anorg. Allg. Chem.* **593**, 46 (1991).
395. D. H. Boal and G. A. Ozin, *J. Chem. Phys.* **55**, 3598 (1971).
396. A. G. Maki and R. Forneris, *Spectrochim. Acta* **23A**, 867 (1967).
- 396a. L. Kloos, P. H. Svensson, and M. J. Taylor, *J. Chem. Soc., Dalton Trans.* 1061 (2000).
397. M. Couzi, J. C. Cornut, and P. V. Huong, *J. Chem. Phys.* **56**, 426 (1972).
398. J. J. Rush, L. W. Schroeder, and A. J. Melveger, *J. Chem. Phys.* **56**, 2793 (1972).
399. B. S. Ault, *J. Phys. Chem.* **82**, 844 (1978).
400. K. Kawaguchi and E. Hirota, *J. Chem. Phys.* **87**, 6838 (1987).
401. J. C. Evans and G. Y.-S. Lo, *J. Phys. Chem.* **70**, 543 (1966).
402. G. C. Stirling, C. J. Ludman, and T. C. Waddington, *J. Chem. Phys.* **52**, 2730 (1970).
403. J. W. Nibler and G. C. Pimentel, *J. Chem. Phys.* **47**, 710 (1967).
404. J. C. Evans and G. Y.-S. Lo, *J. Phys. Chem.* **71**, 3942 (1967).
405. B. S. Ault and L. Andrews, *J. Chem. Phys.* **64**, 1986 (1976).
406. P. N. Noble, *J. Chem. Phys.* **56**, 2088 (1972).
407. B. S. Ault and L. Andrews, *Inorg. Chem.* **16**, 2024 (1977).
408. K. Kaya, N. Mikami, Y. Udagawa, and M. Ito, *Chem. Phys. Lett.* **16**, 151 (1972).
409. W. Kiefer and H. J. Bernstein, *Chem. Phys. Lett.* **16**, 5 (1972).
410. M. E. Heyde, L. Rimai, R. G. Kilponen, and D. Gill, *J. Am. Chem. Soc.* **94**, 5222 (1972).
411. B. S. Ault, *Acc. Chem. Res.* **15**, 103 (1982).
412. B. S. Ault, *J. Phys. Chem.* **83**, 837 (1979).
413. J. C. Evans and G. Y.-S. Lo, *J. Phys. Chem.* **70**, 11 (1966).
414. Z. L. Xiao, R. H. Hauge, and J. L. Margrave, *High. Temp. Sci.* **31**, 59 (1991).
415. Z. L. Xiao, R. H. Hauge, and J. L. Margrave, *J. Phys. Chem.* **95**, 2696 (1991).
416. Z. L. Xiao, R. H. Hauge, and J. L. Margrave, *J. Phys. Chem.* **96**, 636 (1992).

- 417. S. Li, J. van Zee, W. Weltner, M. G. Cory, and M. C. Zerner, *J. Chem. Phys.* **106**, 2055 (1997).
- 418. J. M. Parnis and G. A. Ozin, *J. Phys. Chem.* **93**, 1215 (1989).
- 419. P. Pullumbi, C. Mijoule, L. Manceron, and Y. Bouteiller, *Chem. Phys.* **185**, 13 (1994).
- 420. E. Hirota and H. Ishikawa, *J. Chem. Phys.* **110**, 4254 (1999).
- 421. G. R. Smith and W. A. Guillory, *J. Chem. Phys.* **56**, 1423 (1972).
- 422. D. E. Milligan and M. E. Jacox, *J. Chem. Phys.* **43**, 4487 (1965).
- 423. T. Nakata and S. Matsushita, *J. Phys. Chem.* **72**, 458 (1968).
- 424. A. Müller, R. Kebabcioglu, B. Krebs, P. Bouclier, J. Portier, and P. Hagenmuller, *Z. Anorg. Allg. Chem.* **368**, 31 (1969).
- 425. H. Jacobs and K. M. Hassiepen, *Z. Anorg. Allg. Chem.* **531**, 108 (1985).
- 426. D. Forney, M. E. Jacox, and W. E. Thompson, *J. Chem. Phys.* **98**, 841 (1993).
- 427. B. M. Dinelli, M. W. Crofton, and T. Oka, *J. Mol. Spectrosc.* **127**, 1 (1988).
- 428. W. S. Benedict, N. Gailar, and E. K. Plyler, *J. Chem. Phys.* **24**, 1139 (1956).
- 429. G. E. Walrafen, *J. Chem. Phys.* **40**, 3249 (1964).
- 430. C. Haas and D. F. Hornig, *J. Chem. Phys.* **32**, 1763 (1960); D. F. Hornig, H. F. White, and F. P. Reding, *Spectrochim. Acta* **12**, 338 (1958).
- 431. S. Pinchas and M. Halmann, *J. Chem. Phys.* **31**, 1692 (1959).
- 432. P. A. Staats, H. W. Morgan, and J. H. Goldstein, *J. Chem. Phys.* **24**, 916 (1956).
- 433. I. Kanesaka, H. Hayashi, M. Kita, and K. Kawai, *J. Chem. Phys.* **93**, 6113 (1990).
- 434. H. C. Allen and E. K. Plyler, *J. Chem. Phys.* **25**, 1132 (1956).
- 435. A. J. Tursi and E. R. Nixon, *J. Chem. Phys.* **53**, 518 (1970).
- 436. F. P. Reding and D. F. Hornig, *J. Chem. Phys.* **27**, 1024 (1957).
- 437. A. H. Nielsen and H. H. Nielsen, *J. Chem. Phys.* **5**, 277 (1937).
- 438. D. M. Cameron, W. C. Sears, and H. H. Nielsen, *J. Chem. Phys.* **7**, 994 (1939).
- 439. O. N. Ulenikov, G. A. Onopenko, N. E. Tyabaeva, H. Bürger, and W. Jerzembek, *J. Mol. Spectrosc.* **197**, 100 (1999).
- 440. O. N. Ulenikov, H. Bürger, W. Jerzembek, G. A. Onopenko, E. A. Zhabina, and O. L. Petrunina, *J. Mol. Spectrosc.* **202**, 229 (2000).
- 441. J.-M. Flaud, M. Betrencourt, P. Arcas, H. Bürger, O. Polanz, and W. J. Lafferty, *J. Mol. Spectrosc.* **182**, 396 (1997).
- 442. E. Greinacher, W. Lüttke, and R. Mecke, *Z. Elektrochem.* **59**, 23 (1955).
- 443. M. L. Josien and P. Saumagne, *Bull. Soc. Chim. Fr.* 937 (1956).
- 444. G. E. Walrafen, M. S. Hokmabadi, and W.-H. Yang, *J. Chem. Phys.* **85**, 6964 (1986).
- 445. G. E. Walrafen, *J. Phys. Chem.* **94**, 2237 (1990).
- 446. G. E. Walrafen, *Encyclopedia of Earth System Science*, Vol. 4, Academic Press, San Diego, CA, 1992, p. 463.
- 447. J. E. Bertie, H. J. Labbé, and E. Whalley, *J. Chem. Phys.* **49**, 775, 2141 (1968). J. E. Bertie and E. Whalley, *ibid.* **40**, 1637 (1964).
- 448. G. P. Ayers and A. D. E. Pullin, *Spectrochim. Acta* **32A**, 1629 (1976).
- 449. J. P. Perchard, *Chem. Phys.* **266**, 109 (2001).
- 450. K. Nauta and R. E. Miller, *Science* **287**, 293 (2000).

451. J. P. Devlin, J. Sadlej, and V. Bulch, *J. Phys. Chem. A*, **105**, 974 (2001).
452. W. Klein and M. Jansen, *Z. Anorg. Allg. Chem.* **626**, 136 (2000).
453. A. Dimitrov, K. Seppelt, D. Scheffler, and H. Wilner, *J. Am. Chem. Soc.* **120**, 8711 (1998).
454. K. M. Bulanin, M. O. Bulanin, and A. A. Tsyganenko, *Chem. Phys.* **203**, 127 (1996).
455. O. El-Jaroudi, E. Picquenard, A. Demortier, J.-P. Lelieur, and J. Corset, *Inorg. Chem.* **38**, 2394 (1999).
456. R. J. H. Clark and D. G. Cobbold, *Inorg. Chem.* **17**, 3169 (1978).
457. E. Piquenard, O. El-Jaroudi, and J. Corset, *J. Raman. Spectrosc.* **24**, 11 (1993).
458. P. Lenain, E. Piquenard, J. L. Lesne, and J. Corset, *J. Mol. Struct.* **142**, 355 (1986).
459. L. H. Jones, *Inorganic Vibrational Spectroscopy*, Marcel Dekker, New York, 1971, p. 63.
460. R. Tian, J. C. Facelli, and J. Michl, *J. Phys. Chem.* **92**, 4073 (1988).
461. L. Fang, X. Shen, X. Chen, and J. R. Lombardi, *J. Chem. Phys.* **113**, 7178 (2000).
462. L. Fang, B. Davis, H. Lu, X. Chen, X. Shen, and J. R. Lombardi, *Chem. Phys. Lett.* **352**, 70 (2002).
463. A. Kornath, A. Zoermer, and R. Ludwig, *Inorg. Chem.* **38**, 4696 (1999).
464. L. Fang, B. Davis, H. Lu, and J. R. Lombardi, *J. Phys. Chem. A* **105**, 9375 (2001).
465. T. J. Haslett, K. A. Bosnick, S. Fedrigo, and M. Moskovits, *J. Chem. Phys.* **111**, 6456 (1999).
466. L. Fang, X. Shen, X. Chen, and J. R. Lombardi, *Chem. Phys. Lett.* **332**, 299 (2000).
467. H. Wang, R. Craig, H. Haouari, Y. Liu, J. R. Lombardi, and D. M. Lindsay, *J. Chem. Phys.* **105**, 5355 (1996).
468. R. Guo, K. Balasubramanian, X. Wang, and L. Andrews, *J. Chem. Phys.* **117**, 1614 (2002).
469. M. S. Workentin, B. D. Wagner, F. Negri, M. Z. Zgierski, J. Lusztyk, W. Siebrand, and D. D. M. Wayner, *J. Phys. Chem.* **99**, 94 (1995).
470. D. White, K. S. Seshadri, D. F. Dever, D. E. Mann, and M. J. Linevsky, *J. Chem. Phys.* **39**, 2463 (1963).
471. M. E. Jacox, D. E. Milligan, N. G. Mall, and W. E. Thompson, *J. Chem. Phys.* **43**, 3734 (1965).
472. J. Fulara, M. Grutter, M. Wyss, and J. P. Maier, *J. Phys. Chem. A* **102**, 3459 (1998).
473. J. C. Owrutsky, C. S. Gudeman, C. C. Martner, L. M. Tack, N. H. Rosenbaum, and R. J. Saykally, *J. Chem. Phys.* **84**, 605 (1986).
474. V. E. Bondybey and J. H. English, *J. Chem. Phys.* **67**, 664 (1979).
475. G. M. Begun and W. H. Fletcher, *J. Chem. Phys.* **28**, 414 (1958).
- 475a. K. O. Christe, R. D. Wilson, and W. Sawodny, *J. Mol. Struct.* **8**, 245 (1971).
476. H. Uehara, K. Kawaguchi, and E. Hirota, *J. Chem. Phys.* **83**, 5479 (1985).
477. R. D. Spratley, J. J. Turner, and G. C. Pimentel, *J. Chem. Phys.* **44**, 2063 (1966).
478. H. S. P. Müller and H. Willner, *J. Phys. Chem.* **97**, 10589 (1993).
479. G. Maier and A. Bothur, *Z. Anorg. Allg. Chem.* **621**, 743 (1995).
480. L.-S. Chen, C.-I. Lee, and Y.-P. Lee, *J. Chem. Phys.* **105**, 9454 (1996).
481. E. Isoniemi, L. Khriachtchev, M. Pattersson, and M. Räsänen, *Chem. Phys. Lett.* **311**, 47 (1999).
482. J. Lindenmayer, H. D. Rudolph, and H. Jones, *J. Mol. Spectrosc.* **119**, 56 (1986).

483. K. Johnsson, A. Engdahl, and B. Nelander, *J. Phys. Chem.* **99**, 3965 (1995).
484. H. C. Allen, E. D. Tidwell, and E. K. Plyler, *J. Chem. Phys.* **25**, 302 (1956).
485. J. Pacansky and G. V. Calder, *J. Phys. Chem.* **76**, 454 (1972).
- 485a. P. A. Staats, H. W. Morgan, and J. H. Goldstein, *J. Chem. Phys.* **25**, 582 (1956).
486. D. E. Milligan and M. E. Jacox, *J. Chem. Phys.* **47**, 278 (1967).
487. F. J. Northrup, G. A. Berthady, and R. G. MacDonald, *J. Mol. Spectrosc.* **186**, 349 (1997).
488. N. T. Hunt, D. Collet, Z. Liu, and P. B. Davies, *J. Chem. Phys.* **111**, 5905 (1999).
489. E. R. Lory and R. F. Porter, *J. Am. Chem. Soc.* **93**, 6301 (1971).
490. Y. Kawashima, P. Colarusso, K. Q. Zhang, P. Bernath, and E. Hirota, *J. Mol. Spectrosc.* **192**, 152 (1998).
491. N. H. Rosenbaum, J. C. Owruksy, and R. J. Saykally, *J. Mol. Spectrosc.* **133**, 365 (1989).
492. B. Maier and J. Glatthaar, *Angew. Chem. Int. Ed.* **106**, 473 (1994).
493. L. Khriachtchev, M. Pettersson, M. Runeberg, J. Lundell, and M. Räsänen, *Nature* **406**, 874 (2000).
- 493a. L. Khriachtchev, M. Pettersson, A. Lignell, and M. Räsänen, *J. Am. Chem. Soc.* **123**, 8610 (2001).
494. M. Pettersson, L. Khriachtchev, A. Lignell, M. Räsänen, Z. Bihary, and R. B. Gerber, *J. Chem. Phys.* **116**, 2508 (2002).
495. D. McNaughton and R. Tay-Lim, *J. Mol. Spectrosc.* **209**, 280 (2001).
496. R. E. Dodd and R. Little, *Spectrochim. Acta.* **16**, 1083 (1960).
497. H. Beckers, H. Bürger, P. Paplewski, M. Bogey, J. Demaison, P. Dréan, A. Walters, J. Breidung, and W. Thiel, *Phys. Chem. Chem. Phys.* **3**, 4247 (2001).
498. H. Beckers, M. Bogey, J. Breidung, H. Bürger, J. Demaison, P. Dréan, P. Paplewski, W. Thiel, and A. Walters, *J. Mol. Spectrosc.* **210**, 213 (2001).
499. A. Saouli, I. Dubois, J. F. Blavier, H. Bredohl, G. Blanquet, C. Meyer, and F. Meyer, *J. Mol. Spectrosc.* **165**, 349 (1994).
500. T. B. Freedman and E. R. Nixon, *J. Chem. Phys.* **56**, 698 (1972).
501. D. McNaughton and R. Tay-Lim, *J. Mol. Spectrosc.* **202**, 89 (2002).
502. N. T. Hunt, J. Röpcke, and P. B. Davies, *J. Mol. Spectrosc.* **204**, 120 (2002).
503. K. O. Christe, B. Hoge, J. A. Boatz, G. K. S. Prakash, G. A. Olah, and J. A. Sheehy, *Inorg. Chem.* **38**, 3132 (1999).
504. G. Schallmoser, B. E. Wurfel, A. Thoma, N. Caspary, and V. E. Bondybey, *Chem. Phys. Lett.* **201**, 528 (1993).
505. D. McNaughton and D. N. Bruget, *J. Mol. Spectrosc.* **161**, 336 (1993).
506. W. O. Freitag and E. R. Nixon, *J. Chem. Phys.* **24**, 109 (1956).
507. S. Hemple and E. R. Nixon, *J. Chem. Phys.* **47**, 4273 (1967).
508. Z. K. Ismail, R. H. Hauge, and J. L. Margrave, *J. Chem. Phys.* **57**, 5137 (1972).
509. Z. K. Ismail, R. H. Hauge, and J. L. Margrave, *J. Mol. Spectrosc.* **45**, 304 (1973).
510. W. Beck, *Chem. Ber.* **95**, 341 (1962); **98**, 298 (1965).
511. D. E. Milligan and M. E. Jacox, *J. Chem. Phys.* **47**, 5157 (1967).
512. O. H. Ellestad, P. Klæboe, E. E. Tucker, and J. Songstad, *Acta Chem. Scand.* **26**, 1721 (1972).

513. P. O. Kinell and B. Strandberg, *Acta. Chem. Scand.* **13**, 1607 (1959).
514. H. W. Morgan, *J. Inorg. Nucl. Chem.* **16**, 368 (1960).
515. O. H. Ellestad, P. Klaeboe, and J. Songstad, *Acta Chem. Scand.* **26**, 1724 (1972).
516. S. Mann and M. Jansen, *Z. Anorg. Allg. Chem.* **631**, 153 (1995).
517. G. Becker and K. Hübler, *Z. Anorg. Allg. Chem.* **620**, 405 (1994).
518. R. Ahlrichs, S. Schuck, and H. Schnöckel, *Angw. Chem. Int. Ed.* **27**, 421 (1988).
519. C. Lugez, W. E. Thompson, and M. E. Jacox, *J. Chem. Phys.* **115**, 166 (2001).
520. A. J. Bridgeman, N. Harris, and N. A. Young, *J. Chem. Soc., Chem. Commun.* 1241 (2000).
521. A. Maki, E. K. Plyler, and E. D. Tidwell, *J. Res. Natl. Bur. Stand.* **66A**, 163 (1962).
522. T. Wentink, Jr., *J. Chem. Phys.* **29**, 188 (1958).
523. M. Junker, M. Friesan, and H. Schnöckel, *J. Chem. Phys.* **112**, 1444 (2000).
524. M. Barnes, D. A. Gillett, A. J. Merer, and G. F. Metha, *J. Chem. Phys.* **105**, 6168 (1996).
525. B. Tremblay, M. E. Alikhani, and L. Manceron, *J. Phys. Chem. A* **105**, 11388 (2001).
526. D. E. Milligan and M. E. Jacox, *J. Chem. Phys.* **51**, 277 (1969).
527. M. E. Jacox and D. E. Milligan, *J. Chem. Phys.* **50**, 3252 (1969).
528. J. F. Ogilvie, *Spectrochim. Acta* **23A**, 737 (1967).
529. M. E. Jacox and D. E. Milligan, *J. Chem. Phys.* **46**, 184 (1967).
530. G. Maier, H. P. Reisenauer, and M. de Marco, *Angw. Chem. Int. Ed.* **38**, 108 (1999).
531. J. A. Goleb, H. H. Claassen, M. H. Studier, and E. H. Appelman, *Spectrochim. Acta* **28A**, 65 (1972).
532. I. Schwager and A. Arkell, *J. Am. Chem. Soc.* **89**, 6006 (1967).
533. N. Walker, D. E. Tevault, and R. R. Smardzewski, *J. Chem. Phys.* **69**, 564 (1978).
534. B. Tremblay, M. E. Alikhani, and L. Manceron, *Chem. Phys.* **218**, 37 (1997).
535. R. R. Smardzewski and W. B. Fox, *J. Am. Chem. Soc.* **96**, 304 (1974). *J. Chem. Phys.* **60**, 2104 (1974).
536. U. Magg, J. Lindenmeyer, and H. Jones, *J. Mol. Spectrosc.* **126**, 270 (1987).
537. A. Müller, G. Nagarajan, O. Glemser, and J. Wegener, *Spectrochim. Acta* **23A**, 2683 (1967); A. Müller, N. Mohan, S. J. Cyvin, N. Weinstock, and O. Glemser, *J. Mol. Spectrosc.* **59**, 161 (1976).
538. R. R. Ryan and L. H. Jones, *J. Chem. Phys.* **50**, 1492 (1969); L. H. Jones, L. B. Asprey, and R. R. Ryan, *ibid.* **47**, 3371 (1967).
539. L. H. Jones, R. R. Ryan, and L. B. Asprey, *J. Chem. Phys.* **49**, 581 (1968).
540. J. Laane, L. H. Jones, R. R. Ryan, and L. B. Asprey, *J. Mol. Spectrosc.* **30**, 485 (1969).
541. M. Feuerhahn, W. Hilbig, R. Minkwitz, and U. Engelhardt, *Spectrochim. Acta* **34A**, 1065 (1978).
542. P. Paplewski, H. Bürger, and H. Beckers, *Z. Naturforsch.* **54a**, 507 (1999).
543. R. Ahlrichs, R. Becherer, M. Binnewies, H. Bormann, M. Lakenbrink, S. Schunck, and H. Schnöckel, *J. Am. Chem. Soc.* **108**, 7905 (1986).
544. A. W. Allaf and I. Boustani, *Vib. Spectrosc.* **16**, 69 (1998).

545. D. E. Milligan, M. E. Jacox, A. M. Bass, J. J. Comeford, and D. E. Mann, *J. Chem. Phys.* **42**, 3187 (1965).
546. M. E. Jacox and D. E. Milligan, *J. Chem. Phys.* **43**, 866 (1965).
547. H. S. P. Müller, *Chem. Phys. Lett.* **314**, 396 (1999).
548. H. Schnöckel and S. Schunck, *Z. Anorg. Allg. Chem.* **552**, 163 (1987).
549. H. Schnöckel and S. Schunck, *Z. Anorg. Allg. Chem.* **552**, 155 (1987).
550. C. J. Evans, D. McNaughton, P. Dexter, and W. Lawrance, *J. Mol. Spectrosc.* **187**, 75 (1998).
551. A. M. Zarubaiko and J. V. Gilvert, *J. Phys. Chem.* **97**, 4331 (1993).
552. C. E. Smith, D. E. Milligan, and M. E. Jacox, *J. Chem. Phys.* **54**, 2780 (1971).
553. M. Junker and H. Schnöckel, *J. Chem. Phys.* **110**, 3769 (1999).
554. S. C. Peake and A. J. Downs, *J. Chem. Soc., Dalton Trans.* 859 (1974).
555. G. A. Ozin and A. Vander Voet, *J. Chem. Phys.* **56**, 4768 (1972).
556. G. Maier, H. P. Reisenauer, and M. de Marco, *Chem.-Eur. J.* **6**, 800 (2000).
557. C. O. Della Vedova and H. G. Mack, *Inorg. Chem.* **32**, 948 (1993).
558. L. Krim, E. M. Alikhani, and L. Manceron, *J. Phys. Chem. A* **105**, 7812 (2001).
559. A. Lapinski, J. Spanget-Larsen, J. Waluk, and J. G. Radziszewski, *J. Chem. Phys.* **115**, 1757 (2001).
560. G. Herzberg, *Infrared and Raman Spectra of Polyatomic Molecules*, Van Nostrand, Princeton, NJ, 1945, p. 295.
561. F. P. Reding and D. F. Hornig, *J. Chem. Phys.* **19**, 594 (1951); **22**, 1926, (1954).
562. H. W. Morgan, P. A. Staats, and J. H. Goldstein, *J. Chem. Phys.* **27**, 1212 (1957).
563. S. Sundaram and F. F. Cleveland, *J. Mol. Spectrosc.* **5**, 61 (1960).
564. E. Lee and C. K. Wu, *Trans. Faraday Soc.* **35**, 1366 (1939).
565. G. Spiegel and W. A. Kreiner, *J. Mol. Spectrosc.* **187**, 142 (1998).
566. H. Bürger, W. Jerzembek, H. Ruland, and M. Wirtz, *Mol. Phys.* **98**, 589 (2000).
567. W. H. Haynie and H. H. Nielsen, *J. Chem. Phys.* **21**, 1839 (1953).
568. W. Jerzembek, H. Bürger, L. Constantin, L. Margulés, J. Demaison, J. Breidung, and W. Thiel, *Angew. Chem. Int. Ed.* **41**, 2550 (2002).
569. P. V. Huong and B. Desbat, *J. Raman. Spectrosc.* **2**, 373 (1974).
570. R. C. Taylor and G. L. Vidale, *J. Am. Chem. Soc.* **78**, 5999 (1956).
571. R. Savoie and P. A. Giguère, *J. Chem. Phys.* **41**, 2698 (1964).
572. P. A. Giguère and C. Madec, *Chem. Phys. Lett.* **37**, 569 (1976).
573. C. Xia, M. M. Sanz, and S. C. Foster, *J. Mol. Spectrosc.* **188**, 175 (1998).
574. R. Minkwitz, A. Kotnath, and W. Sawodny, *Angew. Chem. Int. Ed.* **31**, 643 (1992).
575. K. Burczyk and A. J. Downs, *J. Chem. Soc., Dalton Trans.* 2351 (1990).
576. C. Yamada and B. Hirota, *Phys. Rev. Lett.* **56**, 923 (1986).
577. T. Birchall and I. Drammond, *J. Chem. Soc. A* 3162 (1971).
578. C. Cottaz, I. Kleiner, G. Tarrago, L. R. Brown, J. S. Margolis, R. L. Poynter, H. M. Pickett, T. Foucher, P. Drossart, and E. Lellouch, *J. Mol. Spectrosc.* **203**, 285 (2000).
579. M. Snels, L. Fusina, H. Hollenstein, and M. Quack, *Mol. Phys.* **98**, 837 (2000).
580. R. D. Gillard and G. Wilkinson, *J. Chem. Soc.* 1640 (1964).

581. S. Sundaram, F. Suszek, and F. F. Cleveland, *J. Chem. Phys.* **32**, 251 (1960).
582. G. DeAlti, G. Costa, and V. Galasso, *Spectrochim. Acta* **20**, 965 (1964).
583. M. Pariseau, E. Wu, and J. Overend, *J. Chem. Phys.* **39**, 217 (1963).
- 583a. J. M. Headrick, E. G. Diken, R. S. Walters, N. I. Hammer, R. A. Christie, J. Cul, E. M. Myshakin, M. A. Duncan, M. A. Johnson, and K. D. Jordan, *Science* **308**, 1765 (2005).
584. J. P. Perchard, R. B. Bohn, and L. Andrews, *J. Phys. Chem.* **95**, 2707 (1991).
585. J. G. Contreras, J. S. Poland, and D. G. Tuck, *J. Chem. Soc., Dalton Trans.* 922 (1973).
586. D. E. Milligan, M. E. Jacox, and J. J. Comeford, *J. Chem. Phys.* **44**, 4058 (1966).
587. D. E. Milligan, M. E. Jacox, and W. A. Guillory, *J. Chem. Phys.* **49**, 5330 (1968).
588. M. E. Jacox, K. K. Irikura, and W. E. Thompson, *J. Chem. Phys.* **103**, 5308 (1995).
589. M. E. Jacox and D. E. Milligan, *J. Chem. Phys.* **49**, 3130 (1968).
590. W. A. Guillory and C. E. Smith, *J. Chem. Phys.* **53**, 1661 (1970).
591. P. S. Poskozim and A. L. Stone, *J. Inorg. Nucl. Chem.* **32**, 1391 (1970).
592. I. Wharf and D. F. Shriver, *Inorg. Chem.* **8**, 914 (1969).
593. C. J. Kallendorf and B. S. Ault, *J. Phys. Chem.* **85**, 608 (1981).
594. M. J. Taylor, *J. Raman. Spectrosc.* **20**, 663 (1989).
595. B. S. Ault, *J. Phys. Chem.* **85**, 3083 (1981).
596. B. Basak, *Inorg. Chim. Acta* **45**, L47 (1980).
597. J. Shamir and H. H. Hyman, *Spectrochim. Acta* **23A**, 1899 (1967).
598. P. J. Hendra and J. R. Mackenzie, *Chem. Commun.* 760 (1968).
599. W. Sawondy, H. Härtner, R. Minkwitz, and D. Bernstein, *J. Mol. Struct.* **213**, 145 (1989).
600. I. Tornieporth-Oetting and T. Klapötke, *Angew. Chem. Int. Ed. Engl.* **29**, 677 (1990).
601. R. J. H. Clark and D. M. Rippon, *J. Mol. Spectrosc.* **52**, 58 (1974).
602. N. B. Sari-Zizi, H. Bürger, M. Litz, H. Najib, and J. Radtke, *J. Mol. Spectrosc.* **177**, 46 (1996).
603. H. Stammreich, R. Forneris, and Y. Tavares, *J. Chem. Phys.* **25**, 580 (1956).
604. H. Bürger, H. Ruland, J. Demaison, and P. Dréan, *J. Mol. Struct.* **517/518**, 105 (2000).
605. T. M. Klapötke, *Main Group Met. Chem.* **20**, 81 (1997).
606. W. V. F. Brooks, J. Passmore, and E. K. Richardson, *Can. J. Chem.* **57**, 3230 (1979).
607. C. J. Adams and A. J. Downs, *J. Chem. Soc. A* 1534 (1971).
608. A. Loewenschuss, N.-I. Gerull, S. Angermann, and W. Brockner, *Polyhedron* **16**, 1161 (1997).
609. J. Molnar, M. Kolonits, M. Hargittai, R. J. M. Konings, and A. S. Booi, *Inorg. Chem.* **35**, 7639 (1996).
610. E. Denchik, S. C. Nyburg, G. A. Ozin, and J. T. Szymanski, *J. Chem. Soc. A* 3157 (1971).
611. V. A. Maroni and P. T. Cunningham, *Appl. Spectrosc.* **27**, 428 (1973).
612. J. A. Evans and D. A. Long, *J. Chem. Soc. A* 1688 (1968).
613. H. E. Doorenbos, J. C. Evans, and R. O. Kagel, *J. Phys. Chem.* **74**, 3385 (1970).
614. J. Passmore, E. K. Richardson, and P. Taylor, *Inorg. Chem.* **17**, 1681 (1978).
615. E. A. Robinson and J. A. Ciruna, *Can. J. Chem.* **46**, 3197 (1968).
616. D. M. Adams and P. J. Lock, *J. Chem. Soc. A* 145 (1967).
617. J. Kouinis and A. G. Galinos, *Monatsh. Chem.* **108**, 835 (1977).

618. A. Givan and A. Loewenschuss, *J. Raman. Spectrosc.* **6**, 84 (1977).
619. R. J. M. Konings and A. S. Booi, *J. Mol. Struct.* **271**, 183 (1992).
620. A. Kovacs, R. J. M. Konings, and A. S. Booi, *Vib. Spectrosc.* **10**, 65 (1995).
621. L. Peter and B. Meyer, *Inorg. Chem.* **24**, 3071 (1985).
622. B. M. Standury, T. A. Holme, Z. H. Kafafi, and J. L. Margrave, *Chem. Phys. Lett.* **129**, 181 (1986).
623. H. Siebert, *Z. Anorg. Allg. Chem.* **275**, 225 (1955).
624. D. J. Gardiner, R. B. Girling, and R. E. Hester, *J. Mol. Struct.* **13**, 105 (1972).
625. W. Sterzel and W. D. Schnee, *Z. Anorg. Allg. Chem.* **383**, 231 (1971).
626. H. Grothe and H. Willner, *Angew. Chem. Int. Ed.* **33**, 1482 (1994).
627. W. A. Alves and R. B. Faria, *Spectrochim. Acta* **58A**, 1395 (2002).
628. H. H. Claassen and G. Knapp, *J. Am. Chem. Soc.* **86**, 2341 (1964).
629. C. Rocchiciolli, *Hebd. Seances Acad. Sci.* **242**, 2922 (1956); **244**, 2704 (1957); **247**, 1108 (1958); **249**, 236 (1959).
630. J. J. Comeford, D. E. Mann, L. J. Schoen, and D. R. Lide, *J. Chem. Phys.* **38**, 461 (1963).
631. G. E. Moore and R. M. Badger, *J. Am. Chem. Soc.* **74**, 6076 (1952).
632. R. Minkwitz, V. Wölfel, R. Nass, H. Härtner, and W. Sawodny, *Z. Anorg. Allg. Chem.* **570**, 127 (1989).
633. L. Andrews and R. Lascola, *J. Am. Chem. Soc.* **109**, 6243 (1987).
634. J. J. Comeford, *J. Chem. Phys.* **45**, 3463 (1966); J. J. Comeford, D. E. Mann, L. J. Schoen, and D. R. Lide, *ibid.* **38**, 461 (1963).
635. O. N. Ulenikov, E. S. Bekhtereva, G. A. Onopenko, E. A. Sinitsin, H. Bürger, and W. Jerzembek, *J. Mol. Spectrosc.* **208**, 236 (2001).
636. L. Andrews and R. Withnall, *Inorg. Chem.* **28**, 494 (1989).
637. H. Beckers, *Z. Anorg. Allg. Chem.* **619**, 1880 (1993).
638. L. Andrews and T. C. McInnis, *Inorg. Chem.* **30**, 2990 (1991).
639. A. Müller, E. Niecke, B. Krebs, and O. Glemser, *Z. Naturforsch.* **23B**, 588 (1968); A. Müller, K. Königer, S. J. Cyvin, and A. Fadini, *Spectrochim. Acta* **29A**, 219 (1973).
640. C. R. S. Dean, A. Finch, and P. N. Crates, *J. Chem. Soc., Dalton Trans.* 1384 (1972).
641. R. Minkwitz and G. Nowicki, *Angew. Chem. Int. Ed.* **29**, 688 (1990).
642. M. Adelhelm and E. Jacob, *Angew. Chem. Int. Ed.* **16**, 461 (1977).
643. A. Kornath and N. Hartfield, *J. Mol. Spectrosc.* **183**, 336 (1997).
644. D. E. Martz and R. T. Lagemann, *J. Chem. Phys.* **22**, 1193 (1954).
645. R. Steudel and D. Lautenbach, *Z. Naturforsch.* **24**, 350 (1969).
646. H. Stammreich, R. Forneris, and Y. Tavares, *J. Chem. Phys.* **25**, 1277 (1956).
647. R. Minkwitz, G. Nowicki, B. Bäck, and W. Sawodny, *Inorg. Chem.* **32**, 787 (1993).
648. A. Kornath, F. Neumann, and R. Ludwig, *Inorg. Chem.* **36**, 5570 (1997).
649. E. Lork, R. Mews, D. Viets, P. G. Watson, T. Borrmann, A. Vij, J. A. Boatz, and K. O. Christe, *Inorg. Chem.* **40**, 1303 (2001).
650. M. Bahou, S.-F. Chen, and Y.-P. Lee, *J. Phys. Chem. A* **104**, 3613 (2000).
651. D. F. Burow, *Inorg. Chem.* **11**, 573 (1972).

652. R. J. Gillespie, P. H. Spekkens, J. B. Milne, and D. M. Moffett, *J. Fluorine. Chem.* **7**, 43 (1976).
653. L. E. Alexander and I. R. Beattie, *J. Chem. Soc., Dalton Trans.* 1745 (1972).
654. J. A. Rolfe and L. A. Woodward, *Trans. Faraday Soc.* **51**, 779 (1955).
655. A. Simon and R. Paetzold, *Z. Anorg. Allg. Chem.* **301**, 246 (1959); *Naturwissenschaften* **44**, 108 (1957).
656. M. Falk and P. A. Giguère, *Can. J. Chem.* **34**, 1680 (1958).
657. H. S. P. Müller, *J. Mol. Struct.* **517/518**, 335 (2000).
658. J. M. Flaud, H. S. P. Müller, and H. Bürger, *J. Mol. Spectrosc.* **207**, 216 (2001).
659. R. J. Gillespie and P. H. Spekkens, *J. Chem. Soc., Dalton Trans.* 1539 (1977).
660. K. O. Christe, E. C. Curtis, and C. J. Schack, *Inorg. Chem.* **11**, 2212 (1972).
661. K. O. Christe and W. W. Wilson, *Inorg. Chem.* **27**, 2714 (1988).
662. R. J. Gillespie, B. Landa, and G. J. Schrobilgen, *Inorg. Chem.* **15**, 1256 (1976).
663. R. Minkwitz and G. Nowicki, *Z. Naturforsch.* **44B**, 1343 (1989).
664. J. Breidung and W. Thiel, *J. Phys. Chem.* **92**, 5597 (1988).
665. B. S. Ault, *J. Am. Chem. Soc.* **100**, 2426 (1978).
666. R. Steudel and D. Lautenbach, *Z. Naturforsch.* **24B**, 350 (1969).
667. M. Goldstein and G. C. Tok, *J. Chem. Soc. A* 2303 (1971).
668. A. Kaldor and R. F. Porter, *J. Am. Chem. Soc.* **93**, 2140 (1971).
669. J. Vanderryn, *J. Chem. Phys.* **30**, 331 (1959).
670. D. A. Dows, *J. Chem. Phys.* **31**, 1637 (1959).
671. R. J. H. Clark and P. D. Mitchell, *J. Chem. Phys.* **56**, 2225 (1972).
672. D. A. Dows and G. Bottger, *J. Chem. Phys.* **34**, 689 (1961).
673. T. Wentink, Jr. and V. H. Tiensuu, *J. Chem. Phys.* **28**, 826 (1958).
674. G. V. Chertihin and L. Andrews, *J. Phys. Chem.* **97**, 10295 (1993).
675. F. A. Kurth, R. A. Eberlein, H. Schnöckel, A. J. Downs, and C. R. Pulham, *J. Chem. Soc., Chem. Commun.* 1302 (1993).
676. Y. S. Yang and J. S. Shirk, *J. Mol. Spectrosc.* **54**, 39 (1975).
677. I. R. Beattie, H. E. Blayden, S. M. Hall, S. N. Jenny, and J. S. Ogden, *J. Chem. Soc., Dalton Trans.* 666 (1976).
678. I. R. Beattie and J. R. Horder, *J. Chem. Soc. A* 2655 (1969).
679. M. Somer, K. Peters, T. Popp, and H. G. von Schnering, *Z. Anorg. Allg. Chem.* **597**, 201 (1991).
680. P. Pullumbi, Y. Bouteiller, L. Manceron, and C. Mijoule, *Chem. Phys.* **185**, 25 (1994).
681. G. K. Selivanov and A. A. Mal'tsev, *Zh. Strukt. Khim.* **14**, 943 (1973).
682. R. G. Pong, A. E. Shirk, and J. S. Shirk, *J. Mol. Spectrosc.* **66**, 35 (1977).
683. W. Blase, G. Cordier, K. Peters, M. Somer, and H. G. von Schnering, *Angew. Chem. Int. Ed. Engl.* **30**, 326 (1991).
684. J. E. D. Davies and D. A. Long, *J. Chem. Soc. A* 2050 (1968).
685. L. Andrews and G. C. Pimentel, *J. Chem. Phys.* **47**, 3637 (1967).
686. R. Becker and W. Brockner, *Z. Naturforsch.* **39A**, 1120 (1984).
687. J.-H. Choy, Y.-I. Kim, S.-J. Hwang, and P. V. Huong, *J. Phys. Chem. B.* **104**, 7273 (2000).

688. J. E. D. Davies and D. A. Long, *J. Chem. Soc. A*, 2054 (1968).
689. P. Biscarini, L. Fusina, G. Nivellini, and G. Pelizzi, *J. Chem. Soc., Dalton Trans.* 664 (1977).
690. R. D. Wesley and C. W. DeKock, *J. Chem. Phys.* **55**, 3866 (1971).
691. M. Lesiecki, J. W. Nibler, and C. W. DeKock, *J. Chem. Phys.* **57**, 1352 (1972).
692. V. N. Bukhmarina, A. Yu. Gerasomov, and Yu. B. Predtechenski, *Vib. Spectrosc.* **4**, 91 (1992).
693. M. Hargittai, B. Reffy, M. Kolonits, C. J. Marsden, and J.-L. Heully, *J. Am. Chem. Soc.*, **119**, 9042 (1997).
694. C. E. Sjögren and E. Rytter, *Spectrochim. Acta* **41A**, 1277 (1985).
695. L. M. Nxumalo and T. A. Ford, *Vib. Spectrosc.* **6**, 333 (1994).
696. K. Shimizu and H. Shingu, *Spectrochim. Acta* **22**, 1999 (1966).
697. S. Konaka, Y. Murata, K. Kuchitsu, and Y. Morino, *Bull. Chem. Soc. Jpn.* **39**, 1134 (1966).
698. W. C. Steele and J. C. Decius, *J. Chem. Phys.* **25**, 1184 (1956).
699. J. P. Laperches and P. Tarte, *Spectrochim. Acta* **22**, 1201 (1966).
700. P. E. Bethell and N. Sheppard, *Trans. Faraday. Soc.* **51**, 9 (1959).
701. S. Bhagavantum and T. Venkatarayudu, *Proc. Indian. Acad. Sci.* **9A**, 224 (1939).
702. A. Müller and M. Stockburger, *Z. Naturforsch.* **20A**, 1242 (1965).
703. A. Müller, N. Mohan, P. Cristophliemk, I. Tossidis, and M. Dräger, *Spectrochim. Acta*, **29A**, 1345 (1973).
704. A. Müller, G. Gattow, and H. Seidel, *Z. Anorg. Allg. Chem.* **347**, 24 (1966).
705. I. Nakagawa and J. L. Walter, *J. Chem. Phys.* **51**, 1389 (1969).
706. T. Ishiwata, I. Fujiwara, Y. Naruge, K. Obi, and I. Tanaka, *J. Phys. Chem.* **87**, 1349 (1983).
707. R. R. Friedl and S. P. Sander, *J. Phys. Chem.* **91**, 2721 (1987).
708. K. Kawaguchi, T. Ishiwata, I. Tanaka, and E. Hirota, *Chem. Phys. Lett.* **180**, 436 (1991).
709. V. E. Bondybey and J. H. English, *J. Mol. Spectrosc.* **109**, 221 (1985).
710. A. Maki, T. A. Blake, R. L. Sams, N. Vulpanovici, J. Barber, E. T. H. Chrysostom, T. Masiello, J. W. Nibler, and A. Weber, *J. Mol. Spectrosc.* **210**, 240 (2001).
711. A. Kalder, A. G. Maki, A. J. Dorney, and I. M. Mills, *J. Mol. Spectrosc.* **45**, 247 (1973).
712. N. J. Brassington, H. G. M. Edwards, and V. Fawcett, *Spectrochim. Acta* **43A**, 451 (1987).
713. P. LaBonville, R. Kugel, and J. R. Ferraro, *J. Chem. Phys.* **67**, 1477 (1977).
714. M. E. Jacox and D. E. Milligan, *J. Chem. Phys.* **54**, 919 (1971).
715. A. Müller, E. Diemann, E. Krickemeyer, and S. Che, *Naturwissenschaften* **80**, 77 (1993).
716. M. R. Waterland and A. M. Kelly, *J. Chem. Phys.* **113**, 6760 (2000).
717. W.-J. Lo, M. Shen, C. Yu, and Y.-P. Lee, *J. Mol. Spectrosc.* **183**, 119 (1997).
718. B. Tremblay, P. Roy, L. Manceron, M. E. Alikhan, and D. Roy, *J. Chem. Phys.* **104**, 2773 (1996).
719. C. C. Addison and B. M. Gatehouse, *J. Chem. Soc.* 613 (1960).
720. J. R. Ferraro and A. Walker, *J. Chem. Phys.* **45**, 550 (1966).

721. G. E. Walrafen and D. E. Irish, *J. Chem. Phys.* **40**, 911 (1964).
722. G. J. Janz and T. R. Kozlowski, *J. Chem. Phys.* **40**, 1699 (1964).
723. C. J. Peacock, A. Müller, and R. Kebabcioglu, *J. Mol. Struct.* **2**, 163 (1968).
724. P. Thirugnanasambandam and G. J. Srinivasan, *J. Chem. Phys.* **50**, 2467 (1969).
725. R. A. Frey, R. L. Redington, and A. L. K. Aljibury, *J. Chem. Phys.* **54**, 344 (1971).
726. R. J. Gillespie, B. Landa, and G. J. Schrobilgen, *Inorg. Chem.* **15**, 1256 (1976).
727. R. J. Gillespie and G. J. Schrobilgen, *Chem. Commun.* 595 (1977).
728. D. W. Green, G. T. Reedy, and S. D. Gabelnick, *J. Chem. Phys.* **73**, 4207 (1980).
729. K. H. Lee, H. Takeo, S. Kondo, and C. Matsumura, *Bull. Chem. Soc. Jpn.* **58**, 1772 (1985).
730. J. Müller and B. Wittig, *Eur. J. Inorg. Chem.* 1807 (1998).
731. R. Köppe and H. Schnöckel, *J. Chem. Soc., Dalton Trans.* 3393 (1992).
732. R. Köppe, M. Tacke, and H. Schnöckel, *Z. Anorg. Allg. Chem.* **605**, 35 (1991).
733. J. Müller and H. Sternkicker, *J. Chem. Soc., Dalton Trans.* 4149 (1999).
734. H.-J. Himmel, A. J. Downs, and T. M. Greene, *J. Am. Chem. Soc.* **122**, 922 (2000).
735. H.-J. Himmel, *J. Chem. Soc., Dalton Trans.* 2678 (2002).
736. B. S. Ault, *Inorg. Chem.* **21**, 756 (1982).
737. X. Zhang, U. Gross, and K. Seppelt, *Angew. Chem. Int. Ed.* **34**, 1858 (1995).
738. D. L. Bernitt, K. O. Hartman, and I. C. Hisatsune, *J. Chem. Phys.* **42**, 3553 (1965).
739. K. Itoh and H. J. Bernstein, *Can. J. Chem.* **34**, 170 (1956).
740. T. C. Smith, H. Li, and D. J. Clouthier, *J. Chem. Phys.* **114**, 9012 (2001).
741. P. D. Mallinson, D. C. McKean, J. H. Holloway, and I. A. Oxtan, *Spectrochim. Acta* **31A**, 143 (1975).
742. N. C. Craig, *Spectrochim. Acta* **44A**, 1225 (1988).
743. I. Mineu, A. Allouche, M. Cossu, J.-P. Aycard, and J. Pourcin, *Spectrochim. Acta* **51A**, 349 (1995).
744. R. F. Stratton and A. H. Nielsen, *J. Mol. Spectrosc.* **4**, 373 (1960).
745. Y. Xu, J. W. C. Johns, and A. R. W. McKellar, *J. Mol. Spectrosc.* **168**, 147 (1994).
746. I. Barnes, K. H. Becker, and J. Starcke, *Chem. Phys. Lett.* **246**, 594 (1995).
747. J. Overend and J. C. Evans, *Trans. Faraday Soc.* **55**, 1817 (1959).
- 747a. A. Perrin, J.-M. Flaud, H. Burger, G. Pawelke, S. Sander, and H. Willner, *J. Mol. Spectrosc.* **209**, 122 (2001).
748. M. E. Jacox and D. E. Milligan, *J. Mol. Spectrosc.* **58**, 142 (1975).
749. A. J. Downs, *Spectrochim. Acta* **19**, 1165 (1963).
750. H. Bürger and W. Jerzembeck, *J. Mol. Spectrosc.* **188**, 209 (1998).
751. I. S. Butler and A. M. English, *Spectrochim. Acta* **33A**, 545 (1977).
752. A. Haas, B. Koch, N. Welcman, and H. Willner, *Spectrochim. Acta* **32A**, 497 (1976).
753. A. Müller, N. Mohan, P. Cristophliemk, I. Tossidis, and M. Dräger, *Spectrochim. Acta* **29A**, 1345 (1973).
754. M. Junker, A. Wilkening, M. Binnewies, and H. Schnöckel, *Eur. J. Inorg. Chem.* 1531 (1999).
755. H. Beckers, J. Breidung, H. Bürger, R. Köppe, C. Kötting, W. Sander, H. Schnöckel, and W. Thiel, *Eur. J. Inorg. Chem.* 2013 (1999).

756. H. Schnöckel, H. J. Göcke, and R. Köppe, *Z. Anorg. Allg. Chem.* **578**, 159 (1989).
757. R. Köppe and H. Schnöckel, *Z. Anorg. Allg. Chem.* **592**, 179 (1991).
758. W. A. Guillory and M. L. Bernstein, *J. Chem. Phys.* **62**, 1058 (1975).
759. K. O. Christe, C. J. Schack, and R. D. Wilson, *Inorg. Chem.* **13**, 2811 (1974).
760. H. Kruse, F. Hegelund, H. Bürger, and G. Pawelke, *J. Mol. Spectrosc.* **203**, 273 (2000).
- 760a. J. Orphal, M. Morillon-Chapey, and G. Guelachvili, *J. Mol. Spectrosc.* **165**, 315 (1994).
761. E. Ya. Misochko, A. V. Akimov, I. U. Goldschleger, and C. A. Wight, *J. Am. Chem. Soc.* **120**, 11520 (1998).
762. C. A. Wamser, W. B. Fox, B. Sukornick, J. R. Holmes, B. B. Stewart, R. Juurik, N. Vandetkooi, and D. Gould, *Inorg. Chem.* **8**, 1249 (1969).
763. A. Allan, J. L. Duncan, J. H. Holloway, and D. C. McKean, *J. Mol. Spectrosc.* **31**, 368 (1969).
764. R. Minkwitz, D. Bernstein, W. Sawodny, and H. Härtner, *Z. Anorg. Allg. Chem.* **580**, 109 (1990).
765. S. Schunck, H. J. Göcke, R. Köppe, and H. Schnöckel, *Z. Anorg. Allg. Chem.* **579**, 66 (1989).
766. R. Withnall and L. Andrews, *J. Am. Chem. Soc.* **107**, 2567 (1985); **108**, 8118 (1986).
767. D. F. Wolfe and G. L. Humphrey, *J. Mol. Struct.* **3**, 293 (1969).
768. R. G. S. Pong, A. E. Shirk, and J. S. Shirk, *Ber. Bunsenges. Phys. Chem.* **82**, 79 (1978).
769. M. Somer, *Z. Anorg. Allg. Chem.* **626**, 2478 (2000).
770. G. Kliche, H. G. von Schnering, and M. Schwarz, *Z. Anorg. Allg. Chem.* **608**, 131 (1992).
771. A. Kornath, A. Kaufmann, and M. Torheyden, *J. Chem. Phys.* **116**, 3323 (2002).
772. H. G. M. Edwards, *J. Mol. Struct.* **295**, 95 (1993).
773. K. Manzel, W. Schulze, V. Wolfel, and R. Minkwitz, *Z. Naturforsch.* **37B**, 1127 (1982).
774. H. Sontag and R. Weber, *Chem. Phys.* **70**, 23 (1982).
775. V. E. Bondybey and J. H. English, *J. Chem. Phys.* **73**, 42 (1980).
776. H. Wang, R. Craig, H. Haouari, J.-G. Dong, Z. Hu, A. Vivoni, J. R. Lombardi, and D. M. Lindsay, *J. Chem. Phys.* **103**, 3289 (1995).
- 776a. R. C. Burns and R. J. Gillespie, *Inorg. Chem.* **21**, 3877 (1982).
- 776b. R. J. H. Clark, T. J. Dines, and L. T. H. Ferris, *J. Chem. Soc., Dalton Trans.* 2237 (1982).
- 776c. R. Minkwitz, J. Nowicki, W. Sawodny, and K. Härtner, *Spectrochim. Acta* **47A**, 151 (1991).
777. J. Goubeau and K. Laitenberger, *Z. Anorg. Allg. Chem.* **320**, 78 (1963).
778. C. Feldmann and M. Jansen, *Angew. Chem. Int. Ed.* **35**, 1728 (1996).
779. J. E. Rauch and J. C. Decius, *Spectrochim. Acta* **22**, 1963 (1966).
780. G. E. McGraw, D. L. Bernitt, and I. C. Hisatsune, *Spectrochim. Acta* **23A**, 25 (1967).
781. S. T. King and J. Overend, *Spectrochim. Acta* **23A**, 61 (1967).
782. S. T. King and J. Overend, *Spectrochim. Acta* **22A**, 689 (1966).
783. P. A. Giguère and T. K. K. Srinivasan, *J. Raman. Spectrosc.* **2**, 125 (1974).
784. M. Pettersson, S. Tuominen, and M. Räsänen, *J. Phys. Chem. A* **101**, 1166 (1997).
785. D. J. Gardiner, N. J. Lawrence, and J. J. Turner, *J. Chem. Soc. A* 400 (1971).
786. N. Zengin and P. A. Giguère, *Can. J. Chem.* **37**, 632 (1959).

787. R. D. Brown and G. P. Pez, *Spectrochim. Acta* **26A**, 1375 (1970).
788. S. G. Frankiss and D. S. Harrison, *Spectrochim. Acta* **31A**, 161 (1975).
789. R. Steudel, D. Jensen, and B. Plinke, *Z. Naturforsch.* **42b**, 163 (1987).
790. R. Forneris and C. E. Hennies, *J. Mol. Struct.* **5**, 449 (1970).
791. W. A. Guillory and C. E. Hunter, *J. Chem. Phys.* **50**, 3516 (1969).
792. J. R. Ohlsen and J. Laane, *J. Am. Chem. Soc.* **100**, 6948 (1978).
793. D. E. Milligan and M. E. Jacox, *J. Chem. Phys.* **55**, 3404 (1971).
794. N. Wiberg, G. Fischer, and H. Bachhuber, *Angew. Chem. Int. Ed. Engl.* **16**, 780 (1977).
- 794a. A. Engdahl, B. Nelander, and G. Karlström, *J. Phys. Chem. A* **105**, 8393 (2001).
795. W. Kiefer, *Spectrochim. Acta* **27A**, 1285 (1971).
796. R. Steudel, D. Jensen, and B. Plinke, *Z. Naturforsch.* **42B**, 163 (1987).
797. J. A. A. Ketelaar, F. N. Hooge, and G. Blasse, *Recl. Trav. Chim. Pays-Bas* **75**, 220 (1956).
798. H. Borrmann, J. Campbell, D. A. Dixon, H. P. A. Mercier, A. M. Pirani, and G. J. Schrobilgen, *Inorg. Chem.* **37**, 1929 (1998).
799. G. Maier, H. P. Reisenauer, A. Meudt, and H. Egenolf, *Chem. Ber.* **130**, 1043 (1997).
800. T. Drews, W. Koch, and K. Seppely, *J. Am. Chem. Soc.* **121**, 4379 (1999).
801. P. A. Giguère and O. Bain, *J. Phys. Chem.* **56**, 340 (1952).
802. C. A. Frenzel and K. E. Blick, *J. Chem. Phys.* **55**, 2715 (1971).
803. W. Schnick and H. Huppertz, *Z. Anorg. Alla. Chem.* **621**, 1703 (1995).
804. J. H. Teles, G. Maier, B. A. Hess, Jr., L. J. Schaad, M. Winnewisser, and B. P. Winnewisser, *Chem. Ber.* **123**, 753 (1989).
805. S. S. Brown, H. L. Berghout, and F. F. Crim, *J. Chem. Phys.* **107**, 9764 (1997).
806. S. L. Laursen, J. E. Grace, R. DeKock, and S. A. Spronk, *J. Am. Chem. Soc.* **120**, 12583 (1998).
807. M. E. Jacox and D. E. Milligan, *J. Chem. Phys.* **40**, 2457 (1964).
808. T. Pasinszki and N. P. C. Westwood, *J. Phys. Chem. A* **102**, 4939 (1998).
809. M. S. Lowenthal, R. K. Khanna, and M. H. Moore, *Spectrochim. Acta* **58A**, 73 (2002).
810. K. Gholivand, H. Willner, D. Bielefeldt, and A. Haas, *Z. Naturforsch.* **39b**, 1211 (1984).
811. T. C. Devore, *J. Mol. Struct.* **162**, 287 (1987).
812. M. Gerke, G. Schatte, and H. Willner, *J. Mol. Spectrosc.* **135**, 539 (1989).
813. A. Schulz, I. C. Tornieporth-Oetting, and T. M. Klöpötke, *Inorg. Chem.* **34**, 4343 (1995).
814. L. Khriachtchev, J. Lundell, E. Isoniemi, and M. Rasänen, *J. Chem. Phys.* **113**, 4265 (2000).
815. T. Talik, K. G. Tokhadze, and Z. Mielke, *J. Mol. Struct.* **611**, 95 (2002).
816. K. Johnsson, A. Engdahl, and B. Nelander, *J. Phys. Chem.* **100**, 3923 (1996).
817. J. R. Durig and D. W. Wertz, *J. Chem. Phys.* **46**, 3069 (1967).
818. G. R. Draper and R. L. Werner, *J. Mol. Spectrosc.* **50**, 369 (1974).
819. M. Wierzejewska and Z. Mielke, *Chem. Phys. Lett.* **349**, 227 (2001).
820. M. J. Nielsen and A. D. E. Pullin, *J. Chem. Soc.* 604 (1960).
821. P. O. Tchir and R. D. Spratley, *Can. J. Chem.* **53**, 2311 (1975).
822. D.-L. Joo, H. Harjanto, and D. J. Clouthier, *J. Mol. Spectrosc.* **178**, 78 (1996).
823. P. O. Tchir and R. D. Spratley, *Can. J. Chem.* **53**, 2331 (1975).

824. S. L. Laursen, A. E. Delia, and K. Mitchell, *J. Phys. Chem. A* **104**, 3681 (2000).
825. J. M. Coanga, L. Schriver-Mazzuoli, A. Schriver, and P. R. Dahoo, *Chem. Phys.* **276**, 309 (2002).
826. D. Scheffler and H. Willner, *Inorg. Chem.* **37**, 4500 (1998).
827. M. Nonella, J. R. Huber, and T. K. Ha, *J. Phys. Chem.* **91**, 5203 (1987).
828. H. H. Eysel, *J. Mol. Struct.* **5**, 275 (1970).
829. M. Bahou and Y.-P. Lee, *J. Chem. Phys.* **115**, 10694 (2001).
830. E. Isoniemi, L. Khriachtchev, J. Lundell, and M. Räsänen, *Phys. Chem. Chem. Phys.* **4**, 1549 (2002).
831. W. T. Thompson and W. H. Fletcher, *Spectrochim. Acta* **22**, 1907 (1966).
832. W. A. Guillory and C. E. Hunter, *J. Chem. Phys.* **54**, 598 (1971).
833. S. H. Jou, M. Shen, C. Yu, and Y.-P. Lee, *J. Chem. Phys.* **104**, 5745 (1996).
834. B. Nelander, A. Engdahl, and T. Svensson, *Chem. Phys. Lett.* **332**, 403 (2000).
835. J. W. G. Seibter, M. Winnewisser, and B. P. Winnewisser, *J. Mol. Spectrosc.* **180**, 26 (1996).
836. M. C. McCarthy, C. A. Gottlieb, A. L. Cooksy, and P. Thaddeus, *J. Chem. Phys.* **103**, 7779 (1995).
837. L. C. Tornieporth-Oetting, P. Gowik, and T. M. Klapötke, *Angew. Chem. Int. Ed.* **30**, 1485 (1991).
838. D. V. Lanzisera and L. Andrews, *J. Am. Chem. Soc.* **119**, 6392 (1997).
839. A. R. Emery and R. C. Taylor, *J. Chem. Phys.* **28**, 1029 (1958).
840. C. J. H. Schutte, *Spectrochim. Acta* **16**, 1054 (1960). J. A. A. Ketelaar and C. J. H. Schutte, *ibid.* **17**, 1240 (1961).
841. A. E. Shirk and D. F. Shriver, *J. Am. Chem. Soc.* **95**, 5904 (1973).
842. P. Pullumbi, Y. Bouteiller, and L. Manceron, *J. Chem. Phys.* **101**, 3610 (1994).
843. Landolt-Börnstein, *Physikalisch-chemische Tabellen*, Vol. 2, Springer, Berlin, 1951.
844. G. E. MacWood and H. C. Urey, *J. Chem. Phys.* **4**, 402 (1936).
845. H. M. Kaylor and A. H. Nielsen, *J. Chem. Phys.* **23**, 2139 (1955).
846. I. F. Kovalev, *Opt. Spektrosk.* **2**, 310 (1957).
847. R. E. Wilde, T. K. K. Srinivasan, R. W. Haral, and S. G. Sankar, *J. Chem. Phys.* **55**, 5681 (1971).
848. J. H. Meal and M. K. Wilson, *J. Chem. Phys.* **24**, 385 (1956).
849. L. P. Lindemann and M. K. Wilson, *J. Chem. Phys.* **22**, 1723 (1954).
850. I. W. Levin and H. Ziffer, *J. Chem. Phys.* **43**, 4023 (1965).
851. V. M. Krivstun, Yu. A. Kuritsin, and E. P. Snegirev, *Opt. Spektrosk.* **86**, 686 (1999).
852. H. W. Morgan, P. A. Staats, and J. H. Goldstein, *J. Chem. Phys.* **27**, 1212 (1957).
853. J. R. Durig, D. J. Antion, and F. G. Baglin, *J. Chem. Phys.* **49**, 666 (1968).
854. R. Minkwitz, A. Kornath, W. Sawodny, and H. Härtner, *Z. Anorg. Allg. Chem.* **620**, 753 (1994).
855. E. L. Wagner and D. F. Hornig, *J. Chem. Phys.* **18**, 296, 305 (1950); R. C. Plumb and D. F. Hornig, *ibid.* **21**, 366 (1953); **23**, 947 (1955); W. Vedder and D. F. Hornig, *ibid.* **35**, 1560 (1961).
856. A. S. Quist, J. B. Bates, and G. E. Boyd, *J. Phys. Chem.* **76**, 78 (1972).

857. V. A. Maroni, *J. Chem. Phys.* **55**, 4789 (1971).
858. A. S. Quist, J. B. Bates, and G. E. Boyd, *J. Chem. Phys.* **54**, 4896 (1971).
859. R. J. H. Clark, S. Joss, and M. J. Taylor, *Spectrochim. Acta* **42A**, 927 (1986).
860. M. C. Dhamelincourt and M. Migeon, *C. R. Hebd. Seances. Acad. Sci.* **281**, C79 (1975).
861. J. A. Creighton, *J. Chem. Soc.* 6589 (1965).
862. K. O. Christe, M. D. Lind, N. Thorup, D. R. Russell, J. Fawcett, and R. Bau, *Inorg. Chem.* **27**, 2450 (1988).
863. B. Gilbert, G. Mamantov, and G. M. Begun, *Inorg. Nucl. Chem. Lett.* **10**, 1123 (1974).
864. E. Rytter and H. A. Øye, *J. Inorg. Nucl. Chem.* **35**, 4311 (1973).
865. D. H. Brown and D. T. Stewart, *Spectrochim. Acta* **26A**, 1344 (1970).
866. G. M. Begun, C. R. Boston, G. Torsi, and G. Mamantov, *Inorg. Chem.* **10**, 886 (1971).
867. H. A. Øye and W. Bues, *Inorg. Nucl. Chem. Lett.* **8**, 31 (1972).
868. L. A. Woodward and A. A. Nord, *J. Chem. Soc.* 2655 (1955).
869. L. A. Woodward and G. H. Singer, *J. Chem. Soc.* 716 (1958).
870. L. A. Woodward and M. J. Taylor, *J. Chem. Soc.* 4473 (1960).
871. L. A. Woodward and P. T. Bill, *J. Chem. Soc.* 1699 (1955).
872. J. Blixt, J. Glaser, J. Mink, I. Persson, and M. Sandström, *J. Am. Chem. Soc.* **117**, 5089 (1995).
873. D. M. Adams and D. M. Morris, *J. Chem. Soc. A* 694 (1968).
874. R. J. H. Clark and D. M. Rippon, *Chem. Comm.* 1295 (1971). R. J. H. Clark and P. D. Mitchell, *J. Chem. Soc., Faraday Trans. 2*, **71**, 515 (1975).
875. R. R. Haun and W. D. Harkins, *J. Am. Chem. Soc.* **54**, 3917 (1932).
876. H. Stammreich, Y. Tavares, and D. Bassi, *Spectrochim. Acta* **17**, 661 (1961).
877. R. J. H. Clark and T. J. Dines, *Inorg. Chem.* **19**, 1681 (1980).
878. Y. Boudon, H. Bürger, and E. B. Mkadmi, *J. Mol. Spectrosc.* **206**, 172 (2001).
879. R. J. H. Clark and B. K. Hunter, *J. Mol. Struct.* **9**, 354 (1971).
880. K. O. Christe, *Spectrochim. Acta* **36A**, 921 (1980).
881. R. Minkwitz, D. Bernstein, and W. Sawodny, *Angew. Chem. Int. Ed. Engl.* **29**, 181 (1990).
882. R. Minkwitz, D. Lennhoff, W. Sawodny, and H. Härtner, *Z. Naturforsch.* **47b**, 1661 (1992).
883. P. Van Huong, and B. Desbat, *Bull. Soc. Chim. Fr.* 2631 (1972).
884. A. Aubauer, M. Kaupp, T. M. Klapötke, H. Noth, H. Piotrowski, W. Schnick, J. Senker, and M. Suter, *J. Chem. Soc., Dalton Trans.* 1880 (2001).
885. L. Tornieporth-Oetting and T. Klapötke, *J. Chem. Soc., Chem. Commun.* 132 (1990).
886. A. Schulz and T. M. Klapötke, *Spectrochim. Acta* **51A**, 905 (1995).
887. A. Müller and A. Fadini, *Z. Anorg. Allg. Chem.* **349**, 164 (1967).
888. J. Weidlein and K. Dehnicke, *Z. Anorg. Allg. Chem.* **337**, 113 (1965).
889. T. Klapötke, J. Passmore, and E. G. Awere, *J. Chem. Soc., Chem. Commun.* 1426 (1988).
890. I. Tornieporth-Oetting and T. Klapötke, *Angew. Chem. Int. Ed. Engl.* **28**, 1671 (1989).
891. W. J. Casteel, Jr., P. Kolb, N. LeBlond, H. P. A. Mercier, and G. J. Schrobilgen, *Inorg. Chem.* **35**, 929 (1996).

892. A. Sabatini and L. Sacconi, *J. Am. Chem. Soc.* **86**, 17 (1964).
893. I. R. Beattie, T. R. Gilson and G. A. Ozin, *J. Chem. Soc. A* 534 (1969).
894. J. S. Avery, C. D. Burbridge, and D. M. L. Goodgame, *Spectrochim. Acta* **24A**, 1721 (1968).
895. P. L. Goggin, R. J. Goodfellow, and K. Kessler, *J. Chem. Soc., Dalton Trans.* 1914 (1977).
896. G. J. Janz and D. W. James, *J. Chem. Phys.* **38**, 905 (1963).
897. D. A. Long and J. Y. H. Chau, *Trans. Faraday. Soc.* **58**, 2325 (1962).
898. M. M. Metallinou, L. Nalbandian, G. N. Papatheodorou, W. Voigt, and H. H. Emons, *Inorg. Chem.* **30**, 4260 (1991).
899. L. E. Alexander and I. R. Beattie, *J. Chem. Soc., Dalton Trans.* 1745 (1972).
900. R. J. H. Clark, B. K. Hunter, and D. M. Rippon, *Inorg. Chem.* **11**, 56 (1972); R. J. H. Clark and D. M. Rippon, *J. Mol. Spectrosc.* **44**, 479 (1972).
901. A. Büchler, J. B. Berkowitz-Mattuck, and D. H. Dugre, *J. Chem. Phys.* **34**, 2202 (1961).
902. M. F. A. Dove, J. A. Creighton, and L. A. Woodward, *Spectrochim. Acta* **18**, 267 (1962).
903. J. Jacobs, H. S. Müller, H. Willner, E. Jacob, and H. Bürger, *Inorg. Chem.* **31**, 5357 (1992).
904. B. Cuoni, F. P. Emmenegger, C. Rohrbasser, C. W. Schläpfer, and P. Studer, *Spectrochim. Acta* **34A**, 247 (1978).
905. H. G. M. Edwards, M. J. Ware, and L. A. Woodward, *Chem. Commun.* 540 (1968).
906. G. Thiele, D. Honert, and H. Rotter, *Z. Anorg. Allg. Chem.* **616**, 195 (1992).
907. A. Armbruster, H. W. Rotter, and G. Thiele, *Z. Anorg. Allg. Chem.* **622**, 795 (1996).
908. H. G. M. Edwards, L. A. Woodward, M. J. Gall, and M. J. Ware, *Spectrochim. Acta* **26A**, 287 (1970).
909. H.-H. Schmidtke and J. Nover, *Inorg. Chim. Acta* **240**, 231 (1995).
910. R. J. M. Konings, A. S. Booij, A. Kovacs, G. V. Girichev, N. I. Giricheva, and O. G. Krasnova, *J. Mol. Struct.* **378**, 121 (1996).
911. A. Haaland, K.-G. Martinsen, O. Swang, H. V. Volden, A. S. Booij, and R. J. M. Konings, *J. Chem. Soc., Dalton Trans.* 185 (1995).
912. D. M. Adams and P. J. Lock, *J. Chem. Soc. A*, 620 (1967).
913. D. N. Anderson and R. D. Willett, *Inorg. Chim. Acta* **8**, 167 (1974).
914. R. D. Willett, J. R. Ferraro, and M. Choca, *Inorg. Chem.* **13**, 2919 (1974).
915. D. Forster, *Chem. Commun.* 113 (1967).
916. P. L. Goggin and T. G. Buick, *Chem. Commun.* 290 (1967).
917. R. A. Work, III and M. L. Good, *Spectrochim. Acta* **28A**, 1537 (1972).
918. J. T. R. Dunsmuir and A. P. Lane, *J. Chem. Soc. A*, 404, 2781 (1971).
919. R. L. Hunt and B. S. Ault, *Spectrochim. Acta* **37A**, 63 (1981).
920. P. Wermer and B. S. Ault, *Inorg. Chem.* **20**, 970 (1981).
921. V. N. Bakhmarina, Yu. B. Predtchenskii, and L. D. Shcherba, *J. Mol. Struct.* **218**, 33 (1990).
922. G. Maier, H. P. Reisenauer, J. Hu, B. A. Hess, and L. J. Schaad, *Tetrahedron. Lett.* **30**, 4105 (1989).

923. M. E. Jacox and W. E. Thompson, *J. Phys. Chem.* **95**, 2781 (1991).
924. R. J. H. Clark and P. D. Mitchell, *J. Am. Chem. Soc.* **95**, 8300 (1973); *J. Raman. Spectrosc.* **2**, 399 (1974).
925. R. J. H. Clark and P. D. Mitchell, *Chem. Commun.* 762 (1973).
926. T. Kamisuki and S. Maeda, *Chem. Phys. Lett.* **21**, 330 (1973).
927. S. T. King, *J. Chem. Phys.* **49**, 1321 (1968).
928. F. Königer and A. Müller, *J. Mol. Spectrosc.* **56**, 200 (1975).
929. F. Königer, A. Müller, and K. Nakamoto, *Z. Naturforsch.* **30b**, 456 (1975).
930. D. Tevault, J. D. Brown, and K. Nakamoto, *Appl. Spectrosc.* **30**, 461 (1976).
931. A. Müller and B. Krebs, *J. Mol. Spectrosc.* **24**, 180 (1967). A. Müller and A. Fadini, *Z. Anorg. Allg. Chem.* **349**, 164 (1967).
932. L. J. Basile, J. R. Ferraro, P. LaBonville, and M. C. Wall, *Coord. Chem. Rev.* **11**, 21(1973).
933. K. O. Christe, D. A. Dixon, H. P. A. Mercier, J. C. P. Sanders, G. J. Schrobilgen, and W. W. Wilson, *J. Am. Chem. Soc.* **116**, 2850 (1994).
934. S. Chitsaz, K. Dehnicke, G. Frenzen, A. Pilz, and U. Müller, *Z. Anorg. Allg. Chem.* **622**, 2016 (1996).
935. C. J. Adams and A. J. Downs, *J. Chem. Soc. A*, 1534 (1971).
936. G. Y. Ahlajah and M. Goldstein, *J. Chem. Soc. A*, 326 (1970). *Chem. Commun.* 1356 (1968).
937. K. O. Christe, H. Willner, and W. Sawodny, *Spectrochim. Acta* **35A**, 1347 (1979).
938. K. Seppelt, *Z. Anorg. Allg. Chem.* **416**, 12 (1975).
939. C. J. Adams and A. J. Downs, *Spectrochim. Acta* **28A**, 1841 (1972).
940. A. Kovács, K.-G. Martinson, and R. J. M. Konings, *J. Chem. Soc., Dalton Trans.* 1037 (1997).
941. K. O. Christe and W. Sawodny, *Inorg. Chem.* **12**, 2879 (1973).
942. L. E. Alexander and I. R. Beattie, *J. Chem. Soc., Dalton Trans.* 1745 (1972).
943. A. M. Heyns, K. J. Range, and M. Widenauer, *Spectrochim. Acta* **46A**, 1621 (1990).
944. S. D. Ross, *Spectrochim. Acta* **28A**, 1555 (1972).
945. M. Robineau and D. Zins, *C. R. Hebd. Seances Acad. Sci.* **280**, C759 (1975).
946. Landolt-Börnstein, *Physikalisch-chemische Tabellen*, Vol. 2, Springer, Berlin, 1951.
947. D. Fortnum and J. O. Edwards, *J. Inorg. Nucl. Chem.* **2**, 264 (1956).
948. E. Steger and K. Herzog, *Z. Anorg. Allg. Chem.* **331**, 169 (1964).
949. E. Steger and W. Schmidt, *Ber. Bunsenges. Phys. Chem.* **68**, 102 (1964).
950. O. Sala and M. L. A. Temperini, *Chem. Phys. Lett.* **36**, 652 (1975).
951. C. R. Evenson and P. K. Dorhout, *Inorg. Chem.* **40**, 2875 (2001).
952. M. Jansen, *Angew. Chem. Int. Ed. Engl.* **16**, 534 (1977).
953. H. Siebert, *Z. Anorg. Allg. Chem.* **275**, 225 (1954).
954. M. Malchos and M. Jansen, *Z. Naturforsch.* **53b**, 704 (1998).
955. Y. Aoki, H. Konno, H. Tachikawa, and M. Inagaki, *Bull. Chem. Soc. Jpn.* **73**, 1197 (2000).
956. N. A. Chumaevslii, T. A. Ivanova, and V. P. Tarasov, *Russ. J. Inorg. Chem.* **37**, 1067 (1992).

957. H. Siebert, *Z. Anorg. Allg. Chem.* **273**, 21 (1953).
958. R. S. McDowell and L. B. Asprey, *J. Chem. Phys.* **57**, 3062 (1972).
959. F. Gonzalez-Vilchez and W. P. Griffith, *J. Chem. Soc., Dalton Trans.* 1416 (1972).
960. N. Weinstock, H. Schulze, and A. Müller, *J. Chem. Phys.* **59**, 5063 (1973).
961. A. Müller, K. H. Schmidt, K. H. Tytko, J. Bouwma, and F. Jellinek, *Spectrochim. Acta* **28A**, 381 (1972).
962. A. Müller, N. Weinstock, and H. Schulze, *Spectrochim. Acta* **28A**, 1075 (1972); K. H. Schmidt and A. Müller, *ibid.* 1829.
963. A. Müller, B. Krebs, R. Kebabcioğlu, M. Stockburger, and O. Glemser, *Spectrochim. Acta* **24A**, 1831 (1968).
964. H. Homborg and W. Preetz, *Spectrochim. Acta* **32A**, 709 (1976).
965. P. J. Hendra, P. Le Barazer, and A. Crookell, *J. Raman Spectrosc.* **20**, 35 (1989).
966. E. J. Baran and S. G. Manca, *Spectrosc. Lett.* **15**, 455 (1982).
967. A. Müller, E. Diemann, and U. V. K. Rao, *Chem. Ber.* **103**, 2961 (1970).
968. R. S. McDowell, L. B. Asprey, and L. C. Hoskins, *J. Chem. Phys.* **56**, 5712 (1972).
969. R. S. McDowell, *Inorg. Chem.* **6**, 1759 (1967); R. S. McDowell and M. Goldblatt, *ibid.* **10**, 625 (1971).
- 969a. M. Gerken and G. J. Schrobilgen, *Inorg. Chem.* **41**, 198 (2002).
970. E. J. Baran, *Z. Anorg. Allg. Chem.* **399**, 57 (1973).
971. J. O. Edwards, G. C. Morrison, V. F. Ross, and J. W. Schultz, *J. Am. Chem. Soc.* **77**, 266 (1955).
972. N. J. Campbell, J. Flanagan, and W. P. Griffith, *J. Chem. Phys.* **83**, 3712 (1985).
973. E. R. Lippincott, J. A. Psellos, and M. C. Tobin, *J. Chem. Phys.* **20**, 536 (1952).
974. A. Müller, E. J. Baran, and R. O. Carter, *Struct. Bonding. (Berlin)* **26**, 81 (1976).
975. E. J. Baran, *Inorg. Chem.* **20**, 4453 (1981).
976. F. Ramondo, L. Bencivenni, V. Rossi, and H. M. Nagarathna-Naik, *Mol. Phys.* **64**, 1145 (1988).
977. R. Kugel and H. Taube, *J. Phys. Chem.* **79**, 2130 (1975).
978. A. Givan, L. A. Larsen, A. Loewenschuss, and C. J. Nielsen, *J. Mol. Struct.* **509**, 35 (1999).
979. H. Grothe and H. Willner, *Angew. Chem. Int. Ed.* **35**, 768 (1996).
980. M. Chabanel, D. Legoff, and K. Toujaj, *J. Chem. Soc., Farad Trans.* **92**, 4199 (1996).
981. W. Kiefer and H. J. Bernstein, *Mol. Phys.* **23**, 835 (1972).
982. A. Ranade and M. Stockburger, *Chem. Phys. Lett.* **22**, 257 (1973).
983. A. Ranade, W. Krasser, A. Müller, and E. Ahlborn, *Spectrochim. Acta* **30A**, 1341 (1974).
984. R. S. McDowell and L. B. Asprey, *J. Chem. Phys.* **57**, 3062 (1972).
985. K. H. Schmidt and A. Müller, *Coord. Chem. Rev.* **14**, 115 (1974).
986. A. Müller, E. Diemann, R. Jostes, and H. Böge, *Angew. Chem. Int. Ed.* **20**, 934 (1981).
987. E. Johnsen, A. J. Downs, M. J. Goode, T. M. Greene, H.-J. Himmel, M. Müller, S. Parsons, and C. R. Pulham, *Inorg. Chem.* **40**, 4755 (2001).
988. K. O. Christe, E. C. Curtis, and C. J. Schack, *Spectrochim. Acta* **31A**, 1035 (1975).
989. B. S. Ault, *J. Phys. Chem.* **84**, 3448 (1980).

990. R. J. H. Clark and O. H. Ellestad, *J. Mol. Spectrosc.* **56**, 386 (1975).
991. R. H. Mann and P. M. Harris, *J. Mol. Spectrosc.* **45**, 65 (1973).
992. D. Papousek, H. Bürger, A. Rahner, P. Schulz, H. Hollenstein, and M. Quack, *J. Mol. Spectrosc.* **195**, 263 (1999).
993. H. Bürger, S. Biedermann, and A. Ruoff, *Spectrochim. Acta* **30A**, 1655 (1974).
994. J. Goubeau, F. Haenschke, and A. Ruoff, *Z. Anorg. Allg. Chem.* **366**, 113 (1969).
995. F. Lattanzi, C. DiLauro, and H. Bürger, *Mol. Phys.* **72**, 575 (1991).
996. U. Müller and V. Krug, *Z. Naturforsch.* **40b**, 1015 (1985).
997. A. Ruoff, H. Bürger, S. Biedermann, and J. Cichon, *Spectrochim. Acta* **30A**, 1647 (1974).
998. E. C. Curtis, D. Philipovich, and W. H. Maberly, *J. Chem. Phys.* **46**, 2904 (1967).
999. R. Minkwitz and B. Bäck, *Z. Naturforsch.* **49b**, 221 (1994).
1000. A. Finch, P. N. Gates, F. J. Ryan, and F. F. Bentley, *J. Chem. Soc., Dalton Trans.* 1863 (1973).
1001. R. Küster, T. Drews, and K. Seppelt, *Inorg. Chem.* **39**, 2784 (2000).
- 1001a. R. Minkwitz, D. Lennhoff, W. Sawodny, and H. Härtner, *Z. Naturforsch.* **47b**, 1661 (1992).
1002. H. S. Gutowsky and A. D. Liehr, *J. Chem. Phys.* **26**, 329 (1957).
1003. M. L. Delwaulle and F. François, *C. R. Hebd. Seances Acad. Sci.* **220**, 817 (1945).
1004. J. Durand, L. Beys, P. Hillaire, S. Aleonard, and L. Cot, *Spectrochim. Acta* **34A**, 123 (1978).
1005. M. B. Zidan and A. W. Allaf, *Spectrochim. Acta* **58A**, 1577 (2002).
1006. M. Brownstein, P. A. W. Dean, and R. J. Gillespie, *Chem. Commun.* 9 (1970).
1007. F. Königer, A. Müller, and O. Glemser, *J. Mol. Struct.* **46**, 29 (1978).
1008. Y. Tavares-Forneris, and R. Forneris, *J. Mol. Struct.* **24**, 205 (1965).
1009. I. C. Hisatsune and J. Heicklen, *Can. J. Chem.* **53**, 2646 (1975).
1010. C. S. Alleyne, K. O. Mailer, and R. C. Thompson, *Can. J. Chem.* **52**, 336 (1974).
1011. D. J. Stufkens and H. Gerding, *Recl. Trav. Chim. Pays-Bas.* **89**, 417 (1970).
1012. E. Steger, I. C. Ciurea, and A. Fadini, *Z. Anorg. Allg. Chem.* **350**, 225 (1967).
1013. S. Ball and J. Milne, *Can. J. Chem.* **73**, 716 (1995).
1014. M. Černík and K. Dostál, *Z. Anorg. Allg. Chem.* **425**, 37 (1976).
1015. W. F. Murphy and H. Katz, *J. Raman. Spectrosc.* **7**, 76 (1978).
1016. K. Burczyk, H. Bürger, M. LeGuennec, G. Włodarczak, and J. Demaison, *J. Mol. Spectrosc.* **148**, 65 (1991).
1017. H. H. Claassen and E. H. Appelman, *Inorg. Chem.* **9**, 622 (1970).
1018. H. Bürger, G. Pawelke, and E. H. Appelman, *J. Mol. Spectrosc.* **144**, 201 (1990).
1019. J. Goubeau, E. Kilcioglu, and E. Jacob, *Z. Anorg. Allg. Chem.* **357**, 190 (1968).
1020. M. D. Zidan and A. W. Allaf, *Spectrochim. Acta* **56A**, 2693 (2000).
1021. K. D. Scherfise and K. Dehnicke, *Z. Anorg. Allg. Chem.* **538**, 119 (1986).
- 1021a. G. A. Ozin, and D. J. Reynolds, *J. Chem. Soc., Chem. Commun.* 884 (1969).
1022. H. Stammreich, O. Sala, and D. Bassi, *Spectrochim. Acta.* **19**, 593 (1963).
1023. H. Stammreich, O. Sala, and K. Kawai, *Spectrochim. Acta* **17**, 226 (1961).

1024. A. Müller, K. H. Schmidt, E. Ahlborn, and C. J. L. Lock, *Spectrochim. Acta* **29A**, 1773 (1973).
1025. K. H. Schmidt and A. Müller, *Spectrochim. Acta* **28A**, 1829 (1972).
1026. A. Müller, N. Mohan, H. Dornfeld, and C. Tellez, *Spectrochim. Acta* **34A**, 561 (1978).
1027. A. Müller, K. H. Schmidt, and U. Zint, *Spectrochim. Acta* **32A**, 901 (1976).
1028. E. L. Varetti, R. R. Filgueira, and A. Müller, *Spectrochim. Acta* **37A**, 369 (1981).
1029. E. L. Varetti, *J. Raman. Spectrosc.* **22**, 307 (1991).
1030. J. Binenboym, U. El-Gad, and H. Selig, *Inorg. Chem.* **13**, 319 (1974).
1031. A. Guest, H. E. Howard-Lock, and C. J. L. Lock, *J. Mol. Spectrosc.* **43**, 273 (1972).
1032. I. R. Beattie, R. A. Crocombe, and J. S. Ogden, *J. Chem. Soc., Dalton Trans.* 1481 (1977).
1033. A. Müller, B. Krebs, and W. Höltje, *Spectrochim. Acta* **23A**, 2753 (1967).
1034. K. H. Schmidt, V. Flemming, and A. Müller, *Spectrochim. Acta* **31A**, 1913 (1975).
1035. M. Gerken, D. A. Dixon, and G. J. Schrobilgen, *Inorg. Chem.* **41**, 259 (2002).
1036. A. Kornath, D. Kadzimirsz, and R. Ludwig, *Inorg. Chem.* **38**, 3066 (1999).
1037. S. J. Clarke, P. R. Chalker, J. Holman, C. W. Michie, M. Puyet, and M. J. Rosseinsky, *J. Am. Chem. Soc.* **124**, 3337 (2002).
1038. R. H. Bradley, P. N. Brier, and D. E. H. Jones, *J. Chem. Soc. A*, 1397 (1971).
1039. K. Hamada, G. A. Ozin, and E. A. Robinson, *Bull. Chem. Soc. Jpn.* **44**, 2555 (1971).
1040. F. Höfler, *Z. Naturforsch.* **26A**, 547 (1971).
1041. C. A. Clausen and M. L. Good, *Inorg. Chem.* **9**, 220 (1970).
1042. F. Höfler and W. Veigl, *Angew. Chem. Int. Ed. Engl.* **10**, 919 (1971).
1043. K. O. Christe and E. C. Curtis, *Inorg. Chem.* **11**, 2196 (1972).
1044. K. O. Christe, *Inorg. Chem.* **14**, 2821 (1975).
1045. M. Abenoza and V. Tabacik, *J. Mol. Struct.* **26**, 95 (1975).
1046. I. McAlpine and H. Sutcliffe, *Spectrochim. Acta* **25A**, 1723 (1969).
1047. J. E. Drake, C. Riddle, and D. E. Rogers, *J. Chem. Soc. A*, 910 (1969).
1048. D. C. McKean and B. A. Smart, *Spectrochim. Acta* **55A**, 845 (1999).
1049. M.-L. Dubois, M.-B. Delhay, and F. Wallart, *C. R. Hebd. Seances Acad. Sci.* **269B**, 260 (1969).
1050. J. E. Drake and C. Riddle, *J. Chem. Soc. A*, 2114 (1969).
1051. J. Weidlein, *Z. Anorg. Allg. Chem.* **358**, 13 (1968).
1052. A. Kornath, *J. Mol. Spectrosc.* **188**, 63 (1998).
1053. H. Bürger, J. Demaison, F. Hegelund, L. Margulès, and I. Merke, *J. Mol. Struct.* **612**, 133 (2002).
1054. D. E. Martz and R. T. Lagemann, *J. Chem. Phys.* **22**, 1193 (1954).
1055. R. Minkwitz, U. Nass, and J. Sawatzki, *J. Fluorine. Chem.* **31**, 175 (1986).
1056. R. J. Gillespie, J. B. Milne, D. Moffett, and P. Spekkens, *J. Fluorine. Chem.* **7**, 43 (1976).
1057. K. O. Christe and E. C. Curtis, *Inorg. Chem.* **11**, 35 (1972).
1058. R. Bougon, P. Joubert, and G. Tantot, *J. Chem. Phys.* **66**, 1562 (1977).
1059. H. H. Claassen, E. L. Gasner, H. Kim, and J. L. Huston, *J. Chem. Phys.* **49**, 253 (1968).

1060. S. A. Brandan, A. B. Altabef, and E. L. Varetti, *J. Raman Spectrosc.* **27**, 447 (1996).
1061. M. Muller, M. J. F. Leroy, and R. Rohmer, *C. R. Hebd. Seances Acad. Sci.* **270C**, 1458 (1970).
1062. S. D. Brown, G. L. Gard, and T. M. Loehr, *J. Chem. Phys.* **64**, 1219 (1976).
1063. M. Spoliti, J. H. Thirtle, and T. M. Dunn, *J. Mol. Spectrosc.* **52**, 146 (1974).
1064. E. G. Hope, W. Levason, J. S. Ogden, and M. Tajik, *J. Chem. Soc., Dalton Trans.* 1587 (1986).
1065. V. V. Kovba and A. A. Mal'tsev, *Russ. J. Inorg. Chem. (Engl. trans.)* **20**, 11 (1975).
1066. A. Müller, N. Weinstock, K. H. Schmidt, K. Nakamoto, and C. W. Schläpfer, *Spectrochim. Acta* **28A**, 2289 (1972).
1067. K. O. Christe, R. D. Wilson, and E. C. Curtis, *Inorg. Chem.* **12**, 1358 (1973).
1068. G. A. Ozin and A. Vander Voet, *Chem. Commun.* 1489 (1970).
1069. A. Müller, B. Krebs, E. Niecke, and A. Ruoff, *Ber. Bunsenges. Phys. Chem.* **71**, 571 (1967).
1070. M. L. Delwaulle and F. François, *J. Chim. Phys.* **46**, 87 (1949). *Hebd. Seances Acad. Sci.* **226**, 894 (1948).
1071. A. Müller and E. Diemann, *Z. Naturforsch.* **24b**, 353 (1969).
1072. A. Müller and E. Diemann, *Chem. Ber.* **102**, 2603 (1969).
1073. E. Diemann and A. Müller, *Inorg. Nucl. Chem. Lett.* **5**, 339 (1969).
1074. A. Müller and E. Diemann, *Z. Anorg. Allg. Chem.* **373**, 57 (1970).
1075. J. R. Durig and J. W. Clark, *J. Chem. Phys.* **46**, 3057 (1967).
1076. M. L. Delwaulle and F. François, *C. R. Hebd. Seances Acad. Sci.* **222**, 1193 (1946).
1077. A. Müller, E. Niecke, and O. Glemser, *Z. Anorg. Allg. Chem.* **350**, 246 (1967).
1078. T. T. Crow and R. T. Lagemann, *Spectrochim. Acta* **12**, 143 (1958).
1079. G. D. Flesch and H. J. Svec, *J. Am. Chem. Soc.* **80**, 3189 (1958).
1080. K. O. Christe and C. J. Schack, *Inorg. Chem.* **9**, 1852 (1970).
1081. H. Stammreich and R. Forneris, *Spectrochim. Acta* **16**, 363 (1960).
1082. P. Tsao, C. C. Cobb, and H. H. Claassen, *J. Chem. Phys.* **54**, 5247 (1971).
1083. H. Bürger, S. Ma, J. Breidung, and W. Thiel, *J. Chem. Phys.* **104**, 4945 (1996).
1084. P. J. Hendra, *J. Chem. Soc. A* 1298 (1967). *Spectrochim. Acta* **23A**, 2871 (1967).
1085. L. A. Degen and A. J. Rowlands, *Spectrochim. Acta* **47A**, 1263 (1991).
1086. P. L. Goggin and J. Mink, *J. Chem. Soc., Dalton Trans.* 1479 (1974).
1087. Y. M. Bosworth and R. J. H. Clark, *J. Chem. Soc., Dalton Trans.* 381 (1975).
1088. S. F. Parker, H. Herman, A. Zimmerman, and K. P. J. Williams, *Chem. Phys.* **261**, 261 (2000).
- 1088a. Y. Chen, D. H. Christensen, O. F. Nielsen, J. Hyldtoft, and C. J. H. Jacobsen, *Spectrochim. Acta* **51A**, 595 (1995).
1089. R. J. Gillespie, *J. Chem. Educ.* **40**, 295 (1963); **47**, 18 (1970).
1090. H. H. Claassen, C. L. Chernick, and J. G. Malm, *J. Am. Chem. Soc.* **85**, 1927 (1963).
1091. Y. M. Bosworth and R. J. H. Clark, *Inorg. Chem.* **14**, 170 (1975).
1092. J. Hiraishi and T. Shimanouchi, *Spectrochim. Acta* **22**, 1483 (1966).
1093. A. N. Pandey and U. P. Verma, *J. Mol. Struct.* **42**, 171 (1977).

1094. L. V. Konovalov, V. Yu. Kukushkin, V. K. Bel'skii, and V. E. Konovalov, *Russ. J. Inorg. Chem.* (Engl. Transl.) **35**, 863 (1990).
1095. H. Omrani, R. Mercier, and C. Sourisseau, *Spectrochim. Acta* **55A**, 1411 (1999).
- 1095a. E. Suchanek, N. Lange, G. Auffermann, W. Bronger, and H. D. Lutz, *J. Raman Spectrosc.* **30**, 981 (1999).
1096. H. C. Clark, K. R. Dixon, and J. G. Nicolson, *Inorg. Chem.* **8**, 450 (1969).
1097. I. R. Beattie and K. M. Livingston, *J. Chem. Soc. A* 859 (1969).
1098. I. R. Beattie, T. Gilson, K. Livingston, V. Fawcett, and G. A. Ozin, *J. Chem. Soc. A* 712 (1967).
1099. J. I. Bullock, N. J. Taylor, and F. W. Parrett, *J. Chem. Soc., Dalton Trans.* 1843 (1972).
1100. J. A. Creighton and J. H. S. Green, *J. Chem. Soc. A* 808 (1968).
1101. I. R. Beattie, K. M. S. Livingston, and D. J. Reynolds, *J. Chem. Phys.* **51**, 4269 (1969).
1102. N. A. Chumaevskii, *Russ. J. Inorg. Chem* (Engl. transl.) **29**, 1415 (1984).
1103. P. van Huong and B. Desbat, *Bull. Soc. Chim. Fr.* 2631 (1972).
1104. L. C. Hoskins and R. C. Lord, *J. Chem. Phys.* **46**, 2402 (1967).
1105. K. Seppelt, *Z. Anorg. Allg. Chem.* **434**, 5 (1977).
1106. J. Gaunt and J. B. Ainscough, *Spectrochim. Acta.* **10**, 57 (1957).
1107. I. R. Beattie and G. A. Ozin, *J. Chem. Soc. A*, 1691 (1969).
1108. H. Haas and M. Jansen, *Z. Anorg. Allg. Chem.* **626**, 1174 (2000).
1109. T. V. Long, A. W. Herlinger, E. F. Epstein, and I. Bernal, *Inorg. Chem.* **9**, 459 (1970).
1110. C. S. Creaser and J. A. Creighton, *J. Chem. Soc., Dalton Trans.* 1402 (1975).
1111. H. H. Claassen and H. Selig, *J. Chem. Phys.* **44**, 4039 (1965).
1112. E. G. Hope, *J. Chem. Soc., Dalton Trans.* 723 (1990).
1113. R. D. Werder, R. A. Frey, and H. Günthard, *J. Chem. Phys.* **47**, 4159 (1967).
1114. E. M. Nour, *Spectrochim. Acta* **42A**, 1411 (1986).
1115. N. Acquista and S. Abramowitz, *J. Chem. Phys.* **58**, 5484 (1973).
1116. A. M. McNair and B. S. Ault, *Inorg. Chem.* **21**, 2603 (1982).
1117. A. K. Brisdon, J. T. Graham, E. G. Hope, D. M. Jenkins, W. Levason, and J. S. Ogden, *J. Chem. Soc., Dalton Trans.* 1529 (1990).
1118. R. A. Condrate and K. Nakamoto, *Bull. Chem. Soc. Jpn.* **39**, 1108 (1966).
1119. R. R. Holmes, R. M. Deiters, and J. A. Golen, *Inorg. Chem.* **8**, 2612 (1969).
1120. I. W. Levin, *J. Mol. Spectrosc.* **33**, 61 (1970).
1121. H. Selig, J. H. Holloway, J. Tyson, and H. H. Claassen, *J. Chem. Phys.* **53**, 2559 (1970).
1122. D. E. Sands and A. Zalkin, *Acta Crystallogr.* **12**, 723 (1959).
1123. A. Zalkin and D. E. Sands, *Acta Crystallogr.* **11**, 615 (1958).
1124. R. A. Walton and B. J. Brisdon, *Spectrochim. Acta* **23A**, 2489 (1967).
1125. P. M. Boorman, N. N. Greenwood, M. A. Hildon, and H. J. Whitfield, *J. Chem. Soc. A*. 2017 (1967).
1126. A. J. Edwards, *J. Chem. Soc.* 3714 (1964).
1127. L. E. Alexander and I. R. Beattie, *J. Chem. Phys.* **56**, 5829 (1972).
1128. L. E. Alexander, I. R. Beattie, and P. J. Jones, *J. Chem. Soc., Dalton Trans.* 210 (1972).
1129. H. Gerding and H. Houtgraaf, *Recl. Trav. Chim.* **74**, 5 (1955).

1130. R. R. Holmes, *Acc. Chem. Res.* **5**, 296 (1972).
1131. R. R. Holmes, *J. Chem. Phys.* **46**, 3718 3724, 3730 (1967).
1132. C. Macho, R. Minkwitz, J. Rohmann, B. Steger, V. Wölfel, and H. Oberhammer, *Inorg. Chem.* **25**, 2828 (1986).
1133. J. A. Salthouse and T. C. Waddington, *Spectrochim. Acta* **23A**, 1069 (1967).
1134. J. Breidung, W. Thiel, and A. Komornicki, *J. Phys. Chem.* **92**, 5603 (1988).
1135. R. R. Holmes and C. J. Hora, Jr., *Inorg. Chem.* **11**, 2506 (1972).
1136. R. Winkwitz and A. Liedtke, *Inorg. Chem.* **28**, 4238 (1989).
1137. H. Beckers, J. Breidung, H. Bürger, R. Kuna, A. Rahner, W. Schneider, and W. Thiel, *J. Chem. Phys.* **93**, 4603 (1990).
1138. R. Minkwitz and H. Prenzel, *Z. Anorg. Allg. Chem.* **548**, 103 (1987).
1139. R. Minkwitz and H. Prenzel, *Z. Anorg. Allg. Chem.* **534**, 150 (1986).
1140. K. O. Christe, C. J. Schack, and E. C. Curtis, *Spectrochim. Acta* **33A**, 323 (1977).
1141. K. O. Criste, D. A. Dixon, G. J. Schrobilgen, and W. W. Wilson, *J. Am. Chem. Soc.* **119**, 3918 (1997).
1142. M. Gerken, D. A. Dixon, and G. J. Schrobilgen, *Inorg. Chem.* **39**, 4244 (2000).
1143. R. J. Gillespie and G. J. Schrobilgen, *J. Chem. Soc., Chem. Commun.* 595 (1977).
1144. K. O. Criste and W. W. Wilson, *Inorg. Chem.* **27**, 3763 (1988).
1145. W. J. Casteel, D. A. Dixon, H. P. A. Mercier, and G. J. Schrobilgen, *Inorg. Chem.* **35**, 4310 (1996).
1146. N. LeBlond, D. A. Dixon, and G. J. Schrobilgen, *Inorg. Chem.* **39**, 2473 (2000).
1147. D. M. Adams and R. R. Smardzewski, *J. Chem. Soc. A* 714 (1971).
1148. L. E. Alexander and I. R. Beattie, *J. Chem. Soc. A* 3091 (1971).
1149. H. A. Szymanski, R. Yelin, and L. Marabella, *J. Chem. Phys.* **47**, 1877 (1967).
1150. K. O. Christe, E. C. Curtis, C. J. Schack, and D. Pilipovich, *Inorg. Chem.* **11**, 1679 (1972).
1151. T. Schönherr, *Z. Naturforsch.* **43b**, 159 (1988).
1152. O. V. Blinova, S. L. Dobycin, and L. D. Shcherba, *Opt. Spektrosk.* **61**, 756 (1986).
1153. G. M. Begun, W. H. Fletcher, and D. F. Smith, *J. Chem. Phys.* **42**, 2236 (1965).
1154. K. O. Christe, *Spectrochim. Acta* **27A**, 631 (1971).
1155. R. A. Frey, R. L. Redington, and A. L. Khidir Aljibury, *J. Chem. Phys.* **54**, 344 (1971).
1156. N. Acquista and S. Abramowitz, *J. Chem. Phys.* **56**, 5221 (1972).
1157. B. Družina and B. Žemva, *J. Fluorine. Chem.* **39**, 309 (1988).
1158. J. B. Milne and D. Moffett, *Inorg. Chem.* **12**, 2240 (1973).
1159. K. O. Christe and E. C. Curtis, *Inorg. Chem.* **11**, 2209 (1972).
1160. R. Bougon, T. B. Huy, P. Charpin, and G. Tantot, *C. R. Hebd. Seances Acad. Sci.* **283**, C71 (1976).
1161. W. W. Wilson and K. O. Christe, *Inorg. Chem.* **26**, 916 (1987).
1162. J. B. Milne and D. M. Moffett, *Inorg. Chem.* **15**, 2165 (1976).
1163. E. G. Hope, P. J. Jones, W. Levason, J. S. Ogden, M. Tajik, and J. W. Turff, *J. Chem. Soc., Dalton Trans.* 529 (1985).
1164. K. O. Christe, W. W. Wilson, and R. A. Bougon, *Inorg. Chem.* **25**, 2163 (1986).

1165. W. Levason, R. Narayanaswamy, J. S. Ogden, A. J. Rest, and J. W. Turff, *J. Chem. Soc., Dalton Trans.* 2501 (1981).
1166. L. E. Alexander, I. R. Beattie, A. Bukovszky, P. J. Jones, C. J. Marsden, and G. J. Van Schalkwyk, *J. Chem. Soc., Dalton Trans.* 81 (1974).
1167. R. T. Paine and R. S. McDowell, *Inorg. Chem.* **13**, 2366 (1974).
1168. I. R. Beattie, K. M. S. Livingston, D. J. Reynolds, and G. A. Ozin, *J. Chem. Soc. A* 1210 (1970).
1169. K. Iijima and S. Shibata, *Bull. Chem. Soc. Jpn.* **48**, 666 (1975).
1170. R. J. Collin, W. P. Griffith, and D. Pawson, *J. Mol. Struct.* **19**, 531 (1973).
1171. A. K. Brisdon, E. G. Hope, J. H. Holloway, W. Levason, and J. S. Ogden, *J. Fluorine Chem.* **64**, 117 (1993).
1172. W. Preetz and W. Lierka, *Z. Naturforsch.* **48b**, 44 (1993).
1173. M. G. Krishna Pillai and P. Parameswaran Pillai, *Can. J. Chem.* **46**, 2393 (1968).
1174. K. O. Christe, W. W. Wilson, and R. A. Bougon, *Inorg. Chem.* **25**, 2163 (1986).
1175. K. O. Christe, E. C. Curtis, D. A. Dixon, H. P. Mercier, J. C. P. Sanders, and G. J. Schrobilgen, *J. Am. Chem. Soc.* **113**, 3351 (1991).
1176. K. O. Christe, W. W. Wilson, G. W. Drake, D. A. Dixon, J. A. Boatz, and R. S. Gnann, *J. Am. Chem. Soc.* **120**, 4711 (1998).
1177. M. J. Reisfeld, *Spectrochim. Acta* **29A**, 1923 (1973).
1178. E. J. Baran and A. E. Lavat, *Z. Naturforsch.* **36A**, 677 (1981).
1179. S. Milicev, A. Rahten, and H. Borrmann, *J. Raman Spectrosc* **28**, 315 (1997).
1180. T. Barrowcliffe, I. R. Beattie, P. Day, and K. Livingston, *J. Chem. Soc. A*, 1810 (1967).
1181. T. G. Spiro, *Inorg. Chem.* **6**, 569 (1967).
1182. C. Naulin and R. Bougon, *J. Chem. Phys.* **64**, 4155 (1976).
1183. P. Benkič and Z. Mazej, *Z. Anorg. Allg. Chem.* **627**, 1952 (2001).
1184. I. R. Beattie, T. Gilson, K. Livingston, V. Fawcett, and G. A. Ozin, *J. Chem. Soc. A*, 712 (1967).
1185. T. L. Brown, W. G. McDugle, Jr., and L. G. Kent, *J. Am. Chem. Soc.* **92**, 3645 (1970).
1186. M. Debeau and M. Krauzman, *C. R. Hebd. Seances Acad. Sci.* **264B**, 1724 (1967).
1187. I. Wharf and D. F. Shriver, *Inorg. Chem.* **8**, 914 (1969).
1188. A. M. Heyns, *Spectrochim. Acta* **33A**, 315 (1977).
1189. A. S. Muir, *Polyhedron* **10**, 2217 (1991).
1190. A. I. Popov, A. V. Shcharabarin, V. F. Sukhoverkov, and N. A. Chumaevsty, *Z. Anorg. Allg. Chem.* **576**, 242 (1989).
1191. M. Burgard and J. MacCordick, *Inorg. Nucl. Chem. Lett.* **6**, 599 (1970).
1192. Y. M. Bosworth and R. J. H. Clark, *J. Chem. Soc., Dalton Trans.* 1749 (1974).
1193. R. J. H. Clark and M. L. Duarte, *J. Chem. Soc., Dalton Trans.* 790 (1977).
1194. M. A. Hooper and D. W. James, *Aust. J. Chem.* **26**, 1401 (1973).
1195. M. A. Hooper and D. W. James, *J. Inorg. Nucl. Chem.* **35**, 2335 (1973).
1196. T. Surles, L. A. Quaterman, and H. H. Hyman, *J. Inorg. Nucl. Chem.* **35**, 670 (1973).
1197. Y. M. Bosworth, R. J. H. Clark, and D. M. Rippon, *J. Mol. Spectrosc.* **46**, 240 (1973).

1198. H. H. Claassen, G. L. Goodman, J. H. Holloway, and H. Selig, *J. Chem. Phys.* **53**, 341 (1970).
1199. A. Aboumaja, H. Berger, and R. Saint-Loup, *J. Mol. Spectrosc.* **78**, 486 (1979).
1200. O. Reich, S. Hasche, K. Büscher, I. Beckmann, and B. Krebs, *Z. Anorg. Allg. Chem.* **622**, 1011 (1996).
1201. R. W. Berg, F. W. Poulsen, and N. J. Bjerrum, *J. Chem. Phys.* **67**, 1829 (1977).
1202. L.-J. Baker, C. E. F. Rickard, and M. J. Taylor, *Polyhedron* **14**, 401 (1995).
1203. K. O. Christe, W. W. Wilson, R. V. Chirak, J. C. P. Sanders, and G. J. Schrobilgen, *Inorg. Chem.* **29**, 3306 (1990).
1204. K. O. Christe, *Inorg. Chem.* **12**, 1580 (1973).
1205. R. J. Gillespie and G. J. Schrobilgen, *Inorg. Chem.* **13**, 1230 (1974).
1206. R. Bougon, P. Charpin, and J. Soriano, *C. R. Hebd. Seances Acad. Sci.* **272C**, 565 (1971).
1207. N. Bartlett and K. Leary, *Rev. Chim. Minér.* **13**, 82 (1976).
1208. S. Turrell, S. Hafsi, P. Conflant, P. Barbier, M. Drache, and J. C. Champarnaud-Mesjard, *J. Mol. Struct.* **174**, 449 (1988).
1209. R. Becker, A. Lentz, and W. Sawodny, *Z. Anorg. Allg. Chem.* **420**, 210 (1976).
1210. D. M. Adams and D. M. Morris, *J. Chem. Soc. A*, 694 (1968).
1211. I. W. Forrest and A. P. Lane, *Inorg. Chem.* **15**, 265 (1976).
1212. R. J. H. Clark, L. Maresca, and R. J. Puddephatt, *Inorg. Chem.* **7**, 1603 (1968).
1213. P. C. Crouch, G. W. A. Fowles, and R. A. Walton, *J. Chem. Soc. A*, 972 (1969).
1214. P. A. W. Dean and D. F. Evans, *J. Chem. Soc. A*, 698 (1967).
1215. D. M. Adams and D. C. Newton, *J. Chem. Soc. A*, 2262 (1968).
1216. W. von Bronswyk, R. J. H. Clark, and L. Maresca, *Inorg. Chem.* **8**, 1395 (1969).
1217. R. Becker and W. Sawodny, *Z. Naturforsch.* **28b**, 360 (1973).
1218. R. A. Walton and B. J. Brisdon, *Spectrochim. Acta* **23A**, 2222 (1967).
1219. O. L. Keller, *Inorg. Chem.* **2**, 783 (1963).
1220. E. Hahn and R. Hebisich, *Spectrochim. Acta* **47A**, 1097 (1991).
1221. S. M. Horner, R. J. H. Clark, B. Crociani, D. B. Copley, W. W. Horner, F. N. Collier, and S. Y. Tyree, *Inorg. Chem.* **7**, 1859 (1968).
1222. D. Brown and P. J. Jones, *J. Chem. Soc. A*, 247 (1967).
1223. G. A. Ozin, G. W. A. Fowles, D. J. Tidmarsh, and R. A. Walton, *J. Chem. Soc. A*, 642 (1969).
1224. O. L. Keller and A. Chetham-Strode, *Inorg. Chem.* **5**, 367 (1966).
1225. B. Weinstock and G. L. Goodman, *Adv. Chem. Phys.* **11**, 169 (1965).
1226. F. G. Hope, P. J. Jones, W. Levason, J. S. Ogden, M. Tajik, and J. W. Turff, *J. Chem. Soc., Dalton Trans.* 1443 (1985).
1227. H. H. Eysel, *Z. Anorg. Allg. Chem.* **390**, 210 (1972).
1228. R. S. McDowell, R. J. Sherman, L. B. Asprey, and R. C. Kennedy, *J. Chem. Phys.* **62**, 3974 (1975).
1229. R. R. Smardzewski, R. E. Nofle, and W. B. Fox, *J. Mol. Spectrosc.* **62**, 449 (1976).
1230. J. A. Creighton and T. J. Sinclair, *Spectrochim. Acta* **35A**, 507 (1979).

1231. C. D. Flint, *J. Mol. Spectrosc.* **37**, 414 (1971).
1232. E. Jacob and M. Föhnle, *Angew. Chem. Int. Ed. Engl.* **15**, 159 (1976).
1233. J. A. LoMenzo, S. Strobebridge, H. H. Patterson, and E. Engstrom, *J. Mol. Spectrosc.* **66**, 150 (1977).
1234. P. W. Fraiss, C. J. L. Lock, and A. Guest, *Chem. Commun.* 1612 (1970).
1235. G. L. Bottger and C. V. Damsgard, *Spectrochim. Acta* **28A**, 1631 (1972).
1236. L. A. Woodward and M. J. Ware, *Spectrochim. Acta* **20**, 711 (1964).
1237. K. O. Christe, *Inorg. Chem.* **16**, 2238 (1977).
1238. Z. Mazej and K. Lutar, *J. Fluorine. Chem.* **107**, 63 (2001).
1239. M. Debeau and H. Poulet, *Spectrochim. Acta* **25A**, 1553 (1969).
1240. P. J. Hendra and P. J. D. Park, *Spectrochim. Acta* **23A**, 1635 (1967).
1241. L. A. Woodward and M. J. Ware, *Spectrochim. Acta* **19**, 775 (1963).
1242. D. M. Adams and H. A. Gebbie, *Spectrochim. Acta* **19**, 925 (1963).
1243. K. Wieghardt and H. H. Eysel, *Z. Naturforsch.* **25b**, 105 (1970).
1244. J. M. Fletcher, W. E. Gardner, A. C. Fox, and G. Topping, *J. Chem. Soc. A*, 1038 (1967).
1245. W. Preetz and M. Bruns, *Z. Naturforsch.* **38b**, 680 (1983).
1246. Y. M. Bosworth and R. J. H. Clark, *J. Chem. Soc., Dalton Trans.* 1749 (1974).
1247. D. A. Kelly and M. L. Good, *Spectrochim. Acta* **28A**, 1529 (1972).
1248. H. Homborg, *Z. Anorg. Allg. Chem.* **460**, 17 (1980).
1249. N. J. Campbell, V. A. Davis, W. P. Griffith, and T. J. Townend, *J. Chem. Soc., Dalton Trans.* 1673 (1985).
1250. I. J. Ellison and R. D. Gillard, *Polyhedron*. **15**, 339 (1996).
1251. M. Rotger, V. Bourdon, A. T. Nguyen, and D. Avignat, *J. Raman. Spectrosc.* **27**, 145 (1996).
1252. V. Bourdon, M. Rotger, and D. D. Avignat, *J. Mol. Spectrosc.* **175**, 327 (1996).
1253. R. J. H. Clark and P. C. Turtle, *J. Chem. Soc., Dalton Trans.* 2063 (1978).
1254. W. Preetz and H. J. Steinebach, *Z. Naturforsch.* **41b**, 260 (1986).
1255. L. A. Woodward and M. J. Ware, *Spectrochim. Acta* **24A**, 921 (1968).
1256. R. T. Paine, R. S. McDowell, L. B. Asprey, and L. H. Jones, *J. Chem. Phys.* **64**, 3081 (1976).
1257. J. L. Ryan *J. Inorg. Nucl. Chem.* **33**, 153 (1971).
1258. E. Stumpp and G. Piltz, *Z. Anorg. Allg. Chem.* **409**, 53 (1974).
1259. R. N. Mulford, H. J. Dewey, and J. E. Barefield, *J. Chem. Phys.* **94**, 4790 (1991).
1260. B. W. Berringer, J. B. Gruber, T. M. Loehr, and G. P. O'Leary, *J. Chem. Phys.* **55**, 4608 (1971).
1261. H. J. Dewey, J. E. Barefield, and W. W. Rice, *J. Chem. Phys.* **84**, 684 (1986).
1262. S. J. David and K. C. Kim, *J. Chem. Phys.* **89**, 1780 (1988).
1263. S. F. Parker, K. P. J. Williams, M. Bortz, and K. Yvon, *Inorg. Chem.* **36**, 5218 (1997).
1264. D. M. Yost, C. S. Steffens, and S. T. Gross, *J. Chem. Phys.* **2**, 311 (1934).
1265. A. Fadini and S. Kemmler-Sack, *Spectrochim. Acta* **34A**, 853 (1978).
1266. C. J. Adams and A. J. Downs, *Chem. Commun.* 1699 (1970).

1267. L. A. Woodward and J. A. Creighton, *Spectrochim. Acta* **17**, 594 (1961).
1268. M. Bettinelli, L. Disipio, A. Paschetto, G. Ingletto, and A. Montenero, *Inorg. Chim. Acta* **99**, 37 (1985).
1269. M. Bettinelli, L. Disipio, G. Ingletto, and C. Razzetti, *Inorg. Chim. Acta* **133**, 7 (1987).
1270. O. Arp and W. Preetz, *Z. Anorg. Allg. Chem.* **620**, 1391 (1994).
1271. M. Wei, R. D. Willett, and K. W. Hipps, *Inorg. Chem.* **35**, 5300 (1996).
1272. R. D. Hunt, L. Andrews, and L. MacToth, *J. Phys. Chem.* **95**, 1183 (1991).
1273. H. Hamaguchi, I. Harada, and T. Shimanouchi, *Chem. Phys. Lett.* **32**, 103 (1975).
1274. H. Hamaguchi, *J. Chem. Phys.* **69**, 569 (1978).
1275. H. Hamaguchi and T. Shimanouchi, *Chem. Phys. Lett.* **38**, 370 (1976).
1276. B. Weinstock, H. H. Claassen, and C. L. Chernick, *J. Chem. Phys.* **38**, 1470 (1963).
1277. H. Kim, H. H. Claassen, and E. Pearson, *Inorg. Chem.* **7**, 616 (1968).
1278. H. H. Claassen, G. L. Goodman, and H. Kim, *J. Chem. Phys.* **56**, 5042 (1972).
1279. M. Takami, T. Oyama, T. Watanabe, S. Namba, and R. Nakane, *Jpn. J. Appl. Phys.* **23**, L88 (1984).
1280. D. N. Travis, J. C. McGurk, D. McKeown, and R. G. Denning, *Chem. Phys. Lett.* **45**, 287 (1977).
1281. G. Herzberg, *Molecular Spectra and Molecular Structure, Vol II: Infrared and Raman Spectra of Polyatomic Molecules*, Van Nostrand, New York, 1951 p. 446.
1282. K. Takeuchi, H. Tashiro, S. Isomura, T. Oyama, S. Satooka, K. Midorikawa, and S. Namba, *J. Nucl. Sci. Technol.* **23**, 282 (1986).
1283. H. Kim, P. A. Souder, and H. H. Claassen, *J. Mol. Spectrosc.* **26**, 46 (1968).
1284. P. LaBonville, J. R. Ferraro, M. C. Wall, and L. J. Basile, *Coord. Chem. Rev.* **7**, 257 (1972).
1285. P. J. Cresswell, J. E. Fergusson, B. R. Penfold, and D. E. Scaife, *J. Chem. Soc., Dalton Trans.* 254 (1972).
1286. J. Hauck and A. Fadini, *Z. Naturforsch.* **25B**, 422 (1970).
1287. J. Hauck, *Z. Naturforsch.* **25B**, 224, 468, 647 (1970).
1288. P. Ayyub, M. S. Multani, V. R. Palkar, and R. Vijayaraghavan, *Phys. Rev.* **B34**, 8137 (1986).
1289. K. O. Christe, D. A. Dixon, and W. W. Wilson, *J. Am. Chem. Soc.* **116**, 7123 (1994).
1290. C. J. Adams and A. J. Downs, *J. Inorg. Nucl. Chem.* **34**, 1829 (1972).
1291. G. Goetz, M. Deneux, and M. J. F. Leroy, *Bull. Soc. Chim. Fr.* 29 (1971).
1292. J. E. Griffith, *Spectrochim. Acta* **23A**, 2145 (1967).
1293. K. O. Christe, E. C. Curtis, and C. J. Schack, *Spectrochim. Acta* **33A**, 69 (1977).
1294. K. O. Christe, C. J. Schack, D. Pilipovich, E. C. Curtis, and W. Sawodny, *Inorg. Chem.* **12**, 620 (1973).
1295. W. Heilemann, R. Mews, S. Pohl, and W. Saak, *Chem. Ber.* **122**, 427 (1989).
1296. K. O. Christe, C. J. Schack, and E. C. Curtis, *Inorg. Chem.* **11**, 583 (1972).
1297. K. Seppelt, *Z. Anorg. Allg. Chem.* **399**, 87 (1973).
1298. W. V. F. Brooks, M. E. Eshaque, C. Lau, and J. Passmore, *Can. J. Chem.* **54**, 817 (1976).

1299. P. K. Miller, K. D. Abney, A. K. Rappe, O. P. Anderson, and S. H. Strauss, *Inorg. Chem.* **27**, 2255 (1988).
1300. K. Dehnicke, G. Pausewang, and W. Rüdorff, *Z. Anorg. Allg. Chem.* **366**, 64 (1969).
1301. G. A. Ozin, G. W. A. Fowles, D. J. Tidmarsh, and R. A. Walton, *J. Chem. Soc. A*, 642 (1969).
1302. N. LeBlond, H. P. A. Mercier, D. A. Dixon, and G. J. Schrobilgen, *Inorg. Chem.* **39**, 4494 (2000).
1303. R. J. Collin, W. P. Griffith, and D. Pawson, *J. Mol. Struct.* **19**, 531 (1973).
1304. A. Beuter and W. Sawodny, *Z. Anorg. Allg. Chem.* **427**, 37 (1976).
1305. D. M. Adams, G. W. Fraser, D. M. Morris, and R. D. Peacock, *J. Chem. Soc. A*, 1131 (1968).
1306. J. H. Holloway, H. Selig, and H. H. Claassen, *J. Chem. Phys.* **54**, 4305 (1971).
1307. E. G. Hope, W. Levason, and J. S. Ogden, *J. Chem. Soc., Dalton Trans.* 61 (1988).
1308. B. Lorenzen and W. Preetz, *Z. Naturforsch.* **55b**, 45 (2000).
1309. P. Joubert, R. Bougon, and B. Gaudreau, *Can. J. Chem.* **56**, 1874 (1978).
1310. J. P. Brunnette and M. J. F. Leroy, *J. Inorg. Nucl. Chem.* **36**, 289 (1974).
1311. W. Preetz and H. N. von Allwörden, *Z. Naturforsch.* **42b**, 381 (1987); H. N. von Allwörden and W. Preetz, *ibid.* **42a**, 597 (1987).
1312. W. Preetz and K. Irmer, *Z. Naturforsch.* **45b**, 283 (1990).
1313. W. Preetz and A. Wendt, *Z. Naturforsch.* **46b**, 1496 (1991).
1314. W. Preetz, D. Ruf, and D. Tensfeldt, *Z. Naturforsch.* **39b**, 1100 (1984).
- 1314a. B. Lorenzen and W. Preetz, *Z. Anorg. Allg. Chem.* **625**, 1917 (1999).
1315. W. Preetz and W. Kuhr, *Z. Naturforsch.* **44b**, 1221 (1989).
1316. W. Preetz and H.-J. Steinebach, *Z. Naturforsch.* **40b**, 745 (1985).
1317. D. Tensfeldt and W. Preetz, *Z. Naturforsch.* **39b**, 1185 (1984).
1318. B. Lorenzen and W. Preetz, *Z. Anorg. Allg. Chem.* **626**, 667 (2000).
1319. W. Preetz and P. Erhöfer, *Z. Naturforsch.* **44b**, 412 (1989); P. Erhöfer and W. Preetz, *ibid.* 619, 1214.
1320. C. Bruhn, H.-H. Drews, B. Meynhardt, and W. Preetz, *Z. Anorg. Allg. Chem.* **621**, 373 (1995).
1321. W. Preetz and G. Rimkus, *Z. Naturforsch.* **37b**, 579 (1982).
1322. K. Irmer and W. Preetz, *Z. Naturforsch.* **46b**, 1200 (1991).
1323. W. Preetz, G. Peters, and D. Bublit, *Chem. Rev.* **96**, 977 (1996).
1324. W. Abriel and H. Ehrhardt, *Z. Naturforsch.* **43b**, 557 (1988).
1325. W. J. Casteel, Jr., D. A. Dixon, N. LeBlond, H. P. A. Mercier, and G. J. Schrobilgen, *Inorg. Chem.* **37**, 340 (1998).
1326. W. J. Casteel, Jr., D. A. Dixon, N. LeBlond, P. E. Lock, H. P. A. Mercier, and G. J. Schrobilgen, *Inorg. Chem.* **38**, 2340 (1999).
1327. G. J. Schrobilgen, *Chem. Commun.* 894 (1980).
1328. J. H. Holloway, V. Kaucic, D. Martin-Rovet, D. R. Russell, G. J. Schrobilgen, and H. Selig, *Inorg. Chem.* **24**, 678 (1985).
1329. K. O. Christe, D. A. Dixon, J. C. P. Sanders, G. J. Schrobilgen, S. S. Tsai, and W. W. Wilson, *Inorg. Chem.* **34**, 1868 (1995).

1330. K. O. Christe, W. W. Wilson, D. Dixon, and J. A. Boatz, *J. Am. Chem. Soc.* **121**, 3382 (1999).
1331. H. H. Claassen, E. L. Gasner, and H. Selig, *J. Chem. Phys.* **49**, 1803 (1968).
1332. K. O. Christe, J. C. P. Sanders, G. J. Schrobiligen, and W. W. Wilson, *J. Chem. Soc., Chem. Commun.* 837 (1991).
1333. A. R. Mahjoub and K. Seppelt, *J. Chem. Soc., Chem. Commun.* 840 (1991).
1334. H. H. Eysel and K. Seppelt, *J. Chem. Phys.* **56**, 5081 (1972).
1335. G. W. Drake, D. A. Dixon, J. A. Sheehy, J. A. Boatz, and K. O. Christe, *J. Am. Chem. Soc.* **120**, 8392 (1998).
1336. Nguyen-Quy-Dao, *Bull. Soc. Chim. Fr.* 3976 (1968).
1337. K. O. Christe, D. A. Dixon, A. R. Mamjoub, H. P. A. Mercier, J. C. P. Sanders, K. Seppelt, G. J. Schrobiligen, and W. W. Wilson, *J. Am. Chem. Soc.* **115**, 2696 (1993).
1338. K. O. Christe, D. A. Dixon, J. C. P. Sanders, G. J. Schrobiligen, and W. W. Wilson, *Inorg. Chem.* **32**, 4089 (1993).
1339. J. L. Hoard, W. G. Martin, M. E. Smith, and J. E. Whitney, *J. Am. Chem. Soc.* **76**, 3820 (1954).
1340. R. Stomberg and C. Brosset, *Acta. Chem. Scand.* **14**, 441 (1960).
1341. K. O. Hartman and F. A. Miller, *Spectrochim. Acta* **24A**, 669 (1968).
1342. C. W. F. T. Pistorius, *Bull. Soc. Chim. Belg.* **68**, 630 (1959).
1343. H. L. Schlaefer and H. F. Wasgestian, *Theor. Chim. Acta* **1**, 369 (1963).
1344. J. R. Durig, J. W. Thompson, J. D. Witt, and J. D. Odom, *J. Chem. Phys.* **58**, 5339 (1973).
1345. D. E. Mann and L. Fano, *J. Chem. Phys.* **26**, 1665 (1957).
1346. J. D. Odom, J. E. Saunders, and J. R. Durig, *J. Chem. Phys.* **56**, 1643 (1972).
1347. L. A. Minon, K. S. Seshadri, R. C. Taylor, and D. White, *J. Chem. Phys.* **53**, 2416 (1970).
1348. F. Mélen, R. Pokorni, and M. Herman, *Chem. Phys. Lett.* **194**, 181 (1992).
1349. B. Andrews and A. Anderson, *J. Chem. Phys.* **74**, 1534 (1981).
1350. W. G. Fateley, H. A. Bent, and B. Crawford, Jr., *J. Chem. Phys.* **31**, 204 (1959).
1351. G. M. Begun and W. H. Fletcher, *Spectrochim. Acta* **19**, 1343 (1963).
1352. R. J. H. Clark and S. Firth, *Spectrochim. Acta* **58A**, 1731 (2002).
1353. R. E. Hester and R. A. Plane, *Inorg. Chem.* **3**, 513 (1964).
1354. D. N. Shchepkin, L. A. Zhygula, and L. P. Belozerskaya, *J. Mol. Struct.* **49**, 265 (1978).
1355. J. R. Durig, S. F. Bush, and E. E. Mercer, *J. Chem. Phys.* **44**, 4238 (1966).
1356. R. Lascola, R. Withnall, and L. Andrews, *Inorg. Chem.* **27**, 642 (1988).
1357. E. R. Nixon, *J. Phys. Chem.* **60**, 1054 (1956).
1358. S. G. Frankiss, *Inorg. Chem.* **7**, 1931 (1968).
1359. K. H. Rhee, A. M. Snider, Jr., and F. A. Miller, *Spectrochim. Acta* **29A**, 1029 (1973).
1360. S. G. Frankiss and F. A. Miller, *Spectrochim. Acta* **21**, 1235 (1965).
1361. S. G. Frankiss, F. A. Miller, H. Stammreich, and Th. T. Sans, *Spectrochim. Acta* **23A**, 543 (1967).
1362. W. C. Hodgeman, J. B. Weinrach, and D. W. Bennett, *Inorg. Chem.* **30**, 1611 (1991).

1363. M. Somer, D. Thierry, K. Peters, L. Walz, M. Hartweg, and H. G. von Schneering, *Z. Naturforsch.* **46b**, 789 (1991).
1364. A. Hammerschmidt, C. Jansen, K. Küper, C. Püttmann, and B. Krebs, *Z. Anorg. Allg. Chem.* **621**, 1330 (1995).
1365. J. R. Durig, B. M. Gimarc, and J. D. Odom, in J. R. Durig, ed., *Vibrational Spectra and Structure*, Vol. 2, Marcel Dekker, New York, 1975, p. 1.
1366. R. P. Bell and H. C. Longuet-Higgins, *Proc. R. Soc. London Ser. A*, **183**, 357 (1945).
1367. C. Liang, R. D. Davy, and H. F. Schaefer, *Chem. Phys. Lett.* **159**, 393 (1989).
1368. J. L. Duncan, D. C. McKean, and I. Torto, *J. Mol. Spectrosc.* **85**, 16 (1981).
1369. J. L. Domenech, D. Bermejo, J.-M. Flaud, and W. J. Lafferty, *J. Mol. Spectrosc.* **194**, 185 (1999).
1370. A. Snelson, *J. Phys. Chem.* **71**, 3202 (1967).
1371. M. Tranquille and M. Fouassier, *J. Chem. Soc., Faraday Trans. 2*, **76**, 26 (1980).
1372. D. M. Adams and R. G. Churchill, *J. Chem. Soc. A*, 697 (1970).
1373. A. J. Downs, M. J. Goode, and C. R. Pulham, *J. Am. Chem. Soc.* **111**, 1936 (1989).
1374. C. R. Pulham, A. J. Downs, M. J. Goode, D. W. H. Rankin, and H. E. Robertson, *J. Am. Chem. Soc.* **113**, 5149 (1991).
1375. I. R. Beattie, T. Gilson, and P. Cocking, *J. Chem. Soc. A*, 702 (1967).
1376. A. D. Alvarenga, M. L. Saboungi, L. A. Curtis, M. Grimsditch, and L. E. McNeil, *Mol. Phys.* **81**, 409 (1994).
1377. L. Nalbandian and G. N. Papatheodorou, *High Temp. Sci.* **28**, 49 (1988).
1378. R. A. Frey, R. D. Werder, and H. H. Günthard, *J. Mol. Spectrosc.* **35**, 260 (1970).
1379. T. Onishi and T. Shimanouchi, *Spectrochim. Acta* **20**, 721 (1964).
1380. N. N. Greenwood, D. J. Prince, and B. P. Straughan, *J. Chem. Soc. A*, 1694 (1968).
1381. P. L. Goggin, *J. Chem. Soc., Dalton Trans.* 1483 (1974).
1382. B. Schupp and H. L. Keller, *Z. Anorg. Allg. Chem.* **625**, 1944 (1999).
1383. R. Fornieris, J. Hiraishi, F. A. Miller, and M. Uehara, *Spectrochim. Acta* **26A**, 581 (1970).
- 1383a. L. Nalbandian and G. N. Papatheodorou, *Vib. Spectrosc.* **4**, 25 (1992).
1384. M. Jansen, G. Schatte, K. M. Tobias, and H. Winner, *Inorg. Chem.* **27**, 1703 (1988).
1385. B. L. Crawford, W. H. Avery, and J. W. Linnett, *J. Chem. Phys.* **6**, 682 (1938).
1386. G. W. Bethke and M. K. Wilson, *J. Chem. Phys.* **26**, 1107 (1957).
1387. D. C. McKean, *Spectrochim. Acta* **48A**, 1335 (1992).
1388. D. A. Dows and R. M. Hexter, *J. Chem. Phys.* **24**, 1029 (1956).
1389. R. G. Snyder and J. C. Decius, *Spectrochim. Acta* **13**, 280 (1959).
1390. W. G. Palmer, *J. Chem. Soc.* 1552 (1961).
1391. S. J. Cyvin, B. N. Cyvin, C. Wibbelmann, R. Becker, W. Brockner, and M. Parnsen, *Z. Naturforsch.* **40a**, 709 (1985).
1392. W. Brockner, L. Ohse, U. Pätzmann, B. Eisenmann, and H. Schäfer, *Z. Naturforsch.* **40a**, 1248 (1985).
1393. K. Buijs, *J. Chem. Phys.* **36**, 861 (1962).
1394. C. A. Evans, K. H. Tan, S. P. Tapper, and M. J. Taylor, *J. Chem. Soc., Dalton Trans.* 988 (1973).

1395. V. Tosa, A. Ashimine, and K. Takeuchi, *J. Mol. Struct.* **410/411**, 411 (1997).
1396. V. Tosa, S. Isomura, Y. Kuga, and K. Takeuchi, *Vib. Spectrosc.* **8**, 45 (1994).
1397. F. Höfler, W. Sawodny, and E. Hengge, *Spectrochim. Acta* **26A**, 819 (1970).
1398. J. E. Griffiths, *Spectrochim. Acta* **25A**, 965 (1969).
1399. G. A. Ozin, *J. Chem. Soc. A* 2952 (1969).
1400. P. R. Bunker, *J. Chem. Phys.* **47**, 718 (1967).
1401. B. H. Freeland, J. H. Hencher, D. G. Tuck, and J. G. Contreras, *Inorg. Chem.* **15**, 2144 (1976).
1402. S. Mohan and M. Baskaran, *Spectrochim. Acta* **46A**, 757 (1990).
1403. C. Aubauer, G. Engelhardt, T. M. Klapötke, H. Nöth, A. Schulz, and M. Warchhold, *Eur. J. Inorg. Chem.* 2245 (2000).
1404. M. H. Abbas and G. Davidson, *Spectrochim. Acta* **50A**, 1153 (1994).
1405. I. Kanesaka, K. Ozaki, and I. Matsuura, *J. Raman Spectrosc.* **26**, 997 (1995).
1406. W. Bues, K. Buchler, and P. Kuhnle, *Z. Anorg. Allg. Chem.* **325**, 8 (1963).
1407. R. G. Brown and S. D. Ross, *Spectrochim. Acta* **28**, 1263 (1972).
1408. I. R. Beattie, T. R. Gilson, and P. J. Jones, *Inorg. Chem.* **35**, 1301 (1996).
1409. J. Roziere, J.-L. Pascal, and A. Potier, *Spectrochim. Acta* **29A**, 169 (1973).
1410. A. Grodzicki and A. Potier, *J. Inorg. Nucl. Chem.* **35**, 61 (1973).
1411. P. Tarte, M. J. Pottier, and A. M. Proces, *Spectrochim. Acta* **29A**, 1017 (1973).
1412. R. Saez-Puche, M. Bijkerk, F. Fernandez, E. J. Baran, and I. L. Botta, *J. Alloys. Compounds* **184**, 25 (1992).
1413. E. J. Baran, C. Cascales, and R. G. Mercader, *Spectrochim. Acta* **56A**, 1277 (2000).
1414. R. M. Wing and K. P. Callahan, *Inorg. Chem.* **8**, 871 (1969).
1415. E. J. Baran, *J. Mol. Struct.* **48**, 441 (1978).
1416. I. R. Beattie and G. A. Ozin, *J. Chem. Soc. A*, 2615 (1969).
1417. J. D. Witt and R. M. Hammaker, *J. Chem. Phys.* **58**, 303 (1973).
1418. A. Hezel and S. D. Ross, *Spectrochim. Acta* **23A**, 1583 (1967).
1419. R. W. Mooney and R. L. Goldsmith, *J. Inorg. Nucl. Chem.* **31**, 933 (1969).
1420. D. Mascherpa-Corral and A. Potier, *J. Inorg. Nucl. Chem.* **38**, 211 (1976).
1421. B. C. Dave and R. S. Czernuszewicz, *Inorg. Chem.* **33**, 847 (1994).
1422. N. Stock, G. D. Stucky, and A. K. Cheetham, *Z. Naturforsch.* **56b**, 359 (2001).
1423. K. Hassler and W. Köll, *J. Organomet. Chem.* **487**, 223 (1995).
1424. A. Simon and H. Richter, *Z. Anorg. Allg. Chem.* **304**, 1 (1960); **315**, 196, (1962).
1425. F. A. Cotton and G. Wilkinson, *Advanced Inorganic Chemistry*, 3rd ed., Wiley, New York, 1972, p. 552.
1426. R. J. H. Clark and M. L. Franks, *J. Am. Chem. Soc.* **97**, 2691 (1975).
1427. P. S. Santos, M. L. A. Temperini, and O. Sala, *Chem. Phys. Lett.* **56**, 148 (1978).
1428. G. Peters and W. Preetz, *Z. Naturforsch.* **34b**, 1767 (1979).
1429. R. J. H. Clark and M. J. Stead, *Inorg. Chem.* **22**, 1214 (1983).
1430. S. D. Conradson, A. P. Sattelberger, and W. H. Woodruff, *J. Am. Chem. Soc.* **110**, 1309 (1988).
1431. W. Preetz, G. Peters, and L. Rudzik, *Z. Naturforsch.* **34b**, 1240 (1979).

1432. W. Preetz and G. Peters, *Z. Naturforsch.* **35b**, 797 (1980).
1433. D. E. Morris, A. P. Sattelberger, and W. H. Woodruff, *J. Am. Chem. Soc.* **108**, 8270 (1986).
1434. W. Preetz, P. Hollmann, G. Thiele, and H. Hillebrecht, *Z. Naturforsch.* **45b**, 1416 (1990).
1435. W. Preetz, G. Peters, and D. Bublitz, *J. Cluster. Sci.* **5**, 83 (1994).
1436. R. F. Dallinger, *J. Am. Chem. Soc.* **107**, 7202 (1985).
1437. J. R. Schoonover, R. F. Dallinger, P. M. Killough, A. P. Sattelberger, and W. H. Woodruff, *Inorg. Chem.* **30**, 1093 (1991).
1438. J. Shamir, S. Schneider, A. Bino, and S. Cohen, *Inorg. Chim. Acta* **111**, 141 (1986).
1439. R. J. Ziegler and W. M. Risen, Jr., *Inorg. Chem.* **11**, 2796 (1972).
1440. J. D. Black, J. T. R. Dunsmuir, I. W. Forrest, and A. P. Lane, *Inorg. Chem.* **14**, 1257 (1975).
1441. A. Wendt and W. Preetz, *Z. Anorg. Allg. Chem.* **619**, 1669 (1993).
1442. H. J. Steinebach and W. Preetz, *Z. Anorg. Allg. Chem.* **530**, 155 (1985).
1443. P. Hollmann, W. Preetz, H. Hillebrecht, and G. Thiele, *Z. Anorg. Allg. Chem.* **611**, 28 (1992).
1444. I. R. Beattie, T. R. Gilson, and G. A. Ozin, *J. Chem. Soc.* 2765 (1968).
1445. S. E. Butler, P. W. Smith, R. Stranger, and I. E. Grey, *Inorg. Chem.* **25**, 4375 (1986).
1446. D. A. Edwards and R. T. Ward, *J. Chem. Soc. A*, 1617 (1970).
1447. R. C. Burns and T. A. O'Donnell, *Inorg. Chem.* **18**, 3081 (1979).
1448. W. Kelm and W. Preetz, *Z. Anorg. Allg. Chem.* **117**, 568 (1989).
1449. A. Wendt and W. Preetz, *Z. Anorg. Allg. Chem.* **620**, 655 (1994).
1450. P. Hollmann and W. Preetz, *Z. Naturforsch.* **47b**, 1115 (1992).
1451. L. H. Jones and S. A. Ekberg, *Spectrochim. Acta* **36A**, 761 (1980).
1452. D. Hartley and M. J. Ware, *J. Chem. Soc., Chem. Commun.* 912 (1967).
1453. D. Bublitz and W. Preetz, *Z. Anorg. Allg. Chem.* **622**, 1107 (1996).
1454. P. Brückner, W. Preetz, and M. Pünjer, *Z. Anorg. Allg. Chem.* **623**, 8 (1997).
1455. D. Bublitz, W. Preetz, and M. K. Simsek, *Z. Anorg. Allg. Chem.* **623**, 1 (1997).
1456. M. Stallmann and W. Preetz, *Z. Anorg. Allg. Chem.* **625**, 567 (1999); **626**, 258 (2000).
1457. P. M. Boorman and B. P. Straughan, *J. Chem. Soc.* 1514 (1966).
1458. R. A. MacKay and R. F. Schneider, *Inorg. Chem.* **7**, 455 (1968).
1459. P. B. Fleming, J. L. Meyer, W. K. Grindstaff, and R. E. McCarley, *Inorg. Chem.* **9**, 1769 (1970).
1460. R. Mattes, *Z. Anorg. Allg. Chem.* **364**, 279 (1969).
1461. P. Caillet, S. Ihmaine, and C. Perrin, *J. Mol. Struct.* **216**, 27 (1990).
1462. F. J. Farrell, V. A. Maroni, and T. G. Spiro, *Inorg. Chem.* **8**, 2638 (1969).
1463. R. Mattes, H. Bierbüsse, and J. Fuchs, *Z. Anorg. Allg. Chem.* **385**, 230 (1971).
1464. H. Hartl, F. Pickhard, F. Emmerling, and C. Röhr, *Z. Anorg. Allg. Chem.* **627**, 2630 (2001).
1465. A. Proust, R. Thouvenot, M. Chaussade, E. Robert, and P. Gouzerh, *Inorg. Chim. Acta* **224**, 81 (1994).
1466. V. A. Maroni and T. G. Spiro, *J. Am. Chem. Soc.* **89**, 45 (1967). *Inorg. Chem.* **7**, 188 (1968).

1467. T. G. Spiro, D. H. Templeton, and A. Zalkin, *Inorg. Chem.* **8**, 856 (1969).
1468. T. G. Spiro, V. A. Maroni, and C. O. Quicksall, *Inorg. Chem.* **8**, 2524 (1969).
1469. C. Sourisseau, V. Rodriguev, S. Jobic, and R. Brec, *J. Raman Spectrosc.* **30**, 1087 (1999).
1470. J. Ellermeier, C. Näther, and W. Bensch, *Inorg. Chem.* **38**, 4601 (1999).
1471. J. Server-Carrio, J. Bas-Serra, M. E. González-Núñez, A. Garcia-Gastaldi, G. B. Jameson, L. C. W. Baker, and R. Acerete, *J. Am. Chem. Soc.* **121**, 977 (1999).
1472. A. Müller, E. Krickemeyer, H. Bogge, M. Schidotmann, and F. Peters, *Angew. Chem. Int. Ed.* **37**, 3360 (1998).
1473. W. Weltner, Jr. and J. R. W. Warn, *J. Chem. Phys.* **37**, 292 (1962).
1474. L. R. Beattie, P. J. Jones, D. J. Wild, and T. R. Gilson, *J. Chem. Soc., Dalton Trans.* 267 (1987).
1475. A. Karthikeyan, C. A. Martindale, and S. W. Martin, *Inorg. Chem.* **41**, 622 (2002).
1476. A. Kaldor and R. F. Porter, *Inorg. Chem.* **10**, 775 (1971).
1477. J. R. Durig, W. H. Green, and A. L. Marston, *J. Mol. Struct.* **2**, 19 (1968).
1478. J. L. Parsons, *J. Chem. Phys.* **33**, 1860 (1960).
1479. F. A. Grimm and R. F. Porter, *Inorg. Chem.* **8**, 731 (1969).
1480. J. D. Carpenter and B. S. Ault, *J. Phys. Chem.* **96**, 7913 (1992).
1481. R. J. M. Konings, A. S. Booiij, and E. H. P. Cordfunke, *J. Mol. Spectrosc.* **145**, 451 (1991).
1482. B. Tian, G. Wu, and R. Xu, *Spectrochim. Acta* **43A**, 65 (1987).
1483. P. Ney, M. D. Fontana, A. Maillard, and K. Polgar, *J. Phys. Condens. Matter* **10**, 673 (1998).
1484. W. Bues, G. Foerster, and R. Schmitt, *Z. Anorg. Allg. Chem.* **344**, 148 (1966).
1485. F. R. Brown, F. A. Miller, and C. Sourisseau, *Spectrochim. Acta* **32A**, 125 (1976).
1486. J. Thesing, J. Baurmeister, W. Preetz, D. Thiery, and H. G. von Schnering, *Z. Naturforsch.* **46b**, 800 (1991).
1487. W. Preetz and J. Fritze, *Z. Naturforsch.* **39b**, 1472 (1984).
1488. J. Thesing, W. Preetz, and J. Baurmeister, *Z. Naturforsch.* **46b**, 19 (1991).
1489. J. Thesing, M. Stallbaum, and W. Preetz, *Z. Naturforsch.* **46b**, 602 (1991).
1490. V. Lorenzen, W. Preetz, F. Baumann, and W. Kaim, *Inorg. Chem.* **37**, 4011 (1998).
1491. L. A. Leites, S. S. Bukalov, A. P. Kurbakova, M. M. Kaganski, Yu. L. Gaft, N. T. Kuznetsov, and I. A. Zakharova, *Spectrochim. Acta* **38A**, 1047 (1982).
1492. S. J. Cyvin, B. N. Cyvin, and T. Mogstad, *Spectrochim. Acta* **42A**, 985 (1986).
1493. V. F. Kalasinsky, *J. Phys. Chem.* **83**, 3239 (1979).
1494. W. E. Keller and H. L. Johnson, *J. Chem. Phys.* **20**, 1749 (1952).
1495. Y. Matsui and R. C. Taylor, *Spectrochim. Acta* **45A**, 299 (1989).
1496. B. Steuer, G. Peters, and W. Preetz, *Inorg. Chim. Acta* **289**, 70 (1999).
1497. W. Preetz and G. Peters, *Eur. J. Inorg. Chem.* 1831 (1999).
1498. J. Fritze and W. Preetz, *Z. Naturforsch.* **42B**, 293 (1987).
- 1498a. A. J. Downs, T. M. Greene, E. Johnsen, P. T. Brain, C. A. Morrison, S. Parsons, C. R. Pulham, D. W. H. Rankin, K. Aarset, I. M. Mills, E. M. Page, and D. A. Rice, *Inorg. Chem.* **40**, 3484 (2001).
1499. B. Roussel, A. Chapput, and G. Fleury, *J. Mol. Struct.* **31**, 371 (1976).

1500. K. E. Buck, K. Niedenzo, W. Sawodny, T. Takasuka, T. Totani, and H. Watanabe, *Inorg. Chem.* **10**, 1133 (1971).
1501. B. E. Smith, H. F. Shurvell, and B. D. James, *J. Chem. Soc., Dalton Trans.* 711 (1978).
1502. R. T. Paine, R. W. Light, and M. Nelson, *Spectrochim. Acta* **35A**, 213 (1979).
1503. A. G. Csaszar, L. Hedberg, K. Hedberg, R. C. Burns, A. T. Wen, and M. J. McGlinchey, *Inorg. Chem.* **30**, 1371 (1991).
1504. C. J. Dain, A. J. Downs, M. J. Goode, D. G. Evans, K. T. Nicholls, D. W. H. Rankin, and H. E. Robertson, *J. Chem. Soc., Dalton Trans.* 967 (1991).
1505. W. J. Lehmann and I. Shapiro, *Spectrochim. Acta* **17**, 396 (1961).
1506. L. J. Bellamy, W. Gerrard, M. F. Lappert, and R. L. Williams, *J. Chem. Soc.* 2412 (1958).
1507. A. Meller, *Organomet. Chem. Rev.* **2**, 1 (1967).
1508. J. G. Verkade, *Coord. Chem. Rev.* **9**, 1 (1972).
1509. W. Weltner, Jr. and R. J. Van Zee, *Chem. Rev.* **89**, 1713 (1989).
1510. I. Cermak, M. Förderer, I. Cermakova, S. Kalhofer, H. Stopka-Ebeler, G. Monninger, and W. Krätschmer, *J. Chem. Phys.* **108**, 10129 (1998).
1511. A. M. Smith, J. Agreiter, C. Engel, and V. E. Bondybey, *Chem. Phys. Lett.* **207**, 531 (1993).
1512. N. Moazzen-Ahmadi and A. R. W. McKellar, *J. Chem. Phys.* **98**, 7757 (1993).
1513. P. A. Withey, L. N. Shen, and W. R. M. Graham, *J. Chem. Phys.* **95**, 820 (1991).
1514. L. N. Shen, P. A. Withey, and W. R. M. Graham, *J. Chem. Phys.* **94**, 2395 (1991).
1515. N. Moazzen-Ahmadi, J. J. Thong, and A. R. W. McKellar, *J. Chem. Phys.* **100**, 4033 (1994).
1516. M. Vala, T. M. Chandrasekhar, J. Szczepanski, R. J. van Zee, and W. Weltner, Jr., *J. Chem. Phys.* **90**, 595 (1989).
1517. J. Szczepanski and M. Vala, *J. Phys. Chem.* **95**, 2792 (1991).
1518. N. Moazzen-Ahmedi, A. R. W. McKellar, and T. Amano, *J. Chem. Phys.* **91**, 2140 (1989).
1519. J. R. Heath, A. L. Cooksy, M. H. W. Gruebele, C. A. Schuttenmaier, and R. J. Saykally, *Science* **244**, 564 (1989).
1520. N. Moazzen-Ahamadi, S. D. Flett, and A. R. W. McKellar, *Chem. Phys. Lett.* **186**, 291 (1991).
- 1520a. R. H. Kranze and W. R. M. Graham, *J. Chem. Phys.* **98**, 71 (1993).
1521. S. L. Wang, C. M. L. Rittby, and W. R. M. Graham, *J. Chem. Phys.* **107**, 6032 (1997).
1522. J. D. Presilla-Marquez, J. A. Sheehy, J. D. Mills, P. G. Carrick, and C. W. Larson, *Chem. Phys. Lett.* **274**, 439 (1997).
1523. R. H. Kranze, C. M. L. Rittby, and W. R. M. Graham, *J. Chem. Phys.* **105**, 5313 (1996).
1524. J. Szczepanski, S. Ekern, C. Chapo, and M. Vala, *Chem. Phys.* **211**, 359 (1996).
1525. R. H. Kranze, P. A. Withey, C. M. L. Rittby, and W. R. M. Graham, *J. Chem. Phys.* **103**, 6841 (1995).
1526. L. Lapinski and M. Vala, *Chem. Phys. Lett.* **300**, 195 (1999).
1527. T. F. Giesen, A. van Orden, H. J. Hwang, R. S. Fellers, R. A. Provencal, and R. J. Saykally, *Science* **265**, 756 (1994).
1528. M. Vala, Y. M. Chandrasekhar, J. Szczepanski, and R. Pellow, *J. Mol. Struct.* **222**, 209 (1990).

1529. G. A. Rechsteiner, C. Felix, A. K. Ott, O. Hampe, R. P. van Duyne, M. F. Jarrold, and K. Raghavachari, *J. Phys. Chem. A*, **105**, 3029 (2001).
1530. A. K. Ott, G. A. Rechsteiner, C. Felix, O. Hampe, M. F. Jarrold, and R. P. van Duyne, *J. Chem. Phys.* **109**, 9652 (1998).
1531. J. Szczepanski, S. Ekern, and M. Vala, *J. Phys. Chem. A* **101**, 1841 (1997).
1532. J. Szczepanski, M. Vala, L. N. Shen, P. A. Withey, and W. R. M. Graham, *J. Phys. Chem. A* **101**, 8788 (1997).
1533. J. Szczepanski, E. Auerbach, and M. Vala, *J. Phys. Chem. A* **101**, 9296 (1997).
1534. P. Freivogel, M. Grutter, D. Forney, and J. P. Maier, *J. Chem. Phys.* **107**, 4468 (1997).
1535. H. W. Kroto, J. R. Heath, S. C. O'Brien, R. F. Curl, and R. E. Smalley, *Nature* **318**, 162 (1985).
1536. H. W. Kroto, J. E. Fischer, and D. E. Cox, *The Fullerenes*, Pergamon Press, Oxford, UK, 1993.
1537. M. S. Dresselhaus, G. Dresselhaus, and P. C. Eklund, *Science of Fullerenes and Carbon Nanotubes*, Academic Press, San Diego, CA, 1996.
1538. E. J. Maggio, "Bouncing Balls of Carbon: The Discovery and Promise of Fullerenes," in *A Positron Named Priscilla*, National Academy Press, Washington, DC, 1994.
1539. K. Nakamoto and M. A. McKinney, *J. Chem. Educ.* **77**, 775 (2000).
1540. R. E. Stanton and M. D. Newton, *J. Phys. Chem.* **92**, 2141 (1988).
1541. J. P. Hare, T. J. Dennis, H. W. Kroto, R. Taylor, A. W. Allaf, S. Balm, and D. R. Walton, *J. Chem. Soc., Chem. Commun.* 412 (1991).
1542. C. I. Frum, R. Engleman, Jr., H. G. Hedderich, P. F. Bernath, L. D. Lamb, and D. R. Huffman, *Chem. Phys. Lett.* **176**, 504 (1991).
1543. P. H. M. van Loosdrecht, P. J. M. van Bentum, M. A. Verheijen, and G. Meijer, *Chem. Phys. Lett.* **198**, 587 (1992).
1544. S. H. Gallagher, R. S. Armstrong, W. A. Clucas, P. A. Lay, and C. A. Reed, *J. Phys. Chem. A*, **101**, 2960 (1997).
1545. R. L. Garrell, T. M. Herne, C. A. Szafrabski, F. Diederich, F. Ettl, and R. L. Whetten, *J. Am. Chem. Soc.* **113**, 6302 (1991).
1546. R. E. Stanton and M. D. Newton, *J. Phys. Chem.* **92**, 2141 (1988).
1547. D. A. Dixon, B. E. Chase, G. Fitzgerald, and N. Matsuzawa, *J. Phys. Chem.* **99**, 4486 (1995).
1548. S. Guha, J. Menendez, J. B. Page, G. B. Adams, G. S. Spencer, J. P. Lehman, P. Giannozzi, and S. Baroni, *Phys. Rev. Lett.* **72**, 3359 (1994).
1549. S. Guha and K. Nakamoto, *Coord. Chem. Rev.* **249**, 1111 (2005).
1550. P. Zhou, K. A. Wang, A. M. Rao, P. C. Eklund, G. Dresselhaus, and M. S. Dresselhaus, *Phys. Rev.* **B45**, 10838 (1992).
1551. P. C. Eklund, P. Zhou, K.-A. Wang, G. Dresselhaus, and M. S. Dresselhaus, *J. Phys. Chem. Solids* **53**, 1391 (1992).
1552. C. H. Choi, M. Kertesz, and L. Mihaly, *J. Phys. Chem. A* **104**, 102 (2000).
1553. F. N. Tebbe, R. L. Harlow, D. B. Chase, D. L. Thorn, G. C. Campbell, Jr., J. C. Calabrese, N. Herron, R. J. Young, and E. Wasserman, *Science* **256**, 822 (1992).
1554. P. R. Birkett, H. W. Kroto, R. Taylor, D. R. M. Walton, R. Ian Grose, P. J. Hendra, and P. W. Fowler, *Chem. Phys. Lett.* **205**, 399 (1993).

1555. K. Esfarjani, Y. Hashi, J. Onoe, K. Takeuchi, and Y. Kawazoe, *Phys. Rev. B* **57**, 223 (1998).
1556. J. Onoe and K. Takeuchi, *Phys. Rev. B* **54**, 6167 (1996).
1557. G. B. Adams, J. B. Page, O. F. Sankey, and M. O'Keeffe, *Phys. Rev. B* **50**, 17471 (1994).
1558. P. J. Fagan, J. C. Calabrese, and B. Malone, *Science* **252**, 1160 (1991).
- 1558a. B. Chase and P. J. Fagan, *J. Am. Chem. Soc.* **114**, 2252 (1992).
1559. D. S. Bethune, G. Meijer, W. C. Tang, H. J. Rosen, W. G. Golden, H. Seki, C. A. Brown, and M. S. de Vries, *Chem. Phys. Lett.* **179**, 181 (1991).
1560. R. A. Jishi, M. S. Dresselhaus, D. Dresselhaus, K.-A. Wang, P. Zhou, A. M. Rao, and P. C. Eklund, *Chem. Phys. Lett.* **206**, 187 (1993).
1561. S. H. Gallagher, R. S. Armstrong, P. A. Lay, and C. A. Reed, *Chem. Phys. Lett.* **234**, 245 (1995).
1562. Z. Slanina, J. M. Rudziński, M. Togashi, and E. Osawa, *J. Mol. Struct. (Thermochem.)* **202**, 169 (1989).
1563. G. Klepp, F. Borondics, Z. Gillay, N. Kamaras, and L. Forro, *Ferroelectrics* **249**, 117 (2001).
1564. S. Lebedkin, W. E. Hull, A. Soldatov, B. Renker, and M. M. Kappes, *J. Phys. Chem. B* **104**, 4101 (2000).
1565. D. E. Manolopoulos and P. W. Fowler, *J. Chem. Phys.* **96**, 7603 (1992).
1566. T. J. S. Dennis, M. Hulman, K. Kuzmany, and H. Shinohara, *J. Phys. Chem. B* **104**, 5411 (2000).
1567. Y. Yamamoto, M. Saunders, A. Khong, R. J. Cross, Jr., M. Grayson, M. L. Gross, A. F. Benedetto, and R. B. Weisman, *J. Am. Chem. Soc.* **121**, 1591 (1999).
1568. H. Jantoljak, N. Krawez, I. Loa, R. Tellmann, E. E. B. Campbell, A. P. Litvinchuk, and C. Thomsen, *Z. Phys. Chem. (Munich.)* **200**, 157 (1997).
1569. P. Kuran, M. Krause, A. Bartl, and L. Dunsch, *Chem. Phys. Lett.* **292**, 580 (1998).
1570. K. Kobayashi, S. Nagase, and T. Akasaka, *Chem. Phys. Lett.* **261**, 502 (1996).
1571. S. Stevenson, P. W. Fowler, T. Heine, J. C. Duchamp, G. Rice, T. Glass, K. Harich, E. Hajdu, R. Bible, and H. C. Dorn, *Nature* **408**, 427 (2000).
1572. M. Krause, H. Kuzmany, P. Georgi, L. Dunsch, K. Vietze, and G. Seifert, *J. Chem. Phys.* **115**, 6596 (2001).
1573. J. M. Campanera, C. Bo, M. M. Olmstead, A. L. Balch, and J. M. Poblet, *J. Phys. Chem. A* **106**, 12356 (2002).
1574. K. Kobayashi, Y. Sano, and S. Nagase, *J. Comput. Chem.* **22**, 1353 (2001).
1575. M. Inakuma, E. Yamamoto, T. Kai, C.-R. Wang, T. Tomiyama, H. Shinohara, T. J. S. Dennis, M. Hulman, M. Krause, and H. Kuzmany, *J. Phys. Chem. B* **104**, 5072 (2000).
- 1575a. M. Krause, M. Hulman, H. Kuzmany, T. J. S. Dennis, M. Inakuma, and H. Shinohara, *J. Chem. Phys.* **111**, 7976 (1999).
1576. R. Saito, G. Dresselhaus, and M. S. Dresselhaus, *Physical Properties of Carbon Nanotubes*, Imperial College Press, London, 1998.
1577. A. M. Rao, E. Richter, S. Bandow, B. Chase, P. C. Eklund, K. A. Williams, S. Fang, K. B. Subbaswamy, M. Menon, A. Thess, R. E. Smalley, G. Dresselhaus, and M. S. Dresselhaus, *Science* **275**, 187 (1997).

- 1577a. S. Bandow, S. Asaka, Y. Saito, A. M. Rao, L. Grigorian, E. Richter, and P. C. Eklund, *Phys. Rev. Lett.* **80**, 3779 (1998).
1578. J. C. Decius and R. M. Hester, *Molecular Vibrations in Crystals*, McGraw-Hill, New York, 1977, p. 114.
1579. D. S. Knight and W. B. White, *J. Mater. Res.* **4**, 385 (1989).
1580. J. R. Ferraro, *Vibrational Spectroscopy at High External Pressures*, Academic Press, New York, 1984.
1581. A. Tardieu, F. Cansell, and J. P. Petitet, *J. Appl. Phys.* **68**, 3243 (1990).
1582. E. R. Lippincott, F. E. Welsh, and C. E. Weir, *Anal. Chem.* **33**, 137 (1961).
1583. X. X. Bi, P. C. Eklund, J. G. Zhang, A. M. Rao, T. A. Perry, and C. P. Beetz, Jr., *J. Mater. Res.* **5**, 811 (1990).
1584. I. Kiflawi, D. Fisher, H. Kanda, and G. Sittas, *Diamond Relat. Mater.* **5**, 1516 (1996).
1585. W. G. Fateley, F. R. Dollish, N. T. McDevitt, and F. F. Bentley, *Infrared and Raman Selection Rules for Molecular and Lattice Vibrations*, Wiley-Interscience, New York, 1972, p. 163.
1586. F. Tuinstra and J. L. Koenig, *J. Chem. Phys.* **53**, 1126 (1970).
1587. K. Omori, *Sci. Rep. Tohoku. Univ. Ser. 3* **1**, 102 (1961).
1588. J. W. Huang and W. R. M. Graham, *J. Chem. Phys.* **93**, 1583 (1990).
1589. L. N. Shen, T. J. Doyle, and W. R. M. Graham, *J. Chem. Phys.* **93**, 1597 (1990).
- 1589a. J. D. Presilla-Márquez, P. G. Carrick, and C. W. Larson, *J. Chem. Phys.* **110**, 5702 (1999).
1590. P. Botschwina and H. P. Reisenauer, *Chem. Phys. Lett.* **183**, 217 (1991).
1591. R. D. Brown, D. E. Pullin, E. H. N. Rice, and M. Rodler, *J. Am. Chem. Soc.* **107**, 7877 (1985).
1592. W. H. Weber, P. D. Maker, and C. W. Peters, *J. Chem. Phys.* **64**, 2149 (1976).
1593. G. Maier, H. P. Reisenauer, H. Balli, W. Brandt, and R. Janoschek, *Angew. Chem. Int. Ed.* **29**, 905 (1990).
1594. G. Maier, H. P. Reisenauer, U. Schafer, and H. Balli, *Angew. Chem. Int. Ed.* **27**, 566 (1988).
1595. J. B. Bates and W. H. Smith, *Chem. Phys. Lett.* **14**, 362 (1972).
1596. H. W. Kroto and D. McNaughton, *J. Mol. Spectrosc.* **114**, 473 (1985).
1597. E. Suzuki and F. Watari, *Chem. Phys. Lett.* **168**, 1 (1990).
1598. E. Suzuki and F. Watari, *Spectrochim. Acta* **51A**, 779 (1995).
1599. D.-L. Joo, D. J. Clouthier, C. P. Chan, V. W.-M. Lai, E. S. F. Ma, and A. J. Merer, *J. Mol. Spectrosc.* **171**, 113 (1995).
1600. F. Holland and M. Winnewisser, *J. Mol. Spectrosc.* **149**, 45 (1991).
1601. F. Holland, M. Winnewisser, and J. W. Johns, *Can. J. Phys.* **68**, 435 (1990).
1602. J. Szczepanski, R. Hodyss, J. Fuller, and M. Vala, *J. Phys. Chem. A* **103**, 2975 (1999).
1603. R. West, D. Eggerding, J. Perkins, D. Handy, and E. C. Tuazon, *J. Am. Chem. Soc.* **101**, 1710 (1979).
1604. M. Ito and R. West, *J. Am. Chem. Soc.* **85**, 2580 (1963).
1605. H. Torii, M. Tasumi, I. M. Bell, and R. J. H. Clark, *Chem. Phys.* **216**, 67 (1997).
1606. M. J. Taylor, P. N. Gates, and P. M. Smith, *Spectrochim. Acta* **48A**, 205 (1992).

1607. K. W. Hipps and A. T. Aplin, *J. Phys. Chem.* **89**, 5459 (1985).
1608. D. Christen, H. G. Mack, C. J. Marsden, H. Oberhammer, G. Schatte, K. Seppelt, and R. Willner, *J. Am. Chem. Soc.* **109**, 4009 (1987).
1609. R. Minkwitz and A. Werner, *J. Fluorine. Chem.* **39**, 141 (1988).
1610. C. O. Della Vedova, and P. J. Aymonino, *J. Raman. Spectrosc.* **17**, 485 (1986).
1611. E. C. Honea, A. Ogura, C. A. Murray, K. Raghavachari, W. O. Sprenger, M. F. Jarrold, and W. L. Brown, *Nature* **366**, 42 (1993).
1612. S. Li, R. J. van Zee, W. Weltner, and K. Raghavachari, *Chem. Phys. Lett.* **243**, 275 (1995).
1613. G. Kliche, M. Schwarz, and H. G. von Schnering, *Angew. Chem. Int. Ed.* **26**, 349 (1987).
1614. A. van Orden, R. A. Provençal, T. F. Giesen, and R. J. Saykally, *Chem. Phys. Lett.* **237**, 77 (1995).
1615. J. D. Presilla-Marquez, S. C. Gay, C. M. L. Rittby, and W. R. M. Graham, *J. Chem. Phys.* **102**, 6354 (1995).
1616. J. D. Presilla-Marquez and W. R. M. Graham, *J. Chem. Phys.* **100**, 181 (1994).
1617. J. D. Presilla-Marquez and W. R. M. Graham, *J. Chem. Phys.* **96**, 6509 (1992).
1618. J. D. Presilla-Marquez, C. M. L. Rittby, and W. R. M. Graham, *J. Chem. Phys.* **104**, 2818 (1996).
1619. F. Höfler, G. Bauer, and E. Hengge, *Spectrochim. Acta* **32A**, 1435 (1976).
1620. K. Hassler, E. Hengge, and D. Kovar, *Spectrochim. Acta* **34A**, 1193 (1978).
1621. B. Albinsson, H. Teramae, H. S. Plitt, L. M. Goss, H. Schdbaur, and J. Michl, *J. Phys. Chem.* **100**, 8681 (1996).
1622. V. N. Khabashesku, K. N. Kuudin, and J. L. Margrave, *J. Mol. Struct.* **443**, 175 (1998).
1623. N. Wiberg, W. Niedermayer, G. Fischer, H. Nöth, and M. Suter, *Eur. J. Inorg. Chem.* 1066 (2002).
1624. R. Zink, T. F. Maguera, and J. Michl, *J. Phys. Chem. A* **104**, 3829 (2000).
1625. H. Fleischer, K. Hensen, D. Burgdorf, E. Flindt, U. Wannagat, H. Bürger, and G. Pawelke, *Z. Anorg. Allg. Chem.* **621**, 239 (1995).
1626. J. Gnado and P. Dhamelincourt, *J. Raman. Spectrosc.* **24**, 63 (1993).
1627. F. A. Miller, J. Perkins, G. A. Gibbon, and B. A. Swisshelm, *J. Raman. Spectrosc.* **2**, 93 (1974).
1628. J. R. Durig, M. J. Flanagan, and V. F. Kalasinsky, *J. Chem. Phys.* **66**, 2775 (1977).
1629. J. R. Durig, M. J. Flanagan, and V. F. Kalasinsky, *Spectrochim. Acta* **34A**, 63 (1978).
1630. J. R. Durig, Y. S. Li, M. M. Chen, and J. D. Odom, *J. Mol. pectrosc.* **59**, 74 (1976).
1631. J. R. Durig, K. S. Kalasinsky, and V. F. Kalasinsky, *J. Mol. Struct.* **35**, 201 (1976).
1632. K. Hamada, *J. Mol. Struct.* **48**, 191 (1978).
1633. F. Höfler and W. Peter, *Z. Naturforsch.* **30b**, 282 (1975).
1634. M. Friesen, M. Junker, A. Zumbusch, and H. Schnöckel, *J. Chem. Phys.* **111**, 7881 (1999).
1635. M. Sitarz, M. Handke, W. Mozgawa, E. Galuskin, and I. Galuskina, *J. Mol. Struct.* **555**, 357 (2000).
1636. C. Marcolli, P. Laine, R. Buhler, G. Calzaferri, and J. Tomkinson, *J. Phys. Chem. B.* **101**, 1171 (1997).

1637. I. S. Ignat'ev, A. N. Lazarev, T. F. Tenisheva, and B. F. Shechegolev, *J. Mol. Struct.* **244**, 193 (1991).
1638. M. G. M. van der Vis, R. J. M. Konings, A. Oskam, and T. L. Snoeck, *J. Mol. Struct.* **274**, 47 (1992).
1639. J. Dong, L. Miao, and M. Zhou, *Chem. Phys. Lett.* **355**, 31 (2002).
1640. J. Etchepare, *Spectrochim. Acta* **26A**, 2147 (1970).
1641. P. McMillan, *Am. Mineral.* **69**, 622 (1984).
1642. P. K. Dutta and B. Del Barco, *J. Chem. Soc., Chem. Commun.* 1297 (1985).
1643. A. N. Lazarev, *Vibrational Spectra and Structure of Silicates*, Consultants Bureau, New York, 1972.
1644. R. A. Condrate, *J. Non.-Cryst. Solids* **84**, 26 (1986).
1645. R. A. Condrate, "The infrared and Raman Spectra of Glasses," in L. D. Pye, H. J. Stevens, and W. C. LaCourse, eds., *Introduction to Glass Science*, Plenum Press, New York, 1972.
1646. R. K. Sato and P. F. McMillan, *J. Phys. Chem.* **91**, 3494 (1987).
1647. J. B. Bates and A. S. Quist, *J. Chem. Phys.* **56**, 1528 (1972).
1648. A. L. Smith, *Spectrochim. Acta* **16**, 87 (1960).
1649. B. J. Aylett, *Adv. Inorg. Chem. Radiochem.* **11**, 262 (1968).
1650. H. J. Campbell-Ferguson and E. A. V. Ebsworth, *J. Chem. Soc. A*, 705 (1967).
1651. J. Curda, W. Carrillo-Cabrera, A. Schmeding, K. Pevters, M. Somer, and H. G. von Schnering, *Z. Anorg. Allg. Chem.* **623**, 929 (1997).
1652. J. Campbell and G. J. Schrobilgen, *Inorg. Chem.* **36**, 4078 (1997).
1653. M. Somer, W. Carrillo-Cabrera, E. M. Peters, K. Peters, and H. G. von Schnering, *Z. Anorg. Allg. Chem.* **624**, 1915 (1998).
1654. E. A. V. Ebsworth, D. W. H. Rankin, and G. M. Sheldrick, *J. Chem. Soc. A*, 2828 (1968).
1655. S. Pohl and B. Krebs, *Z. Anorg. Allg. Chem.* **424**, 265 (1876).
1656. M. Somer, W. Carrillo-Cabrera, E. M. Peters, K. Peters, M. Kaupp, and H. G. von Schnering, *Z. Anorg. Allg. Chem.* **625**, 37 (1999).
1657. H. Borrmann, J. Campbell, D. A. Dixon, H. P. A. Mercier, A. M. Pirani, and G. J. Schrobilgen, *Inorg. Chem.* **37**, 6656 (1998).
1658. H. Schumann, *Angew. Chem. Int. Ed.* **8**, 937 (1969).
1659. C. H. Bibart and G. E. Ewing, *J. Chem. Phys.* **61**, 1293 (1974).
1660. E. L. Varetta and G. C. Pimentel, *J. Chem. Phys.* **55**, 3813 (1971).
1661. X. Wang and O.-Z. Qin, *Spectrochim. Acta* **54A**, 575 (1998).
1662. C.-I. Lee, Y.-P. Lee, X. Wang, and Q.-Z. Qin, *J. Chem. Phys.* **109**, 10446 (1998).
1663. G. R. Smith and W. A. Guillory, *J. Mol. Spectrosc.* **68**, 223 (1977).
1664. A. Givan and A. Loewenschuss, *J. Chem. Phys.* **93**, 866 (1990).
1665. A. Givan and A. Loewenschuss, *J. Chem. Phys.* **94**, 7562 (1991).
1666. L. Bencivenni, N. Sanna, I. Schriver-Mazzuoli, and A. Schriver, *J. Chem. Phys.* **104**, 7836 (1996).
1667. T. M. Klapötke, A. Schutz, and I. C. Tornieporth-Oetting, *Chem. Ber.* **127**, 2181 (1994).
1668. E. J. Sluys and B. J. van der Veken, *J. Mol. Struct.* **320**, 249 (1994).
1669. A. Stirling, I. Pápai, and J. Mink, *J. Chem. Phys.* **100**, 2910 (1994).

1670. I. Pápai and A. Stirling, *Chem. Phys. Lett.* **253**, 196 (1996).
1671. T. Bremm and M. Jansen, *Z. Naturforsch* **46b**, 1031 (1991); *Z. Anorg. Allg. Chem.* **608**, 49 (1992).
1672. L. K. Keefer, J. L. Flippen-Anderson, C. George, A. P. Shanklin, T. M. Dunama, D. Christodoulou, J. E. Saavedra, E. S. Sagan, and D. S. Bohle, *Nitric Oxide* **5**, 377 (2001).
1673. H. R. Hunt, J. R. Cox, and J. D. Ray, *Inorg. Chem.* **1**, 938 (1962).
1674. K. O. Christe, W. W. Wilson, M. A. Petrie, H. H. Michels, J. C. Bottaro, and R. Gilardi, *Inorg. Chem.* **35**, 5068 (1996).
1675. J. Laane and J. R. Ohlsen, *Prog. Inorg. Chem.* **27**, 465 (1980).
1676. K. O. Christe and C. J. Schack, *Inorg. Chem.* **17**, 2749 (1978).
1677. H. Bürger, H. Niepel, G. Pawelke, and H. Oberhammer, *J. Mol. Struct.* **54**, 159 (1979).
1678. C. O. Della Vedova, S. E. Ulic, A. Ben Altabef, and P. J. Aymonino, *Z. Phys. Chem.* **268**, 445 (1987).
1679. D. Tevautt and R. R. Smardzewski, *J. Phys. Chem.* **82**, 375 (1978).
1680. W. W. Wilson and K. O. Christe, *Inorg. Chem.* **26**, 1573 (1987).
1681. J. R. Durig, G. A. Guirgis, and K. A. Krutules, *J. Mol. Struct.* **328**, 55 (1994).
1682. R. Kopitzky, H. Willner, H.-G. Mack, A. Pfeiffer, and H. Oberhammer, *Inorg. Chem.* **37**, 6208 (1998).
1683. G. Pawelke, R. Dammel, and W. Pull, *Z. Naturforsch.* **47b**, 351 (1992).
1684. R. Minkwitz, W. Meckstroth, and H. Preut, *Z. Anorg. Allg. Chem.* **617**, 136 (1992).
1685. R. R. Friedl, S. P. Sander, and Y. L. Yung, *J. Phys. Chem.* **96**, 7490 (1992).
1686. J. R. Durig, G. A. Guirgis, and K. A. Krutules, *J. Mol. Struct.* **354**, 1 (1995).
1687. M. C. L. Gerry, W. Lewis-Bevan, A. J. Merer, and N. P. C. Westwood, *J. Mol. Spectrosc.* **110**, 153 (1985).
1688. M. Birk and W. Winnewisser, *Chem. Phys. Lett.* **123**, 382 (1986).
1689. M. Nonella, R. P. Müller, and J. R. Huber, *J. Mol. Spectrosc.* **112**, 142 (1985).
1690. R. Withnall and L. Andrews, *J. Phys. Chem.* **92**, 2155 (1988).
1691. D. L. Frasco and E. L. Wagner, *J. Chem. Phys.* **30**, 1124 (1959).
1692. K. O. Christie, W. W. Wilson, D. A. Dixon, S. I. Khan, R. Bau, T. Metzenthin, and R. Lu, *J. Am. Chem. Soc.* **115**, 1836 (1993).
1693. T. Chivers and I. Drummond, *Inorg. Chem.* **13**, 1222 (1974).
- 1693a. W. V. F. Brooks, T. S. Cameron, S. Parsons, J. Passmore, and M. J. Schriver, *Inorg. Chem.* **33**, 6230 (1994).
- 1693b. A. Maaninen, J. Silviri, R. J. Suontamo, J. Konu, R. S. Laitinen, and T. Chivers, *Inorg. Chem.* **36**, 2170 (1997).
1694. J. Bojes, T. Chivers, W. G. Laidlaw, and M. Trsic, *J. Am. Chem. Soc.* **101**, 4517 (1979).
1695. I. Nevitt, H. S. Rzepa, and J. D. Woollins, *Spectrochim. Acta* **45A**, 367 (1989).
1696. R. Steudel, *Z. Naturforsch.* **36a**, 850 (1981).
1697. A. Turowski, R. Appel, W. Sawodny, and K. Molt, *J. Mol. Struct.* **48**, 313 (1978).
1698. J. Adel, C. Ergezinger, R. Figge, and K. Dehnicke, *Z. Naturforsch.* **43b**, 639 (1988).
1699. P. K. Gowik and T. M. Klapötke, *Spectrochim. Acta* **46A**, 1371 (1990).

1700. U. Patt-Siebel, S. Ruangsuttinarupap, U. Müller, J. Pebler, and K. Dehnicke, *Z. Naturforsch.* **41b**, 1191 (1986).
1701. R. S. M. Alvaréz, E. H. Cutin, C. O. Della Védova, R. Mews, R. Haist, and H. Oberhammer, *Inorg. Chem.* **40**, 5188 (2001).
1702. D. E. C. Corbridge, *The Structural Chemistry of Phosphors*, Elsevier, Amsterdam, 1974.
1703. L. C. Thomas, *Interpretation of the Infrared Spectra of Organophosphorus Compounds*, Heyden, London, 1974.
1704. L. C. Thomas and R. A. Chittenden, *Spectrochim. Acta* **26A**, 781 (1970).
1705. J. Goubeau, *Pure Appl. Chem.* **44**, 393 (1975).
1706. I. Krossing, *J. Am. Chem. Soc.* **123**, 4603 (2001).
1707. M. Baudler, S. Akapoglu, D. Ouzounis, F. Wasgestian, B. Meinigke, H. Budzikiewicz, and H. Münster, *Angew. Chem. Int. Ed.* **27**, 280 (1988).
1708. H. G. von Schnering, T. Meyer, W. Hoenle, W. Schmettow, U. Hinze, W. Bauhofer, and G. Kliche, *Z. Anorg. Allg. Chem.* **553**, 261 (1987).
1709. C. Hadenfeldt and K. Hödel, *Z. Anorg. Allg. Chem.* **622**, 1495 (1996).
1710. H. G. von Schnering, M. Somer, G. Kliche, W. Hönle, T. Meyer, J. Wolf, L. Ohse, and P. B. Kempa, *Z. Anorg. Allg. Chem.* **601**, 13 (1991).
1711. Z. Mielke, M. McCluskey, and L. Andrews, *Chem. Phys. Lett.* **165**, 146 (1990).
1712. R. J. M. Konings, E. H. P. Cordfunke, and A. S. Booi, *J. Mol. Spectrosc.* **152**, 29 (1992).
1713. W. P. Griffith and K. J. Rutt, *J. Chem. Soc. A*, 2331 (1968).
1714. N. Santha and V. U. Nayar, *J. Raman Spectrosc.* **21**, 517 (1990).
1715. G. Fomakoye, R. Cahay, and P. Tarte, *Spectrochim. Acta* **46A**, 1245 (1990).
1716. X. Mathew and V. U. Nayar, *J. Raman Spectrosc.* **20**, 633 (1989).
1717. C. I. Cabello and E. J. Baran, *Spectrochim. Acta* **41A**, 1359 (1985).
1718. M. Bagieu-Beucher, A. Durif, and I. C. Guitel, *J. Solid State Chem.* **45**, 159 (1982).
1719. A. R. S. Valentim, B. Engels, S. D. Peyerimhoff, A. Tellenbach, I. S. Strojek, and M. Jansen, *Z. Anorg. Allg. Chem.* **624**, 642 (1998).
1720. G. R. Burns, J. R. Rollo, and R. W. G. Syme, *J. Raman Spectrosc.* **19**, 345 (1988).
1721. W. Bues, M. Somer, and W. Brockner, *Z. Naturforsch.* **36a**, 842 (1981).
1722. M. Gardner, *J. Chem. Soc., Dalton Trans.*, 691 (1973).
1723. G. R. Burns, J. R. Rollo, J. D. Sarfrati, and K. R. Morgan, *Spectrochim. Acta* **47A**, 811 (1991).
1724. G. R. Burns, J. R. Rollo, and J. D. Sarfrati, *Inorg. Chim. Acta* **161**, 35 (1989).
1725. V. Varma, J. P. Fernandes, and C. N. R. Rao, *J. Mol. Struct.* **198**, 403 (1989).
1726. I. C. Hisatsune, *Spectrochim. Acta* **21**, 18 (1965).
1727. T. R. Manley and D. A. Williams, *Spectrochim. Acta* **23A**, 149 (1967).
1728. E. Steger and K. Lunkwitz, *J. Mol. Struct.* **3**, 67 (1969).
1729. H. G. M. Edwards, J. S. Ingman, and D. A. Long, *Spectrochim. Acta* **32A**, 731 (1976).
1730. B. Bley, M. Bodenbinder, G. Balzer, H. Willner, G. Hagele, F. Mistry, and F. Aubke, *Can. J. Chem.* **74**, 2392 (1996).

1731. J. R. Durig, J. Xiao, J. B. Robb, and F. F. D. Daeyaert, *J. Raman Spectrosc.* **29**, 463 (1998).
1732. C. Aubauer, G. Engelhardt, T. M. Klapotke, and A. Schulz, *J. Chem. Soc., Dalton Trans.* 1729 (1999).
1733. J. R. Durig, Z. Shen, and W. Zhao, *J. Mol. Struct.* **375**, 95 (1996).
1734. J. R. Durig, T. K. Gounev, M. S. Lee, and T. S. Little, *J. Mol. Struct.* **327**, 23 (1994).
1735. H.-J. Himmel, A. J. Downs, and T. M. Greene, *Inorg. Chem.* **40**, 396 (2001).
1736. K. O. Christe, C. J. Schack, and E. C. Curtis, *Inorg. Chem.* **15**, 843 (1976).
1737. K. Ohno, H. Matsuura, D. McNaughton, and H. W. Kroto, *J. Mol. Spectrosc.* **111**, 415 (1985).
1738. K. Ohno and H. Matsuura, *J. Mol. Struct.* **242**, 303 (1991).
1739. F. Emmerling and C. Röhr, *Z. Naturforsch.* **57b**, 963 (2002).
1740. S. H. Brumbach and G. M. Rosenblatt, *J. Chem. Phys.* **56**, 3110 (1972).
1741. R. Mercier and C. Sourisseau, *Spectrochim. Acta* **34A**, 337 (1978).
1742. W. P. Griffith, *J. Chem. Soc. A*, 905 (1967).
1743. G. A. Ozin, *J. Chem. Soc. A*, 2307 (1970).
1744. R. A. Work and M. L. Good, *Spectrochim. Acta* **29A**, 1547 (1973).
1745. G. D. Brabson, Z. Mielke, and L. Andrews, *J. Phys. Chem.* **95**, 79 (1991).
1746. M. S. Boumedien, J. Corset, and E. Picquenard, *J. Raman Spectrosc.* **30**, 463 (1999).
1747. P. Lenain, E. Picquenard, J. Corset, D. Jensen, and R. Steudel, *Ber. Bunsenges. Phys. Chem.* **92**, 859 (1988).
1748. R. Steudel and F. Schuster, *J. Mol. Struct.* **44**, 143 (1978).
1749. R. Steudel and H.-J. Mäusle, *Z. Naturforsch.* **33A**, 951 (1978).
1750. R. Steudel, T. Sandow, and J. Steidel, *Z. Naturforsch.* **40b**, 594 (1985).
1751. R. Steudel, *J. Phys. Chem.* **80**, 1516 (1976).
1752. R. Steudel and F. Schuster, *Z. Naturforsch.* **32a**, 1313 (1977).
1753. G. El-Jaroudi, E. Picquenard, A. Demortier, J. P. Lelieur, and J. Corset, *Inorg. Chem.* **39**, 2593 (2000).
1754. T. S. Cameron, R. J. Deeth, I. Dionne, H. Du, H. D. B. Jenkins, I. Krossing, J. Passmore, and H. K. Roobottom, *Inorg. Chem.* **39**, 5614 (2000).
1755. B. Liang and L. Andrews, *J. Phys. Chem. A* **196**, 3738, 6945 (2002).
1756. W. Bubenheim and U. Müller, *Z. Anorg. Allg. Chem.* **620**, 1607 (1994).
1757. R. Steudel and D. F. Eggers, Jr., *Spectrochim. Acta* **31A**, 871 (1975).
1758. R. Steudel and M. Rebsch, *J. Mol. Spectrosc.* **51**, 334 (1974).
1759. A. W. Herlonger and T. V. Long, *Inorg. Chem.* **8**, 2661 (1969).
- 1759a. R. Minkwitz, A. Kornath, W. Sawodny, and J. Hahn, *Inorg. Chem.* **35**, 3622 (1996).
1760. H. Wieser, P. J. Krueger, E. Muller, and J. B. Hyne, *Can. J. Chem.* **47**, 1633 (1969).
1761. K. Stopperka and F. Kilz, *Z. Anorg. Allg. Chem.* **370**, 49 (1969).
1762. E. M. Appelman, L. J. Basile, R. Kim, and J. R. Ferraro, *Spectrochim. Acta* **41A**, 1295 (1985).

1763. Y. P. Kuo, B. M. Cheng, and Y. P. Lee, *Chem. Phys. Lett.* **177**, 195 (1991).
1764. R. Minkwitz, R. Seelbinder, and R. Schöbel, *Angew. Chem. Int. Ed.* **41**, 111 (2002).
1765. E. L. Varetto, *J. Mol. Struct. (Thechem)* **429**, 121 (1998).
1766. W. Huang, R. A. Wheeler, and R. Frech, *Spectrochim. Acta* **50A**, 985 (1994).
1767. S. P. Gejji, K. Hermansson, and J. Lindgren, *J. Phys. Chem.* **98**, 8687 (1994).
1768. R. Steudel, *J. Phys. Chem.* **81**, 343 (1977).
1769. R. Steudel, K. Bergemann, J. Buschmann, and P. Luger, *Angew. Chem. Int. Ed.* **35**, 2537 (1996).
1770. R. Steudel and F. Rose, *Spectrochim. Acta* **33A**, 979 (1977).
1771. R. Steudel, *J. Mol. Struct.* **87**, 97 (1982).
1772. R. Steudel, J. Steidel, and N. Rautenberg, *Z. Naturforsch.* **35b**, 792 (1980).
1773. K. O. Christe, C. J. Schack, and E. C. Curtis, *Spectrochim. Acta* **26A**, 2367 (1970).
1774. R. Kebabcioglu, R. Mews, and O. Glemser, *Spectrochim. Acta* **28A**, 1593 (1972).
1775. R. Steudel, D. Jensen, and B. Plinke, *Z. Naturforsch.* **42b**, 163 (1987).
1776. S. Brownridge, T. S. Cameron, H. Du, C. Knapp, R. Köppe, J. Passmore, J. M. Rautiainen, and H. Schnöckel, *Inorg. Chem.* **44**, 1660 (2005).
1777. R. Minkwitz and J. Nowicki, *Inorg. Chem.* **29**, 2361 (1990).
1778. D. A. Braden, G. L. Gard, and T. J. R. Weakley, *Inorg. Chem.* **35**, 1912 (1996).
1779. R. M. S. Alvarez, E. H. Cutin, R. M. Romano, and C. O. Della Védova, *Spectrochim. Acta* **52A**, 667 (1996).
1780. M. Meyer, *J. Mol. Struct.* **273**, 99 (1992).
1781. G. Młostoń, J. Romański, H. P. Reisenauer, and G. Meier, *Angew. Chem. Int. Ed.* **40**, 393 (2001).
1782. D. J. Clouthier and J. M. Vollmer, *J. Mol. Struct.* **354**, 49 (1995).
1783. R. M. Romano, C. O. Della Védova, A. J. Downs, and T. M. Greene, *J. Am. Chem. Soc.* **123**, 5794 (2001).
1784. J. R. Durig, G. A. Guirgis, and K. A. Krutules, *J. Raman Spectrosc.* **26**, 475 (1995).
1785. S. E. Ulic, N. di Napoli, A. Hermann, H.-G. Mack, and C. O. Della Védova, *J. Raman Spectrosc.* **31**, 909 (2000).
1786. G. D. Brabson and L. Andrews, *J. Phys. Chem.* **96**, 9172 (1992).
1787. R. Steudel, *Z. Naturforsch.* **30a**, 1481 (1975).
1788. V. Müller, C. Crebe, U. Müller, and K. Dehnicke, *Z. Anorg. Allg. Chem.* **619**, 416 (1993).
1789. R. Laitinen, R. Steudel, and E.-M. Strauss, *J. Chem. Soc., Dalton Trans.* 1869 (1985).
1790. A. K. Verma and T. B. Rauchfuss, *Inorg. Chem.* **34**, 6199 (1995).
1791. D. M. Giolando, M. Papavassiliou, J. Pickardt, T. B. Rauchfuss, and R. Steudel, *Inorg. Chem.* **27**, 2596 (1988).
1792. A. Simon and R. Paetzold, *Z. Anorg. Allg. Chem.* **303**, 39, 46, 53, 72, 79 (1960); *Z. Elektrochem.* **64**, 209 (1960).
1793. J. Silviri, T. Chivers, and R. S. Laitinen, *Inorg. Chem.* **32**, 4391 (1993).
1794. J. Campbell, D. P. DiClommo, H. P. A. Mercier, A. M. Pirani, G. J. Schrobilgen, and M. Willuhn, *Inorg. Chem.* **34**, 6265 (1995).

- 1795. H. Borrmann, J. Campbell, D. A. Dixon, H. P. A. Mercier, A. M. Pirani, and G. J. Schrobilgen, *Inorg. Chem.* **37**, 6656 (1998).
- 1796. R. Boese, A. Haas, and C. Limberg, *J. Chem. Soc., Dalton Trans.* 2547 (1993).
- 1797. H. Borrmann, J. Campbell, D. A. Dixon, H. P. A. Mercier, A. M. Pirani, and G. J. Schrobilgen, *Inorg. Chem.* **37**, 1929 (1998).
- 1798. G. W. Drake, G. I. Schmek, and I. W. Kolis, *Inorg. Chem.* **35**, 1740 (1996).
- 1799. B. Casper, D. Christen, H.-G. Mack, H. Oberhammer, G. A. Arguello, R. Julicher, M. Kronberg, and H. Willner, *J. Phys. Chem.* **100**, 3983 (1996).
- 1800. R. Minkwitz and M. Berkei, *Inorg. Chem.* **38**, 5041 (1999).
- 1801. G. R. Clark, M. J. Taylor, and D. Steele, *J. Chem. Soc., Faraday Trans.* **89**, 3597 (1993).
- 1802. R. Minkwitz, M. Berkei, and R. Ludwig, *Inorg. Chem.* **40**, 25 (2001).
- 1803. P. Deplano, F. A. Devillanova, J. R. Ferraro, M. L. Mercuri, V. Lippolis, and E. F. Trogu, *Appl. Spectrosc.* **48**, 1236 (1994).
- 1804. E. M. Nour, L. H. Chen, and J. Laane, *J. Phys. Chem.* **90**, 2841 (1986).
- 1805. R. Poll, J. C. Gordon, R. K. Khanna, and P. E. Fanwick, *Inorg. Chem.* **31**, 3165 (1992).

Appendixes

APPENDIX I. POINT GROUPS AND THEIR CHARACTER TABLES

The following are the character tables of the point groups that appear frequently in this book. The species (or the irreducible representations) of the point group are labeled according to the following rules: *A* and *B* denote nondegenerate species (one-dimensional representation). *A* represents the symmetric species (character = +1) with respect to rotation about the principal axis (chosen as *z* axis), whereas *B* represents the antisymmetric species (character = −1) with respect to rotation about the principal axis; *E* and *F* denote doubly degenerate (two-dimensional representation) and triply degenerate species (three-dimensional representation) respectively. If two species in the same point group differ in the character of *C* (other than the principal axis), they are distinguished by subscripts 1, 2, 3, If two species differ in the character to σ (other than σ_v), they are distinguished by ' and '. If two species differ in the character of *i*, they are distinguished by subscripts *g* and *u*. If these rules allow several different labels, *g* and *u* take precedence over 1, 2, 3, . . . , which in turn take precedence over ' and '. The labels of species of point groups $C_{\infty v}$ and $D_{\infty h}$ (linear molecules) are exceptional and are taken from the notation for the component of the electronic orbital angular momentum along the molecular axis.

C_1	<i>I</i>
<i>A</i>	1

C_2	I	$C_2(z)$		
A	+1	+1	T_z, R_z	$\alpha_{xx}, \alpha_{yy}, \alpha_{zz}, \alpha_{xy}$
B	+1	-1	T_x, T_y, R_x, R_y	α_{yz}, α_{xz}

C_s	I	$\sigma(xy)$		
A'	+1	+1	T_x, T_y, R_z	$\alpha_{xx}, \alpha_{yy}, \alpha_{zz}, \alpha_{xy}$
B'	+1	-1	T_z, R_x, R_y	α_{yz}, α_{xz}

$C_i \equiv S_2$	I	i		
A_g	+1	+1	R_x, R_y, R_z	All components of α
A_u	+1	-1	T_x, T_y, T_x	

C_{2v}	I	$C_2(z)$	$\sigma_v(xz)$	$\sigma_v(yz)$		
A_1	+1	+1	+1	+1	T_z	$\alpha_{xx}, \alpha_{yy}, \alpha_{zz}$
A_2	+1	+1	-1	-1	R_z	α_{xy}
B_1	+1	-1	+1	-1	T_x, R_y	α_{xz}
B_2	+1	-1	-1	+1	T_y, R_x	α_{yz}

C_{2h}	I	$C_2(z)$	$\sigma_h(xy)$	i		
A_g	+1	+1	+1	+1	R_z	$\alpha_{xx}, \alpha_{yy}, \alpha_{zz}, \alpha_{xy}$
A_u	+1	+1	-1	-1	T_z	α_{yz}, α_{xz}
B_g	+1	-1	-1	+1	R_x, R_y	
B_u	+1	-1	+1	-1	T_x, T_y	

$D_2 \equiv V$	I	$C_2(z)$	$C_2(y)$	$C_2(x)$		
A	+1	+1	+1	+1	T_z, R_z T_y, R_y T_x, R_x	$\alpha_{xx}, \alpha_{yy}, \alpha_{zz}$
B_1	+1	+1	-1	-1		α_{xy}
B_2	+1	-1	+1	-1		α_{xz}
B_3	+1	-1	-1	+1		α_{yz}

$D_{2h} \equiv V_h$	I	$\sigma(xy)$	$\sigma(xz)$	$\sigma(yz)$	i	$C_2(z)$	$C_2(y)$	$C_2(x)$		
A_g	+1	+1	+1	+1	+1	+1	+1	+1	R_z T_z R_y T_y R_x T_x	$\alpha_{xx}, \alpha_{yy}, \alpha_{zz}$
A_u	+1	-1	-1	-1	-1	+1	+1	+1		α_{xy}
B_{1g}	+1	+1	-1	-1	+1	+1	-1	-1		
B_{1u}	+1	-1	+1	+1	-1	+1	-1	-1		α_{xz}
B_{2g}	+1	-1	+1	-1	+1	-1	+1	-1		
B_{2u}	+1	+1	-1	+1	-1	-1	+1	-1	α_{yz}	α_{xy}
B_{3g}	+1	-1	-1	+1	+1	-1	-1	+1		
B_{3u}	+1	+1	+1	-1	-1	-1	-1	+1		

C_3	I	C_3	C_3^2		
A	1	1	1	T_z, R_z	$\alpha_{xx} + \alpha_{yy}, \alpha_{zz}$
E	$\begin{Bmatrix} 1 \\ 1 \end{Bmatrix}$	$\begin{Bmatrix} \epsilon \\ \epsilon^* \end{Bmatrix}$	$\begin{Bmatrix} \epsilon^* \\ \epsilon \end{Bmatrix}$	$(T_x, T_y), (R_x, R_y)$	$(\alpha_{xx} - \alpha_{yy}, \alpha_{xy}), (\alpha_{yz}, \alpha_{xz})$

$$\epsilon = e^{2\pi i/3}$$

C_4	I	C_4	C_2	C_4^3		
A	1	1	1	1	T_z, R_z	$\alpha_{xx} + \alpha_{yy}, \alpha_{zz}$
B	1	-1	1	-1		$\alpha_{xx} - \alpha_{yy}, \alpha_{xy}$
E	$\begin{Bmatrix} 1 \\ 1 \end{Bmatrix}$	$\begin{Bmatrix} i \\ -i \end{Bmatrix}$	$\begin{Bmatrix} -1 \\ -1 \end{Bmatrix}$	$\begin{Bmatrix} -i \\ i \end{Bmatrix}$	$(T_x, T_y), (R_x, R_y)$	$(\alpha_{yz}, \alpha_{xz})$

C_5	I	C_5	C_5^2	C_5^3	C_5^4		
A	1	1	1	1	1	T_z, R_z	$\alpha_{xx} + \alpha_{yy}, \alpha_{zz}$
E_1	$\begin{Bmatrix} 1 \\ 1 \end{Bmatrix}$	$\begin{Bmatrix} \epsilon \\ \epsilon^* \end{Bmatrix}$	$\begin{Bmatrix} \epsilon^2 \\ \epsilon^{2*} \end{Bmatrix}$	$\begin{Bmatrix} \epsilon^{2*} \\ \epsilon^2 \end{Bmatrix}$	$\begin{Bmatrix} \epsilon^* \\ \epsilon \end{Bmatrix}$	$(T_x, T_y), (R_x, R_y)$	$(\alpha_{yz}, \alpha_{xz})$
E_2	$\begin{Bmatrix} 1 \\ 1 \end{Bmatrix}$	$\begin{Bmatrix} \epsilon^2 \\ \epsilon^{2*} \end{Bmatrix}$	$\begin{Bmatrix} \epsilon^* \\ \epsilon \end{Bmatrix}$	$\begin{Bmatrix} \epsilon \\ \epsilon^* \end{Bmatrix}$	$\begin{Bmatrix} \epsilon^{2*} \\ \epsilon^2 \end{Bmatrix}$		$(\alpha_{xx} - \alpha_{yy}, \alpha_{xy})$

$$\epsilon = e^{2\pi i/5}$$

C_6	I	C_6	C_3	C_2	C_3^2	C_6^5		
A	1	1	1	1	1	1	T_z, R_z	$\alpha_{xx} + \alpha_{yy}, \alpha_{zz}$
B	1	-1	1	-1	1	-1		
E_1	$\begin{Bmatrix} 1 \\ 1 \end{Bmatrix}$	$\begin{Bmatrix} \epsilon \\ \epsilon^* \end{Bmatrix}$	$\begin{Bmatrix} -\epsilon^* \\ -\epsilon \end{Bmatrix}$	$\begin{Bmatrix} -1 \\ -1 \end{Bmatrix}$	$\begin{Bmatrix} -\epsilon \\ -\epsilon^* \end{Bmatrix}$	$\begin{Bmatrix} \epsilon^* \\ \epsilon \end{Bmatrix}$	$(T_x, T_y), (R_x, R_y)$	$(\alpha_{xz}, \alpha_{yz})$
E_2	$\begin{Bmatrix} 1 \\ 1 \end{Bmatrix}$	$\begin{Bmatrix} -\epsilon^* \\ -\epsilon \end{Bmatrix}$	$\begin{Bmatrix} -\epsilon \\ -\epsilon^* \end{Bmatrix}$	$\begin{Bmatrix} 1 \\ 1 \end{Bmatrix}$	$\begin{Bmatrix} -\epsilon^* \\ -\epsilon \end{Bmatrix}$	$\begin{Bmatrix} -\epsilon \\ -\epsilon^* \end{Bmatrix}$		$(\alpha_{xx} - \alpha_{yy}, \alpha_{xy})$

$$\epsilon = e^{2\pi i/6}$$

S_4	I	S_4	C_2	S_4^3		
A	1	1	1	1	R_z	$\alpha_{xx} + \alpha_{yy}, \alpha_{zz}$
B	1	-1	1	-1	T_z	$\alpha_{xx} - \alpha_{yy}, \alpha_{xy}$
E	$\begin{Bmatrix} 1 \\ 1 \end{Bmatrix}$	$\begin{Bmatrix} i \\ -i \end{Bmatrix}$	$\begin{Bmatrix} -1 \\ -1 \end{Bmatrix}$	$\begin{Bmatrix} -i \\ i \end{Bmatrix}$	$(T_x, T_y), (R_x, R_y)$	$(\alpha_{xz}, \alpha_{yz})$

$S_6 \equiv C_{3i}$	I	C_3	C_3^2	i	S_6^5	S_6		
A_g	1	1	1	1	1	1	R_z	$\alpha_{xx} + \alpha_{yy}, \alpha_{zz}$
E_g	$\begin{Bmatrix} 1 & \epsilon & \epsilon^* & 1 & \epsilon & \epsilon^* \\ 1 & \epsilon^* & \epsilon & 1 & \epsilon^* & \epsilon \end{Bmatrix}$						(R_x, R_y)	$(\alpha_{xx} - \alpha_{yy}, \alpha_{xy}), (\alpha_{xz}, \alpha_{yz})$
A_u	1	1	1	-1	-1	-1	T_z	
E_u	$\begin{Bmatrix} 1 & \epsilon & \epsilon^* & -1 & -\epsilon & -\epsilon^* \\ 1 & \epsilon^* & \epsilon & -1 & -\epsilon^* & -\epsilon \end{Bmatrix}$						(T_x, T_y)	

$\epsilon = e^{2\pi i/3}$

D_3	I	$2C_3(z)$	$3C_2$		
A_1	+1	+1	+1	T_z, R_z $(T_x, T_y), (R_x, R_y)$	$\alpha_{xx} + \alpha_{yy}, \alpha_{zz}$
A_2	+1	+1	-1		
E	+2	-1	0		$(\alpha_{xx} - \alpha_{yy}, \alpha_{xy}), (\alpha_{yz}, \alpha_{xz})$

D_4	I	$2C_4$	$C_2(=C_4^2)$	$2C_2'$	$2C_2''$		
A_1	1	1	1	1	1	T_z, R_z $(T_x, T_y), (R_x, R_y)$	$\alpha_{xx} + \alpha_{yy}, \alpha_{zz}$
A_2	1	1	1	-1	-1		
B_1	1	-1	1	1	-1		$\alpha_{xx} - \alpha_{yy}$
B_2	1	-1	1	-1	1		α_{xy}
E	2	0	-2	0	0		$(\alpha_{xz}, \alpha_{yz})$

D_5	I	$2C_5$	$2C_5^2$	$5C_2$		
A_1	1	1	1	1	T_z, R_z $(T_x, T_y), (R_x, R_y)$	$\alpha_{xx} + \alpha_{yy}, \alpha_{zz}$
A_2	1	1	1	-1		
E_1	2	$2c \frac{2\pi}{5}$	$2c \frac{4\pi}{5}$	0		$(\alpha_{xz}, \alpha_{yz})$
E_2	2	$2c \frac{4\pi}{5}$	$2c \frac{2\pi}{5}$	0		$(\alpha_{xx} - \alpha_{yy}, \alpha_{xy})$

C = cosine

D_6	I	$2C_6$	$2C_3$	C_2	$3C_2'$	$3C_2''$		
A_1	1	1	1	1	1	1	T_z, R_z $(T_x, T_y), (R_x, R_y)$	$\alpha_{xx} + \alpha_{yy}, \alpha_{zz}$
A_2	1	1	1	1	-1	-1		
B_1	1	-1	1	-1	1	-1		
B_2	1	-1	1	-1	-1	1		
E_1	2	1	-1	-2	0	0		$(\alpha_{xz}, \alpha_{yz})$
E_2	2	-1	-1	2	0	0		$(\alpha_{xx} - \alpha_{yy}, \alpha_{xy})$

C_{3v}	I	$2C_2(z)$	$3\sigma_v$		
A_1	+1	+1	+1	T_z	$\alpha_{xx} + \alpha_{yy}, \alpha_{zz}$
A_2	+1	+1	-1	R_z	
E	+2	-1	0	$(T_x, T_y), (R_x, R_y)$	$(\alpha_{xx} - \alpha_{yy}, \alpha_{xy}), (\alpha_{yz}, \alpha_{xz})$

C_{4v}	I	$2C_4(z)$	$C_4^2 \equiv C_2''$	$2\sigma_v$	$2\sigma_d$		
A_1	+1	+1	+1	+1	+1	T_z	$\alpha_{xx} + \alpha_{yy}, \alpha_{zz}$
A_2	+1	+1	+1	-1	-1	R_z	
B_1	+1	-1	+1	+1	-1		$\alpha_{xx} - \alpha_{yy}$
B_2	+1	-1	+1	-1	+1		α_{xy}
E	+2	0	-2	0	0	$(T_x, T_y), (R_x, R_y)$	$(\alpha_{yz}, \alpha_{xz})$

C_{5v}	I	$2C_5$	$2C_5^2$	$5\sigma_v$		
A_1	1	1	1	1	T_z	$\alpha_{xx} + \alpha_{yy}, \alpha_{zz}$
A_2	1	1	1	-1	R_z	
E_1	2	$2c \frac{2\pi}{5}$	$2c \frac{4\pi}{5}$	0	$(T_x, T_y), (R_x, R_y)$	$(\alpha_{xz}, \alpha_{yz})$
E_2	2	$2c \frac{4\pi}{5}$	$2c \frac{2\pi}{5}$	0		$(\alpha_{xx} - \alpha_{yy}, \alpha_{xy})$

c = cosine

C_{6v}	I	$2C_6$	$2C_3$	C_2	$3\sigma_v$	$3\sigma_d$		
A_1	1	1	1	1	1	1	T_z	$\alpha_{xx} + \alpha_{yy}, \alpha_{zz}$
A_2	1	1	1	1	-1	-1	R_z	
B_1	1	-1	1	-1	1	-1		
B_2	1	-1	1	-1	-1	1		
E_1	2	1	-1	-2	0	0	$(T_x, T_y), (R_x, R_y)$	$(\alpha_{xz}, \alpha_{yz})$
E_2	2	-1	-1	2	0	0		$(\alpha_{xx} - \alpha_{yy}, \alpha_{xy})$

$C_{\infty v}$	I	$2C_{\infty}^{\phi}$	$2C_{\infty}^{2\phi}$	$2C_{\infty}^{3\phi}$...	$\infty\sigma_v$		
Σ^+	+1	+1	+1	+1	...	+1	T_z	$\alpha_{xx} + \alpha_{yy}, \alpha_{zz}$
Σ^-	+1	+1	+1	+1	...	-1	R_z	
Π	+2	$2 \cos \phi$	$2 \cos 2\phi$	$2 \cos 3\phi$...	0	$(T_x, T_y), (R_x, R_y)$	$(\alpha_{yz}, \alpha_{xz})$
Δ	+2	$2 \cos 2\phi$	$2 \cos 2 \cdot 2\phi$	$2 \cos 3 \cdot 2\phi$...	0		$(\alpha_{xx} - \alpha_{yy}, \alpha_{xy})$
Φ	+2	$2 \cos 3\phi$	$2 \cos 2 \cdot 3\phi$	$2 \cos 3 \cdot 3\phi$...	0		
...		

ϕ = arbitrary angle

$$\epsilon = e^{2\pi i/3}$$

$$\epsilon = e^{2\pi i/5}$$

C_{6h}	I	C_6	C_3	C_2	C_3^2	C_6^5	i	S_3^5	S_6^5	σ_h	S_6	S_3		
A_g	1	1	1	1	1	1	1	1	1	1	1	1	R_z	$\alpha_{xx} + \alpha_{yy}, \alpha_{zz}$
A_u	1	1	1	1	1	1	-1	-1	-1	-1	-1	-1	T_z	
B_g	1	-1	1	-1	1	-1	1	-1	1	-1	1	-1		
B_u	1	-1	1	-1	1	-1	-1	1	-1	1	-1	1		
E_{1g}	$\left\{ \begin{array}{l} 1 \\ 1 \end{array} \right.$	$\left\{ \begin{array}{l} \epsilon \\ \epsilon^* \end{array} \right.$	$\left\{ \begin{array}{l} -\epsilon^* \\ -\epsilon \end{array} \right.$	$\left\{ \begin{array}{l} -1 \\ -1 \end{array} \right.$	$\left\{ \begin{array}{l} -\epsilon \\ -\epsilon^* \end{array} \right.$	$\left\{ \begin{array}{l} \epsilon^* \\ \epsilon \end{array} \right.$	$\left\{ \begin{array}{l} 1 \\ 1 \end{array} \right.$	$\left\{ \begin{array}{l} \epsilon \\ \epsilon^* \end{array} \right.$	$\left\{ \begin{array}{l} -\epsilon^* \\ -\epsilon \end{array} \right.$	$\left\{ \begin{array}{l} -1 \\ -1 \end{array} \right.$	$\left\{ \begin{array}{l} -\epsilon \\ -\epsilon^* \end{array} \right.$	$\left\{ \begin{array}{l} \epsilon^* \\ \epsilon \end{array} \right.$	(R_x, R_y)	$(\alpha_{xz}, \alpha_{yz})$
E_{1u}	$\left\{ \begin{array}{l} 1 \\ 1 \end{array} \right.$	$\left\{ \begin{array}{l} \epsilon \\ \epsilon^* \end{array} \right.$	$\left\{ \begin{array}{l} -\epsilon^* \\ -\epsilon \end{array} \right.$	$\left\{ \begin{array}{l} -1 \\ -1 \end{array} \right.$	$\left\{ \begin{array}{l} -\epsilon \\ -\epsilon^* \end{array} \right.$	$\left\{ \begin{array}{l} \epsilon^* \\ \epsilon \end{array} \right.$	$\left\{ \begin{array}{l} -1 \\ -1 \end{array} \right.$	$\left\{ \begin{array}{l} -\epsilon \\ -\epsilon^* \end{array} \right.$	$\left\{ \begin{array}{l} \epsilon^* \\ \epsilon \end{array} \right.$	$\left\{ \begin{array}{l} 1 \\ 1 \end{array} \right.$	$\left\{ \begin{array}{l} \epsilon \\ \epsilon^* \end{array} \right.$	$\left\{ \begin{array}{l} -\epsilon^* \\ -\epsilon \end{array} \right.$	(T_x, T_y)	
E_{2g}	$\left\{ \begin{array}{l} 1 \\ 1 \end{array} \right.$	$\left\{ \begin{array}{l} -\epsilon^* \\ -\epsilon \end{array} \right.$	$\left\{ \begin{array}{l} -\epsilon \\ \epsilon^* \end{array} \right.$	$\left\{ \begin{array}{l} 1 \\ 1 \end{array} \right.$	$\left\{ \begin{array}{l} -\epsilon^* \\ -\epsilon \end{array} \right.$	$\left\{ \begin{array}{l} -\epsilon \\ -\epsilon^* \end{array} \right.$	$\left\{ \begin{array}{l} 1 \\ 1 \end{array} \right.$	$\left\{ \begin{array}{l} -\epsilon^* \\ -\epsilon \end{array} \right.$	$\left\{ \begin{array}{l} -\epsilon \\ -\epsilon^* \end{array} \right.$	$\left\{ \begin{array}{l} 1 \\ 1 \end{array} \right.$	$\left\{ \begin{array}{l} -\epsilon^* \\ -\epsilon \end{array} \right.$	$\left\{ \begin{array}{l} -\epsilon \\ -\epsilon^* \end{array} \right.$		$(\alpha_{xx} - \alpha_{yy}, \alpha_{xy})$
E_{2u}	$\left\{ \begin{array}{l} 1 \\ 1 \end{array} \right.$	$\left\{ \begin{array}{l} -\epsilon^* \\ -\epsilon \end{array} \right.$	$\left\{ \begin{array}{l} -\epsilon \\ \epsilon^* \end{array} \right.$	$\left\{ \begin{array}{l} 1 \\ 1 \end{array} \right.$	$\left\{ \begin{array}{l} -\epsilon^* \\ -\epsilon \end{array} \right.$	$\left\{ \begin{array}{l} -\epsilon \\ -\epsilon^* \end{array} \right.$	$\left\{ \begin{array}{l} -1 \\ -1 \end{array} \right.$	$\left\{ \begin{array}{l} \epsilon^* \\ \epsilon \end{array} \right.$	$\left\{ \begin{array}{l} \epsilon \\ \epsilon^* \end{array} \right.$	$\left\{ \begin{array}{l} -1 \\ -1 \end{array} \right.$	$\left\{ \begin{array}{l} \epsilon^* \\ \epsilon \end{array} \right.$	$\left\{ \begin{array}{l} \epsilon \\ \epsilon^* \end{array} \right.$		

$$\epsilon = e^{2\pi i/6}$$

$D_{2d} \equiv V_d$	I	$2S_4(z)$	$S_4^2 \equiv C_2''$	$2C_2$	$2\sigma_d$		
A_1	+1	+1	+1	+1	+1	R_z	$\alpha_{xx} + \alpha_{yy}, \alpha_{zz}$
A_2	+1	+1	+1	-1	-1		
B_1	+1	-1	+1	+1	-1		$\alpha_{xx} - \alpha_{yy}$
B_2	+1	-1	+1	-1	+1	T_z	α_{xy}
E	+2	0	-2	0	0	$(T_x, T_y), (R_x, R_y)$	$(\alpha_{yz}, \alpha_{xz})$

D_{3d}	I	$2S_6(z)$	$2S_6^2 \equiv 2C_3$	$2S_6^3 \equiv S_2 \equiv i$	$3C_2$	$3\sigma_d$		
A_{1g}	+1	+1	+1	+1	+1	+1		$\alpha_{xx} + \alpha_{yy}, \alpha_{zz}$
A_{1u}	+1	-1	+1	-1	+1	-1		
A_{2g}	+1	+1	+1	+1	-1	-1	R_z	
A_{2u}	+1	-1	+1	-1	-1	+1	T_z	
E_g	+2	-1	-1	+2	0	0	(R_x, R_y)	$(\alpha_{xx} - \alpha_{yy}, \alpha_{xy}),$ $(\alpha_{yz}, \alpha_{xz})$
E_u	+2	+1	-1	-2	0	0	(T_x, T_y)	

D_{4d}	I	$2S_8(z)$	$2S_8^2 \equiv 2C_4$	$2S_8^3$	$S_8^4 \equiv C_2''$	$4C_2$	$4\sigma_d$		
A_1	+1	+1	+1	+1	+1	+1	+1	R_z	$\alpha_{xx} + \alpha_{yy}, \alpha_{zz}$
A_2	+1	+1	+1	+1	+1	-1	-1		
B_1	+1	-1	+1	-1	+1	+1	-1		
B_2	+1	-1	+1	-1	+1	-1	+1	T_z	
E_1	+2	$+\sqrt{2}$	0	$-\sqrt{2}$	-2	0	0	(T_x, T_y)	
E_2	+2	0	-2	0	+2	0	0		$(\alpha_{xx} - \alpha_{yy}, \alpha_{xy})$
E_3	+2	$-\sqrt{2}$	0	$+\sqrt{2}$	-2	0	0	(R_x, R_y)	$(\alpha_{yz}, \alpha_{xz})$

D_{5d}	I	$2C_5$	$2C_5^2$	$5C_2$	i	$2S_{10}^3$	$2S_{10}$	$5\sigma_d$		
A_{1g}	1	1	1	1	1	1	1	1	R_z T_z	$\alpha_{xx} + \alpha_{yy}, \alpha_{zz}$
A_{1u}	1	1	1	1	-1	-1	-1	-1		
A_{2g}	1	1	1	-1	1	1	1	-1		
A_{2u}	1	1	1	-1	-1	-1	-1	1		
E_{1g}	2	$2c \frac{2\pi}{5}$	$2c \frac{4\pi}{5}$	0	2	$2c \frac{2\pi}{5}$	$2c \frac{4\pi}{5}$	0	(R_x, R_y)	$(\alpha_{xz}, \alpha_{yz})$
E_{1u}	2	$2c \frac{2\pi}{5}$	$2c \frac{4\pi}{5}$	0	-2	$-2c \frac{2\pi}{5}$	$-2c \frac{4\pi}{5}$	0		
E_{2g}	2	$2c \frac{4\pi}{5}$	$2c \frac{2\pi}{5}$	0	2	$2c \frac{4\pi}{5}$	$2c \frac{2\pi}{5}$	0	(T_x, T_y)	$(\alpha_{xx} - \alpha_{yy}, \alpha_{xy})$
E_{2u}	2	$2c \frac{4\pi}{5}$	$2c \frac{2\pi}{5}$	0	-2	$-2c \frac{4\pi}{5}$	$-2c \frac{2\pi}{5}$	0		

c = cosine

D_{3h}	I	$2C_3(z)$	$3C_2$	σ_h	$2S_3$	$3\sigma_v$		
A'_1	+1	+1	+1	+1	+1	+1	R_z T_z	$\alpha_{xx} + \alpha_{yy}, \alpha_{zz}$
A''_1	+1	+1	+1	-1	-1	-1		
A'_2	+1	+1	-1	+1	+1	-1		
A''_2	+1	+1	-1	-1	-1	+1		
E'	+2	-1	0	+2	-1	0	(T_x, T_y)	$(\alpha_{xx} - \alpha_{yy}, \alpha_{xy})$
E''	+2	-1	0	-2	+1	0		

D_{4h}	I	$2C_4(z)$	$C_4^2 \equiv C_2$	$2C_2'$	$2C_2''$	σ_h	$2\sigma_v$	$2\sigma_d$	$2S_4$	$S_2 \equiv i$		
A_{1g}	+1	+1	+1	+1	+1	+1	+1	+1	+1	+1	R_z T_z	$\alpha_{xx} + \alpha_{yy},$ α_{zz}
A_{1u}	+1	+1	+1	+1	+1	-1	-1	-1	-1	-1		
A_{2g}	+1	+1	+1	-1	-1	+1	-1	-1	+1	+1		
A_{2u}	+1	+1	+1	-1	-1	-1	+1	+1	-1	-1		
B_{1g}	+1	-1	+1	+1	-1	+1	+1	-1	-1	+1		
B_{1u}	+1	-1	+1	+1	-1	-1	-1	+1	+1	-1		
B_{2g}	+1	-1	+1	-1	+1	+1	-1	-1	-1	+1		
B_{2u}	+1	-1	+1	-1	+1	-1	+1	-1	+1	-1		
E_g	+2	0	-2	0	0	-2	0	0	0	+2	(R_x, R_y)	$(\alpha_{yz}, \alpha_{xz})$
E_u	+2	0	-2	0	0	+2	0	0	0	-2	(T_x, T_y)	

D_{5h}	I	$2C_5$	$2C_5^2$	$5C_2$	σ_h	$2S_5$	$2S_5^3$	$5\sigma_v$		
A'_1	1	1	1	1	1	1	1	1	R_z T_z	$\alpha_{xx} + \alpha_{yy}, \alpha_{zz}$
A''_1	1	1	1	1	-1	-1	-1	-1		
A'_2	1	1	1	-1	1	1	1	-1		
A''_2	1	1	1	-1	-1	-1	-1	1		
E'_1	2	$2c \frac{2\pi}{5}$	$2c \frac{4\pi}{5}$	0	2	$2c \frac{2\pi}{5}$	$2c \frac{4\pi}{5}$	0	(T_x, T_y)	$(\alpha_{xz}, \alpha_{yz})$
E''_1	2	$2c \frac{2\pi}{5}$	$2c \frac{4\pi}{5}$	0	-2	$-2c \frac{2\pi}{5}$	$-2c \frac{4\pi}{5}$	0		
E'_2	2	$2c \frac{4\pi}{5}$	$2c \frac{2\pi}{5}$	0	2	$2c \frac{4\pi}{5}$	$2c \frac{2\pi}{5}$	0	(R_x, R_y)	$(\alpha_{xx} - \alpha_{yy}, \alpha_{xy})$
E''_2	2	$2c \frac{4\pi}{5}$	$2c \frac{2\pi}{5}$	0	-1	$-2c \frac{4\pi}{5}$	$-2c \frac{2\pi}{5}$	0		

c = cosine

D_{6h}	I	$2C_6(z)$	$2C_6^2 \equiv 2C_3$	$C_6^3 \equiv C_2$	$3C_2'$	$3C_2''$	σ_h	$3\sigma_v$	$3\sigma_d$	$2S_6$	$2S_3$	$S_6^3 \equiv S_2 \equiv i$		
A_{1g}	+1	+1	+1	+1	+1	+1	+1	+1	+1	+1	+1	+1	R_z T_z	$\alpha_{xx} + \alpha_{yy}$ α_{zz}
A_{1u}	+1	+1	+1	+1	+1	+1	-1	-1	-1	-1	-1	-1		
A_{2g}	+1	+1	+1	+1	-1	-1	+1	-1	-1	+1	+1	+1	(R_x, R_y) (T_x, T_y)	α_{yz}, α_{xz} $(\alpha_{xx} - \alpha_{yy})$ α_{xy}
A_{2u}	+1	+1	+1	+1	-1	-1	-1	+1	+1	-1	-1	-1		
B_{1g}	+1	-1	+1	-1	+1	-1	-1	+1	-1	+1	+1	+1	(R_x, R_y) (T_x, T_y)	α_{yz}, α_{xz} $(\alpha_{xx} - \alpha_{yy})$ α_{xy}
B_{1u}	+1	-1	+1	-1	+1	-1	+1	+1	-1	-1	-1	-1		
B_{2g}	+1	-1	+1	-1	-1	+1	+1	-1	+1	-1	-1	-1	(R_x, R_y) (T_x, T_y)	α_{yz}, α_{xz} $(\alpha_{xx} - \alpha_{yy})$ α_{xy}
B_{2u}	+1	-1	+1	-1	-1	+1	-1	-1	-1	+1	+1	+1		
E_{1g}	+2	+1	-1	-2	0	0	-2	0	0	-1	+1	+2	(R_x, R_y) (T_x, T_y)	α_{yz}, α_{xz} $(\alpha_{xx} - \alpha_{yy})$ α_{xy}
E_{1u}	+2	+1	-1	-2	0	0	+2	0	0	+1	-1	-2		
E_{2g}	+2	-1	-1	+2	0	0	+2	0	0	-1	-1	+2	(R_x, R_y) (T_x, T_y)	α_{yz}, α_{xz} $(\alpha_{xx} - \alpha_{yy})$ α_{xy}
E_{2u}	+2	-1	-1	+2	0	0	-2	0	0	+1	+1	-2		

$\mathbf{D}_{\infty h}$	l	$2C_{\infty}^{\phi}$	$2C_{\infty}^{2\phi}$	$2C_{\infty}^{3\phi}$	\dots	σ_h	∞C_2	$\infty \sigma_v$	$2S_{\infty}^{\phi}$	$2S_{\infty}^{2\phi}$	\dots	$S_2 \equiv i$		
Σ_g^+	+1	+1	+1	+1	\dots	+1	+1	+1	+1	+1	\dots	+1		$\alpha_{xx} + \alpha_{yy}, \alpha_{zz}$
Σ_u^+	+1	+1	+1	+1	\dots	-1	-1	+1	-1	-1	\dots	-1	T_z	
Σ_g^-	+1	+1	+1	+1	\dots	+1	-1	-1	+1	+1	\dots	+1	R_z	
Σ_u^-	+1	+1	+1	+1	\dots	-1	+1	-1	-1	-1	\dots	-1		
Π_g	+2	$2 \cos \phi$	$2 \cos 2\phi$	$2 \cos 3\phi$	\dots	-2	0	0	-2	-2	\dots	+2	(R_x, R_y)	$(\alpha_{yz}, \alpha_{xz})$
Π_u	+2	$2 \cos \phi$	$2 \cos 2\phi$	$2 \cos 3\phi$	\dots	+2	0	0	+2	+2	\dots	-2	(T_x, T_y)	$(\alpha_{xx} - \alpha_{yy}, \alpha_{xy})$
Δ_g	+2	$2 \cos 2\phi$	$2 \cos 4\phi$	$2 \cos 6\phi$	\dots	+2	0	0	+2	+2	\dots	+2		
Δ_u	+2	$2 \cos 2\phi$	$2 \cos 4\phi$	$2 \cos 6\phi$	\dots	-2	0	0	-2	-2	\dots	-2		
Φ_g	+2	$2 \cos 3\phi$	$2 \cos 6\phi$	$2 \cos 9\phi$	\dots	-2	0	0	-2	-2	\dots	+2		
Φ_u	+2	$2 \cos 3\phi$	$2 \cos 6\phi$	$2 \cos 9\phi$	\dots	+2	0	0	+2	+2	\dots	-2		
\dots	\dots	\dots	\dots	\dots	\dots	\dots	0	0	\dots	\dots	\dots	\dots		

$\phi = \text{arbitrary angle}$

T	I	4C₃	4C₃²	3C₂		
A	1	1	1	1		$\alpha_{xx} + \alpha_{yy} + \alpha_{zz}$
E	$\begin{Bmatrix} 1 & \epsilon & \epsilon^* & 1 \\ 1 & \epsilon^* & \epsilon & 1 \end{Bmatrix}$					$(2\alpha_{zz} - \alpha_{xx} - \alpha_{yy}, \alpha_{xx} - \alpha_{yy})$
F	3	0	0	-1	$(R_x, R_y, R_z), (T_x, T_y, T_z)$	$(\alpha_{xy}, \alpha_{xz}, \alpha_{yz})$

$\epsilon = e^{2\pi i/3}$

T_h	I	4C₃	4C₃²	3C₂	i	4S₆	4S₆⁵	3σ_v		
A_g	1	1	1	1	1	1	1	1		$\alpha_{xx} + \alpha_{yy} + \alpha_{zz}$
A_u	1	1	1	1	-1	-1	-1	-1		
E_g	$\begin{Bmatrix} 1 & \epsilon & \epsilon^* & 1 & 1 & \epsilon & \epsilon^* & 1 \\ 1 & \epsilon^* & \epsilon & 1 & 1 & \epsilon^* & \epsilon & 1 \end{Bmatrix}$									$(2\alpha_{zz} - \alpha_{xx} - \alpha_{yy}, \alpha_{xx} - \alpha_{yy})$
E_u	$\begin{Bmatrix} 1 & \epsilon & \epsilon^* & 1 & -1 & -\epsilon & -\epsilon^* & -1 \\ 1 & \epsilon^* & \epsilon & 1 & -1 & -\epsilon^* & -\epsilon & -1 \end{Bmatrix}$									
F_g	3	0	0	-1	3	0	0	-1	(R_x, R_y, R_z)	$(\alpha_{xy}, \alpha_{yz}, \alpha_{xz})$
F_u	3	0	0	-1	-3	0	0	1	(T_x, T_y, T_z)	

$\epsilon = e^{2\pi i/3}$

T_d	I	8C₃	6σ_d	6S₄	3S₄² ≡ 3C₂		
A₁	+1	+1	+1	+1	+1		$\alpha_{xx} + \alpha_{yy} + \alpha_{zz}$
A₂	+1	+1	-1	-1	+1		
E	+2	-1	0	0	+2		$(\alpha_{xx} + \alpha_{yy} - 2\alpha_{zz}, \alpha_{xx} - \alpha_{yy})$
F₁	+3	0	-1	+1	-1	(R_x, R_y, R_z)	
F₂	+3	0	+1	-1	-1	(T_x, T_y, T_z)	$(\alpha_{xy}, \alpha_{yz}, \alpha_{xz})$

O	I	6C₄	3C₂(= C₄²)	8C₃	6C₂		
A₁	1	1	1	1	1		$\alpha_{xx} + \alpha_{yy} + \alpha_{zz}$
A₂	1	-1	1	1	-1		
E	2	0	2	-1	0		$(2\alpha_{zz} - \alpha_{xx} - \alpha_{yy}, \alpha_{xx} - \alpha_{yy})$
F₁	3	1	-1	0	-1	$(R_x, R_y, R_z), (T_x, T_y, T_z)$	
F₂	3	-1	-1	0	1		$(\alpha_{xy}, \alpha_{yz}, \alpha_{xz})$

O_h	I	$8C_3$	$6C_2$	$6C_4$	$3C_4^2 \equiv 3C_2'$	$S_2 \equiv i$	$6S_4$	$8S_6$	$3\sigma_h$	$6\sigma_d$		
A_{1g}	+1	+1	+1	+1	+1	+1	+1	+1	+1	+1	$\alpha_{xx} + \alpha_{yy} + \alpha_{zz}$	
A_{1u}	+1	+1	+1	+1	+1	-1	-1	-1	-1	-1		
A_{2g}	+1	+1	-1	-1	+1	+1	-1	+1	+1	-1		
A_{2u}	+1	+1	-1	-1	+1	-1	+1	-1	-1	+1		
E_g	+2	-1	0	0	+2	0	0	-1	+2	0	$(\alpha_{xx} + \alpha_{yy} - 2\alpha_{zz}, \alpha_{xx} - \alpha_{yy})$	
E_u	+2	-1	0	0	+2	-2	0	+1	-2	0		
F_{1g}	+3	0	-1	+1	-1	+3	+1	0	-1	-1	(R_x, R_y, R_z)	
F_{1u}	+3	0	-1	+1	-1	-3	-1	0	+1	+1	(T_x, T_y, T_z)	
F_{2g}	+3	0	+1	-1	-1	+3	-1	0	-1	+1	$(\alpha_{xy}, \alpha_{yz}, \alpha_{xz})$	
F_{2u}	+3	0	+1	-1	-1	-3	+1	0	+1	-1		

I_h	I	$12C_5$	$12C_5^2$	$20C_3$	$15C_2$	i	$12S_{10}$	$12S_{10}^3$	$20S_6$	$15\sigma_v$		
A_g	1	1	1	1	1	1	1	1	1	1	$\alpha_{xx} + \alpha_{yy} + \alpha_{zz}$	(R_z, R_y, R_z) (T_x, T_y, T_z)
A_u	1	1	1	1	1	-1	-1	-1	-1	-1		
F_{1g}	3	$2c\frac{\pi}{5}$	$2c\frac{3\pi}{5}$	0	-1	3	$2c\frac{3\pi}{5}$	$2c\frac{\pi}{5}$	0	-1		
F_{1u}	3	$2c\frac{\pi}{5}$	$2c\frac{3\pi}{5}$	0	-1	-3	$-2c\frac{3\pi}{5}$	$-2c\frac{\pi}{5}$	0	1		
F_{2g}	3	$2c\frac{3\pi}{5}$	$2c\frac{\pi}{5}$	0	-1	3	$2c\frac{\pi}{5}$	$2c\frac{3\pi}{5}$	0	-1		
F_{2u}	3	$2c\frac{3\pi}{5}$	$2c\frac{\pi}{5}$	0	-1	-3	$-2c\frac{\pi}{5}$	$-2c\frac{3\pi}{5}$	0	1		
G_g	4	-1	-1	1	0	4	-1	-1	1	0		
G_u	4	-1	-1	1	0	-4	1	1	-1	0		
H_g	5	0	0	-1	1	5	0	0	-1	1		
H_u	5	0	0	-1	1	-5	0	0	1	-1		
$(2\alpha_{zz} - \alpha_{xx} - \alpha_{yy}, \alpha_{xx} - \alpha_{yy}, \alpha_{xx} - \alpha_{yy}, \alpha_{xy}, \alpha_{yz}, \alpha_{xz})$												

$c = \cosine$; G and H denote four- and five-fold degenerate species, respectively

APPENDIX II. MATRIX ALGEBRA

II.1. Definition of a Matrix

A matrix is an array of numbers or symbols for numbers. In general, it is written as:

$$\mathbf{A} = \begin{bmatrix} a_{11} & a_{12} & a_{13} & \cdots & a_{1n} \\ a_{21} & a_{22} & a_{23} & \cdots & a_{2n} \\ a_{31} & a_{32} & a_{33} & \cdots & a_{3n} \\ \vdots & \vdots & \vdots & & \vdots \\ a_{m1} & a_{m2} & a_{m3} & \cdots & a_{mn} \end{bmatrix} = [a_{ij}]$$

Here, the square brackets indicate that these elements constitute a matrix. \mathbf{A} and $[a_{ij}]$ indicate the same matrix in abbreviated forms. In the latter, a_{ij} denotes the element in the i th row and j th column. If $m = n$, it is called a *square matrix*. In a square matrix, the set of elements a_{ij} with $i = j$ are called the *diagonal elements*. If all the diagonal elements are one and all the *off-diagonal elements* are zero, such a matrix is called a *unit (or identity) matrix*, and expressed as \mathbf{E} (or \mathbf{I}). A *diagonal matrix*, \mathbf{D} , is similar to the unit matrix except that the diagonal elements are not necessarily equal. Thus

$$\mathbf{E} = \begin{bmatrix} 1 & 0 & 0 \\ 0 & 1 & 0 \\ 0 & 0 & 1 \end{bmatrix} \quad \mathbf{D} = \begin{bmatrix} d_{11} & 0 & 0 \\ 0 & d_{22} & 0 \\ 0 & 0 & d_{33} \end{bmatrix}$$

A matrix is called *symmetric* if the relationship $a_{ij} = a_{ji}$ holds for all off-diagonal elements. If $a_{ij} = -a_{ji}$, it is called *antisymmetric*.

If $m \neq n$, the matrix is called a *rectangular matrix*. Among them, the one-column matrix and one-row matrix shown below are important.

$$\mathbf{X} = \begin{bmatrix} x_1 \\ x_2 \\ x_3 \end{bmatrix} \quad \tilde{\mathbf{X}} = [x_1 \quad x_2 \quad x_3]$$

Sometimes, the former is called a *vector*. The tilde sign over \mathbf{X} in the latter indicates a *transpose* of a matrix in which the elements are interchanged across the diagonal. In the case of a 2×2 matrix, we have

$$\mathbf{A} = \begin{bmatrix} a_{11} & a_{12} \\ a_{21} & a_{22} \end{bmatrix} \quad \tilde{\mathbf{A}} = \begin{bmatrix} a_{11} & a_{21} \\ a_{12} & a_{22} \end{bmatrix}$$

II.2. Addition and Subtraction

When two matrices are of same dimensions, they can be added or subtracted by the rule that $u_{ij} = a_{ij} \pm b_{ij}$. If B is

$$\mathbf{B} = \begin{bmatrix} b_{11} & b_{12} \\ b_{21} & b_{22} \end{bmatrix}$$

then

$$\mathbf{U} = \mathbf{A} \pm \mathbf{B} = \begin{bmatrix} a_{11} \pm b_{11} & a_{12} \pm b_{12} \\ a_{21} \pm b_{21} & a_{22} \pm b_{22} \end{bmatrix}$$

II.3. Multiplication

Two matrices can be multiplied only if the number of columns of the first matrix \mathbf{B} is equal to the number of rows of the second matrix \mathbf{A} . Each element of the resulting matrix, $\mathbf{U} = \mathbf{BA}$, is given by

$$u_{ij} = \sum_{k=1}^n b_{ik} a_{kj}$$

For example

$$\mathbf{BA} = \begin{bmatrix} b_{11}a_{11} + b_{12}a_{21} & b_{11}a_{12} + b_{12}a_{22} \\ b_{21}a_{11} + b_{22}a_{21} & b_{21}a_{12} + b_{22}a_{22} \end{bmatrix}$$

If \mathbf{X} is a column matrix and $\tilde{\mathbf{X}}$ is its transpose, then

$$\mathbf{AX} = \begin{bmatrix} a_{11} & a_{12} \\ a_{21} & a_{22} \end{bmatrix} \begin{bmatrix} x_1 \\ x_2 \end{bmatrix} = \begin{bmatrix} a_{11}x_1 + a_{12}x_2 \\ a_{21}x_1 + a_{22}x_2 \end{bmatrix}$$

$$\tilde{\mathbf{X}}\mathbf{AX} = \begin{bmatrix} x_1 & x_2 \end{bmatrix} \begin{bmatrix} a_{11}x_1 + a_{12}x_2 \\ a_{21}x_1 + a_{22}x_2 \end{bmatrix} = a_{11}x_1^2 + a_{12}x_1x_2 + a_{21}x_1x_2 + a_{22}x_2^2$$

It should be noted that matrix multiplication is generally *not commutative*. Namely, \mathbf{BA} is not necessarily equal to \mathbf{AB} . For example

$$\begin{bmatrix} 1 & 2 \\ 3 & 4 \end{bmatrix} \begin{bmatrix} 1 & 0 \\ 2 & 1 \end{bmatrix} = \begin{bmatrix} 5 & 2 \\ 11 & 4 \end{bmatrix}$$

$$\begin{bmatrix} 1 & 0 \\ 2 & 1 \end{bmatrix} \begin{bmatrix} 1 & 2 \\ 3 & 4 \end{bmatrix} = \begin{bmatrix} 1 & 2 \\ 5 & 8 \end{bmatrix}$$

However, the *associative law* holds for matrix multiplication. Thus

$$\mathbf{A}(\mathbf{B} + \mathbf{C}) = \mathbf{AB} + \mathbf{AC} \quad \text{and} \quad (\mathbf{AB})\mathbf{C} = \mathbf{A}(\mathbf{BC})$$

If a constant λ is multiplied to \mathbf{A} , each element of \mathbf{A} is multiplied by λ :

$$\lambda\mathbf{A} = \begin{bmatrix} \lambda a_{11} & \lambda a_{12} \\ \lambda a_{21} & \lambda a_{22} \end{bmatrix}$$

II.4. Division

Division by a matrix is accomplished as multiplication of its reciprocal (or inverse) matrix. For example, the division of \mathbf{B} by \mathbf{A} is written as

$$\mathbf{U} = \mathbf{B}/\mathbf{A} = \mathbf{BA}^{-1}$$

Here, \mathbf{A}^{-1} is the reciprocal matrix of \mathbf{A} , which is defined as

$$\mathbf{AA}^{-1} = \mathbf{A}^{-1}\mathbf{A} = \mathbf{E}$$

Only the square matrix can have its reciprocal matrix. The reciprocal of the product matrix is given by

$$(\mathbf{BA})^{-1} = \mathbf{A}^{-1}\mathbf{B}^{-1}$$

If $\mathbf{A} = \tilde{\mathbf{A}}^{-1}$ (i.e., $\tilde{\mathbf{A}}\mathbf{A} = \mathbf{E}$), such a square matrix is called an *orthogonal matrix*. For example

$$\begin{bmatrix} 1/\sqrt{3} & 1/\sqrt{3} & 1/\sqrt{3} \\ 2/\sqrt{6} & -1/\sqrt{6} & -1/\sqrt{6} \\ 0 & 1/\sqrt{2} & -1/\sqrt{2} \end{bmatrix}, \quad \begin{bmatrix} \cos \phi & \sin \phi & 0 \\ -\sin \phi & \cos \phi & 0 \\ 0 & 0 & 1 \end{bmatrix}$$

II.5. Determinant

The determinant $|\mathbf{A}|$ of a square matrix \mathbf{A} is defined as

$$|\mathbf{A}| = \begin{vmatrix} a_{11} & a_{12} & a_{13} & \cdots & a_{1n} \\ a_{21} & a_{22} & a_{23} & \cdots & a_{2n} \\ a_{31} & a_{32} & a_{33} & \cdots & a_{3n} \\ \vdots & \vdots & \vdots & & \vdots \\ a_{n1} & a_{n2} & a_{n3} & \cdots & a_{nn} \end{vmatrix} = \sum (-1)^h a_{1a} a_{2b} \cdots a_{nk}$$

Here, h is the number of exchanges necessary to bring the sequence a, b, \dots, k back to the natural order, $1, 2, \dots, n$, and the summation is taken over all permutations of a, b, \dots, k . For example

$$\begin{vmatrix} a_{11} & a_{12} & a_{13} \\ a_{21} & a_{22} & a_{23} \\ a_{31} & a_{32} & a_{33} \end{vmatrix} = a_{11}a_{22}a_{33} + a_{12}a_{23}a_{31} + a_{13}a_{21}a_{32} \\ - a_{13}a_{22}a_{31} - a_{11}a_{23}a_{32} - a_{12}a_{21}a_{33}$$

Here, the dotted lines indicate how to obtain positive terms. *Three different lines* were used to show how the products on the right side were obtained. Likewise, the negative terms can be obtained by changing the direction of the dotted lines by 90° . As shown above, vertical lines are used to express the determinant. It can be shown that

$$|\mathbf{AB}| = |\mathbf{A}||\mathbf{B}|$$

II.6. Eigenvalues (Characteristic Values)

If \mathbf{A} is a square matrix of dimension n and \mathbf{E} is the unit matrix of the same dimension, then

$$|\mathbf{A} - \lambda\mathbf{E}| = 0$$

is called the *characteristic equation* of the matrix \mathbf{A} . For example, the characteristic equation for \mathbf{A} given below is written as

$$\mathbf{A} = \begin{bmatrix} a & b \\ b & a \end{bmatrix} \quad \begin{vmatrix} a-\lambda & b \\ b & a-\lambda \end{vmatrix} = 0$$

Expansion of the characteristic equation gives

$$\lambda^2 - 2a\lambda + a^2 - b^2 = 0$$

The two eigenvalues of this equation are

$$\lambda_1 = a + b, \quad \lambda_2 = a - b$$

More generally, the characteristic equation of a matrix \mathbf{A} having the dimension $n \times n$ is written as

$$\lambda^n + c_1\lambda^{n-1} + c_2\lambda^{n-2} + \dots + c_{n-1}\lambda + c_n = 0$$

There are two simple relationships between the coefficients c_1, c_2, \dots, c_n and eigenvalues:

$$a_{11} + a_{22} + \dots + a_{nn} = -c_1 = \lambda_1 + \lambda_2 + \dots + \lambda_n$$

$$|\mathbf{A}| = \pm c_n = \lambda_1\lambda_2 \dots \lambda_n \quad (+ \text{ for even } n; - \text{ for odd } n)$$

These relationships are readily confirmed by the example above, given for a 2×2 matrix.

II.7. Eigenvectors

If λ_a is an eigenvalue of \mathbf{A} , a vector, \mathbf{l}_a , which satisfies the relation

$$\mathbf{A}\mathbf{l}_a = \mathbf{l}_a\lambda_a$$

is called an *eigenvector* of \mathbf{A} . As an example, consider the 2×2 matrix mentioned above. The \mathbf{l}_1 for λ_1 is

$$\begin{bmatrix} a & b \\ b & a \end{bmatrix} \begin{bmatrix} l_{11} \\ l_{21} \end{bmatrix} = \begin{bmatrix} l_{11} \\ l_{21} \end{bmatrix} (a + b)$$

Then, we obtain $l_{11} = l_{21}$. Their absolute values can be determined only by using the normalization condition:

$$l_{11}^2 + l_{21}^2 = 1$$

Then

$$l_{11} = l_{21} = 1/\sqrt{2}$$

Using the same procedure, we obtain

$$l_{12} = 1/\sqrt{2} \quad \text{and} \quad l_{22} = -1/\sqrt{2}$$

for λ_2 . If we assemble these two results by columns, we have

$$\begin{bmatrix} a & b \\ b & a \end{bmatrix} \begin{bmatrix} 1/\sqrt{2} & 1/\sqrt{2} \\ 1/\sqrt{2} & -1/\sqrt{2} \end{bmatrix} = \begin{bmatrix} 1/\sqrt{2} & 1/\sqrt{2} \\ 1/\sqrt{2} & -1/\sqrt{2} \end{bmatrix} \begin{bmatrix} a+b & 0 \\ 0 & a-b \end{bmatrix}$$

More generally, this is written as

$$\mathbf{A}\mathbf{L} = \mathbf{L}\mathbf{\Lambda}$$

By multiplying \mathbf{L}^{-1} on both sides, we obtain

$$\mathbf{L}^{-1}\mathbf{A}\mathbf{L} = \mathbf{L}^{-1}\mathbf{L}\mathbf{\Lambda} = \mathbf{\Lambda}$$

It is seen that the \mathbf{L} matrix can transform the \mathbf{A} matrix into a diagonal matrix with its eigenvalues as the diagonal elements. As shown above, the \mathbf{L} matrix can be calculated once the λ values of the \mathbf{A} matrix are obtained.

APPENDIX III. GENERAL FORMULAS FOR CALCULATING THE NUMBER OF NORMAL VIBRATIONS IN EACH SPECIES

Most of these tables were reproduced from G. Herzberg, *Molecular Spectra and Molecular Structure*, Vol. II (Ref. 1 of Chapter 1).

For the derivations of these tables, see K. Nakamoto and M. A. McKinney, *J. Chem. Educ.* **77**, 775 (2000).

TABLE A. Point Groups Including Only Nondegenerate Vibrations

Point Group	Total Number of Atoms	Species	Number of Vibrations ^a
C₂	$2m + m_0$	A B	$3m + m_0 - 2$ $3m + 2m_0 - 4$
C_s	$2m + m_0$	A' A''	$3m + 2m_0 - 3$ $3m + m_0 - 3$
C_i ≡ S₂	$2m + m_0$	A _g A _u	$3m - 3$ $3m + 3m_0 - 3$
C_{2v}	$4m + 2m_{xz} + 2m_{yz} + m_0$	A ₁ A ₂ B ₁ B ₂	$3m + 2m_{xz} + 2m_{yz} + m_0 - 1$ $3m + m_{xz} + m_{yz} - 1$ $3m + 2m_{xz} + m_{yz} + m_0 - 2$ $3m + m_{xz} + 2m_{yz} + m_0 - 2$
C_{2h}	$4m + 2m_h + 2m_2 + m_0$	A _g A _u B _g B _u	$3m + 2m_h + m_2 - 1$ $3m + m_h + m_2 + m_0 - 1$ $3m + m_h + 2m_2 - 2$ $3m + 2m_h + 2m_2 + 2m_0 - 2$
D₂ ≡ V	$4m + 2m_{2x} + 2m_{2y} + 2m_{2z} + m_0$	A B ₁ B ₂ B ₃	$3m + m_{2x} + m_{2y} + m_{2z}$ $3m + 2m_{2x} + 2m_{2y} + m_{2z} + m_0 - 2$ $3m + 2m_{2x} + m_{2y} + 2m_{2z} + m_0 - 2$ $3m + m_{2x} + 2m_{2y} + 2m_{2z} + m_0 - 2$
D_{2h} ≡ V_h	$8m + 4m_{xy} + 4m_{xz} + 4m_{yz} + 2m_{2x} + 2m_{2y} + 2m_{2z} + m_0$	A _g A _u B _{1g} B _{1u} B _{2g} B _{2u} B _{3g} B _{3u}	$3m + 2m_{xy} + 2m_{xz} + 2m_{yz} + m_{2x} + m_{2y} + m_{2z}$ $3m + m_{xy} + m_{xz} + m_{yz}$ $3m + 2m_{xy} + m_{xz} + m_{yz} + m_{2x} + m_{2y} - 1$ $3m + m_{xy} + 2m_{xz} + 2m_{yz} + m_{2x}$ $\quad + m_{2y} + m_{2z} + m_0 - 1$ $3m + m_{xy} + 2m_{xz} + m_{yz} + m_{2x} + m_{2z} - 1$ $3m + 2m_{xy} + m_{xz} + 2m_{yz} + m_{2x} + m_{2y}$ $\quad + m_{2z} + m_0 - 1$ $3m + m_{xy} + m_{xz} + 2m_{yz} + m_{2y} + m_{2z} - 1$ $3m + 2m_{xy} + 2m_{xz} + m_{yz} + m_{2x}$ $\quad + m_{2y} + m_{2z} + m_0 - 1$

^aNote that m is always the number of sets of equivalent nuclei not on any element of symmetry; m_0 is the number of nuclei lying on all symmetry elements present; m_{xy} , m_{xz} , m_{yz} are the numbers of sets of nuclei lying on the xy , xz , yz plane, respectively, but not on any axes going through these planes; m_2 is the number of sets of nuclei on a twofold axis but not at the point of intersection with another element of symmetry; m_{2x} , m_{2y} , m_{2z} are the numbers of sets of nuclei lying on the x , y , or z axis if they are twofold axes, but not on all of them; m_h is the number of sets of nuclei on a plane σ_h but not on the axis perpendicular to this plane.

TABLE B. Point Groups Including Degenerate Vibrations

Point Group	Total Number of Atoms	Species	Number of Vibrations ^a
D₃	$6m + 3m_2 + 2m_3 + m_0$	A_1 A_2 E	$3m + m_2 + m_3$ $3m + 2m_2 + m_3 + m_0 - 2$ $6m + 3m_2 + 2m_3 + m_0 - 2$
C_{3v}	$6m + 3m_v + m_0$	A_1 A_2 E	$3m + 2m_v + m_0 - 1$ $3m + m_v - 1$ $6m + 3m_v + m_0 - 2$
C_{4v}	$8m + 4m_v + 4m_d + m_0$	A_1 A_2 B_1 B_2 E	$3m + 2m_v + 2m_d + m_0 - 1$ $3m + m_v + m_d - 1$ $3m + 2m_v + m_d$ $3m + m_v + 2m_d$ $6m + 3m_v + 3m_d + m_0 - 2$
C_{∞v}	m_0	Σ^+ Σ^- Π Δ, Φ, \dots	$m_0 - 1$ 0 $m_0 - 2$ 0
D_{2d} ≡ V_d	$8m + 4m_d + 4m_2$ $+ 2m_4 + m_0$	A_1 A_2 B_1 B_2 E	$3m + 2m_d + m_2 + m_4$ $3m + m_d + 2m_2 - 1$ $3m + m_d + m_2$ $3m + 2m_d + 2m_2 + m_4 + m_0 - 1$ $6m + 3m_d + 3m_2 + 2m_4 + m_0 - 2$
D_{3d}	$12m + 6m_d + 6m_2$ $+ 2m_6 + m_0$	A_{1g} A_{1u} A_{2g} A_{2u} E_g E_u	$3m + 2m_d + m_2 + m_6$ $3m + m_d + m_2$ $3m + m_d + 2m_2 - 1$ $3m + 2m_d + 2m_2 + m_6 + m_0 - 1$ $6m + 3m_d + 3m_2 + m_6 - 1$ $6m + 3m_d + 3m_2 + m_6 + m_0 - 1$
D_{4d}	$16m + 8m_d + 8m_2$ $+ 2m_8 + m_0$	A_1 A_2 B_1 B_2 E_1 E_2 E_3	$3m + 2m_d + m_2 + m_8$ $3m + m_d + 2m_2 - 1$ $3m + m_d + m_2$ $3m + 2m_d + 2m_2 + m_8 + m_0 - 1$ $6m + 3m_d + 3m_2 + m_8 + m_0 - 1$ $6m + 3m_d + 3m_2$ $6m + 3m_d + 3m_2 + m_8 - 1$
D_{3h}	$12m + 6m_v + 6m_h + 3m_2$ $+ 2m_3 + m_0$	A'_1 A''_1 A'_2 A''_2 E' E''	$3m + 2m_v + 2m_h + m_2 + m_3$ $3m + m_v + m_h$ $3m + m_v + 2m_h + m_2 - 1$ $3m + 2m_v + m_h + m_2 + m_3 + m_0 - 1$ $6m + 3m_v + 4m_h + 2m_2$ $+ m_3 + m_0 - 1$ $6m + 3m_v + 2m_h + m_2 + m_3 - 1$

TABLE B. (Continued)

Point Group	Total Number of Atoms	Species	Number of Vibrations ^a
D_{4h}	$16m + 8m_v + 8m_d + 8m_h$ $+ 4m_2 + 4m'_2 + 2m_4 + m_0$	A_{1g} A_{1u} A_{2g} A_{2u} B_{1g} B_{1u} B_{2g} B_{2u} E_g E_u	$3m + 2m_v + 2m_d + 2m_h$ $+ m_2 + m'_2 + m_4$ $3m + m_v + m_d + m_h$ $3m + m_v + m_d + 2m_h + m_2 + m'_2 - 1$ $3m + 2m_v + 2m_d + m_h + m_2$ $+ m'_2 + m_4 + m_0 - 1$ $3m + 2m_v + m_d + 2m_h + m_2 + m'_2$ $3m + m_v + 2m_d + m_h + m'_2$ $3m + m_v + 2m_d + 2m_h + m_2 + m'_2$ $3m + 2m_v + m_d + m_h + m_2$ $6m + 3m_v + 3m_d + 2m_h + m_2$ $+ m'_2 + m_4 - 1$ $6m + 3m_v + 3m_d + 4m_h + 2m_2$ $+ 2m'_2 + m_4 + m_0 - 1$
D_{5h}	$20m + 10m_v + 10m_h$ $+ 5m_2 + 2m_5 + m_0$	A'_1 A''_1 A'_2 A''_2 E'_1 E''_1 E'_2 E''_2	$3m + 2m_v + 2m_h + m_2 + m_5$ $3m + m_v + m_h$ $3m + m_v + 2m_h + m_2 - 1$ $3m + 2m_v + m_h + m_2 + m_5 + m_0 - 1$ $6m + 3m_v + 4m_h + 2m_2 + m_5$ $+ m_0 - 1$ $6m + 3m_v + 2m_h + m_2 + m_5 - 1$ $6m + 3m_v + 4m_h + 2m_2$ $6m + 3m_v + 2m_h + m_2$
D_{6h}	$24m + 12m_v + 12m_d$ $+ 12m_h + 6m_2 + 6m'_2$ $+ 2m_6 + m_0$	A_{1g} A_{1u} A_{2g} A_{2u} B_{1g} B_{1u} B_{2g} B_{2u} E_{1g} E_{1u} E_{2g} E_{2u}	$3m + 2m_v + 2m_d + 2m_h$ $+ m_2 + m'_2 + m_6$ $3m + m_v + m_d + m_h$ $3m + m_v + m_d + 2m_h + m_2 + m'_2 - 1$ $3m + 2m_v + 2m_d + m_h + m_2 + m'_2$ $+ m_6 + m_0 - 1$ $3m + m_v + 2m_d + m_h + m'_2$ $3m + 2m_v + m_d + 2m_h + m_2 + m'_2$ $3m + 2m_v + m_d + m_h + m_2$ $3m + m_v + 2m_d + 2m_h + m_2 + m'_2$ $6m + 3m_v + 3m_d + 2m_h$ $+ m_2 + m'_2 + m_6 - 1$ $6m + 3m_v + 3m_d + 4m_h + 2m_2 + 2m'_2$ $+ m_6 + m_0 - 1$ $6m + 3m_v + 3m_d + 4m_h + 2m_2 + 2m'_2$ $6m + 3m_v + 3m_d + 2m_h + m_2 + m'_2$
D_{∞h}	$2m_\infty + m_0$	Σ_g^+ Σ_u^+ Σ_g^-, Σ_u^- Π_g Π_u $\Delta_g, \Delta_u, \dots$ Φ_g, Φ_u, \dots	m_∞ $m_\infty + m_0 - 1$ 0 $m_\infty - 1$ $m_\infty + m_0 - 1$ 0 0

(Continued)

TABLE B. (Continued)

Point Group	Total Number of Atoms	Species	Number of Vibrations ^a
T_d	$24m + 12m_d + 6m_2$ $+ 4m_3 + m_0$	A_1 A_2 E F_1 F_2	$3m + 2m_d + m_2 + m_3$ $3m + m_d$ $6m + 3m_d + m_2 + m_3$ $9m + 4m_d + 2m_2 + m_3 - 1$ $9m + 5m_d + 3m_2 + 2m_3 + m_0 - 1$
O_h	$48m + 24m_h + 24m_d$ $+ 12m_2 + 8m_3 + 6m_4 + m_0$	A_{1g} A_{1u} A_{2g} A_{2u} E_g E_u F_{1g} F_{1u} F_{2g} F_{2u}	$3m + 2m_h + 2m_d + m_2 + m_3 + m_4$ $3m + m_h + m_d$ $3m + 2m_h + m_d + m_2$ $3m + m_h + 2m_d + m_2 + m_3$ $6m + 4m_h + 3m_d + 2m_2 + m_3 + m_4$ $6m + 2m_h + 3m_d + m_2 + m_3$ $9m + 4m_h + 4m_d + 2m_2$ $+ m_3 + m_4 - 1$ $9m + 5m_h + 5m_d + 3m_2 + 2m_3$ $+ 2m_4 + m_0 - 1$ $9m + 4m_h + 5m_d + 2m_2 + 2m_3 + m_4$ $9m + 5m_h + 4m_d + 2m_2 + m_3 + m_4$
T_h	$24m + 12m_v + 8m_3$ $+ 6m_2 + m_0$	A_g A_u E_g E_u F_g F_u	$3m + 2m_v + m_3 + m_2$ $3m + m_v + m_3$ $3m + 2m_v + m_3 + m_2$ $3m + m_v + m_3$ $9m + 4m_v + 3m_3 + 2m_2 - 1$ $9m + 5m_v + 3m_3 + 3m_2 + m_0 - 1$
I_h	$120m + 60m_v + 30m_2$ $+ 20m_3 + 12m_5 + m_0$	A_g A_u F_{1g} F_{1u} F_{2g} F_{2u} G_g G_u H_g H_u	$3m + 2m_v + m_2 + m_3 + m_5$ $3m + m_v$ $9m + 4m_v + 2m_2 + m_3 + m_5 - 1$ $9m + 5m_v + 3m_2 + 2m_3$ $+ 2m_5 + m_0 - 1$ $9m + 4m_v + 2m_2 + m_3$ $9m + 5m_v + 3m_2 + 2m_3 + m_5$ $12m + 6m_v + 3m_2 + 2m_3 + m_5$ $12m + 6m_v + 3m_2 + 2m_3 + m_5$ $15m + 8m_v + 4m_2 + 3m_3 + 2m_5$ $15m + 7m_v + 3m_2 + 2m_3 + m_5$

^aNote that m is the number of sets of nuclei not any element of symmetry; m_0 is the number of nuclei on all elements of symmetry; m_2, m_3, m_4, \dots are the numbers of sets of nuclei on a twofold, threefold, fourfold, and so on, axis but not on any other element of symmetry that does not wholly coincide with that axis; m'_2 is the number of sets of nuclei on a twofold axis called C'_2 in the previous character tables; m_v, m_d, m_h are the numbers of sets of nuclei on planes $\sigma_v, \sigma_d, \sigma_h$, respectively, but not on any other element of symmetry.

APPENDIX IV. DIRECT PRODUCTS OF IRREDUCIBLE REPRESENTATIONS

As shown in Sec. 1.10, the characters for direct products can be obtained by multiplying the corresponding characters of two representations and resolving the result into those of the irreducible representations by using Eq. 1.74. This procedure, however, can be greatly simplified if we use the following rules (Ref. 3 of Chapter 1).

1. General Rules

$$\begin{array}{llll}
 A \times A = A, & B \times B = A, & A \times B = B, & A \times E = E \\
 B \times E = E, & A \times F = F, & B \times F = F & \\
 g \times g = g, & u \times u = g, & u \times g = u & \\
 ' \times ' = ', & " \times " = ', & ' \times " = " & \\
 A \times E_1 = E_1, & A \times E_2 = E_2, & B \times E_1 = E_2, & B \times E_2 = E_1
 \end{array}$$

2. Subscripts on A or B

$$1 \times 1 = 1, \quad 2 \times 2 = 1, \quad 1 \times 2 = 2 \quad \text{except for } \mathbf{D}_2 \text{ and } \mathbf{D}_{2h}$$

where

$$1 \times 2 = 3, \quad 2 \times 3 = 1, \quad 1 \times 3 = 2$$

3. Doubly Degenerate Representations

For \mathbf{C}_3 , \mathbf{C}_{3h} , \mathbf{C}_{3v} , \mathbf{D}_3 , \mathbf{D}_{3h} , \mathbf{D}_{3d} , \mathbf{C}_6 , \mathbf{C}_{6h} , \mathbf{C}_{6v} , \mathbf{D}_6 , \mathbf{D}_{6h} , \mathbf{S}_6 , \mathbf{O} , \mathbf{O}_h , \mathbf{T} , \mathbf{T}_d , \mathbf{T}_h .

$$\begin{array}{l}
 E_1 \times E_1 = E_2 \times E_2 = A_1 + A_2 + E_2 \\
 E_1 \times E_2 = B_1 + B_2 + E_1
 \end{array}$$

For \mathbf{C}_4 , \mathbf{C}_{4v} , \mathbf{C}_{4h} , \mathbf{D}_{2d} , \mathbf{D}_4 , \mathbf{D}_{4h} , and \mathbf{S}_4

$$E \times E = A_1 + A_2 + B_1 + B_2$$

For groups in the lists above that have symbols A , B , or E without subscripts, read $A_1 = A_2 = A$, and so on.

4. Triply Degenerate Representations

For \mathbf{T}_d , \mathbf{O} , \mathbf{O}_h :

$$\begin{array}{l}
 E \times F_1 = E \times F_2 = F_1 + F_2 \\
 F_1 \times F_1 = F_2 \times F_2 = A_1 + E + F_1 + F_2 \\
 F_1 \times F_2 = A_2 + E + F_1 + F_2
 \end{array}$$

For T and T_h , drop subscripts 1 and 2 from A and F .

5. Linear Molecules ($C_{\infty v}$ and $D_{\infty h}$)

$$\begin{aligned}
\Sigma^+ \times \Sigma^+ &= \Sigma^- \times \Sigma^- = \Sigma^+, & \Sigma^+ \times \Sigma^- &= \Sigma^- \\
\Sigma^+ \times \Pi &= \Sigma^- \times \Pi = \Pi & \Sigma^+ \times \Delta &= \Sigma^- \times \Delta = \Delta \\
\Pi \times \Pi &= \Sigma^+ + \Sigma^- + \Delta \\
\Delta \times \Delta &= \Sigma^+ + \Sigma^- + \Gamma \\
\Pi \times \Delta &= \Pi + \Phi
\end{aligned}$$

Using rule 3, in C_{3v} , we find that $E \times E = A_1 + A_2 + E$ (Sec. 1.10). Similarly, using rules 1 and 3, in D_{4h} , we find that $E_u \times E_u = A_{1g} + A_{2g} + B_{1g} + B_{2g}$ (Sec. 1.23).

APPENDIX V. NUMBER OF INFRARED- AND RAMAN-ACTIVE STRETCHING VIBRATIONS FOR MX_nY_m -TYPE MOLECULES

Compound	Structure	Point Group	IR or Raman	M–X Stretching	M–Y Stretching
MX_6	Octahedral	O_h	IR R	F_{1u} A_{1g}, E_g	
MX_5Y	Octahedral	C_{4v}	IR R	$2A_1, E$ $2A_1, B_1, E$	A_1 A_1
<i>trans</i> - MX_4Y_2	Octahedral	D_{4h}	IR R	E_u A_{1g}, B_{1g}	A_{2u} A_{1g}
<i>cis</i> - MX_4Y_2	Octahedral	C_{2v}	IR R	$2A_1, B_1, B_2$ $2A_1, B_1, B_2$	A_1, B_1 A_1, B_1
<i>mer</i> - MX_3Y_3	Octahedral	C_{2v}	IR R	$2A_1, B_2$ $2A_1, B_2$	$2A_1, B_1$ $2A_1, B_1$
<i>fac</i> - MX_3Y_3	Octahedral	C_{3v}	IR R	A_1, E A_1, E	A_1, E A_1, E
MX_5	Trigonal–bipyramidal	D_{3h}	IR R	A''_2, E' $2A'_1, E'$	
MX_5	Tetragonal–pyramidal	C_{4v}	IR R	$2A_1, E$ $2A_1, B_1, E$	
MX_4	Tetrahedral	T_d	IR R	F_2 A_1, F_2	
MX_3Y	Tetrahedral	C_{3v}	IR R	A_1, E A_1, E	A_1 A_1
MX_2Y_2	Tetrahedral	C_{2v}	IR R	A_1, B_1 A_1, B_1	A_1, B_2 A_1, B_2
Polymeric $MX_2Y_2^a$	Octahedral	C_i	IR R	$2A_u$ $2A_g$	A_u A_g
MX_4	Square–planar	D_{4h}	IR R	E_u A_{1g}, B_{2g}	
MX_3Y	Planar	C_{2v}	IR R	$2A_1, B_1$ $2A_1, B_1$	A_1 A_1

APPENDIX V. (Continued)

Compound	Structure	Point Group	IR or Raman	M–X Stretching	M–Y Stretching
<i>trans</i> -MX ₂ Y ₂	Planar	D _{2h}	IR R	B _{3u} A _g	B _{2u} A _g
<i>cis</i> -MX ₂ Y ₂	Planar	C _{2v}	IR R	A ₁ , B ₂ A ₁ , B ₂	A ₁ , B ₂ A ₁ , B ₂
MX ₃	Pyramidal	C _{3v}	IR R	A ₁ , E A ₁ , E	
MX ₃	Planar	D _{3h}	IR R	E' A' ₁ , E'	

^aBridging through X atoms.

APPENDIX VI. DERIVATION OF EQ. 1.113

Using the rectangular coordinates, we write the kinetic energy as

$$2T = \tilde{\mathbf{X}}\mathbf{M}\dot{\mathbf{X}} \quad (\text{A.1})$$

where

$$\mathbf{X} = \begin{bmatrix} x_1 \\ y_1 \\ z_1 \\ x_2 \\ \vdots \\ z_N \end{bmatrix} \quad \text{and} \quad \mathbf{M} = \begin{bmatrix} m_1 & & & & & \\ & m_1 & & & & \\ & & m_1 & & & \\ & & & m_2 & & \\ & & & & \ddots & \\ & & & & & m_N \end{bmatrix}$$

By definition, the momentum p_{x_1} conjugated with x_1 is given by

$$p_{x_1} = \frac{\partial T}{\partial \dot{x}_1} = m_1 \dot{x}_1$$

$p_{y_1} \cdots p_{z_N}$ take similar forms. Using the conjugate momenta, we write T as

$$\begin{aligned} 2T &= \frac{1}{m_1} p_{x_1}^2 + \frac{1}{m_1} p_{y_1}^2 + \cdots + \frac{1}{m_N} p_{z_N}^2 \\ &= \tilde{\mathbf{P}}_x \mathbf{M}^{-1} \mathbf{P}_x \end{aligned} \quad (\text{A.2})$$

where

$$\mathbf{P}_x = \begin{bmatrix} p_{x1} \\ p_{y1} \\ \vdots \\ p_{zN} \end{bmatrix} \quad \text{and} \quad \mathbf{M}^{-1} = \begin{bmatrix} \mu_1 & & & \\ & \mu_1 & & \\ & & \ddots & \\ & & & \mu_N \end{bmatrix}$$

The column matrix \mathbf{P}_x can be expressed as

$$\mathbf{P}_x = \mathbf{M}\dot{\mathbf{X}} \quad (\text{A.3})$$

Define a set of conjugate momenta \mathbf{P} associated with internal coordinates, \mathbf{R} . As is shown at the end of this appendix, we have

$$\mathbf{P}_x = \tilde{\mathbf{B}}\mathbf{P} \quad (\text{A.4})$$

Equations A.3 and A.4 give

$$\mathbf{M}\dot{\mathbf{X}} = \tilde{\mathbf{B}}\mathbf{P} \quad (\text{A.5})$$

Equation 1.118 in Chapter 1 gives

$$\mathbf{R} = \mathbf{B}\mathbf{X} \quad \text{and} \quad \dot{\mathbf{R}} = \mathbf{B}\dot{\mathbf{X}} \quad (\text{A.6})$$

By inserting Eq. A.5 into Eq. A.6, we obtain

$$\dot{\mathbf{R}} = \mathbf{B}\mathbf{M}^{-1}\tilde{\mathbf{B}}\mathbf{P} \quad (\text{A.7})$$

Using Eq. A.4, we write Eq. A.2 as

$$2T = \tilde{\mathbf{P}}\mathbf{B}\mathbf{M}^{-1}\tilde{\mathbf{B}}\mathbf{P} \quad (\text{A.8})$$

If we define

$$\mathbf{G} = \mathbf{B}\mathbf{M}^{-1}\tilde{\mathbf{B}} \quad (\text{Eq. 1.117 in Chapter 1})$$

Eq. A.8 is written as

$$2T = \tilde{\mathbf{P}}\mathbf{G}\mathbf{P} \quad (\text{A.9})$$

If Eq. 1.117 is combined with Eq. A.7, we obtain

$$\dot{\mathbf{R}} = \mathbf{G}\mathbf{P}$$

or

$$\mathbf{G}^{-1}\dot{\mathbf{R}} = \mathbf{G}^{-1}\mathbf{G}\mathbf{P} = \mathbf{P} \quad (\text{A.10})$$

Using Eq. A.10, Eq. A.9 can be written

$$\begin{aligned} 2T &= \tilde{\mathbf{R}}\tilde{\mathbf{G}}^{-1}\mathbf{G}\mathbf{G}^{-1}\dot{\mathbf{R}} \\ &= \tilde{\mathbf{R}}\mathbf{G}^{-1}\dot{\mathbf{R}} \quad (\text{Eq. 1.113 in chapter 1}) \end{aligned}$$

VI.1. Derivation of Eq. A.4

The momentum p_{R_k} conjugated with the internal coordinate R_k is given by

$$p_{R_k} = \frac{\partial T}{\partial \dot{R}_k}, \quad k = 1, 2, \dots, s$$

If we denote the coordinates corresponding to the translational and rotational motions of the molecule by R_j^0 and its conjugate momentum by $p_{R_j}^0$

$$p_{R_j}^0 = \frac{\partial T}{\partial \dot{R}_j^0}, \quad j = 1, 2, \dots, 6$$

then the momentum p_{x1} in terms of rectangular coordinates is written as

$$\begin{aligned} p_{x1} &= \frac{\partial T}{\partial \dot{x}_1} = \sum_k^s \frac{\partial T}{\partial \dot{R}_k} \frac{\partial R_k}{\partial x_1} + \sum_j^6 \frac{\partial T}{\partial \dot{R}_j^0} \frac{\partial R_j^0}{\partial x_1} \\ &= \sum_k^s p_{R_k} B_{k,x1} + \sum_j^6 p_{R_j}^0 \frac{\partial R_j^0}{\partial x_1} \end{aligned}$$

The second term becomes zero since the momenta corresponding to the translational and rotational motions are zero. Thus, we have

$$\begin{aligned} p_{x1} &= \sum_k^s p_{R_k} B_{k,x1} \\ p_{y1} &= \sum_k^s p_{R_k} B_{k,y1} \\ &\vdots \\ p_{zN} &= \sum_k^s p_{R_k} B_{k,zN} \end{aligned}$$

In matrix form, this is written as

$$\mathbf{P}_x = \tilde{\mathbf{B}}\mathbf{P} \quad (\text{A.4})$$

APPENDIX VII. THE G AND F MATRIX ELEMENTS OF TYPICAL MOLECULES

In the following tables, F represents F matrix elements in the GVF field, whereas F^* denotes those in the UBF field. In the latter, $F' = -\frac{1}{10}F$ was assumed for all cases, and the *molecular tension* (Refs. 89–91 of Chapter 1) was ignored.

VII.1. Bent XY_2 Molecules (C_{2v})

A_1 species—infrared- and Raman-active:

$$G_{11} = \mu_y + \mu_x(1 + \cos\alpha)$$

$$G_{12} = -\frac{\sqrt{2}}{r}\mu_x \sin\alpha$$

$$G_{22} = \frac{2}{r^2} [\mu_y + \mu_x(1 - \cos\alpha)]$$

$$F_{11} = f_r + f_{rr}$$

$$F_{12} = (\sqrt{2})r f_{r\alpha}$$

$$F_{22} = r^2 f_{\alpha}$$

$$F_{11}^* = K + 2F \sin^2 \frac{\alpha}{2}$$

$$F_{12}^* = (0.9)(\sqrt{2})rF \sin \frac{\alpha}{2} \cos \frac{\alpha}{2}$$

$$F_{22}^* = r^2 \left[H + F \left\{ \cos^2 \frac{\alpha}{2} + (0.1) \sin^2 \frac{\alpha}{2} \right\} \right]$$

B_2 species—infrared- and Raman-active:

$$G = \mu_y + \mu_x(1 - \cos\alpha)$$

$$F = f_r - f_{rr}$$

$$F^* = K - (0.2)F \cos^2 \frac{\alpha}{2}$$

VII.2. Pyramidal XY_3 Molecules (C_{3v})

A_1 species—infrared- and Raman-active:

$$\begin{aligned}
 G_{11} &= \mu_y + \mu_x(1 + 2 \cos \alpha) \\
 G_{12} &= -\frac{2(1 + 2 \cos \alpha)(1 - \cos \alpha)}{r \sin \alpha} \mu_x \\
 G_{22} &= \frac{2}{r^2} \left(\frac{1 + 2 \cos \alpha}{1 + \cos \alpha} \right) [\mu_y + 2\mu_x(1 - \cos \alpha)] \\
 F_{11} &= f_r + 2f_{rr} \\
 F_{12} &= r(2f_{r\alpha} + f'_{r\alpha}) \\
 F_{22} &= r^2(f_\alpha + 2f_{\alpha\alpha}) \\
 F_{11}^* &= K + 4F \sin^2 \frac{\alpha}{2} \\
 F_{12}^* &= (1.8)rF \sin \frac{\alpha}{2} \cos \frac{\alpha}{2} \\
 F_{22}^* &= r^2 \left[H + F \left(\cos^2 \frac{\alpha}{2} + (0.1) \sin^2 \frac{\alpha}{2} \right) \right]
 \end{aligned}$$

E species—infrared- and Raman-active:

$$\begin{aligned}
 G_{11} &= \mu_y + \mu_x(1 - \cos \alpha) \\
 G_{12} &= \frac{1(1 - \cos \alpha)^2}{r \sin \alpha} \mu_x \\
 G_{22} &= \frac{1}{r^2(1 + \cos \alpha)} [(2 + \cos \alpha)\mu_y + (1 - \cos \alpha)^2 \mu_x] \\
 F_{11} &= f_r - f_{rr} \\
 F_{12} &= r(-f_{r\alpha} + f'_{r\alpha}) \\
 F_{22} &= r^2(f_\alpha - f_{\alpha\alpha}) \\
 F_{11}^* &= K + \left(\sin^2 \frac{\alpha}{2} - (0.3) \cos^2 \frac{\alpha}{2} \right) F \\
 F_{12}^* &= -(0.9)rF \sin \frac{\alpha}{2} \cos \frac{\alpha}{2} \\
 F_{22}^* &= r^2 \left[H + F \left(\cos^2 \frac{\alpha}{2} + (0.1) \sin^2 \frac{\alpha}{2} \right) \right]
 \end{aligned}$$

Here $f_{r\alpha}$ denotes interaction between Δr and $\Delta\alpha$ having a common bond (e.g., Δr_1 and $\Delta\alpha_{12}$ or $\Delta\alpha_{31}$); $f'_{r\alpha}$ denotes interaction between Δr and $\Delta\alpha$ having no common bonds (e.g., Δr_1 and $\Delta\alpha_{23}$); see Fig. 1.20c.

VII.3. Planar XY_3 Molecules (D_{3h})

A'_1 species—Raman-active:

$$\begin{aligned} G &= \mu_y \\ F &= f_r + 2f_{rr} \\ F^* &= K + 3F \end{aligned}$$

A''_2 species—infrared-active:

$$\begin{aligned} G &= \frac{9}{4r^2}(\mu_y + 3\mu_x) \\ F &= F^* = r^2 f_\theta \end{aligned}$$

E' species—infrared- and Raman-active:

$$\begin{aligned} G_{11} &= \mu_y + \frac{3}{2}\mu_x \\ G_{12} &= \frac{3\sqrt{3}}{2r}\mu_x \\ G_{22} &= \frac{3}{2r^2}(2\mu_y + 3\mu_x) \\ F_{11} &= f_r - f_{rr} \\ F_{12} &= r(f'_{r\alpha} - f_{r\alpha}) \\ F_{22} &= r^2(f_\alpha - f_{\alpha\alpha}) \\ F_{11}^* &= K + 0.675F \\ F_{12}^* &= -(0.9)\frac{\sqrt{3}}{4}rF \\ F_{22}^* &= r^2(H + 0.325F) \end{aligned}$$

The symbols $f_{r\alpha}$ and $f'_{r\alpha}$ are defined in VII.2; f_θ denotes the force constant for the out-of-plane mode (see Fig. 1.20f).

VII.4. Tetrahedral XY_4 Molecules (T_d)

A_1 species—Raman-active:

$$\begin{aligned} G &= \mu_y \\ F &= f_r + 3f_{rr} \\ F^* &= K + 4F \end{aligned}$$

E species—Raman-active:

$$\begin{aligned} G &= \frac{3\mu_y}{r^2} \\ F &= r^2(f_\alpha - 2f_{\alpha\alpha} + f'_{\alpha\alpha}) \\ F^* &= r^2(H + 0.4F) \end{aligned}$$

F_2 species—infrared- and Raman-active:

$$\begin{aligned} G_{11} &= \mu_y + \frac{4}{3}\mu_x \\ G_{12} &= -\frac{8}{3r}\mu_x \\ G_{22} &= \frac{1}{r^2} \left(\frac{16}{3}\mu_x + 2\mu_y \right) \\ F_{11} &= f_r - f_{rr} \\ F_{12} &= (\sqrt{2})r(f_{r\alpha} - f'_{r\alpha}) \\ F_{22} &= r^2(f_\alpha - f'_{\alpha\alpha}) \\ F_{11}^* &= K + \frac{6}{5}F \\ F_{12}^* &= \frac{3}{5}rF \\ F_{22}^* &= r^2(H + 0.4F) \end{aligned}$$

where $f_{\alpha\alpha}$ denotes interaction between two $\Delta\alpha$ having a common bond; $f'_{\alpha\alpha}$ denotes interaction between two $\Delta\alpha$ having no common bond.

VII.5. Square-Planar XY_4 Molecules (D_{4h})

A_{1g} species—Raman-active:

$$\begin{aligned} G &= \mu_y \\ F &= f_r + 2f_{rr} + f'_{rr} \\ F^* &= K + 2F \end{aligned}$$

B_{1g} species—Raman-active:

$$G = \mu_y$$

$$F = f_r - 2f_{rr} + f'_{rr}$$

$$F^* = K - 0.2F$$

B_{2g} species—Raman-active:

$$G = \frac{4\mu_y}{r^2}$$

$$F = r^2(f_\alpha - 2f_{\alpha\alpha} + f'_{\alpha\alpha})$$

$$F^* = r^2(H + 0.55F)$$

E_u species—infrared-active:

$$G_{11} = 2\mu_x + \mu_y$$

$$G_{12} = -\frac{2\sqrt{2}}{r}\mu_x$$

$$G_{22} = \frac{2}{r^2}(\mu_y + 2\mu_x)$$

$$F_{11} = f_r - f'_{rr}$$

$$F_{12} = (\sqrt{2})r(f_{r\alpha} - f'_{r\alpha})$$

$$F_{22} = r^2(f_\alpha - f'_{\alpha\alpha})$$

$$F_{11}^* = K + 0.9F$$

$$F_{12}^* = (\sqrt{2})r(0.45)F$$

$$F_{22}^* = r^2(H + 0.55F)$$

The symbol f_{rr} denotes interaction between two Δr perpendicular to each other; f'_{rr} denotes interaction between two Δr on the same straight line. In addition, a square-planar XY_4 molecule has two out-of-plane vibrations in the A_{2u} and B_{2u} species.

VII.6. Octahedral XY_6 Molecules (O_h)

A_{1g} species—Raman-active:

$$G = \mu_y$$

$$F = f_r + 4f_{rr} + f'_{rr}$$

$$F^* = K + 4F$$

E_g species—Raman-active:

$$\begin{aligned} G &= \mu_y \\ F &= f_r - 2f_{rr} + f'_{rr} \\ F^* &= K + 0.7F \end{aligned}$$

F_{1u} species—infrared-active:

$$\begin{aligned} G_{11} &= \mu_y + 2\mu_x \\ G_{12} &= -\frac{4}{r}\mu_x \\ G_{22} &= \frac{2}{r^2}(\mu_y + 4\mu_x) \\ F_{11} &= f_r - f'_{rr} \\ F_{12} &= 2rf_{r\alpha} \\ F_{22} &= r^2(f_\alpha + 2f_{\alpha\alpha}) \\ F_{11}^* &= K + 1.8F \\ F_{12}^* &= 0.9rF \\ F_{22}^* &= r^2(H + 0.55F) \end{aligned}$$

F_{2g} species—Raman-active:

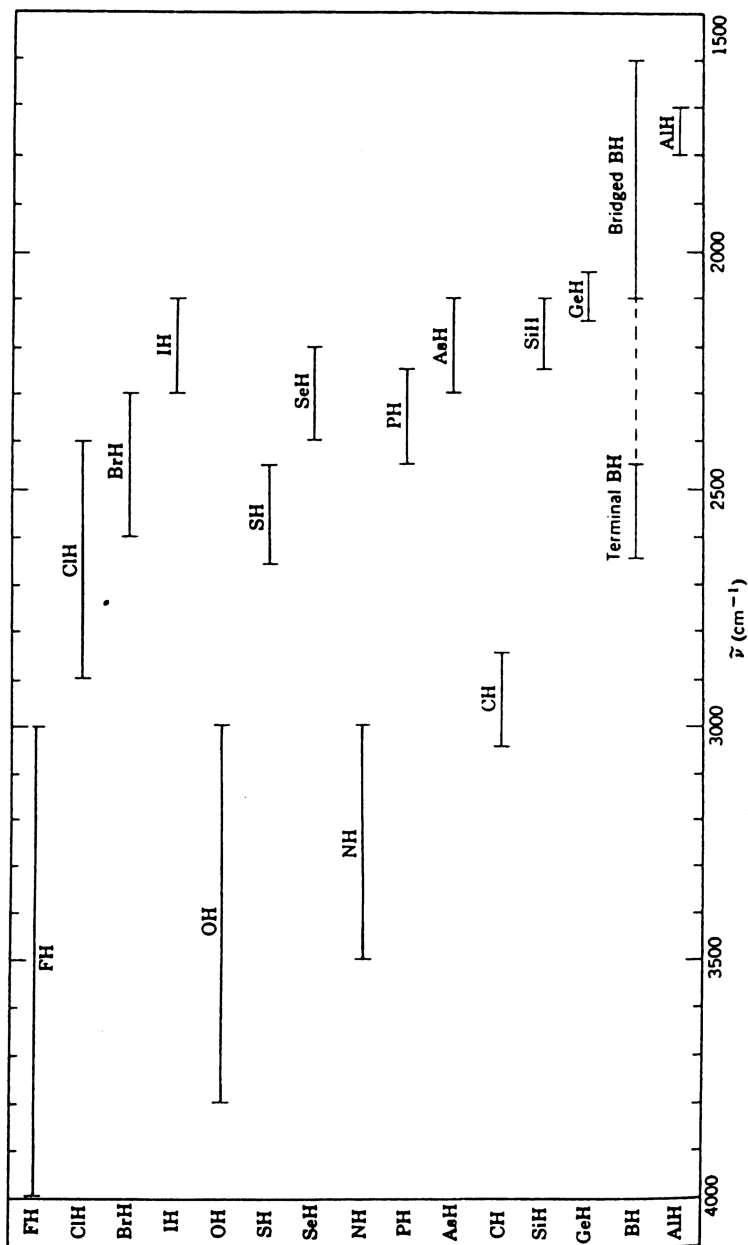
$$\begin{aligned} G &= \frac{4\mu_y}{r^2} \\ F &= r^2(f_\alpha - 2f'_{\alpha\alpha}) \\ F^* &= r^2(H + 0.55F) \end{aligned}$$

F_{2u} species—inactive:

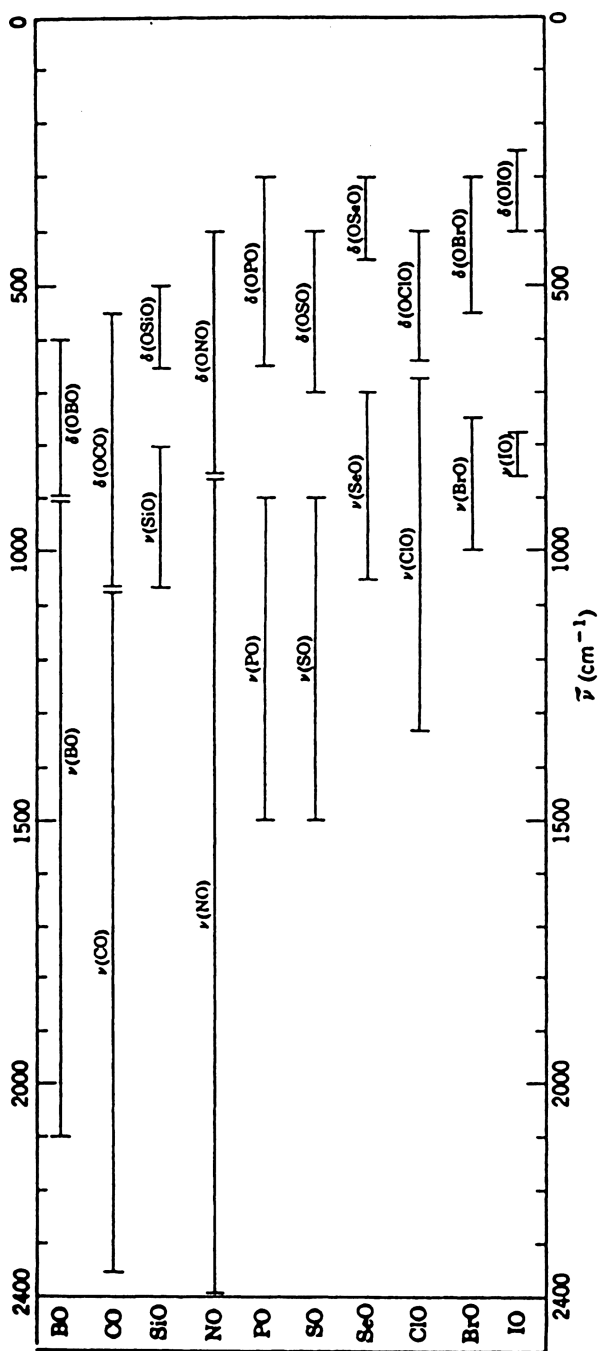
$$\begin{aligned} G &= \frac{2\mu_y}{r^2} \\ F &= r^2(f_\alpha - 2f_{\alpha\alpha}) \\ F^* &= r^2(H + 0.55F) \end{aligned}$$

The symbol f_{rr} denotes interaction between two Δr perpendicular to each other, whereas f'_{rr} denotes those between two Δr on the same straight line; $f_{\alpha\alpha}$ denotes interaction between two $\Delta\alpha$ perpendicular to each other, whereas $f'_{\alpha\alpha}$ denotes those between two $\Delta\alpha$ on the same plane. Only the interaction between two $\Delta\alpha$ having a common bond was considered.

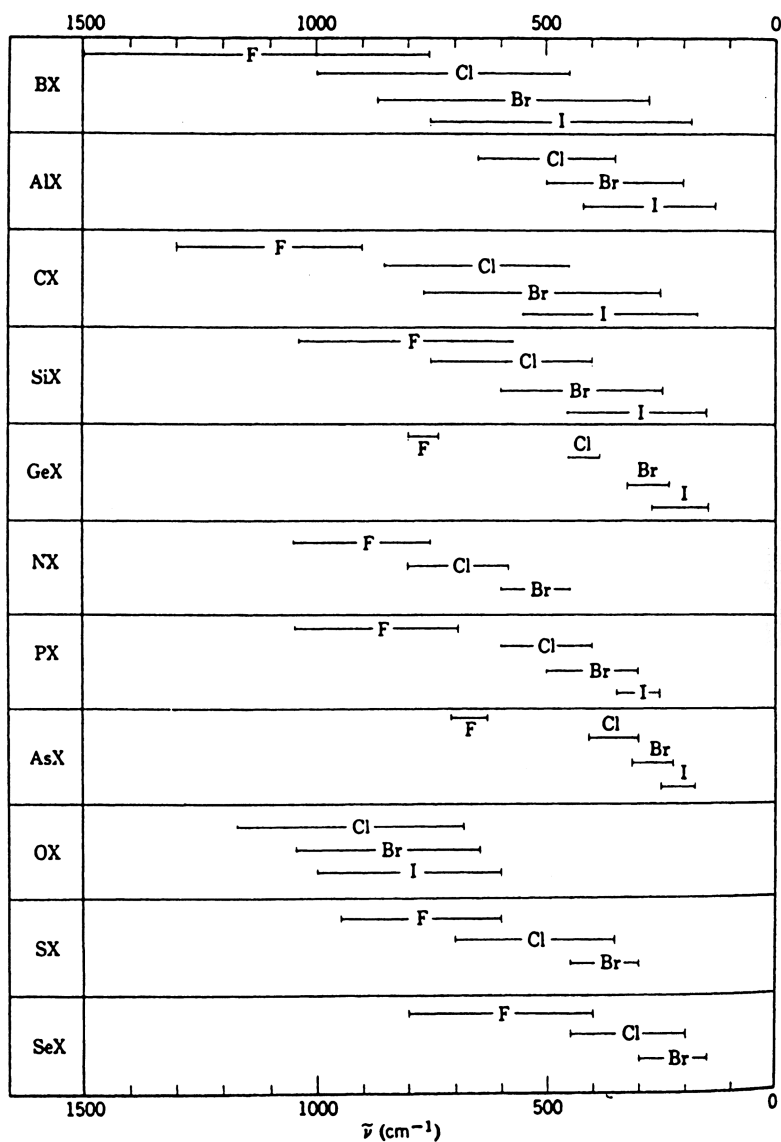
APPENDIX VIII. GROUP FREQUENCY CHARTS



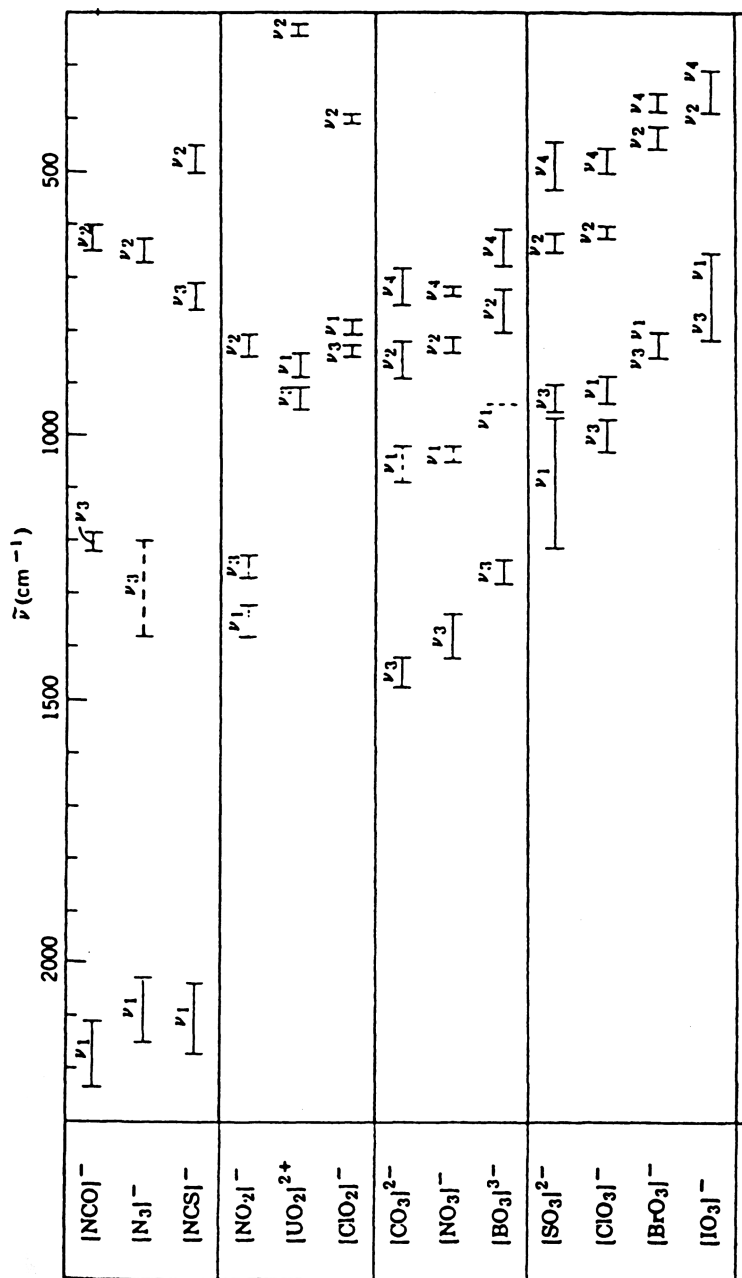
(a) Hydrogen stretching frequencies



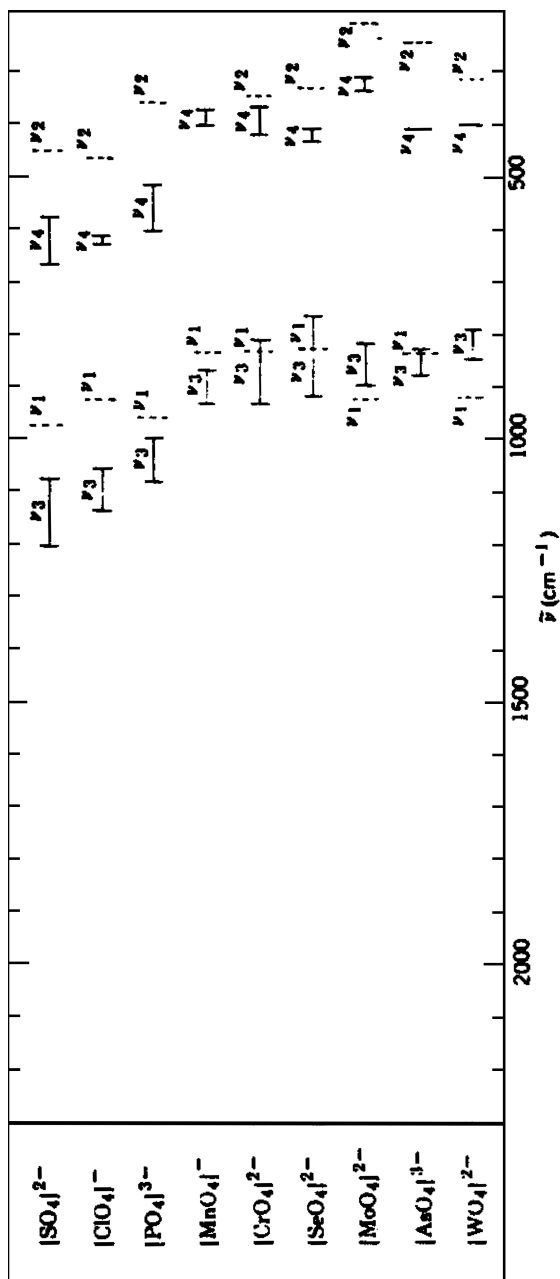
(b) Oxygen stretching and bending frequencies



(c) Halogen (X) stretching frequencies



(Continued)

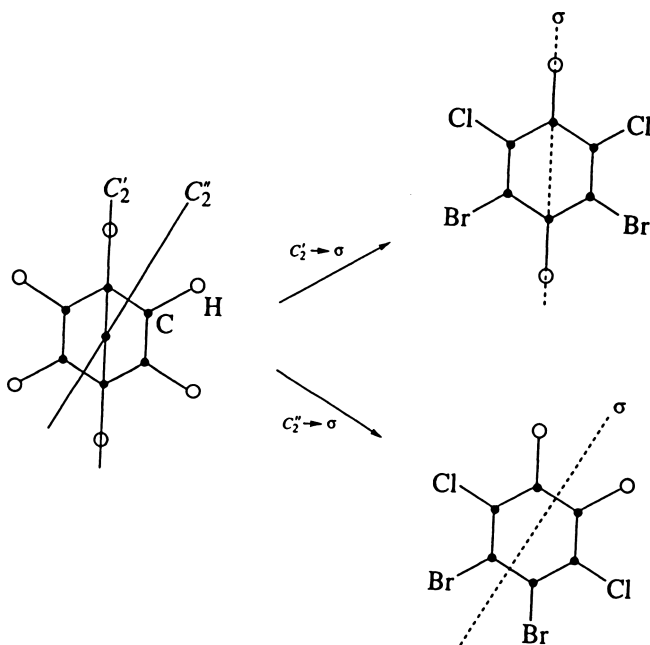


(d) Characteristic frequencies of some inorganic ions. (Broken lines indicate Raman-active vibrations.)

APPENDIX IX. CORRELATION TABLES

The following tables were reproduced with permission from the book by W. G. Fateley, F. R. Dollish, N. T. McDevitt, and F. F. Bentley (Ref. 15 in Chapter 1). In some cases, more than one correlation is available between a pair of point groups. Then, it is necessary to specify the choice of symmetry operation from a larger group. For example, in the table of $C_{4v} \rightarrow C_s$ correlation, σ_v and σ_d are written above C_s to show two different possibilities: the first (σ_v) and second (σ_d) columns are used when the σ_v and σ_d planes, respectively, of the parent molecule become the (sole) σ plane of the C_s molecule.

In the $D_{6h} \rightarrow C_{2v}$ correlation, two different correlations exist depending upon whether the C_2' or C_2'' axis of the D_{6h} molecule becomes the (sole) C_2 axis of the C_{2v} molecule.



In using the correlation tables for the purpose of the correlation method (Sec. 1.27), the rules given below must be followed. Those species of the point groups C_{3h} , C_{4h} , C_{5h} , C_{6h} , C_6 , S_4 , S_6 , S_8 , T , and T_h marked with an asterisk (*) will not use the coefficient 2 of the E_i species in this correlation procedure only. Also, for those species of the point group T and T_h marked with a double dagger (\ddagger) a coefficient 2 will be added to the E_i term related to the F_i species of the point group.

C_{2h}	C_2	C_s	C_i
A_g	A	A'	A_g
B_g	B	A''	A_g
A_u	A	A''	A_u
B_u	B	A'	A_u

C_{2v}	C_2	$\sigma(zx)$ C_s	$\sigma(yz)$ C_s
A_1	A	A'	A'
A_2	A	A''	A''
B_1	B	A'	A''
B_2	B	A''	A'

D_2	C_2^z	C_2^y	C_2^x
A	A	A	A
B_1	A	B	B
B_2	B	A	B
B_3	B	B	A

D_{2d}	S_4	$C_2 \rightarrow C_2(z)$ D_2	C_{2v}	C_2 C_2	C_2' C_2	C_s
A_1	A	A	A_1	A	A	A'
A_2	A	B_1	A_2	A	B	A''
B_1	B	A	A_2	A	A	A''
B_2	B	B_1	A_1	A	B	A'
E	E	$B_2 + B_3$	$B_1 + B_2$	$2B$	$A + B$	$A' + A''$

D_{2h}	$C_2(z)$ D_2	$C_2(y)$ C_{2v}	$C_2(x)$ C_{2v}	$C_2(z)$ C_{2h}	$C_2(y)$ C_{2h}	$C_2(x)$ C_{2h}	$C_2(z)$ C_2	$C_2(y)$ C_2	$C_2(x)$ C_2	$\sigma(xy)$ C_i	$\sigma(zx)$ C_s	$\sigma(yz)$ C_s	C_i
A_g	A	A_1	A_1	A_1	A_g	A_g	A	A	A	A'	A'	A'	A_g
B_{1g}	B_1	A_2	B_2	B_1	A_g	B_g	A	B	B	A'	A''	A''	A_g
B_{2g}	B_2	B_1	A_2	B_2	B_g	A_g	B	A	B	A''	A'	A''	A_g
B_{3g}	B_3	B_2	B_1	A_2	B_g	B_g	B	B	A	A''	A''	A'	A_g
A_u	A	A_2	A_2	A_2	A_u	A_u	A	A	A	A''	A''	A''	A_u
B_{1u}	B_1	A_1	B_1	B_2	A_u	B_u	A	B	B	A''	A'	A'	A_u
B_{2u}	B_2	B_2	A_1	B_1	B_u	A_u	B	A	B	A'	A''	A'	A_u
B_{3u}	B_3	B_1	B_2	A_1	B_u	B_u	B	B	A	A'	A'	A''	A_u

C_{3h}	C_3	C_s	C_1
A'	A	A'	A
E'	E	$2A'^*$	$2A^*$
A''	A	A''	A
E''	E	$2A''^*$	$2A^*$

C_{3v}	C_3	C_s
A_1	A	A'
A_2	A	A''
E	E	$A' + A''$

D_3	C_3	C_2
A_1	A	A
A_2	A	B
E	E	$A + B$

D_{3d}	D_3	C_{3v}	$S_6 \equiv C_{3i}$	C_3	C_{2h}	C_2	C_s	C_i
A_{1g}	A_1	A_1	A_g	A	A_g	A	A'	A_g
A_{2g}	A_2	A_2	A_g	A	B_g	B	A''	A_g
E_g	E	E	E_g	E	$A_g + B_g$	$A + B$	$A' + A''$	$2A_g$
A_{1u}	A_1	A_2	A_u	A	A_u	A	A''	A_u
A_{2u}	A_2	A_1	A_u	A	B_u	B	A'	A_u
E_u	E	E	E_u	E	$A_u + B_u$	$A + B$	$A' + A''$	$2A_u$

D_{3h}	C_{3h}	D_3	C_{3v}	$\overbrace{\sigma_h \rightarrow \sigma_v(z,y)}^{C_{2v}}$	C_3	C_2	σ_h C_s	σ_v C_s
A_1^1	A'	A_1	A_1	A_1	A	A	A_1	A'
A_2^1	A'	A_2	A_2	B_2	A	B	A'	A''
E'	E'	E	E	$A_1 + B_2$	E	$A + B$	$2A'$	$A' + A''$
A''_1	A''	A_1	A_2	A_2	A	A	A''	A''
A''_2	A''	A_2	A_1	B_1	A	B	A''	A'
E''	E''	E	E	$A_2 + B_1$	E	$A + B$	$2A''$	$A' + A''$

C_4	C_2	C_{4h}	C_4	S_4	C_{2h}	C_2	C_s	C_i	C_1
A	A	A_g	A	A	A_g	A	A'	A_g	A
B	A	B_g	B	B	A_g	A	A'	A_g	A
E	$2B$	E_g	E	E	$2B_u^*$	$2B^*$	$2A''^*$	$2A_g^*$	$2A^*$
		A_u	A	B	A_u	A	A''	A_u	A
		B_u	B	A	A_u	A	A''	A_u	A
		E_u	E	E	$2B_u^*$	$2B^*$	$2A'^*$	$2A_u^*$	$2A^*$

C_{4v}	C_4	σ_v C_{2v}	σ_d C_{2v}	C_2	σ_v C_s	σ_d C_s
A_1	A	A_1	A_1	A	A'	A'
A_2	A	A_2	A_2	A	A''	A''
B_1	B	A_1	A_2	A	A'	A''
B_2	B	A_2	A_1	A	A''	A'
E	E	$B_1 + B_2$	$B_1 + B_2$	$2B$	$A' + A''$	$A' + A''$

D_4	C_2' D_2	C_2'' D_2	C_4	C_2	C_2' C_2	C_2'' C_2
A_1	A	A	A	A	A	A
A_2	B_1	B_1	A	A	B	B
B_1	A	B_1	B	A	A	B
B_2	B_1	A	B	A	B	A
E	$B_2 + B_3$	$B_2 + B_3$	E	$2B$	$A + B$	$A + B$

D_{4d}	D_4	C_{4v}	S_8	C_4	C_{2v}	C_2 C_2	C_2' C_2	C_s
A_1	A_1	A_1	A	A	A_1	A	A	A'
A_2	A_2	A_2	A	A	A_2	A	B	A''
B_1	A_1	A_2	B	A	A_2	A	A	A''
B_2	A_2	A_1	B	A	A_1	A	B	A'
E_1	E	E	E_1	E	$B_1 + B_2$	$2B$	$A + B$	$A' + A''$
E_2	$B_1 + B_2$	$B_1 + B_2$	E_2	$2B$	$A_1 + A_2$	$2A$	$A + B$	$A' + A''$
E_3	E	E	E_3	E	$B_1 + B_2$	$2B$	$A + B$	$A' + A''$

D_{4h}	D_4	C_2' D_{2d}	C_2'' D_{2d}	C_{4v}	C_{4h}	C_2' D_{2h}	C_2'' D_{2h}	C_4	S_4	C_2' D_2	C_2'' D_2	C_{2v} C_{2v}	C_{2v} C_{2v}
A_{1g}	A_1	A_1	A_1	A_1	A_g	A_g	A_g	A	A	A	A	A_1	A_1
A_{2g}	A_2	A_2	A_2	A_2	A_g	B_{1g}	B_{1g}	A	A	B_1	B_1	A_2	A_2
B_{1g}	B_1	B_1	B_2	B_1	B_g	A_g	B_{1g}	B	B	A	B_1	A_1	A_2
B_{2g}	B_2	B_2	B_2	B_2	B_g	B_{1g}	A_g	B	B	B_1	A	A_2	A_1
E_g	E	E	E	E	E_g	$B_{2g} + B_{3g}$	$B_{2g} + B_{3g}$	E	E	$B_2 + B_3$	$B_2 + B_3$	$B_1 + B_2$	$B_1 + B_2$
A_{1u}	A_1	B_1	B_1	A_2	A_u	A_u	A_u	A	B	A	A	A_2	A_2
A_{2u}	A_2	B_2	B_2	A_1	A_u	B_{1u}	B_{1u}	A	B	B_1	B_1	A_1	A_1
B_{1u}	B_1	A_1	A_2	B_2	B_u	A_u	B_{1u}	B	A	A	B_1	A_2	A_1
B_{2u}	B_2	A_2	A_1	B_1	B_u	B_{1u}	A_u	B	A	B_1	A	A_1	A_2
E_u	E	E	E	E	E_u	$B_{2u} + B_{3u}$	$B_{2u} + B_{3u}$	E	E	$B_2 + B_3$	$B_2 + B_3$	$B_1 + B_2$	$B_1 + B_2$

\mathbf{D}_{4h}	C_2' \mathbf{C}_{2v}	C_2'' \mathbf{C}_{2v}	C_2 \mathbf{C}_{2h}	C_2' \mathbf{C}_{2h}	C_2'' \mathbf{C}_{2h}	C_2 \mathbf{C}_2	C_2' \mathbf{C}_2	C_2'' \mathbf{C}_2	σ_h \mathbf{C}_s	σ_v \mathbf{C}_s	σ_d \mathbf{C}_s	\mathbf{C}_i
A_{1g}	A_1	A_1	A_g	A_g	A_g	A	A	A	A'	A'	A'	A_g
A_{2g}	B_1	B_1	A_g	B_g	B_g	A	B	B	A'	A''	A''	A_g
B_{1g}	A_1	B_1	A_g	A_g	B_g	A	A	B	A'	A'	A''	A_g
B_{2g}	B_1	A_1	A_g	B_g	A_g	A	B	A	A'	A''	A'	A_g
E_g	$A_2 + B_2$	$A_2 + B_2$	$2B_g$	$A_g + B_g$	$A_g + B_g$	$2B$	$A + B$	$A + B$	$2A''$	$A' + A''$	$A' + A''$	$2A_g$
A_{1u}	A_2	A_2	A_u	A_u	A_u	A	A	A	A''	A''	A''	A_u
A_{2u}	B_2	B_2	A_u	B_u	B_u	A	B	B	A''	A'	A'	A_u
B_{1u}	A_2	B_2	A_u	A_u	B_u	A	A	B	A''	A''	A'	A_u
B_{2u}	B_2	A_2	A_u	B_u	A_u	A	B	A	A''	A'	A''	A_u
E_u	$A_1 + B_1$	$A_1 + B_1$	$2B_u$	$A_u + B_u$	$A_u + B_u$	$2B$	$A + B$	$A + B$	$2A'$	$A' + A''$	$A' + A''$	$2A_u$

S_4	C_2	C_1	C_{5h}	C_5	C_s	C_1
A	A	A	A'	A	A'	A
B	A	A	E'_1	E_1	$2A'^*$	$2A^*$
E	$2B^*$	$2A^*$	E'_2	E_2	$2A'^*$	$2A^*$
			A''	A	A''	A
			E''_1	E_1	$2A''$	$2A^*$
			E''_2	E_2	$2A''^*$	$2A^*$

C_{5v}	C_5	C_s	D_5	C_5	C_2
A_1	A	A'	A_1	A	A
A_2	A	A''	A_2	A	B
E_1	E_1	$A' + A''$	E_1	E_1	$A + B$
E_2	E_2	$A' + A''$	E_2	E_2	$A + B$

D_{5d}	D_5	C_{5v}	C_5	C_2	C_s	C_i
A_{1g}	A_1	A_1	A	A	A'	A_g
A_{2g}	A_2	A_2	A	B	A''	A_g
E_{1g}	E_1	E_1	E_1	$A + B$	$A' + A''$	$2A_g$
E_{2g}	E_2	E_2	E_2	$A + B$	$A' + A''$	$2A_g$
A_{1u}	A_1	A_2	A	A	A''	A_u
A_{2u}	A_2	A_1	A	B	A'	A_u
E_{1u}	E_1	E_1	E_1	$A + B$	$A' + A''$	$2A_u$
E_{2u}	E_2	E_2	E_2	$A + B$	$A' + A''$	$2A_u$

D_{5h}	D_5	C_{5v}	C_{5h}	C_5	$\overbrace{\sigma_h \rightarrow \sigma(XZ)}^{C_{2v}}$	C_2	σ_h C_s	σ_v C_s
A'_1	A_1	A_1	A'	A	A_1	A	A'	A'
A'_2	A_2	A_2	A'	A	B_1	B	A'	A''
E'_1	E_1	E_1	E'_1	E_1	$A_1 + B_2$	$A + B$	$2A'$	$A' + A''$
E'_2	E_2	E_2	E'_2	E_2	$A_1 + B_2$	$A + B$	$2A'$	$A' + A''$
A''_2	A_1	A_2	A''	A	A_2	A	A''	A''
A''_2	A_2	A_1	A''	A	B_2	B	A''	A'
E''_1	E_1	E_1	E''_1	E_1	$A_2 + B_2$	$A + B$	$2A''$	$A' + A''$
E''_2	E_2	E_2	E''_2	E_2	$A_2 + B_2$	$A + B$	$2A''$	$A' + A''$

C₆	C₃	C₂	C₁
<i>A</i>	<i>A</i>	<i>A</i>	<i>A</i>
<i>B</i>	<i>A</i>	<i>B</i>	<i>A</i>
<i>E₁</i>	<i>E</i>	<i>2B*</i>	<i>2A*</i>
<i>E₂</i>	<i>E</i>	<i>2A*</i>	<i>2A*</i>

C_{6h}	C₆	C_{3h}	S₆ ≡ C_{3i}	C_{2h}	C₃	C₂	C_s	C_i	C₁
<i>A_g</i>	<i>A</i>	<i>A'</i>	<i>A_g</i>	<i>A_g</i>	<i>A</i>	<i>A</i>	<i>A'</i>	<i>A_g</i>	<i>A</i>
<i>B_g</i>	<i>B</i>	<i>A''</i>	<i>A_g</i>	<i>B_g</i>	<i>A</i>	<i>B</i>	<i>A''</i>	<i>A_g</i>	<i>A</i>
<i>E_{1g}</i>	<i>E₁</i>	<i>E''</i>	<i>E_g</i>	<i>2B_g*</i>	<i>E</i>	<i>2B*</i>	<i>2A'*</i>	<i>2A_g*</i>	<i>2A*</i>
<i>E_{2g}</i>	<i>E₂</i>	<i>E'</i>	<i>E_g</i>	<i>2A_g*</i>	<i>E</i>	<i>2A*</i>	<i>2A'*</i>	<i>2A_g*</i>	<i>2A*</i>
<i>A_u</i>	<i>A</i>	<i>A''</i>	<i>A_u</i>	<i>A_u</i>	<i>A</i>	<i>A</i>	<i>A''</i>	<i>A_u</i>	<i>A</i>
<i>B_u</i>	<i>B</i>	<i>A'</i>	<i>A_u</i>	<i>B_u</i>	<i>A</i>	<i>B</i>	<i>A'</i>	<i>A_u</i>	<i>A</i>
<i>E_{1u}</i>	<i>E₁</i>	<i>E'</i>	<i>E_u</i>	<i>2B_u*</i>	<i>E</i>	<i>2B*</i>	<i>2A'*</i>	<i>2A_u*</i>	<i>2A*</i>
<i>E_{2u}</i>	<i>E₂</i>	<i>E''</i>	<i>E_u</i>	<i>2A_u*</i>	<i>E</i>	<i>2A*</i>	<i>2A''*</i>	<i>2A_u</i>	<i>2A*</i>

C_{6v}	C₆	σ_v C_{3v}	σ_d C_{3v}	$\overbrace{\sigma_v \rightarrow \sigma(ZX)}^{\text{C}_{2v}}$ C_{2v}	C₃	C₂	σ_v C_s	σ_d C_s
<i>A₁</i>	<i>A</i>	<i>A₁</i>	<i>A₁</i>	<i>A₁</i>	<i>A</i>	<i>A</i>	<i>A'</i>	<i>A'</i>
<i>A₂</i>	<i>A</i>	<i>A₂</i>	<i>A₂</i>	<i>A₂</i>	<i>A</i>	<i>A</i>	<i>A''</i>	<i>A''</i>
<i>B₁</i>	<i>B</i>	<i>A₁</i>	<i>A₂</i>	<i>B₁</i>	<i>A</i>	<i>B</i>	<i>A'</i>	<i>A''</i>
<i>B₂</i>	<i>B</i>	<i>A₂</i>	<i>A₁</i>	<i>B₂</i>	<i>A</i>	<i>B</i>	<i>A''</i>	<i>A'</i>
<i>E₁</i>	<i>E₁</i>	<i>E</i>	<i>E</i>	<i>B₁ + B₂</i>	<i>E</i>	<i>2B</i>	<i>A' + A''</i>	<i>A' + A''</i>
<i>E₂</i>	<i>E₂</i>	<i>E</i>	<i>E</i>	<i>A₁ + A₂</i>	<i>E</i>	<i>2A</i>	<i>A' + A''</i>	<i>A' + A''</i>

D₆	C₆	<i>C'</i> ₂ D₃	<i>C''</i> ₂ D₃	D₂	C₃	C₂	<i>C'</i> ₂ C₂	<i>C''</i> ₂ C₂
<i>A₁</i>	<i>A</i>	<i>A₁</i>	<i>A₁</i>	<i>A</i>	<i>A</i>	<i>A</i>	<i>A</i>	<i>A</i>
<i>A₂</i>	<i>A</i>	<i>A₂</i>	<i>A₂</i>	<i>B₁</i>	<i>A</i>	<i>A</i>	<i>B</i>	<i>B</i>
<i>B₁</i>	<i>B</i>	<i>A₁</i>	<i>A₂</i>	<i>B₂</i>	<i>A</i>	<i>B</i>	<i>A</i>	<i>B</i>
<i>B₂</i>	<i>B</i>	<i>A₂</i>	<i>A₁</i>	<i>B₃</i>	<i>A</i>	<i>B</i>	<i>B</i>	<i>A</i>
<i>E₁</i>	<i>E₁</i>	<i>E</i>	<i>E</i>	<i>B₂ + B₃</i>	<i>E</i>	<i>2B</i>	<i>A + B</i>	<i>A + B</i>
<i>E₂</i>	<i>E₂</i>	<i>E</i>	<i>E</i>	<i>A + B₁</i>	<i>E</i>	<i>2A</i>	<i>A + B</i>	<i>A + B</i>

D_{6d}	D_6	C_{6v}	C_6	D_{2d}	D_3	C_{3v}	D_2	C_{2v}	S_4	C_3	C_2	C_2''	C_s
A_1	A_1	A_1	A	A_1	A_1	A_1	A	A_1	A	A	A	A	A'
A_2	A_2	A_2	A	A_2	A_2	A_2	B_1	A_2	A	A	A	B	A''
B_1	A_1	A_2	A	B_1	A_1	A_2	A	A_2	B	A	A	A	A''
B_2	A_2	A_1	A	B_2	A_2	A_1	B_1	A_1	B	A	A	B	A'
E_1	E_1	E_1	E_1	E	E	E	$B_2 + B_3$	$B_1 + B_2$	E	E	$2B$	$A + B$	$A' + A''$
E_2	E_2	E_2	E_2	$B_1 + B_2$	E	E	$A + B_1$	$A_1 + A_2$	$2B$	E	$2A$	$A + B$	$A' + A''$
E_3	$B_1 + B_2$	$B_1 + B_2$	$2B$	E	$A_1 + A_2$	$A_1 + A_2$	$B_2 + B_3$	$B_1 + B_2$	E	$2A$	$2B$	$A + B$	$A' + A''$
E_4	E_2	E_2	E_2	$A_1 + A_2$	E	E	$A + B_1$	$A_1 + A_2$	$2A$	E	$2A$	$A + B$	$A' + A''$
E_5	E_1	E_1	E_1	E	E	E	$B_2 + B_3$	$B_1 + B_2$	E	E	$2B$	$A + B$	$A' + A''$

	$\overbrace{\sigma_h \rightarrow \sigma(xy)}^{\sigma_v \rightarrow \sigma(yz)} \quad D_{2h}$									
D_{6h}	D_6	C'_{2h}	C'_{2h}	C'_{2h}	C'_{2h}	C'_{2h}	C'_{2h}	C'_{2h}	C'_{2h}	C'_{2h}
A_{1g}	A_1	A'_1	A_1	A_g	A_1	A_g	A	A'	A_1	A_g
A_{2g}	A_2	A'_2	A_2	A_g	A_2	A_g	A	A'	A_2	A_g
B_{1g}	B_1	A''_1	B_2	B_g	A_1	A_{2g}	B	A''	A_2	A_g
B_{2g}	B_2	A''_2	B_1	B_g	A_2	A_{1g}	B	A''	A_1	A_g
E_{1g}	E_1	E''	E_1	E_{1g}	E_g	E_g	E_1	E'	E	E_g
E_{2g}	E_2	E'	E_2	E_{2g}	E_g	E_g	E_2	E'	E	E_g
A_{1u}	A_1	A''_1	A_2	A_u	A_{1u}	A_{1u}	A	A''	A_2	A_u
A_{2u}	A_2	A''_2	A_1	A_u	A_{2u}	A_{2u}	A	A''	A_1	A_u
B_{1u}	B_1	A'_1	B_2	B_u	A_1	A_{2u}	B	A'	A_2	A_u
B_{2u}	B_2	A'_2	B_1	B_u	A_2	A_{1u}	B	A'	A_1	A_u
E_{1u}	E_1	E'	E_1	E_{1u}	E_u	E_u	E_1	E'	E	E_u
E_{2u}	E_2	E''	E_2	E_{2u}	E_u	E_u	E_2	E'	E	E_u

D_{6h}	C_2 C_{2v}	C'_2 C_{2v}	C''_2 C_{2v}	C_2 C_{2h}	C'_2 C_{2h}	C''_2 C_{2h}	C_3	C_2 C_2	C'_2 C_2	C''_2 C_2	σ_h C_s	σ_d C_s	σ_v C_s	C_i
A_{1g}	A_1	A_1	A_1	A_g	A_g	A_g	A	A	A	A	A'	A'	A'	A_g
A_{2g}	A_2	B_2	B_1	A_g	B_g	B_g	A	A	B	B	A'	A''	A''	A_g
B_{1g}	B_1	A_2	B_2	B_g	A_g	B_g	A	B	A	B	A''	A'	A'	A_g
B_{2g}	B_2	B_1	A_2	B_g	B_g	A_g	A	B	B	A	A''	A'	A'	A_g
E_{1g}	$B_1 + B_2$	$A_2 + B_1$	$B_2 + A_2$	$2B_g$	$A_g + B_g$	$A_g + B_g$	E	$2B$	$A + B$	$A + B$	$2A''$	$A' + A''$	$A' + A''$	$2A_g$
E_{2g}	$A_1 + A_2$	$A_1 + B_2$	$A_1 + B_1$	$2A_g$	$A_g + B_g$	$A_g + B_g$	E	$2A$	$A + B$	$A + B$	$2A'$	$A' + A''$	$A' + A''$	$2A_g$
A_{1u}	A_2	A_2	A_2	A_u	A_u	A_u	A	A	A	A	A''	A''	A''	A_u
A_{2u}	A_1	B_1	B_2	A_u	B_u	B_u	A	A	B	B	A''	A'	A'	A_u
B_{1u}	B_2	A_1	B_1	B_u	A_u	B_u	A	B	A	B	A'	A''	A''	A_u
B_{2u}	B_1	B_2	A_1	B_u	B_u	A_u	A	B	B	A	A'	A'	A''	A_u
E_{1u}	$B_2 + B_1$	$A_1 + B_2$	$B_1 + A_1$	$2B_u$	$A_u + B_u$	$A_u + B_u$	E	$2B$	$A + B$	$A + B$	$2A'$	$A' + A''$	$A' + A''$	$2A_u$
E_{2u}	$A_2 + A_1$	$A_2 + B_1$	$A_2 + B_2$	$2A_u$	$A_u + B_u$	$A_u + B_u$	E	$2A$	$A + B$	$A + B$	$2A''$	$A' + A''$	$A' + A''$	$2A_u$

$C_{3i} \equiv S_6$	C_3	C_i	C_1
A_g	A	A_g	A
E_g	E	$2A_g^*$	$2A^*$
A_u	A	A_u	A
E_u	E	$2A_u^*$	$2A^*$

S_8	C_4	C_2	C_1
A	A	A	A
B	A	A	A
E_1	E	$2B$	$2A$
E_2	$2B$	$2A$	$2A$
E_3	E	$2B$	$2A$

$C_{\infty v}^\dagger$	C_{6v}	C_{4v}	C_{3v}	C_{2v}
$A_1 \equiv \Sigma^+$	A_1	A_1	A_1	A_1
$A_2 \equiv \Sigma^-$	A_2	A_2	A_2	A_2
$E_1 \equiv \Pi$	E_1	E	E	$B_1 + B_2$
$E_2 \equiv \Delta$	E_2	$B_1 + B_2$	E	$A_1 + A_2$
$E_3 \equiv \Phi$	$B_2 + B_1$	E	$A_1 + A_2$	$B_1 + B_2$
$E_4 \equiv \Gamma$	E_2	$A_1 + A_2$	E	$A_1 + A_2$
...				

$D_{\infty h}^\dagger$	D_{6h}	C_{6v}	C_{3v}	D_{4h}	C_{4v}	C_{2v}	$C_{\infty v}$
Σ_g^+	A_{1g}	A_1	A_1	A_{1g}	A_1	A_1	$\Sigma^+ \equiv A_1$
Σ_g^-	A_{2g}	A_2	A_2	A_{2g}	A_2	A_2	$\Sigma^- \equiv A_2$
Π_g	E_{1g}	E_1	E	E_g	E	$B_1 + B_2$	$\Pi \equiv E_1$
Δ_g	E_{2g}	E_2	E	$B_{1g} + B_{2g}$	$B_1 + B_2$	$A_1 + B_2$	$\Delta \equiv E_2$
...							
Σ_u^+	A_{2u}	A_1	A_1	A_{2u}	A_1	A_1	$\Sigma^+ \equiv A_1$
Σ_u^-	A_{1u}	A_2	A_2	A_{1u}	A_2	A_2	$\Sigma^- \equiv A_2$
Π_u	E_{1u}	E_1	E	E_u	E	$B_1 + B_2$	$\Pi \equiv E_1$
Δ_u	E_{2u}	E_2	E	$B_{1u} + B_{2u}$	$B_1 + B_2$	$A_1 + A_2$	$\Delta \equiv E_2$
...							

[†]The z axis of $C_{\infty v}$ and $D_{\infty h}$ groups must coincide with z axis of the point group.

T	D_2	C_3	C_2	C_1
A	A	A	A	A
E	$2A^*$	E	$2A^*$	$2A^*$
F	$B_1 + B_2 + B_3$	$A + E_\dagger^*$	$A + 2B$	$3A$

T_d	T	D_{2d}	C_{3v}	S_4	D_2	C_{2v}	C_3	C_2	C_s
A_1	A	A_1	A_1	A	A	A_1	A	A	A'
A_2	A	B_1	A_2	B	A	A_2	A	A	A''
E	E	$A_1 + B_1$	E	$A + B$	$2A$	$A_1 + A_2$	E	$2A$	$A' + A''$
F_1	F	$A_2 + E$	$A_2 + E$	$A + E$	$B_1 + B_2 + B_3$	$A_2 + B_1 + B_2$	$A + E$	$A + 2B$	$A' + 2A''$
F_2	F	$B_2 + E$	$A_1 + E$	$B + E$	$B_1 + B_2 + B_3$	$A_1 + B_1 + B_2$	$A + E$	$A + 2B$	$2A' + A''$

T_h	T	D_{2h}	$S_6 \equiv C_{3i}$	D_2	C_{2v}	C_{2h}	C_3	C_2	C_s	C_i	C_1
A_g	A	A_g	A_g	A	A_1	A_g	A	A	A'	A_g	A
E_g	E	$2A_g^*$	E_g	$2A^*$	$2A_1^*$	$2A_g^*$	E	$2A^*$	$2A'^*$	$2A_g^*$	$2A^*$
F_g	F	$B_{1g} + B_{2g} + B_{3g}$	$A_g + E_g^\dagger$	$B_1 + B_2 + B_3$	$A_2 + B_1 + B_2$	$A + 2B_g$	$A + E_1^\dagger$	$A + 2B$	$A' + 2A''$	$3A_g$	3A
A_u	A	A_u	A_u	A	A_2	A_u	A	A	A''	A_u	A
E_u	E	$2A_u^*$	E_u	$2A^*$	$2A_2^*$	$2A_u^*$	E	$2A^*$	$2A''^*$	$2A_u^*$	$2A^*$
F_u	F	$B_{1u} + B_{2u} + B_{3u}$	$A_u + E_u^\dagger$	$B_1 + B_2 + B_3$	$A_1 + B_1 + B_2$	$A_u + 2B_u$	$A + E_1^\dagger$	$A + 2B$	$2A' + A''$	$3A_u$	3A

O	T	D ₄	D ₃	C ₄	$\overbrace{3C_2}^{D_2}$	$\overbrace{C_2, 2C'_2}^{D_2}$	C ₃	C ₂	C' ₂
A ₁	A	A ₁	A ₁	A	A	A	A	A	A
A ₂	A	B ₁	A ₂	B	A	B ₁	A	A	B
E	E	A ₁ + B ₁	E	A + B	2A	A + B ₁	E	2A	A + B
F ₁	F	A ₂ + E	A ₂ + E	A + E	B ₁ + B ₂ + B ₃	B ₁ + B ₂ + B ₃	A + E	A + 2B	A + 2B
F ₂	F	B ₂ + E	A ₁ + E	B + E	B ₁ + B ₂ + B ₃	A + B ₂ + B ₃	A + E	A + 2B	2A + B

O _h	O	T _d	T _h	T	D _{3d}	D _{4h}	C _{3v}	D ₃	C _{3i} ≡ S ₆
A _{1g}	A ₁	A ₁	A _g	A	A _{1g}	A _{1g}	A ₁	A ₁	A _g
A _{2g}	A ₂	A ₂	A _g	A	A _{2g}	B _{1g}	A ₂	A ₂	A _g
E _g	E	E	E _g	E	E _g	A _{1g} + B _{1g}	E	E	E _g
F _{1g}	F ₁	F ₁	F _g	F	A _{2g} + E _g	A _{2g} + E _g	A ₂ + E	A ₂ + E	A _g + E _g
F _{2g}	F ₂	F ₂	F _g	F	A _{1g} + E _g	B _{2g} + E _g	A ₁ + E	A ₁ + E	A _g + E _g
A _{1u}	A ₁	A ₂	A _u	A	A _{1u}	A _{1u}	A ₂	A ₁	A _u
A _{2u}	A ₂	A ₁	A _u	A	A _{2u}	B _{1u}	A ₁	A ₂	A _u
E _u	E	E	E _u	E	E _u	A _{1u} + B _{1u}	E	E	E _u
F _{1u}	F ₁	F ₂	F _u	F	A _{2u} + E _u	A _{2u} + E _u	A ₁ + E	A ₂ + E	A _u + E _u
F _{2u}	F ₂	F ₁	F _u	F	A _{1u} + E _u	B _{2u} + E _u	A ₂ + E	A ₁ + E	A _u + E _u

O _h	C ₃	C ₂ , σ _d D _{2d}	C' ₂ , σ _h D _{2d}	C _{4v}	D ₄	C _{4h}	S ₄	C ₄
A _{1g}	A	A ₁	A ₁	A ₁	A ₁	A _g	A	A
A _{2g}	A	B ₁	B ₂	B ₁	B ₁	B _g	B	B
E _g	E	A ₁ + B ₁	A ₁ + B ₂	A ₁ + B ₁	A ₁ + B ₁	A _g + B _g	A + B	A + B
F _{1g}	A + E	A ₂ + E	A ₂ + E	A ₂ + E	A ₂ + E	A _g + E _g	A + E	A + E
F _{2g}	A + E	B ₂ + E	B ₁ + E	B ₂ + E	B ₂ + E	B _g + E _g	B + E	B + E
A _{1u}	A	B ₁	B ₁	A ₂	A ₁	A _u	B	A
A _{2u}	A	A ₁	A ₂	B ₂	B ₁	B _u	A	B
E _u	E	A ₁ + B ₁	A ₂ + B ₁	A ₂ + B ₂	A ₁ + B ₁	A _u + B _u	A + B	A + B
F _{1u}	A + E	B ₂ + E	B ₂ + E	A ₁ + E	A ₂ + E	A _u + E _u	B + E	B + E
F _{2u}	A + E	A ₂ + E	A ₁ + E	B ₁ + E	B ₂ + E	B _u + E _u	A + E	B + E

O_h	$3C_2$ D_{2h}	$C_{2,2C'_2}$ D_{2h}	C_{2, σ_h} C_{2v}	C_{2, σ_d} C_{2v}	C'_2, σ_h C_{2v}	$3C_2$ D_2	$C_{2,2C'_2}$ D_2
A_{1g}	A_g	A_g	A_1	A_1	A_1	A	A
A_{2g}	A_g	B_{1g}	A_1	A_2	B_1	A	B_1
E_g	$2A_g$	$A_g + B_{1g}$	$2A_1$	$A_1 + A_2$	$A_1 + B_1$	$2A$	$A + B_1$
F_{1g}	$B_{1g} + B_{2g} + B_{3g}$	$B_{1g} + B_{2g} + B_{3g}$	$A_2 + B_1 + B_2$	$A_2 + B_1 + B_2$	$A_2 + B_1 + B_2$	$B_1 + B_2 + B_3$	$B_1 + B_2 + B_3$
F_{2g}	$B_{1g} + B_{2g} + B_{3g}$	$A_{1g} + B_{2g} + B_{3g}$	$A_2 + B_1 + B_2$	$A_1 + B_1 + B_2$	$A_1 + A_2 + B_2$	$B_1 + B_2 + B_3$	$A + B_2 + B_3$
A_{1u}	A_u	A_u	A_2	A_2	A_2	A	A
A_{2u}	A_u	B_{2u}	A_2	A_1	B_2	A	B_1
E_u	$2A_u$	$A_u + B_{1u}$	$2A_2$	$A_1 + A_2$	$A_2 + B_2$	$2A$	$A + B_1$
F_{1u}	$B_{1u} + B_{2u} + B_{3u}$	$B_{1u} + B_{2u} + B_{3u}$	$A_1 + B_1 + B_2$	$A_1 + B_1 + B_2$	$A_1 + B_1 + B_2$	$B_1 + B_2 + B_3$	$B_1 + B_2 + B_3$
F_{2u}	$B_{1u} + B_{2u} + B_{3u}$	$A_u + B_{2u} + B_{3u}$	$A_1 + B_1 + B_2$	$A_2 + B_1 + B_2$	$A_1 + A_2 + B_1$	$B_1 + B_2 + B_3$	$A + B_2 + B_3$

O_h	C_{2, σ_h} C_{2h}	C'_{2, σ_h} C_{2h}	σ_h C_s	σ_d C_s	C_2 C_2	C'_2 C_2	C_i	C_1
A_{1g}	A_g	A_g	A'	A'	A	A	A_g	A
A_{2g}	A_g	B_g	A'	A''	A	B	A_g	A
E_g	$2A_g$	$A_g + B_g$	$2A'$	$A' + A''$	$2A$	$A + B$	$2A_g$	$2A$
F_{1g}	$A_g + 2B_g$	$A_g + 2B_g$	$A' + A''$	$A' + 2A''$	$A + 2B$	$A + 2B$	$3A_g$	$3A$
F_{2g}	$A_g + 2B_g$	$2A_g + B_g$	$A' + 2A''$	$2A' + A''$	$A + 2B$	$2A + B$	$3A_g$	$3A$
A_{1u}	A_u	A_u	A''	A''	A	A	A_u	A
A_{2u}	A_u	B_u	A''	A'	A	B	A_u	A
E_u	$2A_u$	$A_u + B_u$	$2A''$	$A' + A''$	$2A$	$A + B$	$2A_u$	$2A$
F_{1u}	$A_u + 2B_u$	$A_u + 2B_u$	$2A' + A''$	$2A' + A''$	$A + 2B$	$A + 2B$	$3A_u$	$3A$
F_{2u}	$A_u + 2B_u$	$2A_u + B_u$	$2A' + A''$	$A' + 2A''$	$A + 2B$	$2A + B$	$3A_u$	$3A$

I_h	I	C_5	C_3	C_2	C_1
A_g	A	A	A	A	A
A_u	A	A	A	A	A
F_{1g}	F_1	$A + E_1$	$A + E$	$A + 2B$	$3A$
F_{1u}	F_1	$A + E_1$	$A + E$	$A + 2B$	$3A$
F_{2g}	F_2	$A + E_2$	$A + E$	$A + 2B$	$3A$
F_{2u}	F_2	$A + E_2$	$A + E$	$A + 2B$	$3A$
G_{1g}	G_1	$E_1 + E_2$	$2A + E$	$2A + 2B$	$4A$
G_{1u}	G_1	$E_1 + E_2$	$2A + E$	$2A + 2B$	$4A$
H_g	H	$A + E_1 + E_2$	$A + 2E$	$3A + 2B$	$5A$
H_u	H	$A + E_1 + E_2$	$A + 2E$	$3A + 2B$	$5A$

APPENDIX X. SITE SYMMETRY FOR THE 230 SPACE GROUPS

The tables of site symmetry for the 230 space groups shown below were reproduced with permission from the book of J. R. Ferraro and J. S. Ziomek (Ref. 9 of Chapter I). The number in front of the point group notation represents the number of distinct sets of sites, and those in parentheses indicates the number of equivalent sites for each distinct set. Since the number of sites for C_p , C_{pv} ($p = 1, 2, 3, \dots$) and C_s is infinite, no coefficients are given in front of these point group notations.

Space group	Site symmetries	
1 $P1$	C_1^1	$C_1(1)$
2 $P\bar{1}$	C_i^1	$8C_i(1); C_1(2)$
3 $P2$	C_2^1	$4C_2(1); C_1(2)$
4 $P2_1$	C_2^2	$C_1(2)$
5 B_2 or C_2	C_2^3	$2C_2(1); C_1(2)$
6 Pm	C_s^1	$2C_s(1); C_1(2)$
7 Pb or Pc	C_s^2	$C_1(2)$
8 Bm or Cm	C_s^3	$C_s(1); C_1(2)$
9 Bb or Cc	C_4^4	$C_1(2)$
10 $P2/m$	C_{2h}^1	$8C_{2h}(1); 4C_2(2); 2C_s(2); C_1(4)$
11 $P2_1/m$	C_{2h}^2	$4C_i(2); C_s(2); C_1(4)$

(Continued)

(Continued)

Space group		Site symmetries
12 $B2/m$ or $C2/m$	C_{2h}^3	$4C_{2h}(1); 2C_i(2); 2C_2(2); C_s(2); C_1(4)$
13 $P2/b$ or $P2/c$	C_{2h}^4	$4C_i(2); 2C_2(2); C_1(4)$
14 $P2_1/b$ or $P2_1/c$	C_{2h}^5	$4C_i(2); C_1(4)$
15 $B2/b$ or $C2/c$	C_{2h}^6	$4C_i(2); C_2(2); C_1(4)$
16 $P222$	D_2^1	$8D_2(1); 12C_2(2); C_1(4)$
17 $P222_1$	D_2^2	$4C_2(2); C_1(4)$
18 $P2_12_12$	D_2^3	$2C_2(2); C_1(4)$
19 $P2_12_12_1$	D_2^4	$C_1(4)$
20 $C222_1$	D_2^5	$2C_2(2); C_1(4)$
21 $C222$	D_2^6	$4D_2(1); 7C_2(2); C_1(4)$
22 $F222$	D_2^7	$4D_2(1); 6C_2(2); C_1(4)$
23 $I222$	D_2^8	$4D_2(1); 6C_2(2); C_1(4)$
24 $I2_12_12_1$	D_2^9	$3C_2(2); C_1(4)$
25 $Pmm2$	C_{2v}^1	$4C_{2v}(1); 4C_s(2); C_1(4)$
26 $Pmc2_1$	C_{2v}^2	$2C_s(2); C_1(4)$
27 $Pcc2$	C_{2v}^3	$4C_2(2); C_1(4)$
28 $Pma2$	C_{2v}^4	$2C_2(2); C_s(2); C_1(4)$
29 $Pca2_1$	C_{2v}^5	$C_1(4)$
30 $Pnc2$	C_{2v}^6	$2C_2(2); C_1(4)$
31 $Pmn2_1$	C_{2v}^7	$C_s(2); C_1(4)$
32 $Pba2$	C_{2v}^8	$2C_2(2); C_1(4)$
33 $Pna2_1$	C_{2v}^9	$C_1(4)$
34 $Pnn2$	C_{2v}^{10}	$2C_2(2); C_1(4)$
35 $Cmm2$	C_{2v}^{11}	$2C_{2v}(1); C_2(2); 2C_s(2); C_1(4)$
36 $Cmc2_1$	C_{2v}^{12}	$C_s(2); C_1(4)$
37 $Ccc2$	C_{2v}^{13}	$3C_2(2); C_1(4)$
38 $Amm2$	C_{2v}^{14}	$2C_{2v}(1); 3C_s(2); C_1(4)$
39 $Abm2$	C_{2v}^{15}	$2C_2(2); C_s(2); C_1(4)$
40 $Ama2$	C_{2v}^{16}	$C_2(2); C_s(2); C_1(4)$
41 $Aba2$	C_{2v}^{17}	$C_2(2); C_1(4)$
42 $Fmm2$	C_{2v}^{18}	$C_{2v}(1); C_2(2); 2C_s(2); C_1(4)$
43 $Fdd2$	C_{2v}^{19}	$C_2(2); C_1(4)$
44 $Imm2$	C_{2v}^{20}	$2C_{2v}(1); 2C_s(2); C_1(4)$
45 $Iba2$	C_{2v}^{21}	$2C_2(2); C_1(4)$
46 $Ima2$	C_{2v}^{22}	$C_2(2); C_s(2); C_1(4)$
47 $Pmmm$	D_{2h}^1	$8D_{2h}(1); 12C_{2v}(2); 6C_s(4); C_1(8)$
48 $Pnnn$	D_{2h}^2	$4D_2(2); 2C_i(4); 6C_2(4); C_1(8)$
49 $Pccm$	D_{2h}^3	$4C_{2h}(2); 4D_2(2); 8C_2(4); C_s(4); C_1(8)$
50 $Pban$	D_{2h}^4	$4D_2(2); 2C_i(4); 6C_2(4); C_1(8)$
51 $Pmma$	D_{2h}^5	$4C_{2h}(2); 2C_{2v}(2); 2C_2(4); 3C_s(4); C_1(8)$
52 $Pnna$	D_{2h}^6	$2C_i(4); 2C_2(4); C_1(8)$
53 $Pmna$	D_{2h}^7	$4C_{2h}(2); 3C_2(4); C_s(4); C_1(8)$

(Continued)

Space group		Site symmetries
54 <i>Pcca</i>	D_{2h}^8	$2C_4(4); 3C_2(4); C_1(8)$
55 <i>Pbam</i>	D_{2h}^9	$4C_{2h}(2); 2C_2(4); 2C_2(4); C_1(8)$
56 <i>Pccn</i>	D_{2h}^{10}	$2C_4(4); 2C_2(4); C_1(8)$
57 <i>Pbcm</i>	D_{2h}^{11}	$2C_4(4); C_2(4); C_s(4); C_1(8)$
58 <i>Pnnm</i>	D_{2h}^{12}	$4C_{2h}(2); 2C_2(4); C_s(4); C_1(8)$
59 <i>Pmmm</i>	D_{2h}^{13}	$2C_{2v}(2); 2C_4(4); 2C_s(4); C_1(8)$
60 <i>Pbcn</i>	D_{2h}^{14}	$2C_4(4); C_2(4); C_1(8)$
61 <i>Pbca</i>	D_{2h}^{15}	$2C_4(4); C_1(8)$
62 <i>Pnma</i>	D_{2h}^{16}	$2C_4(4); C_s(4); C_1(8)$
63 <i>Cmcm</i>	D_{2h}^{17}	$2C_{2h}(2); C_{2v}(2); C_4(4); C_2(4); 2C_s(4); C_1(8)$
64 <i>Cmca</i>	D_{2h}^{18}	$2C_{2h}(2); C_4(4); 2C_2(4); C_s(4); C_1(8)$
65 <i>Cmmm</i>	D_{2h}^{19}	$4D_{2h}(1); 2C_{2h}(2); 6C_{2v}(2); C_2(4); 4C_s(4); C_1(8)$
66 <i>Cccm</i>	D_{2h}^{20}	$2D_2(2); 4C_{2h}(2); 5C_2(4); C_s(4); C_1(8)$
67 <i>Cmma</i>	D_{2h}^{21}	$2D_2(2); 4C_{2h}(2); C_{2v}(2); 5C_2(4); 2C_s(4); C_1(8)$
68 <i>Ccca</i>	D_{2h}^{22}	$2D_2(2); 2C_4(4); 4C_2(4); C_1(8)$
69 <i>Fmmm</i>	D_{2h}^{23}	$2D_{2h}(1); 3C_{2h}(2); D_2(2); 3C_{2v}(2); 3C_2(4); 3C_s(4); C_1(8)$
70 <i>Fddd</i>	D_{2h}^{24}	$2D_2(2); 2C_4(4); 3C_2(4); C_1(8)$
71 <i>Immm</i>	D_{2h}^{25}	$4D_{2h}(1); 6C_{2v}(2); C_4(4); 3C_s(4); C_1(8)$
72 <i>Ibam</i>	D_{2h}^{26}	$2D_2(2); 2C_{2h}(2); C_4(4); 4C_2(4); C_s(4); C_1(8)$
73 <i>Ibca</i>	D_{2h}^{27}	$2C_4(4); 3C_2(4); C_1(8)$
74 <i>Imma</i>	D_{2h}^{28}	$4C_{2h}(1); C_{2v}(2); 2C_2(4); 2C_s(4); C_1(8)$
75 <i>P4</i>	C_4^1	$2C_4(1); C_2(2); C_1(4)$
76 <i>P4₁</i>	C_4^2	$C_1(4)$
77 <i>P4₂</i>	C_4^3	$3C_2(2); C_1(4)$
78 <i>P4₃</i>	C_4^4	$C_1(4)$
79 <i>I4</i>	C_4^5	$C_4(1); C_2(2); C_1(4)$
80 <i>I4₁</i>	C_4^6	$C_2(2); C_1(4)$
81 $P\bar{4}$	S_4^1	$4S_4(1); 3C_2(2); C_1(4)$
82 $I\bar{4}$	S_4^2	$4S_4(1); 2C_2(2); C_1(4)$
83 <i>P4/m</i>	C_{4h}^1	$4C_{4h}(1); 2C_{2h}(2); 2C_4(2); C_2(4); 2C_s(4); C_1(8)$
84 <i>P4₂/m</i>	C_{4h}^2	$4C_{2h}(2); 2S_4(2); 3C_2(4); C_s(4); C_1(8)$
85 <i>P4/n</i>	C_{4h}^3	$2S_4(2); C_4(2); 2C_4(4); C_2(4); C_1(8)$
86 <i>P4₂/n</i>	C_{4h}^4	$2S_4(2); 2C_4(4); 2C_2(4); C_1(8)$
87 <i>I4/m</i>	C_{4h}^5	$2C_{4h}(1); C_{2h}(2); S_4(2); C_4(2); C_4(4); C_2(4); C_s(4); C_1(8)$
88 <i>I4₁/a</i>	C_{4h}^6	$2S_4(2); 2C_4(4); C_2(4); C_1(8)$
89 <i>P422</i>	D_4^1	$4D_4(1); 2D_2(2); 2C_4(2); 7C_2(4); C_1(8)$
90 <i>P42₁2</i>	D_4^2	$2D_2(2); C_4(2); 3C_2(4); C_1(8)$
91 <i>P4₁22</i>	D_4^3	$3C_2(4); C_1(8)$
92 <i>P4₁2₁2</i>	D_4^4	$C_2(4); C_1(8)$
93 <i>P4₂22</i>	D_4^5	$6D_2(2); 9C_2(4); C_1(8)$
94 <i>P4₂2₁2</i>	D_4^6	$2D_2(2); 4C_2(4); C_1(8)$
95 <i>P4₃22</i>	D_4^7	$3C_2(4); C_1(8)$

(Continued)

(Continued)

Space group		Site symmetries
96 $P4_32_12$	D_4^8	$C_2(4); C_1(8)$
97 $I422$	D_4^9	$2D_4(1); 2D_2(2); C_4(2); 5C_2(4); C_1(8)$
98 $I4_122$	D_4^{10}	$2D_2(2); 4C_2(4); C_1(8)$
99 $P4mm$	C_{4v}^1	$2C_{4v}(1); C_{2v}(2); 3C_s(4); C_1(8)$
100 $P4bm$	C_{4v}^2	$C_4(2); C_{2v}(2); C_s(4); C_1(8)$
101 $P4_2cm$	C_{4v}^3	$2C_{2v}(2); C_2(4); C_s(4); C_1(8)$
102 $P4_2nm$	C_{4v}^4	$C_{2v}(2); C_2(4); C_s(4); C_1(8)$
103 $P4cc$	C_{4v}^5	$2C_4(2); C_2(4); C_1(8)$
104 $P4nc$	C_{4v}^6	$C_4(2); C_2(4); C_1(8)$
105 $P4_2mc$	C_{4v}^7	$3C_{2v}(2); 2C_s(4); C_1(8)$
106 $P4_2bc$	C_{4v}^8	$2C_2(4); C_1(8)$
107 $I4mm$	C_{4v}^9	$C_{4v}(1); C_{2v}(2); 2C_s(4); C_1(8)$
108 $I4cm$	C_{4v}^{10}	$C_4(2); C_{2v}(2); C_s(4); C_1(8)$
109 $I4_1md$	C_{4v}^{11}	$C_{2v}(2); C_s(4); C_1(8)$
110 $I4_1cd$	C_{4v}^{12}	$C_2(4); C_1(8)$
111 $P\bar{4}2m$	D_{2d}^1	$4D_{2d}(1); 2D_2(2); 2C_{2v}(2); 5C_2(4); C_s(4); C_1(8)$
112 $P\bar{4}2c$	D_{2d}^2	$4D_2(2); 2S_4(2); 7C_2(4); C_1(8)$
113 $P\bar{4}2_1m$	D_{2d}^3	$2S_4(2); C_{2v}(2); C_2(4); C_s(4); C_1(8)$
114 $P\bar{4}2_1c$	D_{2d}^4	$2S_4(2); 2C_2(4); C_1(8)$
115 $P\bar{4}m2$	D_{2d}^5	$4D_{2d}(1); 3C_{2v}(2); 2C_2(4); 2C_s(4); C_1(8)$
116 $P\bar{4}c2$	D_{2d}^6	$2D_2(2); 2S_4(2); 5C_2(4); C_1(8)$
117 $P\bar{4}b2$	D_{2d}^7	$2S_4(2); 2D_2(2); 4C_2(4); C_1(8)$
118 $P\bar{4}n2$	D_{2d}^8	$2S_4(2); 2D_2(2); 4C_2(4); C_1(8)$
119 $I\bar{4}m2$	D_{2d}^9	$4D_{2d}(1); 2C_{2v}(2); 2C_2(4); C_s(4); C_1(8)$
120 $I\bar{4}c2$	D_{2d}^{10}	$D_2(2); 2S_4(2); D_2(2); 4C_2(4); C_1(8)$
121 $I\bar{4}2m$	D_{2d}^{11}	$2D_{2d}(1); D_2(2); S_4(2); C_{2v}(2); 3C_2(4); C_s(4); C_1(8)$
122 $I\bar{4}2d$	D_{2d}^{12}	$2S_4(2); 2C_2(4); C_1(8)$
123 $P4/mmm$	D_{4h}^1	$4D_{4h}(1); 2D_{2h}(2); 2C_{4v}(2); 7C_{2v}(4); 5C_s(8); C_1(16)$
124 $P4/mcc$	D_{4h}^2	$D_4(2); C_{4h}(2); D_4(2); C_{4h}(2); C_{2h}(4); D_2(4); 2C_4(4); 4C_2(8); C_s(8); C_1(16)$
125 $P4/nbm$	D_{4h}^3	$2D_4(2); 2D_{2d}(2); 2C_{2h}(4); C_4(4); C_{2v}(4); 4C_2(8); C_s(8); C_1(16)$
126 $P4/nnc$	D_{4h}^4	$2D_4(2); D_2(4); S_4(4); C_4(4); C_{4h}(8); 4C_2(8); C_1(8)$
127 $P4/mbm$	D_{4h}^5	$2C_{4h}(2); 2D_{2h}(2); C_4(4); 3C_{2v}(4); 3C_s(8); C_1(16)$
128 $P4/mnc$	D_{4h}^6	$2C_{4h}(2); C_{2h}(4); D_2(4); C_4(4); 2C_2(8); C_s(8); C_1(16)$
129 $P4/nmm$	D_{4h}^7	$2D_{2d}(2); C_{4v}(2); 2C_{2h}(4); C_{2v}(4); 2C_2(8); 2C_s(8); C_1(16)$
130 $P4/ncc$	D_{4h}^8	$D_2(4); S_4(4); C_4(4); C_{4h}(8); 2C_2(8); C_1(16)$
131 $P4_2/mmc$	D_{4h}^9	$4D_{2h}(2); 2D_{2d}(2); 7C_{2v}(4); C_2(8); 3C_s(8); C_1(16)$
132 $P4_2/mcm$	D_{4h}^{10}	$D_{2h}(2); D_{2d}(2); D_{2h}(2); D_{2d}(2); D_2(4); C_{2h}(4); 4C_{2v}(4); 3C_2(8); 2C_s(8); C_1(16)$
133 $P4_2/nbc$	D_{4h}^{11}	$3D_2(4); S_4(4); C_{4h}(8); 5C_2(8); C_1(16)$

(Continued)

Space group		Site symmetries
134 $P4_2/nnm$	D_{4h}^{12}	$2D_{2d}(2); 2D_2(4); 2C_{2h}(4); C_{2v}(4); 5C_2(8); C_s(8); C_1(16)$
135 $P4_2/mbc$	D_{4h}^{13}	$C_{2h}(4); S_4(4); C_{2h}(4); D_2(4); 3C_2(8); C_s(8); C_1(16)$
136 $P4_2/mnm$	D_{4h}^{14}	$2D_{2h}(2); C_{2h}(4); S_4(4); 3C_{2v}(4); C_2(8); 2C_s(8); C_1(16)$
137 $P4_2/nmc$	D_{4h}^{15}	$2D_{2d}(2); 2C_{2v}(4); C_4(8); C_2(8); C_s(8); C_1(16)$
138 $P4_2/nmc$	D_{4h}^{16}	$D_2(4); S_4(4); 2C_{2h}(4); C_{2v}(4); 3C_2(8); C_s(8); C_1(16)$
139 $I4/mmm$	D_{4h}^{17}	$2D_{4h}(1); D_{2h}(2); D_{2d}(2); C_{4v}(2); C_{2h}(4); 4C_{2v}(4); C_2(8); 3C_s(8); C_1(16)$
140 $I4/mcm$	D_{4h}^{18}	$D_4(2); D_{2d}(2); C_{4h}(2); D_{2h}(2); C_{2h}(4); C_4(4); 2C_{2v}(4); 2C_2(8); 2C_s(8); C_1(16)$
141 $I4_1/amd$	D_{4h}^{19}	$2D_{2d}(2); 2C_{2h}(4); C_{2v}(4); 2C_2(8); C_s(8); C_1(16)$
142 $I4_1/acd$	D_{4h}^{20}	$S_4(4); D_2(4); C_4(8); 3C_2(8); C_1(16)$
143 $P3$	C_3^1	$3C_3(1); C_1(3)$
144 $P3_1$	C_3^2	$C_1(3)$
145 $P3_2$	C_3^3	$C_1(3)$
146 $R3$	C_3^4	$C_3(1); C_1(3)$
147 $P\bar{3}$	C_{3i}^1	$2C_3(1); 2C_3(2); 2C_i(3); C_1(6)$
148 $R\bar{3}$	C_{3i}^2	$2C_3(1); C_3(2); 2C_i(3); C_1(6)$
149 $P312$	D_3^1	$6D_3(1); 3C_3(2); 2C_2(3); C_1(6)$
150 $P321$	D_3^2	$2D_3(1); 2C_3(2); 2C_2(3); C_1(6)$
151 $P3_112$	D_3^3	$2C_2(3); C_1(6)$
152 $P3_121$	D_3^4	$2C_2(3); C_1(6)$
153 $P3_212$	D_3^5	$2C_2(3); C_1(6)$
154 $P3_221$	D_3^6	$2C_2(3); C_1(6)$
155 $R32$	D_3^7	$2D_3(1); C_3(2); 2C_2(3); C_1(6)$
156 $P3ml$	C_{3v}^1	$3C_{3v}(1); C_s(3); C_1(6)$
157 $P1m$	C_{3v}^2	$C_{3v}(1); C_3(2); C_s(3); C_1(6)$
158 $P3cl$	C_{3v}^3	$3C_3(2); C_1(6)$
159 $P31c$	C_{3v}^4	$2C_3(2); C_1(6)$
160 $R3m$	C_{3v}^5	$C_{3v}(1); C_s(3); C_1(6)$
161 $R3c$	C_{3v}^6	$C_3(2); C_1(6)$
162 $P31m$	D_{3d}^1	$2D_{3d}(1); 2D_3(2); C_{3v}(2); 2C_{2h}(3); C_3(4); 2C_2(6); C_s(6); C_1(12)$
163 $P\bar{3}1c$	D_{3d}^2	$D_3(2); C_3(2); 2D_3(2); 2C_3(4); C_4(6); C_2(6); C_1(12)$
164 $P\bar{3}m1$	D_{3d}^3	$2D_{3d}(1); 2C_{3v}(2); 2C_{2h}(3); 2C_2(6); C_s(6); C_1(12)$
165 $P\bar{3}c1$	D_{3d}^4	$D_3(2); C_3(2); 2C_3(4); C_4(6); C_2(6); C_1(12)$
166 $P\bar{3}m$	D_{3d}^5	$2D_{3d}(1); C_{3v}(2); 2C_{2h}(3); 2C_2(6); C_s(6); C_1(12)$
167 $R\bar{3}c$	D_{3d}^6	$D_3(2); C_3(2); C_3(4); C_4(6); C_2(6); C_1(12)$
168 $P6$	C_6^1	$C_6(1); C_3(2); C_2(3); C_1(6)$
169 $P6_1$	C_6^2	$C_1(6)$
170 $P6_5$	C_6^3	$C_1(6)$
171 $P6_2$	C_6^4	$2C_2(3); C_1(6)$

(Continued)

(Continued)

Space group		Site symmetries
172 $P6_4$	C_6^5	$2C_2(3); C_1(6)$
173 $P6_3$	C_6^6	$2C_3(3); C_1(6)$
174 $P6$	C_{3h}^1	$6C_{3h}(1); 3C_3(2); 2C_s(3); C_1(6)$
175 $P6/m$	C_{6h}^1	$2C_{6h}(1); 2C_{3h}(2); C_6(2); 2C_{2h}(2); C_3(4);$ $C_2(6); 2C_s(6); C_1(12)$
176 $P6_3/m$	C_{6h}^2	$C_{3h}(2); C_3(2); 2C_{3h}(2); 2C_3(4); C_6(6);$ $C_s(6); C_1(12)$
177 $P622$	D_6^1	$2D_6(1); 2D_3(2); C_6(2); 2D_2(3); C_3(4);$ $5C_2(6); C_1(12)$
178 $P6_122$	D_6^2	$2C_2(6); C_1(12)$
179 $P6_522$	D_6^3	$2C_2(6); C_1(12)$
180 $P6_222$	D_6^4	$4D_2(3); 6C_2(6); C_1(12)$
181 $P6_422$	D_6^5	$4D_2(3); 6C_2(6); C_1(12)$
182 $P6_322$	D_6^6	$4D_3(2); 2C_3(4); 2C_2(6); C_1(12)$
183 $P6mm$	C_{6v}^1	$C_{6v}(1); C_{3v}(2); C_{2v}(3); 2C_s(6); C_1(12)$
184 $P6cc$	C_{6v}^2	$C_6(2); C_3(4); C_2(6); C_1(12)$
185 $P6_3cm$	C_{6v}^3	$C_{3v}(2); C_3(4); C_s(6); C_1(12)$
186 $P6_3mc$	C_{6v}^4	$2C_{3v}(2); C_s(6); C_1(12)$
187 $P\bar{6}m2$	D_{3h}^1	$6D_{3h}(1); 3C_{3v}(2); 2C_{2v}(3); 3C_s(6); C_1(12)$
188 $P\bar{6}c2$	D_{3h}^2	$D_3(2); C_{3h}(2); D_3(2); C_{3h}(2); D_3(2); C_{3h}(2); 3C_3(4);$ $C_2(6); C_s(6); C_1(12)$
189 $P\bar{6}2m$	D_{3h}^3	$2D_{3h}(1); 2C_{3h}(2); C_{3v}(2); 2C_{2v}(3); C_3(4); 3C_s(6); C_1(12)$
190 $P\bar{6}2c$	D_{3h}^4	$D_3(2); 3C_{3h}(2); 2C_3(4); C_2(6); C_s(6); C_1(12)$
191 $P6/mmm$	D_{6h}^1	$2D_{6h}(1); 2D_{3h}(2); C_{6v}(2); 2D_{2h}(3); C_{3v}(4);$ $5C_{2v}(6); 4C_s(12); C_1(24)$
192 $P6/mcc$	D_{6h}^2	$D_6(2); C_{6h}(2); D_3(4); C_{3h}(4); C_6(4); D_2(6); C_{2h}(6); C_3(8);$ $3C_2(12); C_s(12); C_1(24)$
193 $P6_3/mcm$	D_{6h}^3	$D_{3h}(2); D_{3d}(2); C_{3h}(4); D_3(4); C_6(4); C_{2h}(6); C_{2v}(6);$ $C_3(8); C_2(12); 2C_s(12); C_1(24)$
194 $P6_3/mmc$	D_{6h}^4	$D_{3d}(2); 3D_{3h}(2); 2C_{3v}(4); C_{2h}(6); C_{2v}(6); C_2(12);$ $2C_s(12); C_1(24)$
195 $P23$	T^1	$2T(1); 2D_2(3); C_3(4); 4C_2(6); C_1(12)$
196 $F23$	T^2	$4T(1); C_3(4); 2C_2(6); C_1(12)$
197 $I23$	T^3	$T(1); D_2(3); C_3(4); 2C_2(6); C_1(12)$
198 $P2_13$	T^4	$C_3(4); C_1(12)$
199 $I2_13$	T^5	$C_3(4); C_2(6); C_1(12)$
200 $Pm\bar{3}$	T_h^1	$2T_h(1); 2D_{2h}(3); 4C_{2v}(6); C_3(8); 2C_s(12); C_1(24)$
201 $Pn\bar{3}$	T_h^2	$T(2); 2C_3(4); D_2(6); C_3(8); 2C_2(12); C_1(24)$
202 $Fm\bar{3}$	T_h^3	$2T_h(1); T(2); C_{2h}(6); C_{2v}(6); C_3(8); C_2(12);$ $C_s(12); C_1(24)$
203 $Fd\bar{3}$	T_h^4	$2T(2); 2C_3(4); C_3(8); C_2(12); C_1(24)$
204 $Im\bar{3}$	T_h^5	$T_h(1); D_{2h}(3); C_3(4); 2C_{2v}(6); C_3(8); C_s(12); C_1(24)$
205 $Pa\bar{3}$	T_h^6	$2C_3(4); C_3(8); C_1(24)$
206 $Ia\bar{3}$	T_h^7	$2C_3(4); C_3(8); C_2(12); C_1(24)$

(Continued)

Space group		Site symmetries
207 $P4_32$	O^1	$2O(1); 2D_4(3); 2C_4(6); C_3(8); 3C_2(12); C_1(24)$
208 $P4_232$	O^2	$T(2); 2D_3(4); 3D_2(6); C_3(8); 5C_2(12); C_1(24)$
209 $F432$	O^3	$2O(1); T(2); D_2(6); C_4(6); C_3(8); 3C_2(12); C_1(24)$
210 $F4_132$	O^4	$2T(2); 2D_3(4); C_3(8); 2C_2(12); C_1(24)$
211 $I432$	O^5	$O(1); D_4(3); D_3(4); D_2(6); C_4(6); C_3(8); 3C_2(12); C_1(24)$
212 $P4_332$	O^6	$2D_3(4); C_3(8); C_2(12); C_1(24)$
213 $P4_132$	O^7	$2D_3(4); C_3(8); C_2(12); C_1(24)$
214 $I4_132$	O^8	$2D_3(4); 2D_2(6); C_3(8); 3C_2(12); C_1(24)$
215 $P4_3m$	T_d^1	$2T_d(1); 2D_{2d}(3); C_{3v}(4); 2C_{2v}(6); C_2(12); C_s(12); C_1(24)$
216 $F4_3m$	T_d^2	$4T_d(1); C_{3v}(4); 2C_{2v}(6); C_s(12); C_1(24)$
217 $I4_3m$	T_d^3	$T_d(1); D_{2d}(3); C_{3v}(4); S_4(6); C_{2v}(6); C_2(12); C_s(12); C_1(24)$
218 $P4_3n$	T_d^4	$T(2); D_2(6); 2S_4(6); C_3(8); 3C_2(12); C_1(24)$
219 $F4_3c$	T_d^5	$2T(2); 2S_4(6); C_3(8); 2C_2(12); C_1(24)$
220 $I4_3d$	T_d^6	$2S_4(6); C_3(8); C_2(12); C_1(24)$
221 $Pm3m$	O_h^1	$2O_h(1); 2D_{4h}(3); 2C_{4v}(6); C_{3v}(8); 3C_{2v}(12); 3C_s(24); C_1(48)$
222 $Pn3n$	O_h^2	$O(2); D_4(6); C_3(8); S_4(12); C_4(12); C_3(16); 2C_2(24); C_1(48)$
223 $Pm3n$	O_h^3	$T_h(2); D_{2h}(6); 2D_{2d}(6); D_3(8); 3C_{2v}(12); C_3(16); C_2(24); C_s(24); C_1(48)$
224 $Pn3m$	O_h^4	$T_d(2); 2D_{3d}(4); D_{2d}(6); C_{3v}(8); D_2(12); C_{2v}(12); 3C_2(24); C_s(24); C_1(48)$
225 $Fm3m$	O_h^5	$2O_h(1); T_d(2); D_{2h}(6); C_{4v}(6); C_{3v}(8); 3C_{2v}(12); 2C_s(24); C_1(48)$
226 $Fm3c$	O_h^6	$O(2); T_h(2); D_{2d}(6); C_{4h}(6); C_{2v}(12); C_4(12); C_3(16); C_2(24); C_s(24); C_1(48)$
227 $Fd3m$	O_h^7	$2T_d(2); 2D_{3d}(4); C_{3v}(8); C_{2v}(12); C_s(24); C_2(24); C_1(48)$
228 $Fd3c$	O_h^8	$T(4); D_3(8); C_3(8); S_4(12); C_3(16); 2C_2(24); C_1(48)$
229 $Im3m$	O_h^9	$O_h(1); D_{4h}(3); D_{3d}(4); D_{2d}(6); C_{4v}(6); C_{3v}(8); 2C_{2v}(12); C_2(24); 2C_s(24); C_1(48)$
230 $Ia3d$	O_h^{10}	$C_3(8); D_3(8); D_2(12); S_4(12); C_3(16); 2C_2(24); C_1(48)$

Note the following equivalent nomenclatures:

 $C_i \equiv S_2$ $C_2 \equiv C_{1h}$ $D_2 \equiv V$ $D_{2h} \equiv V_h$ $D_{2d} \equiv V_d$ $C_{3i} \equiv S_6$

Index

Since the number of compounds included in this volume is numerous, entries for most of individual compounds are collected under general entries such as vibrational frequencies and sulfur compounds. Normal modes of vibration, infrared and Raman spectra included are found under respective general titles.

- Ab initio* calculation of force constants, 106
- Accidental degeneracy, 58
- Acoustical branch, 131
- Aluminosilicates, 278
- Anharmonicity, 11
- Anharmonicity corrections, 103, 149
- Anisotropy of polarization, 92
- Anomalous polarization (*ap*), 94, 104, 229
- Antimony compounds, 290
- Anti-Stokes line, 8
- Antisymmetric vibration, 29
- Aragonite, 122
- Arsenic compounds, 290
- A-term resonance, 99
- Axis of symmetry. *p*-fold (C_p), 22
- Badger's rule, 14
- Band assignments, 82
- Bismuth compounds, 290
- B**-matrix, 60
- Bohr's frequency condition, 1
- Boron compounds, 254
- Boron hydrides (boranes), 255
- Bravais lattices, 117
- Brillouin zone, 131
- B-term resonance, 99
- Buckminsterfullerene (C_{60}), 259
- Calcite, 122, 126
- Carbonate radical (CO_3), 181
- Carbon clusters (small), 258
- Carbon compounds, 258
- Carbon oxide anions, 276
- Cartesian coordinate, 107
- Center of symmetry (*i*), 22
- Ceramic superconductors, 136
- Character (χ), 41
- Character tables, 355

- Chlorine isotope pattern, 199
 Class 36
 Combination bands, 5, 11
 Correlation method, 124
 Correlation tables, 119, 127, 393
 Crystallographic point groups, 116
 Crystals, vibrational analysis, 119
 Cubic potential, 11
 C_5 , 258
 C_{60} , 259
 C_{60} dimer, 263
 C_{70} , 264
 $C_{60}Br_{24}$, 263
 $C_{60}K_3$, 263
 C_{84} , 265
- Decius formula, 64
 Degenerate vibration, 26
 Density functional theory(DFT), 106
 Depolarization (dp), 92
 Depolarization ratio, 81, 92
 Diamond, 272
 Diazene (N_2H_2), 189
 Dichroism, infrared, 134
 Dipole moment, changes, 31
 Dispersion curves, 131, 134
- Electromagnetic spectrum, 3
 E-matrix, 60
 Endohedral fullerenes, 267
 Energy level diagram, 4
 Excitation profile, 105
- Factor group analysis, 123
 Fermi resonance, 58
 F-matrix, 59, 382
 Force constants, 10
 Force field, 71
 Frank-Condon factor, 100
 Fundamental vibrations, 5
- Gas phase, infrared spectra, 109
 Generalized coordinate (q), 15
 Generalized valence force (GVF) field, 72
 Germanium compounds, 276
 GF matrix method, 58
 GF matrix elements, 382
 Glide plane, 118
- G-matrix, 59, 382
 Gordy's rule, 14
 Group, 34
 Group frequencies, 82
 Group frequency charts, 286, 292, 388
 Group theory, 34
 g-vibration, 34
- Halogeno compounds, 296
 Harmonic oscillator, 10
 Herman–Mauguin (HM) notation, 119
 Hermite polynomial, 11
 Herschbach-Laurie equation, 15
 Hot bands, 5
 Hydronium (OH_3^+) ion, 174
- Ice, 168
 Identity (I), 22
 Improper rotation, 43
 Inert gas matrix, 109
 Infrared dichroism, 134
- Infrared spectra**
 $B_3N_3H_6$ (borazine), 257
 $[B_6X_6]Cs_2$, (X = Cl, Br and I), 256
 C_5 , 260
 C_{60} , 261
 C_{70} , 266
 C_{84} , 267
 $CaCO_3$ (calcite), 134
 $[ClO_3]K$, 179
 $Cr(CO)_6$, 111
 $Eu@C_{74}$, 268
 $GeCl_4$, 199
 HArF, 173
 H_2NCN (cyanamide), 283
 $[IO_3]K$, 179
 MF_6 , (M = Mo, Te, Ru and Rh), 230
 NH_3 , 4
 NH_4Cl , 195
 NiF_2 , 163
 NNO , 174
 $[OsF_6Cl_{6-n}]^{2-}$, (n = 2~4), 236
 $[PbF_3]M$ (M = Na, K, Rb, Cs), 115
 $P_4N_4Cl_8$, 291
 $Sc(CO)_n$, 114
 $Sc_3N@C_{80}$, 270
 Si_6H_{12} , 278
 SiO_2 (α -quartz), 280

- $^{235}\text{UF}_6/^{238}\text{UF}_6$, 232
 US_n , 113
 XeF_4 , 212
 Inert gas matrices, 109
 Intensity
 Infrared absorption, 88
 Raman scattering, 94
 Internal coordinate, 46, 59
 Internal symmetry coordinate, 108
 Internal tension, 73
 Inverse polarization (*ip*), 94
 Inversion doubling, 176
 Irreducible representation, 37
 Direct products of, 377

 Kronecker's delta (δ_{ij}), 38

 Lagrange's equation, 16
 Laser-ablated metal vapor, 112
 Laser lines, 7
 \mathbf{L} -matrix, 85
 Lattice vibrations, 129

 Matrix algebra, 368
 Matrix co-condensation reaction, 112
 Matrix effect, 112
 Maxwell–Boltzmann distribution law, 5, 9, 97
 Metal cluster compounds, 250
 Metal isotope spectroscopy, 79, 81
 Molecular spectra, origin of, 1
 Multiplication table, 36
 Mutual exclusion rule, 34

 Nanotubes, 271
 Nitrogen compounds, 279
 Nonsymmetric vibration, 29
 Normal coordinate (Q), 17
 Normal coordinate analysis (NCA), 58
Normal modes of vibration
 CH_3X molecule, 83
 CH_2X_2 molecule, 84
 WXYZ (bent) molecule, 192
 X_3 (triangular) molecule, 170
 X_4 (square-planar) molecule, 188
 X_4 (tetrahedral) molecule, 187
 XY_2 (bent) molecule, 30, 31
 XY_2 (linear) molecule, 28, 33
 XY_3 (planar) molecule, 181
 XY_3 (pyramidal) molecule, 174
 XY_4 (square-planar) molecule, 210
 XY_4 (tetrahedral) molecule, 194
 XY_5 (trigonal–bipyramidal) molecule, 214
 XY_6 (octahedral) molecule, 221
 X_2Y_2 (nonlinear) molecule, 189
 X_2Y_6 (bridged) molecule, 241
 X_2Y_6 (ethane-type) molecule, 243
 XYZ (linear) molecule, 160
 ZXY $_4$ (tetragonal–pyramidal) molecule, 217
 Normal vibration, 15, 18
 number in each species, 39, 373

 Optical branch, 131
 Orbital valence force (OVF) field, 74
 Order of group (h), 37
 Orthogonal matrix, 108
 Overtone bands, 5, 11

 Parabolic potential, 10
 Phosphorus compounds, 285
 Plane of symmetry (σ), 22
 Point groups, 23, 25–28, 355
 Polarizability, 32
 Polarizability ellipsoid, 32, 33
 Polarizability tensor, 32
 Polarized infrared spectra, 134
 Polarized Raman spectra, 134
 Potential energy curve, 10
 Potential energy distribution (PED), 87
 Potential field, 71
 Pressure broadening, 89
 Product rule, 78
 Proper rotation, 42

 Raman scattering, 6
Raman spectra
 $[\text{B}_6\text{X}_6]\text{Cs}_2$, ($\text{X} = \text{Cl}, \text{Br}, \text{I}$), 256
 CaCO_3 (calcite), 136
 Carbon nanotubes, 273
 CCl_4 , 9, 93
 C_{60} , 261, 262
 C_{70} , 266
 Eu@C_{74} , 268
 I_2 , 102
 $[\text{IrCl}_6]^{2-}$, 230
 MF_6 ($\text{M} = \text{Mo}, \text{Tc}, \text{Ru}, \text{Rh}$), 230

Raman spectra (*Continued*)

N_2 polymer, 158
 $[\text{N}_5]^+[\text{AsF}_6]^-$, 157
 $[\text{NO}_3]\text{K}$, 183
 N_4X_4 ($\text{X} = \text{S}, \text{Se}$), 285
 $[\text{OsF}_n\text{Cl}_{6-n}]^{2-}$ ($n = 2\sim 4$), 236
 $\text{Pb}_6\text{O}(\text{OH})_6(\text{ClO}_4)_4\text{H}_2\text{O}$, 252
 $\text{P}_4\text{N}_4\text{Cl}_8$, 291
 $\text{Sc}_2@\text{C}_{84}$, 271
 $\text{Sc}_3\text{N}@\text{C}_{80}$, 270
 Si_n ($n = 4, 6, 7$), 277
 Si_6H_{12} , 278
 SiO_2 (α -quartz), 280
 $(\text{SNH})_4$, 295
 $[\text{SnX}_3]^-$ ($\text{X} = \text{Cl}, \text{Br}, \text{I}$), 178
 $[\text{SO}_4]\text{K}_2$, 203
 TiI_4 , 103
 XeF_4 , 212
 $\text{YBa}_2\text{Cu}_3\text{O}_{7-\delta}$, 139
 Rayleigh scattering, 6
 Redlich-Teller product rule, 78
 Reduced mass (μ), 9
 Reducible representation, 37
 Redundant condition, 46
 Representation of the group (Γ), 36
 Resonance fluorescence, 8
 Resonance Raman scattering, 8
Resonance Raman(RR) spectra
 I_2 , 102
 $\text{Ni}(\text{OEP})$, 105
 $[\text{Re}_2\text{F}_8]^{2-}$, 248
 TiI_4 , 103
R-matrix, 60
 Rotational spectra, 3, 4
 Rotational-vibrational spectrum, 232
 Rotation-reflection axis (S_p), 22

 Salt-molecule reaction, 114
 Schönflies(S) notation, 117
 Schrödinger wave equation, 10, 21
 Screw axis, 118
 Secular equation, 75
 Selection rules, 25, 49
 Selenium compounds, 292
 Silanone (H_2SiO), 187
 Silicates, 278
 Silicon clusters, 276
 Silicon compounds, 276
 Similarity transformation, 37

Simultaneous transition, 191
 Site group analysis, 122
 Site symmetry, 122, 407
S-matrix, 62
 Space group, 118, 120
 Stokes line, 8
 Structure determination, 56
 Subgroup, 119
 Sulfate radical(SO_4), 203
 Sulfur compounds, 292
 Sum rule, 78
S vector, 62
 Symmetric vibration, 29
 Symmetry coordinate, 67
 Symmetry elements, 21, 24
 Symmetry in crystals, 115
 Symmetry of normal vibration, 26
 Symmetry operation, 22

Taylor's series, 16
 Theoretical calculation of vibrational frequencies, 106
 Time-resolved resonance Raman (TR^3) spectroscopy, 248
 Totally symmetric vibration, 29
 Triply degenerate vibration, 26
 T-shaped molecules, 184

 UF_6 , 229, 232
U-matrix, 66
 Urey-Bradley force (UBF) field, 72
 u -vibration, 34

van der Waals complexes, 159

Vibrational coupling, 84

Vibrational frequencies

WXYZ molecules, 193
 X_2 molecules, 150, 155
 X_3 (linear, bent, triangular) molecules, 169
 X_4 (tetrahedral) molecules, 188
 X_4 (square-planar) molecules, 188
 XXY (bent, linear) molecules, 170
 XY molecules, 151, 156
 XY_2 (bent, linear) molecules, 161, 164, 168
 XY_3 (planar) molecules, 182, 183
 XY_3 (pyramidal) molecules, 175, 177, 179
 XY_4 (distorted tetrahedral) molecules, 201
 XY_4 (square-planar) molecules, 211
 XY_4 (tetrahedral molecules), 194, 196, 202

- XY_5 (tetragonal pyramidal) molecules, 218
 XY_5 (trigonal bipyramidal) molecules, 215
 XY_6 (octahedral) molecules, 223, 233
 XY_7 (pentagonal bipyramidal) molecules, 238
 X_2Y (linear, bent) molecules, 170
 X_2Y_2 molecules, 190
 X_2Y_4 molecules, 239
 X_2Y_6 (ethane-type) molecules, 245
 X_2Y_6 (non-planar, bridged) molecules, 242
 X_2Y_6 (planar, bridged) molecules, 243
 X_2Y_7 molecules, 246
 X_2Y_9 molecules, 249
 XY_4WZ (octahedral) molecules, 234
 XYZ (bent) molecules, 172
 XYZ (linear) molecules, 171
 XY_5Z (octahedral) molecules, 234
 XY_5Z_2 (pentagonal-bipyramidal) molecules, 238
 $ZWXY_2$ (tetrahedral) molecules, 209
 ZXY_2 (planar) molecules, 185
 ZXY_2 (pyramidal) molecules, 180
 ZXY_3 (tetrahedral) molecules, 205
 ZXY_4 (tetragonal pyramidal) molecules, 218
 ZXY_4 (trigonal bipyramidal) molecules, 215
 Z_2XY_2 (tetrahedral) molecules, 207
 $ZXYW$ (planar) molecules, 185
Vibrational quantum number (ν), 11
Water (H_2O) molecule, 30, 33
Water, liquid, 167
Xenon hexafluoride (XeF_6), 229, 231
Xenon pentafluoride anion ($[XeF_5]^-$), 57
Xenon tetrafluoride (XeF_4), 56
X-matrix, 60
Zero-point energy, 3